

NASA Conference Publication 10105, Part 1
DOT/FAA/RD-92/19-I

Airborne Wind Shear Detection and Warning Systems

*Fourth Combined Manufacturers'
and Technologists' Conference*

ORIGINAL PAGE
COLOR PHOTOGRAPH

N93-19590
--THRU--
N93-19612
Unclas

G3/03 0137624

(NASA-CP-10105-Pt-1) AIRBORNE WIND
SHEAR DETECTION AND WARNING
SYSTEMS: FOURTH COMBINED
MANUFACTURERS' AND TECHNOLOGISTS'
CONFERENCE, PART 1 (NASA) ~~577~~

666p

488704



Compiled by
Dan D. Vicroy
and Roland L. Bowles
NASA Langley Research Center
Hampton, Virginia

Robert H. Passman
Federal Aviation Administration
Washington, D.C.

Proceedings of a conference sponsored by the
National Aeronautics and Space Administration
and the Federal Aviation Administration
and held in Williamsburg, Virginia
April 14-16, 1992

SEPTEMBER 1992

NASA

National Aeronautics and
Space Administration

Langley Research Center
Hampton, Virginia 23665-5225

FOREWORD

The Fourth Combined Manufacturers' and Technologists' Conference was hosted jointly by NASA Langley Research Center (LaRC) and the Federal Aviation Administration (FAA) in Williamsburg, Virginia on April 14-16, 1992. The meeting was co-chaired by Dr. Roland Bowles of LaRC and Robert Passman of the FAA. Dan Vicroy of LaRC served as the Technical Program Chairperson and Carol Lightner of the Bionetics Corporation was the Administrative Chairperson.

The purpose of the meeting was to transfer significant ongoing results of the NASA/FAA joint Airborne Wind Shear Program to the technical industry and to pose problems of current concern to the combined group. It also provided a forum for manufacturers to review forward-look technology concepts and for technologists to gain an understanding of the problems encountered by the manufacturers during the development of airborne equipment and the FAA certification requirements.

The present document has been compiled to record the essence of the technology updates and discussions which followed each. Updates are represented here through the unedited duplication of the vugraphs, which were generously provided by the respective speakers. When time was available questions were taken from the floor; if time was not available questions were requested in writing. The questions and answers are included at the end of each presentation. A general question and answer session was conducted at the end of each day and is included at the end of report along with closing remarks.

TABLE OF CONTENTS

Part 1

FOREWORD	i
TABLE OF CONTENTS	iii
WELCOMING ADDRESS	1
<i>Jack Howell, FAA Technical Center</i>	
SESSION I. -- NASA Flight Tests	
Program Overview / 1991 Flight Test Objectives	7
<i>Dr. Roland Bowles, NASA Langley Research Center</i>	
Flight Test Operations	23
<i>Mike Lewis, NASA Langley Research Center</i>	
NASA Wind Shear Flight Test In Situ Results	45
<i>Rosa Oseguera, NASA Langley Research Center</i>	
Air/Ground Wind Shear Information Integration - Flight Test Results	59
<i>David Hinton, NASA Langley Research Center</i>	
Doppler Radar Results	115
<i>E. Bracalente, NASA Langley Research Center</i>	
Flight Test of an Infrared Wind Shear Detector	141
<i>Dr. Burnell McKissick, NASA Langley Research Center</i>	
SESSION II. -- Hazard Characterization	
Wind Shear Hazard Determination	195
<i>Mike Lewis, NASA Langley Research Center</i>	
Three-Dimensional Numerical Simulation of the 20 June 1991, Orlando Microburst	213
<i>Dr. Fred Proctor, NASA Langley Research Center</i>	
A "Numerical Field Experiment" Approach for Determining Probabilities of Microburst Intensity	245
<i>Dr. Kelvin Droegemeier, University of Oklahoma</i> <i>Terry Zweifel, Honeywell</i>	
SESSION III. -- Reactive System Technology	
An Approach to Evaluating Reactive Airborne Wind Shear Systems	287
<i>Joe Gibson, Martin Marietta</i>	
Panel Discussion	303
<i>Kirk Baker, Federal Aviation Administration</i> <i>Dr. Roland Bowles, NASA Langley Research Center</i> <i>Joe Gibson, Martin Marietta</i> <i>Howard Glover, Sundstrand</i> <i>Doug Ormiston, Boeing</i> <i>Rosa Oseguera, NASA Langley Research Center</i> <i>Dr. Paul Robinson, Lockheed Engineering & Sciences</i> <i>Terry Zweifel, Honeywell</i>	

SESSION IV. -- Airborne Doppler Radar / Industry

RDR-4D Doppler Weather Radar With Forward Looking Wind Shear Detection Capability	317
<i>Steve Grasley, Allied-Signal Aerospace</i>	
Airborne Doppler Radar Research at Rockwell International	357
<i>Roy Robertson, Rockwell International</i>	
Acquisition and Use of Orlando, Florida and Continental Airbus Radar Flight Test Data	373
<i>Mike Eide, Westinghouse Electric</i>	
<i>Bruce Mathews, Westinghouse Electric</i>	

SESSION V. -- Doppler Related Research

Vertical Wind Estimation from Horizontal Wind Measurements.....	391
<i>Dan Vicroy, NASA Langley Research Center</i>	
Microburst Characteristics Determined from 1988-91 TDWR Testbed Measurements	417
<i>Paul Biron, MIT Lincoln Laboratory</i>	
<i>Mark Isaminger, MIT Lincoln Laboratory</i>	
Algorithms for Airborne Doppler Radar Wind Shear Detection	457
<i>Jeff Gillberg, Honeywell</i>	
<i>Mitch Pockrandt, Honeywell</i>	
<i>Peter Symosek, Honeywell</i>	
<i>Earl Benser, Honeywell</i>	

SESSION VI. -- Airborne Doppler Radar / NASA

NASA Experimental Airborne Doppler Radar and Real Time Processor for Wind Shear Detection	477
<i>P. Schaffner, NASA Langley Research Center</i>	
<i>Dr. M. Richards, Georgia Institute of Technology</i>	
<i>W. Jones, NASA Langley Research Center</i>	
<i>L. Crittenden, Research Triangle Institute</i>	
Ground Clutter Measurements Using the NASA Airborne Doppler Radar: Description of Clutter at the Denver and Philadelphia Airports.....	499
<i>S. Harrah, NASA Langley Research Center</i>	
<i>Dr. V. Delnore, Lockheed Lockheed Engineering & Sciences</i>	
<i>M. Goodrich, Lockheed Lockheed Engineering & Sciences</i>	
<i>C. Von Hagel, NASA Langley Research Center</i>	
Spectrum Characteristics of Denver and Philadelphia Ground Clutter and the Problem of Distinguishing Wind Shear Targets from Moving Clutter	517
<i>A. Mackenzie, NASA Langley Research Center</i>	
Comparison of Simulated and Actual Wind Shear Radar Data Products.....	541
<i>Dr. C. Britt, Research Triangle Institute</i>	
<i>L. Crittenden, Research Triangle Institute</i>	
NASA Airborne Radar Wind Shear Detection Algorithm and the Detection of Wet Microbursts in the Vicinity of Orlando, Florida	561
<i>Dr. C. Britt, Research Triangle Institute</i>	
<i>E. Bracalente, NASA Langley Research Center</i>	
Signal Processing for Airborne Doppler Radar Detection of Hazardous Wind Shear as Applied to NASA 1991 Radar Flight Experiment Data.....	587
<i>Dr. E. Baxa, Clemson University</i>	

Part 2*

SESSION VII. -- Airborne LIDAR Technology

Two Micron Laser Development for Atmospheric Remote Sensing at NASA Langley Research Center	617
<i>Philip Brockman, NASA Langley Research Center</i>	
NASA/LMSC Instrument Design & Fabrication	633
<i>Dr. Russel Targ, Lockheed Missiles and Space</i>	
NASA/LMSC Coherent LIDAR Airborne Shear Sensor: System Capabilities and Flight Test Plans	659
<i>Dr. Paul Robinson, Lockheed Engineering & Sciences</i>	
Solid-State Coherent Laser Radar Wind Shear Measuring Systems	673
<i>R. Milton Huffaker, Coherent Technologies</i>	

SESSION VIII. -- Passive Infrared Technology

Development of the Advance Warning Airborne System (AWAS)	687
<i>Pat Adamson, Turbulence Prediction Systems</i>	
A Millimeter-Wave Radiometer for Detecting Microbursts.....	781
<i>Dr. Robert McMillan, Georgia Tech Research Institute</i>	
Colorado State University Research.....	805
<i>Dr. Pete Sinclair, Colorado State University</i>	

SESSION IX. -- Terminal Doppler Weather Radar

The Orlando TDWR Testbed and Airborne Wind Shear Data Comparison Results.....	811
<i>Dr. Steve Campbell, MIT Lincoln Laboratory</i>	
<i>Anthony Berke, MIT Lincoln Laboratory</i>	
<i>Michael Matthews, MIT Lincoln Laboratory</i>	
TDWR 1991 Program Review	847
<i>Kim Elmore, National Center for Atmospheric Research</i>	

SESSION X. -- Flight Management Research

Experimental Evaluation of Candidate Graphical Microburst Alert Displays.....	879
<i>Craig Wanke, Massachusetts Institute of Technology</i>	
<i>Dr. R. John Hansman, Massachusetts Institute of Technology</i>	
Wind Shear Related Research at Princeton University	905
<i>Dr. Robert Stengel, Princeton University</i>	

SESSION XI. -- Regulation, Certification and System Standards

Systems Issues in Airborne Doppler Radar/LIDAR Certification	959
<i>Dr. James Evans, MIT Lincoln Laboratory</i>	
FAA Regulatory / System Standards / Certification Status.....	971
<i>Frank Rock, Federal Aviation Administration</i>	
Results of In-service Evaluation of Wind Shear Systems	977
<i>Todd Murr, Northwest Airlines</i>	

* Published under separate cover.

In-service Evaluation of Wind Shear Systems	997
<i>Capt. Sam Shirck, Continental Airlines</i>	

Advanced Technology Wind Shear Prediction System Evaluation.....	1007
<i>Capt. Greg Gering, American Airlines</i>	

GENERAL QUESTIONS AND ANSWERS.....	1017
------------------------------------	------

APPENDIX - List of Attendees	1029
------------------------------------	------

WELCOMING ADDRESS

Jack Howell

Deputy Director, FAA Technical Center

Good morning, Ladies and Gentlemen, and welcome to the Fourth Combined Manufacturers' and Technologists' Airborne Wind Shear Review meeting. I am very happy to be here today; in fact, I have reached a point in my life where I am very happy to be anywhere on the green side of the grass. I am even more happy to have the opportunity to be the keynote speaker today to talk about a topic that is very important to our aviation system. As the keynote speaker, I feel it is my duty to welcome you to this event, to congratulate you for the next 3 days and for the near future, and -- perhaps most important of all -- to stop speaking on time so that we can get on with the conference.

The welcome is already complete. Secondly, I do want to congratulate you on your many accomplishments. I have been observing the process that has provided us with Wind Shear protection for a number of years, and I have found it to be a very impressive process -- one that could well serve as a model for other undertakings. I view the process as being represented by an equilateral triangle with industry, NASA, and FAA at each apex. Each side, then, represents a particular relationship.

The FAA-NASA relationship is a long-term relationship that exists in the form of memoranda of agreements between the two agencies. This relationship needs to be maintained and nurtured to keep the team of experts working together on an advanced sensor program and to use the synergy that emerges from that relationship to prompt congress to provide adequate funding for this important project.

The FAA-industry relationship, with the exemption 5256 program in place, is a good example of participation between the FAA and industry to accomplish important safety goals involved in the development of predictive Wind Shear systems while simultaneously being mindful of technology, manufacturing, and implementation realities.

In the NASA-industry relationship NASA passes data and information back and forth while maintaining confidentiality in these relationships. In the predictive Wind Shear systems, for example, micro-burst models have been transferred to industry. To me, as a senior executive of the federal sector, this represents Technology Transfer as mandated by our Congress.

At each apex I have also observed an internal review process which for the FAA includes R&D, Air Traffic, Flight Standards, and certification personnel.

I also recognize that these working relationships did not come into existence nor achieve success overnight. Instead, they were steadily built by several individuals who developed strong

personal working relationships along with the business relationships.

As we evolve our managerial styles to involve concepts of Total Quality Management, I feel I should ask this question: what are the measurables? The measurables are at least five.

1. FAR 121.358 which mandates implementation of Wind Shear devices and the 5256 exemption process that permits certain exceptions.
2. There are ground-based and airborne units operating in the system; these represent manifestations of Technology Transfer as I mentioned earlier.
3. We are, I am told, about 1 year ahead of schedule in the Flight Program.
4. And, most important of all, is the fact that we have not had a fatal accident where Wind Shear was a contributing factor since 1985.
5. On the other hand, we do have four very famous saves at Denver in 1988.

So I am convinced your congratulations are deserved.

Now lets talk about the current program. I see in my review that by employing a 4-prong attack aimed at:

1. Hazard characterization;
2. Detection and warning;
3. Recovery flight techniques; and
4. Crew Training on those recovery flight techniques, we are well on the way to providing a solution to this Wind Shear problem. This is important because just as each accident is the result of a series or chain of events involving mechanical, procedural, and/or performance failures so also can this same model be held for a save. Thus it is very likely that any one element of our 4-prong approach may have already interrupted a chain of events that could have led to a disaster.

I see also that we are:

1. Combining technologies; these combinations may lead to site-specific ground-based solutions; similarly these combinations may also lead to aircraft-specific procedures. But, what we want to avoid is site-specific aircraft procedures.
2. Next I see that we have a certain amount of competition. Competition that exists for the purpose of optimization and not duplication is good. This competition exists between airborne and ground-based systems and between predictive and reactive systems.
3. Lastly I see we are expanding the capabilities of the associated technologies for applications to other problem areas. These areas include clear air turbulence; wake vortex

detection; mountain wave or rotor or other orographic flow studies; low visibility surface operations; and the detection and the avoidance of volcanic ash clouds.

Now comes a piece of the presentation I did not warn you about -- a Challenge. If you are sitting there pretty smug, complacent, or content to stay focused on things that make you comfortable, I offer you the opportunity to review with me some of the macro events of the last 1.5 years. First of all, who would have ever guessed it would be possible to coalesce world opinion against a single nation to the extent that we could have a war because that nation had invaded another? Who could have ever forecast the disintegration of the USSR into the UFFR (the union of fewer and fewer republics)? Isn't it sad to realize that our own children's quality of life is in jeopardy because of the status of the national and global economies, and who would ever guess that a state presidential primary could ever have "undecided" as the top vote-getter?

My point is that we are embroiled in a world of change, and we had all better be prepared to lead, follow, or get out of the way. And so, in conclusion, I would like to leave you with two challenges.

1. For those of you in the federal sector -- I challenge you to elevate your thinking to the next level of management; focus your analytical skills on the economic realities of a shrinking budget; learn how to leverage those precious R&D dollars and to take advantage of the DOD capabilities and availability's; seek solutions to administrative with the same vigor you use in seeking solutions to technical problems. For, and you can mark my words, if you don't do it, some unqualified person will.

2. And for those of you in the public sector -- I challenge you to respond to FAA's Acting Deputy Administrator, Mr. Joe Del Balzo's challenge that he issued during the Awards Luncheon at ATCA '91: don't be satisfied with just bringing problems to the FAA; instead, be prepared to be part of the development of solutions just as you have done in the Wind Shear Protection Program. Don't let Technology Transfer be a one-way process; instead, do some reverse engineering and send back to us some certification suggestions so that we regulators can do a better job of both regulating and stimulating the industry by using uniform criteria.

In summary, then, let me conclude by saying I welcome you to this review; I congratulate you on what you have accomplished so far; I approve of the program that you have outlined for yourselves, and I urge you to get ready for change. Lastly, I hope that you have a very good conference and that you enjoy your stay in Williamsburg.

Session I. NASA Flight Tests

PRECEDING PAGE BLANK NOT FILMED

1

1993010402

168

Session I. NASA Flight Tests

N93-19591

Program Overview / 1991 Flight Test Objectives

Dr. Roland Bowles, NASA Langley Research Center

PRECEDING PAGE BLANK NOT FILMED

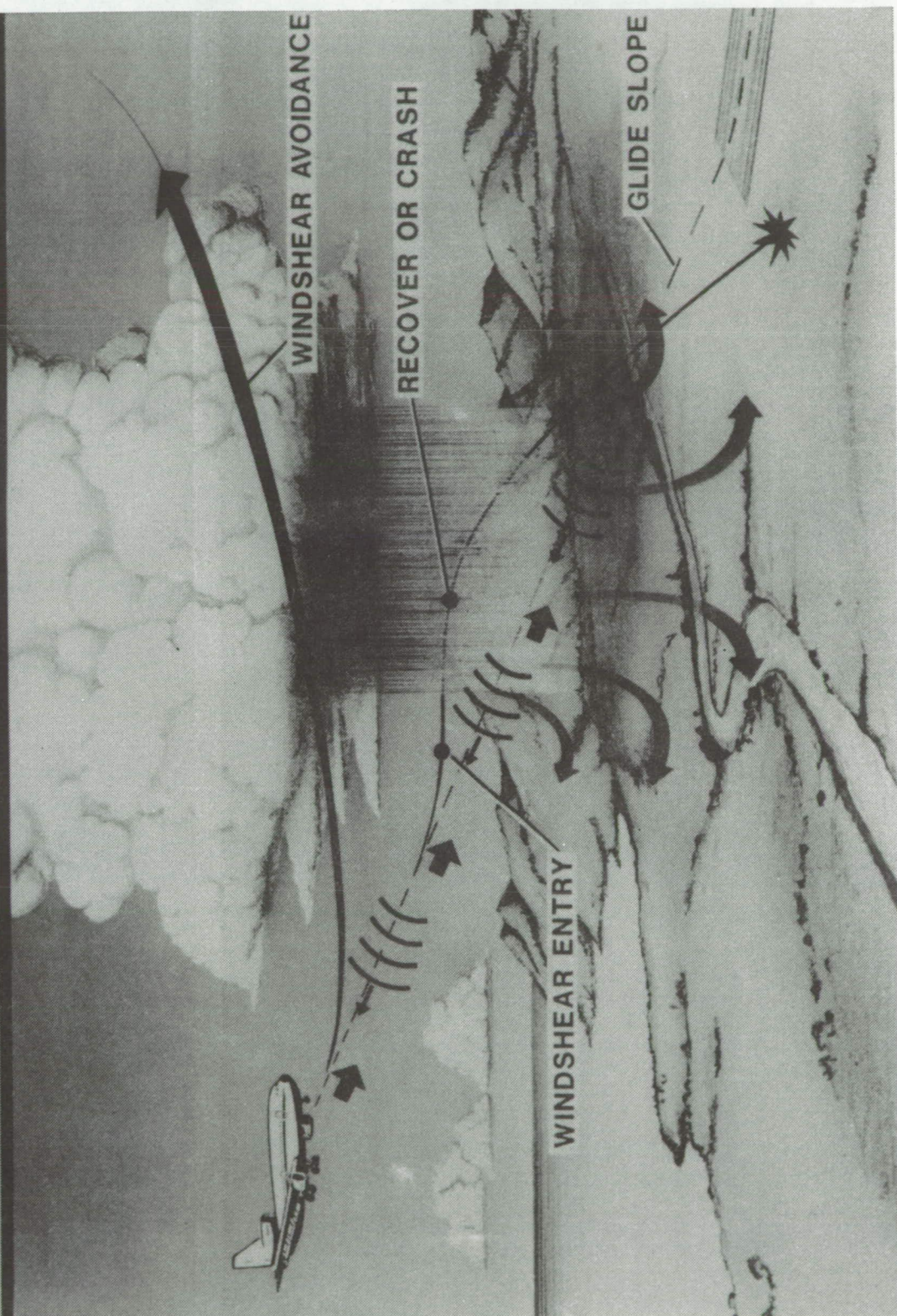
WIND SHEAR PROGRAM

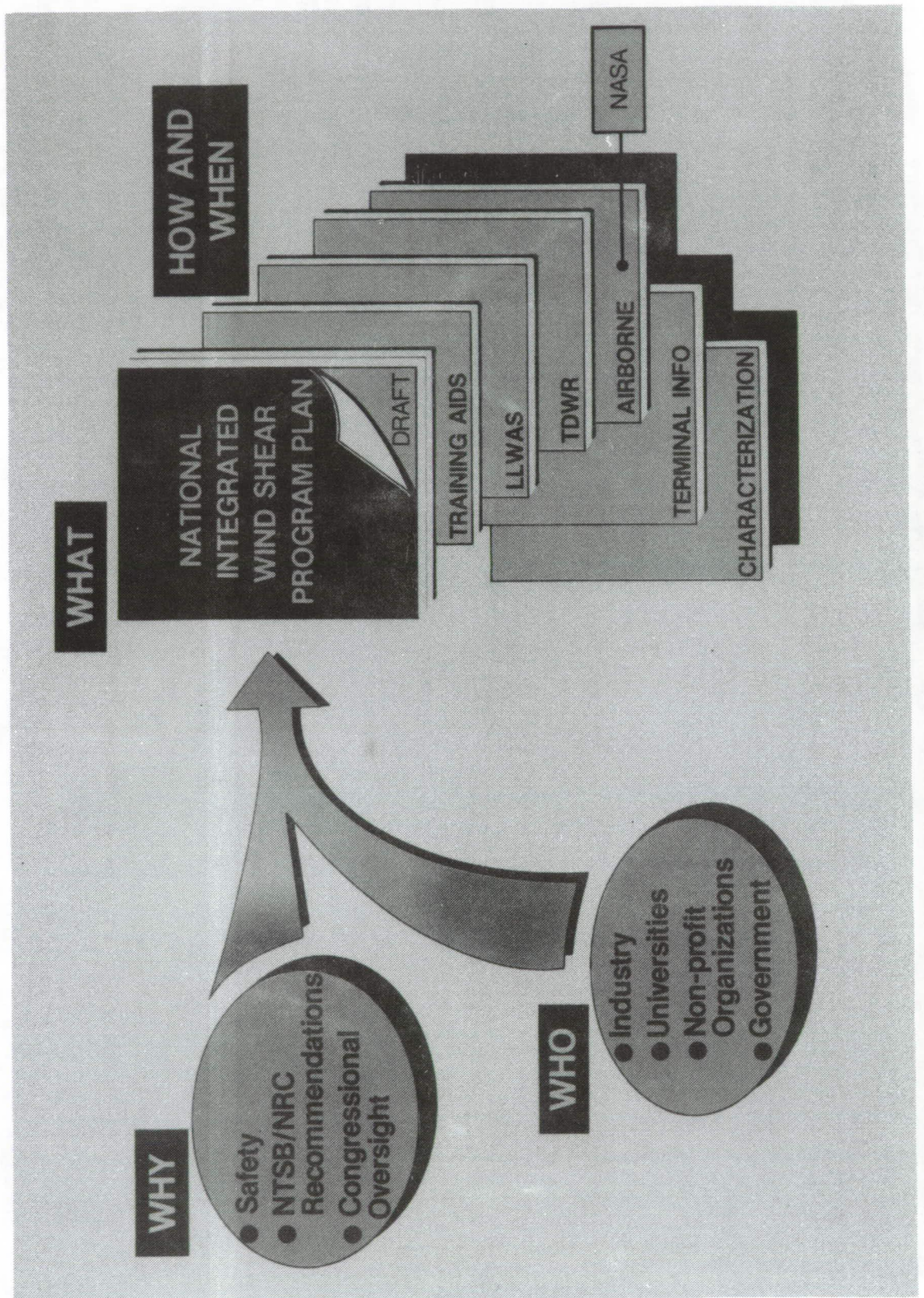
JOINT NASA/FAA AIRBORNE WIND SHEAR DETECTION AND AVOIDANCE PROGRAM



Dr. Roland Bowles
Wind Shear Program Office
NASA Langley

THE WINDSHEAR PROBLEM



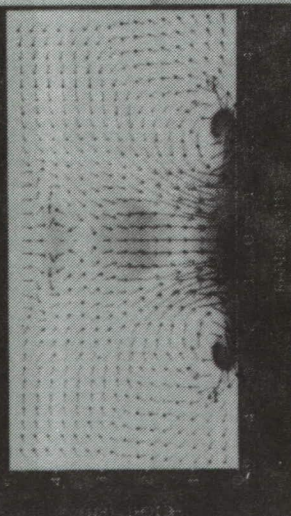


NASA/FAA WINDSHEAR PROGRAM OBJECTIVES

- **TO DEVELOP AND VALIDATE TECHNOLOGY LEADING TO
REDUCED RISKS ASSOCIATED WITH WINDSHEAR &
HEAVY RAIN THROUGH AIRBORNE DETECTION AND
AVOIDANCE**
- **SUPPORT NATIONAL AVIATION POLICY INITIATIVES TO
REDUCE WIND SHEAR HAZARDS THROUGH COCKPIT
INTEGRATION OF TDWR AND AIRBORNE DETECTION
SYSTEMS**

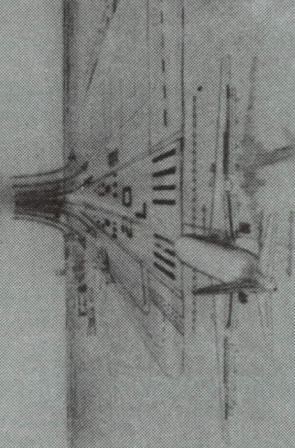
NASA/FAA AIRBORNE WIND SHEAR PROGRAM ELEMENTS

Hazard Characterization



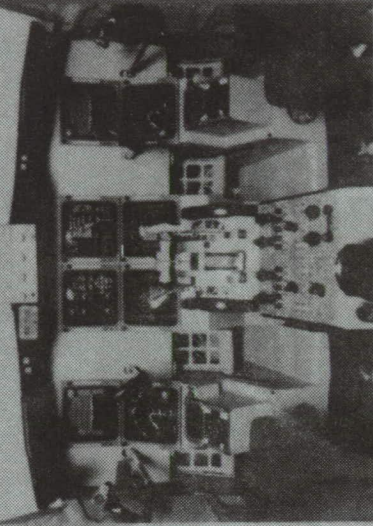
- Wind Shear Physics/Modeling
- Heavy Rain Aerodynamics
- Impact on Flight Characteristics

Sensor Technology



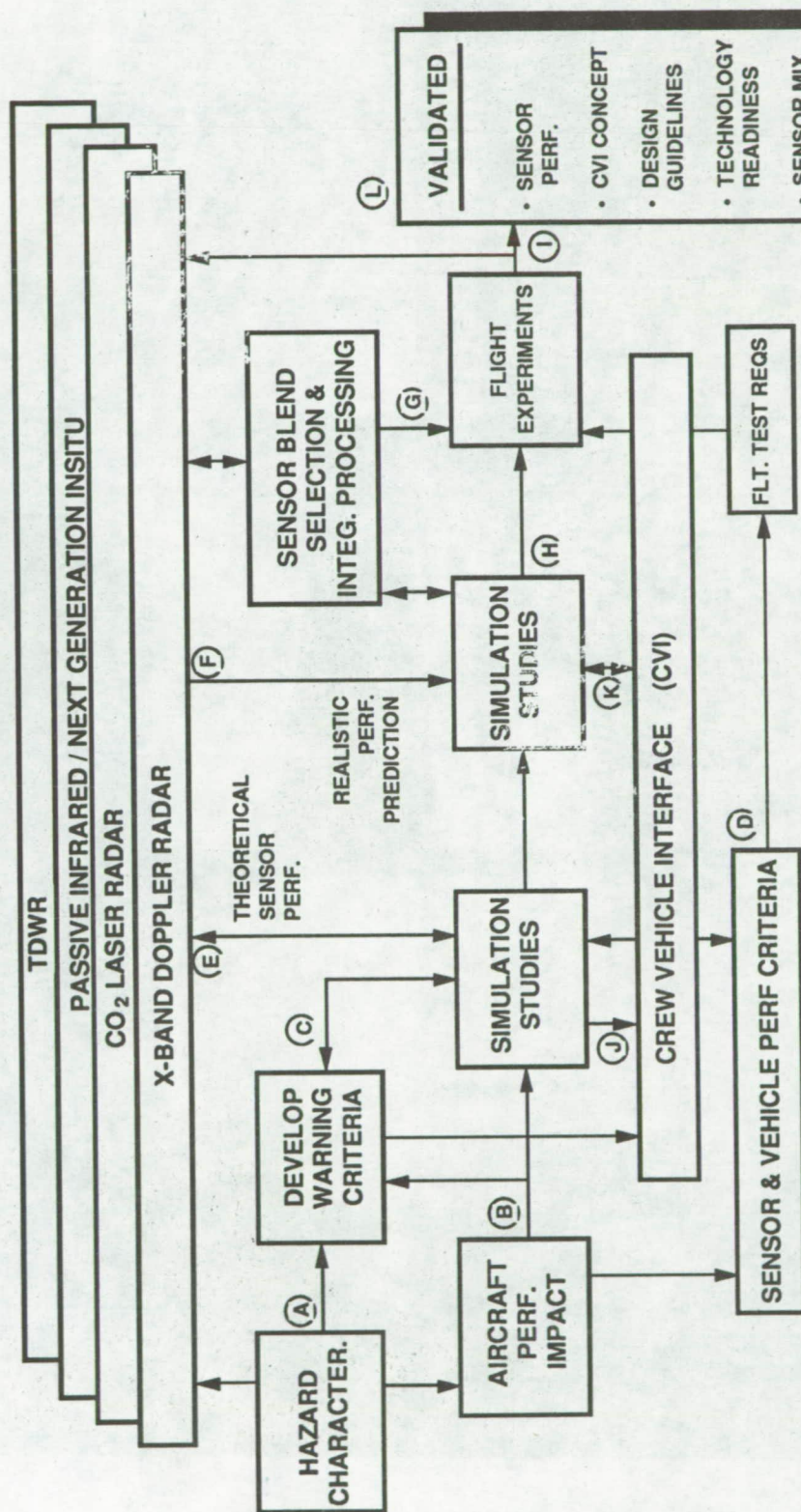
- 2nd Generation Reactive
- Airborne Doppler RADAR/LIDAR
- Airborne Passive INFRARED
- Sensor Information Fusion
- Flight Performance Evaluation

Flight Management Systems



- System Performance Requirements
- Guidance/Display Concepts
- TDWR Information Data Link/Display
- Pilot Factors/Procedures

WIND SHEAR PROGRAM ROADMAP



A VALIDATED MATH MODEL CHARACTERIZING HAZARD, LARGE SCALE HEAVY RAIN TESTS

B PREDICTED AIRCRAFT PERFORMANCE IN WIND SHEAR/HEAVY RAIN

C WARNING CRITERIA DEFINED

D PERFORMANCE GOALS FOR SYSTEM ESTABLISHED

E THEORETICAL SENSOR FEASIBILITY/PERFORMANCE ESTABLISHED

F REALISTIC SENSOR PERFORMANCE DEFINED

G SENSOR INFORMATION REQUIREMENTS AND MIX ESTABLISHED

H SYSTEM PERFORMANCE, OPERATING PROCEDURES & DESIGN GUIDELINES ESTABLISHED

I FLIGHT VALIDATED SENSOR PERFORMANCE, OPER. PROCEDURES, & DESIGN GUIDELINES

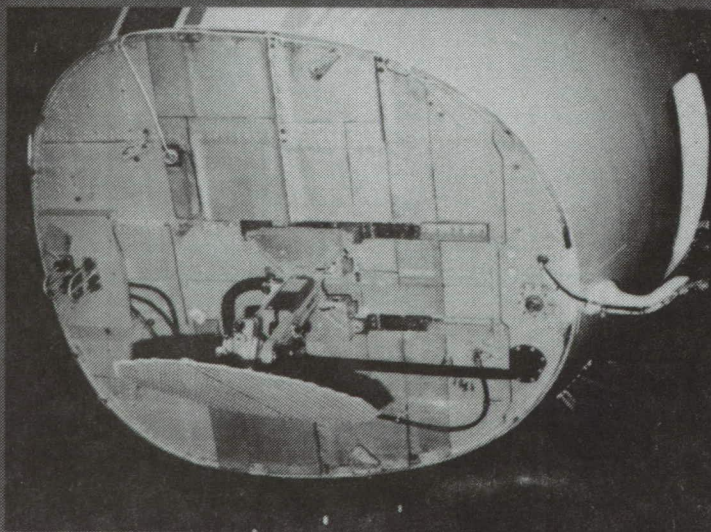
J FLT. CREW ALERTING PROTOCOLS AND OPERATING PROCEDURES PRESENT

K PREDICTED SYSTEM PERFORMANCE WITH KEY VARIABLES PRESENT

L RESEARCH PRODUCTS IN SUPPORT OF ELIMINATING WIND SHEAR RISK

AIRBORNE WINDSHEAR SENSORS

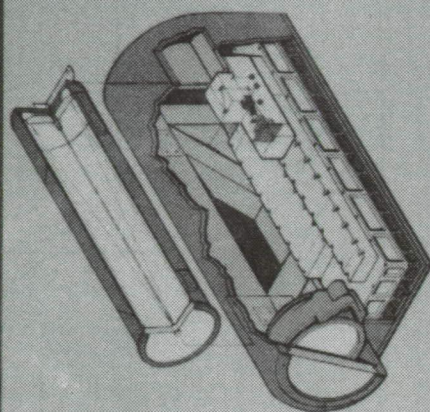
Doppler Radar



Infrared Radiometer



Doppler Lidar



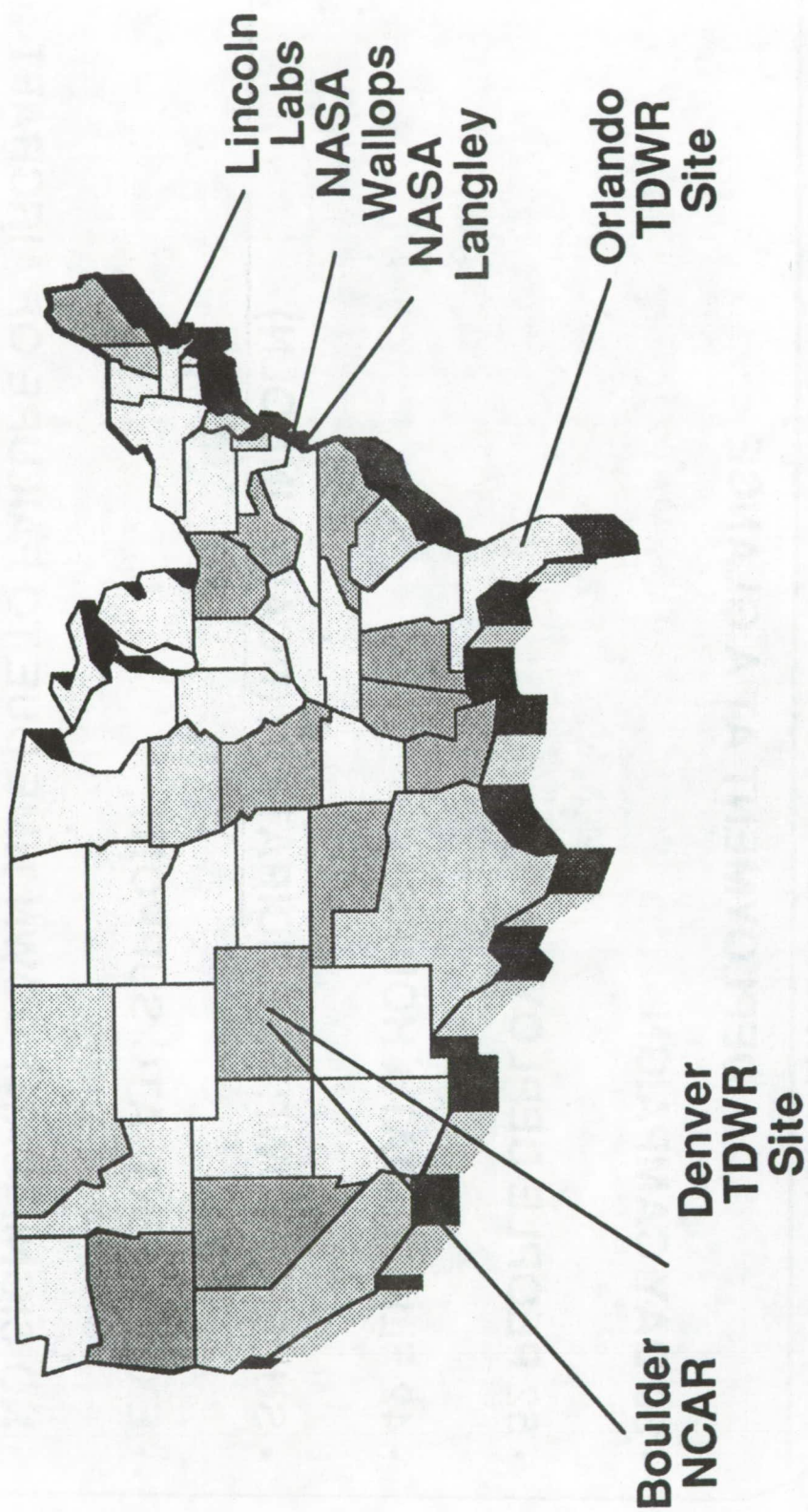
1991 WIND SHEAR FLIGHT EXPERIMENTS

DEPLOYMENT AT A GLANCE

- 30 DAY CAMPAIGN**
- 52 PEOPLE DEPLOYED**
- 42 FLIGHT DATA HOURS**
- SUPERB TDWR PARTICIPATION (NCAR, LINCOLN)**
- EXCELLENT ATC SUPPORT**
- NO SIGNIFICANT DOWN TIME DUE TO FAILURE OF AIRCRAFT
OR RESEARCH SYSTEMS**
- A GOOD PLAN RESULTED IN A SAFE OPERATION WHICH
YIELDED EXCELLENT DATA**

91 WIND SHEAR DEPLOYMENT

OPERATIONAL SITES/KEY PARTICIPANTS



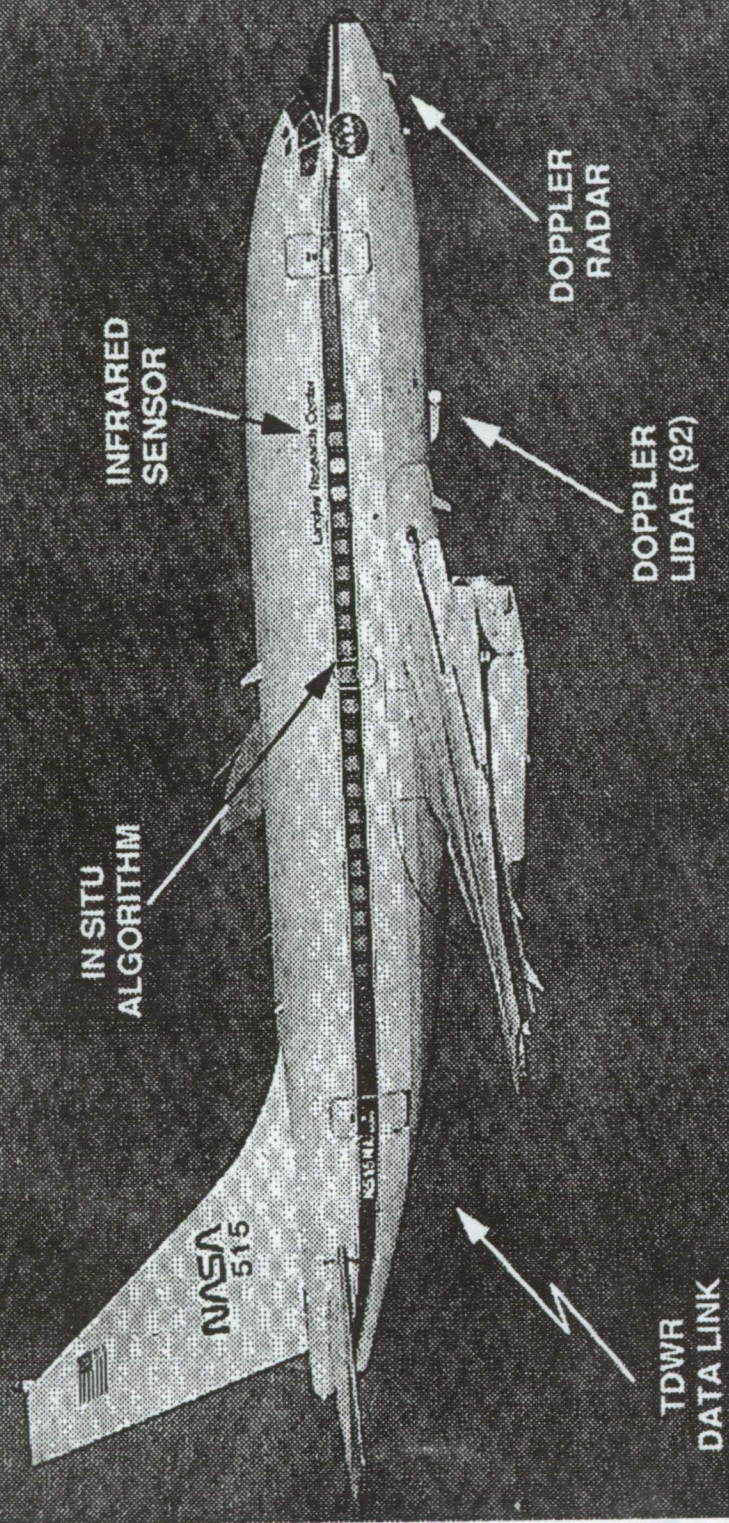
OPERATIVE WIND SHEAR DETECTION SYSTEMS

91 FLIGHT EXPERIMENTS

<u>AIRBORNE TECHNOLOGY</u>	<u>FEATURES / CAPABILITY</u>
<ul style="list-style-type: none"> • PULSED DOPPLER MICROWAVE RADAR 	<ul style="list-style-type: none"> • ADVANCED HARDWARE PERFORMANCE • EXCELLENT CLUTTER REJECTION • REAL-TIME HAZARD DISPLAY
<ul style="list-style-type: none"> • INFRARED RADIOMETER 	<ul style="list-style-type: none"> • REAL-TIME DETECTION ALGORITHM • THERMAL FEATURE IDENTIFICATION • SUCCESSFUL MICROBURST DETECTION
<ul style="list-style-type: none"> • IN SITU TRUTH MEASUREMENT 	<ul style="list-style-type: none"> • ADVANCED ALGORITHM PERFORMANCE EXCEEDS FAA REQUIREMENTS • EXCELLENT GUST REJECTION CHARACTERISTICS • MANEUVER MOTION IMMUNITY
<ul style="list-style-type: none"> • TDWR / AIRCRAFT DATA COMMUNICATION AND DISPLAY 	<ul style="list-style-type: none"> • NASA HAZARD ALGORITHM • DATA LINK COMMUNICATION • EHSI DISPLAY OF HAZARD

WIND SHEAR AIRBORNE SENSORS PROGRAM

RESEARCH AIRCRAFT SENSOR INSTALLATIONS



1991 TEST RESULTS SUMMARY

- ACQUIRED OUTSTANDING HIGH RESOLUTION MEASUREMENTS OF MICROBURST DYNAMICS AND STRUCTURE
- ACCOMPLISHED FIRST EVER IN SITU DETECTION SYSTEM CORRELATION WITH INDEPENDENT MEASUREMENTS
- ACCOMPLISHED FIRST EVER AIRBORNE RADAR DETECTION OF HAZARDOUS WIND SHEAR
- HIGH QUALITY CLUTTER MEASUREMENTS PROVIDE BASIS FOR NATIONAL CERTIFICATION STANDARDS
- DEMONSTRATED PERFORMANCE BENEFITS AND UTILITY OF TDWR DATA LINK CONCEPT

1992 FLIGHT TESTS EXPECTATIONS

- PULSED DOPPLER LIDAR SYSTEM ON BOARD
- FULL SENSOR COMPLEMENT INSTALLED
- SIGNIFICANTLY ENHANCED RADAR PROCESSOR INSTALLED
- IR INSTRUMENT INCLUDES 1991 'LESSONS LEARNED'
- TDWR DATA LINK ENHANCED
- FLIGHT OPERATIONS TO INCLUDE 1991 'LESSONS LEARNED'
- LOCAL, ORLANDO, AND DENVER TEST SITES
- END-TO-END WIND SHEAR DETECTION PERFORMANCE EVALUATION
 - COMMON HAZARD PROCESSING
 - UNIFIED ALERTS
 - INTEGRATED DISPLAY

Program Overview / 1991 Flight Test Objectives

Questions and Answers

Q: Bob Otto (Lockheed) - A potential recommendation for carrying out a sensor comparison program would be to use all candidate sensors (TDWR, reactive, radar, IR, etc.) to determine F-factor as a function of space and time for the same microburst event. A reference or ground truth needs to be decided upon. It may be TDWR or reactive data properly processed. Then the sensors can be evaluated and compared. A parametric evaluation can be done for wet and dry, different microburst spatial sizes and temporal duration, different microburst strengths and various parameters of the event. Please comment on this recommendation and tell what the actual plan will be.

A: Roland Bowles (NASA Langley) - The easy answer is that we don't write those plans, but we certainly feel sensitive to the need to help the FAA put together a technical rationale. That is our job. We are not going to dictate how you are going to get your systems approved, but we are going to be in the background along with the other programs operating out of the FAA like the Lincoln and the NCAR program. Wherever we can get relevant and pertinent data to bare on the subject we are going to get it.

Q: Bob Otto (Lockheed) - I have attended all of the wind shear conferences that you have had and each time I come here I see a great deal of progress being made. I have this vision that at some point we are going to be able to take all the data from all the different sensors for the same type of microburst events and compare all these different sensors and say this sensor works best in this regime, this sensor works best for that regime. In other words, trying to accumulate enough scientific data and try to make a valid comparison among all these different sensors. I think NASA is in a unique position to do that sort of thing. I am just asking if that is what you really want to do or should do in order to satisfy the program objectives?

A: Roland Bowles (NASA Langley) - Our job was basically three fold: a) Define the relevant technologies appropriate to airborne hazard detection and avoidance. b) Out of that admissible list, decide through priority structure what we think the system requirement is going to end up to be and realize in hardware and software those candidates and c) fly them off and compare against suitable environments that we can call truth. I don't call TDWR ground truth. I call TDWR another estimate of what is out there. But I'll tell you what I do think the truth is, I believe it is the airplane. Newton as alive and well. That is why we are stressing a great deal using our In Situ data. Brac showed some results that were extremely encouraging. The data that he showed yesterday had the antenna looking down two degrees below the horizon. There were range gates out there in the ground. In fact, the strongest event we incurred was right over top of the interstate in Orlando. So we had plenty of stuff around to reject or mess it up. When the radar took a snapshot and made a prediction 8 kilometers out and subsequently the airplane flew through that environment and you compare the results, we can even see the latency in the reactive alert due to the gust rejection filtering and it is right on the money. That was based on a snapshot 30 to 40 seconds earlier. So that is one means by which you can judge the validity in the prediction. We do not see anything coming off of the TDWR that is inconsistent with what we are seeing in the air, when we fly in the vicinity or an appropriate neighborhood of the event.

Now, we did fly through icons last year where there just wasn't anything in them. That is another problem that I think Steve is going to address tomorrow. I think this is a good question. I look at it as, what would be the appropriate mix that industry would have to place on the FAA doorstep between flight results, simulation results, and those test procedures that will be outlined in the Interim Standards document and or a TSO, if we ever get to one. I think it is the mix that is important. But, it is going to cost the industry money. Knowing Kurt and his people, I don't think anyone is going to be able to back in on this one. There is a lot of homework to be done. I think we are on the right track. The NASA laser, built by UTAS and integrated by Lockheed, is going to get a good ride. I guarantee you it will get a fair objective comparison. This year we have refined the algorithms throughout the airplane and have been pulling all the data together on a common basis of measurement and display. There are a lot of events that we threw away last year that we will take this year. If things cooperate reasonably well we are going to have a good summer and it will get a fair ride.

Session I. NASA Flight Tests

1993010403
22P

N93-19592

Flight Test Operations

Mike Lewis, NASA Langley Research Center

WIND SHEAR PROGRAM

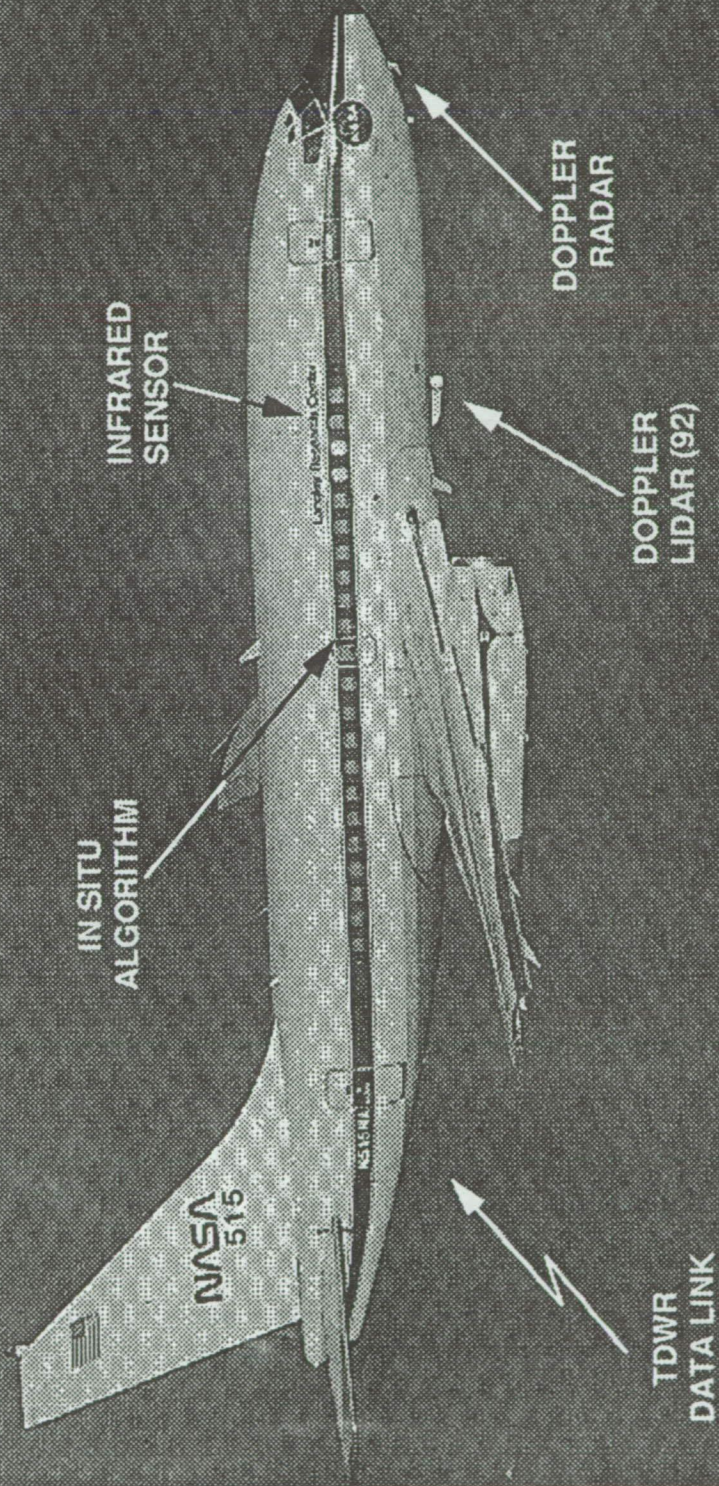
JOINT NASA/FAA AIRBORNE WIND SHEAR DETECTION AND AVOIDANCE PROGRAM

1991 FLIGHT EXPERIMENTS

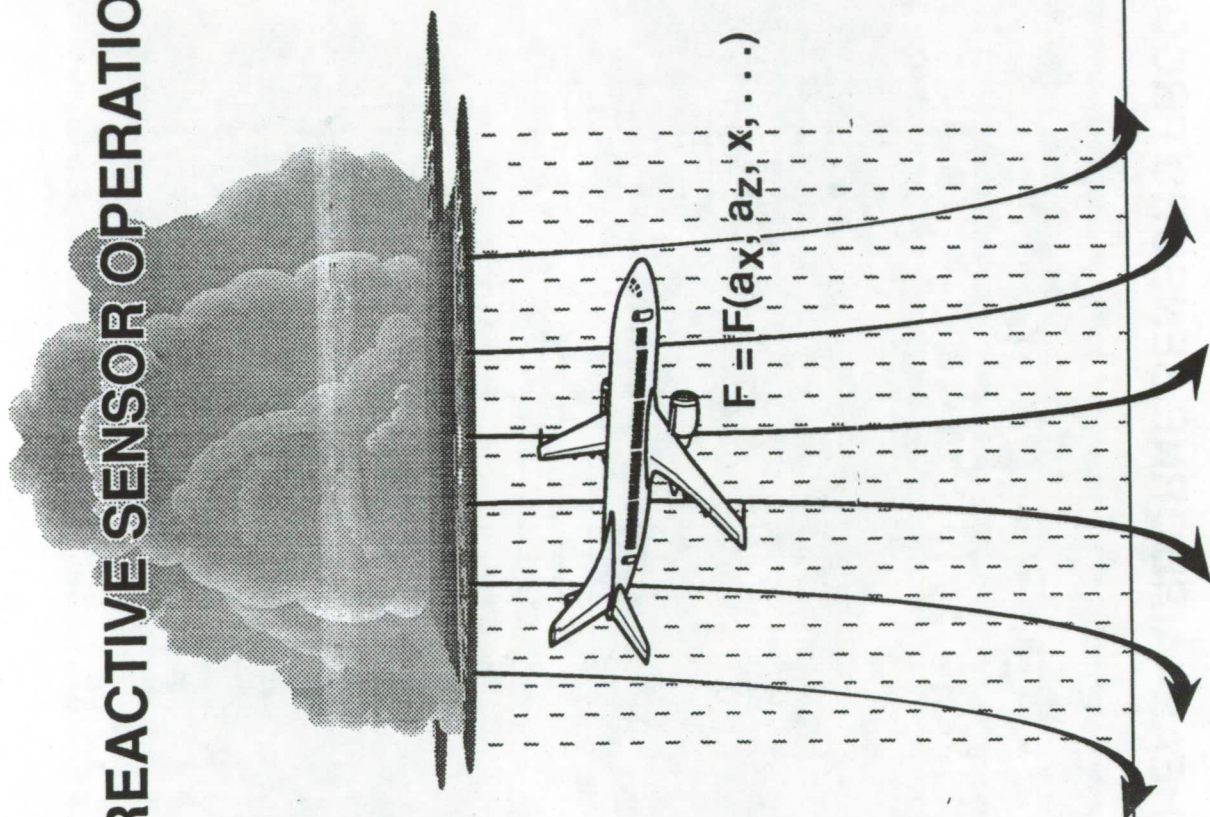
Michael S. Lewis
Flight Systems Directorate
NASA Langley



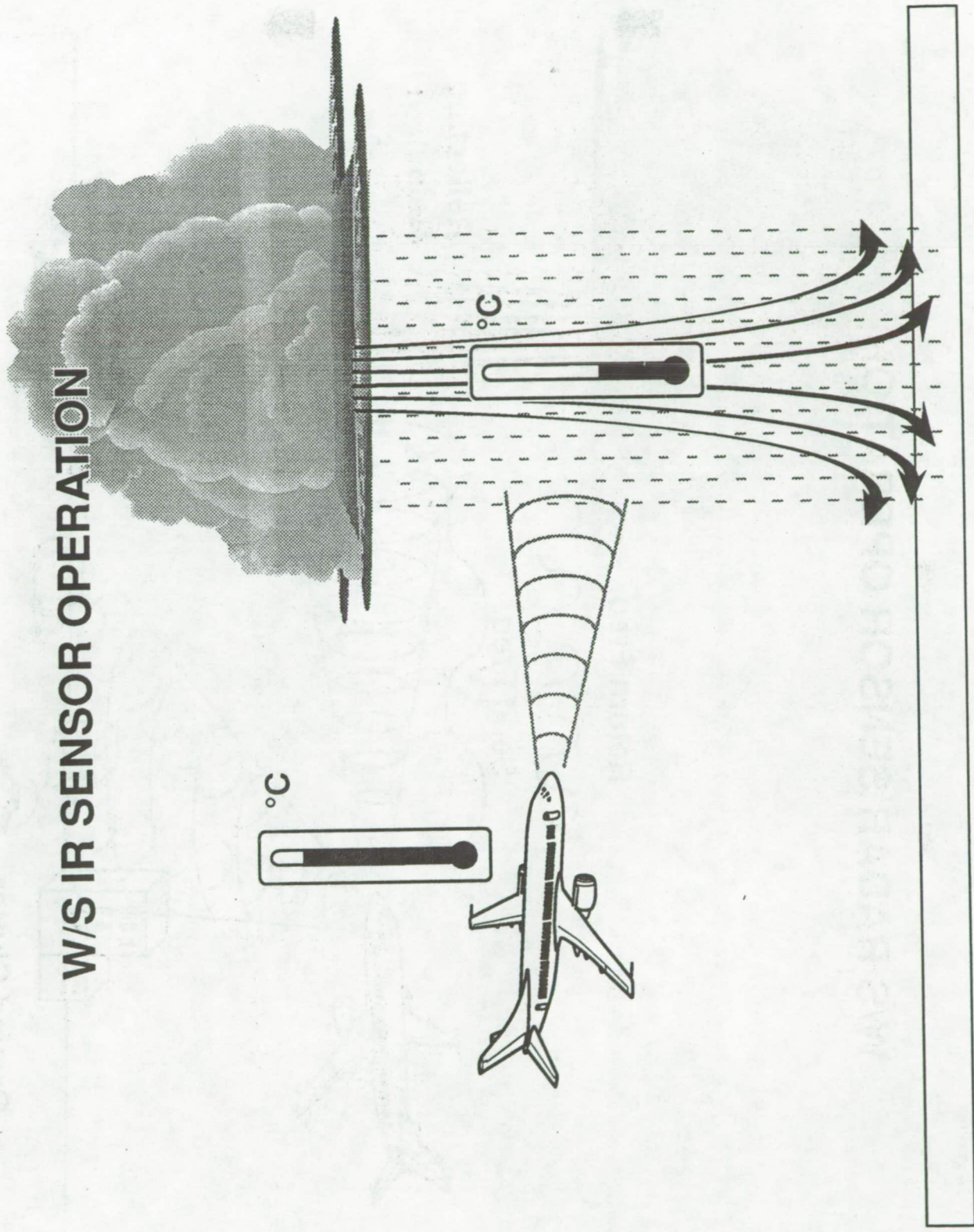
RESEARCH AIRCRAFT SENSOR INSTALLATIONS



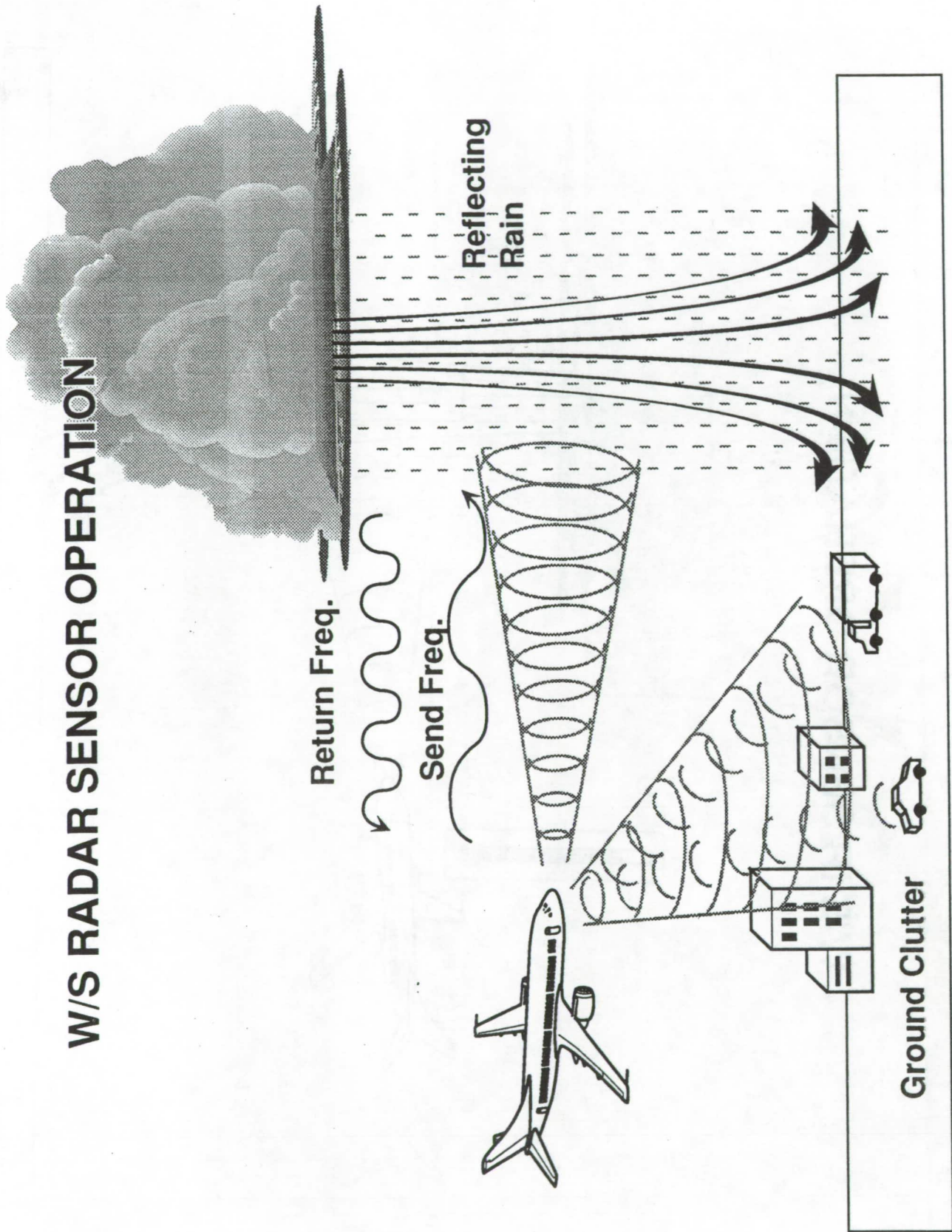
W/S REACTIVE SENSOR OPERATION



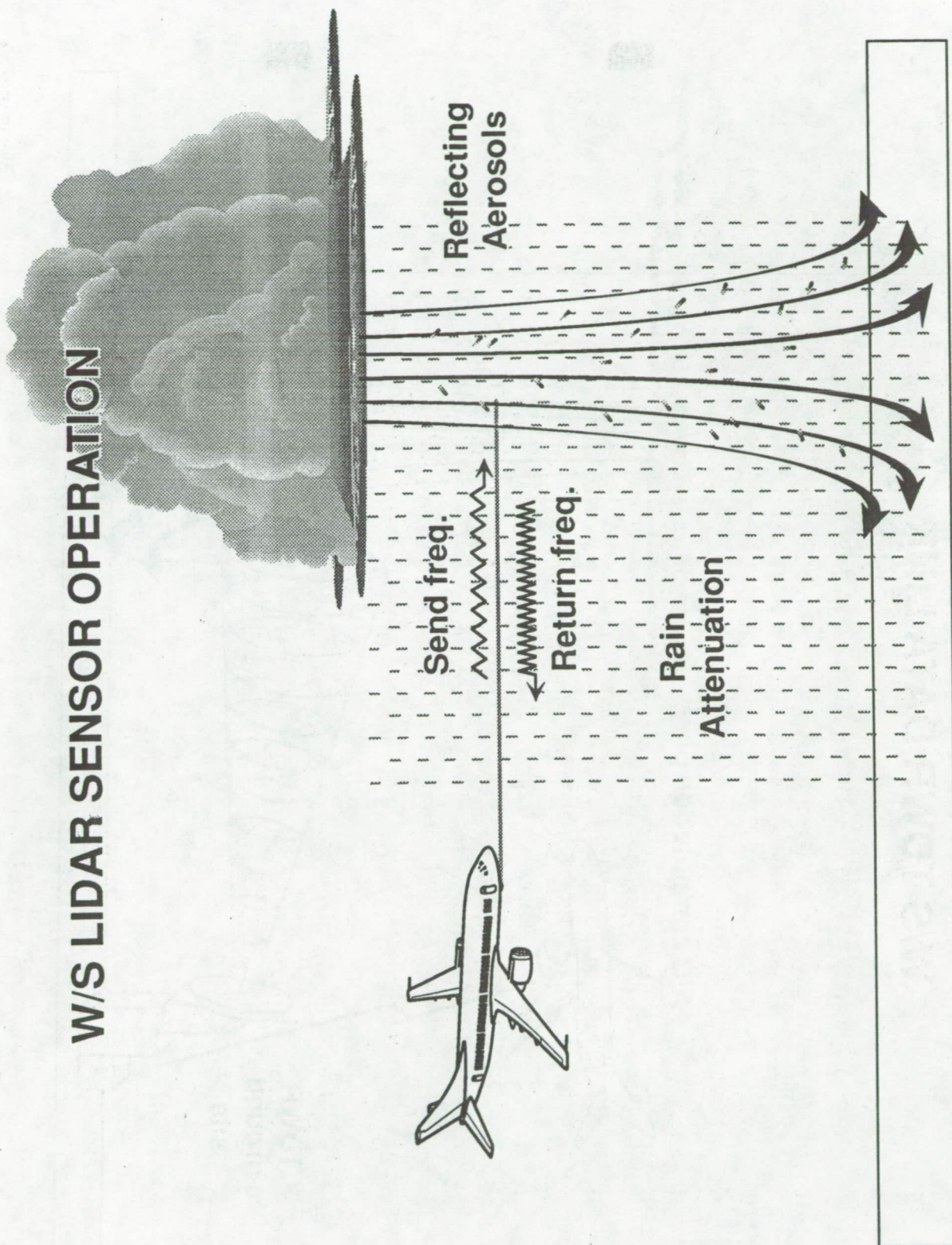
W/S IR SENSOR OPERATION



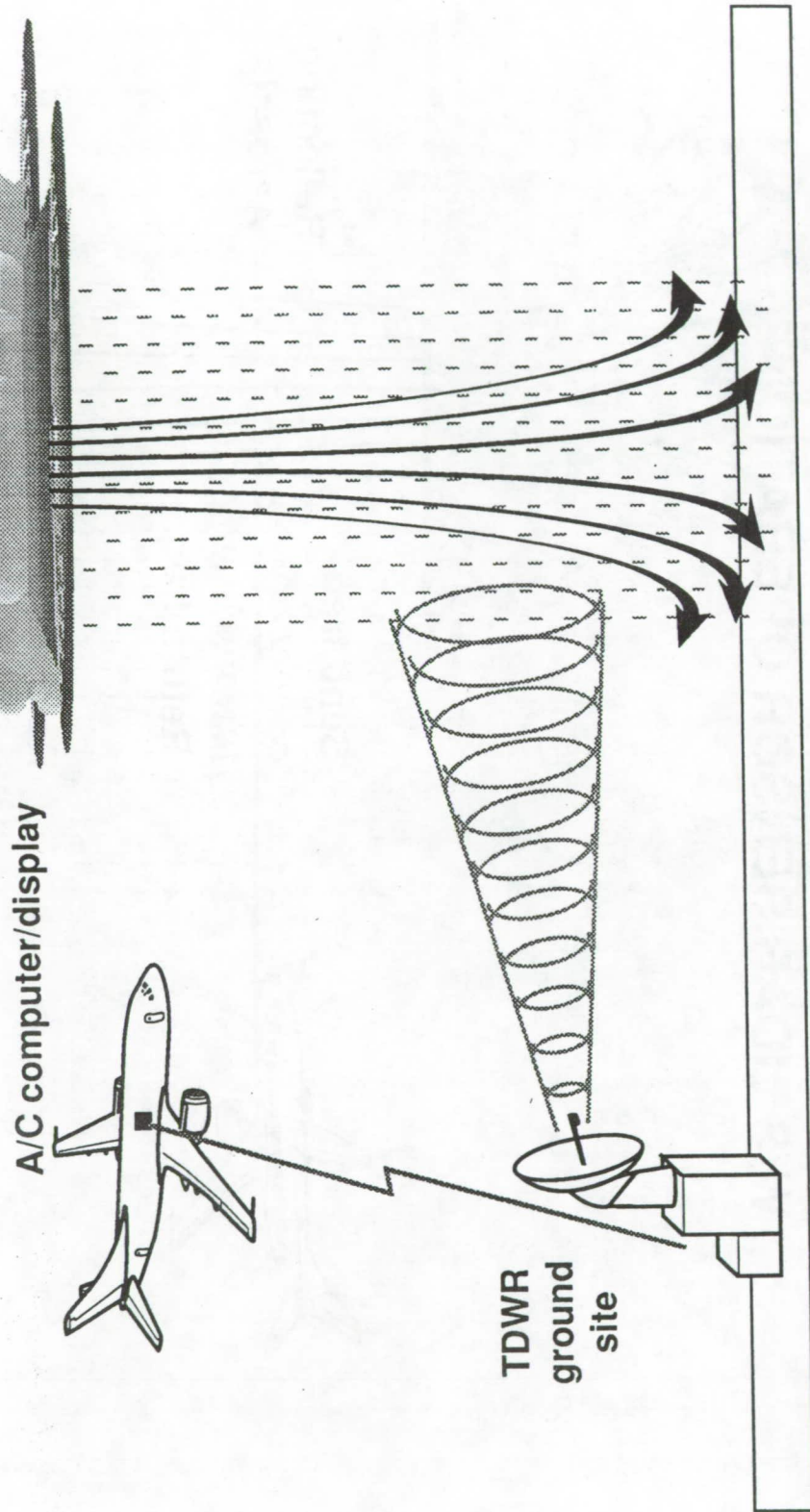
W/S RADAR SENSOR OPERATION



W/S LIDAR SENSOR OPERATION



W/S TDWR DATA LINK



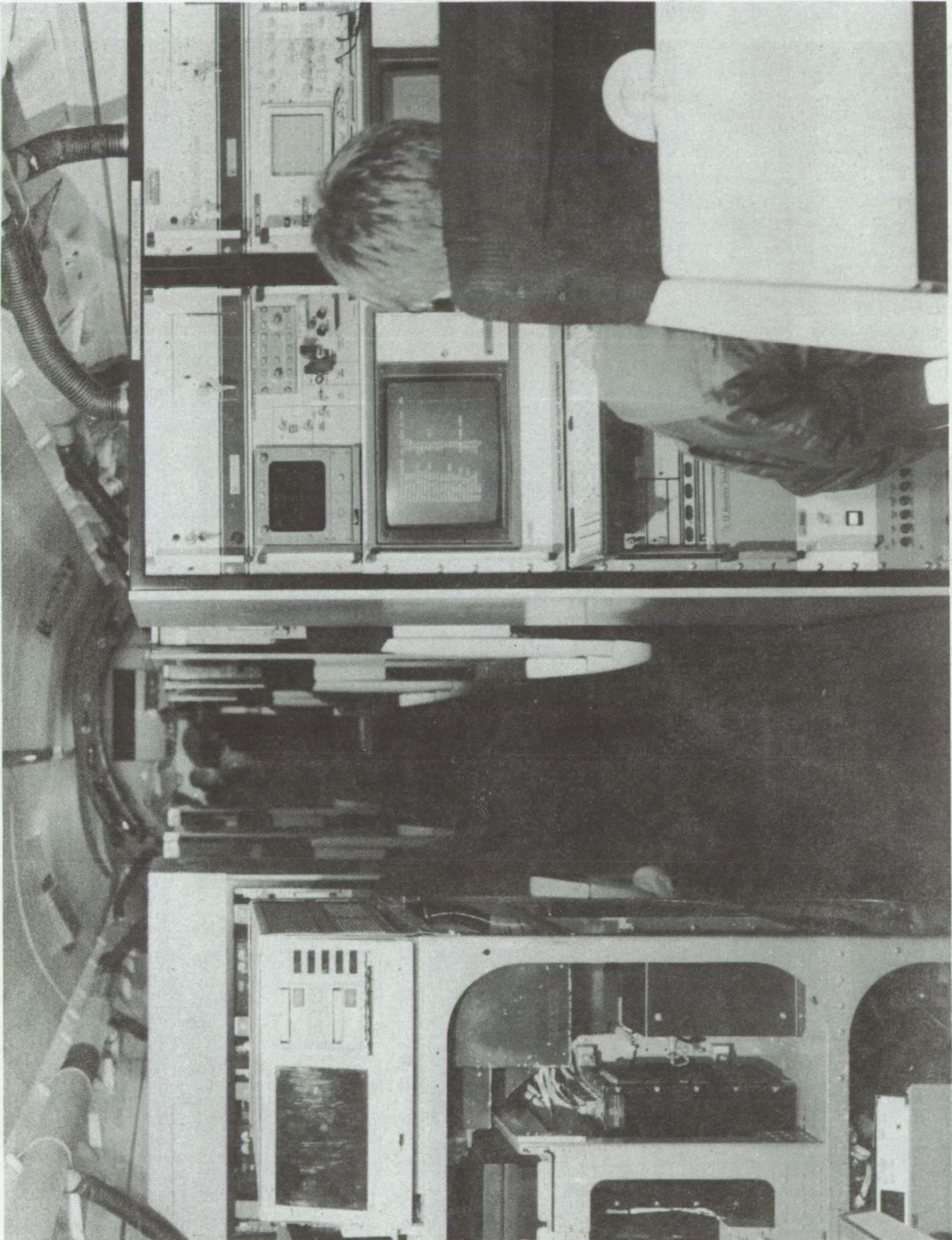
1991 FLIGHT TEST SUMMARY

- INSTRUMENT SYSTEM CHECKOUT (- 2/91)
- CLEAR WEATHER DATA FLIGHTS (2/91 -4/91)
- LOCAL IN/NEAR WEATHER FLIGHTS (5/91)
- DEPLOYMENT PREPARATION FLIGHTS (5/91)
- ORLANDO (6/91), DENVER (7/91) DEPLOYMENTS
 - FULL SAFETY, FLIGHT OPERATIONS REVIEWS
 - ATC, GROUND SITE, TDWR PREPARATIONS
 - 50+ PERSONNEL AT EACH SITE

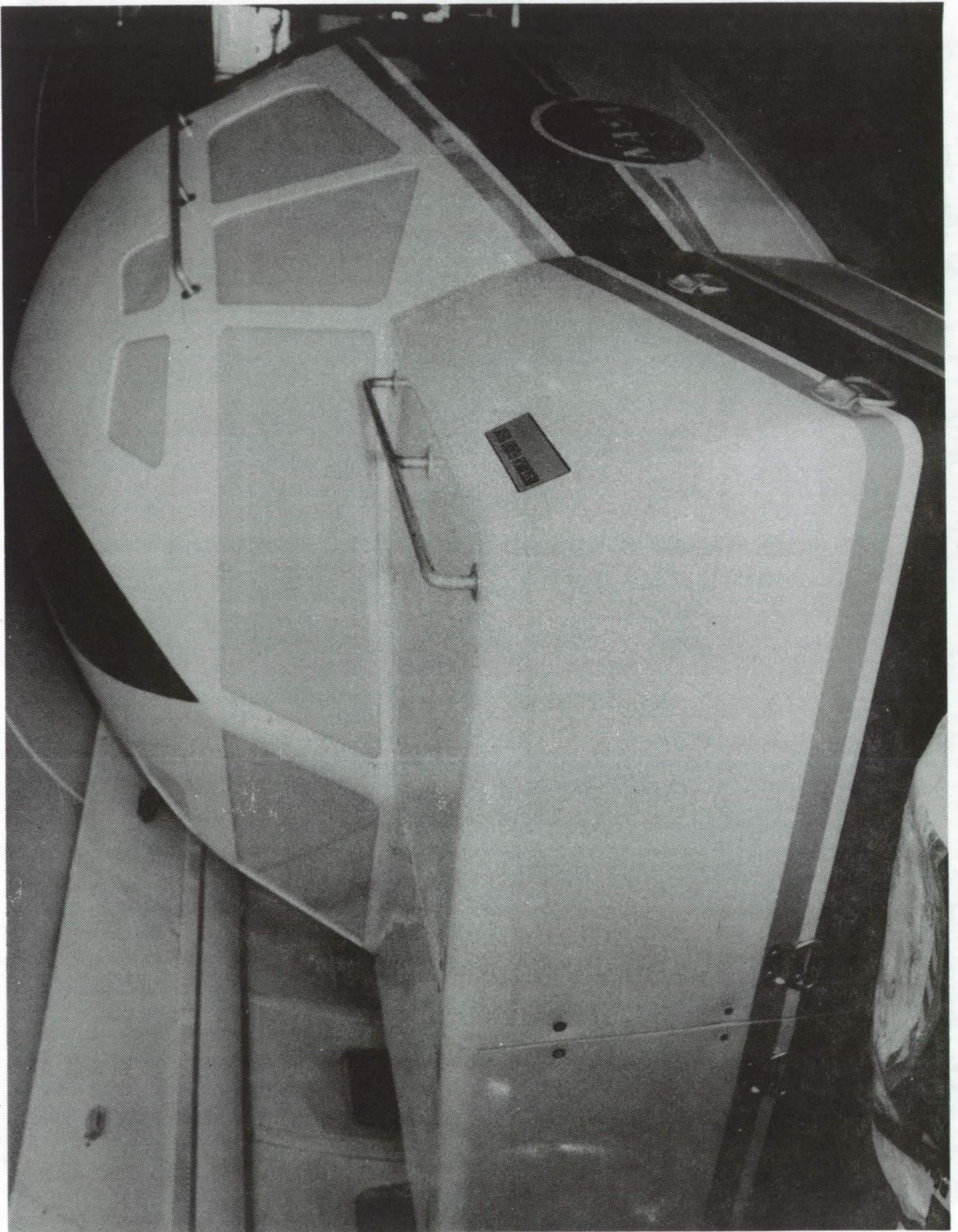
1991 DEPLOYMENT GOALS

- 1.) EVALUATE AND DEMONSTRATE OPERATIONAL FEASIBILITY OF TDWR/AIRCRAFT DATA COMMUNICATION AND AIRBORNE ALGORITHM PERFORMANCE
- 2.) CONDUCT REAL APERTURE RADAR MEASUREMENT OF FIXED AND MOVING CLUTTER
- 3.) TEST AND EVALUATE WIND SHEAR DETECTION PERFORMANCE OF CANDIDATE AIRBORNE SYSTEMS IN REALISTIC ATMOSPHERIC AND OPERATIONAL CONDITIONS

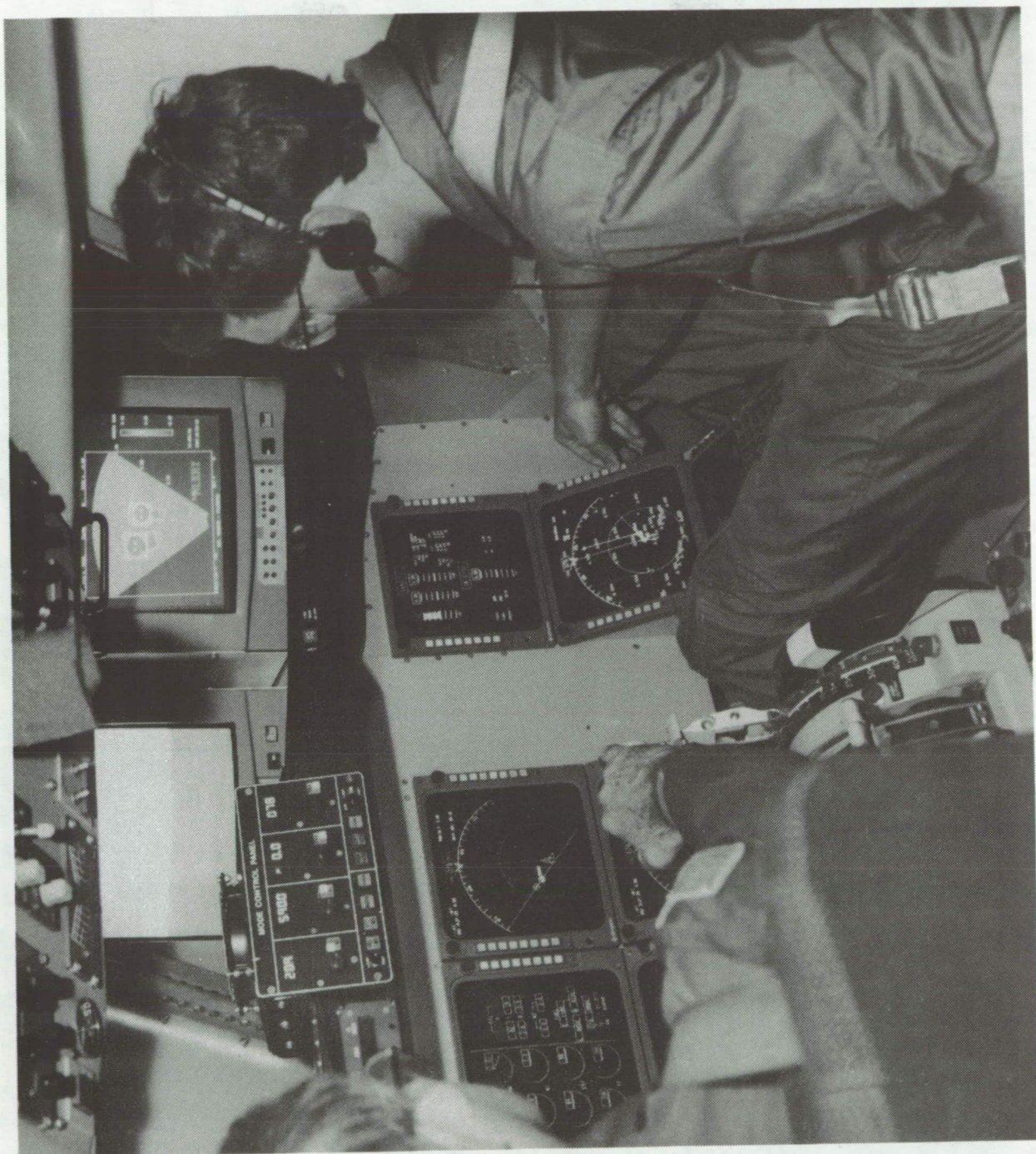
ORIGINAL PAGE
BLACK AND WHITE PHOTOGRAPH



ORIGINAL PAGE
BLACK AND WHITE PHOTOGRAPH

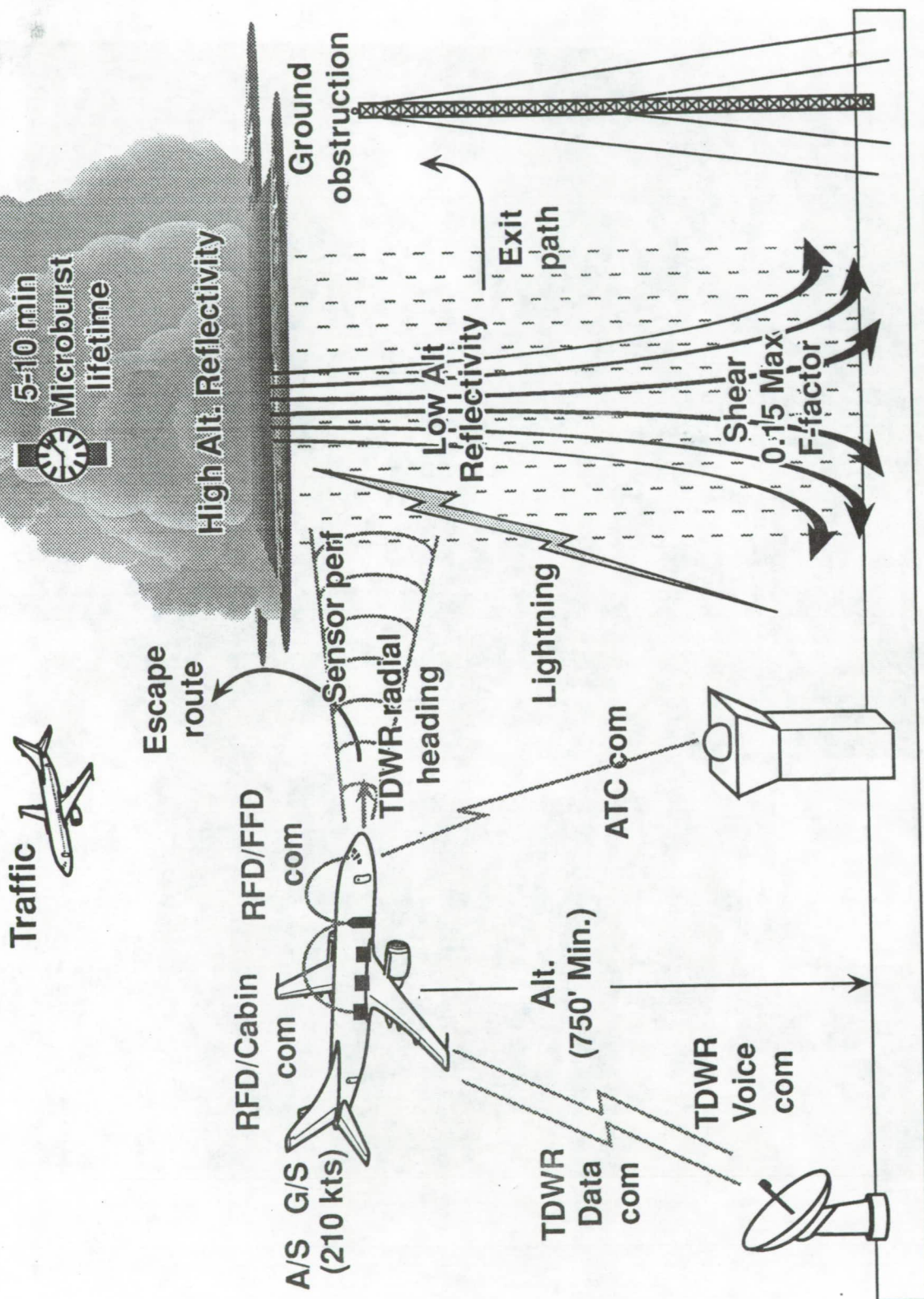


ORIGINAL PAGE
BLACK AND WHITE PHOTOGRAPH



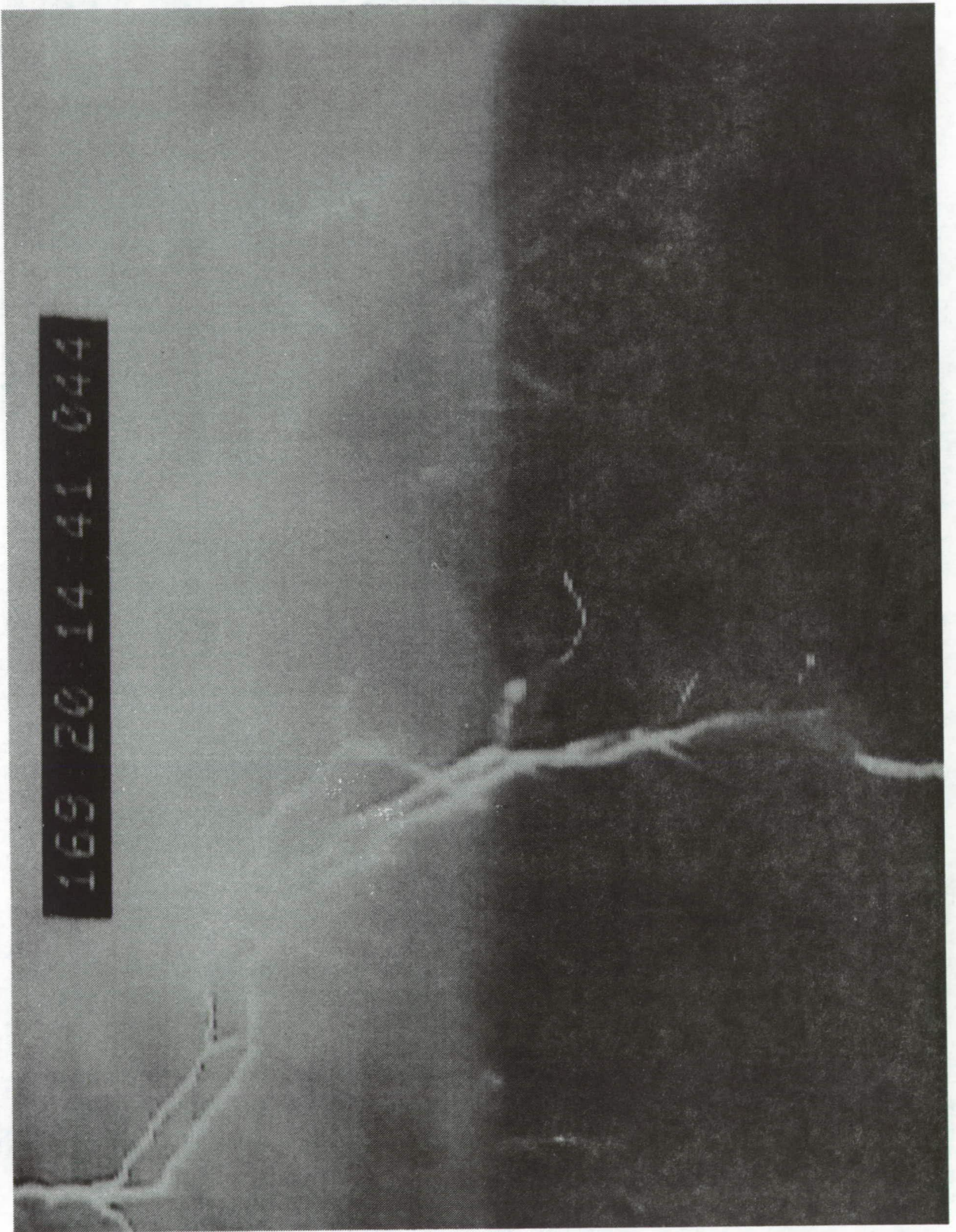
WIND SHEAR FLIGHT OPERATIONS

36



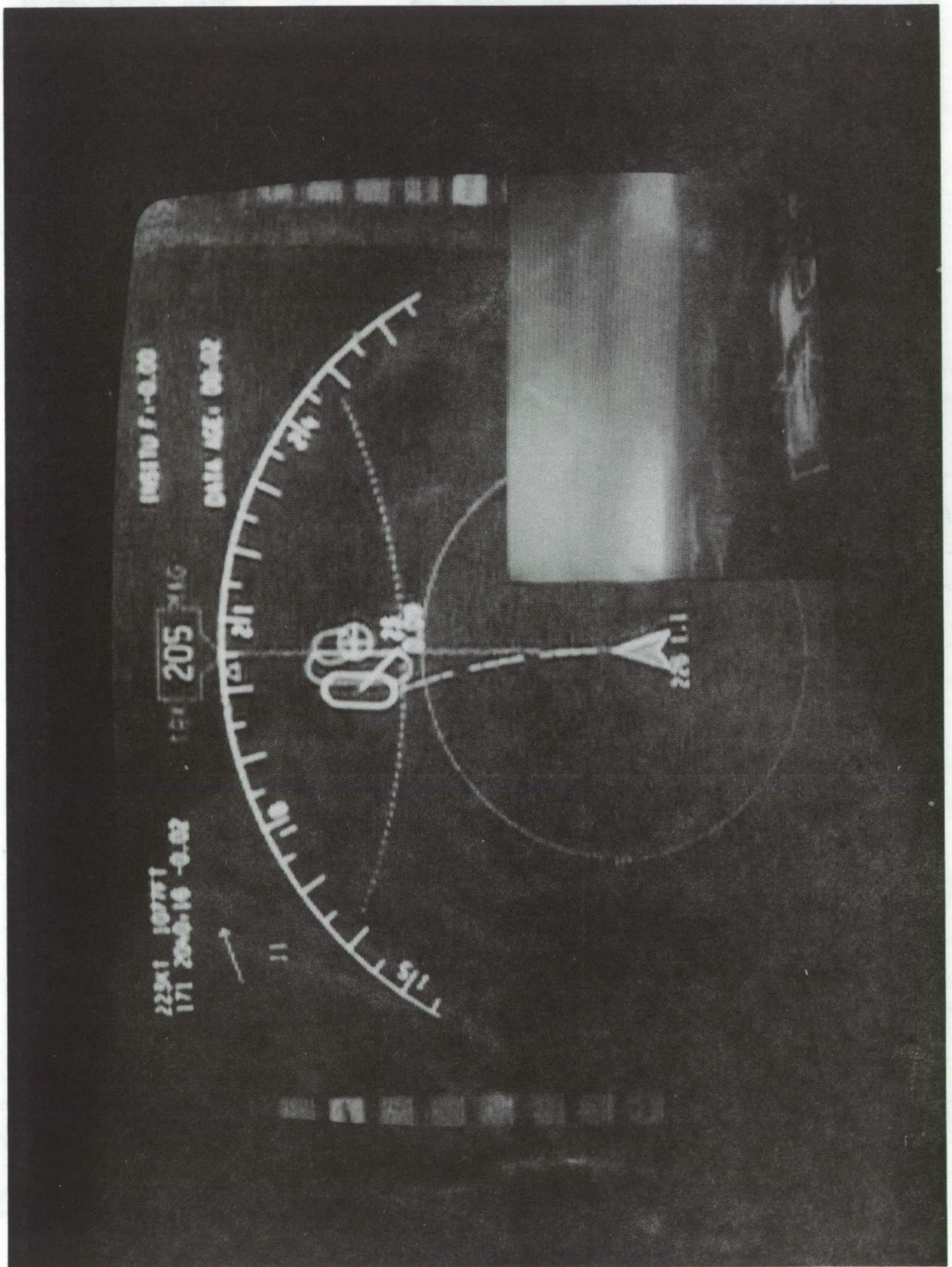
170:20:36:10:101

ORIGINAL PAGE
BLACK AND WHITE PHOTOGRAPH



171:20:40:15:362

ORIGINAL PAGE
BLACK AND WHITE PHOTOGRAPH



WIND SHEAR AIRBORNE SENSORS PROGRAM

1991 DEPLOYMENT GOALS/ACCOMPLISHMENTS

- 1.) EVALUATE AND DEMONSTRATE OPERATIONAL FEASIBILITY OF TDWR/AIRCRAFT DATA COMMUNICATION AND AIRBORNE ALGORITHM PERFORMANCE
 - FEASIBILITY AND UTILITY OF TDWR DATA LINK DEFINITELY DEMONSTRATED
- 2.) CONDUCT REAL APERTURE RADAR MEASUREMENT OF FIXED AND MOVING CLUTTER
 - 100% OF REQUIRED AIRPORT CLUTTER DATA COLLECTED
- 3.) TEST AND EVALUATE WINDSHEAR DETECTION PERFORMANCE OF CANDIDATE AIRBORNE SYSTEMS IN REALISTIC ATMOSPHERIC AND OPERATIONAL CONDITIONS WITH ALL VARIABLES PRESENT
 - MULTIPLE SHEAR APPROACHES AND PENETRATIONS FLOWN
 - APPROX. 19 MICROBURST WIND SHEAR PENETRATIONS, >30 RAIN SHAFT (WEAK DIVERGENCE) PENETRATIONS, >5 PROXIMITY APPROACHES TO LARGE STORM CELLS
 - APPROXIMATELY 8 STRONG GUST FRONT PENETRATIONS
 - MAXIMUM IN SITU F-FACTOR ENCOUNTERED = 0.17, MINIMUM = -0.24
 - CLASSIC 'DRY' TYPE MICROBURST NOT ENCOUNTERED IN DENVER, THOUGH DRY GUST FRONT MEASUREMENTS PROVIDE NEARLY EQUIVALENT DATA

1991 TEST RESULTS SUMMARY

- **ACQUIRED OUTSTANDING HIGH RESOLUTION MEASUREMENTS OF MICROBURST DYNAMICS AND STRUCTURE**
- **ACCOMPLISHED FIRST EVER IN SITU DETECTION SYSTEM CORRELATION WITH INDEPENDENT MEASUREMENTS**
- **ACCOMPLISHED FIRST EVER AIRBORNE RADAR DETECTION OF HAZARDOUS WIND SHEAR**
- **HIGH QUALITY CLUTTER MEASUREMENTS PROVIDE BASIS FOR NATIONAL CERTIFICATION STANDARDS**
- **DEMONSTRATED PERFORMANCE BENEFITS AND UTILITY OF TDWR DATA LINK CONCEPT**

1992 FLIGHT TESTS EXPECTATIONS

- PULSED DOPPLER LIDAR SYSTEM ON BOARD
- FULL SENSOR COMPLEMENT INSTALLED
- SIGNIFICANTLY ENHANCED RADAR PROCESSOR INSTALLED
- IR INSTRUMENT INCLUDES 1991 'LESSONS LEARNED'
- TDWR DATA LINK ENHANCED
- FLIGHT OPERATIONS TO INCLUDE 1991 'LESSONS LEARNED'
- LOCAL, ORLANDO, AND DENVER TEST SITES
- END-TO-END WIND SHEAR DETECTION PERFORMANCE EVALUATION
 - COMMON HAZARD PROCESSING
 - UNIFIED ALERTS
 - INTEGRATED DISPLAY

1993010404

140

Session I. NASA Flight Tests

N93-19593

NASA Wind Shear Flight Test In Situ Results
Rosa Oseguera, NASA Langley Research Center

PRECEDING PAGE BLANK NOT FILMED

NASA WINDSHEAR FLIGHT TEST IN SITU RESULTS

Presented By:
Rosa M. Oseguera
NASA Langley Research Center
at
4th Combined Manufacturers' and Technologists'
Airborne Windshear Review Meeting
April 14-16, 1992

OUTLINE

- **BACKGROUND**
 - OBJECTIVES
 - DESIGN REQUIREMENTS
- **IMPLEMENTATION**
- **RESULTS**
 - ALGORITHM TESTING
 - MICROBURST FLIGHTS
- **SUMMARY**

OBJECTIVES

- **PROVIDE MEASUREMENT STANDARD FOR FORWARD-LOOK SENSOR EVALUATION**
- **DEMONSTRATE OPERATIONAL UTILITY**

The main objectives in developing the NASA in situ windshear detection algorithm were to provide a measurement standard for validation of forward-look sensors under development, and to demonstrate the algorithm's ability to operate with a suitably low nuisance alert rate. It was necessary to know exactly how the algorithm was implemented and what parameters and filtering were used, in order to be able to fully test its effectiveness and correlate in situ results with forward-look sensor data.

DESIGN REQUIREMENTS

- **MINIMIZE AIRCRAFT-INDUCED HAZARD INDEX DUE TO:**
 - CONFIGURATION CHANGES
 - THRUST EXCURSIONS
 - MANEUVERING FLIGHT
 - TURNS IN STEADY WIND
- **MINIMIZE NON-HAZARDOUS ATMOSPHERE-INDUCED HAZARD INDEX**
 - TUNE TO APPROPRIATE SCALE OF MOTION
 - GUST REJECTION / TIME-TO-ALERT TRADE-OFFS
 - LOW NUISANCE ALERT RATE
- **EMPLOY CURRENTLY AVAILABLE STANDARD SHIP-SET SENSORS**

The major design requirements are 1) minimize effects of aircraft-induced motions, such as those shown in the first bullet item, and 2) minimize the effects of non-hazardous atmospheric motions, which is done using gust-rejection filters. The second item shows the major issues addressed in development of the filters, such as tuning the filters to the larger-scale motions associated with windshear, choosing an acceptable trade-off between improving the gust-rejection characteristics and decreasing the latency in the system, and maintaining a low nuisance alert rate; 3) implementing the system using currently available, standard sensors, to make the implementation feasible on any inertially-equipped airplane.

WIND SHEAR HAZARD INDEX

● THEORY

– POTENTIAL CLIMB ANGLE $\gamma_p = \frac{T - D}{mg} - F$

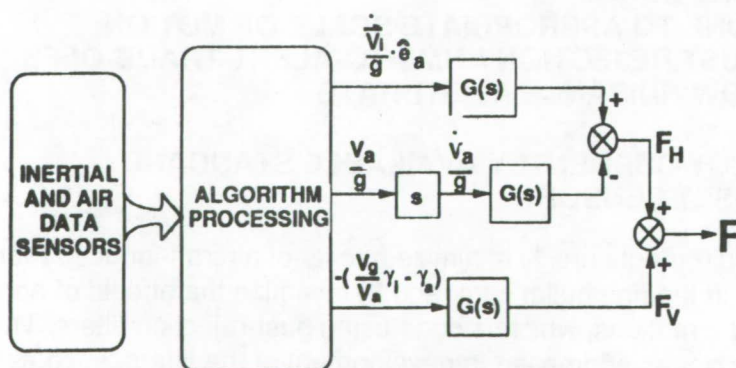
– HAZARD INDEX $F = \frac{\dot{\mathbf{w}} \cdot \mathbf{e}_a}{g} - \frac{w_h}{v_a}$

● IN SITU IMPLEMENTATION

$$F = \left\{ \frac{\dot{\mathbf{v}}_i \cdot \mathbf{e}_a - \dot{v}_a}{g} \right\} - \frac{w_h}{v_a}$$

The method for quantifying the windshear hazard is by computing the windshear hazard index (F-factor), which is shown as it relates to an airplane's potential climb angle and ratio of thrust-minus-drag to weight. The definition of F-factor (second equation) is shown as a function of the wind vector dot product with a unit vector in the direction of the airspeed vector, vertical wind component, and true airspeed. The bottom equation shows the general full 3-dimensional implementation of an in situ algorithm, with F computed from aircraft-measured parameters such as inertial velocity rate and airspeed rate, rather than wind measurements. The NASA implementation was realized in full 3-D form, to not degrade its performance in any flight regime.

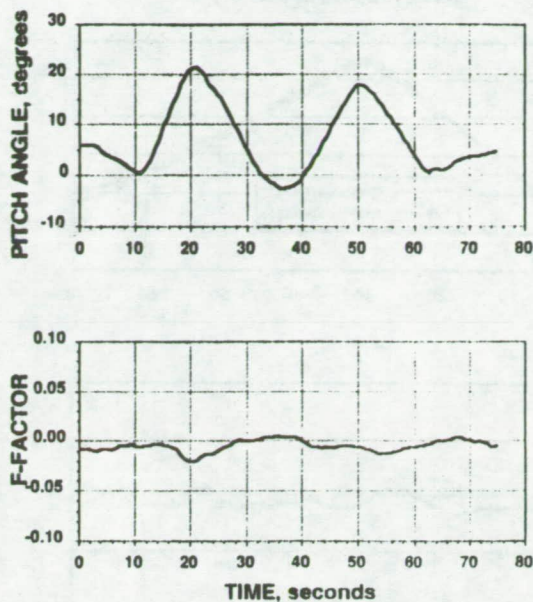
CONCEPTUAL REPRESENTATION OF NASA IN SITU F-FACTOR ALGORITHM



This shows the how the in situ algorithm is implemented on NASA's B-737-100, where the Algorithm Processing represents the first part of the in situ algorithm, which produces the three terms shown. These terms are then filtered (shown as G(s) boxes) to give horizontal, vertical, and total in situ F-factor.

PUSHOVER/PULL-UP

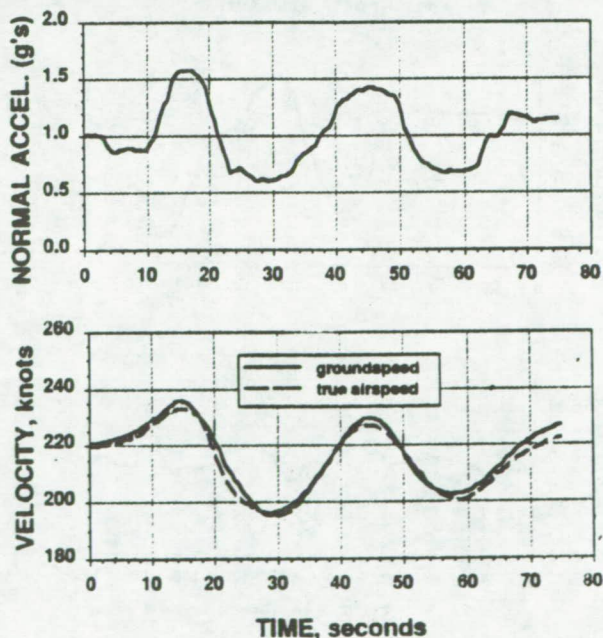
(FLIGHT DATA, 23 MAY 91)



The in situ algorithm was flight-tested locally, with maneuvers intended to induce significant changes in specific state variables to ensure the algorithm's ability to reject aircraft maneuvering effects. This figure shows a pushover/pullup maneuver, where the airplane was pitched up and down in a porpoising type of motion to induce high normal acceleration changes. Ideally, F-factor (bottom plot) should be close to zero, with allowances for acceptable levels of turbulence and signal noise, and well below the FAA-established alert threshold level of $F=0.105$. As shown, there was no adverse effect of the pitching motion on the in situ F-factor measurement.

PUSHOVER/PULL-UP

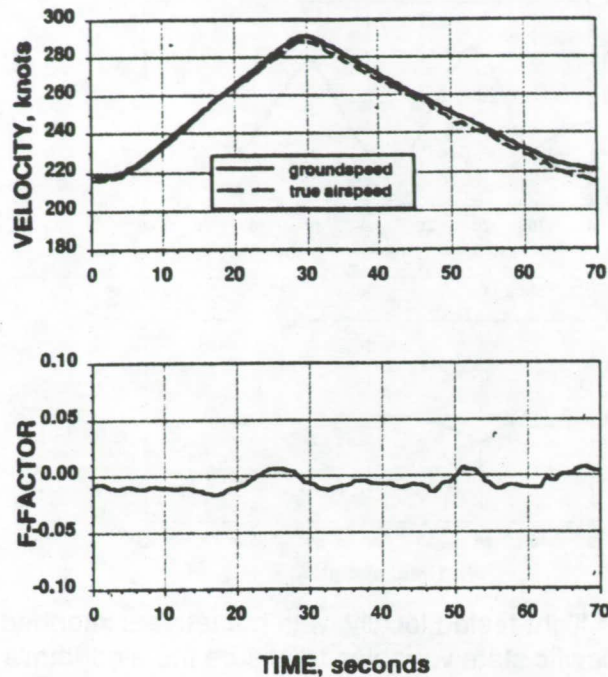
(FLIGHT DATA, 23 MAY 91)



The top figure shows the range of measured normal acceleration, which equals 1.0 g in level, unaccelerated flight. This maneuver induced an increase of 0.6 g and decrease of 0.4 g from the nominal value. True airspeed and groundspeed (bottom plot) are close in value, indicated there was no significant wind.

ACCELERATION/DECELERATION

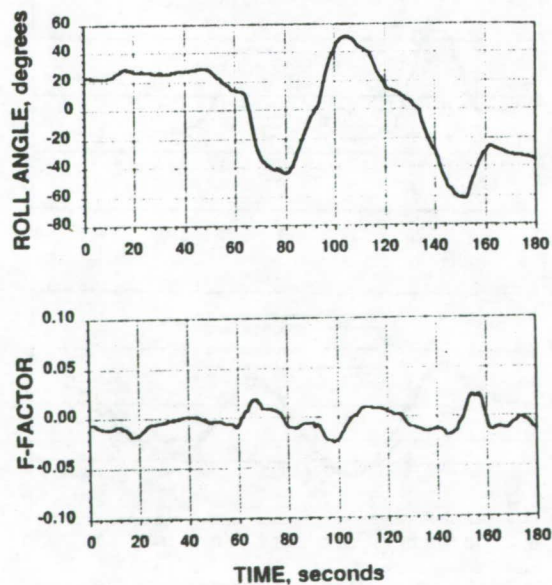
(FLIGHT DATA, 29 MAY 91)



The effect of changing longitudinal acceleration was tested by executing abrupt accelerations and decelerations, where the maximum rate of change was sustained over at least 50 knots change in airspeed. The effect of this motion did not appear to cause any adverse effect on the F-factor (bottom plot) computed by the algorithm.

TURNING FLIGHT

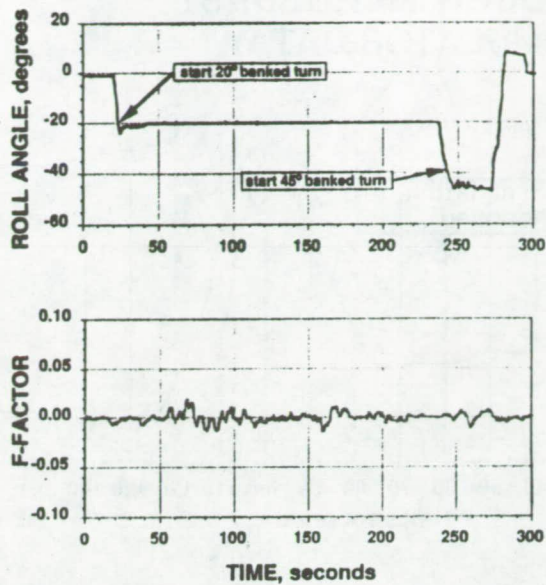
(FLIGHT DATA, 23 MAY 91)



The effectiveness of the 3-D implementation was tested by executing turns at high bank angles. The top figure shows a number of partial turns, at high bank angles and through abrupt changes in direction.

TURNING IN STEADY WIND

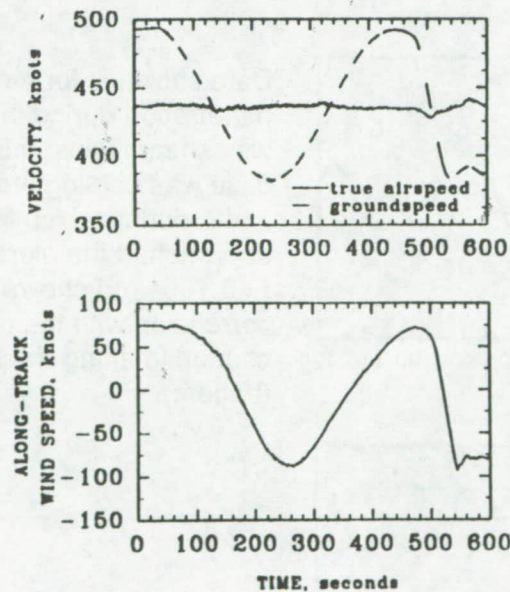
(FLIGHT DATA, 2 OCT 90)



A final maneuvering test was turning in a steady wind condition. The top plot shows the bank angle for the two turns executed in a steady wind of greater than 60 knots. The first was through a 360° heading change at 20° bank, the second through 180° heading at 45° bank. F-factor (bottom plot) shows no adverse effect of this maneuver.

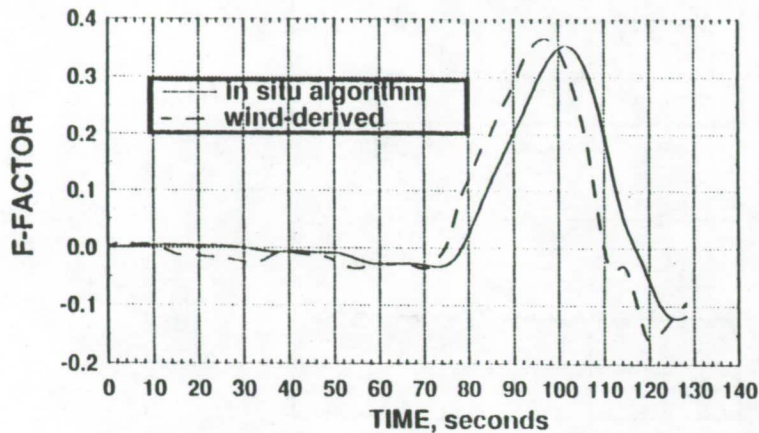
TURNING IN STEADY WIND

(FLIGHT DATA, 2 OCT 90)



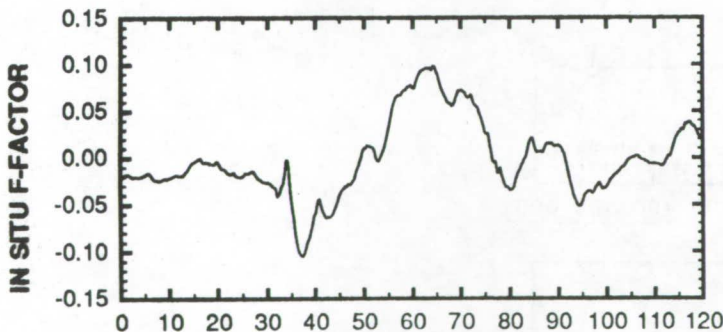
These plots show the effect of the turns in steady wind on the airplane's velocity. The top plot shows true airspeed was constant, while groundspeed varied throughout the turns. The bottom plot shows the along-track wind measured by the airplane, varying by 150 knots over 20 seconds ($t=250$ to 270 sec), and indicates the algorithm's ability to reject the change of longitudinal wind, rather than measure it as a shear.

LANDING APPROACH THROUGH MICROBURST (SIMULATOR DATA)

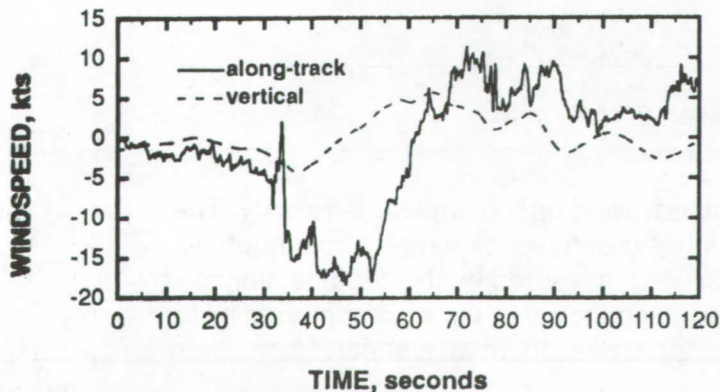


After having shown in flight that the algorithm rejected aircraft maneuvering effects, it was necessary to show that it could also detect a windshear, which was done in simulation, as shown. The in situ F-factor shows some lag and attenuation of the peak, which is primarily due to the effect of the gust-rejection filters, and was expected. Wind-derived F-factor is an instantaneous F-factor computed directly from the known winds.

MICROBURST PENETRATION FLIGHT DATA, 20 JUN 91

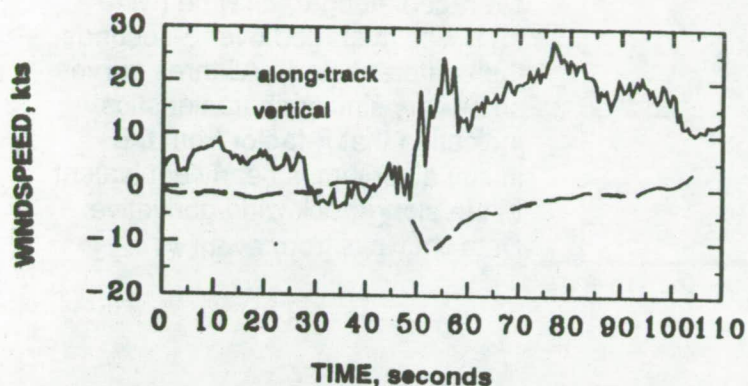
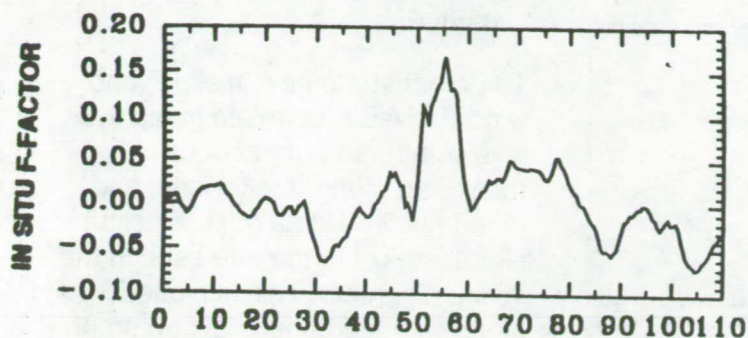


Data shown is for a microburst penetration during the 1991 NASA windshear flights; this particular case was catalogued as event #142, during which in situ F-factor approached the alert threshold of $F=0.105$, and showed good correlation with the observed change in along-track windspeed (bottom).



MICROBURST PENETRATION

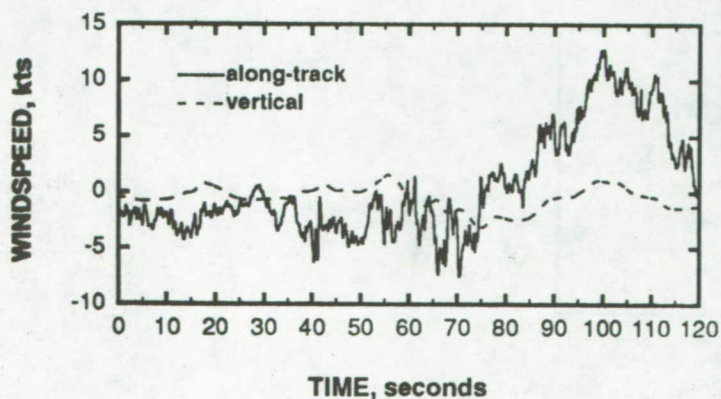
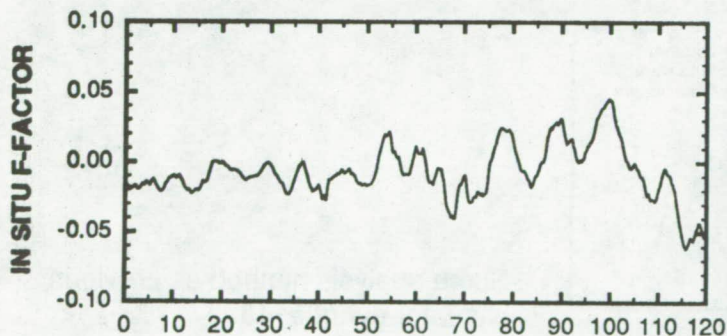
FLIGHT DATA, 17 JUN 91



Data shown is for microburst penetration, event #143, with a peak in situ F of 0.167. Along-track and vertical wind time histories show characteristics of passing near the core of a microburst.

MICROBURST PENETRATION

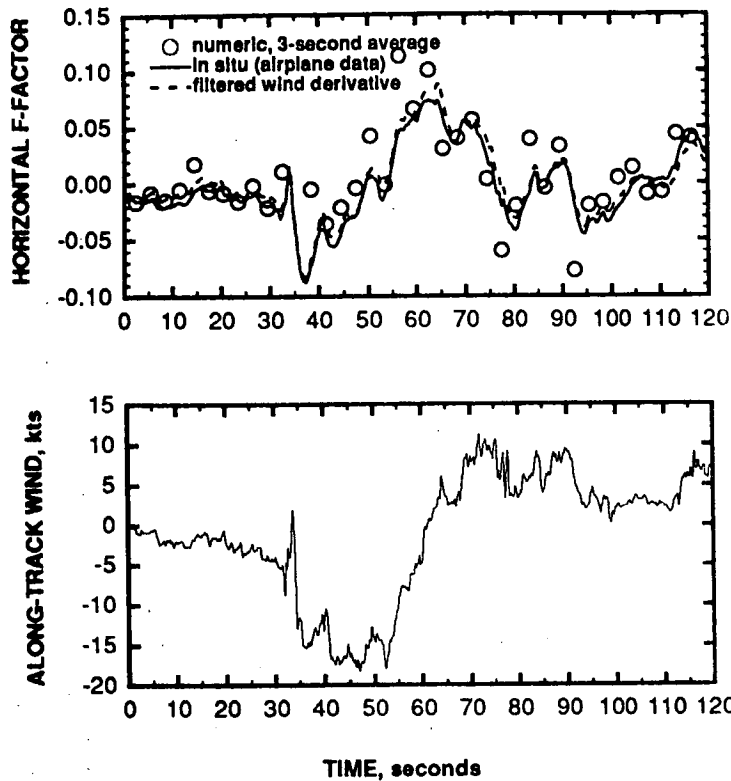
FLIGHT DATA, 17 JUN 91



Data shown is for microburst penetration, event #97. In this case, in situ F peaked at about 0.05, though along-track wind shows a general headwind-to-tailwind trend. The time scale of this event shows that the in situ algorithm is tuned to windshear that is hazardous to the airplane's climb performance, whereas this event was over a longer time scale (or distance), and as such was not a hazard to the airplane. The smaller-scale fluctuations in along-track wind (period of about 10 sec) are evident in the in situ F-factor plot (between $t=75\text{sec}$ and end of run).

MICROBURST PENETRATION

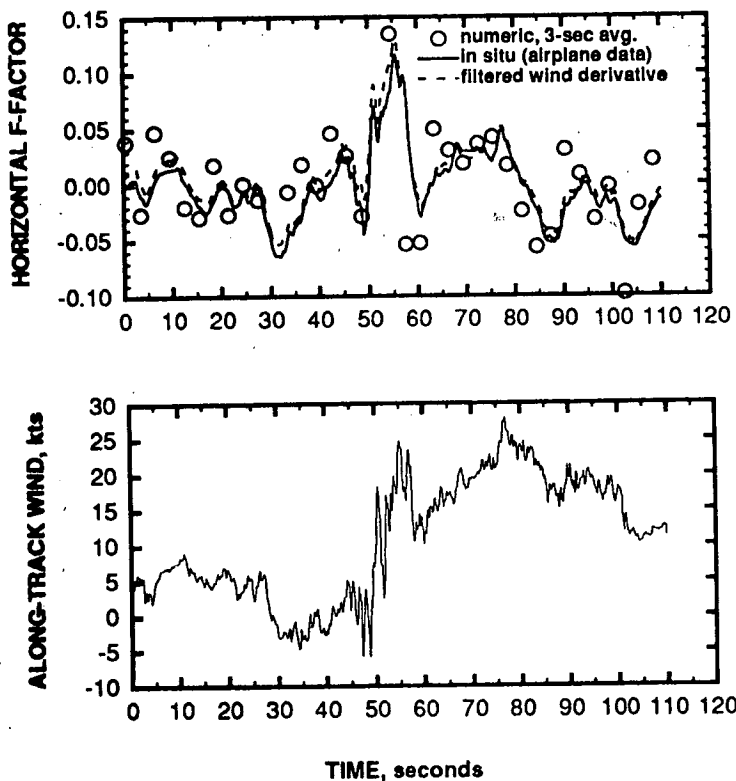
FLIGHT DATA, 20 JUN 91



To demonstrate how in situ F and wind-derived F correlate in-flight, F was computed from aircraft-measured along-track winds, and differentiated with a gust-rejection filter identical to the one used in the in situ algorithm. This is plotted along with the horizontal portion of in situ F-factor (top plot), and an unfiltered numerical differentiation of averaged along-track wind (wind data was averaged over 3-seconds, then differentiated). All three curves show very similar characteristics, indicating that F-factor from the in situ algorithm is nearly equivalent to the along-track wind derivative. Data shown is from event #142.

MICROBURST PENETRATION

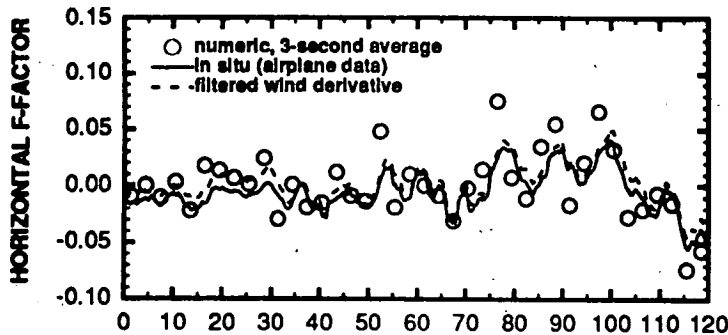
FLIGHT DATA, 20 JUN 91



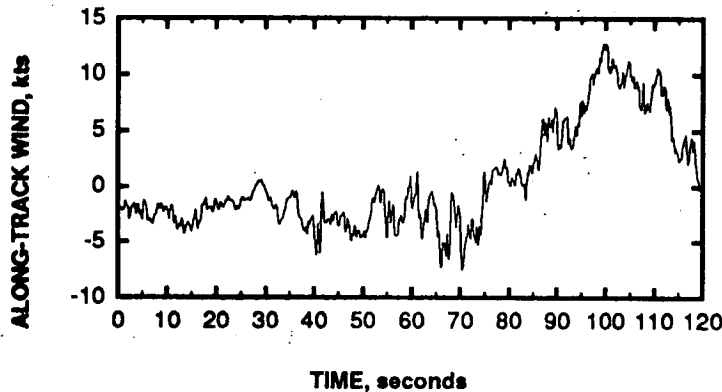
Same analysis method as previous case, for event #143.

MICROBURST PENETRATION

FLIGHT DATA, 17 JUN 91



Same analysis method as for previous case, for event #97.



ALGORITHM PERFORMANCE TO DATE

- OVER 100 FLIGHT HOURS COMPLETED
- APPROXIMATELY 320 TAKE-OFFS AND LANDINGS
- NO NUISANCE ALERTS GENERATED
- ALERTS GENERATED DURING MICROBURST PENETRATIONS CONFIRMED BY GROUND RADAR
- IN SITU HAZARD INDEX CONFIRMED BY WIND MEASUREMENTS

The in situ algorithm's performance is summarized as shown. The algorithm has operated on NASA's B737 for over 100 flight hours, included over 320 take-offs and landings. No nuisance alerts were generated during low-level flight (below 1400'AGL), which included flight in convective weather, gust fronts, and aggressive maneuvering; alerts were generated during microburst penetrations, and confirmed by an independent measurement (ground radar); analysis of in situ hazard index measurement showed that it compared well with hazard index from measured along-track wind.

SUMMARY

OBJECTIVES MET

- VALIDATED IN SITU ALGORITHM AS MEASUREMENT STANDARD FOR FORWARD-LOOK SENSOR EVALUATION
- DEMONSTRATED OPERATIONAL UTILITY

DESIGN REQUIREMENTS MET

- MINIMIZED AIRCRAFT MANEUVER-INDUCED ERRORS IN HAZARD INDEX
- MINIMIZED EFFECTS OF TURBULENCE AND NON-HAZARDOUS ATMOSPHERIC MOTIONS
- STANDARD SENSOR IMPLEMENTATION

Results can be summarized by re-stating objectives and design requirements, which were satisfied as originally set forth.

NASA Wind Shear Flight Test In Situ Results

Questions and Answers

Q: Pete Sinclair (Colorado State University) - I think you might want to be a little cautious about estimating the total F-factor from just the long track winds. Our flight measurements indicate that the vertical term can be as large or larger than the horizontal component and that can throw the F-factor to values above 0.15. Yours looks like that is suppressed quite a bit in the traces you have shown us.

A: Rosa Oseguera (NASA Langley) - Maybe there is a little bit of a misunderstanding. The overall F-factor that we were showing; the first one I showed, is a total F-factor. We are including the vertical term in there. The last slides that I showed were strictly for comparison purposes with the along-track winds. In those slides I was just using the horizontal portion of the F-factor to compare with. That is really all that we are computing from along-track winds. For the purpose of comparing with the forward-look sensors and for providing the alert, the total F-factor was used and that included the vertical term. In fact, that was shown on the block diagram. I just did not clearly point it out. The third term that was computed there was the vertical part of the F-factor.

Q: Pete Sinclair (Colorado State University) - How do you measure the vertical component?

A: Rosa Oseguera (NASA Langley) - It is computed from the difference between inertial flight-path angle and airmass flight-path angle, and groundspeed and airspeed. Roland did you want to expand on that?

Roland Bowles (NASA Langley) - The whole point is that we want to reject certain scales of motion. This measurement is the difference between the airmass and the inertial flight-path angles. This was a fourteen knot peak downdraft in that microburst. When you look at the airplane performance loss the In Situ system peaked out at about fourteen hundred feet per minute, which is about fourteen knots. In other words, that was the measurement of that microburst.

Pete Sinclair (Colorado State University) - What I am saying Roland, is that your system may not be seeing all of the vertical term?

Roland Bowles (NASA Langley) - We don't want it to see all of the vertical term. We don't want small scale turbulence to trip the system. We are not making a wind measurement, we are making a total energy change measurement on the airplane. That is what is hazardous to the airplane.

Pete Sinclair (Colorado State University) - But that vertical term is part of the total hazard to the airplane.

Roland Bowles (NASA Langley) - Sure, at the right scale. This was a small scale microburst. The vertical channel there shows you how the vertical term is estimated. Notice, we are not making wind measurements and processing winds. We are pulling from the backbone sensors on

an airplane, the accelerometers and air-data system. We are not making a wind measurement and then processing the winds. You do not see winds anywhere in there. That's the key.

Q: Jim Evans (MIT) - There is a different issue which I think one has to be concerned about and that is the altitudes at which this testing was done. We know that some microburst have big thick outflows and some of them have much stronger outflows near the surface. We will be showing examples of that later in the conference. One of the questions that comes up is most of this testing was done at the minimum altitude of 1,000 feet, and yet in the context of the guidance we had for TDWR/LLWAS users group, that is the altitude at which people start to get concerned about Wind Shear. One of the questions that would come up is whether the agreement would be as good if you flew down at lower altitudes where we see much more evidence of strong pitching moments. If you look at the Dallas/Fort Worth crash traces for example, you see very strong eddies and things that were definitely affecting the plane at low altitude. So one of the questions I think you would have to ask is, to what extent can you extrapolate the measurements here, at about 1,000 feet altitude, down to much lower altitudes?

A: Roland Bowles (NASA Langley) - That is a good question. The evidence shows that the total energy change to the airplane stays about the same, because the vertical wind component diminishes as a function of altitude where as the horizontal gradient may peak at about 80 to 100 meters, but the overall performance loss is about the same; at normal approach speeds. We were making measurements at the point at which we were testing our sensors. We are not trying to characterize the relative threat level, we were making the In Situ measurement to use as a standard of goodness to compare to the predictions made by the remote sensors.

Dan Vicroy (NASA Langley) - The other point I would like to make is that the F-factor is a performance measurement and in reference to your comment about the pitching moment, that is more of a handling qualities problem and the F-factor is not going to reflect that at all.

Roland Bowles (NASA Langley) - Again, it is a scale of motion you are trying to identify.

Pat Adamson (Turbulence Prediction Systems) - This is just a point of clarification. The F-factor that you guys are talking about is slightly larger because of the airspeed you were flying. The airspeed plays a big factor in the magnitude of F.

1993010405

62P

Session I. NASA Flight Tests

N 93 - 19594

Air/Ground Wind Shear Information Integration - Flight Test Results
David Hinton, NASA Langley Research Center

Air/Ground Wind Shear Information Integration - Flight Test Results

David A. Hinton
NASA Langley Research Center

**Presented at Fourth Combined
Manufacturers' and Technologists'
Airborne Wind Shear Review Meeting
Williamsburg, VA**

April 14, 1992

Air/Ground Wind Shear Information Integration Flight Test Results

David A. Hinton

ABSTRACT

An element of the NASA/FAA wind shear program is the integration of ground-based microburst information on the flight deck, to support airborne wind shear alerting and microburst avoidance. NASA conducted a wind shear flight test program in the summer of 1991 during which airborne processing of Terminal Doppler Weather Radar (TDWR) data was used to derive microburst alerts. High level microburst products were extracted from TDWR, transmitted to a NASA Boeing 737 in flight via data link, and processed to estimate the wind shear hazard level (F-factor) that would be experienced by the aircraft in the core of each microburst. The microburst location and F-factor were used to derive a situation display and alerts. The situation display was successfully used to maneuver the aircraft for microburst penetrations, during which in situ "truth" measurements were made. A total of 19 penetrations were made of TDWR-reported microburst locations, resulting in 18 airborne microburst alerts from the TDWR data and two microburst alerts from the airborne in situ measurements. The primary factors affecting alerting performance were spatial offset of the flight path from the region of strongest shear, differences in TDWR measurement altitude and airplane penetration altitude, and variations in microburst outflow profiles. Predicted and measured F-factors agreed well in penetrations near microburst cores. Although improvements in airborne and ground processing of the TDWR measurements would be required to support an airborne executive-level alerting protocol, the feasibility of airborne utilization of TDWR data link data has been demonstrated.

OUTLINE

- **Introduction and System Concept**
- **Flight Test Procedure**
- **Results**
 - **F-factor Algorithm Performance**
 - **System Alerting Performance**
- **1992 Enhancements**
- **Summary**

Research Goal

Under the terms of the Integrated Wind Shear Program, NASA, the FAA and industry have jointly developed solutions to the wind shear hazard to commercial transports. The NASA efforts are concentrated in airborne aspects such as hazard characterization, aircraft performance impact, advanced in situ and forward-look sensor technology, and flight deck integration. The FAA efforts have been concentrated in ground side aspects such as crew training (ref. 1) and ground-based detection systems such as low-level wind shear alerting systems and Terminal Doppler Weather Radar (TDWR). The TDWR system has proven its capability to detect the microburst phenomenology in tests and operational demonstrations, but experiences suggest (ref. 2) that the information is not reaching flight crews in a timely matter or in a form that is compatible with existing and planned onboard wind shear detection systems.

In 1990 a Memorandum of Agreement between NASA and the FAA was implemented with a major program element to "Demonstrate the practicality and utility of real-time assimilation and synthesis of ground-derived wind shear data to support executive level cockpit warning and crew-centered information display." The goal can be divided into subgoals of identifying ground-based information products required on the flight deck to derive a crew-centered hazard index and rapidly transmitting this data to the flight deck.

Research Goal

Reduce wind shear risk through integration of TDWR and airborne system capabilities.

Approach:

- Identify TDWR information products required for airborne processing of wind shear hazard index and executive-level crew alerting.**
- Demonstrate feasibility of data link and airborne utilization of TDWR information in an operational environment.**

Ground Rules

Ground rules were established for the conduct of this program. The key ground rule was that neither the existing TDWR system nor the current division of responsibilities and roles between air traffic control and pilots would be altered. The TDWR system was to remain unchanged because years of testing have demonstrated its microburst detection capability, the system design was essentially frozen for production, and even minor changes would be prohibitively expensive. Rather than change the system, those high level products produced by TDWR that are required for airborne processing were to be identified and provided to an aircraft via data link. The emphasis was to provide an executive level warning (requiring immediate corrective or compensatory action by the crew). Such a warning requires a very low nuisance alarm rate, on the order of 1 nuisance per 250 hours of system operation. A nuisance is defined as an alert received when system alert threshold conditions exist but do not produce a hazard to the aircraft.

The air/ground roles of the proposed system are tailored to reflect current ATC/pilot roles. The TDWR is to classify events as a microburst and provide location and microburst parameters to the airborne system. The airborne component will quantify the threat, compare to a threshold, and annunciate. The concept is analogous to other ground systems providing meteorological data such as runway visual range, wind, and ceiling. The decision to continue is made on the aircraft based on required minima and operating procedures.

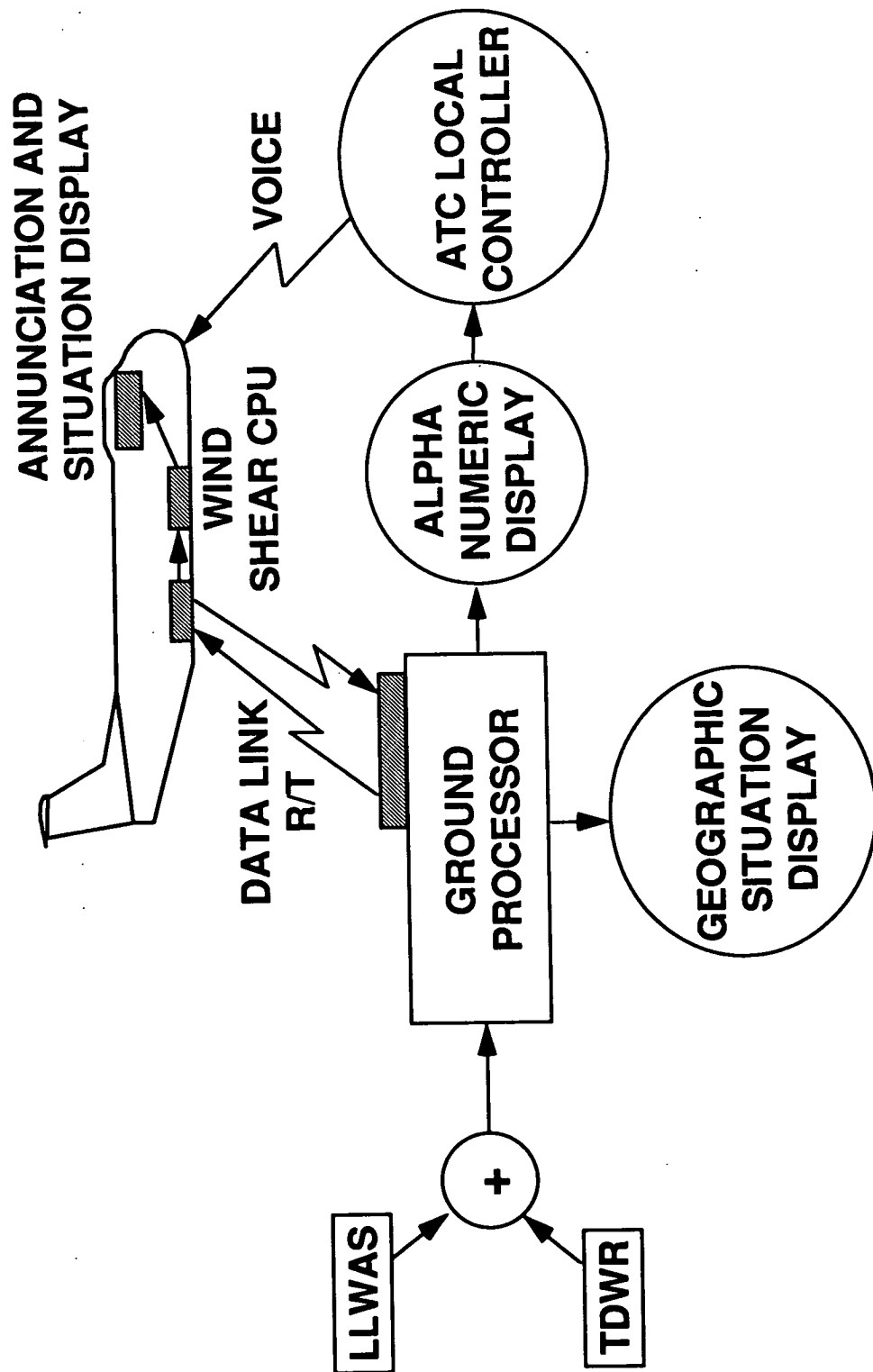
Ground Rules

- Do not change the ground systems or current ATC/pilot roles.
- Identify ground products needed for uplink to support time critical information processing and display.
- Task tailored air/ground roles for TDWR integration:
 - Ground: Classify and locate
 - Airborne: Quantify and annunciate
- Downlink status of airborne warning to ATC.
- Focus research on technology integration/evaluation.

System Architecture

The baseline TDWR system consists of a radar, a ground processor to identify regions of divergence and classify them as microbursts, a geographic situation display to depict microburst locations relative to runways and approach paths to the ATC tower supervisor, and an alphanumeric ribbon display for presenting wind shear and microburst information to the local controller for voice transmission to pilots. A typical message from the local controller is "Microburst alert, threshold wind 140 at 5, expect a 50 knot loss two mile final." The additions to the TDWR system required to support the NASA alerting concept are a cockpit server software package to extract the necessary TDWR data for transmission over a data link, the data link receiver/transmitter, airborne algorithms to compute the wind shear hazard from TDWR supplied data, and annunciation and display. Only air to ground data link is required to provide airborne alerting. The intent of the down link is to provide the ATC system with information that a wind shear alert has been generated by the airborne system. No changes to the existing TDWR system are required to support this concept.

System Architecture



Operational Concept

The current TDWR operational concept is to detect microbursts by examining radar-observed wind velocity information for regions of divergence. When the radar detects a divergence of greater than 15 meters per second over a distance of at least 1 kilometer, a shape algorithm draws a microburst icon around the divergence region. "Wind shear" icons are drawn around divergence regions of at least 7.5 meters per second. The microburst is then quantified for ATC and pilots by the divergence value. The actual hazard to the aircraft depends heavily, though, on the scale length of the divergence, i.e., the change of wind per unit distance, or shear (ref. 3). Existing airborne wind shear systems as well as those under development derive an F-factor hazard index (ref. 3) that is based on wind change per unit distance and down draft. To provide airborne executive level alerting from TDWR information, an estimate must be made of the wind shear in the microburst and the down draft component. The information required for this estimate are readily available from the TDWR system. Since (at a readily available level) the TDWR produces a single velocity and distance number for each microburst, insufficient data are available to estimate the shear along arbitrary paths through the event. The airborne F-factor estimate tested in this study describes the threat only in the core of the event. The core F-factor estimate is then combined on the aircraft with microburst location information to determine if an alert should be given.

Operational Concept

- Using available high-level TDWR products, estimate shear and F-factor in 1 kilometer region about core of microburst outflow.
- Combine F-factor and microburst location with respect to aircraft, to derive executive-level warning and situation display.
- System does not predict F-factor along arbitrary flight path, only predicts hazard in core of outflow.

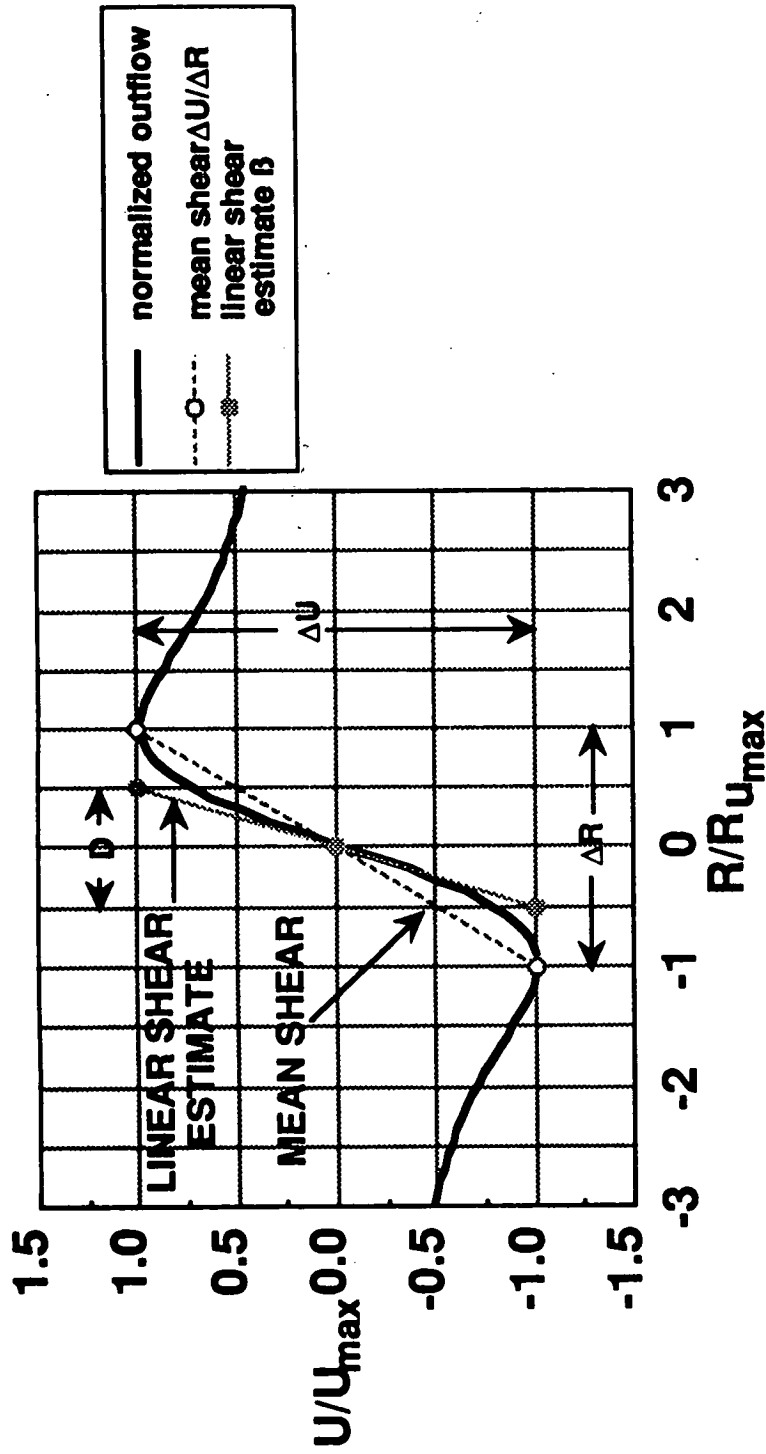
Least-Square Estimate of Linear Shear

The wind shear within a microburst can be estimated from the wind change and scale length information provided by the TDWR and an assumed wind profile. The TDWR information describes the endpoints of the peak-to-peak winds and the assumed wind profile is used to derive information about the wind field between the peaks. The horizontal wind profile of the analytical Oseguera/Bowles microburst model described in reference 4 was used to estimate the least-squares shear value over a distance D about the core of the microburst. Since aircraft performance degradation from wind shear requires shear lengths on the order of 1 kilometer, or greater, a value of 1 kilometer for D was used in the experiment.

The microburst F-factor can be estimated from the shear value just determined and an estimate of the down draft in the event. Mass continuity considerations are used to estimate down draft over the same interval as the shear. The resulting equations, as originally derived by Bowles (ref. 3) are shown on the adjacent figure. The information required from the TDWR to estimate F-factor is the wind change (ΔU), the scale length of the wind change (ΔR) and the altitude of the radar beam in the microburst core.

Each microburst icon is composed of numerous divergence segments, each one degree apart in radar azimuth. Each divergence segment has its own wind change and length. In this experiment the ΔU and ΔR sent to the aircraft was determined as follows. If 5 or fewer segments define an icon then send the maximum ΔU value. If this test fails then if 20 or fewer segments define an icon send the second largest ΔU value. If more than 20 segments define an icon then send the 90th percentile segment ΔU value. In practice, nearly all icons consisted of less than 20 segments and either the largest or next largest divergence value was normally sent. The ΔR value was determined by examining the shear value of each segment in the icon and choosing the 85th percentile shear value. A ΔR value was then determined that would produce this 85th percentile shear when divided into the transmitted ΔU value. As an example, one icon penetrated in the 1991 flight tests (event 143) was defined by 4 segments having ΔU values of 17.1, 18.9, 22.6, and 20.2 meters/second and ΔR values of 3140, 3460, 4500, and 4210 meters, respectively. The corresponding shear values were 5.45, 5.46, 5.02, and 4.80 meters/second/kilometer. Since four segments defined the icon the largest ΔU value (22.6) was transmitted. The 85th percentile shear value was the second largest (5.45) which produced a transmitted ΔR value of 4150 meters (rounded to the nearest 10 meters).

LEAST SQUARE ESTIMATE OF LINEAR SHEAR



$$\beta = 4.1925 \frac{\Delta U}{\Delta R} \left[\left(\frac{\Delta R}{D} \right)^2 - \left(\frac{\Delta R}{D} \right)^3 \frac{\sqrt{\pi}}{2.2424} \operatorname{erf} \left(1.1212 \frac{D}{\Delta R} \right) \right]$$

$$F = \beta \left[\frac{V_G}{g} + \frac{2h}{V} \right]$$

Alert Criteria

The TDWR data link provided the required data to estimate the microburst core F-factor and to depict the TDWR-derived microburst icons on a cockpit moving map display. In order to issue an executive-level alert, a microburst icon must exist on the projected instantaneous trajectory of the aircraft (defined by the centerline of the track-up moving map display), the range to the icon must be less than 1.5 nautical miles, and the core F-factor estimate must be at least 0.105. Note that in a classical microburst wind field the strongest wind gradient and F-factor exists in the core of the event, where the winds are weakest, while very weak wind gradients and F-factors exist in the vicinity of peak wind outflow. Since the TDWR-produced microburst shapes tend to enclose the peak-to-peak wind field, it is logical to assume that the shapes will overestimate the region of strong shear. Since insufficient data was available to determine which region within the icon contained the strongest shear, an alert was generated when any part of an icon intersected the flight path. The alert threshold is consistent with thresholds specified in FAA TSO-C117 for the certification of reactive wind shear devices and the 1.5 mile range is consistent with proposed crew procedures and the supporting alerting strategies.

Alert Criteria

Executive level alert is given when:

- 1. A TDWR microburst icon intersects extended flight path.**
- 2. The F-factor of that icon is at least 0.105.**
- 3. The range to the icon is less than 1.5 nautical mile.**

Flight Test Procedure

The TDWR data link concept was tested during NASA combined sensor flight tests conducted at Orlando, Florida and Denver, Colorado in June and July of 1991. The tests provided the opportunity to measure microburst winds with an array of remote sensors (TDWR, airborne radar, and infrared) and correlate those remote measurements with aircraft in situ wind shear measurements taken during microburst penetration. In addition to the TDWR research aspect, the TDWR system was also used operationally to predict microbursts, maneuver the aircraft for penetrations, and monitor flight safety criteria such as storm reflectivity values. Both for flight safety and for later data correlation, microburst penetrations were conducted on a track either toward or away from the TDWR to minimize the effects of any microburst asymmetry.

The flight tests were conducted in cooperation with the MIT Lincoln Laboratory at Orlando and the National Center for Atmospheric Research (NCAR) at Denver. Both Lincoln Lab and NCAR developed cockpit server software to extract the required parameters from the TDWR and format the data for transmission to a NASA ground station via modem and dedicated phone lines. Only low cost hardware was required to complete the data link to the aircraft. The data was transmitted at 1200 baud over an MFJ Enterprises MFJ-1270B TNC packet radio system. The data transmitted over the data link consisted of the ΔU , ΔR , radar beam altitude, and coordinates of each microburst icon, as well as overhead data such as the GMT time of the beginning of the TDWR radar scan, number of icons in the data link message, and checksum. Each data link message required 14 bytes for overhead data plus 25 bytes per microburst icon. This data was transmitted approximately once every 60 seconds and the elapsed time between the beginning of a TDWR radar antennae sweep and the receipt of that data onboard the aircraft was on the order of 30 seconds. Onboard the aircraft the icons were displayed on a moving map display and used to maneuver the aircraft for microburst penetrations.

Flight Test Procedure

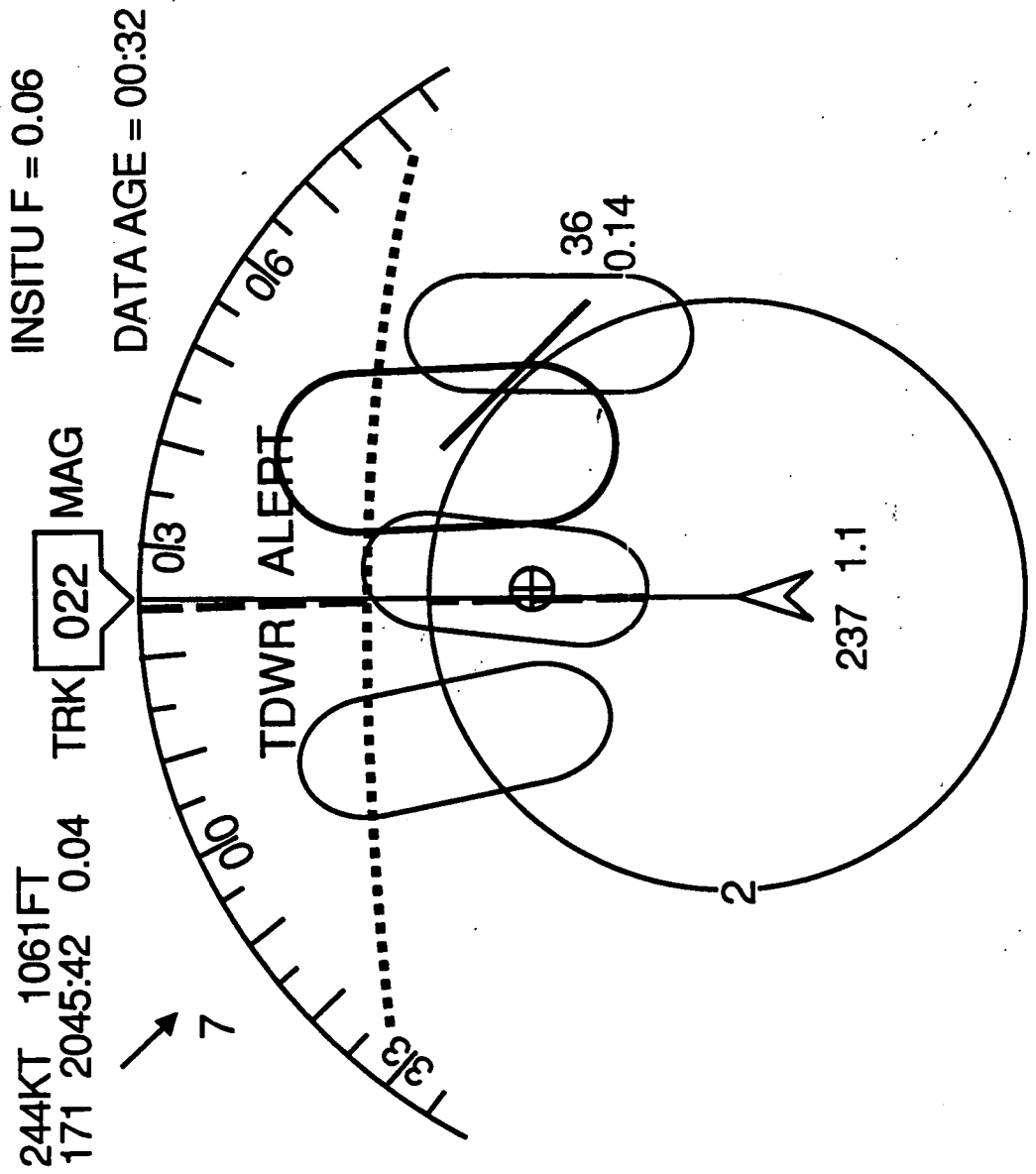
TDWR information integration concept tested during combined sensor flight tests at Orlando and Denver onboard NASA Boeing 737, summer 1991.

- Cockpit server TDWR software developed by MIT Lincoln Lab/NCAR.**
- Data provided via 1200 baud modem to VHF packet radio system. Required data = Delta V, diameter, radar beam altitude, and location and shape of each microburst icon.**
- TDWR data and alerts displayed on moving map display. Display used to maneuver aircraft for encounters.**

Moving Map Display

The TDWR icon information was presented on a moving map display, along with supporting flight state parameters, and recorded on video tape for later analysis. The supporting data included the TDWR data age (elapsed time since last data link reception) and in situ F-factor in the upper right corner; true airspeed, time, radar altitude and inertial wind vector in the upper left corner; groundspeed and barometric altitude below the ownship symbol; and magnetic track angle above the track scale. Microburst alerts generated by the onboard computation and criteria were displayed by the message "TDWR ALERT" in red letters just below the track scale. The wind change and F-factor of each icon were shown numerically by labels that stepped from one icon to the next at the rate of about one icon per second (to reduce display clutter) and by color coding the icons. White was used to draw icons with F less than 0.105, amber for icons between 0.105 and 0.15 F, and red for icons with F-factors at or above 0.15. Also shown on the display were the limits of TDWR coverage and a waypoint which could be transmitted from the TDWR operator to accurately locate places of interest such as gust front boundaries, microburst cores, or predicted microburst locations. This display is not intended to represent a format that should be implemented for fleet operational use. The display was intended as an aid to data analysis as well as a tool for situational awareness during research flights.

The accompanying display sketch was drawn from a video tape of the approach to event 143 on June 20, 1991. Four microburst icons are ahead of the airplane and a waypoint transmitted by the TDWR operator is on the flight path at a range of about 1.5 miles. The aircraft has a groundspeed of 237 knots and the radar altimeter value is 1061 feet. A TDWR alert has been generated by onboard logic and is displayed. The dotted line just beyond the nearest icon represents a 30 kilometer range ring from the TDWR site, which is behind the aircraft.



Results

The simple data link hardware proved very reliable at both deployment locations both while on the ground preparing for takeoff as well as while flying at low altitude 30 to 40 kilometers from the antennae site. The situation display combined with voice information from the TDWR proved invaluable for 15 to 30 minute projections of the weather situation, positioning the aircraft to intercept microbursts that were being predicted but not yet developed, maneuvering with respect to active microbursts, and subsequent data analysis. The situation display was used for maneuvering the airplane to penetrate active microbursts and for assessing the strength of those microbursts before penetration. The voice link was used for other operational data such as reflectivity at the surface and aloft, short term microburst predictions, and general weather trends.

During the two week deployment at Orlando the NASA aircraft penetrated 19 weather events that were generating TDWR icons at the time of penetration. Numerous other events were also encountered such as gust fronts, rain shafts, and divergent flows that had not yet strengthened to the point of generating an icon or decaying microbursts that were no longer producing icons. These other events are not included in this analysis. During a three week deployment at Denver the only observed microbursts were above flight safety reflectivity limits or could not be reached. Hence all data presented here is from the 19 icon penetrations in the Orlando area.

The data is analyzed from two perspectives. The first issue was the performance of the F-factor estimation algorithm. The second issue was the overall alerting performance of the TDWR system (TDWR, airborne processing, and alerting criteria) during the flight tests.

Results

- TDWR data link proved reliable
- Situation display extremely useful for aircraft positioning as well as post-flight data analysis.
- 19 microburst icons penetrated at Orlando, none at Denver.
- Results analyzed for F-factor algorithm performance and for alerting performance.

F-Factor Algorithm Performance

While the overall alerting performance analysis uses data from all 19 icon penetrations, evaluation of the F-factor estimation algorithm can be done only in those cases where the airplane passed through the region described by the estimator, which is in or very near the core of the microburst. Early in the flight tests it became apparent that the TDWR depicts microbursts with multiple icons, typically three or four, to locate areas of larger and smaller divergence (ΔU magnitude). All icons associated with a microburst were treated equally by the airborne F-factor estimator although not all icons contained a center of divergence. Observation by TDWR operators, who could observe flight path as well as radar reflectivity and doppler velocity in real time, indicated that penetration of an icon could miss the divergence core by a kilometer or more. Later flights used the TDWR operator waypoint data link function to help locate the desired cores of the microbursts.

To evaluate the F-factor algorithm a selection criteria was established to determine which penetration data sets were applicable. The selection was based on TDWR radar velocity plots overlaid with aircraft trajectory. To include a penetration in the F-factor data set two criteria must be met; 1) that the TDWR velocity plot show a well-defined microburst outflow, and 2) that the flight path intersect the core of this outflow. Only five of the 19 events satisfied this criteria. Three of the five events were achieved during multiple penetrations of a single microburst on the final day of test flights, at growing, near peak, and decaying periods of the event. Event numbers were assigned to each data block of interest during the deployments. The five core penetrations are events 81, 134, 142, 143, and 144.

For comparisons between the F-factor estimator and in situ measurements, the TDWR radar scan taken closest to the time of airplane penetration was chosen. The average error between the TDWR F-factor estimator and in situ was only 0.02 F with the largest error being 0.04 F. The primary factors affecting the estimation, to be discussed in more detail, were differences between TDWR radar measurement altitude and airplane altitude in the microburst, and errors in estimating the one kilometer shear from TDWR peak-to-peak winds.

All TDWR radar reflectivity, velocity, and shear maps were provided to NASA by the MIT Lincoln Laboratory.

F-factor Algorithm Performance

Event selection criteria:

- Using TDWR velocity plots with aircraft trajectory overlay, determine that:

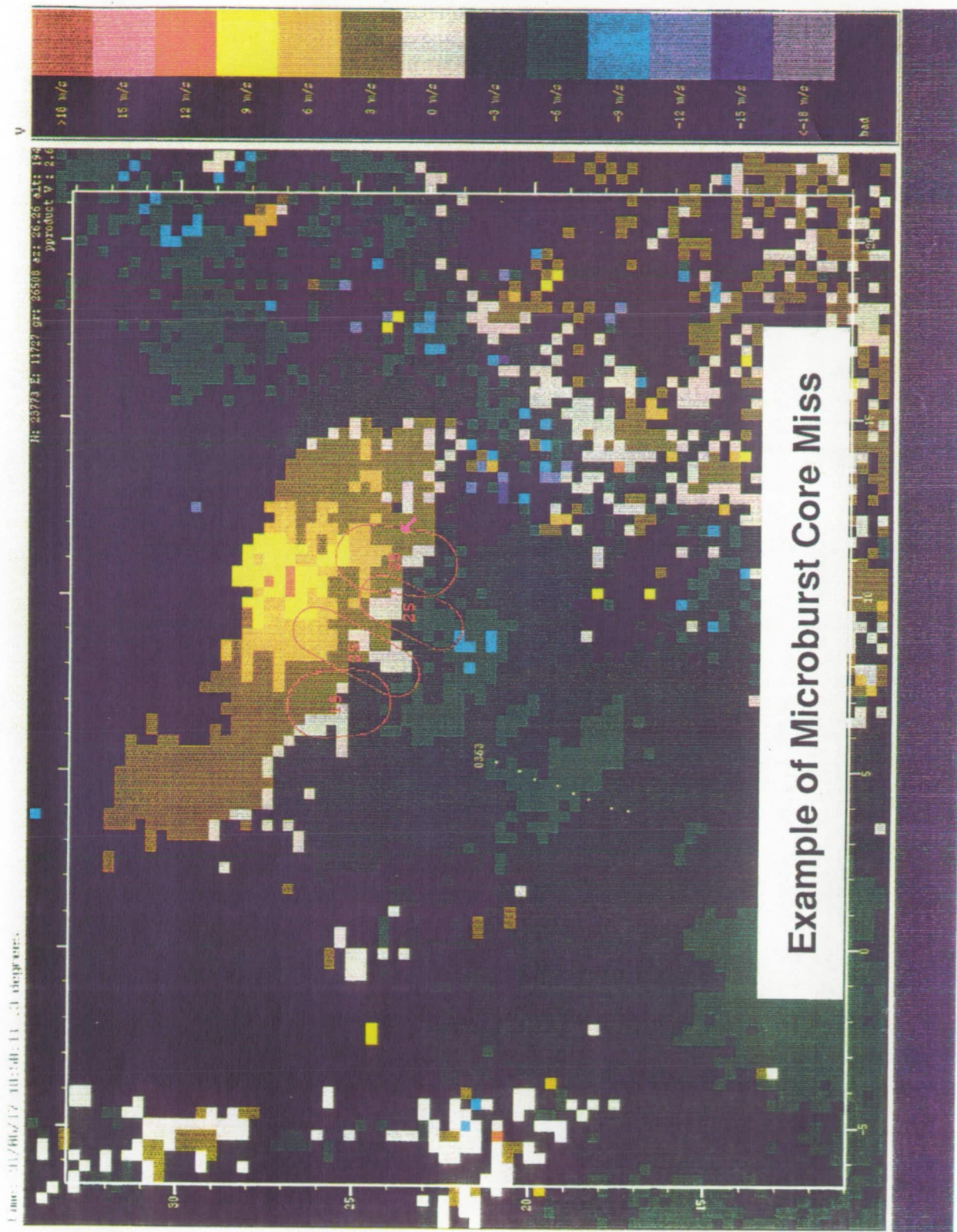
1. A well-defined outflow existed.
2. Aircraft path intersected core of outflow.

Criteria met by 5 of 19 microburst icon penetrations:

- F-factor estimate from TDWR data agreed with in situ F-factor within 0.04, with average error of 0.02.
- Principle factors affecting hazard index estimate were measurement altitude and shear estimate from TDWR information.

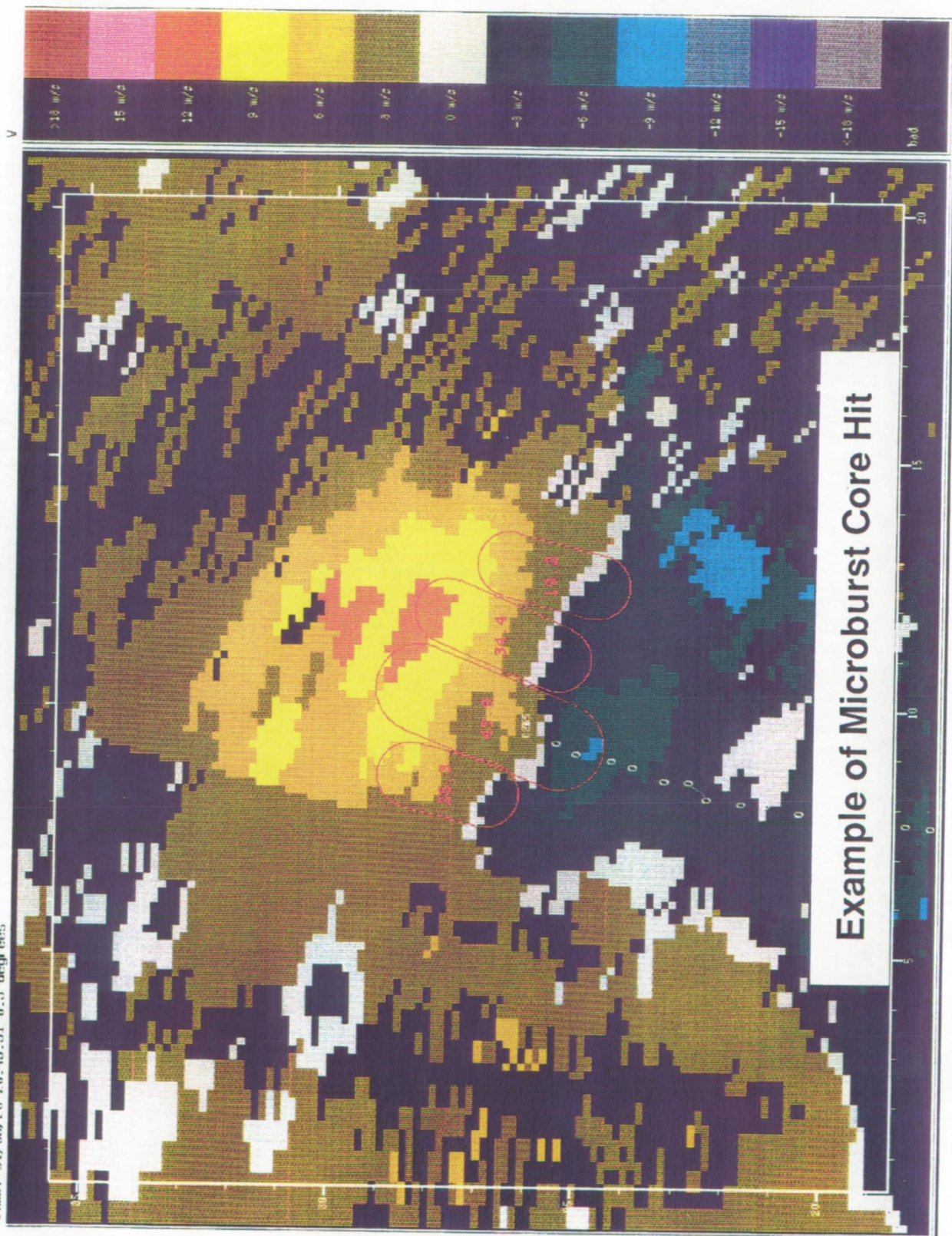
TDWR Plot of Missed Microburst Core and Microburst Core Penetration

These two plots show examples of a microburst icon penetration that did not encounter the core region described by the F-factor estimation algorithm and a penetration through a microburst core. The first event is not included in the set of five core penetrations. The second plot shows the airplane in the core of the penetration cataloged as event 142. Note in the second plot that the flight path passes through the doublet of highest doppler velocity return.



ORIGINAL PAGE
 COLOR PHOTOGRAPH

time: 91/06/20 20:45:51 0.3 degrees



PRECEDING PAGE BLANK NOT FILMED

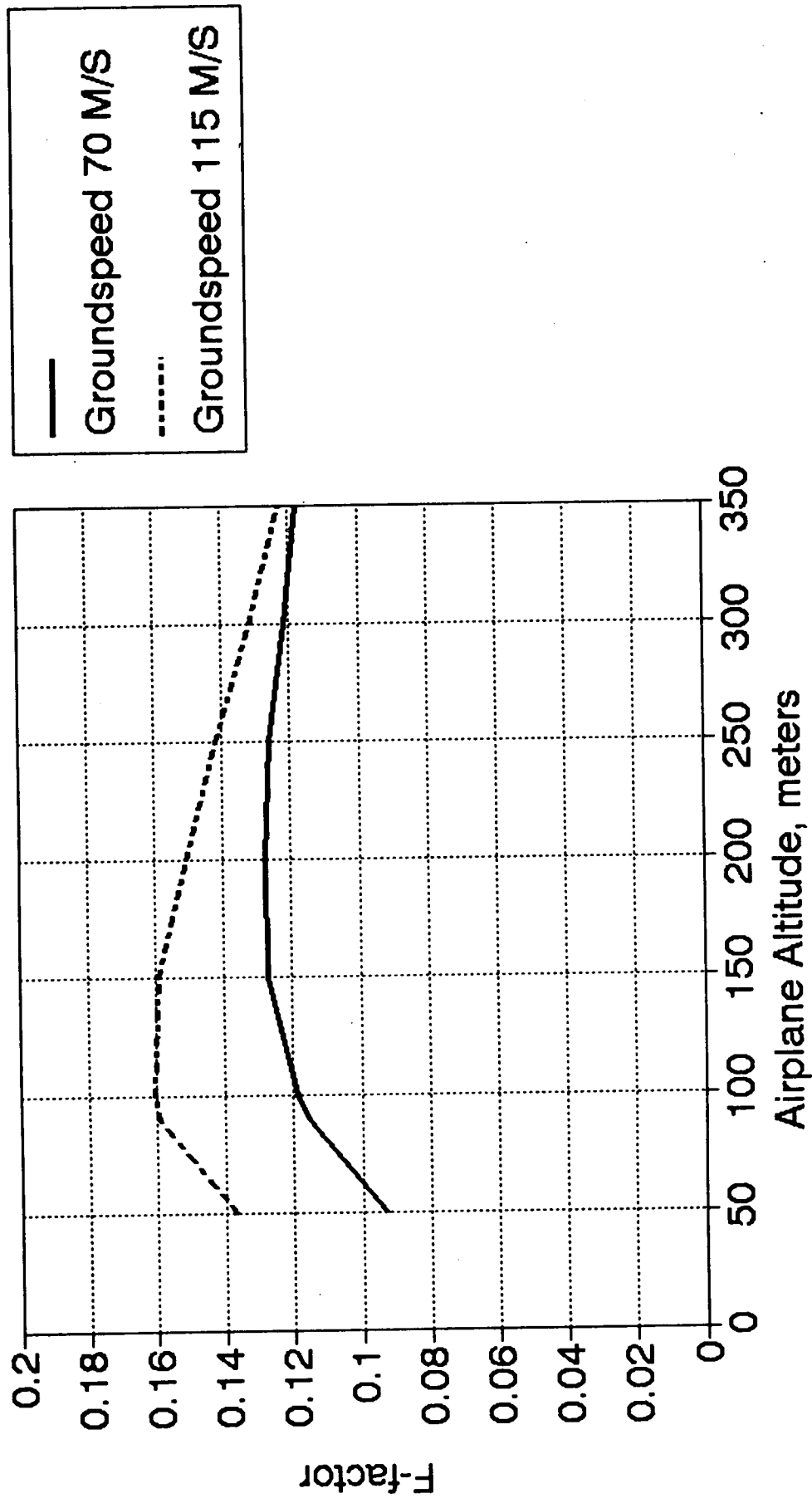
ORIGINAL PAGE
COLOR PHOTOGRAPH

Speed and Altitude Effect on F-Factor

As the altitude of microburst penetration increases above the altitude of maximum outflow, the horizontal wind change decreases while the down draft increases. Since the F-factor experienced by the airplane is proportional to horizontal wind gradient multiplied by groundspeed and down draft divided by airspeed, the horizontal component of F-factor tends to decrease with increasing altitude while the vertical component tends to increase with altitude. At normal approach speeds the change in the two components tend to be of similar magnitude. The result is that the F-factor does not vary greatly with altitude above the altitude of maximum outflow up to altitudes where microbursts no longer pose a safety threat (about 1000 to 1500 feet). Below the altitude of maximum microburst outflow both horizontal winds and vertical winds decrease, leading to reduced F-factor. At the high speeds used in the microburst flights, however, the down draft contributes less to the total F-factor and the measured F-factor does tend to decrease with altitude. The plot shows variation in the altitude-corrected TDWR F-factor estimation with altitude at a groundspeed of 70 and 115 meters per second (136 knots and 223 knots) for a given microburst. The two speeds approximate normal approach speed and the NASA microburst penetration speed. The plot assumes that the altitude of maximum outflow is 90 meters and that the radar measurement is taken at that altitude. At 70 meters/second the change in F-factor from 90 meters to 350 meters is less than 0.01, while at 115 meters/second the change is nearly 0.04. The equation used to provide the TDWR altitude correction is presented next.

Speed and Altitude Effect on F-Factor

Altitude-Corrected TDWR F-Factor



F-Factor Altitude Effect

The trend of relatively constant F-factor with variations in altitude was used as an assumption in the TDWR F-factor estimation algorithm. Although aircraft speed was used in the F-factor algorithm, the altitude of the aircraft was not included in any way. The divergence measured by the radar was used directly and the altitude of the radar beam in the microburst was used in the estimation of the vertical wind. In effect, the F-factor estimate was assuming a penetration at the radar beam altitude. In the events penetrated the radar beam was typically at altitudes of 150 to 220 meters above ground, depending on range of the event from the radar, while the airplane typically flew through the event at 300 to 350 meters above ground. The analytical microburst models described in references 4 and 5 include a shaping function which describes the change in microburst outflow with altitude. These models base the shaping function on mass continuity, boundary layer friction, and vertical wind profiles produced by the Terminal Area Simulation System (TASS) numerical microburst model, which has been extensively validated against observed microburst data (references 6 and 7). The shaping function $p(h)$ provides the ratio of outflow speed to maximum outflow speed at any arbitrary altitude. Given this shaping function, the shear estimate (β) at any altitude can be expressed as the shear at the altitude of maximum outflow multiplied by $p(h)$.

$$\beta = \beta' p(h) \quad (1)$$

Where β' is the shear at the altitude of maximum outflow. We can express F at any altitude as:

$$F_1 = \beta' p(h_1) (V/g + 2h_1/V) \quad (2)$$

and

$$F_2 = \beta' p(h_2) (V/g + 2h_2/V) \quad (3)$$

or by rearranging 2 and 3:

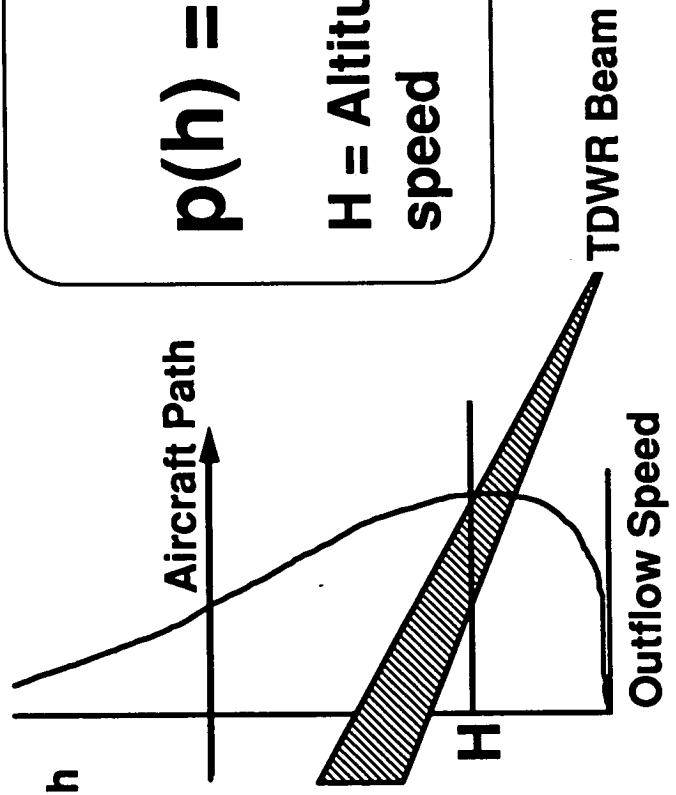
$$F_2 = F_1 p(h_2) (V/g + 2h_2/V) \quad (4)$$

$$\frac{F_2}{p(h_1) (V/g + 2h_1/V)}$$

Equation 4 was used as an altitude correction algorithm where F_1 is the uncorrected TDWR F-factor estimation, h_1 is the TDWR radar beam altitude, and h_2 is the airplane altitude. F_2 then becomes the F-factor estimate at the airplane altitude.

F-factor Altitude Effect

TDWR measurement of wind divergence taken at different altitude than aircraft penetration. Altitude shaping function in NASA analytical wind shear model can provide correction.



$$p(h) = \frac{e^{-0.22h/H} - e^{-2.75h/H}}{0.7386}$$

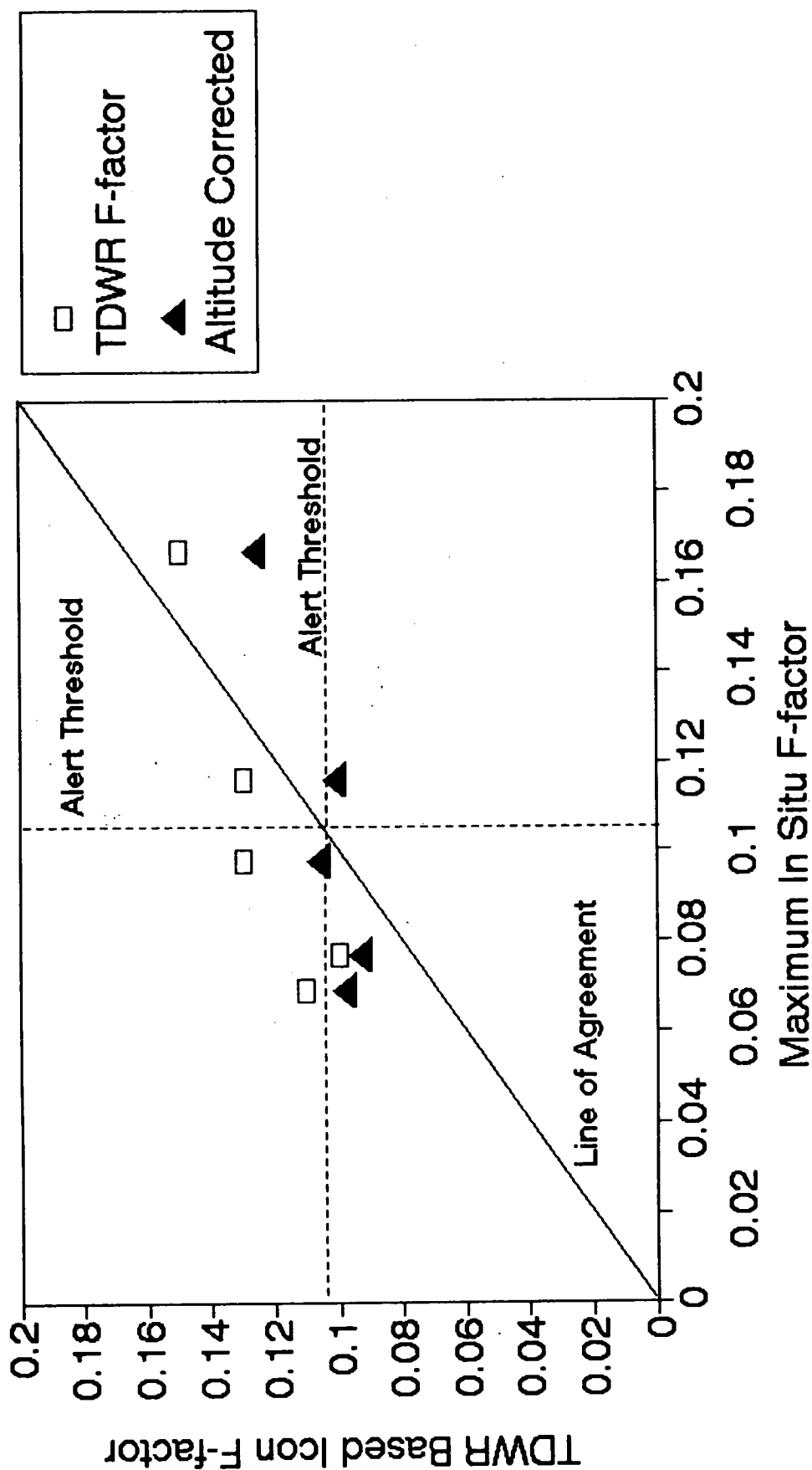
H = Altitude of maximum outflow speed

TDWR Based F-Factor and In Situ F-Factor

Shown in this plot is the F-factor estimated from TDWR data for each of the five core penetrations compared to the maximum in situ F-factor experienced during that event. Both the uncorrected TDWR F-factor and the altitude-corrected F-factor are shown. Also depicted are the alert thresholds of each sensor (0.105) and the ideal "line of agreement". The in situ and TDWR F-factors can be directly compared in this manner since both are tuned to a scale length that affects airplane performance. In the case of the in situ measurement this scale length sensitivity is achieved through gust-rejection filtering. With the exception of the rightmost point (event 143) the TDWR F-factor overestimates the in situ F-factor. When the altitude correction is applied though, the lower four events agree well. Considering that the two measurements are taken by different sensors on different platforms, and at slightly different times, the agreement is excellent. Of course much more data is needed to begin to assign statistical significance to this data. The reason for the relatively large TDWR underestimate of the F-factor for event 143 is related to shear estimation from TDWR products and will be discussed next.

TDWR Based F and In Situ F

Microburst Core Penetrations



Shear Estimation from TDWR Data

Event 143 showed a substantial F-factor underestimate from the airborne algorithms when subjected to the altitude correction formula. The issue that arises is whether the altitude correction formula was incorrect in this case or whether another factor is involved. Examination of the moving map display video tape showed that the peak in situ F-factor was reached in the first third of the distance through the icon, as opposed to the center of the icon as would be expected. A plot of the along-track component of inertial winds as recorded on the aircraft during the penetration shows that the wind profile did not match the assumed profile between the peak winds. In particular, an intermediate peak in the wind was experienced about halfway through the event. This peak was nearly as large in magnitude as the peak outflow on the far side of the microburst.

The ground rules associated with this experiment prohibited changes to the ground system and led to shear estimation from information about the peak wind points. This requires an assumption about the wind profile between the peaks which, as is demonstrated here, will not always be true. In particular, pulsing microbursts may generate a microburst within a macroburst. The shear between the peak-to-peak winds may be low, but a smaller region of intense shear may exist within the outflow. This pulsing phenomena is observed both in field measurements and in TASS numerical simulation microbursts and may be very common (references 2 and 8).

The TDWR system is capable of directly locating regions of strong shear, as demonstrated by shear plots produced by MIT Lincoln Laboratory for post-flight data analysis, but the current alerting strategy does not require nor utilize this capability. Properly implemented, shear-based alerting could enhance the location of hazardous shears and improve the quantification of the hazard to aircraft.

Shear Estimation from TDWR Data

- Ground rule to avoid changing the ground systems led to estimation of shear from:
 1. Data about outflow peaks.
 2. Assumed wind profile through microburst.
- In some cases assumed wind profile may not exist, i.e. microburst within macroburst, complex flow fields.
- TDWR can produce spatial shear measurement, not currently provided to users.

Event 142 Along-Track Wind Profile and Shear Plot

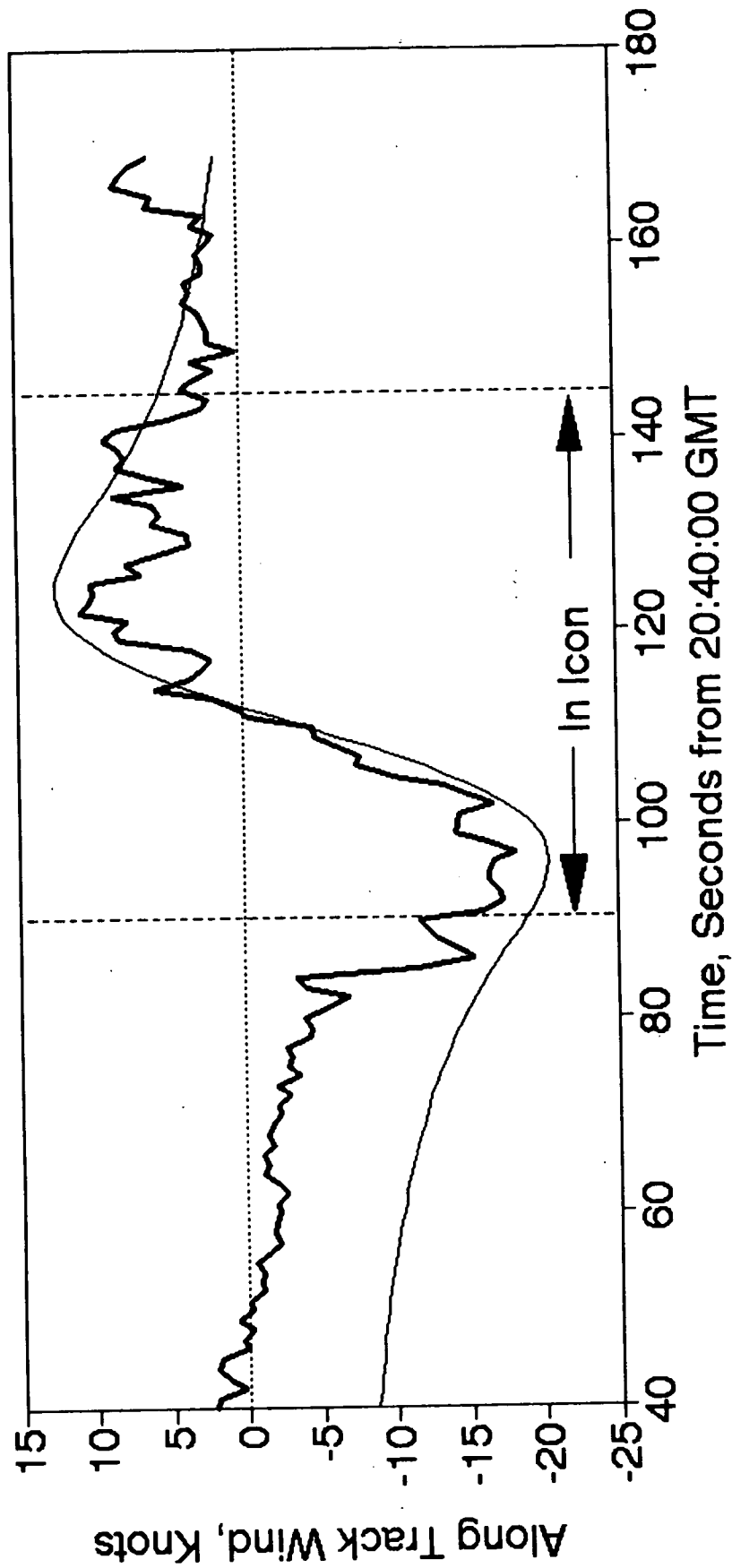
Shown in the next graph and plot are the along-track component of inertial winds experienced by the aircraft during penetration of event 142 and the corresponding TDWR shear map plot.

Superimposed on the inertial wind graph is the wind output of the Oseguera-Bowles analytical wind model. The inputs to the model are the ΔU and ΔR values provided by the TDWR for this shear. Although the in situ winds were somewhat less than predicted by the TDWR, the profile in the microburst core matches the shape of the predicted profile. Event 142 is the third data point from the left in the "TDWR Based F and In Situ F" plot shown earlier, and produced excellent agreement between predicted and actual F-factor when corrected for altitude.

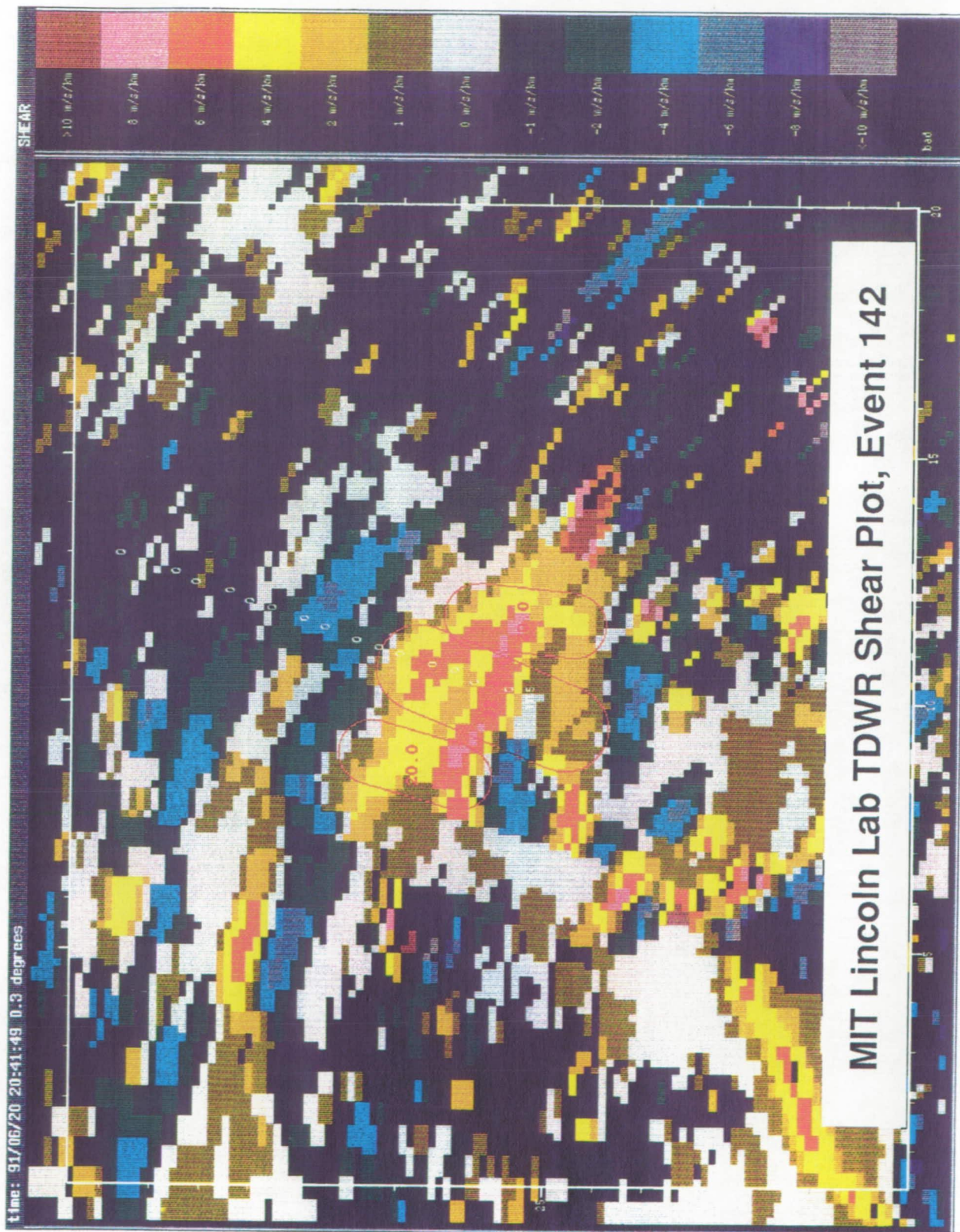
The shear (meters/second per kilometer) of event 142 and airplane flight track are shown in the plot. This plot was generated from TDWR velocity data and provided to NASA by MIT Lincoln Laboratory. The shear plot agrees with aircraft in situ data in showing the region of strong shear in the center of the microburst icon.

Along-Track Wind Profile

Event 142 Microburst Encounter



— Aircraft Wind — Model Wind



PRECEDING PAGE BLANK NOT FILMED

Event 143 Along-Track Wind Profile and Shear Plot

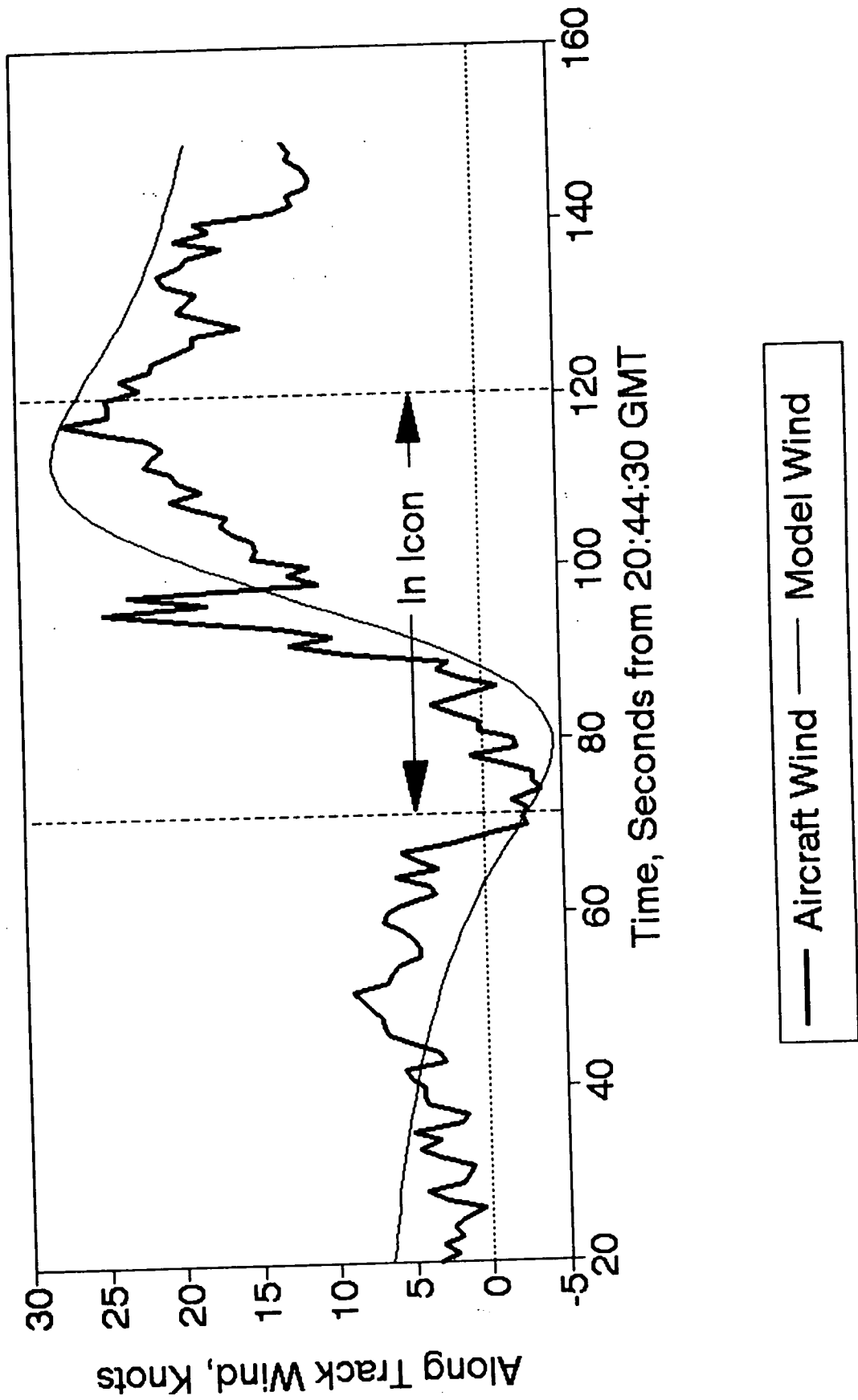
The inertial winds experienced by the aircraft in event 143 are shown followed by the corresponding TDWR shear map plot. This is the same microburst as in event 142 but penetrated about four minutes later while traveling on a reciprocal track.

The event has expanded and a new outflow surge has developed. Event 143 is the rightmost data point in the "TDWR Based F and In Situ F" plot shown earlier. The inputs to the model winds in this case are the TDWR reported ΔU (corrected by the altitude shaping function) and ΔR . Since the TDWR-reported winds significantly overestimated the winds encountered, the altitude-corrected ΔU is shown in order to more closely match the inertial wind peaks and compare the wind profiles. This plot shows a significantly greater than predicted shear in the first half of the icon penetration. This intermediate peak in the wind profile is responsible for the altitude corrected TDWR F-factor underestimate.

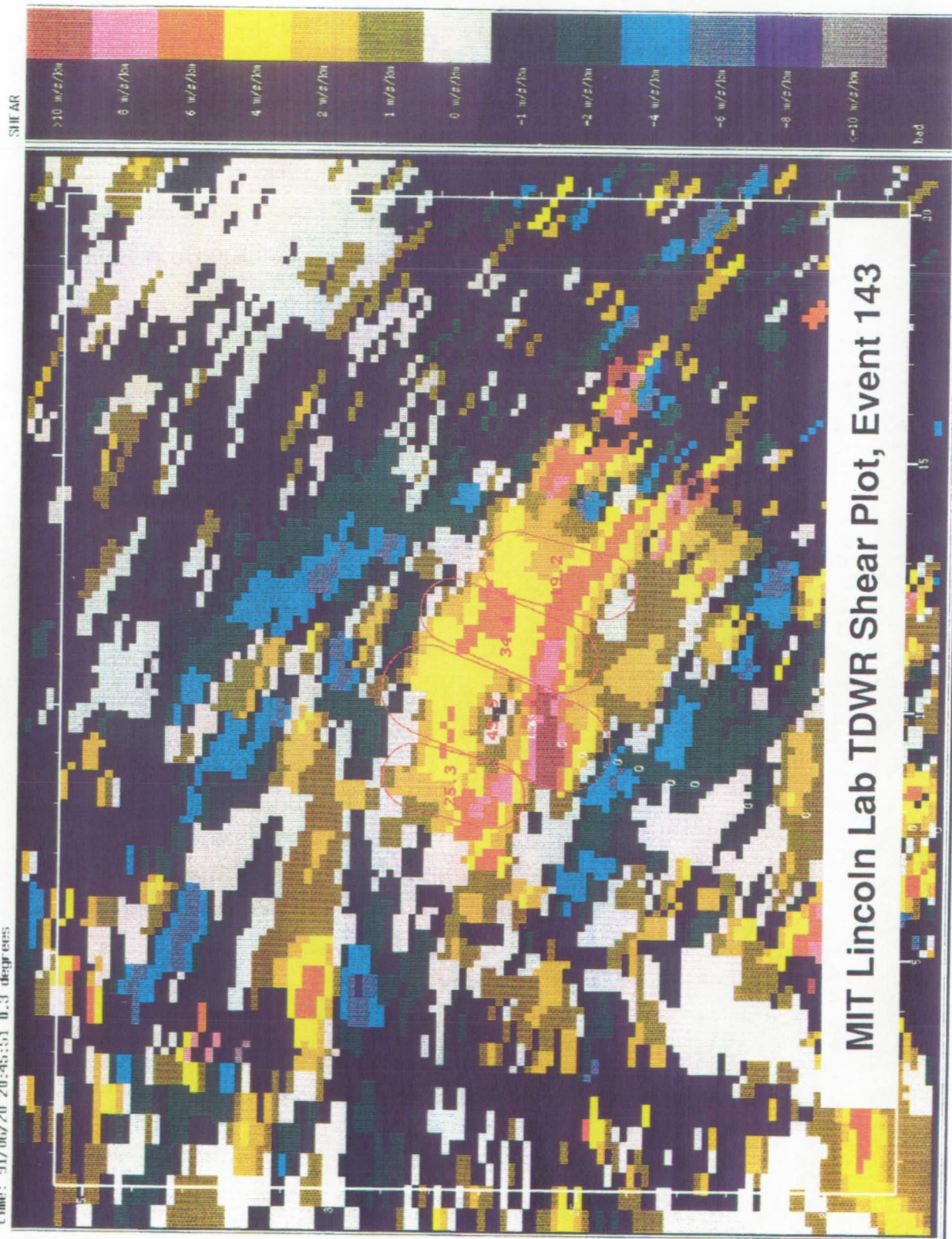
The shear in event 143 and airplane flight track are shown in the plot. The shear plot agrees with aircraft in situ data in showing the region of strong shear in the southern portion of the microburst icon. The flight data correlates very well with the shear plots and suggests that the TDWR is capable of accurately locating shear and measuring shear magnitude. Detailed data about microburst shear is available in the TDWR system but not made available in the current alerting strategy and data link system tested. Provision of this type of data to end users could better quantify the hazard and eliminate the need to estimate shear from wind measurements in airborne applications.

Along-Track Wind Profile

Event 143 Microburst Encounter



Time: 91/06/20 20:45:51 0.3 degrees



Discrete Alerting Performance

To evaluate the overall alerting performance of the TDWR data link system as tested, all 19 microburst icon penetrations were considered. Out of these 19 events, 18 produced airborne TDWR alerts while only 2 produced in situ alerts. By far the predominant factor producing this nuisance alert rate is the spatial effect of not penetrating the microburst core in most of the events. The F-factor estimation is not valid for any arbitrary path in the vicinity of the microburst. Although a separate F-factor was computed for each icon, the division of one microburst into multiple icons was such that any given icon did not necessarily contain the core of a microburst downflow. Penetration of these icons resulted in a significantly lower in situ F-factor than predicted. The second factor affecting alerting performance was the altitude effect described earlier. When adjusted for altitude, fewer icons exceed the alert threshold.

The final factor affecting alerting performance was temporal. A microburst can grow or decay in the one minute interval between updates. In the penetration of event 142 the airborne TDWR alert was received after the airplane entered the microburst event and a new data link update was received. Since this event did not exceed the in situ alert threshold the TDWR alert was counted as a nuisance alert rather than a late or missed alert. Although nuisance alerts caused by decaying events are probably inevitable with any remote or forward look sensor, the issue arises as to the possibility that an alert will be missed on a significant event. This type of missed alert requires that the F-factor increase from below threshold to a truly hazardous level between TDWR updates, and that the airplane enter the event between those updates. Insufficient data was gathered during the flight tests to estimate the frequency of this occurrence, although the potential for this situation was demonstrated in an aborted microburst approach when the TDWR F-factor estimate increased from 0.18 to 0.26 between updates.

Discrete Alerting Performance

Microburst shape penetrations:	19
Airborne TDWR alerts:	18
In Situ alerts:	2

Primary factors affecting alerting performance:

- Spatial, many icon penetrations missed microburst core.**
- Altitude difference, measurement and encounter.**
- Temporal, intensity changes between updates.**

Plans for 1992 Research Flights

Numerous changes are being made to the TDWR processing and the flight operation to enhance system performance and data opportunities during the planned 1992 wind shear flight tests. The altitude correction technique developed during this data analysis will be implemented onboard the aircraft for real-time application. Appropriate limits will be set in the altitude correction so that the algorithm functions realistically while on the ground or when the airplane is loitering at a higher altitude than would be used for penetration. On the ground the algorithm will calculate an F-factor applicable to an initial climb speed and altitude. At high altitude the F-factor will be applicable to the altitude range used for penetrations. The alert criteria will also be modified to prevent alerts during ground taxi due to microbursts near the airport as well as when airborne above 1500 feet. In 1991 numerous alerts were received while the aircraft was on the ground and microbursts were ahead (none of these alerts are included in the analysis.) In 1992 these alerts will not be given unless the airspeed is at least 60 knots, indicating that takeoff roll is in progress. Of course the microburst icons will always be displayed.

To increase the number of microburst core penetrations, the aircraft coordinator at the TDWR site will be provided with a real-time range/azimuth display of shear. This display, along with the waypoint feature of the data link, will be used to communicate the most promising locations to the airborne crew. At the suggestion of Dr. Steve Campbell of MIT Lincoln Laboratory, a "waypoint-with-shear" data link product will be tested. The concept is to make a direct one-kilometer shear estimate at the TDWR site of a region about the designated waypoint, and transmit this shear value to the aircraft for use in F-factor estimation. This will eliminate the process of estimating shear from the peaks of the wind outflow for events marked with such a waypoint. The normal F-factor processing of the microburst icons will continue to be performed for all events.

Finally, the demonstration of an "automated pilot report" capability on the data link is planned. In numerous events (ref. 2) pilots have encountered wind shear and not provided timely pilot reports to ATC. The controllers and subsequent aircraft may not have the benefit of knowing why the earlier aircraft missed the approach. The automated pilot report will downlink the status of wind shear alerts from onboard systems. In the NASA flight tests this alert information will terminate at the TDWR site and will not actually be provided to ATC.

Plans for 1992 Research Flights

- Provide real-time altitude correction.
- Modify alert criteria to prevent alerts at high altitude or during taxi.
- Provide TDWR aircraft coordinator with real-time shear map to enhance ability to hit core of microbursts.
- Evaluate F-factor estimate from direct TDWR measurement of 1 kilometer shear in vicinity of waypoint (MIT Lincoln Lab suggestion).
- Downlink "automatic pilot report" from aircraft to NASA ground station.

Summary

This experiment demonstrated the feasibility of transmitting ground-based wind shear information to an aircraft via data link, processing that information on the aircraft to estimate the wind shear hazard index (F-factor), then providing the information on a moving map display for operational use. In the limited number of microburst core penetrations experienced, the estimated F-factor compared very favorably to the actual in situ F-factor. More cases are needed to show statistical significance.

As the current system was implemented, the executive level alerting performance was inadequate due to an excessive number of nuisance alerts. These nuisance alerts were due to inadequate data being available to the alerting process to precisely locate the region of strong shear, and the aircraft trajectory not intersecting those regions. The information required to minimize this limitation is resident within the TDWR system but not planned as an output product of production TDWR systems. More complete use of the ground system capabilities may greatly improve the utility of the TDWR microburst information to the end users.

References

1. Federal Aviation Administration: Windshear Training Aid, Example Windshear Training Program, February 1987.
2. Schlickemaier, Herbert W.: Windshear Case Study: Denver, Colorado, July 11, 1988, DOT/FAA/DS-89/19, November 1989.
3. Bowles, Roland L.: Reducing Windshear Risk Through Airborne Systems Technology, Paper Presented at the 17th Congress of the International Council of the Aeronautical Sciences, Stockholm, Sweden, September 9-14, 1990.
4. Oseguera, Rosa M. and Bowles, Roland L.: A Simple, Analytic 3-Dimensional Downburst Model Based on Boundary Layer Stagnation Flow, NASA TM-100632, July 1988.
5. Vicroy, Dan D.: A Simple, Analytical, Axisymmetric Microburst Model for Down draft Estimation, NASA TM-104053, DOT/FAA/RD-91/10, February, 1991.
6. Proctor, F. H.: The Terminal Area Simulation System, Volume 1: Theoretical Formulation, NASA CR 4046, 1987.
7. Proctor, F. H.: The Terminal Area Simulation System, Volume 2: Verification Experiments, NASA CR 4047, 1987.
8. Proctor, F. H. and Bowles, R. L.: Three-Dimensional Simulation of the Denver 11 July, 1988 Microburst-Producing Storm, Accepted for Publication in Meteorology and Atmospheric Physics.

Summary

- Demonstrated feasibility of data link and airborne use of TDWR microburst information.
- F-factor estimation from TDWR data reasonable in very limited number of microburst core penetrations.
- Alerting performance inadequate "as is" for executive level crew warning. Improved shear location required.
- Results suggest that full capabilities of ground system should be used to provide shear data to users, airborne F-factor estimation may be improved given data link of shear values.
- Altitude correction required for radar data at research speeds.

Air/Ground Wind Shear Information Integration - Flight Test Results

Questions and Answers

Q: Norm Crabill (Aero Space Consultants) - The shape of these icons sort of bothers me a little bit. I was wondering if the racetrack pattern has it's long axis along the radius vector from the Doppler. Is that correct?

A: Dave Hinton (NASA Langley) - In these cases it did.

Q: Norm Crabill (Aero Space Consultants) - So that is a limitation of the single site ground determination of the velocity field. If you were making an approach to a runway that was at right angles to that, you are not going to get a lot of information. What have you concluded about TDWR siting relative to the runway? How do you use this information to help you site the TDWR now that they are being deployed?

A: Dave Hinton (NASA Langley) - We did not try in our analysis to do that. Our ground rules were not to change the TDWR system, so we did not look into siting issues per say. There are some very good historical reasons for why those shapes are the way they are, and I'll let Steve Cambell cover that.

A: Steve Cambell (MIT Lincoln Laboratory) - That is a good point Norm. Basically, what we originally started out with was a big region that we identified as a microburst. Then we decided to do a better job of isolating where the strong velocity change was by dividing this shape up in the azimuthal direction. I will talk a little bit about this on Thursday, and about some of the ideas we have for doing a better job of localizing the region of peak shear. But you make a very good point, and that is one of the things we are currently looking at; how we can improve that shape representation.

Q: Norm Crabill (Aero Space Consultants) - What about the question of TDWR siting, and some practical situations?

A: Steve Cambell (MIT Lincoln Laboratory) - That is another issue too. We have done extensive testing where we use dual Doppler Radars to determine the shear for approach or departure paths and we have been able to show that we can do a pretty good job of estimating the shear or the change in velocity along the flight path with a single TDWR. The deployed TDWR's will be deployed in conjunction with the enhanced LLWAS system, which is a surface base anemometer system. If you have a situation with a highly asymmetric microburst then the LLWAS system should be able to detect it. Now we have also studied this issue of how likely is it that the outflow would be highly asymmetric. Generally, in the South East they are not very asymmetric. You do see asymmetric ones in places like Denver though; so in that case we think that the surface sensor would be a fail safe for making sure we detect the strong shear of any region perpendicular to the radar beam.

Norm Crabill (Aero Space Consultants) - Well of course the LLWAS alarm at Dallas was after the fact.

Steve Cambell (MIT Lincoln Laboratory) - I should point out that we are integrating with the enhanced LLWAS system. The current six station LLWAS is not really adequate for microburst detection. The enhanced LLWAS system have something like a 13 to 16 stations. It's a much more extensive LLWAS network which covers most of the approach and departure paths. It also has a different algorithm than that used in the current Phase I LLWAS. We have been able to show that when you integrate TDWR and the enhance LLWAS there is a very high probability of detecting a hazardous wind shear along any arbitrary path. So we are very confident. Both systems work very well and when you combine the two you have an extremely reliable system. We have been able to verify that against our dual Doppler measurements, and other measurements.

Norm Crabill (Aero Space Consultants) - Dual Doppler is handy, but you won't have it at those forty-six sites.

Steve Cambell (MIT Lincoln Laboratory) - The dual Doppler is for the purpose of generating the truth so we know what actually happened. We are validating our single Doppler with the surface sensors against dual Doppler.

Q: Sam Shirck (Continental Airlines) - With respect to the TDWR results, is it possible that in the future airborne radar systems may data link their view of the wind shear situations to the ground based TDWR, since the airborne systems have a better viewing angle and a much enhanced update rate?

A: Dave Hinton (NASA Langley) - I think it certainly would be possible to down link the data to the ground base system. The primary obstacle standing in the way is going to be the lack of a system driver for doing that. Within the context of the program we are doing, we have a charter not to change the ground system. Now, if there is a system requirement to do that, it could possibly be done. There are a couple of technical issues involved; one is the data rate that would be required to get that amount of information down, and secondly a lot of dual and triple Doppler analysis' have been done of numerous events and that can take, I would expect, a significant amount of post processing. To do the triple Doppler analysis in real time would probably be a very large computational effort. So it is a question of a system driver plus the effort involved to do it.

Jim Evans (MIT) - Where the ground systems are going in the relatively near future is toward what is called integrated terminal weather systems, which in fact tries to integrate information from all the available ground and airborne systems. We are already talking about ingesting winds and temperature data out of planes. I don't think it is a big issue to transmit that information down over a Mode S data link. I think what you would do is that you would formulate it as a message, it would then come up as an additional piece of alert information that could be passed along in much the same style and thereby provided automatically to succeeding planes. I do not think you would have to get into dual or triple Doppler analysis.

Dave Hinton (NASA Langley) - Obviously, you could operate such a system at various levels, triple Doppler being the most complex. Another way would be to simply look at alert regions and use those in some manner. Which Jim, if I understand, is what you are referring to.

Jim Evans (MIT) - I think I would try that for starters, because I think the others would be fairly complicated. One of the issues that you would get into immediately on dual or triple Doppler, with an airborne weather radar at X-band, would be the whole question about how well you had unfolded your velocities. You don't have to unfold absolutely to get shear regions, but you could be off by a whole fold without any trouble at all.

Q: Norm Crabill (Aero Space Consultants) - I would like to revisit the question of TDWR siting. I don't know to whom I should address the question, but if you have an airport like O'Hare with intersecting runways, where do you put the terminal Doppler radar?

A: Jim Evans (MIT) - It is fairly simple. What we have used as the criteria in siting the TDWR is to look at the runway usage during circumstances when there is weather, and try to line up the TDWR to look along those runways. We then do an adjustment in cases where there are split runway regions. O'Hare is certainly the ugliest case one can point to. In most of the others, it is a fairly reasonable site. We have tried to consider looking up the runways the maximum amount of the time consistent with when the weather was going to be present. It is a lively task of course, in a place like Leguardia, just trying to find a place to put the radar. I think we have been very successful.

Q: Norm Crabill (Aero Space Consultants) - If you have intersecting runways and low weather, and conditions conducive to microbursts, is there any intent to restrict the operations to the runway that is favored by the terminal Doppler weather radar?

A: Jim Evans (MIT) - Again, we don't see the need to do that. What we have been trying to do is assess the performance by taking dual Doppler measurements of the winds along the runway. There is certainly ample reason to believe that dual Doppler does a very good job of estimating the winds. What we do is we look at the winds along the runways no matter what there orientation is, whether the TDWR has a good look angle or a bad look angle, and assess the accuracy of the warnings. For example, if the actual wind along the center line of the path had more than a 30 knot wind change over a suitably small distance we would check to see if we are issuing an alert or not. It is a very high probability that we do, no matter what the orientation of the runway is. That is what we have seen for Denver, Kansas City, and Orlando. In that process we use runways that we have lousy look angles to. The reason that we know what the winds are is because we have dual and in some cases triple Doppler data to tell us what the winds are. That is the way we are trying to assess it. Are we giving it a timely warning for that runway? Sure, it is a little better on the ones that you have a nicer look angle, but it doesn't mean that you are not detecting, very reliably, all the ones at any angle you want to imagine a runway to be.

Norm Crabill (Aero Space Consultants) - Someone keeps bringing up in this discussion, dual Doppler. My understanding is that there is only one TDWR per airport.

Jim Evans (MIT) - Let me again make it clear what is being done. From a research basis, we go to airports with two and three radars and we evaluate quantitatively our performance. We score a single radar's ability to give accurate warnings on all the runways. You say, how did you know what was there. The reason we know what was there is that we had dual or triple Doppler. Now when we go out in the actual operational system there is only one radar at the airport. But, we

believe we know what its performance is going to be. This summer will be our seventh year of testing with dual Doppler data. We think by doing this testing over a wide variety of airports and geographic regions and having synthetic runways as well as real runways, we have a very good handle on the performance of the system. That is the rule. It isn't that a operational system has dual or triple Doppler, it is that we have done careful experiments with dual and triple Doppler and supporting mesonet systems. Is there a microburst the radar can't measure. We have gone out and tried to address that number in this phase. That is what we are quoting from and we hope the past is a prediction of the future. Of course, the world may change. This is one of the most carefully tested systems that I know of.

Q: Norm Crabill (Aero Space Consultants) - Yes, I agree there has been a lot of testing. What has been the result for Chicago where will the radar be located?

A: Jim Evans (MIT) - We have not done dual Doppler testing yet at O'Hare. The radar will be almost due south of O'Hare. There is an ARSR site down there it is roughly to the east of Midway. It is a location that will give a good look at both Midway and O'Hare.

199 3010406
42P

N93-19595

Session I. NASA Flight Tests

Doppler Radar Results

E. Bracalente, NASA Langley Research Center

PRECEDING PAGE BLANK NOT FILMED



Doppler Radar Results

E. Bracalente, NASA LaRC

Fourth Combined Manufacturers' & Technologists' Airborne Wind Shear Review Meeting 4-14,16-92

NASA Flight Tests Airborne Doppler Radar Results

Presentation Outline

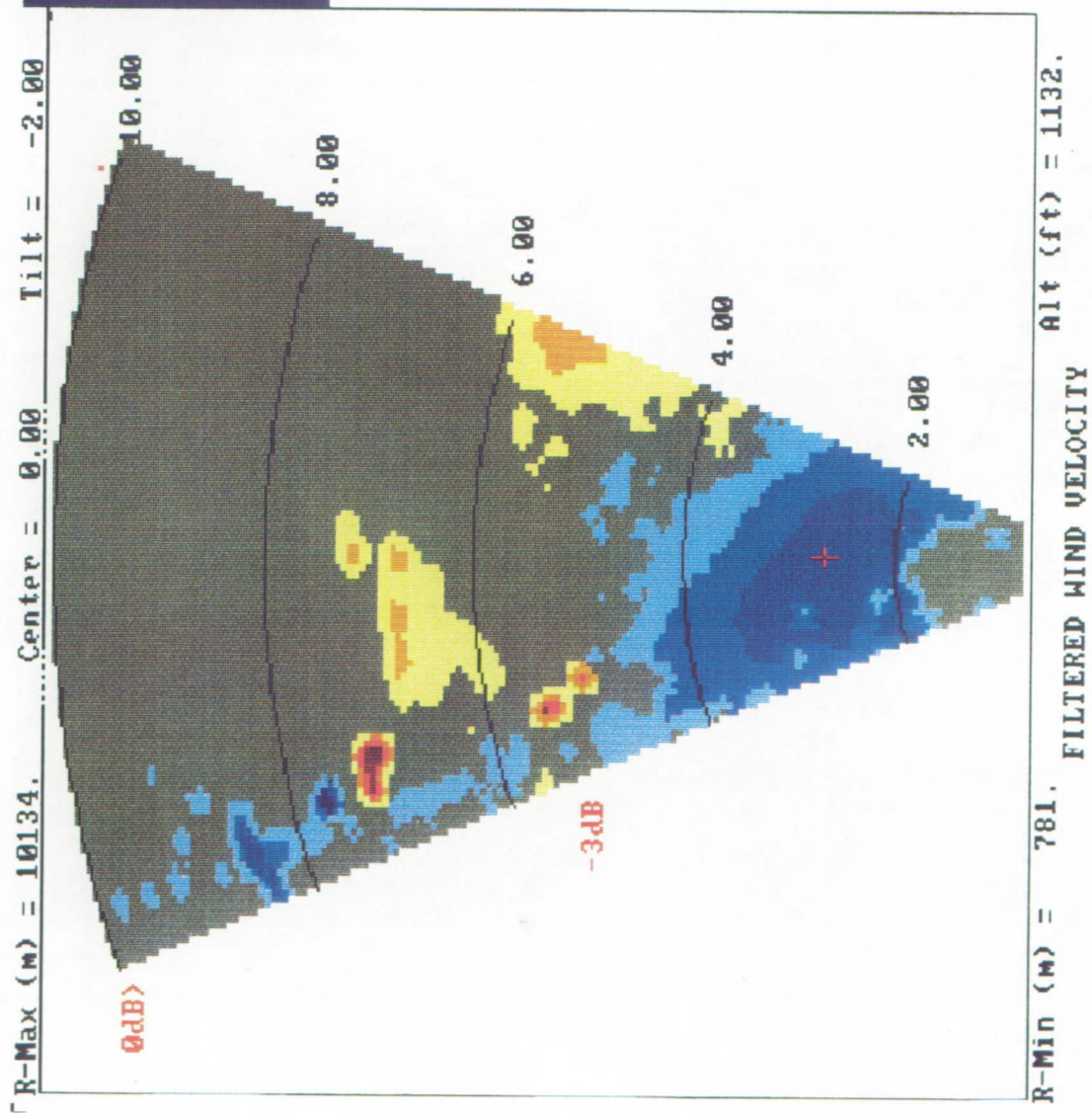
- 1. Summary of Radar Flight Data Collected**
- 2. Video of Combined Aft Cockpit, Nose Camera, & Radar Hazard Displays**
- 3. Comparison of Airborne Radar F-factor measurements with In Situ and TDWR F-factors for Some sample Events**
- 4. Summary Wind Shear Detection Performance**

1991 RADAR FLIGHT DATA COLLECTED

FLIGHT TESTS	TOTAL DATA RUNS	CLUTTER RUNS	WEATHER RUNS	RAW I&Q DATA	PROCESSED RADAR DATA
LOCAL	147	105	10	1.85E+10	1.76E+09
PHILA	46	46	0	5.31E+09	5.06E+08
ORLANDO	124	15	109	1.41E+10	1.34E+09
DENVER	99	62	37	1.27E+10	1.21E+09
TOTAL	416	228	156	5.06E+10	4.82E+09

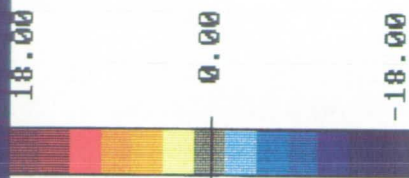
EVENTS SHOWN IN THE FOLLOWING RADAR AZIMUTH SCANS

ORLANDO, JUNE 20, 1991				
DISPLAY NO	EVENT	ANTENNA TILT ANGLE, deg	PARAMETER DISPLAYED	AVERAGE F-FACTOR
1	142	-2	VELOCITY	.1
2	142	-2	F-FACTOR	
3	143	-2	VELOCITY	.16
4	143	-2	F-FACTOR	
5	144	-1	VELOCITY	.1
6	144	-1	F-FACTOR	
7	148	-3	F-FACTOR	.13
8	149	-1	F-FACTOR	.14
9	150	AUTO	F-FACTOR	.06
DENVER, JULY 10, 1991				
10	175	0	VELOCITY	.11
11	175	0	F-FACTOR	



#CURSOR#

LAT 28.5974
 LON -81.2117
 RG 2710.
 AZ 0.
 TILT -7.32
 FRM 1009.
 BIN 14.
 VAL -10.33



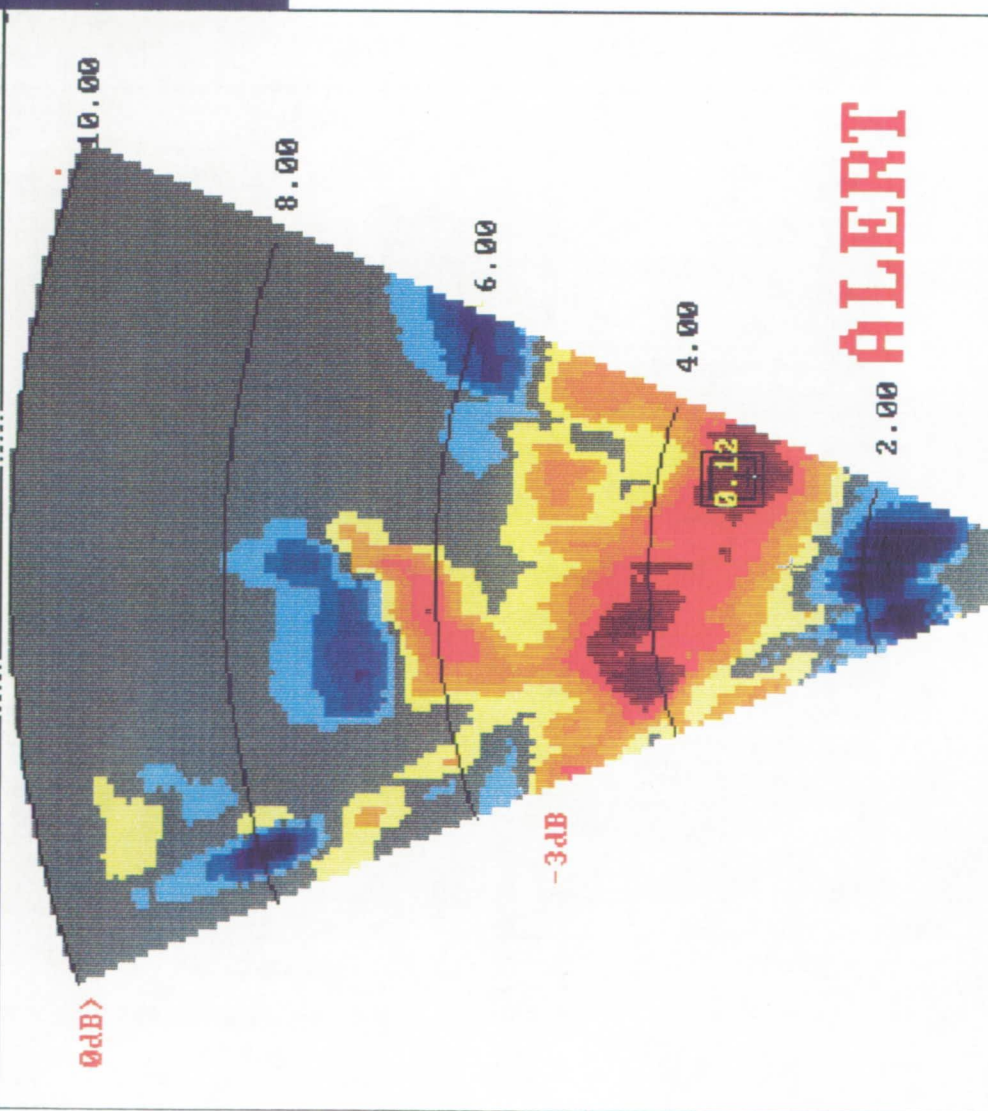
DATE 6:20:91

TIME 20:41:15

FRAME # 1050

ORIGINAL PAGE
 COLOR PHOTOGRAPH

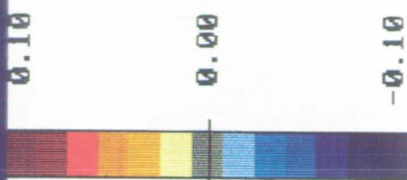
R-Max (m) = 10134. Center = 0.00 Tilt = -2.00



R-Min (m) = 781. TOTAL 1000m F-FACTOR Alt (ft) = 1132.

CURSOR

LAI	28.5957
LON	-81.2203
RG	3211.
AZ	14.
TILT	-6.17
FRM	1037.
BIN	18.
VAL	0.15



DATE 6:20:91

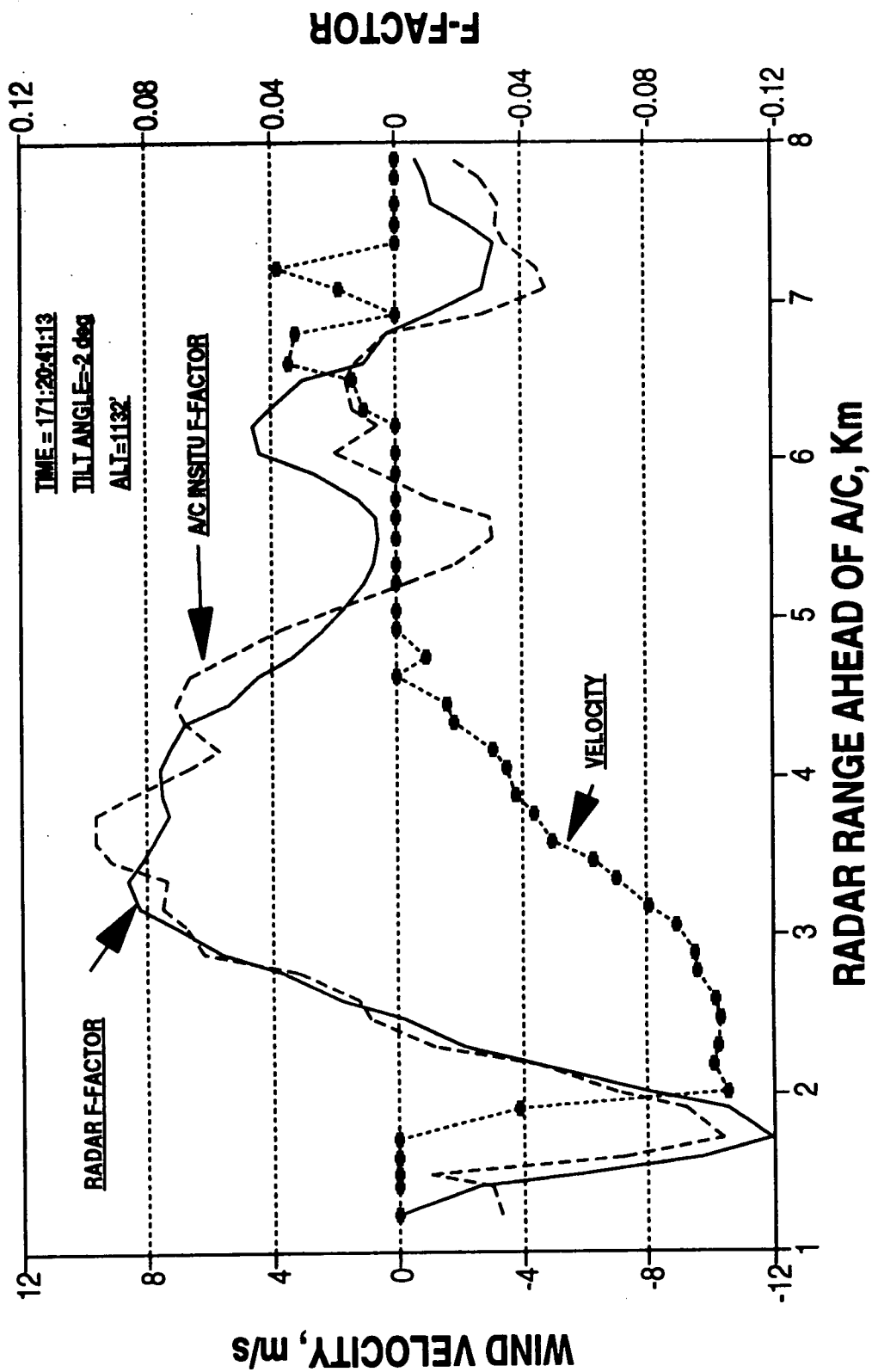
TIME 20:41:15

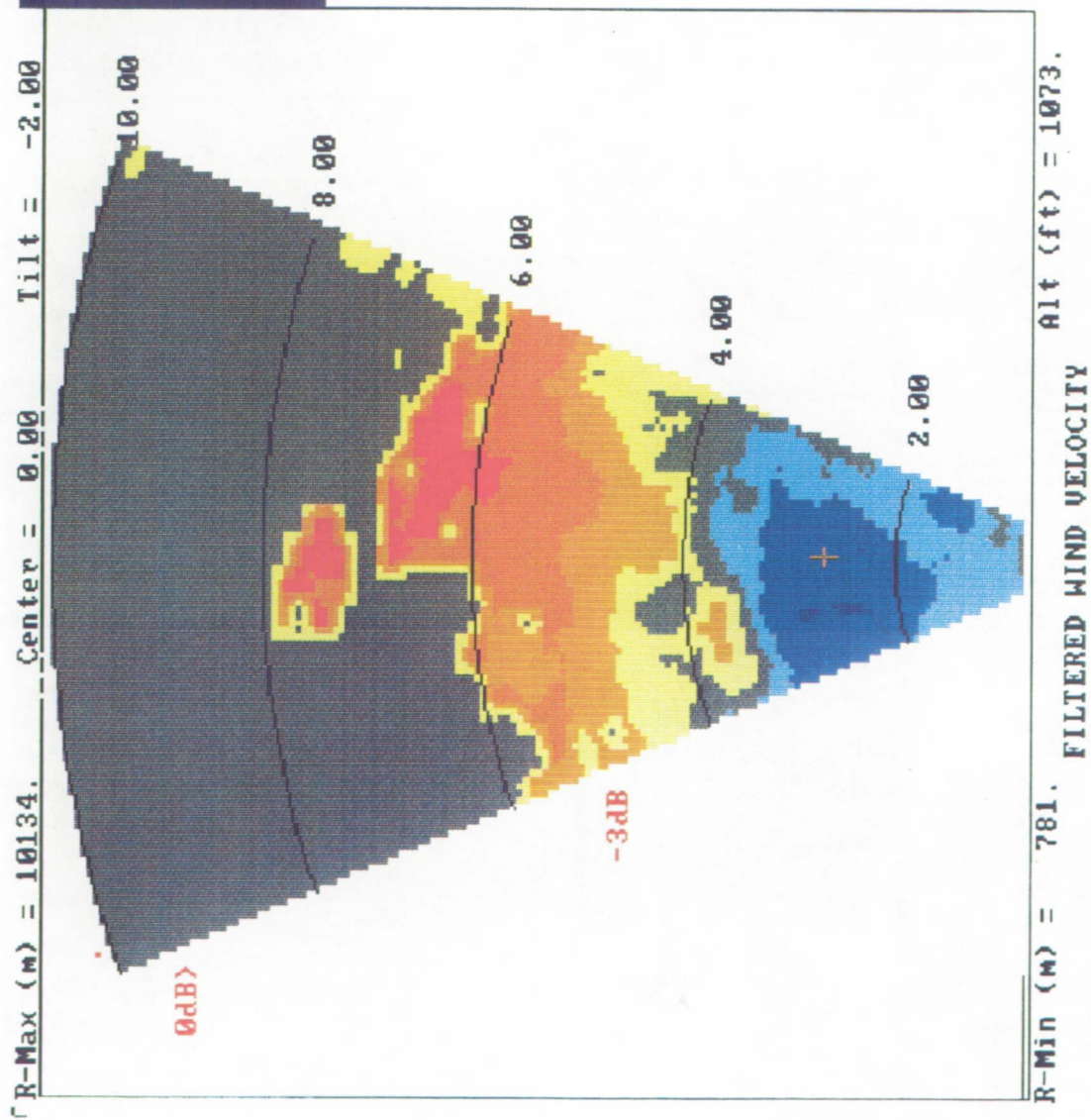
FRAME # 1050

ORIGINAL PAGE
COLOR PHOTOGRAPH

RADAR WIND SPEED & 1KM AVE F-FACTOR & INSITU F-FAC: EVENT 142

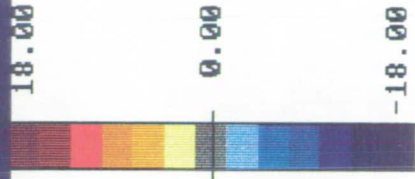
0 & +/- 2 deg AZ RNG LINE AVE





CURSOR

LAT	28.5715
LON	-81.2319
RG	2710.
AZ	0.
TILT	-6.93
FRM	1386.
BIN	14.
VAL	-6.28

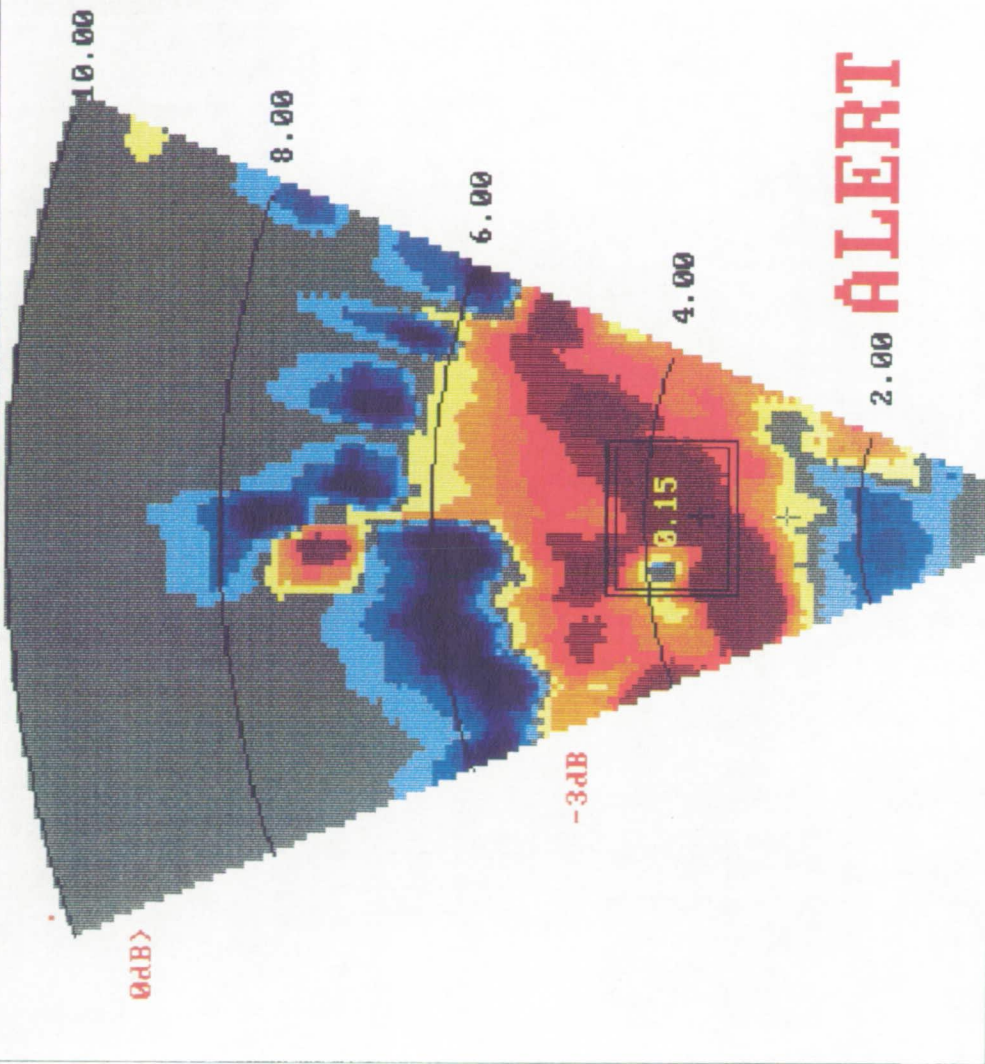


DATE 6:20:91

TIME 20:45:32

FRAME # 1428

R-Max (m) = 10134. Center = 0.00 Tilt = -2.00



R-Min (m) = 781. TOTAL 1000m F-FACTOR Alt (ft) = 1073.

CURSOR

LAI 28.5786
LON -81.2295
RG 3529.
AZ 0
TILT -5.32
FRM 1386.
BIN 20.
VAL 0.16



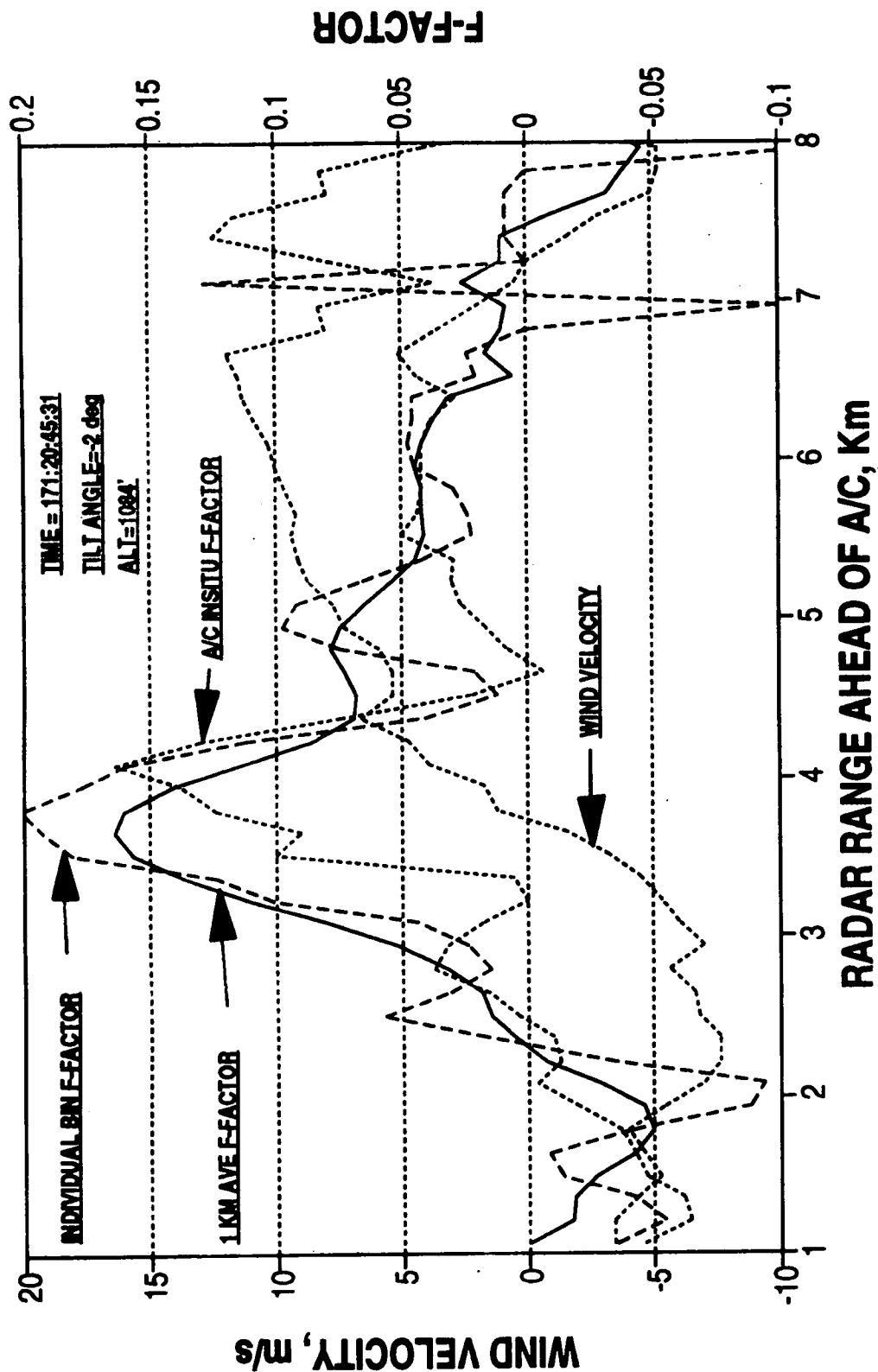
DATE 6:20:91

TIME 20:45:32

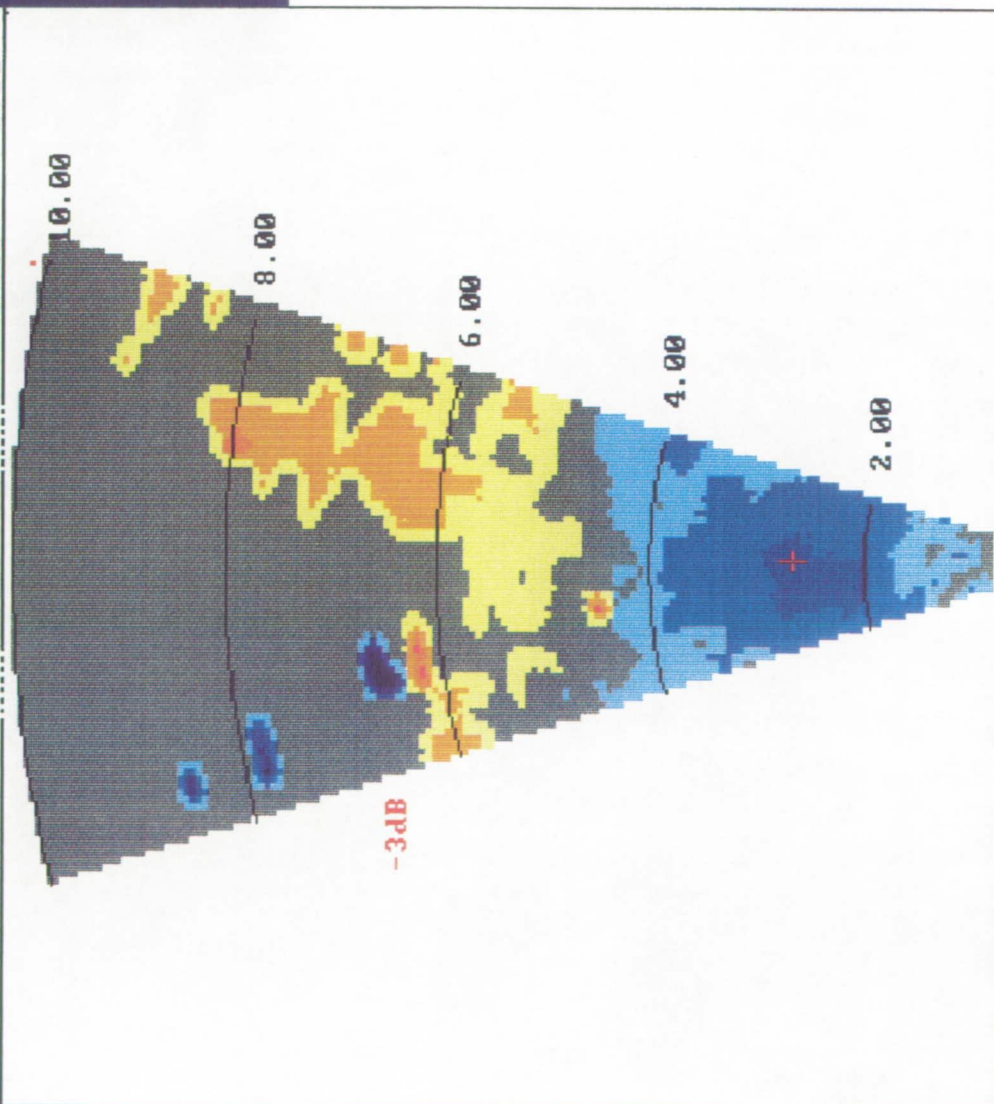
FRAME # 1428

RADAR MEASURED WIND SPEED & F-FACTORS & A/C INSITU F-FACTOR: EVENT 143

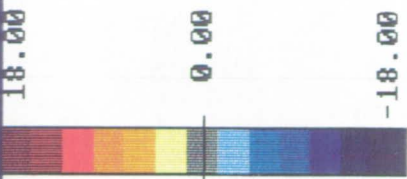
0 & ± 2 deg AZ RING LINE AVE



R-Max (m) = 10134. Center = 0.00 Tilt = -1.00



#CURSOR*
 LAT 28.5935
 LON -81.2089
 RG 2710.
 AZ 0.
 TILT -6.81
 FRM 2597.
 BIN 4.
 VAL -9.37



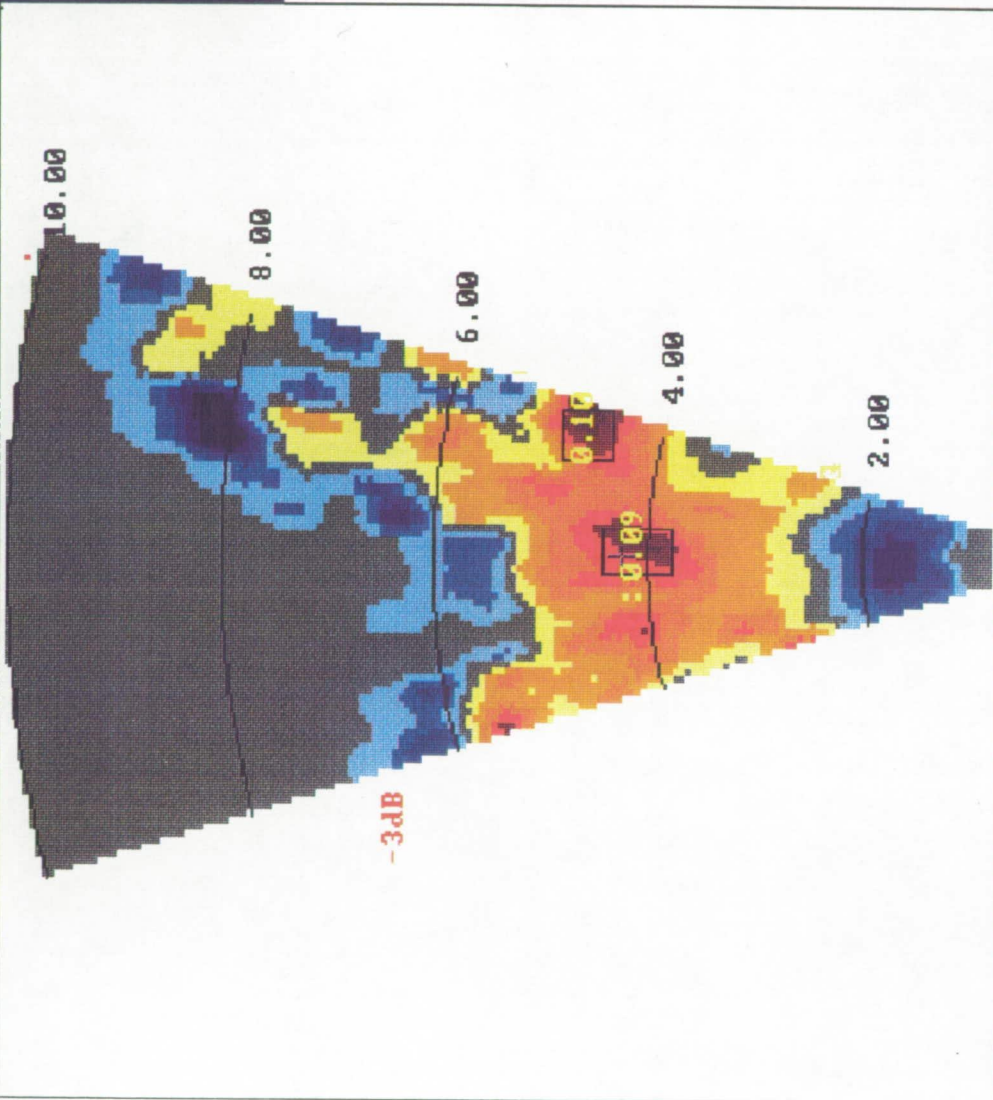
DATE 6:20:91

TIME 20:51:33

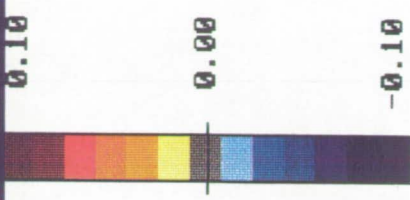
FRAME # 2627

R-Min (m) = 781. FILTERED WIND VELOCITY Alt (ft) = 1054.

R-Max (m) = 10134. Center = 0.00 Tilt = -1.00



CURSOR
 LAT 28.5
 LON -81.2123
 RG 4289.
 AZ 0.
 TILT -4.30
 FRM 2597.
 BIN 25.
 VAL 0.09



DATE 6:20:91

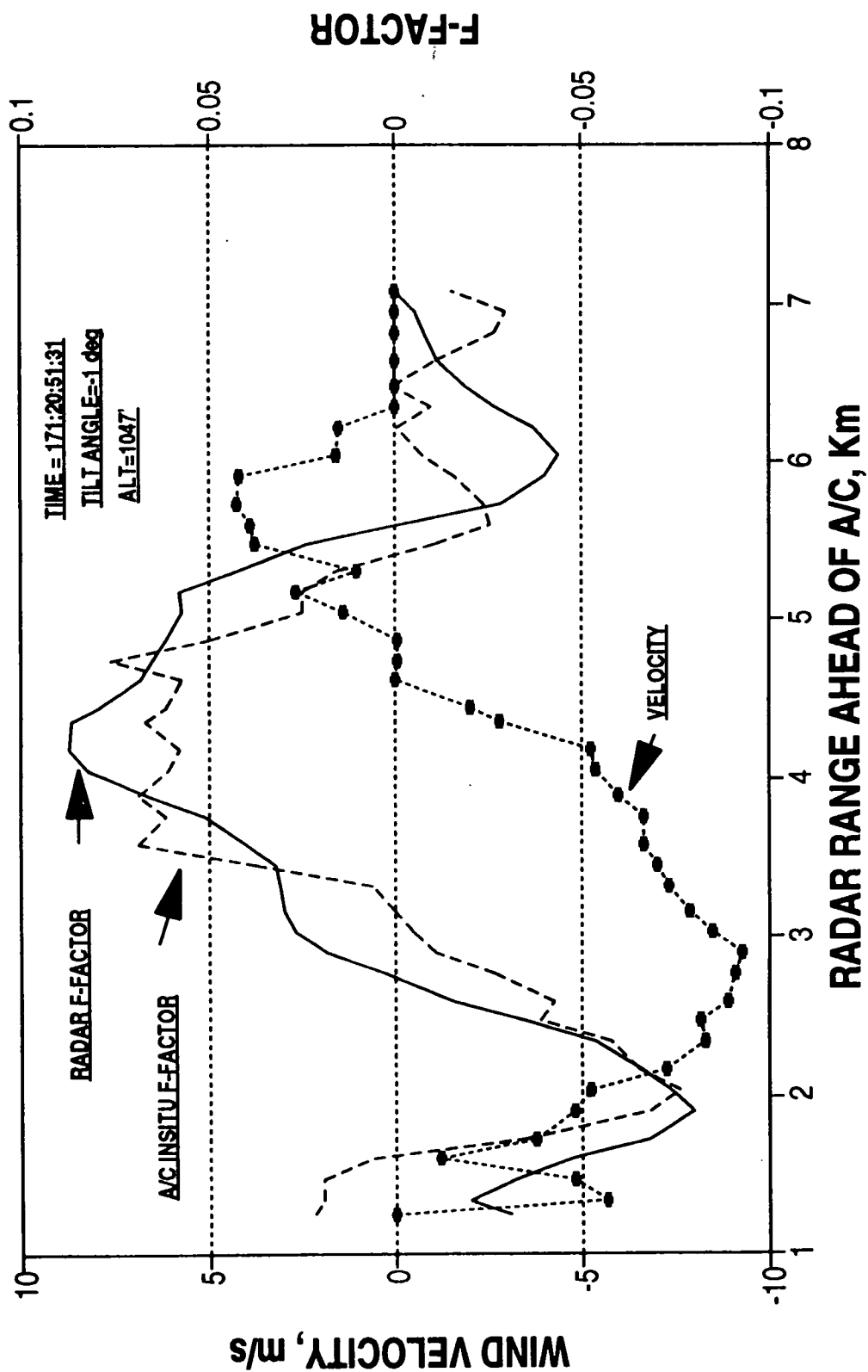
TIME 20:51:33

FRAME # 2627

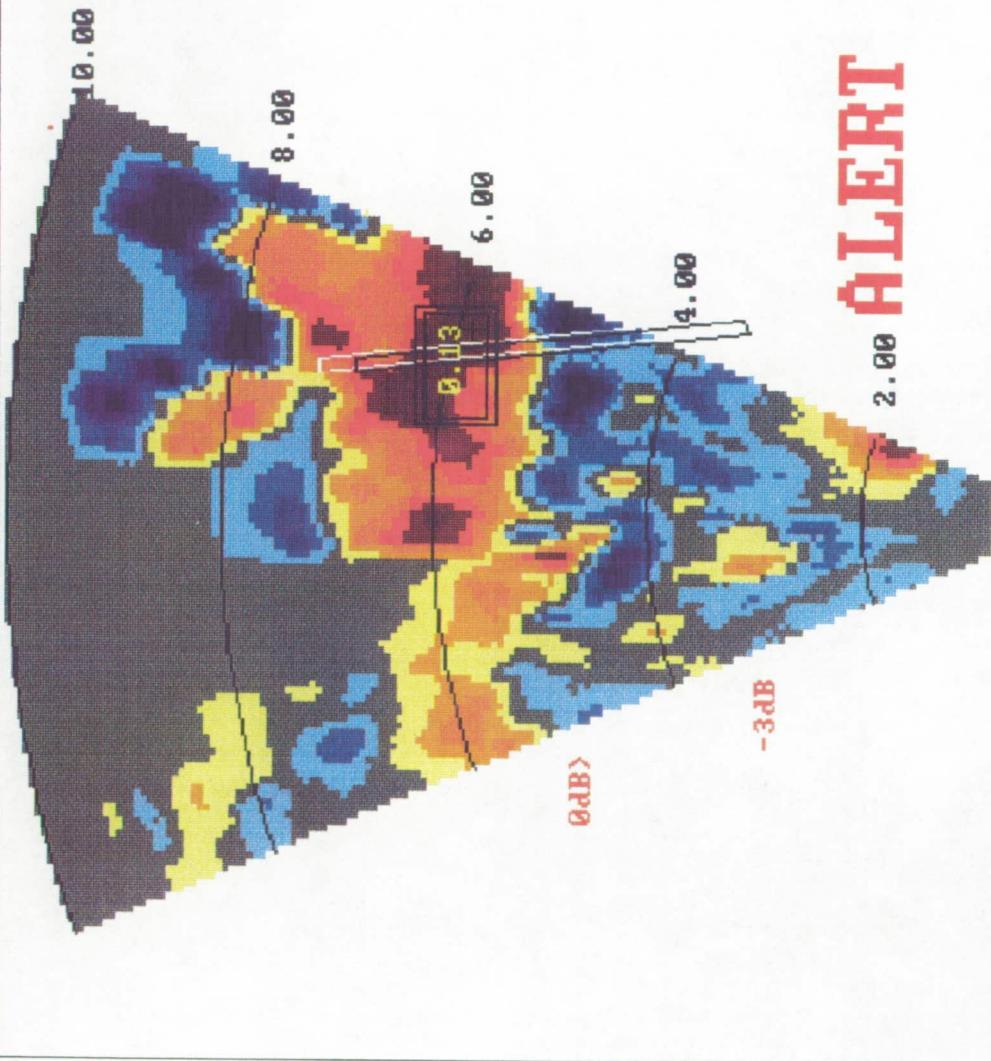
R-Min (m) = 781. TOTAL 1000m F-FACTOR Alt (ft) = 1054.

RADAR WIND SPEED & 1KM ALONG RNG AVE F-FAC, & A/C INSITU F-FAC: EVENT 144

0 & +/-2 deg AZ RNG LINE AVE



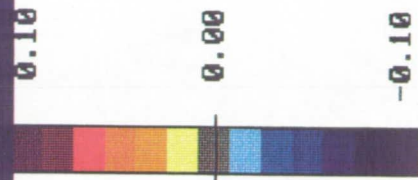
R-Max (m) = 10134. Center = 0.00 Tilt = -3.00



R-Min (m) = 781. TOTAL 1000m F-FACTOR Alt (ft) = 863.

CURSOR

LAT 28.4182
LON -81.3057
RG 5906.
AZ 15.
TILT -2.55
FRM 688.
BIN 37.
VAL 0.13

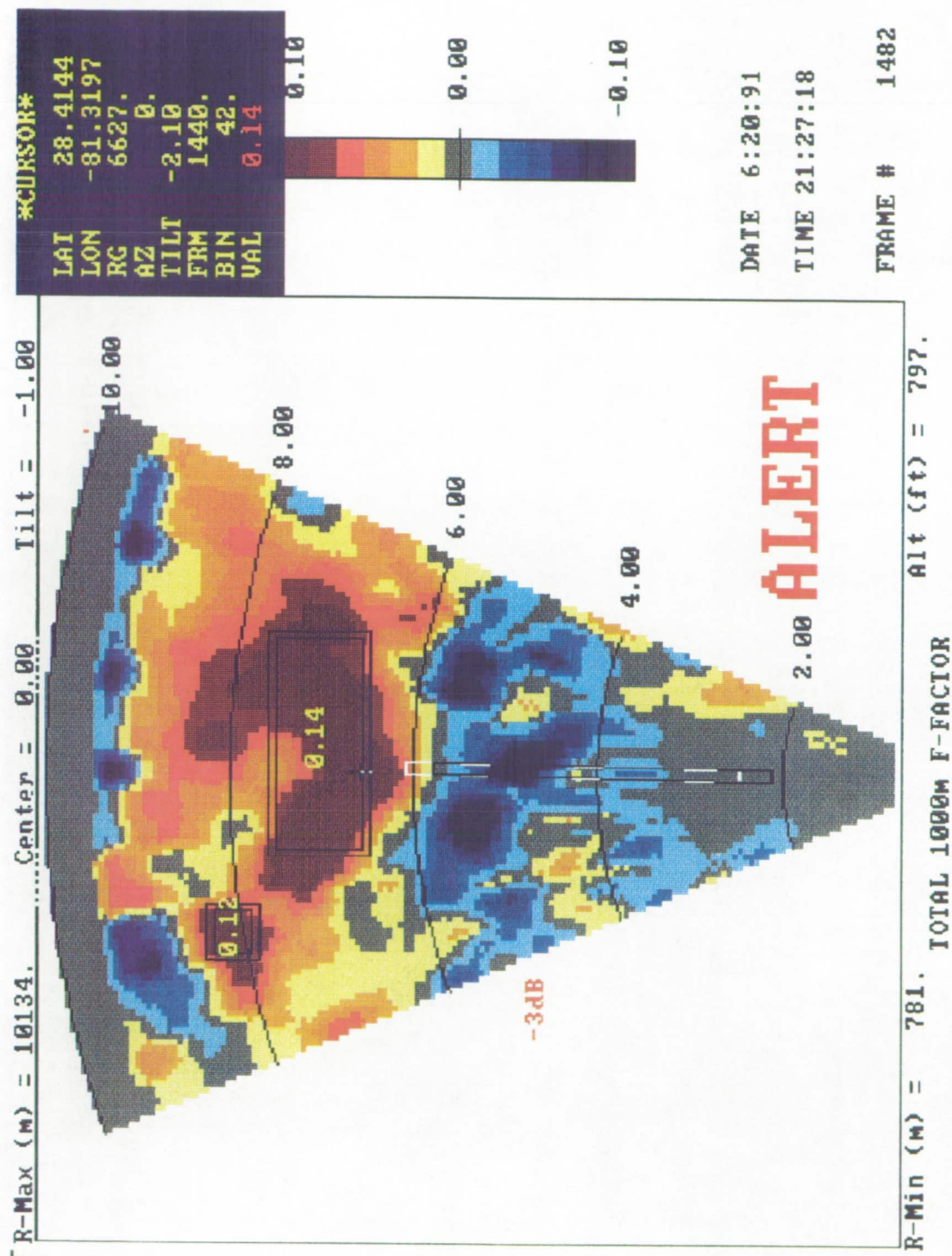


DATE 6:20:91

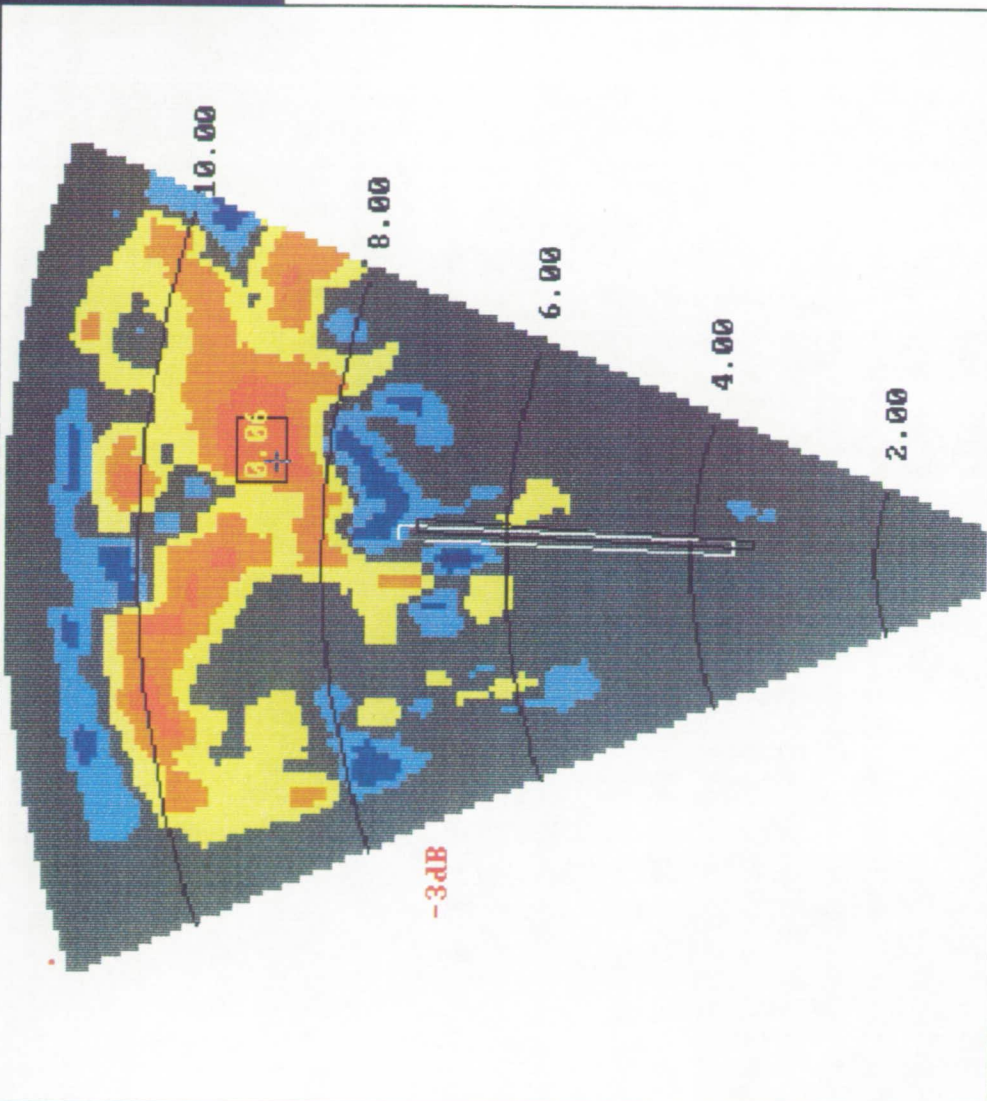
TIME 21:20:31

FRAME # 698

ORIGINAL PAGE
COLOR PHOTOGRAPH



R-Max (m) = 11573. Center = 0.00 Tilt = 0.00



R-Min (m) = 781. TOTAL 1000m F-FACTOR Alt (ft) = 727.

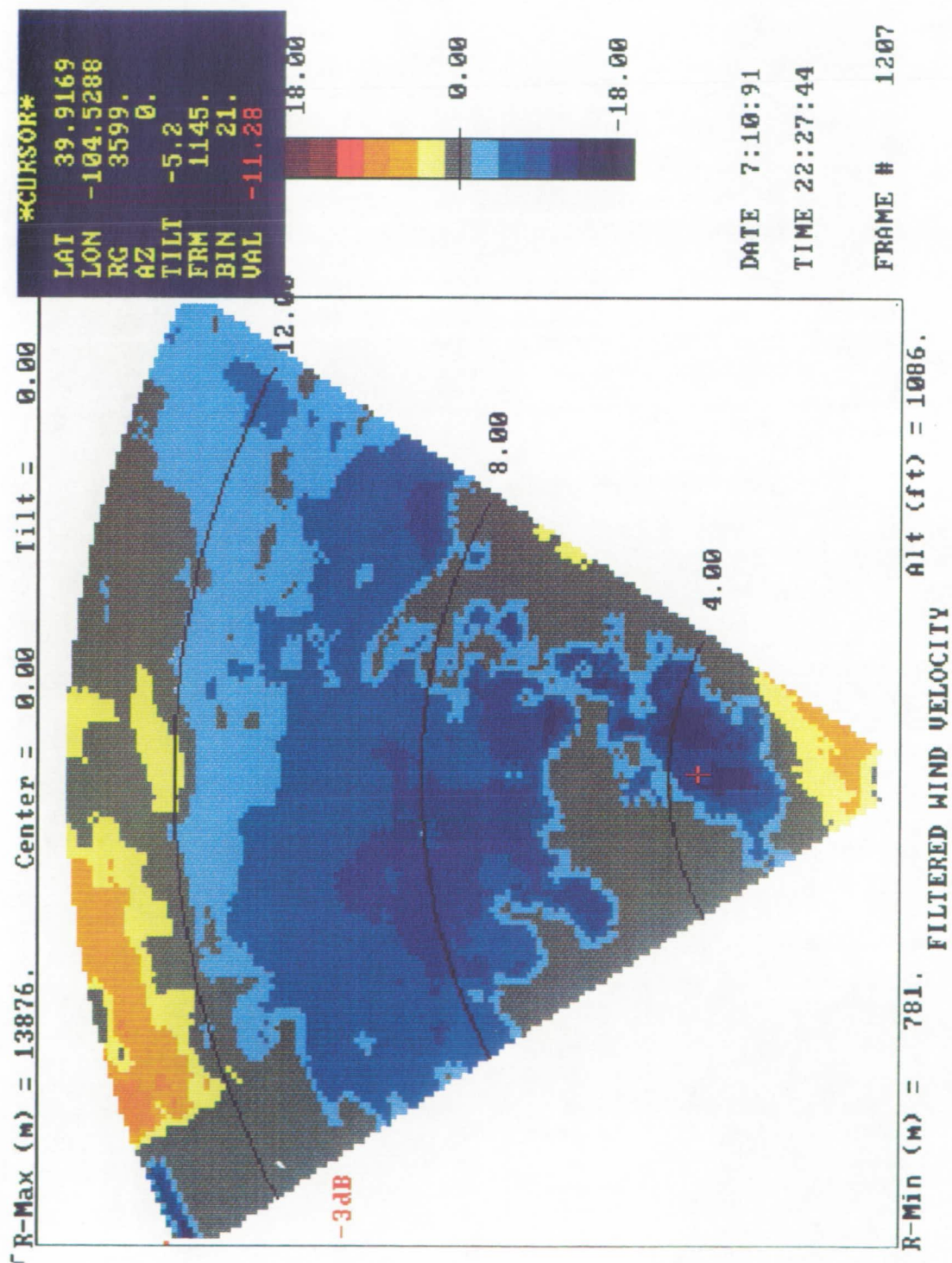
CURSOR
 LAT 28.4076
 LON -81.3319
 RG 8590.
 AZ 6.
 TILT -1.48
 FRM 3881.
 BIN 55.
 VAL 0.07



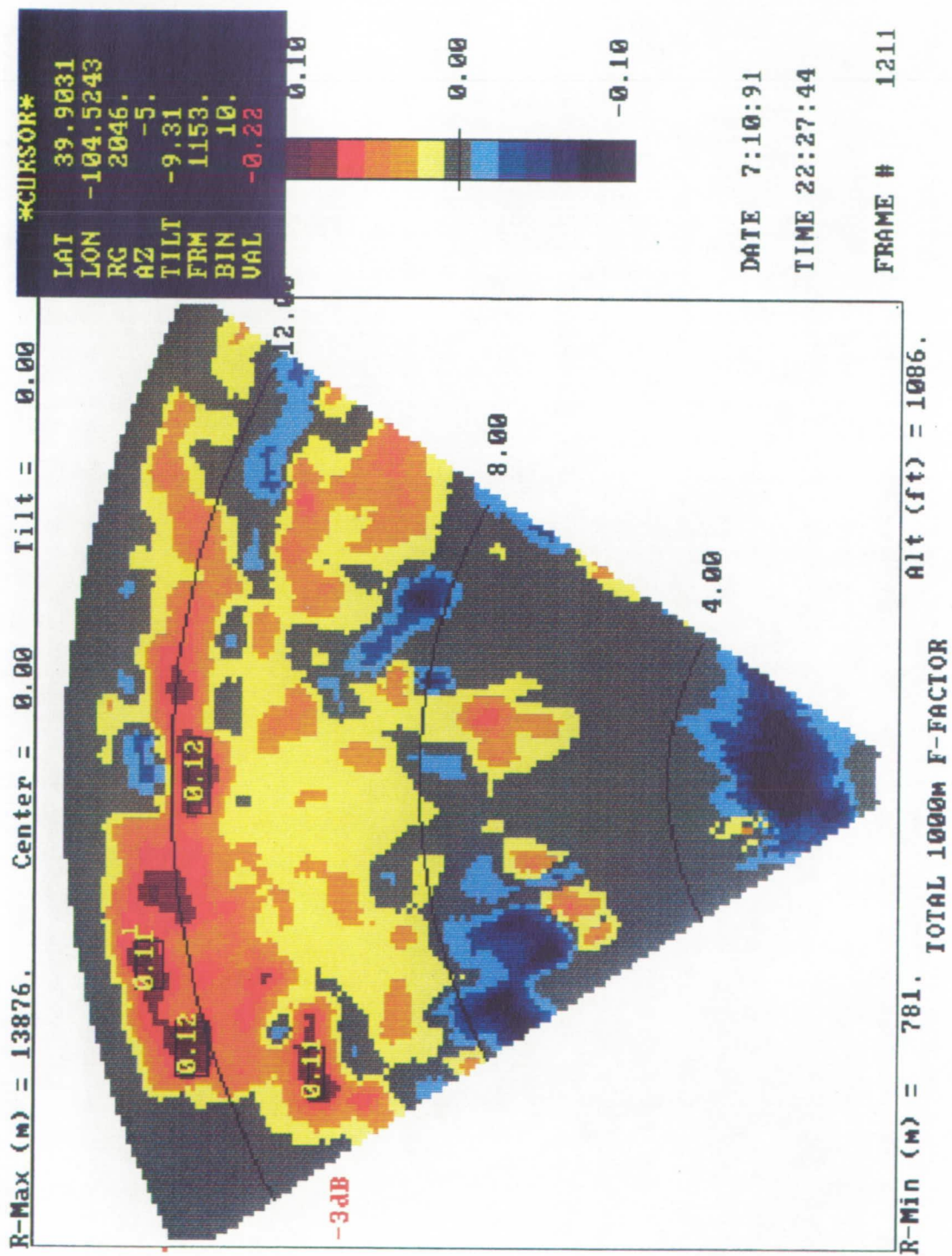
DATE 6:20:91

TIME 21:36: 2

FRAME # 3937

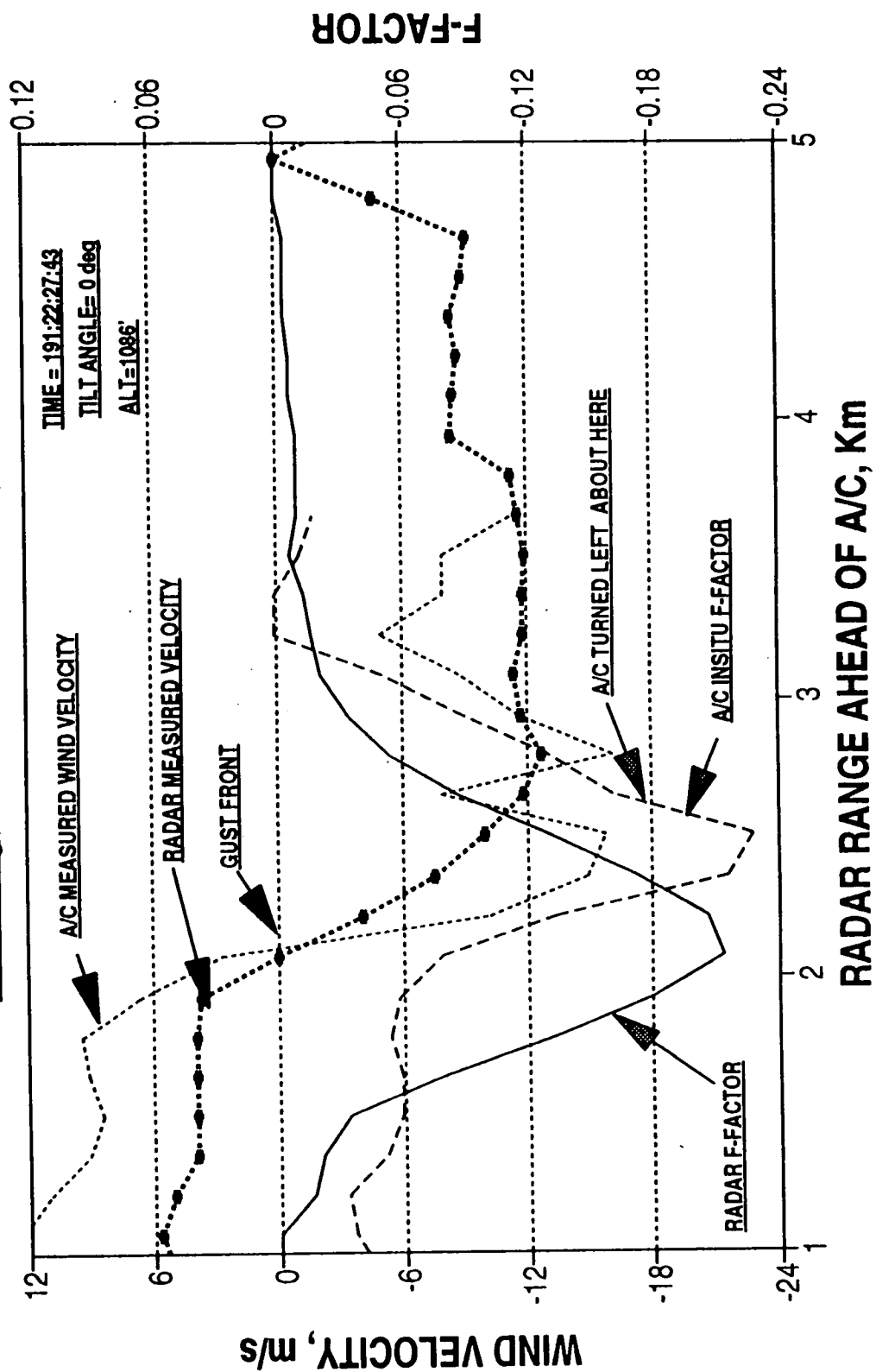


ORIGINAL PAGE
COLOR PHOTOGRAPH

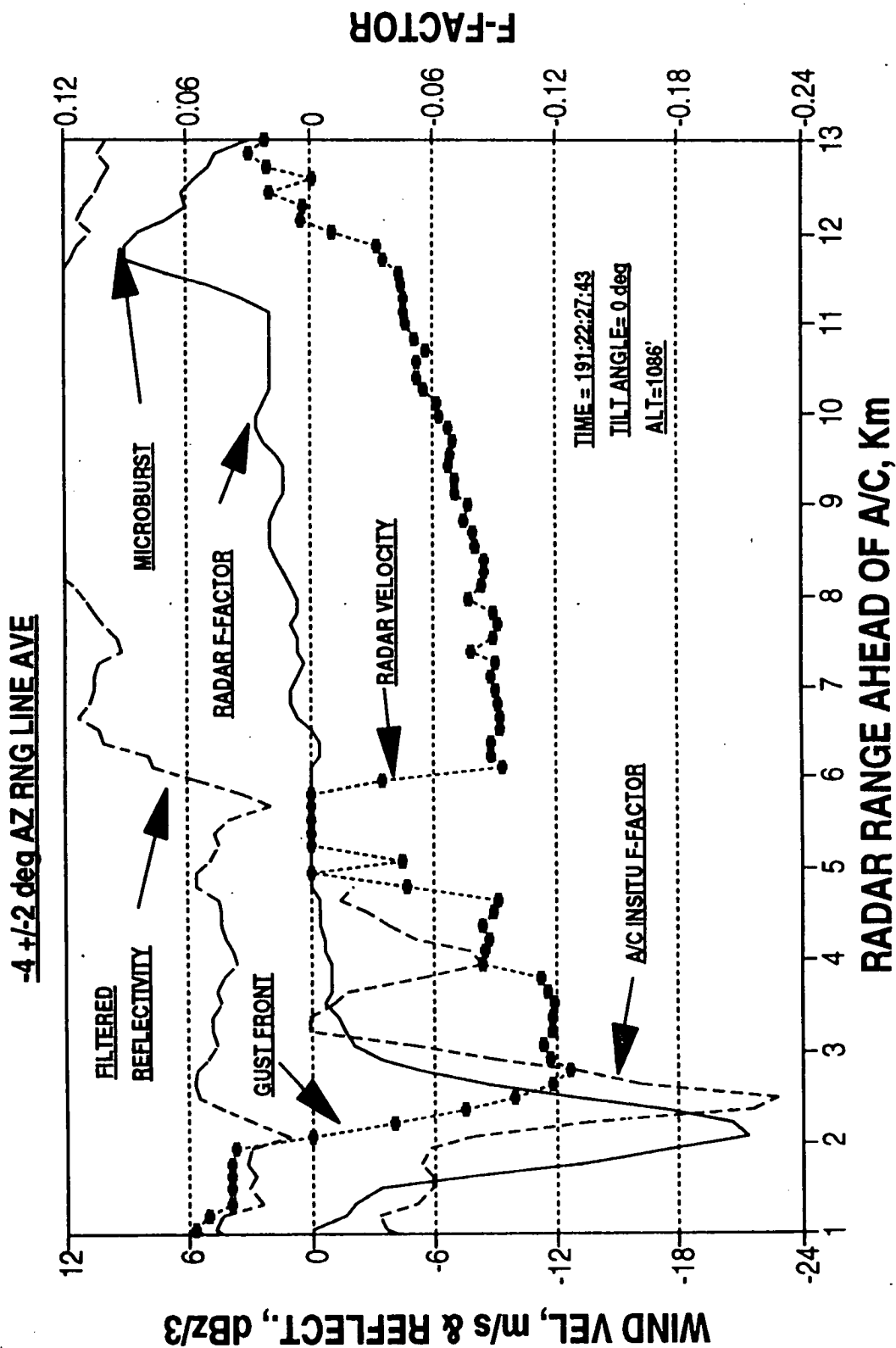


RADAR WIND SPEED & 1KM AVE F-FACTOR & A/C WIND SPD & INSITU F-FAC: EVENT 175

-4 & +/-2 deg AZ RNG LINE AVE



RADAR REFLECT., WIND SPEED, & 1KM AVE F-FAC, & A/C INSITU F-FAC: EVENT 175



SIGNIFICANT WIND SHEAR EVENTS 1991 ORLANDO FLIGHT EXP. RADAR, TDWR, & A/C INSITU F-FACTOR COMPARISONS

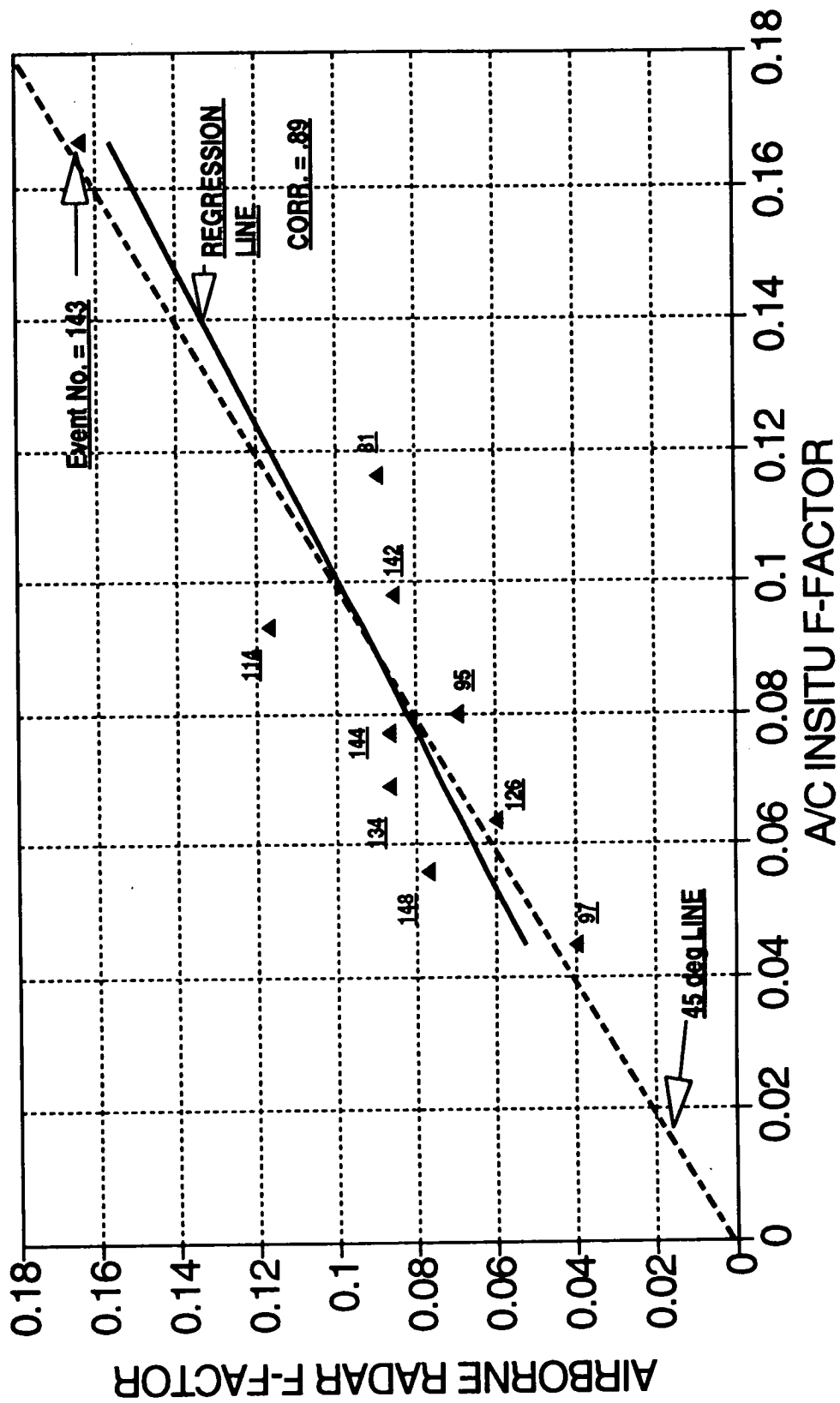
RADAR AND TDWR COMPARISONS

EVENT NUMBER	RADAR FILE NAME	TILT ANGLE deg	DATE	TIME	RADAR F-FACTOR WITHIN AZ SCAN			TDWR F-FACTOR
					MIN	MAX	AVE	
79	OR4W4S1.M6	0	6/15/91	166:19:28:48	0.07	0.09	0.08	0.094
80	OR4W6S1.M6	0	6/15/91	166:19:37:51	0.06	0.08	0.07	0.08
81	OR4W8S1.M6	2.25	6/15/91	166:19:51:46	0.05	0.10	0.09	0.11
86	Q4W15S14.M7	0	6/15/91	166:20:30:27	0.08	0.10	0.10	0.1
95	OR6W1S4.M6	-2	6/17/91	168:18:31:05	0.13	0.16	0.14	0.13
97	OR6W4S3.M6	-1	6/17/91	168:18:50:17	0.12	0.16	0.12	0.09
101	OR6W6S4.M6	-2	6/17/91	168:19:20:00	0.05	0.07	0.07	0.10
106	OR7W1S3.M6	-1	6/18/91	169:19:09:59	0.06	0.09	0.08	0.15
114	OR7W14S1.M6	0	6/18/91	169:20:23:15	0.11	0.15	0.13	0.11
115	OR7W15S3.M6	-1	6/18/91	169:20:25:59	0.11	0.14	0.12	0.086
118	OR7W20S3.M6	-1	6/18/91	169:20:52:16	0.12	0.14	0.13	0.10
126	OR8W1S4.M6	-2	6/19/91	170:17:27:13	0.08	0.12	0.10	0.11
127	OR8W2S3.M6	-1	6/19/91	170:17:34:23	0.06	0.07	0.06	0.11
134	OR8W15S1.M6	0	6/19/91	170:20:51:20	0.12	0.14	0.13	0.096
142	OR9W7S4.M6	-2	6/20/91	171:20:40:49	0.09	0.13	0.10	0.11
143	OR9W8S4.M6	-2	6/20/91	171:20:45:15	0.13	0.17	0.16	0.13
144	OR9W9S3.M6	-1	6/20/91	171:20:51:26	0.08	0.10	0.10	0.094
145	OR9W10S4.M6	-3.5	6/20/91	171:20:57:18	0.05	0.07	0.06	0.095
148	OR9W14S1.M6	-3	6/20/91	171:21:20:25	0.12	0.18	0.13	0.13
150	OR9W16S8.M16	AUTO	6/20/91	171:21:35:00	0.05	0.07	0.06	0.07
149	OR9W15S3.M6	-1	6/20/91	171:21:27:24	0.13	0.16	0.14	0.2

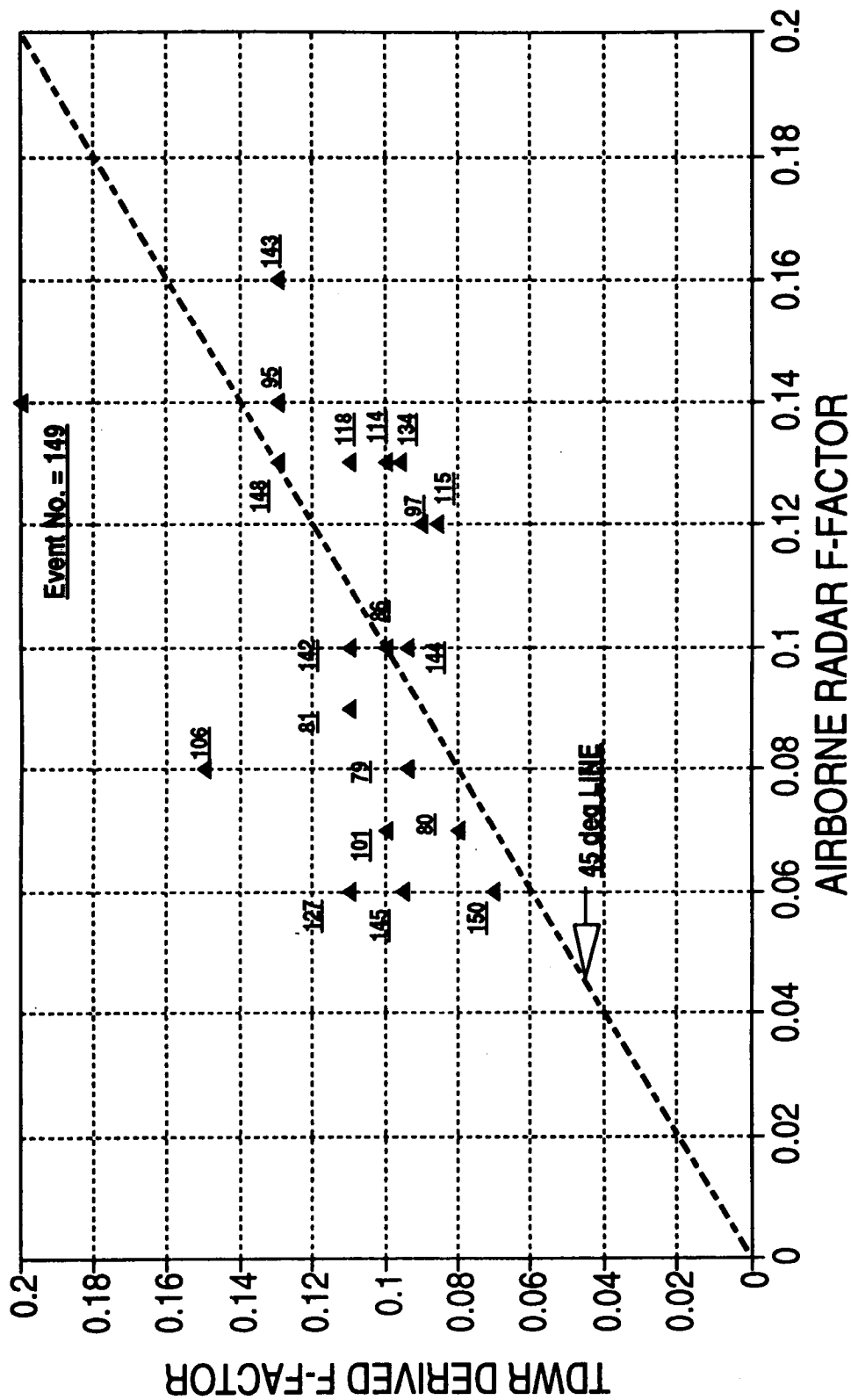
RADAR AND INSITU COMPARISONS

					RADAR LEAST SQ F-FACT	RADAR MEASURE F-FACT	INSITU F-FACT
97	OR6W4S3.M6	-1	6/17/91	168:18:50:17	0.0526	0.040	0.045
148	OR9W14S1.M6	-3	6/20/91	171:21:20:50	0.0619	0.077	0.056
126	OR8W1S4.M6	-2	6/19/91	170:17:27:27	0.0687	0.060	0.064
134	OR8W15S1.M6	0	6/19/91	170:20:51:59	0.0729	0.087	0.069
144	OR9W9S3.M6	-1	6/20/91	171:20:51:32	0.0797	0.087	0.077
95	OR6W1S4.M6	-2	6/17/91	168:18:31:05	0.0820	0.070	0.080
114	OR7W14S1.M6	0	6/18/91	169:20:23:17	0.0933	0.117	0.093
142	OR9W7S4.M6	-2	6/20/91	171:20:41:14	0.0976	0.086	0.098
81	OR4W8S1.M6	2.25	6/15/91	166:19:52:00	0.1128	0.090	0.116
143	OR9W8S4.M6	-2	6/20/91	171:20:45:31	0.1562	0.164	0.167

AIRBORNE RADAR & A/C INSITU F-FACTOR COMPARISONS



AIRBORNE RADAR & TDWR F-FACTOR COMPARISONS



NASA Flight Tests Airborne Doppler Radar Results

Performance Summary

- 1. Data from over 200 clutter and 150 weather event runs were collected. The weather events included approximately 30 microbursts and 20 gust fronts.**
- 2. No false hazard alerts resulted from any clutter targets.**
- 3. All microburst events were detected by the airborne radar. For the microbursts penetrated by the A/C (approx. 15), the airborne radar derived F-factor showed excellent agreement with the In Situ measured F-factor.**
- 4. Gust fronts with approximately 5 dBz or higher reflectivity levels were also detected.**
- 5. Sample comparisons of airborne radar data with TDWR data showed comparable results.**
- 6. Wet microbursts can be accurately detected in the presence of severe ground clutter. Dry microburst performance will be evaluated using radar simulation program with dry U-Burst models and possible Denver ground and flight experiments.**

Doppler Radar Results

Questions and Answers

Q: Anthony Berke (MIT Lincoln Laboratory) - I am curious to know why you had the antenna depressed two degrees or so when you were usually trying to do level flight penetrations?

A: Brac Bracalente (NASA Langley) - Primarily because we wanted to first look down into the event, and secondly, to get some clutter into the signal. We were really doing it over a range of tilt angles, 0, -1, -2, -3. We were collecting data with different conditions so we could evaluate the effects of clutter under those conditions, and to get extra data down in the event. Obviously in some of the comparisons with the In Situ where the antenna was tilted down, the In Situ flew above where we saw the measurement; there will be some differences there. We tried to compare with the In Situ when we were as close to the airplane as possible so the difference in altitude was not great.

Q: Pat Adamson (Turbulence Prediction Systems) - To create total F-factor numbers you estimate or infer the vertical component of the winds. Is that correct? If so, how do you deal with asymmetric events and with the different altitudes where vertical and horizontal winds trade-off?

A: Brac Bracalente (NASA Langley) - That is correct, we do that. Right now we are using an algorithm that Dan Vicroy and Fred Proctor came up with. There is going to be a presentation tomorrow by Dan on that vertical estimation. Basically we take the horizontal wind measurement and multiply it by a factor which takes altitude into consideration. Basically, it is estimating the vertical based on the horizontal component and the altitude at which we made the measurement. As far as the asymmetric events and the different altitudes, Dan will talk about all that tomorrow. It is pretty straightforward. Everything I showed up here did include a vertical estimation in the F-factors.

Q: Pat Adamson (Turbulence Prediction Systems) - What is the sensitivity of the radar? In Denver, 10% of the dry microburst were from -10 to 0 dBZ.

A: Brac Bracalente (NASA Langley) - As I pointed out in the presentation, we did not see any dry microburst, but we did see some low reflectivity gust fronts. I showed one example where the reflectivity was down in the 5 to 10 dBZ range and we were able to detect that. There wasn't extremely strong clutter in that particular region. We think we will be able to work down into the 0 maybe 5 dBZ level, out to three or four kilometers. That is what we are shooting for this summer. Hopefully we will get those kind of events so we can collect some data and see what we can do.

Q: Pat Adamson (Turbulence Prediction Systems) - When flying at 230 knots, is it easier or harder to suppress clutter than at 140 knots?

A: Brac Bracalente (NASA Langley) - I don't know that we see much difference since we zero out the velocity of the aircraft. The spectrum width of the clutter might be a little bit wider at 230 knots. It doesn't really have much effect on our ability to suppress the clutter or to operate the radar.

54p

1993010407
488714

Session I. NASA Flight Tests

N93-19596

Flight Test of an Infrared Wind Shear Detector
Dr. Burnell McKissick, NASA Langley Research Center

FLIGHT TEST OF AN INFRARED
WINDSHEAR DETECTOR

by

BURNELL T. M^cKISSICK
NASA, Langley Research Center
Hampton, VA 23665

Fourth Combined Manufacturers'
and Technologists' Airborne
Wind Shear Review Meeting
Fort Magruder Inn
Williamsburg, Virginia

COMMENTS ON "TOPICS DISCUSSED" SLIDE

The "TOPICS DISCUSSED" slide presents an outline of the presentation. The 5 microburst core penetrations are presented because they represent the only penetrations through the core of a microburst during the Orlando and Denver deployments and therefore the greatest opportunity of detecting a hazardous wind shear.

TOPICS DISCUSSED

- Introduction
- 5 Microburst Core Penetrations
- AWAS III Overall Performance
- Issues of Concern

COMMENTS ON "BACKGROUND" SLIDE

The central problem that is addressed in infrared wind shear detection is the relationship between air temperature change and wind shear. Efforts to draw a link between the two physical phenomena date back to 1954 to work done by Fawbush and Miller. Sinclair, Kuhn and others measured air temperatures around storms during the late 1970's. Sinclair has continued to develop passive infrared technology to measure air temperatures and infer wind shear hazards. Modelling of microbursts by Proctor produced an empirical relationship between temperature change and maximum horizontal wind outflow speed. Finally, Adamson developed a passive infrared wind shear detector which is a part of the NASA/FAA wind shear program and the subject of this presentation.

BACKGROUND

"Can detection of ambient air temperature changes lead to the detection of hazardous wind shears"

-Fawbush and Miller(1954):
Peak Gust= $7+3.06T-0.007T^2-0.00284T^3$

-Foster(1958): $W_0 = -(-gz\delta T_0/T_m)^{1/2}$

-Sinclair and others(late 1970's to present):
infrared radiometer flown on NASA Learjet (1982)

-Proctor(mid 1980's to present): microburst modelling; $u_{\max} = -2.5\Delta T$

-Adamson(mid 1980's to present): development of a passive infrared sensor for wind shear detection

-IR sensor is an integral part of the NASA/FAA wind shear detection and warning research program

NASA SPONSORSHIP OF TPS INFRARED SYSTEM DEVELOPMENT

Phase I SBIR (1987)

- Determined that a passive infrared sensor is feasible for windshear detection
- Passive infrared has considerable commercial potential

Phase II SBIR(1989-1991)

- Flight test of AWAS I on NASA 515 in 1989-1990
- Development of AWAS III
- AWAS III flown on FAA sponsored UND Cessna Citation through microbursts at Orlando

Flight test of AWAS III on NASA 515 at Orlando and
Denver in 1991

COMMENTS ON "MICROBURST TEMPERATURE MEASUREMENTS, GLOBAL AND LOCAL" SLIDE

AWAS III computes a delta temperature (DT) which is a measurement of a far field temperature (T_{far}) minus a near field (T_{near}): $DT = T_{far} - T_{near}$. T_{near} is close to the aircraft while T_{far} is nominally 4 kilometers ahead of the aircraft. If the DT measured by AWAS III is used in Proctor's relationship, for example:

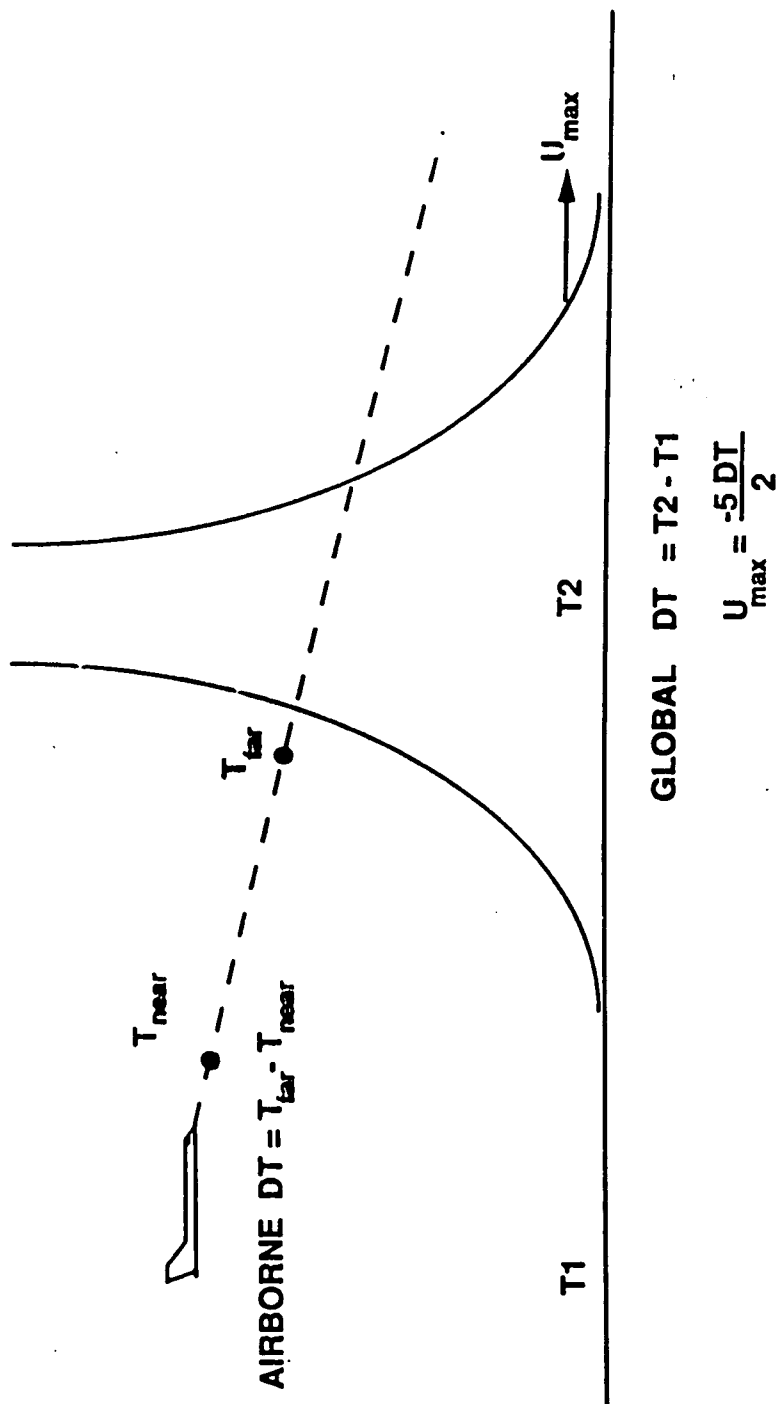
$$U_{max} = -5DT/2,$$

U_{max} becomes an estimate of maximum radial outflow. DT is a point (local) measurement of $T_{far} - T_{near}$. The ΔT in Proctor's equation is a temperature difference between minimum temperature in the core of a microburst and air temperature outside the microburst at the surface, a global difference. There is no assurance that

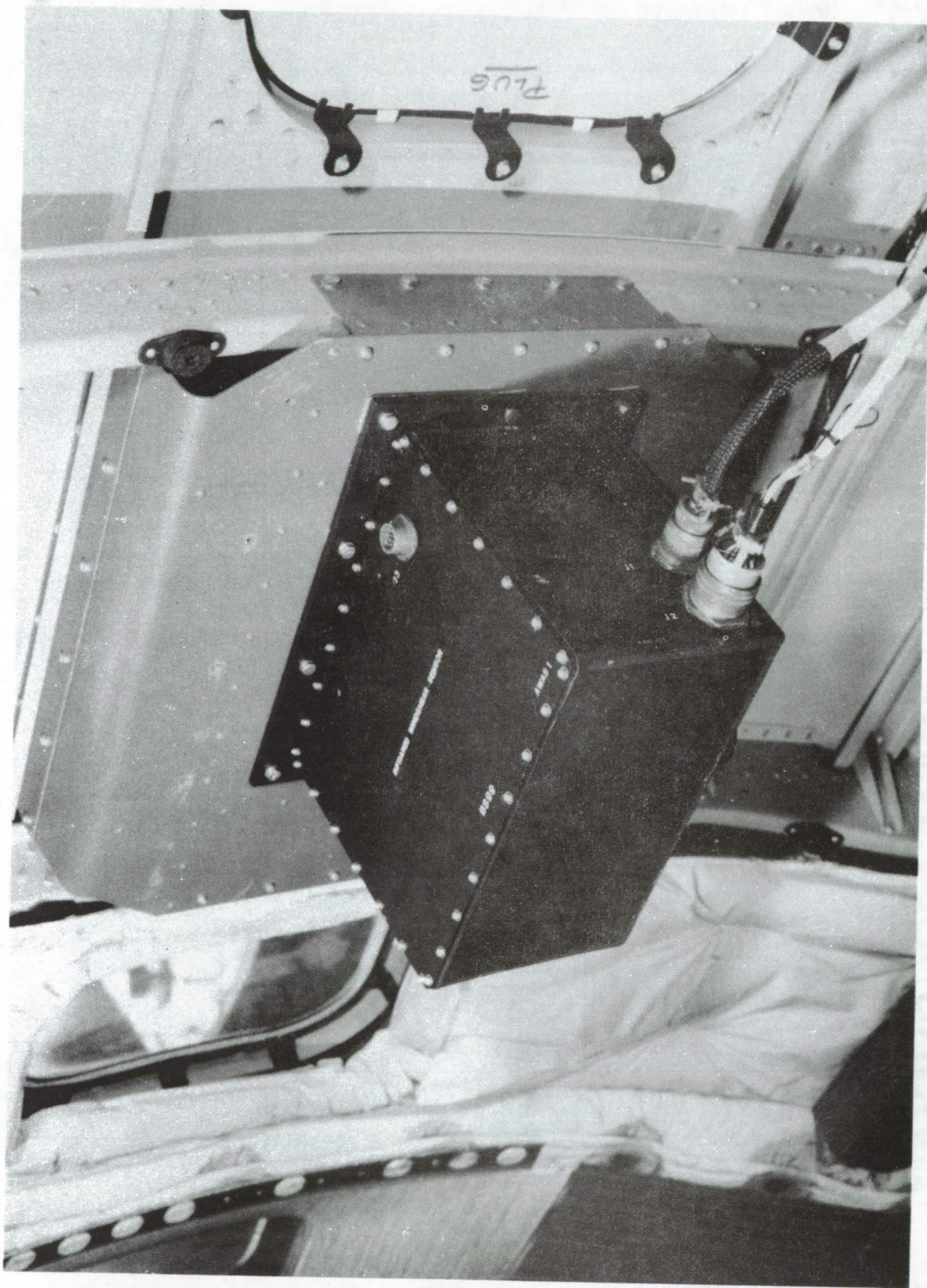
$$DT = \Delta T$$

or that Proctor's relationship will hold for every microburst. The next two slides are pictures of AWAS III as it is installed on NASA Langley's Boeing 737. The first of the two slides is an exterior view of AWAS III while the second slide shows how AWAS looks from the inside of the airplane.

MICROBURST TEMPERATURE MEASUREMENTS, GLOBAL AND LOCAL



ORIGINAL PAGE
BLACK AND WHITE PHOTOGRAPH



ORIGINAL PAGE
BLACK AND WHITE PHOTOGRAPH



COMMENTS ON "OUTPUT OF AWAS III" SLIDE

AWAS III provides more parameters than are listed on this slide. The ones listed were used during the research presented in this talk.

OUTPUT OF AWAS III

Near Field Temperature—Approx. 100 meters ahead
of the aircraft

Far field temperature—Nominally 4 kilometers
ahead of the aircraft

Delta Temperature—Spectral measurement of far field
minus near field temperatures

Thermal Hazard Index—A local hazard index based on
outside air temperature

IR Hazard Index—A predictive hazard index based on
Delta Temperature

COMMENTS ON "5 MICROBURST CORE PENETRATIONS AT ORLANDO" SLIDE

Some pertinent information on the 5 core penetrations is presented on this slide. For example, the penetration labeled as event 143 occurred on June 20, 1991. The in situ F-factor had a peak value of .167 and the thermal hazard index had a peak value of .14. Both indices gave a wind shear alert. The thermal hazard index is an in situ index based on air temperature measured from aircraft sensors.

5 MICROBURST CORE PENETRATIONS AT ORLANDO

Event #	Date	Peak Values		Type of Alert
		<u>In situ</u>	<u>Thermal</u>	
81	6/15/91	.116	.12	Insitu
134	6/19/91	.069	.13	Thermal
142	6/20/91	.098	.13	Thermal
143	6/20/91	.167	.14	Insitu Thermal
144	6/20/91	.077	.13	Thermal

COMMENTS ON "METHOD OF ANALYSIS" SLIDE

The basis of the analysis of the 5 events is the correlation between pairs of important variables: OAT (outside air temperature), LLWSR (thermal hazard index), LLWS2 (predictive hazard index based on infrared measurements), D2 (infrared measured $T_{far} - T_{near}$, basis of LLWS2), Pitch (aircraft Euler angle) and FE3 (in situ F-factor based on inertial and air data measurements). Estimating correlation coefficients and performing detailed comparisons of time series can determine if AWAS III generated predictive wind shear indices. The analysis of event 143 using these techniques will be presented in this talk.

METHOD OF ANALYSIS

Correlation of OAT, LLWSR, LLWS2, D2, Pitch and FE3

Assumption

—Temp. Fields are Constant During an Event

Goal of Analysis is to Determine if AWAS III

Generates Predictive windshear hazard indices

COMMENTS ON "RESULTS FROM 5 CORE PENETRATIONS" AND "COMPUTED LOOK DIST:FLT TST 91" SLIDES

One of the first things that is noticeable from AWAS III generated data are short computed look distances. The slide named "COMPUTED LOOK DIST:FLT TST 91" shows this data for the Orlando and Denver deployments. Estimates of the correlation coefficients between D2 and temperature give evidence that D2 is measuring t_{near} . Because of this, D2 cannot provide a predictive response to wind shear. Several possible explanations exist for the short look distances. One of the first possible explanations is that the flights were through heavy rain which resulted in shortened look distances. Flights at Denver were not through rain, but the computed look distances were small for many of those events. Another possible explanation was that the installation of AWAS III on the NASA Boeing 737 resulted in short look distances. The NASA installation is different than that of American and Northwest airlines, but no one knows how or if the NASA installation affected look distances. In order to eliminate any possible installation effect, TPS redesigned NASA's installation of AWAS III so that it is more like that of American and Northwest airlines for the 1992 deployments.

In the 5 core penetrations there were 4 thermal alerts given due to large drops in measured ambient air temperature. For example, the measured temperature drop for event 143 was approximately 10°C. A temperature drop of this magnitude would correspond to a larger wind shear than experienced in event 143. All of the microburst events of the Orlando deployment involved flying through heavy rain and aircraft temperature probes are affected by rain. Rain effects cause the measured temperature drops to be larger than the true temperature drops. Large measured drops in temperature may have been a contributing factor in the four thermal alerts in the five core penetrations.

RESULTS FROM 5 CORE PENETRATIONS

Computed Look Distance Shorter than Expected

Infrared Detectors Measure Near Field Temperature

No Predictive Response Due to the Infrared Detectors

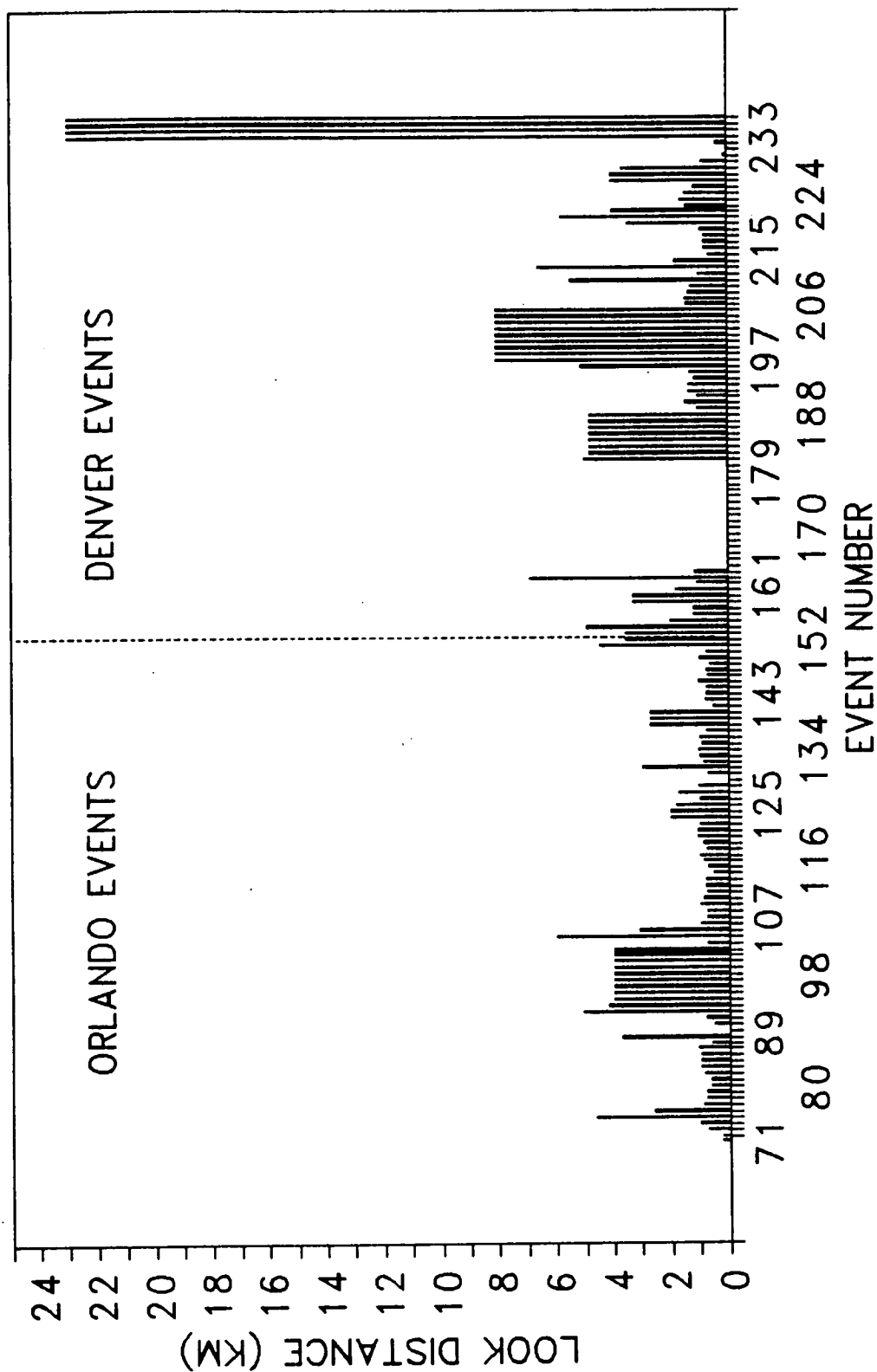
Rain affected Measurement of OAT

4 Thermal Alerts

2 Insitu Alerts

COMPUTED LOOK DIST:FLT TST 91

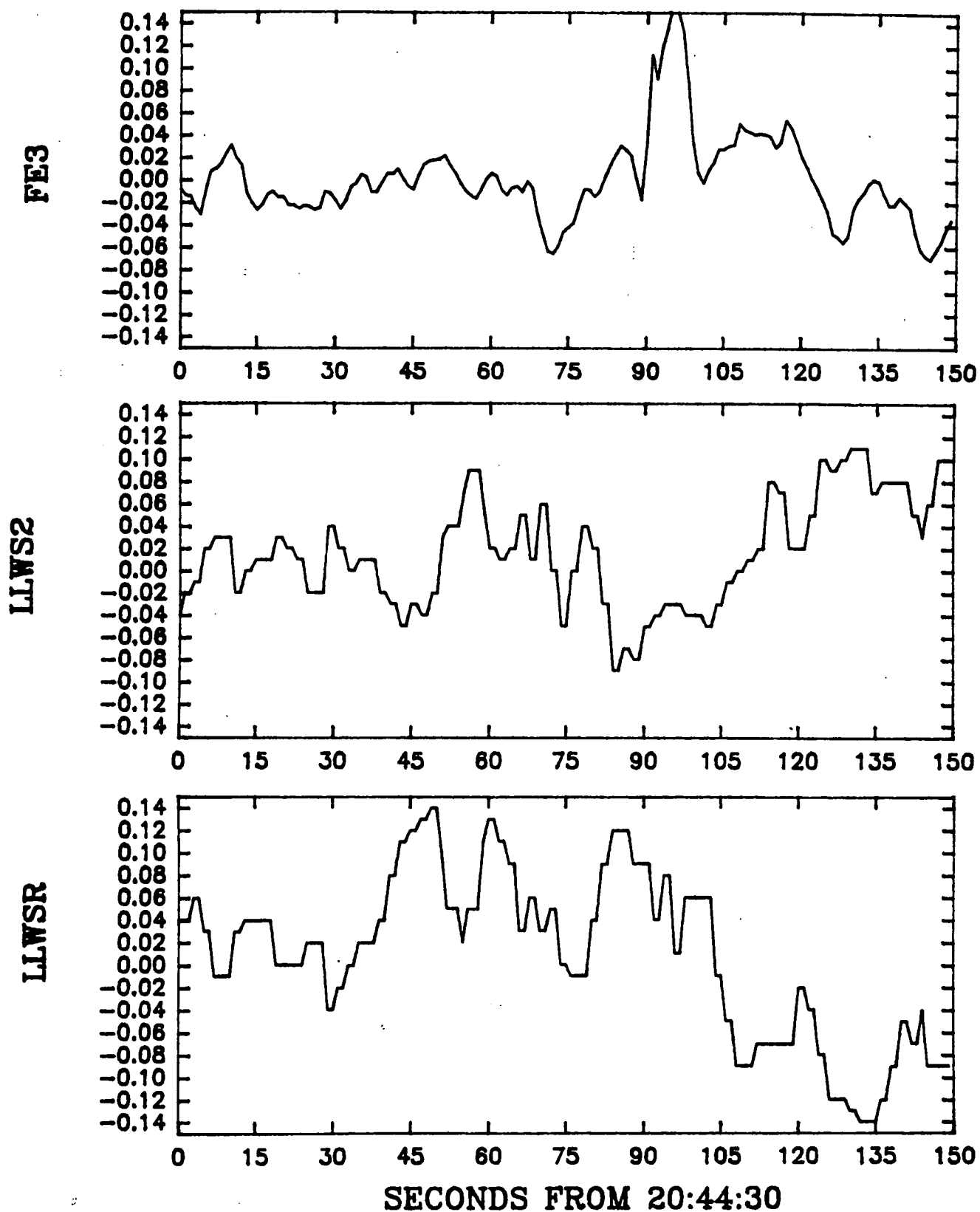
NOTE: ZERO INDICATES NO DATA AVAILABLE



COMMENTS ON "FE3...FOR A MICROBURST PENETRATION" SLIDE

This is the first of a series of slides that present a detailed analysis of event 143. In this slide, time histories of the hazard indices FE3, LLWS2 and LLWSR are shown. At approximately 95 seconds after the beginning of the event FE3 alerts for a wind shear. There are peaks in LLWS2, but these peaks are not a predictive response to wind shear. This will be shown in the subsequent analysis. LLWSR generates an alert at about 50 seconds after the beginning of event 143 or about 45 seconds before the alert caused by FE3. This may be due to the rain effect on the temperature measurement since heavy rain was encountered before penetrating the microburst.

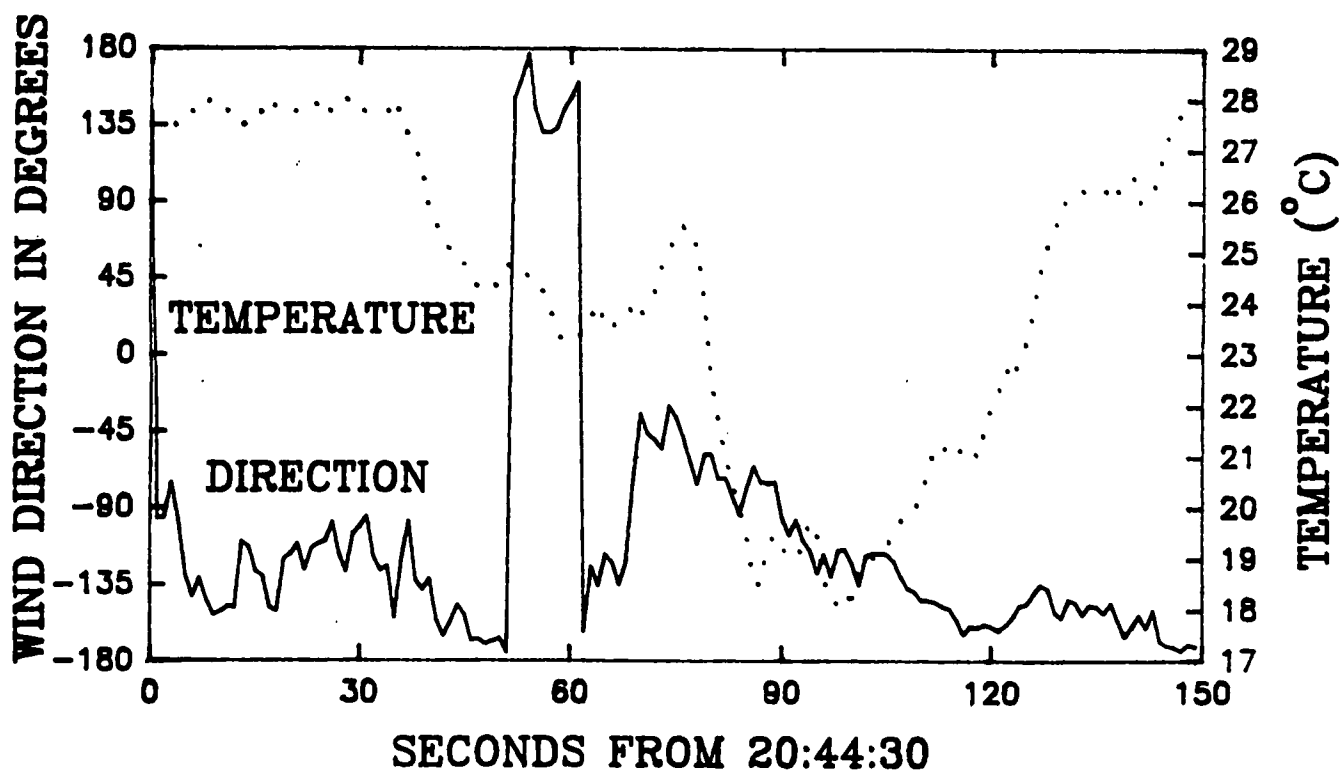
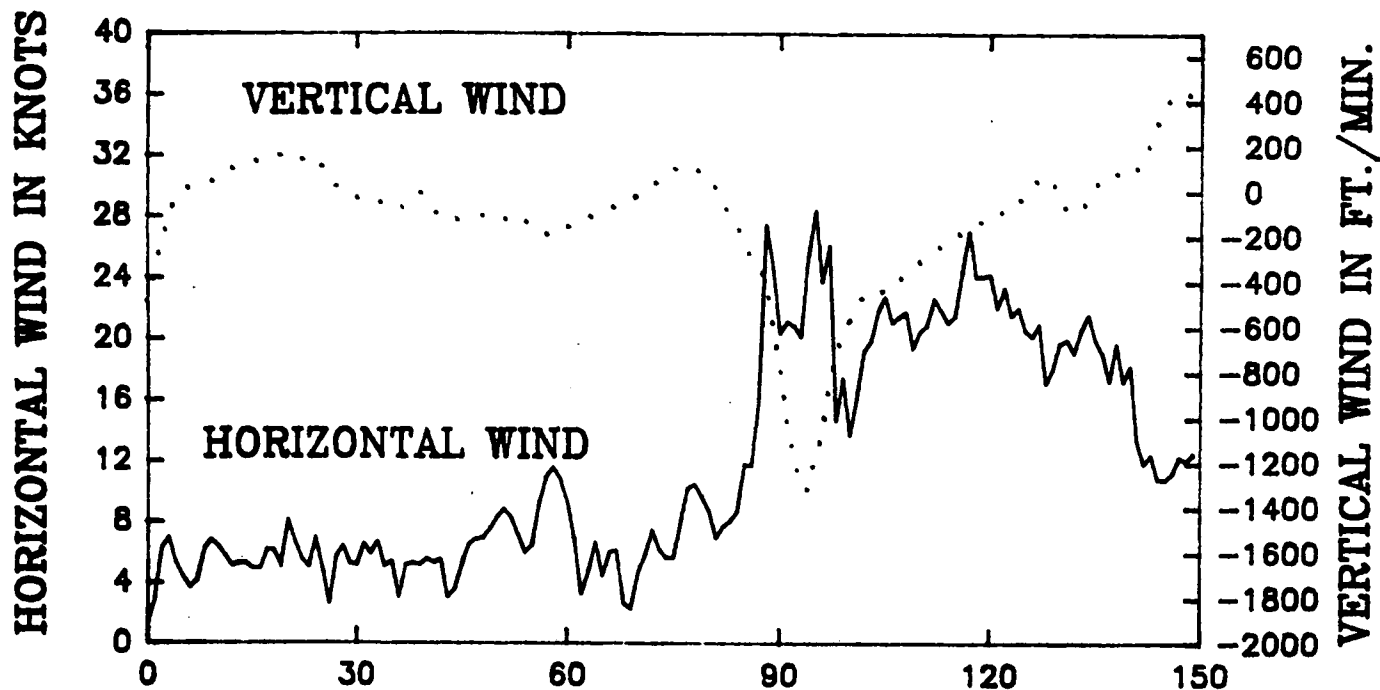
FE3 , LLWS2 ,TLLWS2 AND LLWSR for #143
FLIGHT 612 ON 6/20/91 AT ORLANDO
FOR A MICROBURST PENETRATION



COMMENTS ON "WIND SPEED..." SLIDE

At approximately 90 seconds after the start of event 143 a substantial down draft is encountered. Temperature begins to drop around 35 seconds after the start of the event. As stated before, the drop in measured temperature may be due to the rain effect on the aircraft temperature probe.

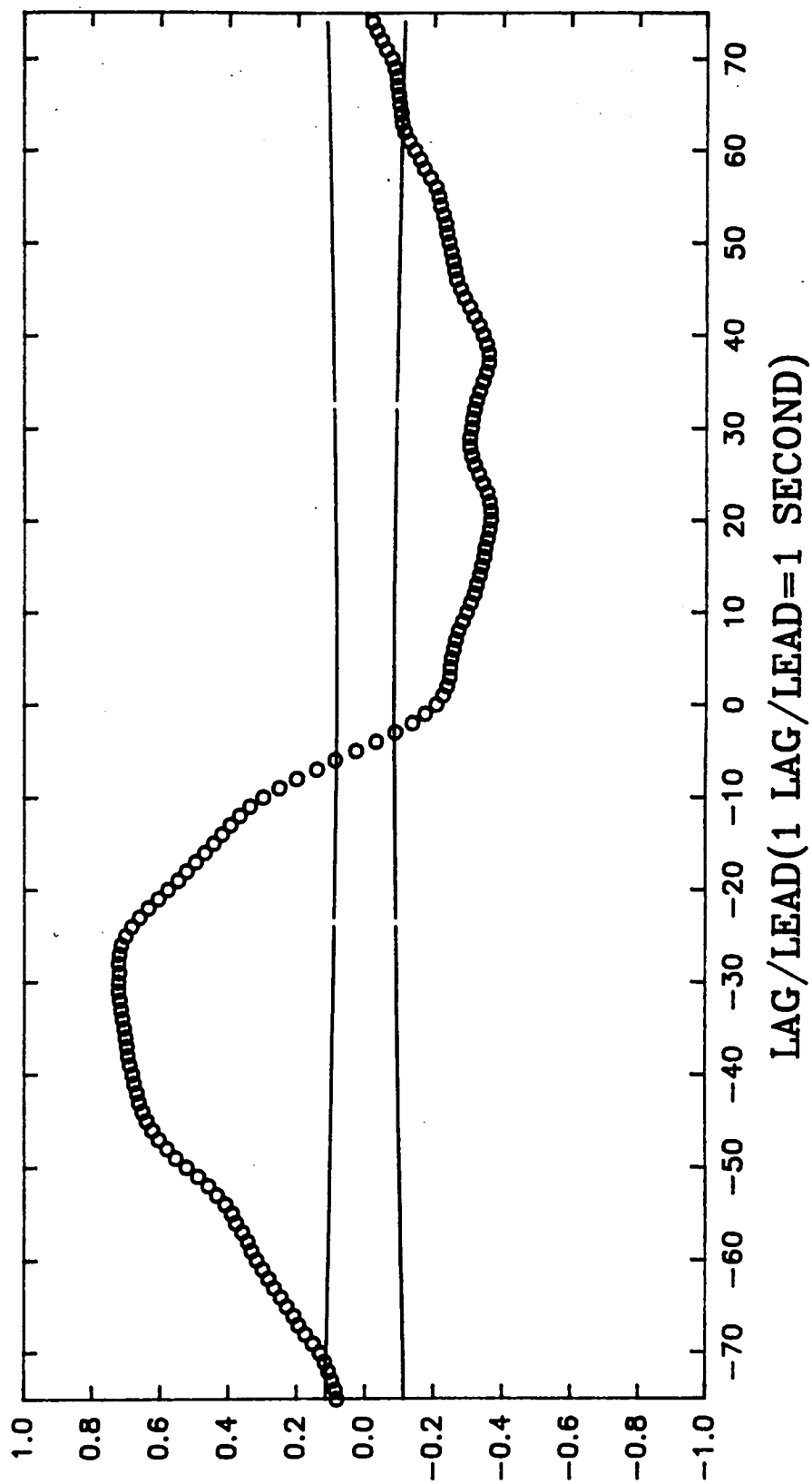
WIND SPEED, DIRECTION AND TEMP. for #143 FLIGHT 612 ON 6/20/91 AT ORLANDO FOR A MICROBURST PENETRATION



**COMMENTS ON "...CROSS CORRELATION OF LLWSR AND
TEMPERATURE" SLIDE**

Normally the correlation at zero lag is much stronger than what is shown in this slide. LLWSR is a function of temperature and usually has a correlation coefficient of about .6.

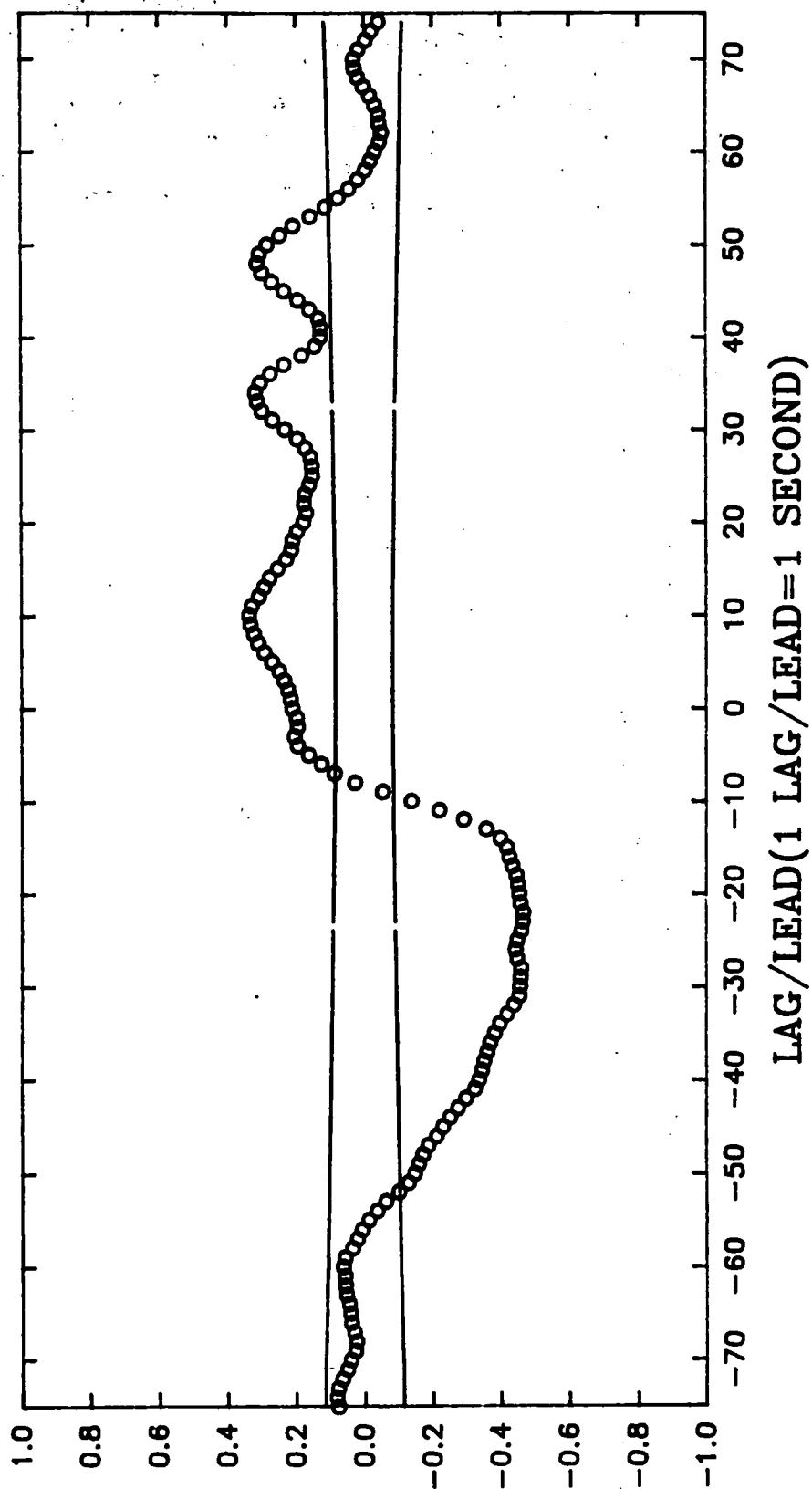
CROSS CORRELATION COEFFICIENT FOR #143 WITH +/- ONE STANDARD ERROR CROSS CORRELATION OF LLSWR AND TEMPERATURE



COMMENTS ON "...CROSS CORRELATION OF LLWSR AND FE3" SLIDE

The three peaks in the cross correlation coefficient correspond to the three peaks in LLWSR correlating with the one peak in FE3. Peaks in LLWSR occurred at 10, 34 and 48 seconds before the peak in FE3. LLWSR is based upon measured temperature which may be affected by rain. Therefore, the peaks in LLWSR may be due to rain effects.

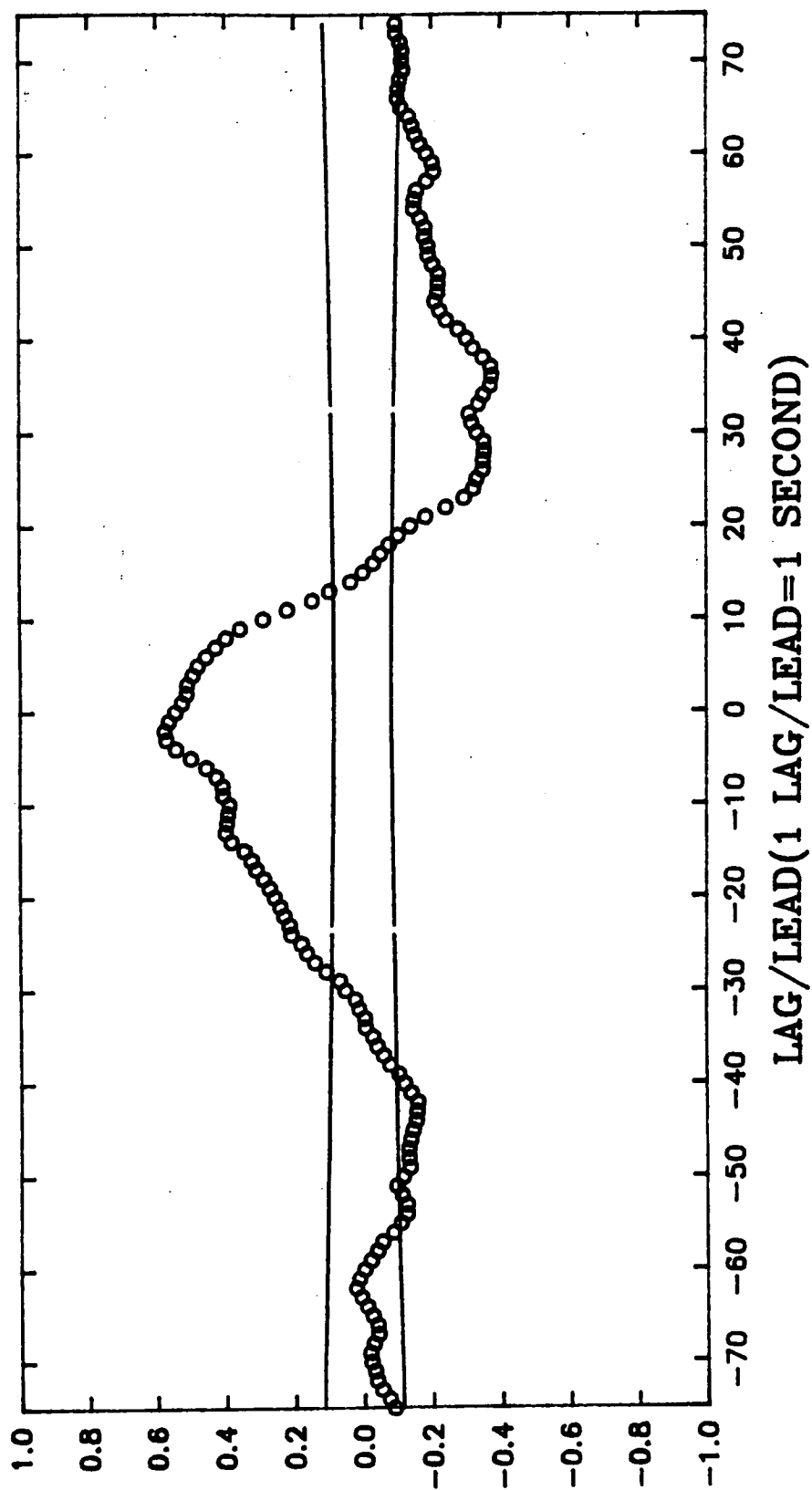
CROSS CORRELATION COEFFICIENT FOR #143
WITH +/- ONE STANDARD ERROR
CROSS CORRELATION OF LLSWR AND FE3



COMMENTS ON "...CROSS CORRELATION OF D2 AND PITCH" SLIDE

D2 and pitch have a correlation coefficient of approximately .6 near zero lag. This indicates a strong pitch effect in the D2 measurement. Also, this positive correlation is evidence that D2 is following a near field temperature. The reasoning goes as such: as the aircraft pitches up (increased pitch) a colder temperature is sensed (temperature decreases) since the sensor is not pitch stabilized. But, since $D2 = t_{far} - t_{near}$, pitch is correlating with $-t_{near}$ which gives a positive correlation coefficient. This is evidence that D2 was primarily measuring near field temperature.

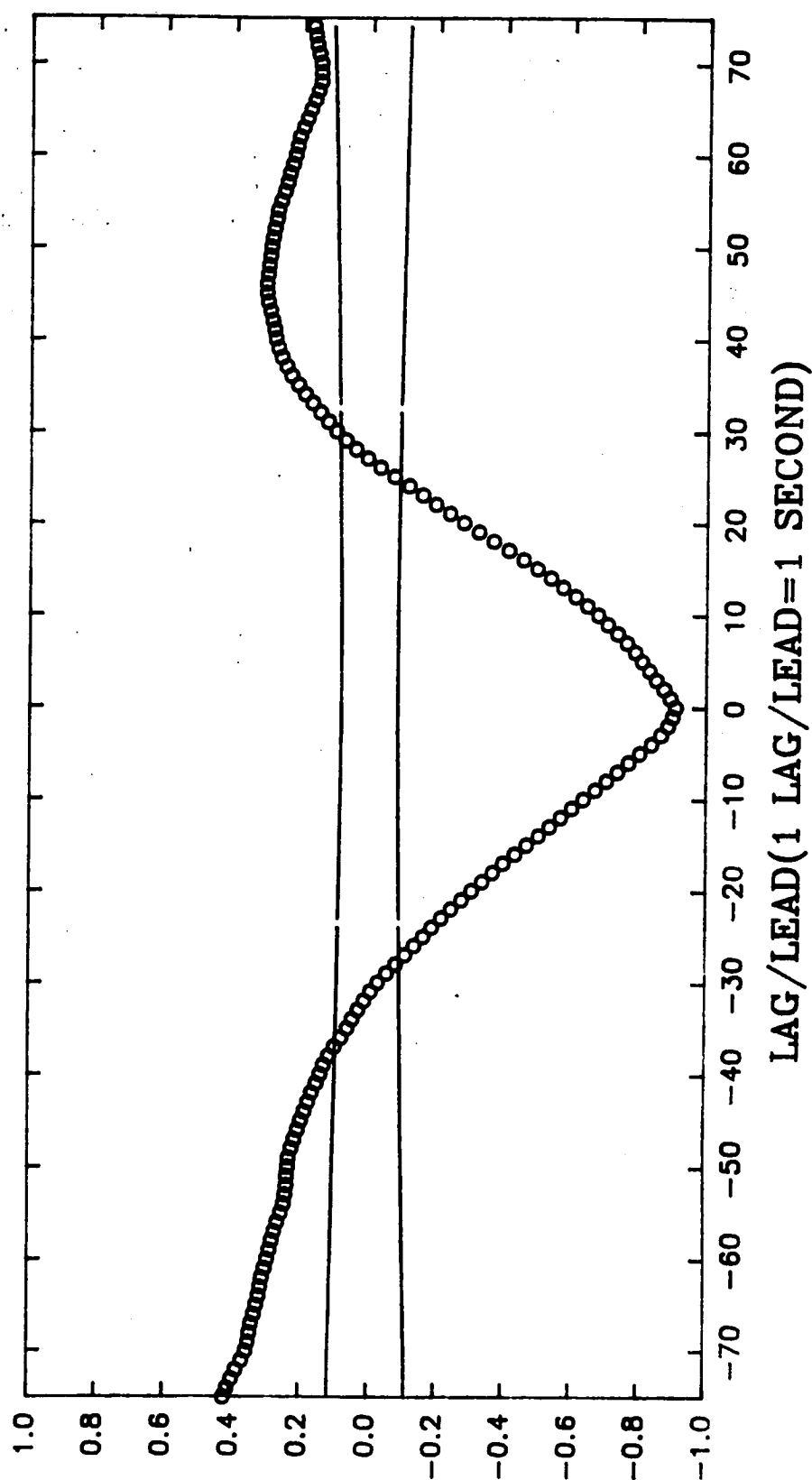
CROSS CORRELATION COEFFICIENT FOR #143
WITH +/- ONE STANDARD ERROR
CROSS CORRELATION OF D2 AND PITCH



**COMMENTS ON "...CROSS CORRELATION OF
D2 AND TEMPERATURE" SLIDE**

In this slide D2 shows very strong correlation with temperature at the aircraft. There also seems to be much weaker correlation of D2 with a far field temperature 45 seconds ahead of the aircraft. This is additional evidence that D2 was primarily measuring near field temperature.

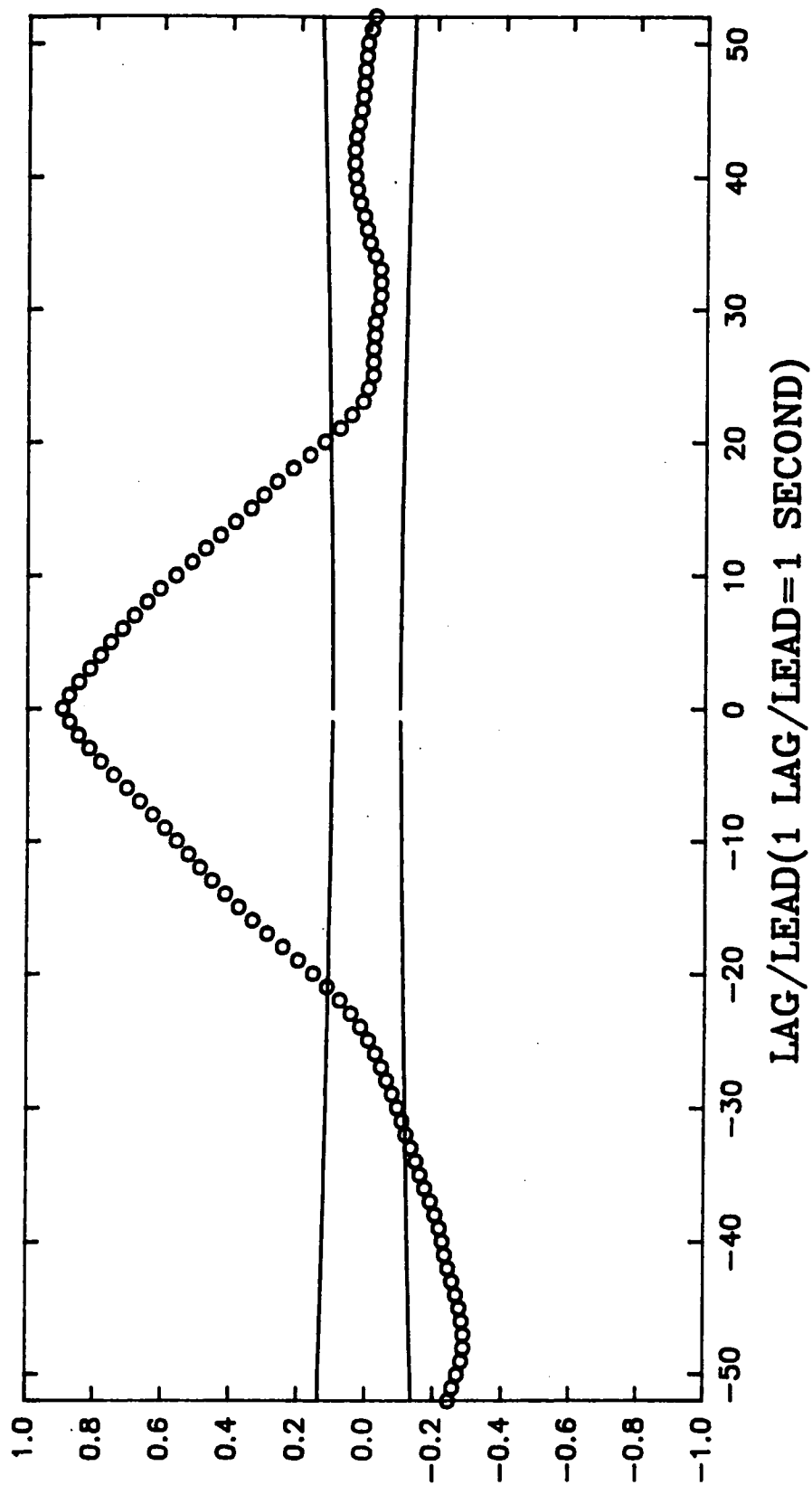
CROSS CORRELATION COEFFICIENT FOR #143
WITH +/- ONE STANDARD ERROR
CROSS CORRELATION OF D2 AND TEMPERATURE



COMMENTS ON "...CROSS CORRELATION OF D2 AND $T(t+45)-T(t)$ " SLIDE

A pseudo $t_{\text{far}} - t_{\text{near}}$ is formed by computing $T(t+45)-T(t)$, temperature 45 seconds ahead of the aircraft minus temperature at the aircraft. D2 shows a very strong correlation with $T(t+45)-T(t)$, but not as strong as the correlation with temperature at the aircraft as shown in the previous slide. Strong correlation between D2 and $T(t+45)-T(t)$ may mean that D2 is measuring a far field temperature 45 seconds ahead of the aircraft minus a near field temperature at the aircraft. A look at the appropriate time series will show that D2 was measuring near field temperature.

CROSS CORRELATION COEFFICIENT FOR #143 WITH +/- ONE STANDARD ERROR CROSS CORRELATION OF D2 AND $T(t+45) - T(t)$

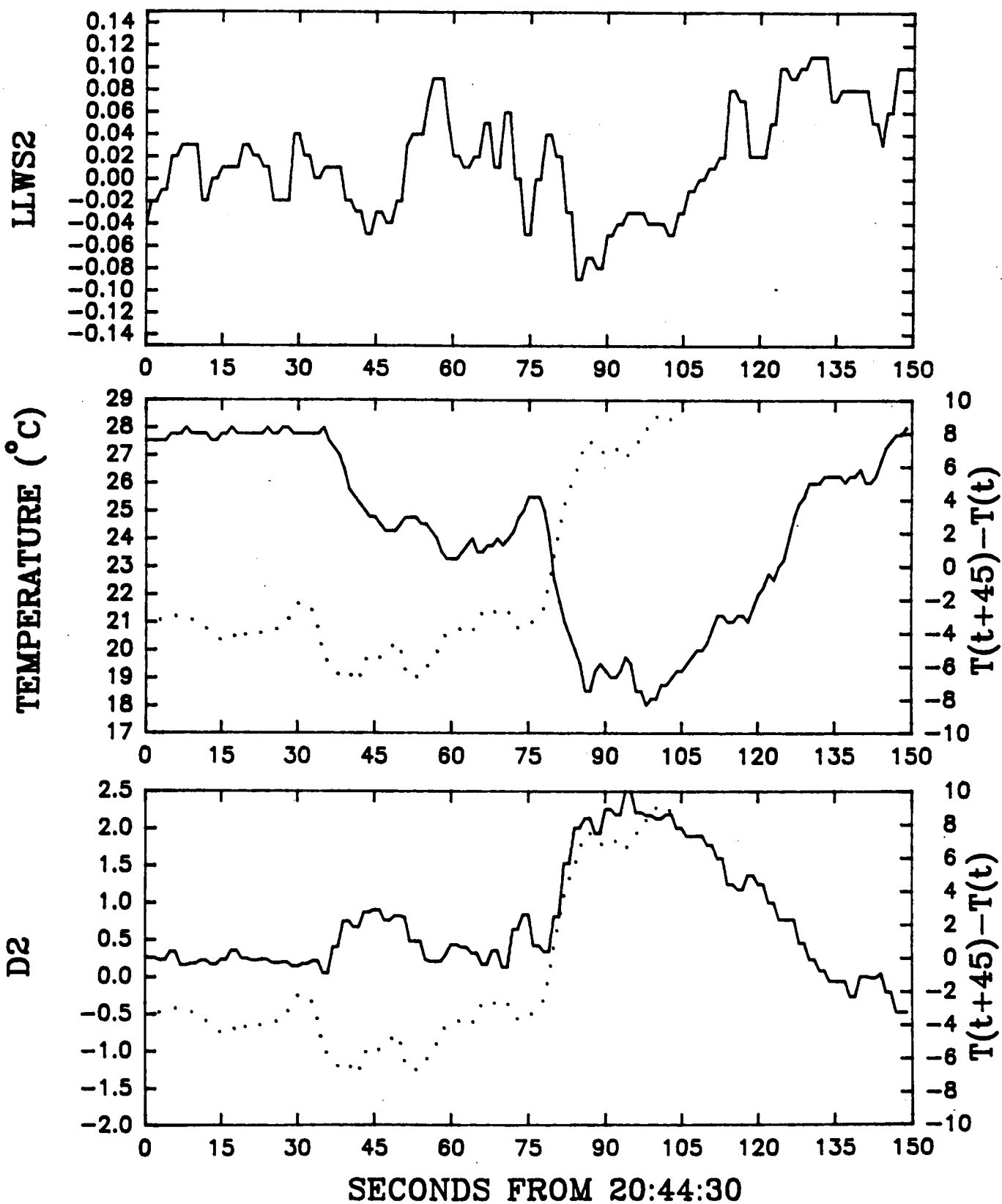


$T(t)$ = TEMP. AT TIME t SECONDS

COMMENTS ON "LLWS2, TEMPERATURE...FOR A MICROBURST PENETRATION" SLIDE

The correlation of D2 and $T(t-45)-T(t)$ does not represent a predictive response to temperature changes. D2 was measuring near field temperature. In the bottom graph of this slide D2 (the solid line) and $T(t-45)-T(t)$ (the dotted line) are plotted against time. The middle graph has outside air temperature (solid line) and $T(t+45)-T(t)$ versus time. Comparing the two graphs shows that D2 varies inversely with temperature. After approximately 35 seconds from beginning of event 143 the aircraft encounters the cold air outflow; D2 becomes a measurement of near field temperature and LLWS2 is responding to near field temperature changes. In the first 35 seconds of event 143 the temperature and D2 are essentially constant and the variation in LLWS2 is system noise. The positive correlation between D2 and $T(t+45)-T(t)$ is due to their behavior after 75 seconds from the start of event 143. During this period both variables are increasing with time and D2 (between 75 and 90 seconds) correlates positively with temperature beyond 120 seconds. Since the aircraft is in the cold air outflow, this correlation does not represent a predictive response to temperature but is termed a nonsense correlation.

LLWS2, TEMPERATURE, AND D2 FOR #143 FLIGHT 612 ON 6/20/91 AT ORLANDO FOR A MICROBURST PENETRATION



COMMENTS ON "FREQUENCY...FOR ALL EVENTS" SLIDE

The in situ algorithm (FE3) alerted twice or 1.14% of the time. AWAS III alerted 32 times or 18.18% of the events contained AWAS alerts. There was one event (number 143) that had a common alert. The alert rates are statistically different based on a χ^2 test.

FREQUENCY TABLE FOR ORLANDO AND DENVER DEPLOYMENTS FOR ALL EVENTS

		FE3		
		ALERTS	NO ALERTS	
AWAS III	ALERTS	1 .005682	31 .176136	.1818
	NO ALERTS	1 .005682	143 .8125	
		.011364		

COMMENTS ON "AWAS III THERMAL ALERTS" SLIDE

All of AWAS' alerts were thermal alerts. A large number of alerts occurred during rain cell penetrations which may have been caused by rain effects as previously stated and radar clutter runs which were low passes over runways followed by go-arounds.

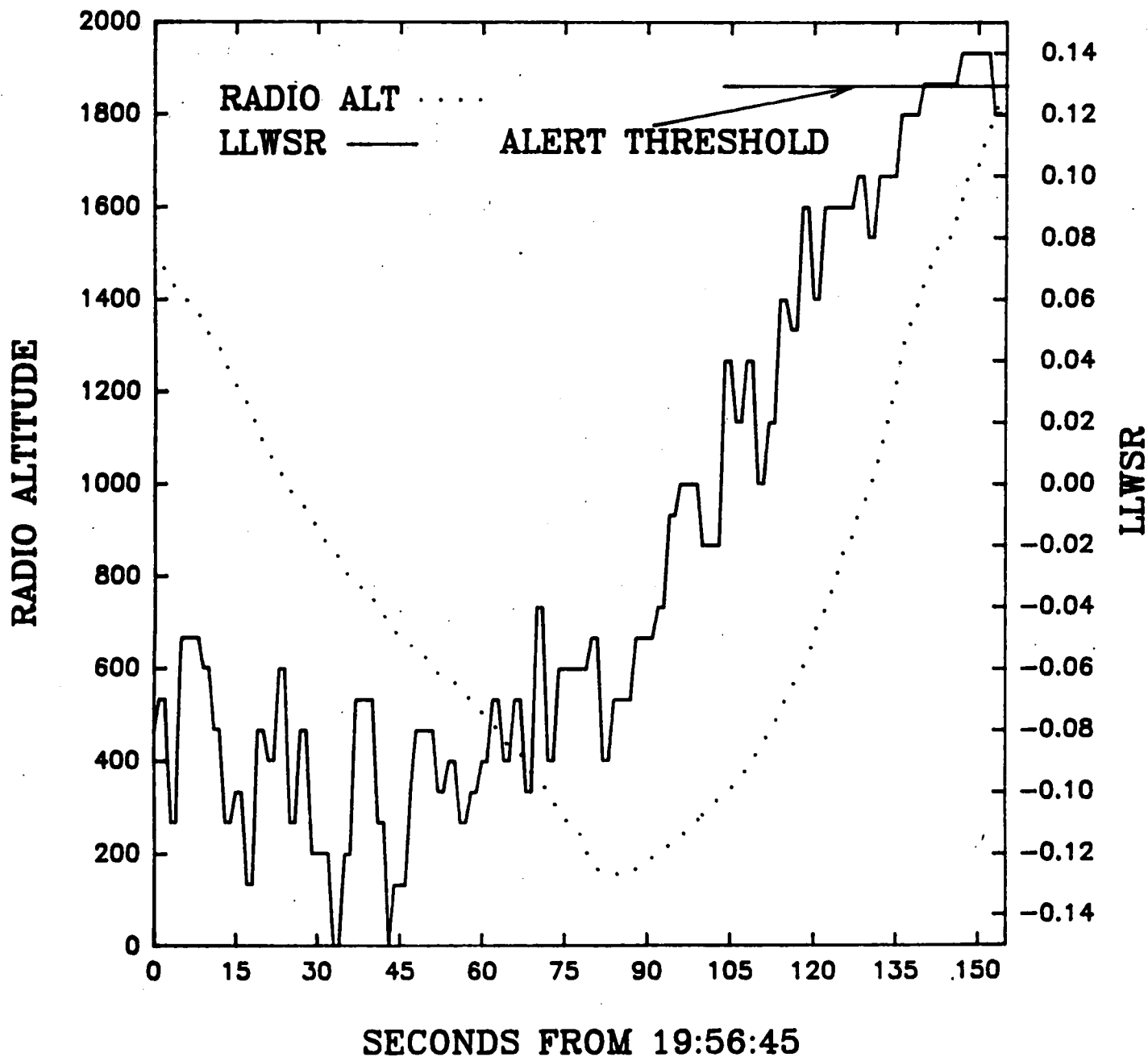
AWAS III THERMAL ALERTS

Event Type	Number of Events
-----	-----
Microburst	9
Rain Cell	11
Gust Front	1
Go-around	10
Other	1
-----	-----
Total	32

COMMENTS ON "...FOR A GO-AROUND" SLIDE

This slide shows the typical behavior of AWAS III during a go-around. The thermal hazard index is not compensated for the change in temperature that occurs when the aircraft is climbing during a go-around.

RADIO ALTITUDE AND LLWSR FOR #190 FLIGHT 618 ON 7/11/91 AT DENVER FOR A GO-AROUND



COMMENTS ON "AWAS III CONCERNS" SLIDE

A number of issues relating to AWAS III performance need to be addressed. Some have already been mentioned during this presentation. NASA's installation of AWAS III was different than that of other installations. The TPS/NASA designed installation used a periscope and AWAS III was in a pressurized passenger compartment of the aircraft. The other installations did not use a periscope and were not in a pressurized part of the aircraft. No one is sure if AWAS III's performance was affected by possible installation effects. All of our penetrations were done with air speeds much higher than approach and landing speeds. AWAS III's hazard indices are based on normal approach and landing speeds of around 140 knots. AWAS III's performance during the go-arounds points to the need for thermal hazard alerts are probably caused by rain affecting temperature probe measurements. The hazard indices from AWAS III appear to contain a lot of noise. Filtering of the indices would reduce the noise level and possibly change the threshold for alerting.

AWAS III CONCERNS

NASA Installation of AWAS III

- Unheated mirror
- Mirror replaced twice
- Window (KRS-5) had to be cleaned
- Rain in periscope may lower look distance

Airspeed of 230 kts. during penetrations

Lapse rate compensation

Effect of rain on OAT measurements

Filtering of data

Threshold for alerting

COMMENTS ON "AWAS III CHANGES FOR 1992 DEPLOYMENTS" SLIDE

Numerous changes are being made to AWAS and to the NASA 737 installation. One of the biggest changes is a TPS redesigned periscope mount. NASA's installation would be more like those of other AWAS III installations. The KRS-5 window is being moved from the bottom of the periscope to the top of the periscope. This will put the window in the same relationship to the reflector as all other installations. Also the NASA installation will have a heated reflector. TPS is developing hazard indices based on microburst penetration speeds in excess of 200 knots. Also, AWAS III will have a new method of compensating for pitch affects (lapse rate effects caused by aircraft pitching) and compensation for lapse rate effects on OAT measurements. And finally, filtering is introduced into the computations of the hazard indices.

AWAS III CHANGES FOR 1992 DEPLOYMENTS

TPS Redesigned Periscope

TPS Developing Hazard Indices for
Flight Test Airspeeds

New Lapse Rate Computation

Enhanced Lapse Rate Compensation
for OAT

Indices Based on Filtered Data

COMMENTS ON "CONCLUSIONS" SLIDE

The AWAS III system functioned according to specifications. Flight profile modes changed when they should have and there were no system errors. There is a need for compensating for rain effects on the thermal hazard index and possible installation effects are uncertain. Various operational and installation uncertainties do not allow NASA to make conclusive statements regarding AWAS III's performance of the wind shear predictive function.

CONCLUSIONS

AWAS III System Operated Without Failures

Numerous Thermal Alerts From Rain Contamination of OAT Measurements

Installation Effects On AWAS III's Performance Are Unknown

Results Are Not Fully Conclusive For 1991

Flight Test of an Infrared Wind Shear Detector

Questions and Answers

Bob McMillan (Georgia Tech) - I have more of a comment than a question. I would like to tell you why I think the look distance was shorter in Orlando than in Denver. I think it was probably water vapor. There are just thousands of water vapor lines scattered through the infrared. I am sure that the humidity was higher in Orlando. So it was not liquid water so much as maybe water vapor.

Burnell McKissick (NASA Langley) - There were lots of events that contained short look distances for Denver too.

Pat Adamson (Turbulence Prediction Systems) - We had similar data in Orlando in 1990 and we had considerably longer look distances. Two things that I think are important, one is that these look distances are radically different than the installation on a research aircraft that we flew in 1990, a Cessna Citation, and they are radically different from both the Northwest and the American Airlines installations. The second one that I think I should mention, is when we talk about OAT effects, the wet bulb/dry bulb effect on an OAT probe is radically increased as a function of airspeed. So when we talk about overshoots from OAT at 230 or 240 knots it is considerably different than the overshoot at 140 knots. They are quite different in that sense. As far as look distance is concerned, these were very different. We had a meeting a few weeks ago to look at these issues and the first thing we noticed was that we did not have any look distance in this installation. That is one of the things that we will be looking at this year.

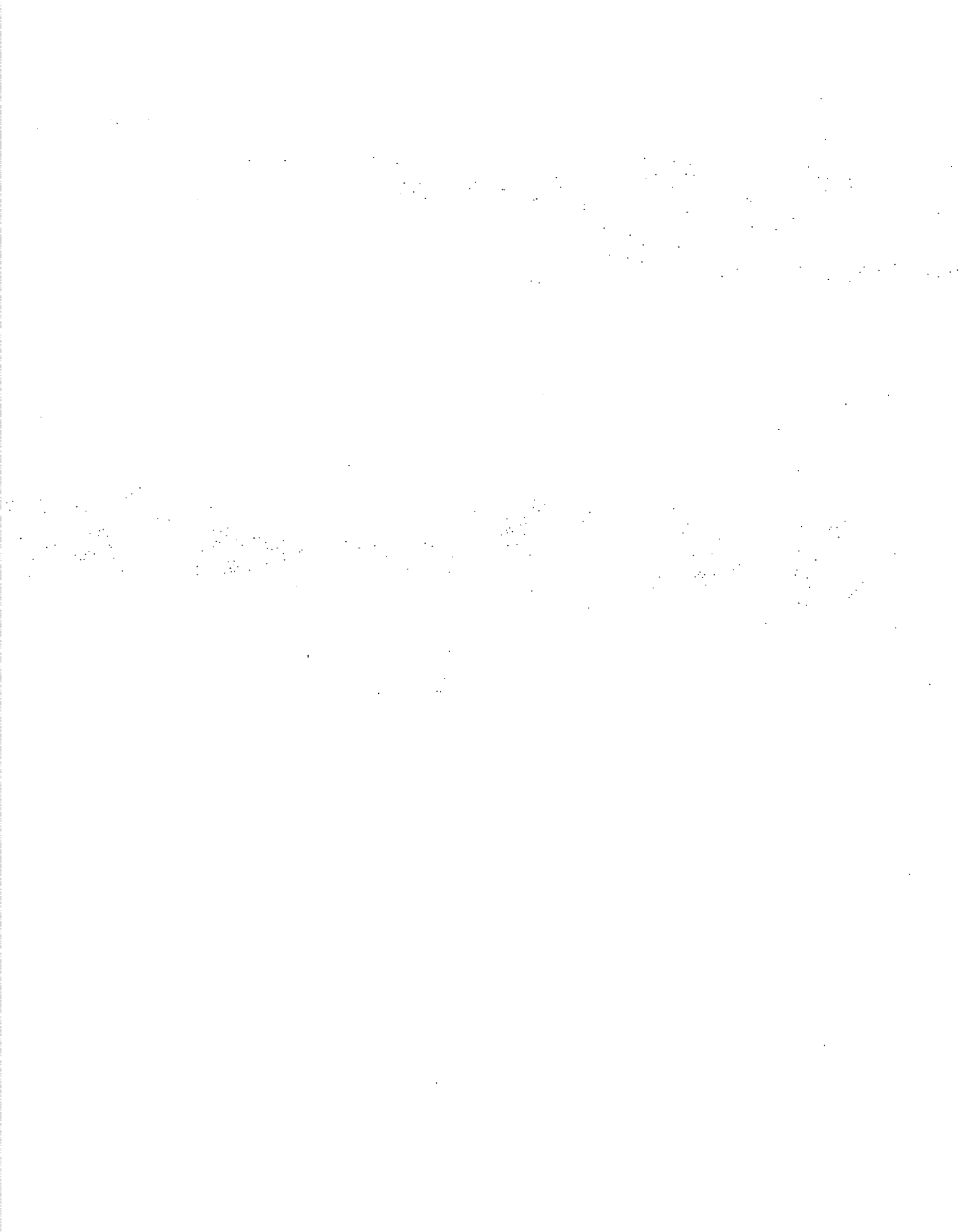
Q: Russell Targ (Lockheed) - In the very beginning and again at the end you said the jury is still out as to whether the temperature sensing scheme will actually measure microburst. What is your criterion going to be for you to determine whether or not this technology does what you want it to do? What are you looking to see?

A: Burnell McKissick (NASA Langley) - We are looking to see alerts at the appropriate time which match up with alerts generated by our In Situ system. So we are sort of bottom lining the whole thing with an alert at the right time, and the right event. Will it indicate a wind shear where there is actually a wind shear. The issue of relating the temperature measurements to the wind shear is one that people are still working on, and it is very interesting, but we are sort of at the bottom line of the whole thing.

Q: Russell Targ (Lockheed) - You show a mixture of missed alerts and false alarms and I am wondering how much of that is acceptable in your quantitative judgment?

A: Burnell McKissick (NASA Langley) - Well, certainly we would like to see less. No one wants to see false alarms. I would like to see less alerts from my stand point, and just a clearer picture of the whole thing. I am not going to say it won't work, there is indication that there is a possibility for it. But there is also room for improvement as there are in the other sensors too.

Session II. Hazard Characterization



1993010408 488715
188

Session II. Hazard Characterization

N93-19597

Wind Shear Hazard Determination
Mike Lewis, NASA Langley Research Center

WIND SHEAR HAZARD DETERMINATION

MICHAEL S. LEWIS

DEPUTY MANAGER

NASA/FAA WIND SHEAR
AIRBORNE SENSORS PROGRAM

4/14/92

**F-FACTOR RELATIONSHIP WITH
AIRCRAFT PERFORMANCE**

$$\gamma_p = \frac{T-D}{W} - F$$

• F = LOSS OF POTENTIAL GAMMA DUE TO WIND SHEAR
(RADIAN; 0.10 RAD = ~6 DEG.)

• F IS ADDITIVE WITH (T-D)/W

TYPICAL INSTALLED (T-D)/W	0.17 (2 ENGINE)
	0.13 (3 ENGINE)
	0.11 (4 ENGINE)

F-FACTOR FORMULATIONS

$$F = \frac{\dot{W}_I \hat{e}_a}{g} \frac{W_h}{V_a} \quad (3-D)$$

$$\approx \frac{1}{g} \frac{\partial W_x}{\partial t} \frac{W_h}{V_a} \quad (2-D, \text{ SMALL GAMMA})$$

$$\approx \frac{V_g \partial W_x}{g \partial x} \frac{W_h}{V_a} \quad (\text{DOPPLER})$$

- ALL OF THESE EQUATIONS DETERMINE SHEAR MAGNITUDE
- NONE OF THESE EQUATIONS DETERMINE SHEAR HAZARD
- TURBULENCE PRODUCES LARGE F - FACTOR VALUES:
 - THEY ARE OF SHORT DURATION
 - THEY ARE TYPICALLY FOLLOWED BY EQUALLY LARGE NEGATIVE VALUES

WIND SHEAR HAZARD
IS A FUNCTION OF F-FACTOR
MAGNITUDE AND DURATION

- WHAT MAGNITUDE?
- HOW LONG?

THE FBAR INDEX

DEFINE $\bar{F} = \frac{1}{L} \int_0^L F dx$

THEN, $\bar{F} = \frac{1}{L} \int_0^L \left(\frac{T-D}{W} \right) dx - \frac{\Delta(V_a^2)}{2 g L} - \frac{\Delta h}{L}$

ASSUME:

INITIAL GAMMA ((T-D)/W):
(MAX GAMMA 0.17, 0.13, 0.11)

PILOT DELAY:

ENGINE RESPONSE TIME:

INITIAL A/S

2 ENGINE:

3 ENGINE:

4 ENGINE:

AIRSPEED LOSS:

REQUIRED GAMMA:

ACCEPTABLE DEVIATION

FROM REQ'D GAMMA:

TAKEOFF

0 DEG

0 SEC

0 SEC

125 KTS

135 KTS

145 KTS

15 KTS

1 DEG

0 FT

LANDING

-3 DEG

5 SEC

3 SEC

140 KTS

150 KTS

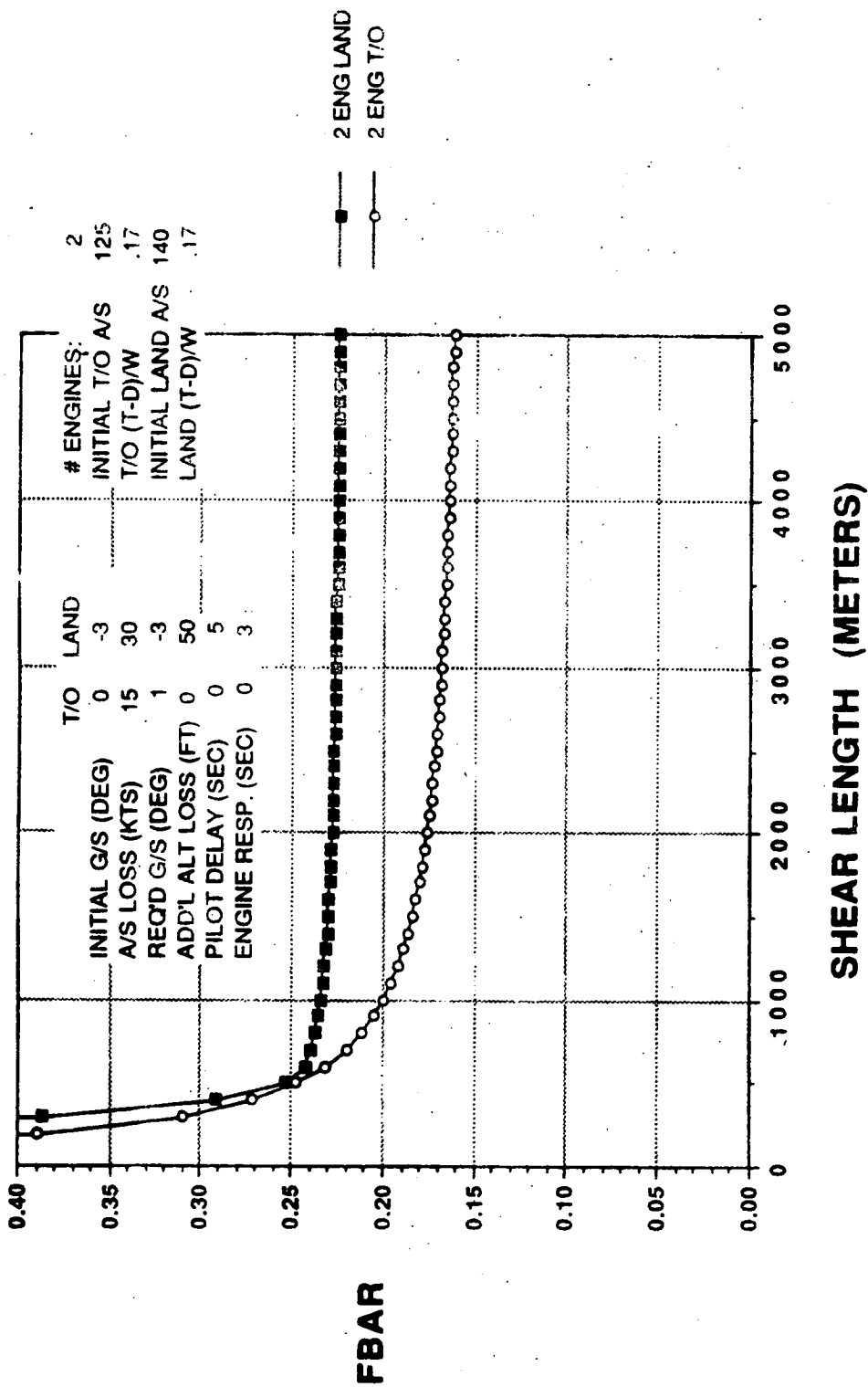
160 KTS

30 KTS

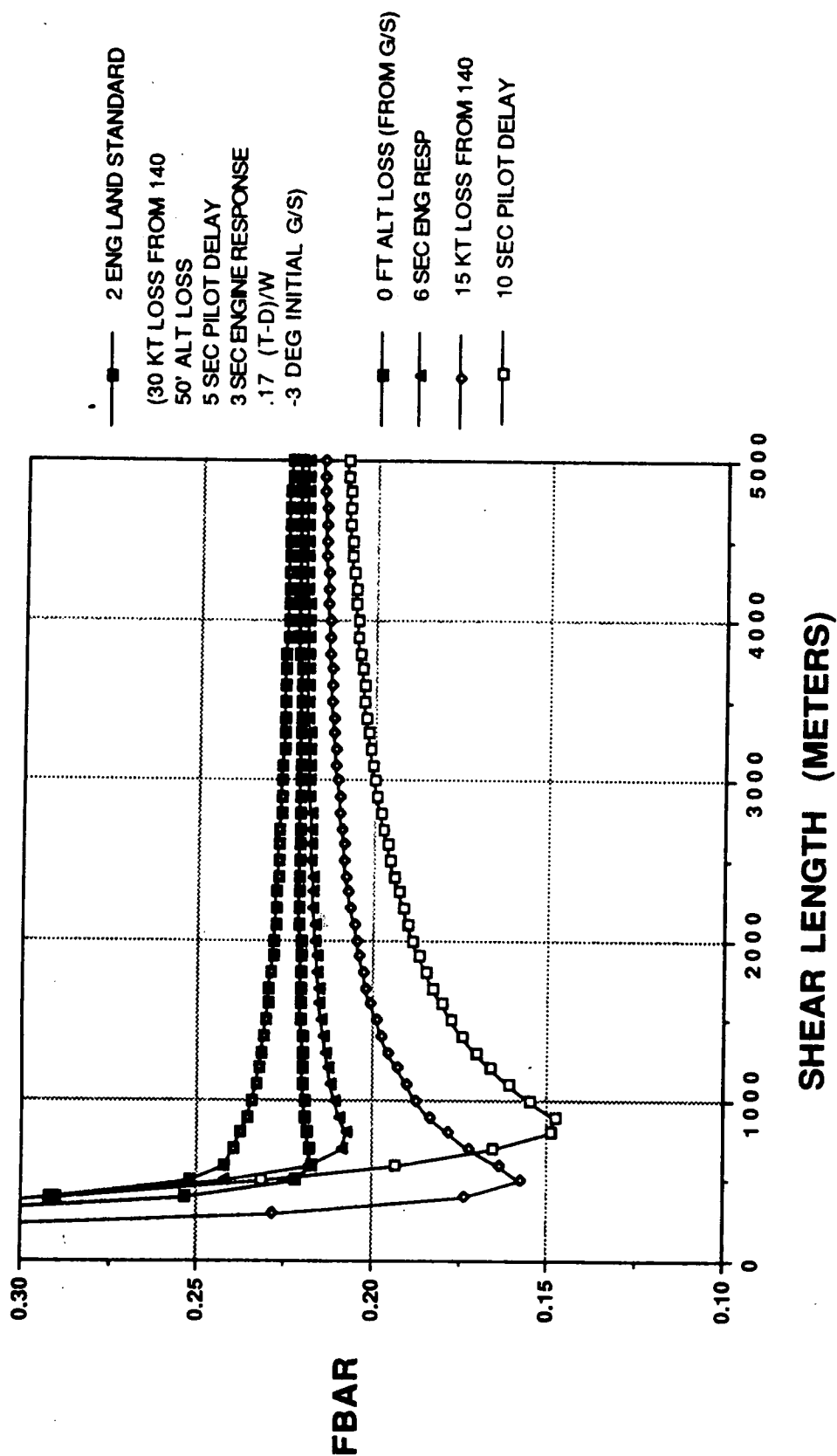
-3 DEG

50 FT

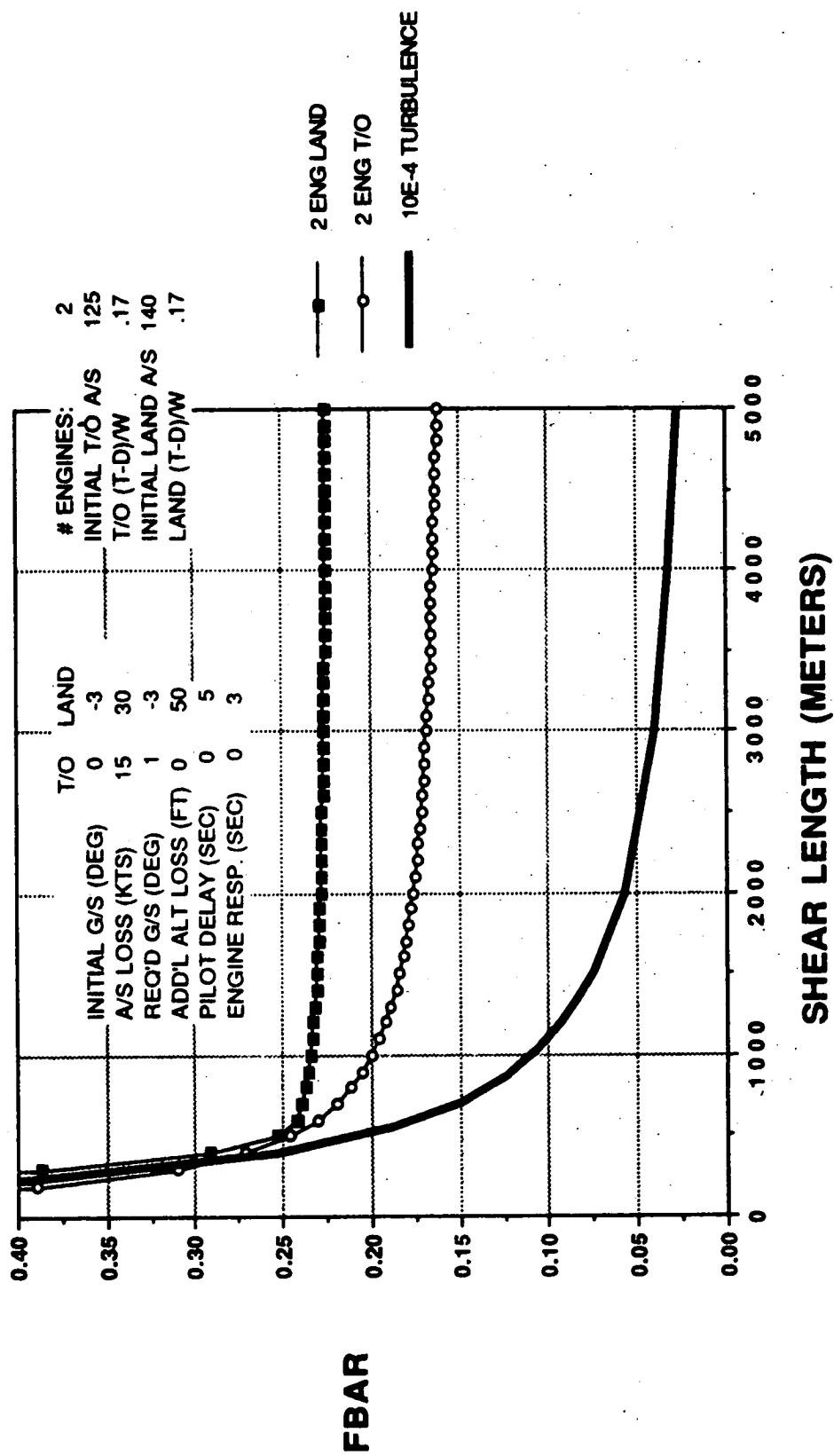
F-FACTOR HAZARD LIMIT



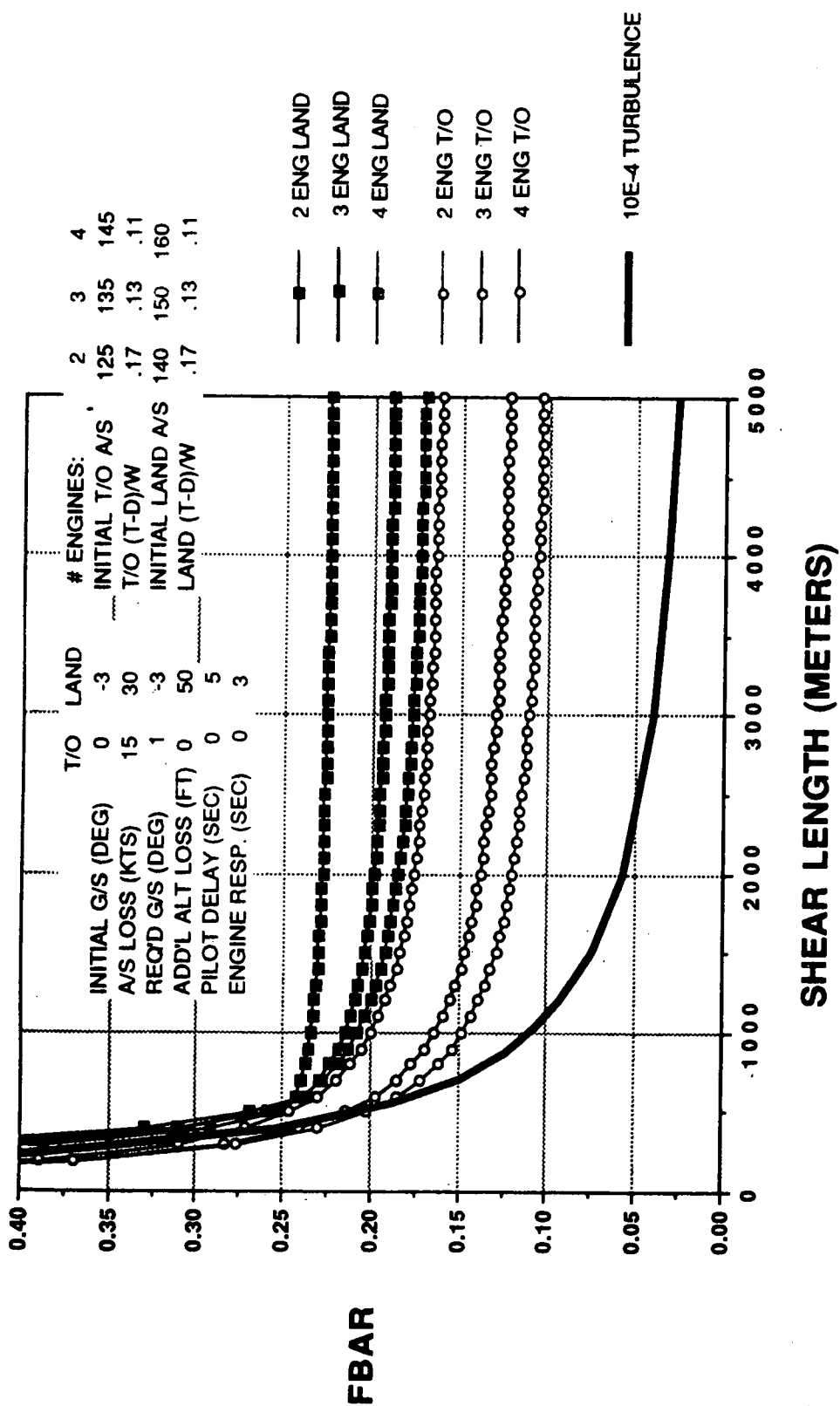
F-FACTOR HAZARD LIMIT PARAMETER SENSITIVITY



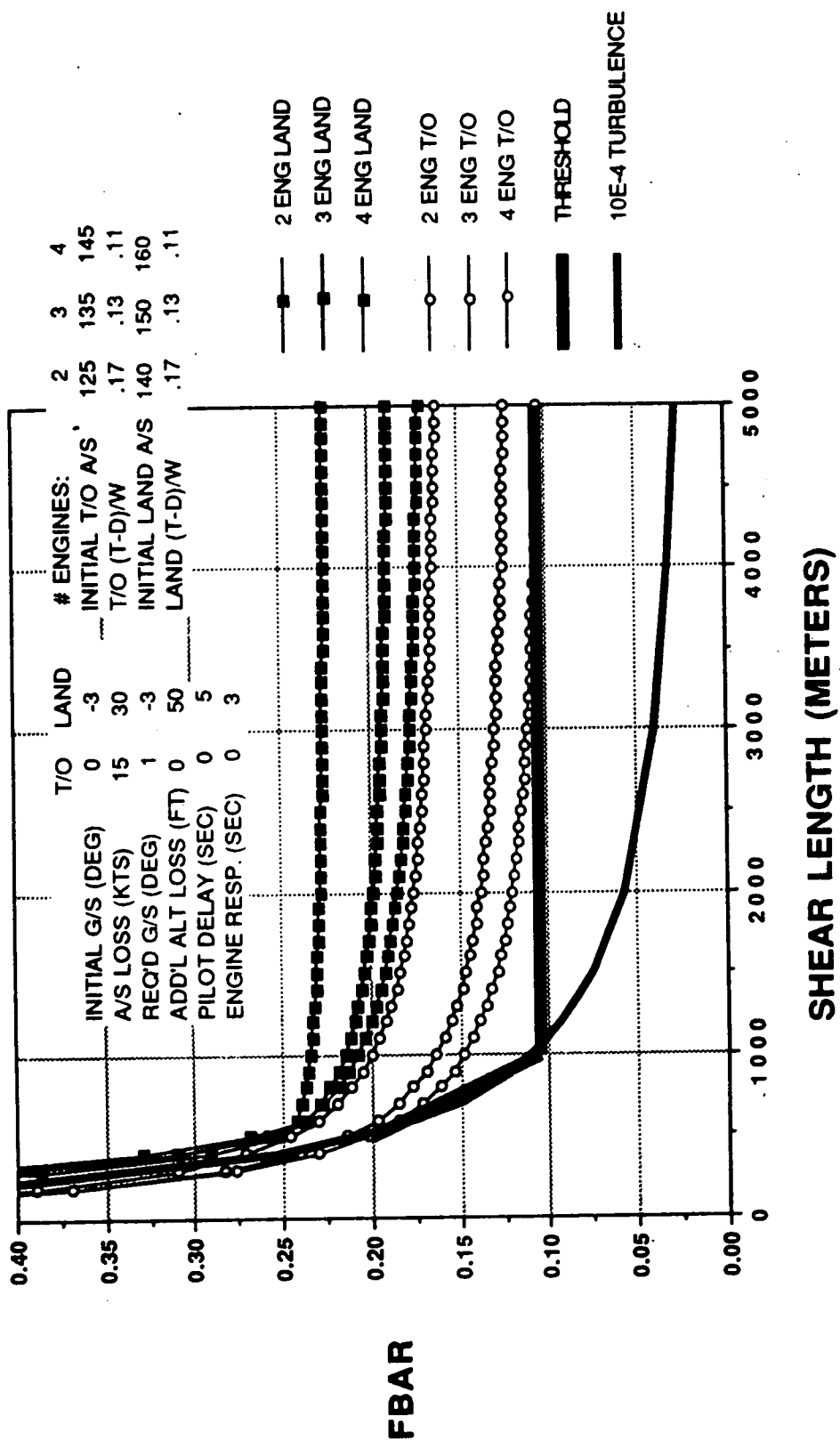
F-FACTOR HAZARD LIMIT



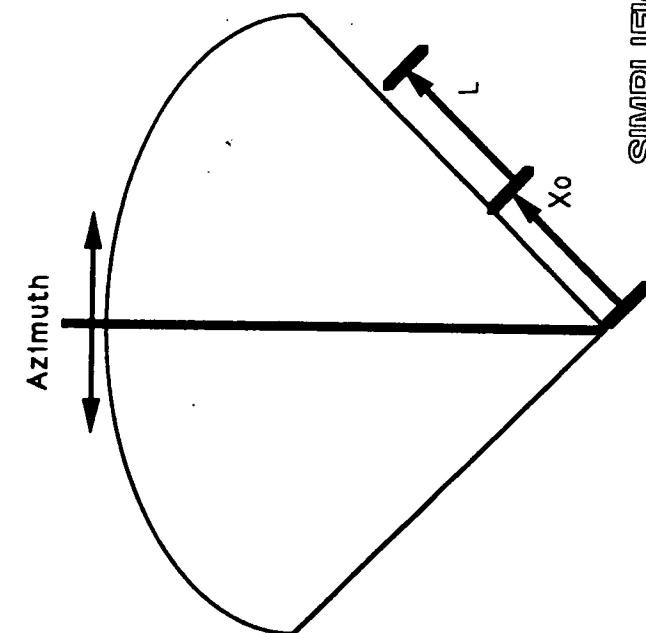
F-FACTOR HAZARD LIMIT



F-FACTOR HAZARD LIMIT



FBAR WITH DOPPLER SENSORS



$$\bar{F} = \frac{1}{L} \int_{x_0}^{x_0+L} F \, dx$$

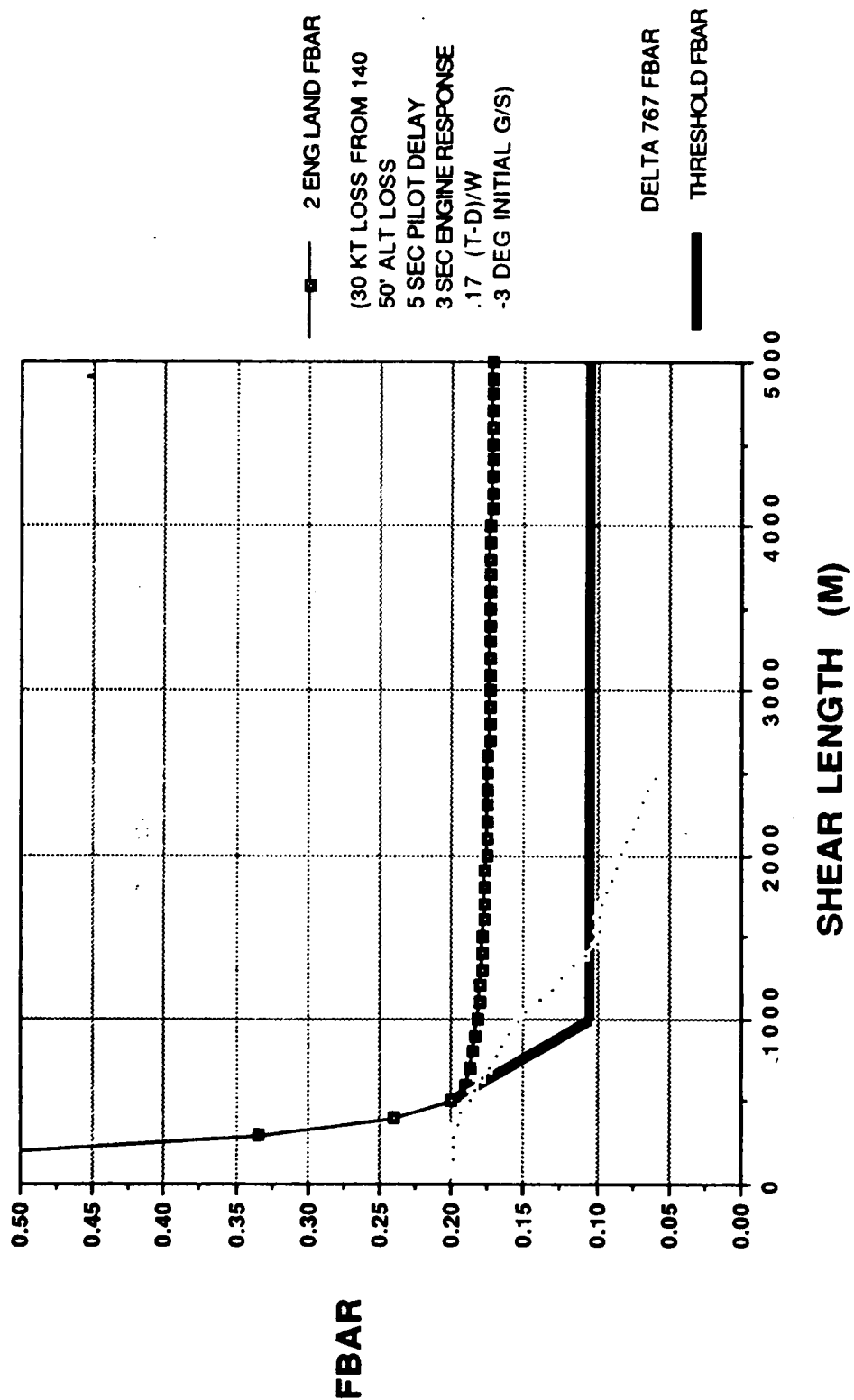
EVALUATE EVERY SCAN:

- AT EVERY AZIMUTH,
- FOR EVERY x_0 ,
- AND EVERY L

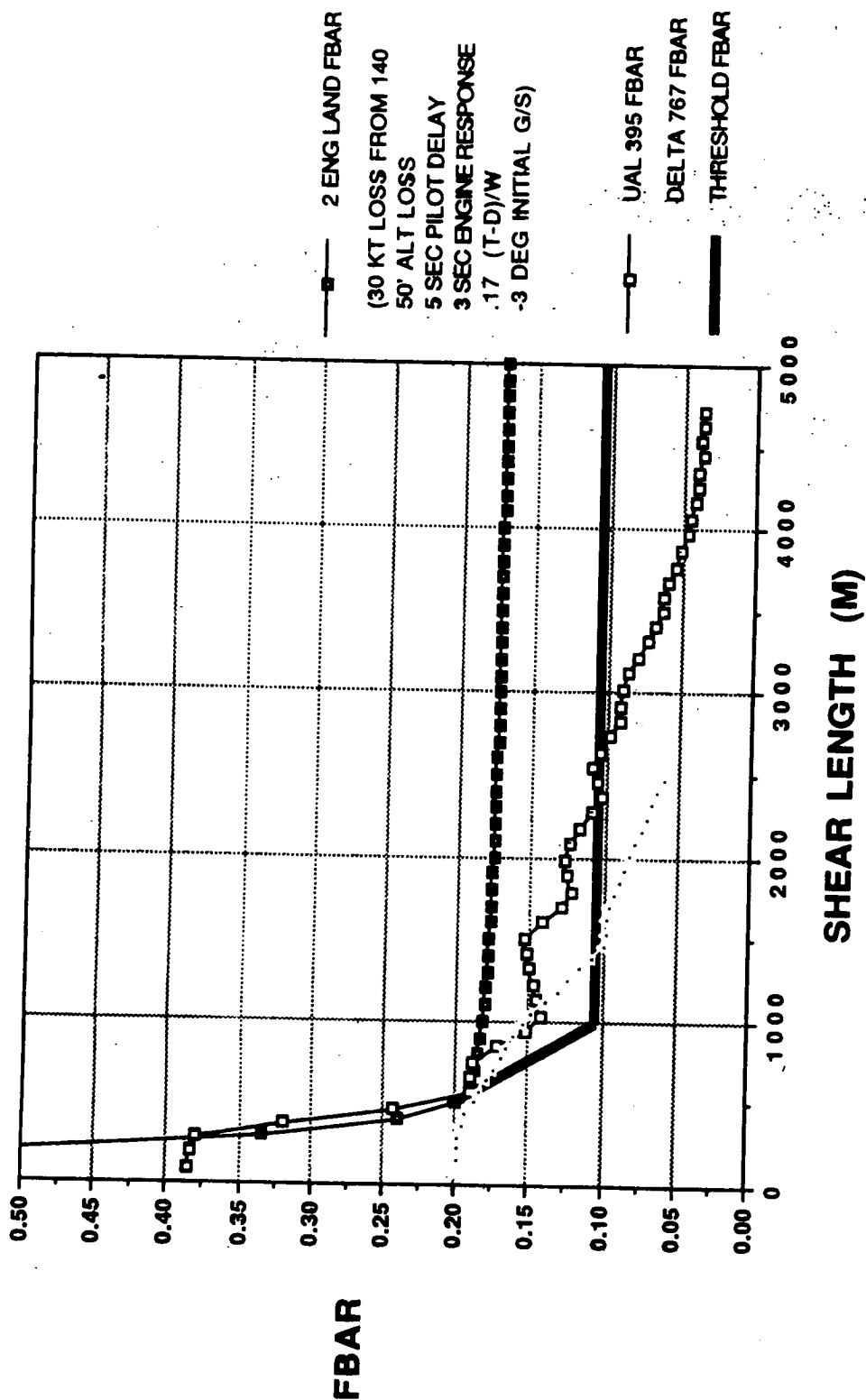
SIMPLIFICATIONS/PRACTICAL CONSIDERATIONS:

- TEST ONLY $L = 1000 \text{ M}$
- REQUIRE MINIMUM CONTIGUOUS AZIMUTH EXCEED.
- REQUIRE MULTIPLE SCAN EXCEEDANCES
- OTHERS

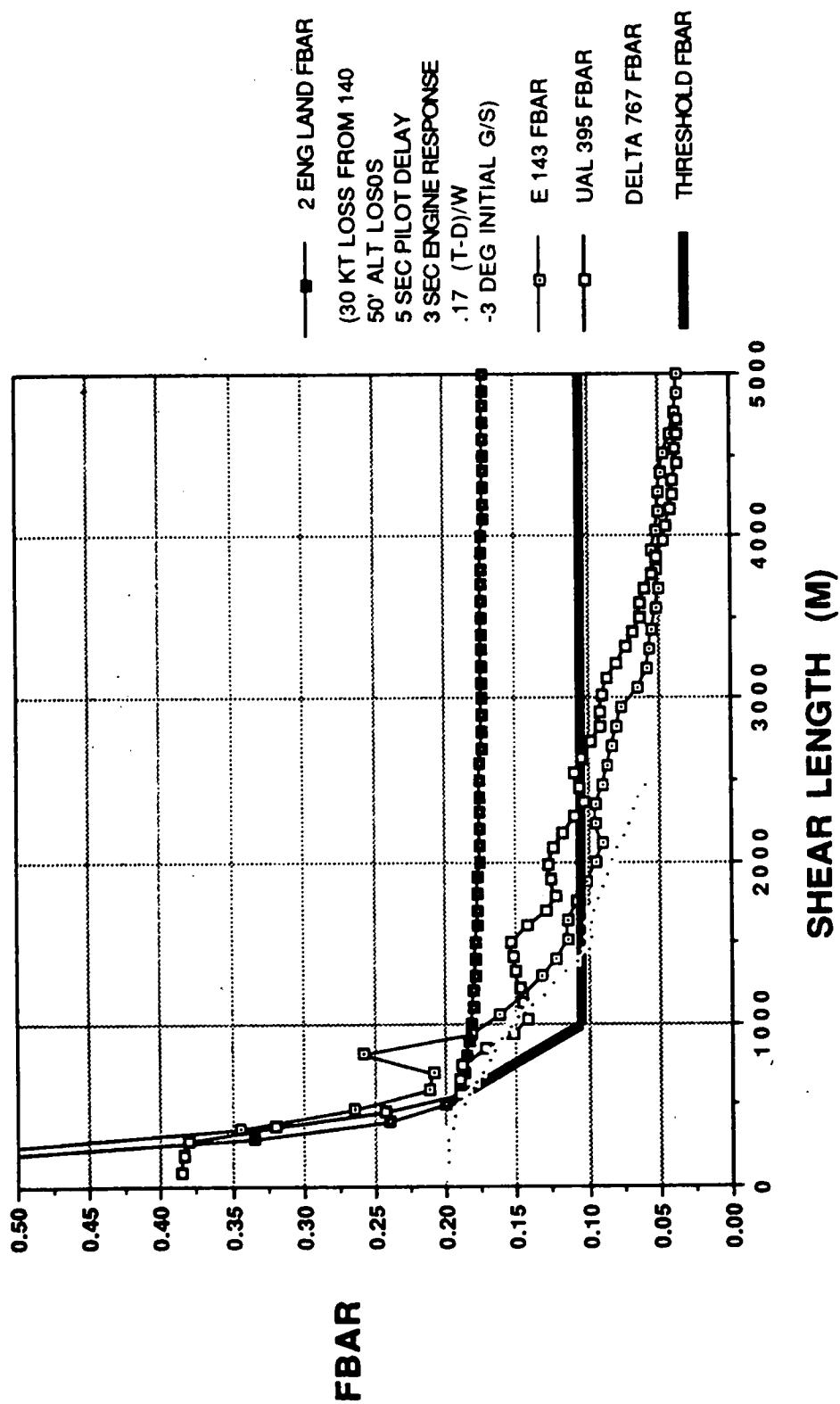
FBAR PROFILE COMPOSITE



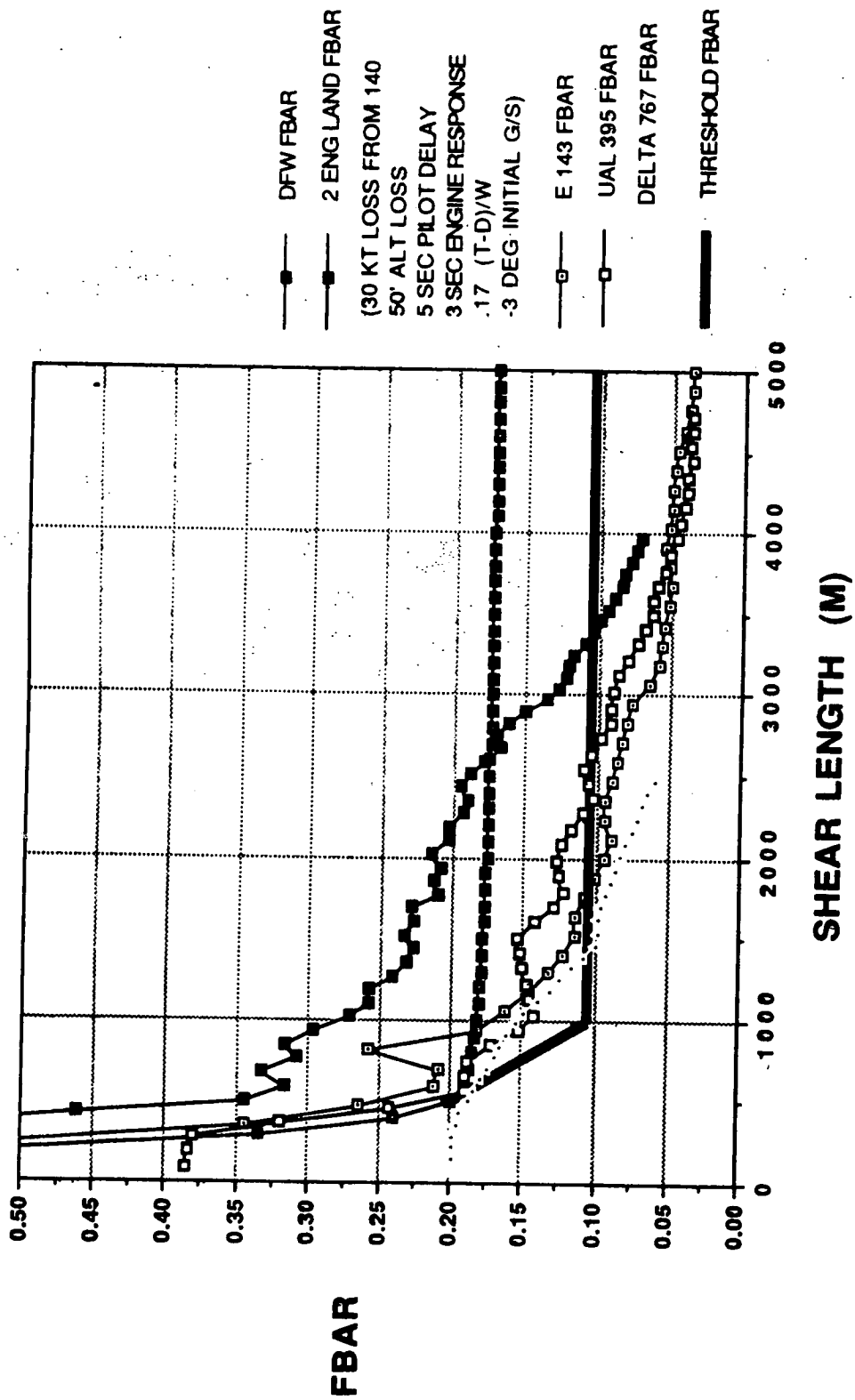
FBAR PROFILE COMPOSITE



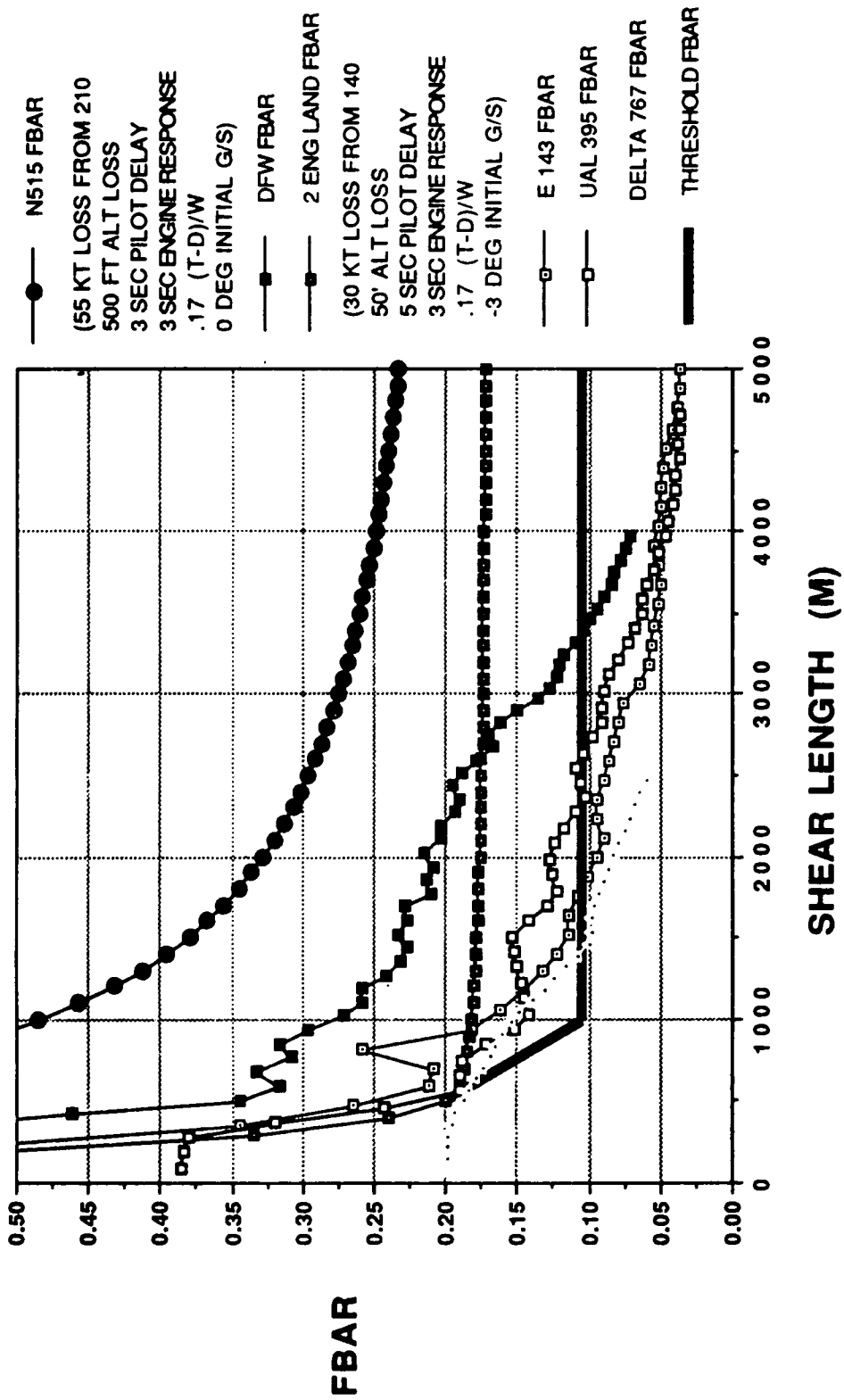
FBAR PROFILE COMPOSITE



FBAR PROFILE COMPOSITE



FBAR PROFILE COMPOSITE



1993010409

Session II. Hazard Characterization

N93-19598

488717

44P

Three-Dimensional Numerical Simulation of the 20 June 1991, Orlando Microburst
Dr. Fred Proctor, NASA Langley Research Center

PRECEDING PAGE BLANK NOT FILMED

THREE-DIMENSIONAL NUMERICAL SIMULATION OF THE 20 JUNE 1991, ORLANDO MICROBURST

FRED H. PROCTOR

NASA-LANGLEY RESEARCH CENTER
Flight Management Division
HAMPTON, VA 23665

14 APRIL 1992

**FOURTH COMBINED MANUFACTURERS' AND TECHNOLOGISTS'
WIND SHEAR REVIEW MEETING**

OUTLINE OF ORLANDO 20 JUNE 1991 SIMULATION

I. INTRODUCTION

A. TASS MODEL DESCRIPTION

B. INITIAL CONDITIONS

II. RESULTS OF 3-D CASE STUDY

A. DESCRIPTION OF MICROBURST EVOLUTION

B. COMPARISON WITH OBSERVATIONS

C. EVOLUTION OF F-FACTOR FIELDS

**D. COMPARISON OF TEMPERATURE VS
F-FACTOR FIELDS**

III. SUMMARY

EXTENDED ABSTRACT

On June 20, 1991, NASA's Boeing 737, equipped with in-situ and look-ahead wind-shear detection systems, made direct low-level penetrations (300-350 m AGL) through a microburst during several stages of its evolution. This microburst was located roughly 20 km northeast of Orlando International Airport and was monitored by a Terminal Doppler Weather Radar (TDWR) located about 10 km south of the airport. The first NASA encounter with this microburst (Event #142), at ~2041 UTC, was during its intensification phase. At flight level, in-situ measurements indicated a peak 1-km (averaged) F-factor of ~0.1. The second NASA encounter (Event #143) occurred at ~2046 UTC, about the time of microburst peak intensity. It was during this penetration that a peak 1-km F-factor of ~.17 was encountered, which was the largest in-situ measurement of the 1991 summer deployment. By the third encounter (Event #144), at ~2051 UTC, the microburst had expanded into a macroburst. During this phase of evolution, an in-situ 1-km F-factor of 0.08 was measured. Details of these encounters from the perspective of on-board radar, in-situ observation, on-board infrared sensor and TDWR are discussed by various authors elsewhere in the conference proceedings. The focus of this paper is to examine this microburst *via* numerical simulation from an unsteady, three-dimensional meteorological cloud model. The simulated high-resolution data fields of wind, temperature, radar reflectivity factor, and precipitation are closely examined so as to derive information not readily available from "observations" and to enhance our understanding of the actual event. Characteristics of the simulated microburst evolution are compared with TDWR and in-situ measurements.

The model used in the simulation is the Terminal Area Simulation¹ (TASS), which has been previously applied to a number of microburst case studies.^{2,3,4,5,6,7,8} Characteristics of the model are listed in Slide 1 and Tables 1 and 2. The initial conditions for this simulation are listed in Slide 2, and the input sounding for ambient temperature, humidity, and wind is shown in Slide 3. The ambient sounding, observed near the location and time of the microburst, indicates a moist, convectively unstable environment with weak and variable winds.

Results from the simulation are shown in the remaining figures and are summarized in the final slide. The results indicate a high-reflectivity (wet) microburst of moderate intensity whose evolution and structure compare favorably with observations. This microburst, which is generated from the simulated parent

storm, may be characterized by three phases of evolution: 1) an intensification phase, 2) a peak-intensity phase, and 3) a macroburst phase. The intensification phase is initiated by rain forming through collection-coalescence and is associated with increasing values of hazard and velocity differential. According to the model simulation, and verified from "observations", the strongest region of wind-shear hazard at this time is in the northern region of the outflow. The first NASA encounter of the actual microburst took place during this phase of evolution. Several minutes later during the peak-intensity phase, a second surge of heavy rain shifted the strongest hazard regions to the southern portion of the outflow. According to the simulation this second surge was associated with melting of graupel aloft and generated the overall strongest downdraft speeds and wind-shear. During this phase of development, the microburst was again encountered by NASA (Event #143), and in-situ and model data show a complex asymmetric F-factor field. The complex hazard field exists, even though the simulation shows a nearly symmetric *region* of outflow. The model data also indicates that regions of upflow and performance-increase (positive F-factor) are embedded within the microburst outflow, as was true in an earlier case-simulation of another Florida microburst⁶. Hence, hazard regions may be asymmetric and complex even in the weak ambient wind conditions typical of Florida's summer season. Following the time of peak outflow and wind-shear hazard, the outflow continues to expand becoming a macroburst, although with embedded microbursts. The model simulation, in-situ (Event #144), and TDWR data indicate that the embedded microbursts are of weaker magnitude than the primary microburst during intense phase (at least true for this case study).

Local correlation between F-factor and either temperature drop or temperature gradient is not apparent in the data from the simulation. However, as predicted by the empirical formula for maximum wind differential from temperature drop^{5,9}, the simulated temperature drop of about 6°C at the surface corresponds to the simulated peak wind change (at 70 m AGL) of 32 m/s. At flight level (roughly 325 m AGL) and at 37 min simulation time, the maximum temperature drop was 3.5°C, almost half the magnitude of the temperature drop at the ground. Hence as shown in the axisymmetric experiment of wet microburst, the magnitude of temperature drop is greatest near the ground and markedly decreases with altitude^{4,5}.

REFERENCES

1. Proctor, F. H., 1987: *The Terminal Area Simulation System. Volume I: Theoretical formulation.* NASA Contractor Rep. 4046, NASA, Washington, DC, 176 pp. [Available from NTIS]
2. Proctor, F. H., 1987: *The Terminal Area Simulation System. Volume II: Verification Experiments.* NASA Contractor Rep. 4047, NASA, Washington, DC, 112 pp. [Available from NTIS]
3. Proctor, F. H., 1988: Numerical simulation of the 2 August 1985 DFW microburst with the three-dimensional Terminal Area Simulation System. Preprints Joint Session of 15th Conf. on Severe Local Storms and Eighth Conf. on Numerical Weather Pred., Baltimore, Amer. Meteor. Soc., J99-J102.
4. Proctor, F. H., 1988: Numerical simulations of an isolated microburst. Part I: Dynamics and structure. J. Atmos. Sci., **45**, 3137-3160.
5. Proctor, F. H., 1989: Numerical simulations of an isolated microburst. Part II: Sensitivity experiments. J. Atmos. Sci., **46**, 2143-2165.
6. Proctor, F. H., 1990: Three-dimensional numerical simulation of a Florida microburst: The 7 July 1990 Orlando event. *Airborne Wind Shear Detection and Warning Systems, Third Combined Manufacturers' and Technologists' Airborne Wind Shear Review Meeting*, Hampton, VA, NASA Conf. Publication 10060, Part I, 81-103. [Available from NTIS]
7. Proctor, F. H., and R. L. Bowles, 1990: Three-dimensional simulation of the Denver 11 July storm of 1988: An intense microburst event. Preprints, 16th Conf. on Severe Local Storms and the Conf. on Atmos. Electricity, Kananaskis Park, Amer. Meteor. Soc., 373-378.
8. Proctor, F. H., and R. L. Bowles, 1992: Three-dimensional simulation of the Denver 11 July 1988 microburst-producing storm. Accepted for publication in Meteorol. and Atmos. Phys., **47**.
9. Proctor, F. H., 1989: A relation between peak temperature drop and velocity differential in a microburst. Preprints Third International Conf. on the Aviation Wea. System., Anaheim, Amer. Meteor. Soc., 5-8.

TERMINAL AREA SIMULATION SYSTEM (TASS)

[ALSO KNOWN AS THE NASA WINDSHEAR MODEL]

- o 3-D TIME DEPENDENT EQUATIONS FOR COMPRESSIBLE NONHYDROSTATIC FLUIDS**
- o PROGNOSTIC EQUATIONS FOR 11 VARIABLES**
 - 1. 3-COMPONENTS OF VELOCITY**
 - 2. PRESSURE**
 - 3. POTENTIAL TEMPERATURE**
 - 4. WATER VAPOR**
 - 5. LIQUID CLOUD DROPLETS**
 - 6. CLOUD ICE CRYSTALS**
 - 7. RAIN**
 - 8. SNOW**
 - 9. HAIL/GRAUPEL**
- o 1st-ORDER SUBGRID TURBULENCE CLOSURE WITH RICHARDSON NUMBER DEPENDENCY**
- o SURFACE FRICTION LAYER BASED ON MONIN-OBUKHOV SIMILARITY THEORY**
- o OPEN LATERAL BOUNDARY CONDITIONS ALLOWING MINIMAL REFLECTION**
- o BULK PARAMETERIZATIONS OF CLOUD MICROPHYSICS**

SLIDE 1

Table 1. Sallent Characteristics of TASS 2.4

Compressible, nonhydrostatic equation set
Non-Boussinesq formulation for density variations
Three-dimensional staggered grid with stretched vertical spacing
Movable, storm-centering mesh
Explicit time-split, second-order, Adams-Bashforth time differencing and second-order quadratic-conservative space differencing for velocity and pressure
Fourth-order quadratic-conservative space differencing and third-order Adams-Bashforth time differencing for temperature and water-vapor equations
Third-order time/space differencing with upstream-biased quadratic interpolation for liquid and frozen water substance equations
Radiation boundary conditions applied to open lateral boundaries
Filter and Sponge applied to top four rows in order to diminish gravity wave reflection at top boundary
No explicit numerical filtering applied to interior points
Surface friction layer based on Monin-Obukhov Similarity theory
Smagorinsky subgrid-turbulence closure with Richardson number dependence
Liquid and ice-phase microphysics
Inverse-exponential size distributions assumed for rain, hail/graupel, and snow
Raindrop intercept function of amount of rainwater ⁵
Snow treated as spherical, low-density graupel-like snow particles
Wet and dry hail growth
Accumulated precipitation advected opposite of grid motion, so as to remain ground relative

Table 2. Cloud Microphysical Interactions

Accretion of cloud droplets by rain

Condensation of water vapor into cloud droplets

Berry-Reinhardt formulation for autoconversion of cloud droplet water into rain

Evaporation of rain and cloud droplets

Spontaneous freezing of supercooled cloud droplets and rain

Initiation of cloud ice crystals

Ice crystal and snow growth due to riming

Vapor deposition and sublimation of hail/graupel, snow, and cloud ice crystals

Accretion by hail/graupel of cloud droplets, cloud ice crystals, rain, and snow

Contact freezing of supercooled rain resulting from collisions with cloud ice crystals or snow

Production of hail/graupel from snow riming

Melting of cloud ice crystals, snow, and hail/graupel

Shedding of unfrozen water during hail wet growth

Shedding of water from melting hail/graupel and snow

Conversion of cloud ice crystals into snow

Accretion by snow of cloud droplets, cloud ice crystals, and rain

Evaporation or vapor condensation on melting hail/graupel and snow

Orlando, FL, 20 June 1991, Simulation

INPUT DATA / ASSUMPTIONS

PHYSICAL DOMAIN SIZE

- O X,Y: 15 KM x 15 KM
- O Z: 18 KM

COMPUTATIONAL RESOLUTION

- O HORIZONTAL - 150 M (103 X 103 GRID POINTS)
- O VERTICAL - 70 M NEAR GROUND STRETCHING TO
440 M AT 18 KM (72 LEVELS)

CONVECTIVE INITIATION AT MODEL TIME ZERO

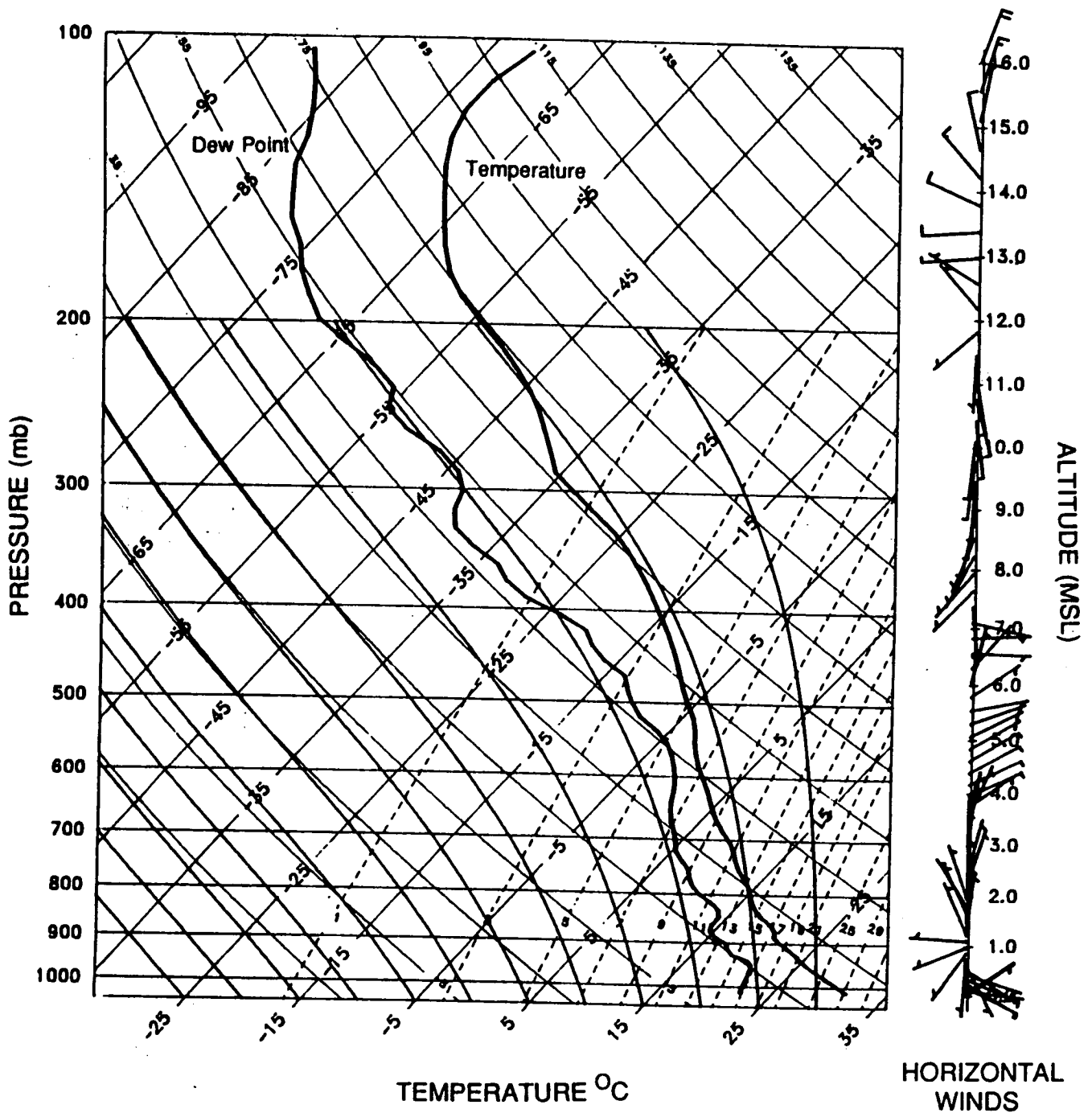
- O SPHEROIDAL THERMAL IMPULSE
- O DIMENSIONS - 7 KM HORIZONTAL x 1.25 KM VERTICAL
- O AMPLITUDE - 1.5° C

**SOUNDING OBSERVED NEAR TIME AND LOCATION OF STORM
(from special rawinsonde launch 2035 UTC)**

**SUB-CLOUD HUMIDITY AND TEMPERATURE MODIFIED USING
NASA AIRCRAFT MEASUREMENTS TAKEN NEAR THE TIME AND
LOCATION OF THE STORM**

SLIDE 2

Orlando, Fl, 20 June 1991
Special sounding - 2035 UTC



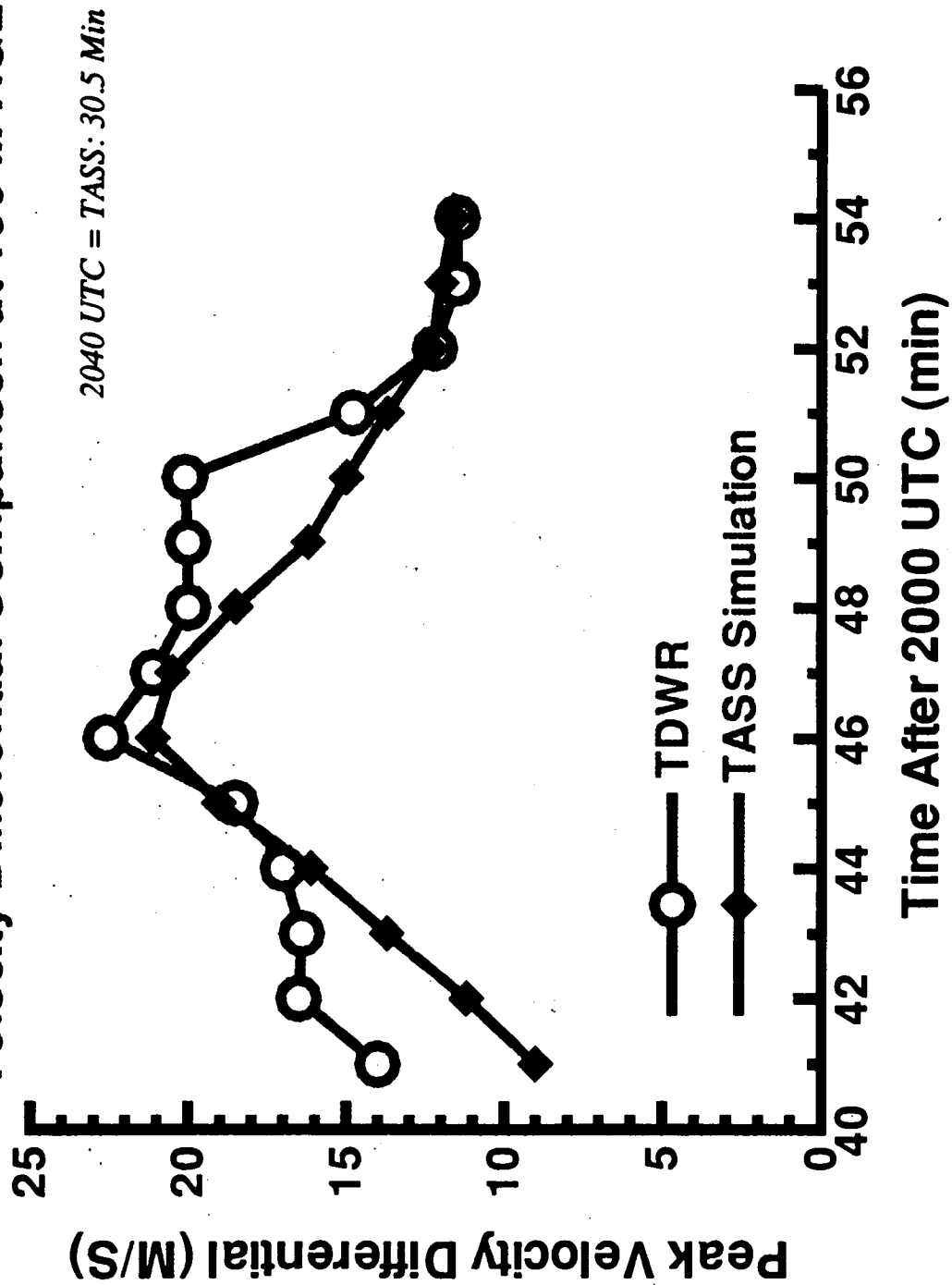
SLIDE 3

20 JUNE 1991 MICROBURST

- O MICROBURST ENCOUNTERED BY NASA AIRCRAFT 3 TIMES**
 - 1. FIRST ENCOUNTER (~2041 UTC) DURING INTENSIFICATION STAGE (EVENT #142).**
 - 2. 2ND ENCOUNTER (~2046) DURING PEAK INTENSITY (EVENT #143).**
 - 3. 3RD ENCOUNTER (~2051) DURING MACROBURST STAGE (EVENT #144).**
- O DURING INTENSIFICATION PHASE, MODEL AND OBSERVED RESULTS SHOW STRONGEST SHEAR AND DOWNFLOW IN NORTHERN REGION OF OUTFLOW.**
- O MODEL AND OBSERVED RESULTS INDICATE MAXIMUM SHEAR AND DOWNFLOW IN SOUTHERN REGION OF OUTFLOW DURING PEAK INTENSITY.**
- O MODEL RESULTS INDICATE MICROBURST INITIATED BY RAIN FORMED THROUGH COLLECTION-COALESCENCE.**
- O ACCORDING TO MODEL SIMULATION, THE MICROBURST IS ENHANCED DURING PEAK-INTENSITY PHASE BY A SECOND SURGE OF PRECIPITATION.**
- O THIS SECOND SURGE -- ASSOCIATED WITH RAIN FROM MELTING GRAUPEL -- GENERATES STRONGEST SHEAR AND DOWNDRAFT SPEEDS IN SOUTHERN SECTOR.**

20 JUN 1991 ORLANDO MICROBURST

Velocity Differential Comparison at 190 M AGL



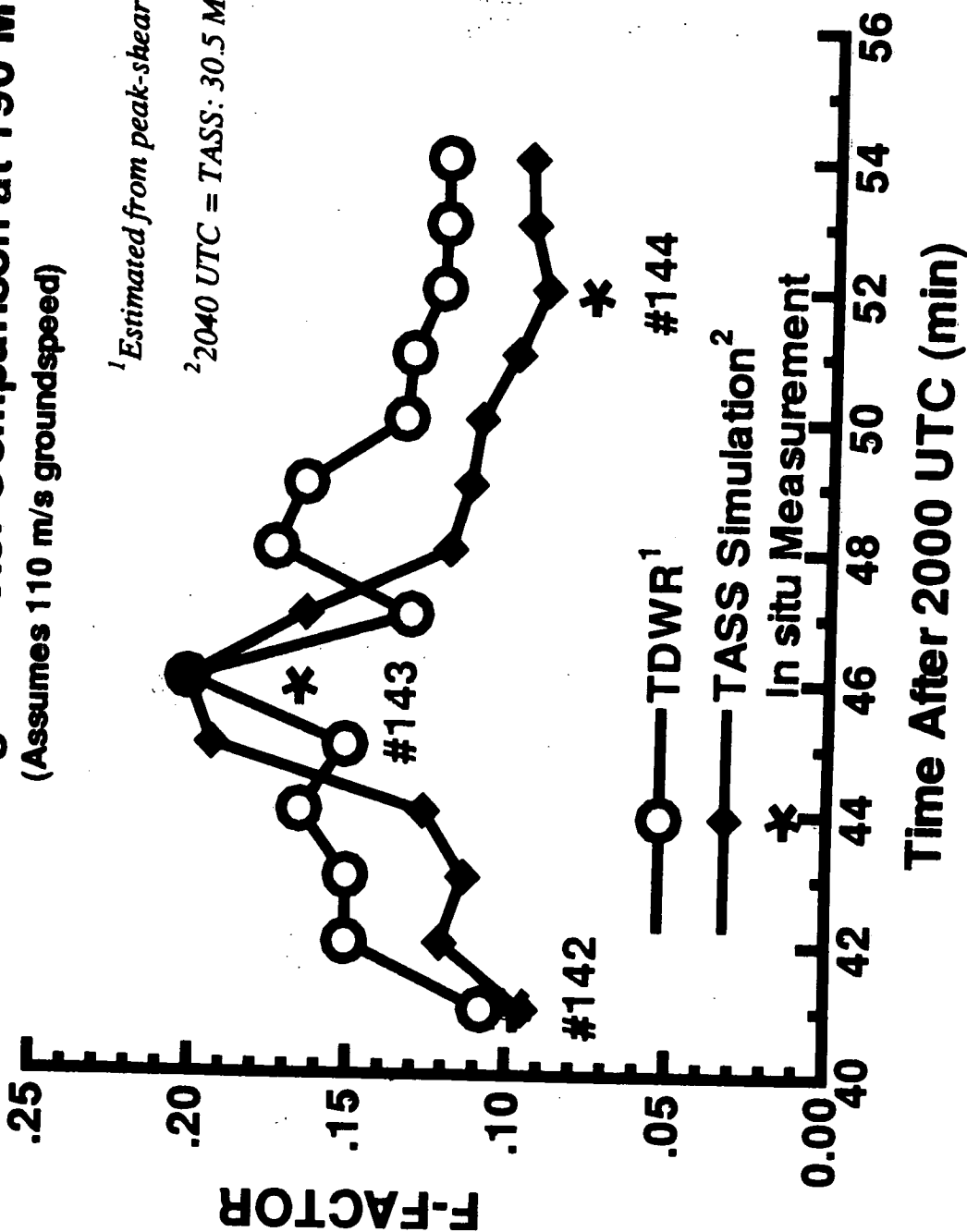
20 JUN 1991 ORLANDO MICROBURST

Peak 1-Km Avg F-Factor Comparison at 190 M AGL

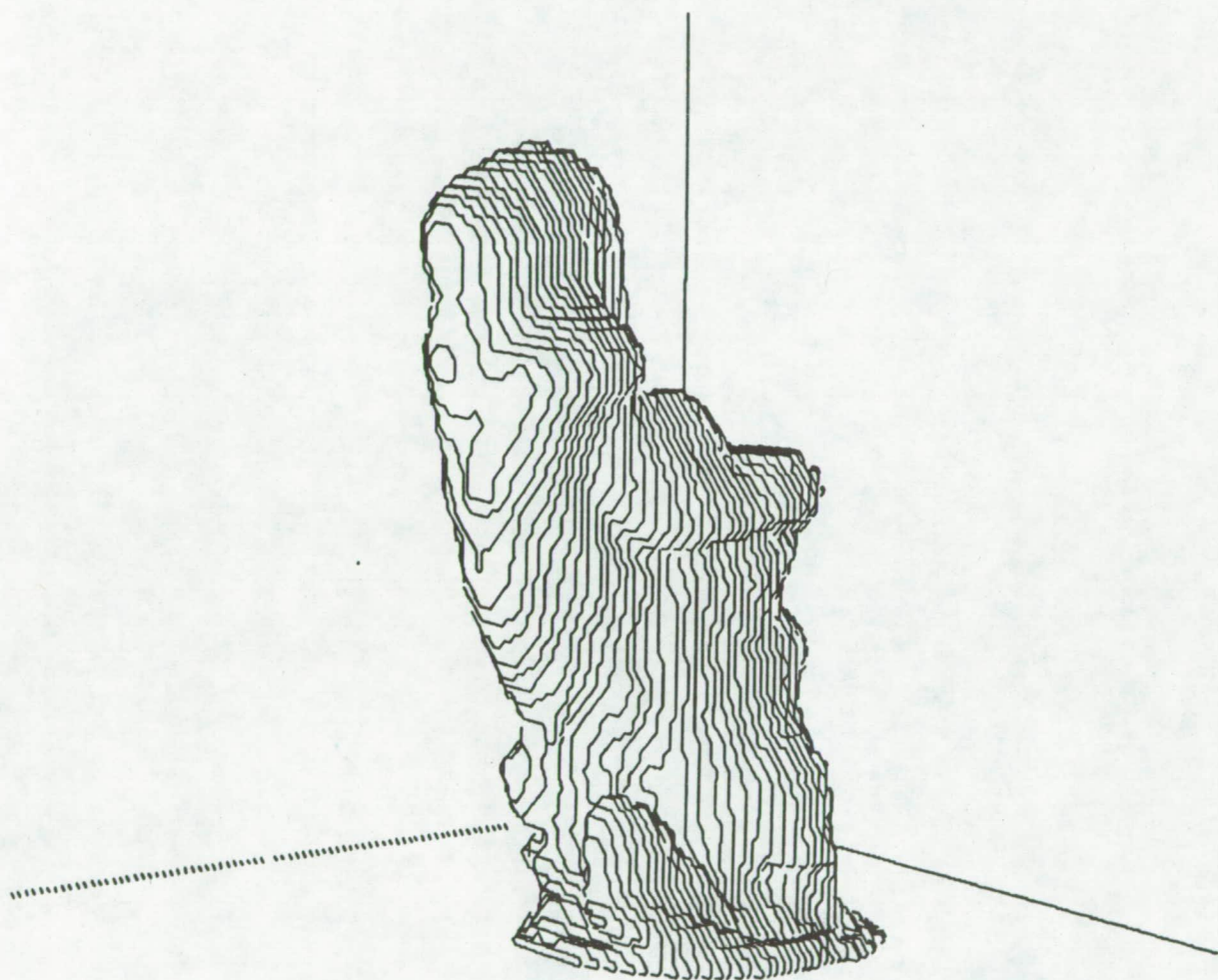
(Assumes 110 m/s groundspeed)

¹ Estimated from peak-shear segments

² 2040 UTC = TASS: 30.5 Min



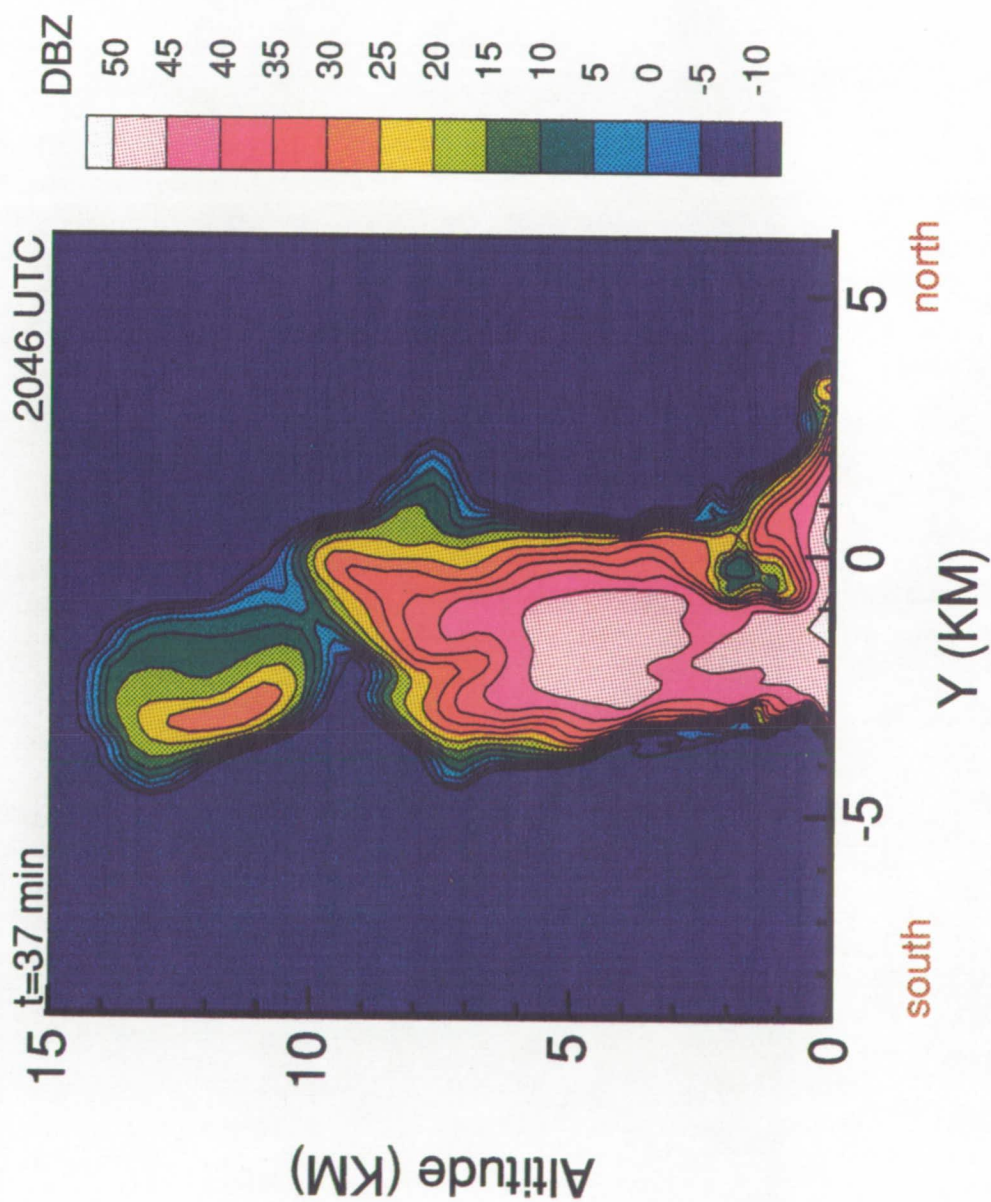
**TASS 3-D SIMULATION -- ORLANDO MICROBURST
3-D PERSPECTIVE OF STORM**



**10 DBZ RADAR REFLECTIVITY SURFACE VIEWED FROM NE
AT 36 MIN (2045 UTC)
STORM TOP AT 14 KM**

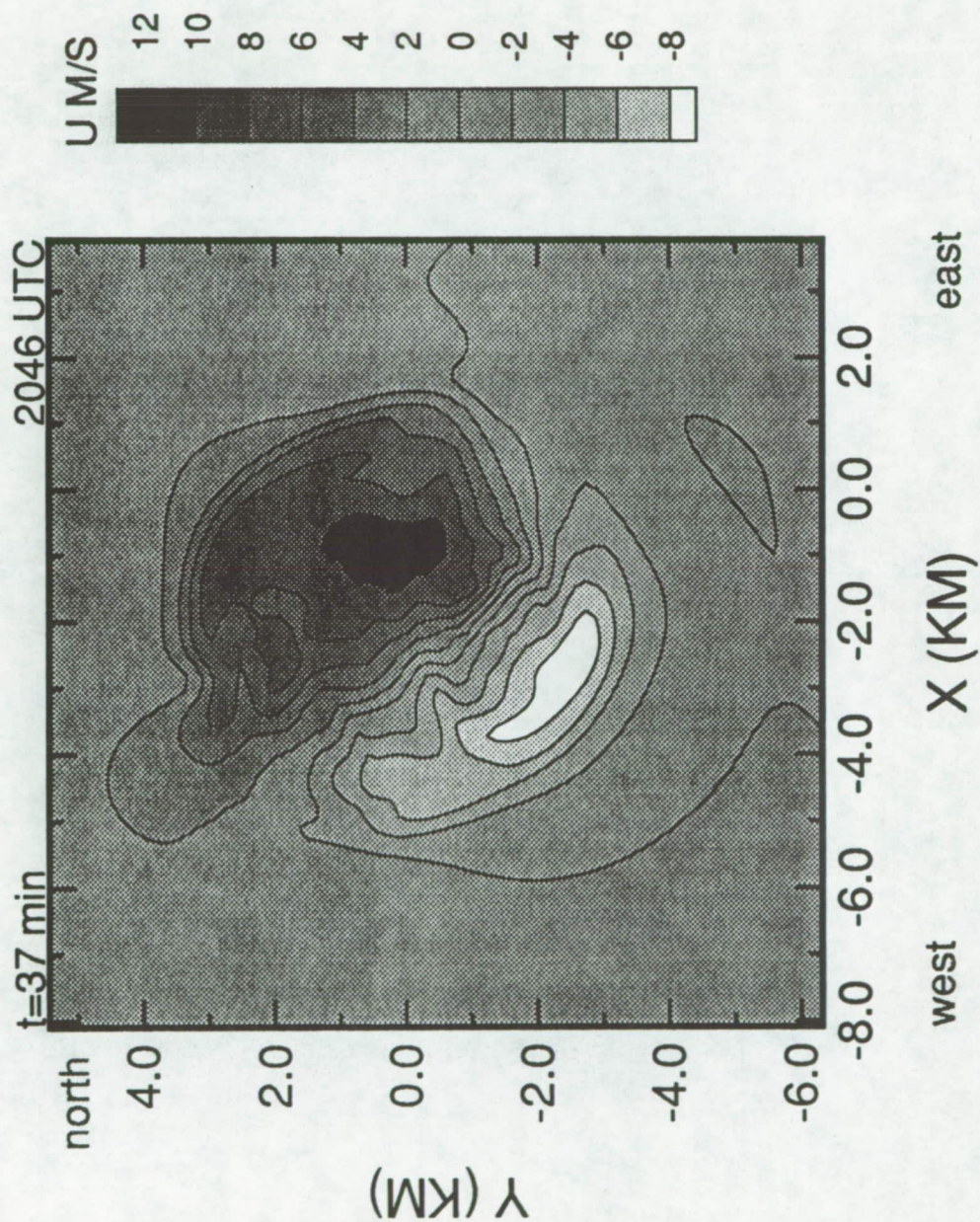
ORLANDO 20 JUNE 1991 MICROBURST SIMULATION

VERTICAL CROSS-SECTION OF RADAR REFLECTIVITY



ORIGINAL PAGE
COLOR PHOTOGRAPH

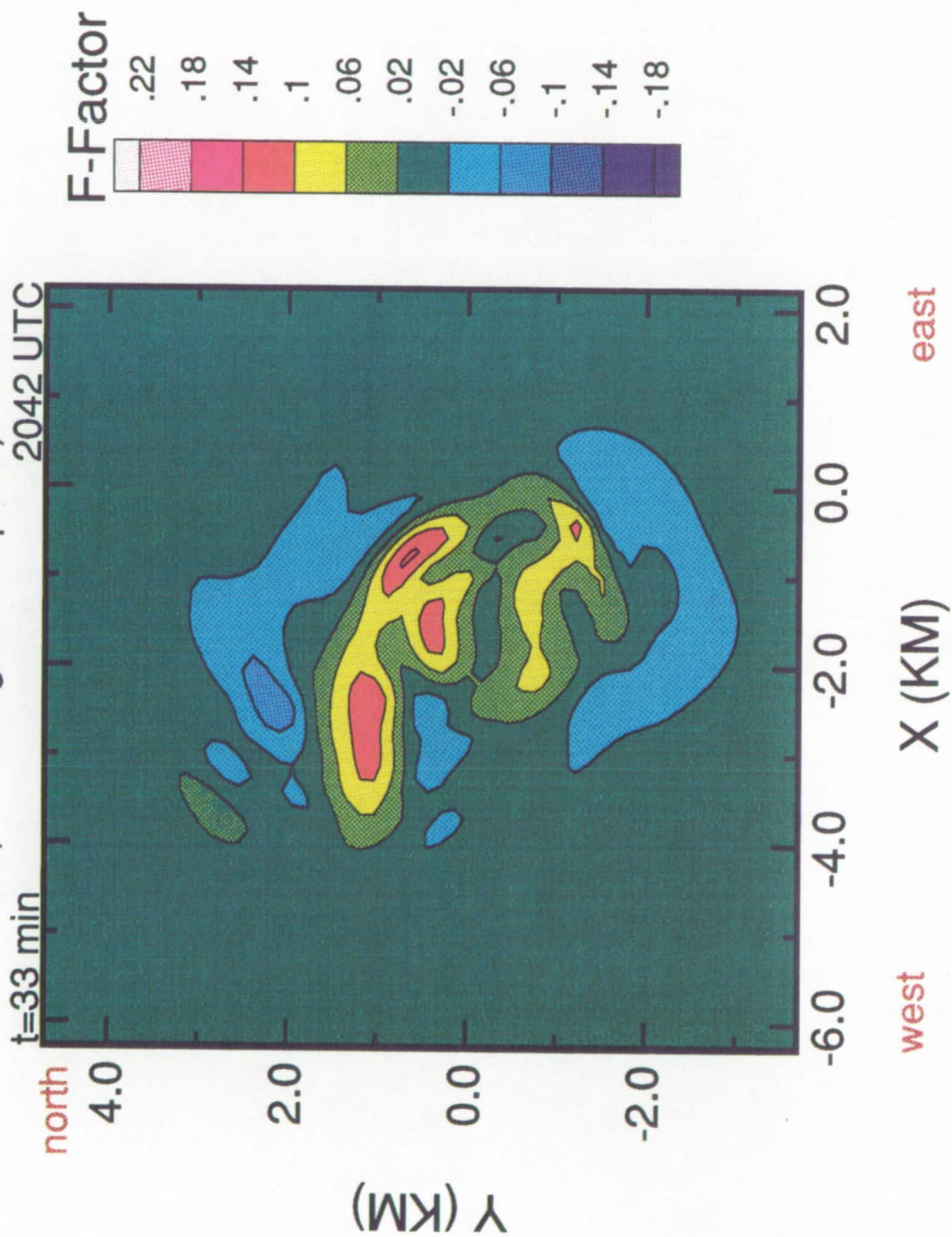
ORLANDO 20 JUNE 1991 MICROBURST SIMULATION VELOCITY ALONG TDWR RADIAL AT 190 M AGL



ORLANDO 20 JUNE 1991 MICROBURST SIMULATION

NORTH-SOUTH F-FACTOR AT 325 M AGL

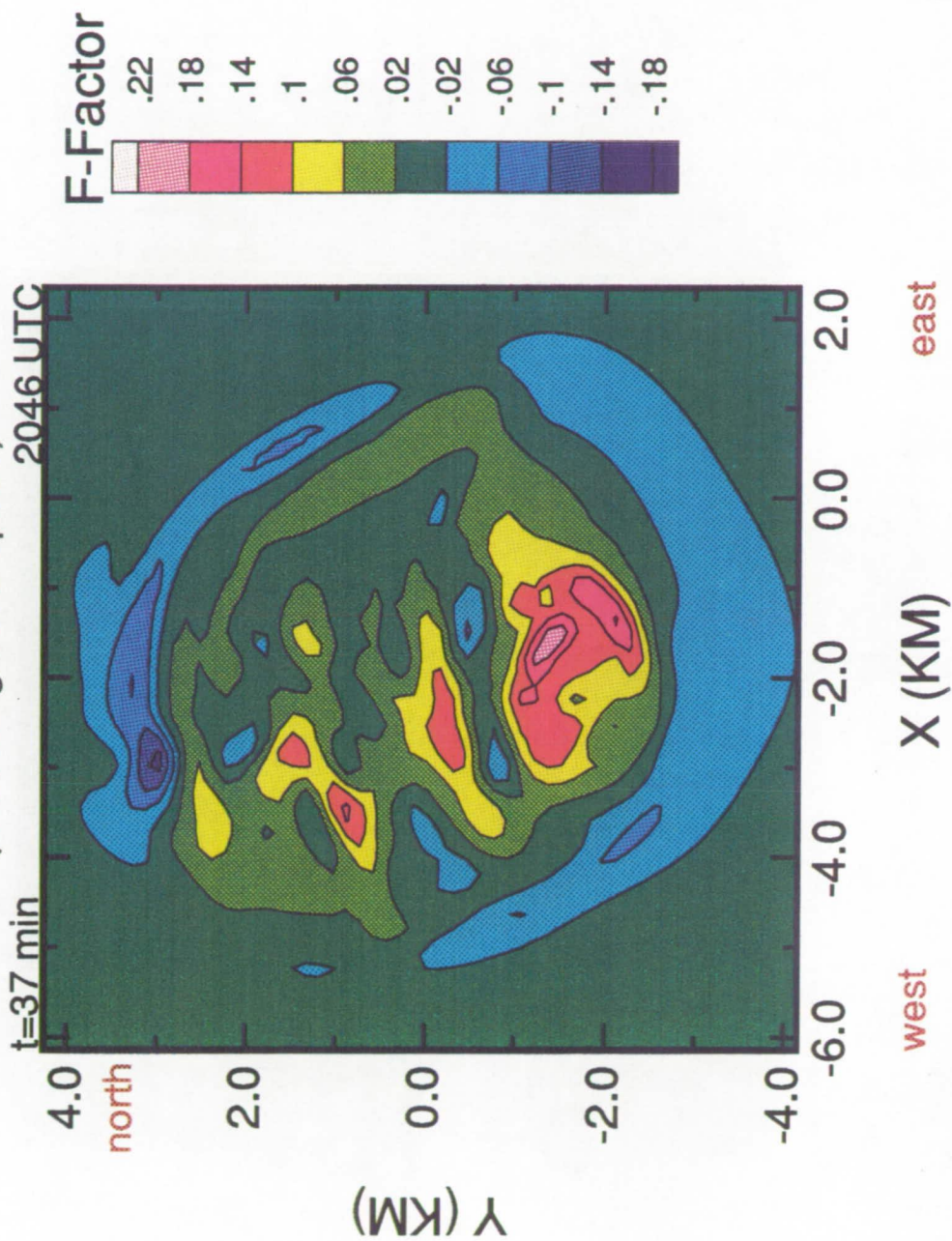
(110 m/s ground speed)



ORLANDO 20 JUNE 1991 MICROBURST SIMULATION

NORTH-SOUTH F-FACTOR AT 325 M AGL

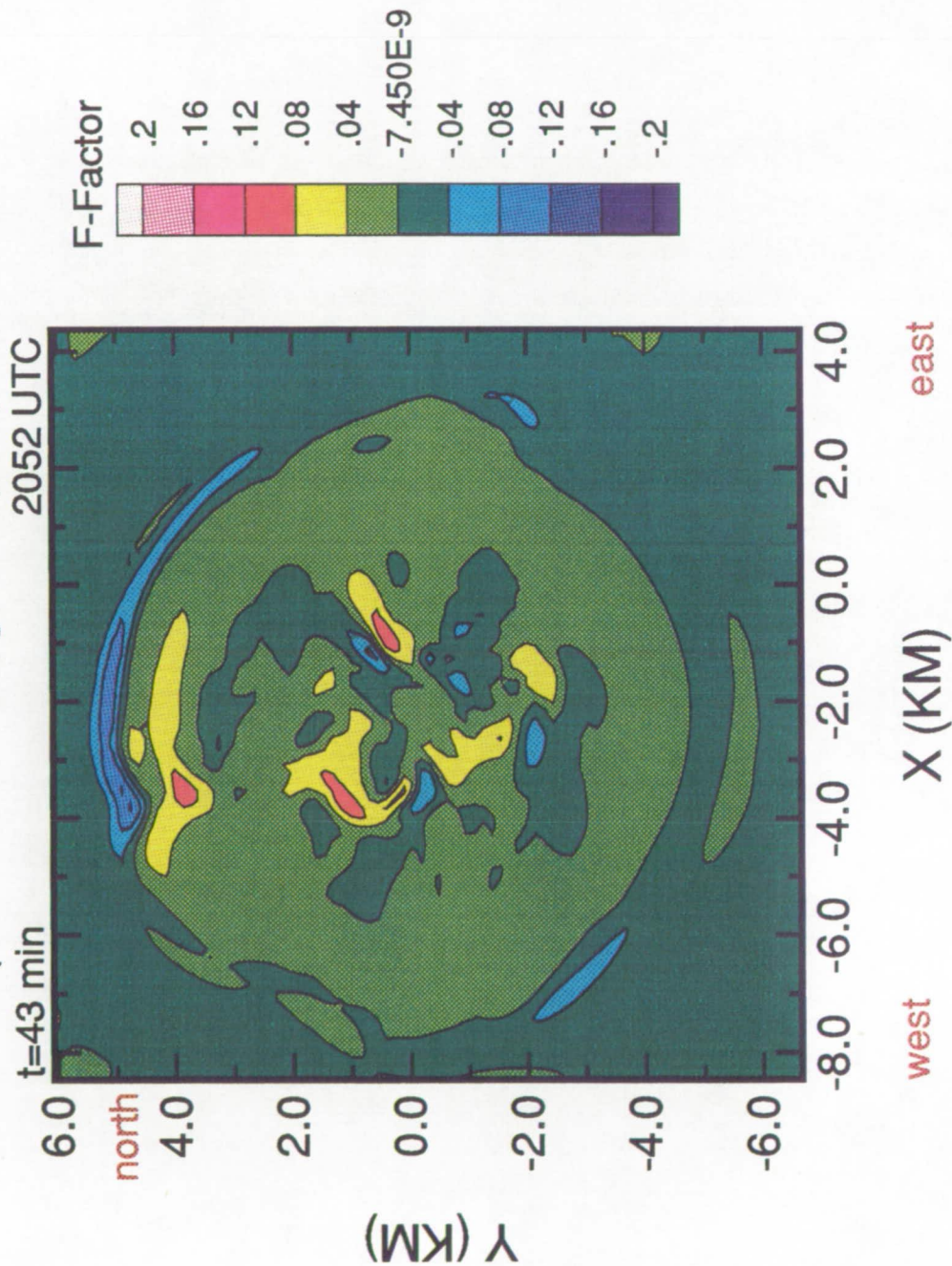
(110 m/s ground speed)



ORLANDO 20 JUNE 1991 MICROBURST SIMULATION

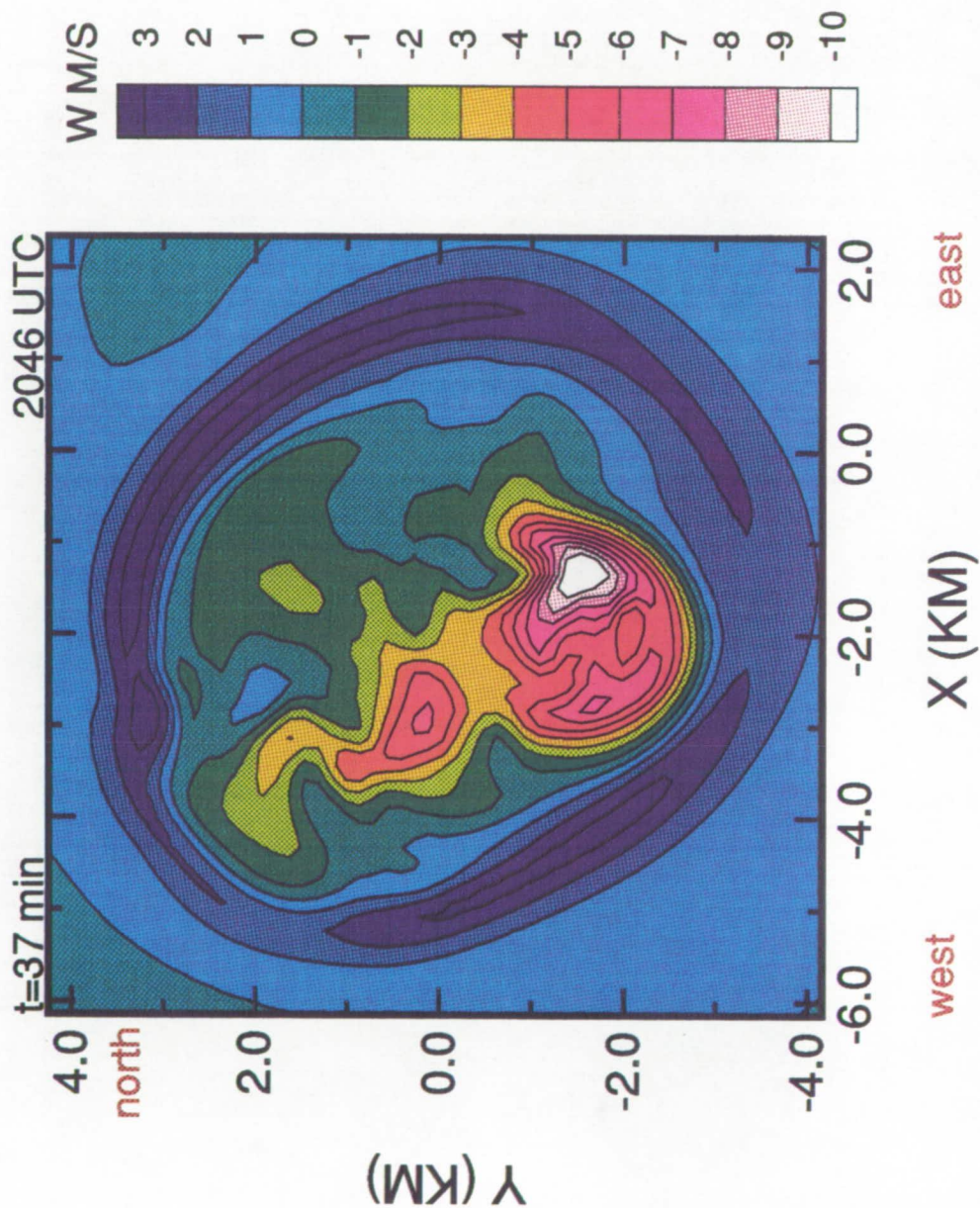
NORTH SOUTH F-FACTOR AT 325 M AGL

(assumes 110 m/s groundspeed)



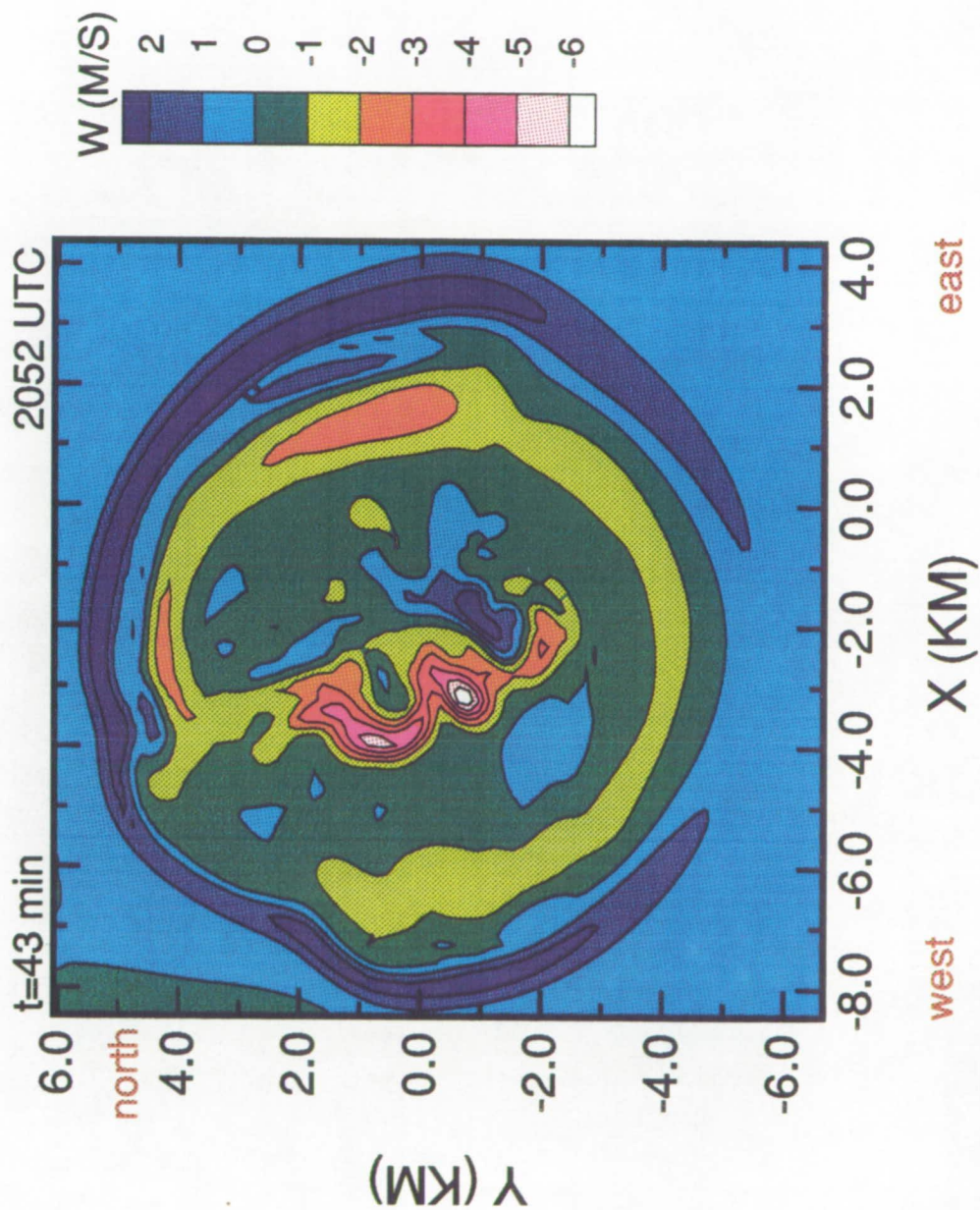
ORLANDO 20 JUNE 1991 MICROBURST SIMULATION

VERTICAL VELOCITY AT 325 M AGL

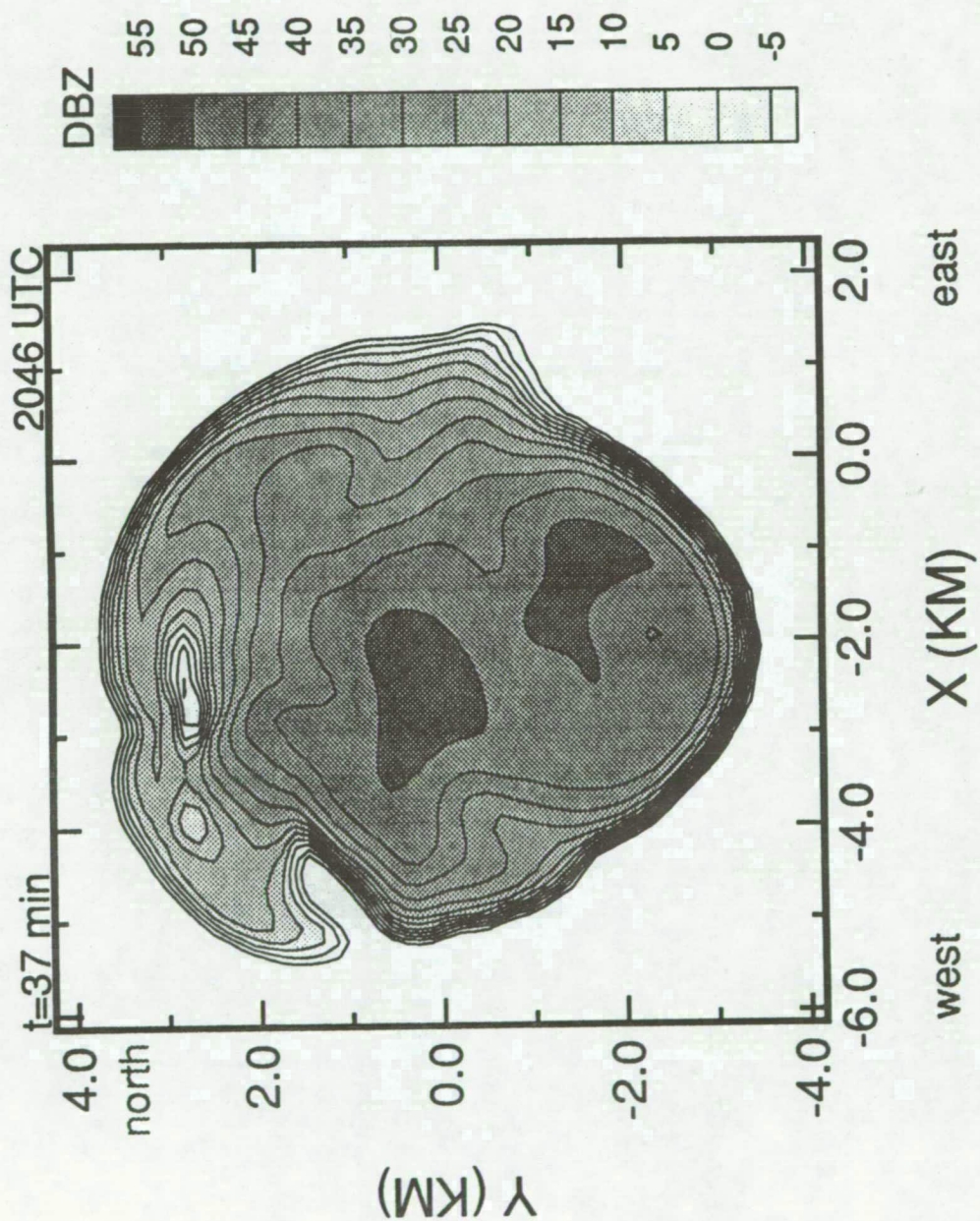


ORLANDO 20 JUNE 1991 MICROBURST SIMULATION

VERTICAL VELOCITY AT 325 M AGL

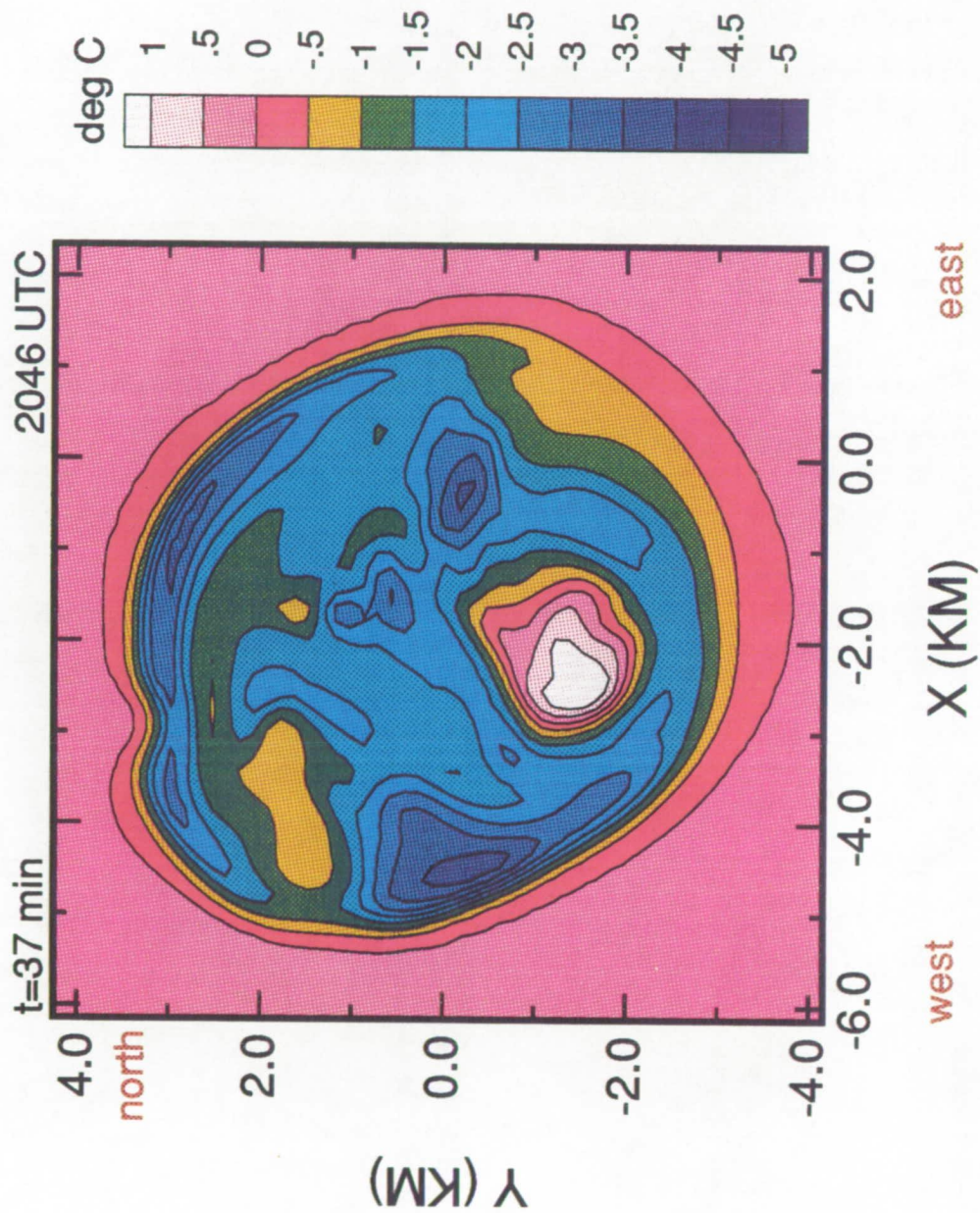


ORLANDO 20 JUNE 1991 MICROBURST SIMULATION **RADAR REFLECTIVITY AT 150 M AGL**

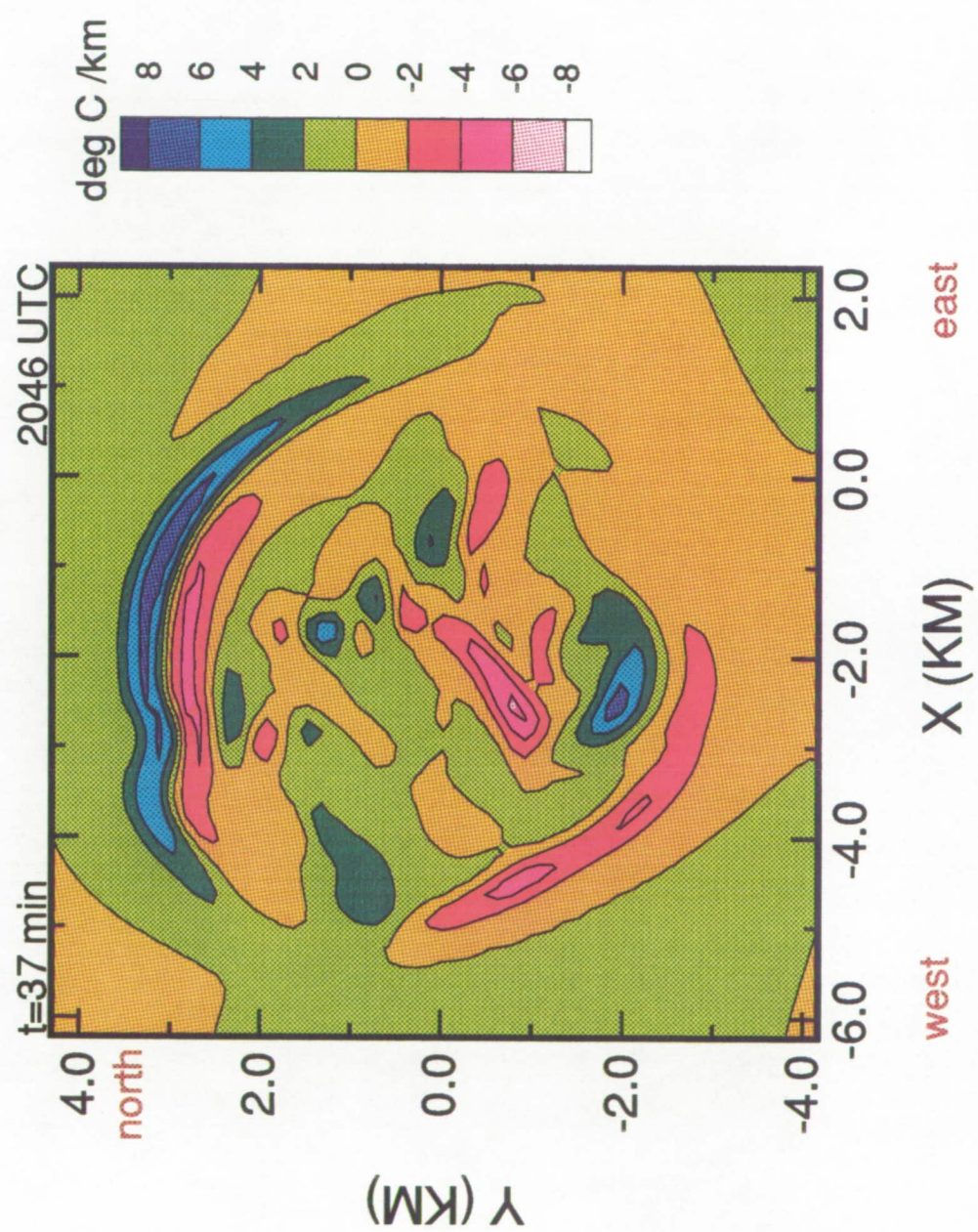


ORLANDO 20 JUNE 1991 MICROBURST SIMULATION

TEMPERATURE DEVIATION FROM AMBIENT AT 325 M AGL



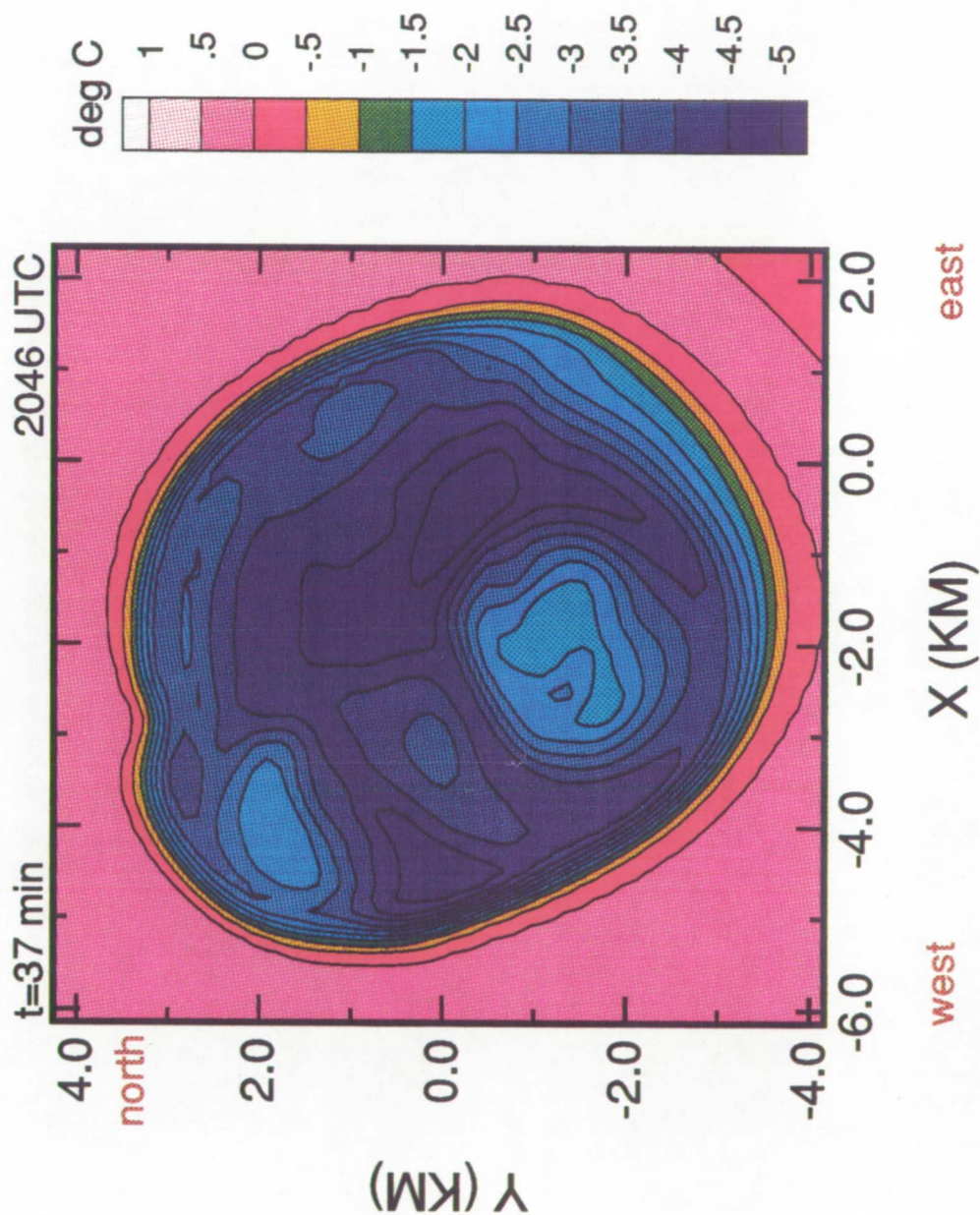
ORLANDO 20 JUNE 1991 MICROBURST SIMULATION N-S TEMPERATURE GRADIENT AT 325 M AGL



ORIGINAL PAGE
COLOR PHOTOGRAPH

ORLANDO 20 JUNE 1991 MICROBURST SIMULATION

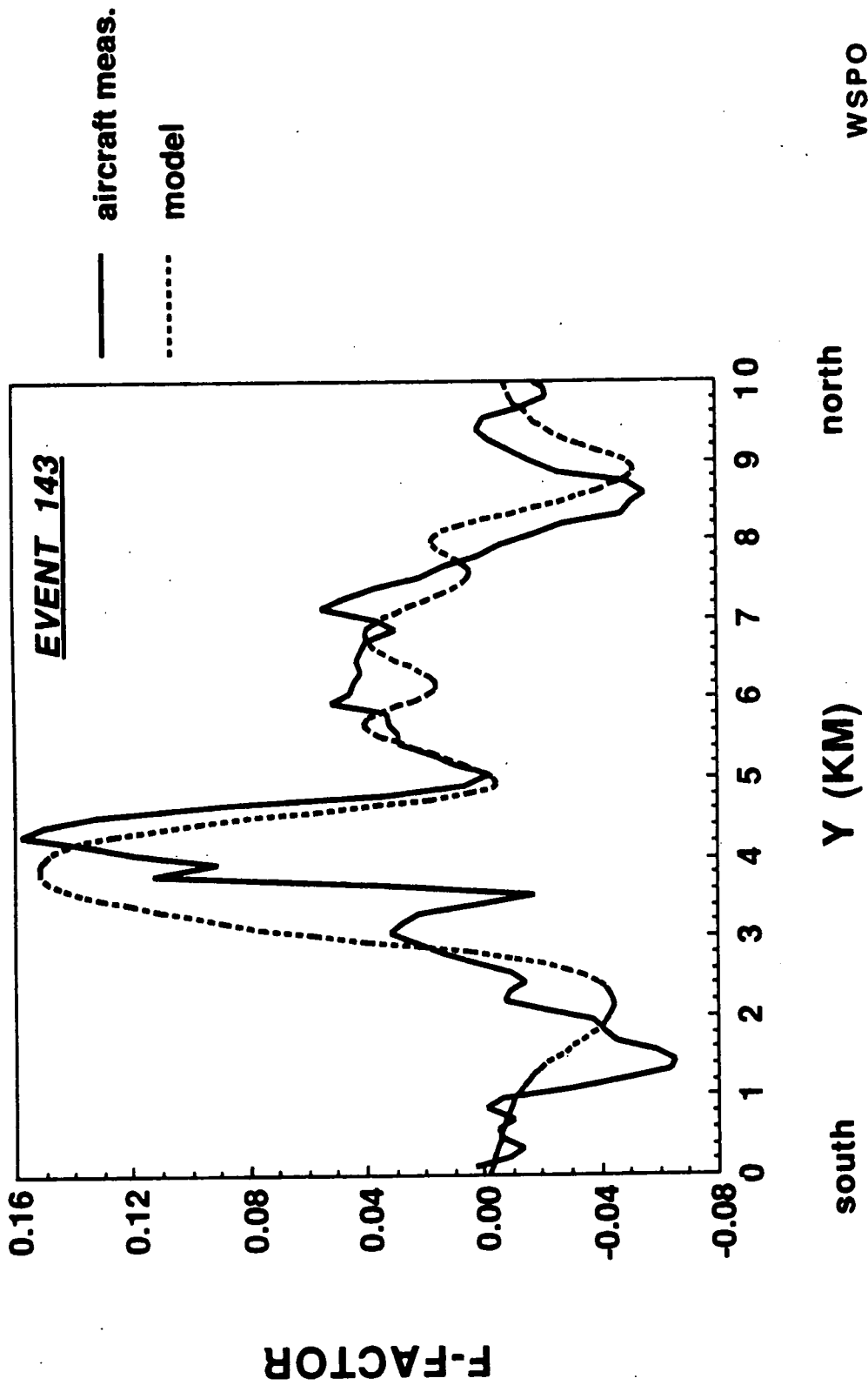
TEMPERATURE DEVIATION FROM AMBIENT AT 75 M AGL



ORIGINAL PAGE
COLOR PHOTOGRAPH

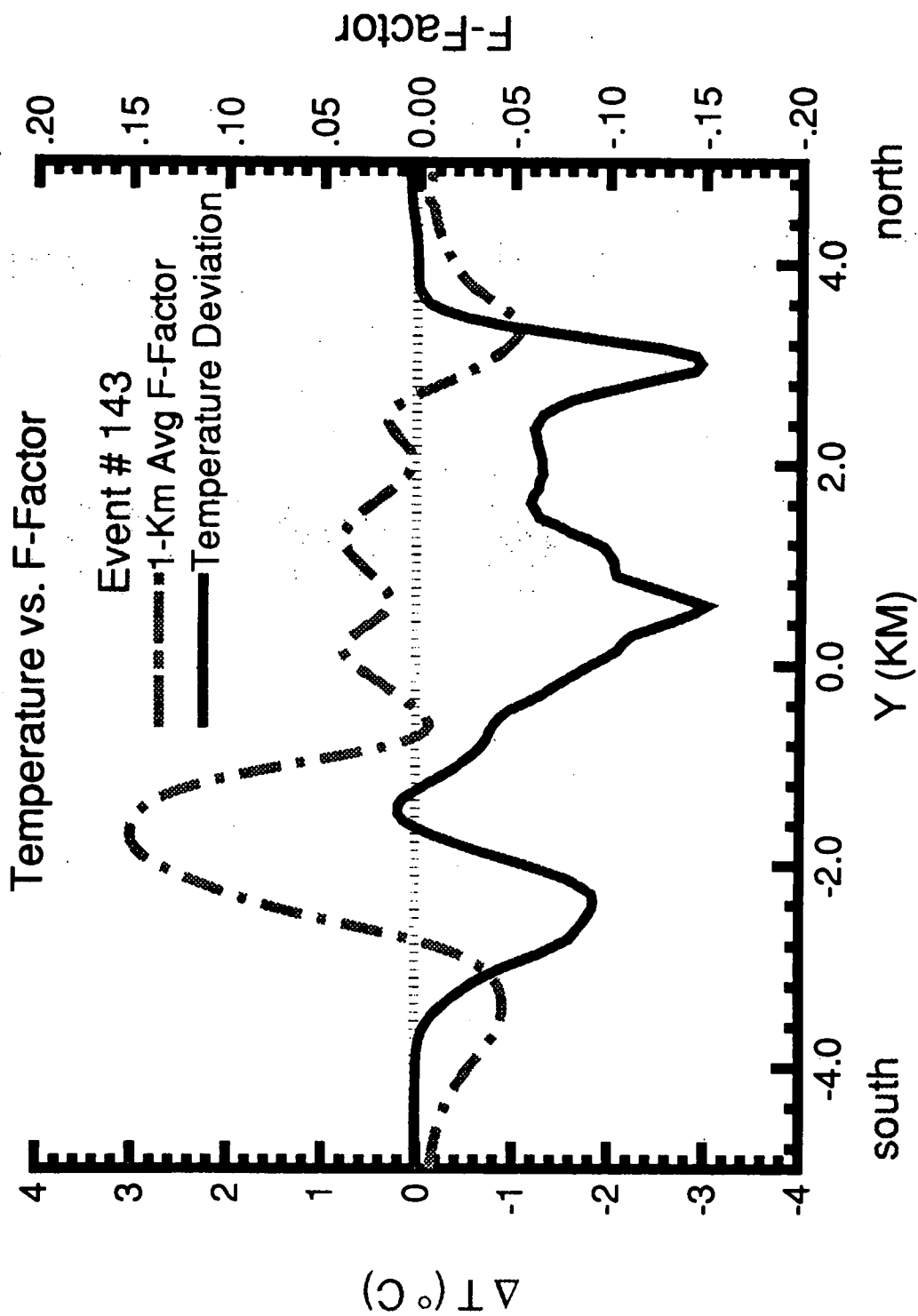
ORLANDO 20 JUNE MICROBURST SIMULATION

1-KM AVG. F-FACTOR AT 2046 UTC MODEL TIME



ORLANDO 20 JUNE MICROBURST SIMULATION

X = -1.5 KM, 325 M AGL, AND 37 MIN (2046 UTC)



ORLANDO 20 JUNE 1991 MICROBURST SIMULATION

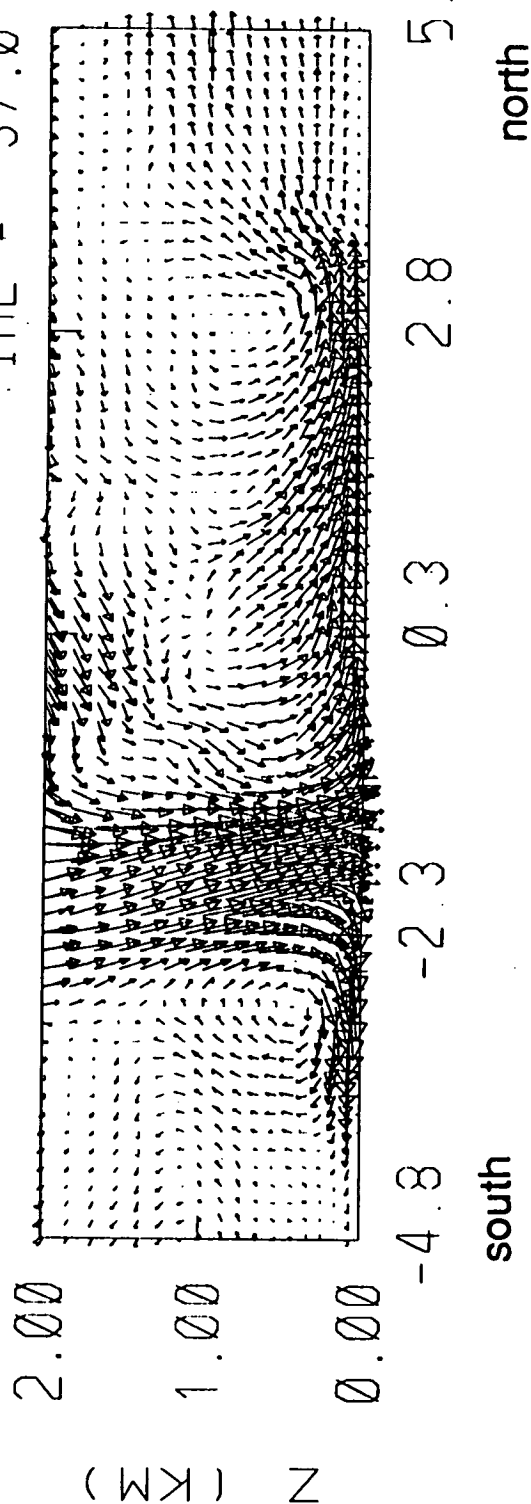
Wind Vectors

South-North Vertical Cross Section at 37 min (2046 UTC)

OR_ 30

X = -1.63

TIME = 37.0



Y (KM)

20 m/s

SUMMARY OF ORLANDO SIMULATION

- O WET MICROBURST WITH HAZARDOUS WIND SHEAR**
- O GOOD AGREEMENT BETWEEN SIMULATION AND OBSERVATION OF EVENT**
- O COMPLEX MICROBURST STRUCTURE:**
 - 1. MULTIPLE DOWNDRAFT SURGES**
 - 2. MULTIPLE DIVERGENCE CENTERS EMBEDDED WITHIN OUTFLOW**
 - 3. AREAS OF UPWARD MOTION EMBEDDED WITHIN OUTFLOW**
 - 4. NONCLASSIC OUTFLOW AND F-FACTOR PROFILES**
- O MODELED ΔV FUNCTION OF ALTITUDE AND DIRECTION OF SEGMENT: PEAK ΔV OF 32.0 M/S ALONG EAST-WEST SEGMENT AT 70 M AGL .VS. 21.1 M/S ALONG SIMULATED TDWR RADIAL (NNE - SSW SEGMENT AT 190 M AGL)**
- O PEAK TEMPERATURE DROP OF $\sim 6^{\circ}$ C OCCURS AT TIME OF MICROBURST PEAK INTENSITY**
- O SIMULATED RAINFALL RATES EXCEED 5 IN/HR AND 1-Km AVERAGED F-FACTORS EXCEED .15**
- O REGION OF PEAK WIND-SHEAR HAZARD DOES NOT CORRELATE LOCALLY WITH PEAK TEMPERATURE DROP**

Three-Dimensional Numerical Simulation of the 20 June 1991, Orlando Microburst Questions and Answers

Q: Not recorded

A: Fred Proctor (NASA Langley) - All my fields are assumed to be horizontally homogenous, in other words, they are constant horizontally but they vary in the vertical. There have been a lot of studies that have shown that storms are really determined by the vertical structure of the atmosphere. That is really what is playing a larger role in creating all these complex fields. The winds change direction with height as well as the temperature and humidity and so forth. Exactly how it's doing that I can't answer.

Q: (Unknown) - Have you correlated the DT measurements you have with the downdraft component of the F-factor as opposed to the total?

A: Fred Proctor (NASA Langley) - I haven't looked at that; I can't tell you.

Q: Kim Elmore (NCAR) - Did the downdraft initiate at the minimum QE level, since it was an area of a lot of coalescence? I was curious as to how deep it was?

A: Fred Proctor (NASA Langley) - I haven't looked at that yet, but usually in storms of this type I find them to form really close to the freezing level, wherever that may be.

Q: Kim Elmore (NCAR) - But it is still the evaporation of rain drops that is the primary driving force?

A: Fred Proctor (NASA Langley) - In this case yes.

Q: Kim Elmore (NCAR) - Is that common for the southeastern storms?

A: Fred Proctor (NASA Langley) - I would say it is probably a primary effect in most of the storms, but certainly not in all of them. You could get one in an atmosphere that was somewhat stable, relative to these. If you had relatively heavy rain fall rates, then you could probably drive them by mass loading.

Q: Kim Elmore (NCAR) - I was going to ask you how much of a role precipitation loading played?

A: Fred Proctor (NASA Langley) - I did not do that analysis for this storm, but I did for the one I presented at the last conference and the mass loading was a pretty small percentage of the total. Even though, in that storm, we had rainfall rates of 9 or 10 inches an hour. That was the Orlando 1990 Storm.

1993010410

Session II. Hazard Characterization

N 93 - 19599

488720

428

A "Numerical Field Experiment" Approach for Determining Probabilities of Microburst Intensity

Dr. Kelvin Droegemeier, University of Oklahoma

Terry Zweifel, Honeywell

A "NUMERICAL FIELD EXPERIMENT"

APPROACH

FOR

DETERMINING PROBABILITIES OF

MICROBURST INTENSITY

**KELVIN DROEGEMEIER
UNIVERSITY OF OKLAHOMA**

AND

**TERRY ZWEIFEL
HONEYWELL, INC.**

OVERVIEW

- SEVERAL INVESTIGATORS HAD DETERMINED THAT SOME ATMOSPHERIC PARAMETERS WERE RELATED TO THE FORMATION AND SEVERITY OF MICROBURSTS.
- FOR EXAMPLE, CARACENA POINTED OUT THE RELATIONSHIP BETWEEN A DRY ADIABATIC LAPSE RATE AND MICROBURSTS IN "THE CRASH OF DELTA FLIGHT 191 AT DALLAS-FORT WORTH INTERNATIONAL AIRPORT".
- THESE EARLY INVESTIGATIONS LED TO THE IDEA THAT NUMERIC MODELING OF MICROBURSTS WITH VARYING ATMOSPHERIC PARAMETERS MIGHT DEFINE "SIGNATURES" THAT COULD LEAD TO DETERMINING THE PROBABILITY OF MICROBURST INTENSITY.
- THE IDEA WAS THAT, BY USING ALREADY AVAILABLE SENSORS (SUCH AS STATIC AIR TEMPERATURE, PRESSURE ALTITUDE, RADAR REFLECTIVITY) ONBOARD AN AIRCRAFT, A RELIABLE PREDICTION OF MICROBURST EXISTENCE AND INTENSITY COULD BE FORMED.
- SUCH DATA COULD BE USED TO CREATE AN "EXPERT METEOROLOGIST" USING EITHER AI OR OTHER TECHNIQUES THAT COULD BE USED IN EITHER REACTIVE OR LOOK-AHEAD SYSTEMS TO VARY SENSITIVITY THRESHOLDS AND COORDINATE THE INPUTS FROM DIFFERENT DETECTING SYSTEMS.

OVERVIEW

■ TO THIS END, HONEYWELL CONTRACTED WITH DR. KELVIN DROEGEMEIER AND THE UNIVERSITY OF OKLAHOMA IN 1990 TO RUN THE MICROBURST SIMULATIONS.

■ THE QUESTIONS TO BE ADDRESSED WERE:

USING THE SENSOR SET AVAILABLE TO THE AIRCRAFT (E.G. TEMPERATURE, RADAR REFLECTIVITY, ETC.), CAN WE CALCULATE THE PROBABILITY THAT

(1) A MICROBURST COULD BE FORMED?

(2) THE RESULTANT WINDS WOULD BE OF SUFFICIENT MAGNITUDE TO THREATEN THE AIRCRAFT?

■ OVER A TWO YEAR PERIOD, A DATA SET OF 1800 MICROBURST SIMULATIONS WAS ACCUMULATED.

■ VERIFICATION OF THE MICROBURST SIMULATION WAS OBTAINED USING THE RESULTS OF OTHER INDEPENDENT RESEARCHERS AND ACTUAL COMPARISON TO MICROBURST EVENTS IN ORLANDO AND DENVER.

■ SOME OF THE RESULTS FROM THE SIMULATION HAVE ALREADY BEEN INCORPORATED INTO HONEYWELL'S WINDSHEAR DETECTION AND GUIDANCE SYSTEM WITH EXCELLENT RESULTS.

The ***Numerical Field Experiment*** **Methodology**

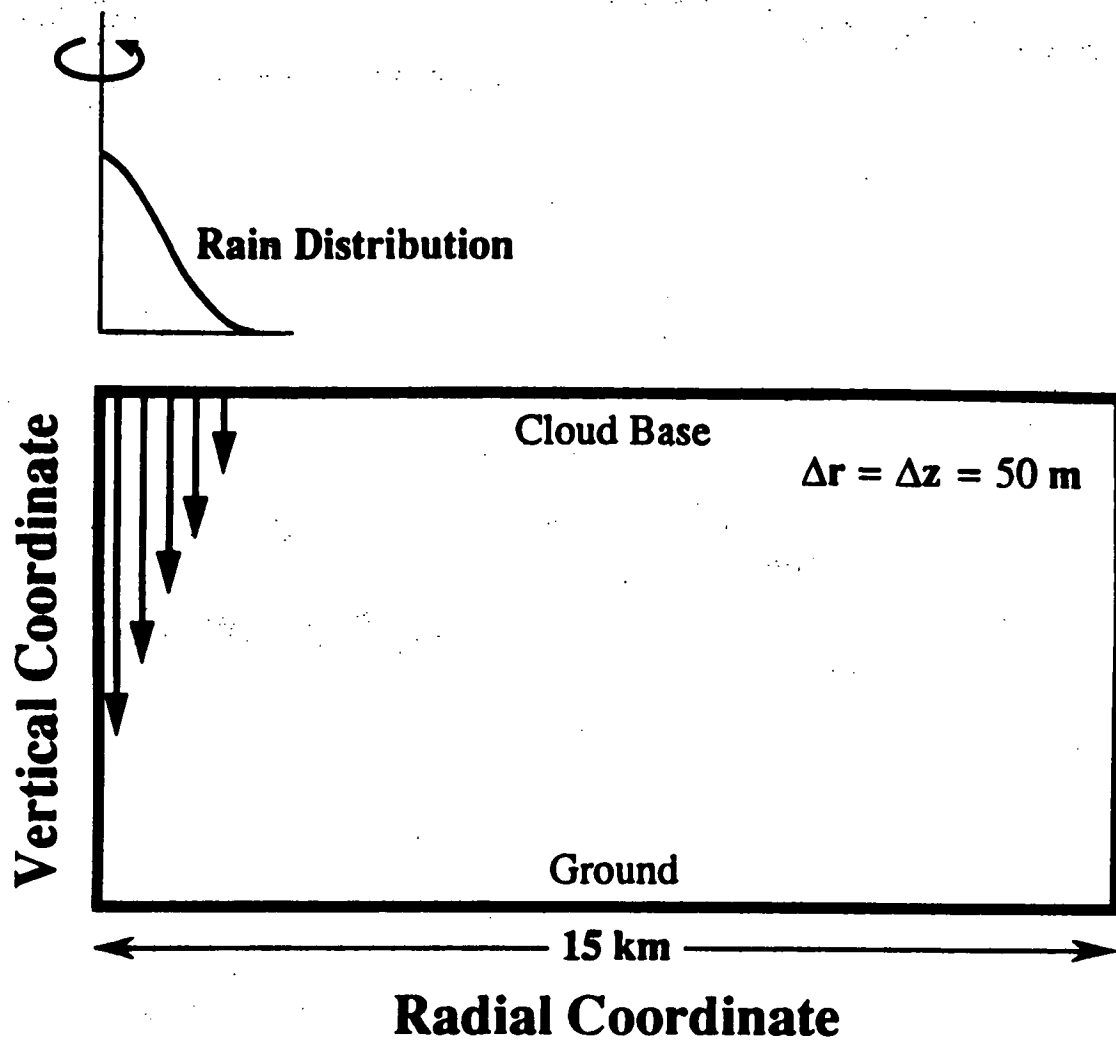
**Use a Numerical Model to Simulate a Large
Population of Physically Plausible
Scenarios Similar to What Might be Anticipated
During a Field Observing Program**

Goals of Study

- **Better understand how various physical parameters interact to determine microburst intensity**
- **Determine probabilities of microburst occurrence under a variety of conditions**
- **Validate results against observations**

Experiment Design

- Axisymmetric Numerical Cloud Model
- Warm Rain Microphysics
- No Ambient Wind
- Zero Ambient Humidity
- Simulate Only the Sub-Cloud Region
- Continuous Influx of Rainwater at Model Top (Cloud Base)



Parameter Space

Cloud Base Height (0.5, 1, 2, 3, 4 km AGL)

Sub-Cloud Lapse Rate (70, 80, 90, 100% D.A.)

Surface Temperature (55, 65, 75, 85, 95, 105 F)

Cloud Base Reflectivity (20, 30, 40, 50, 60 dBz)

Rainshaft Radius (0.5, 1.0, 2.0 km)

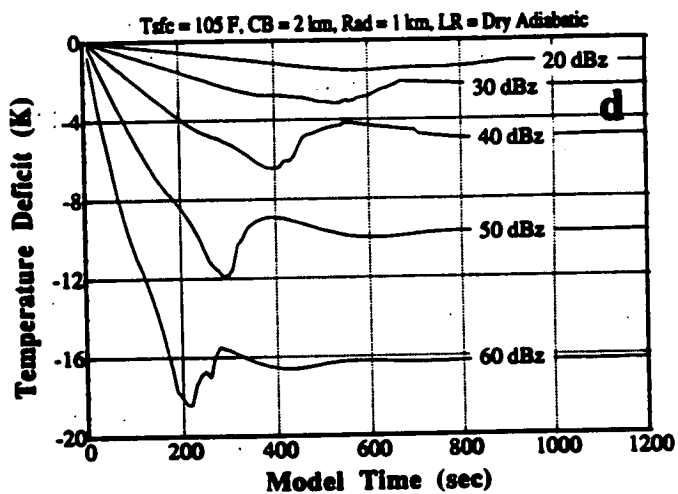
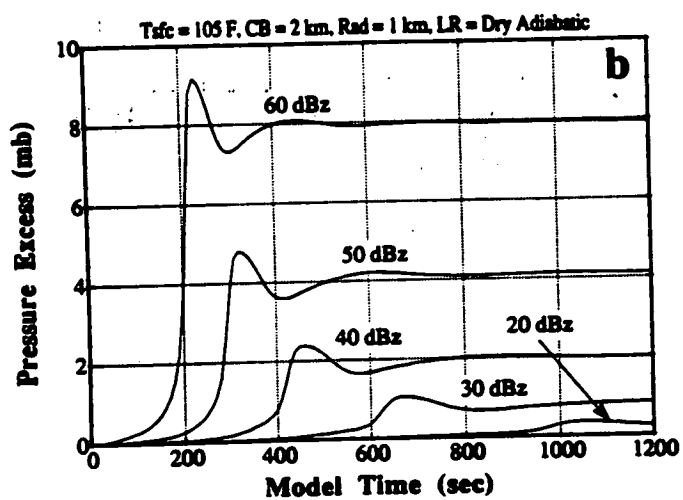
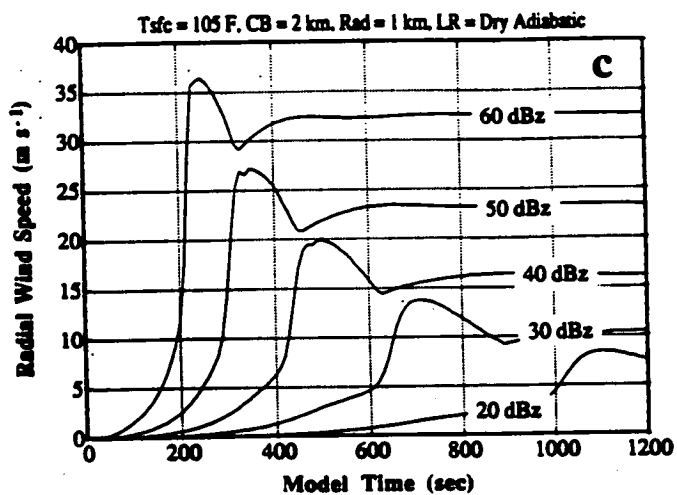
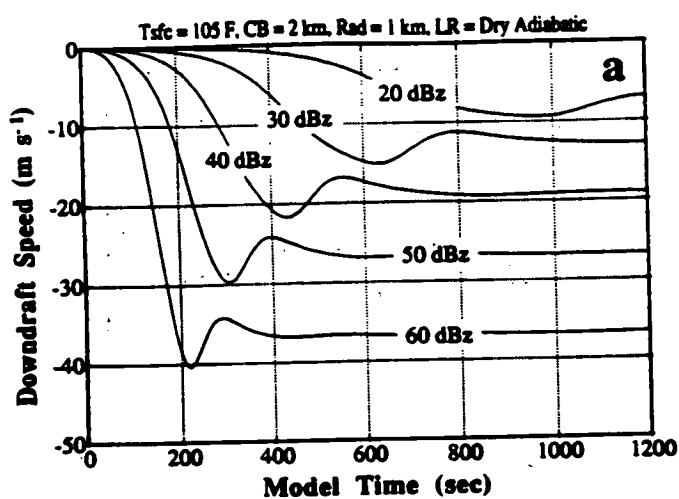
All Combinations → 1800 Simulations

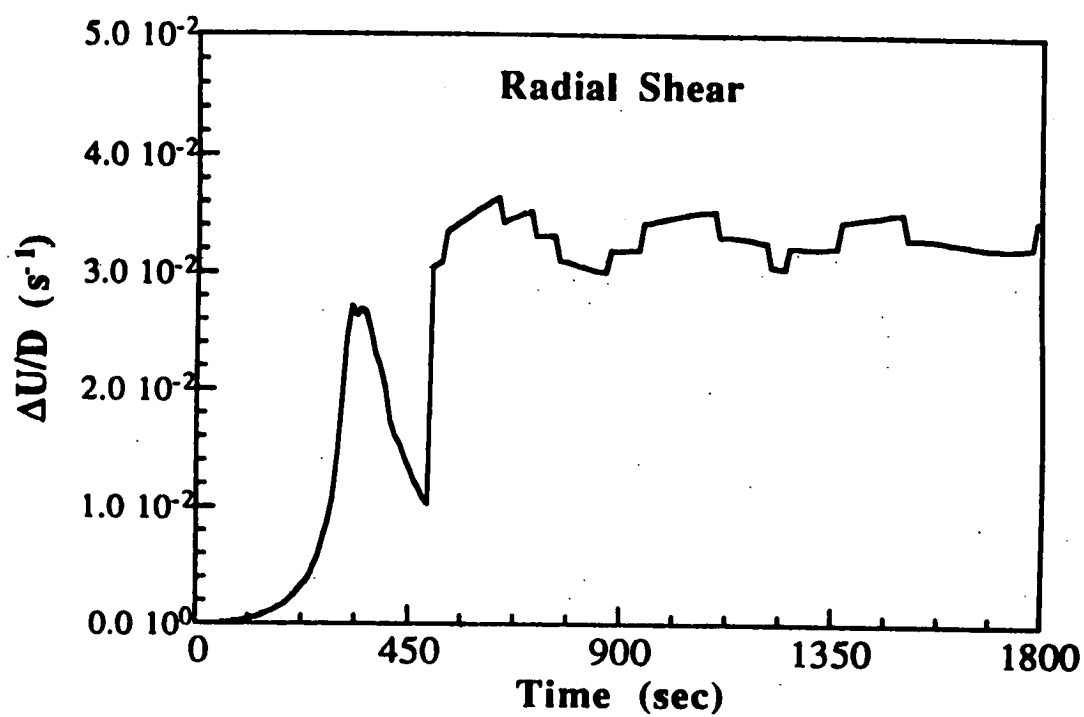
- **Each Run for 20 Minutes**
- **Max's & Min's of all Fields Saved Every 10 s**

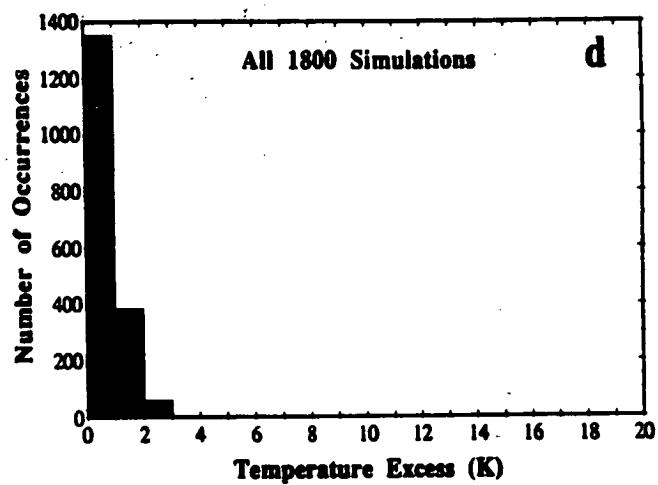
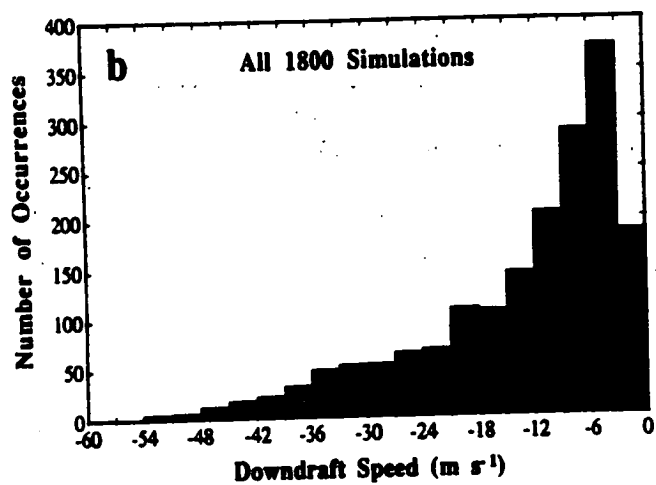
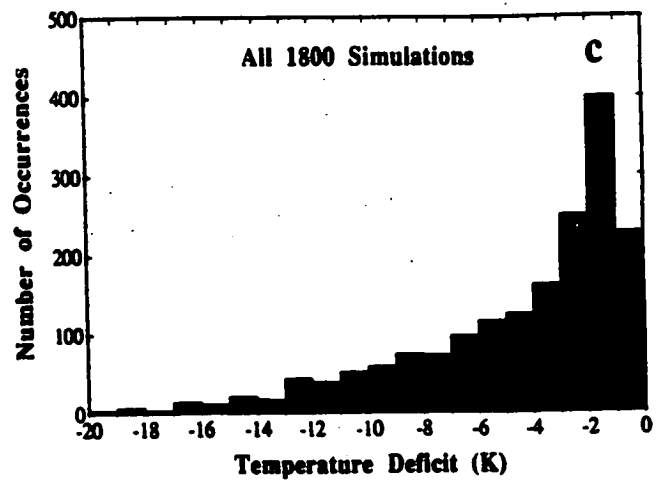
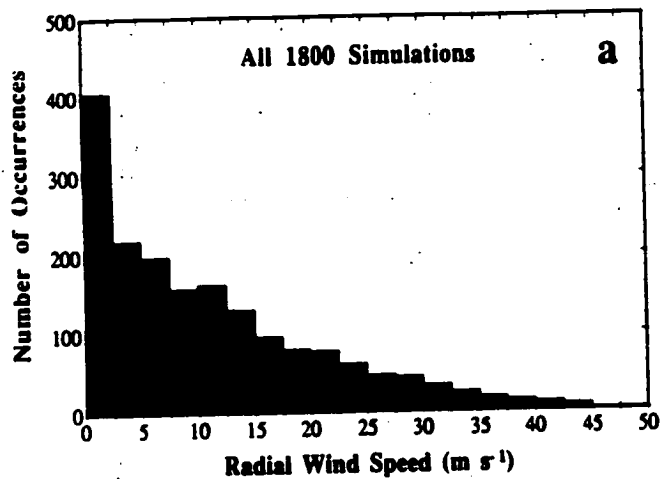
Model Validation

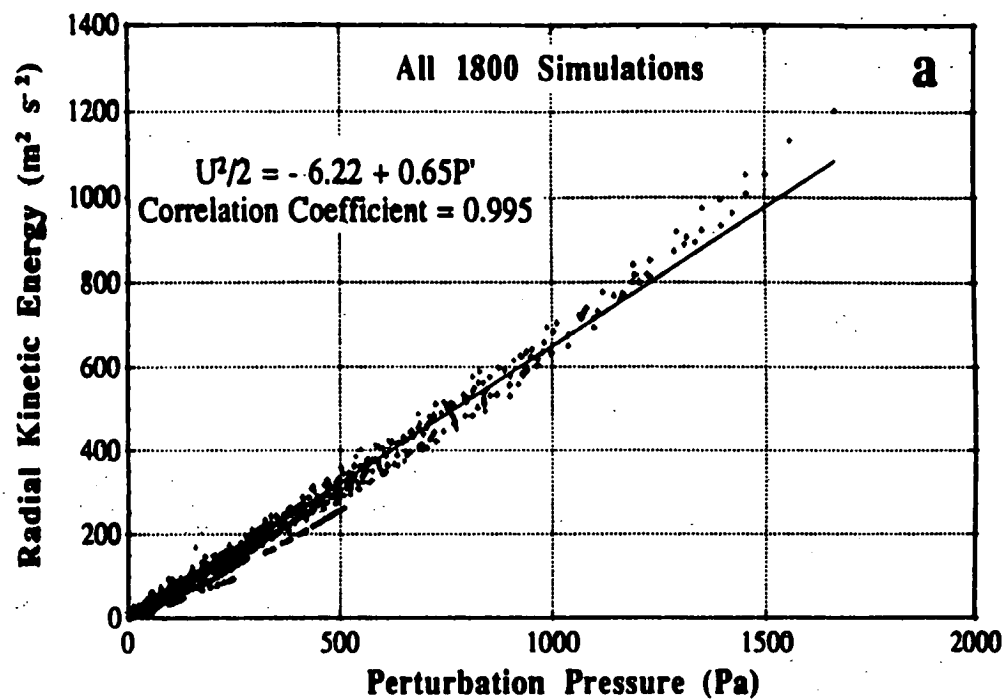
- NCSA Bakeoff - Tested Against Some 15 Codes
- Independent Tests with Krueger Axisymmetric and Klemp & Wilhelmson 3-D

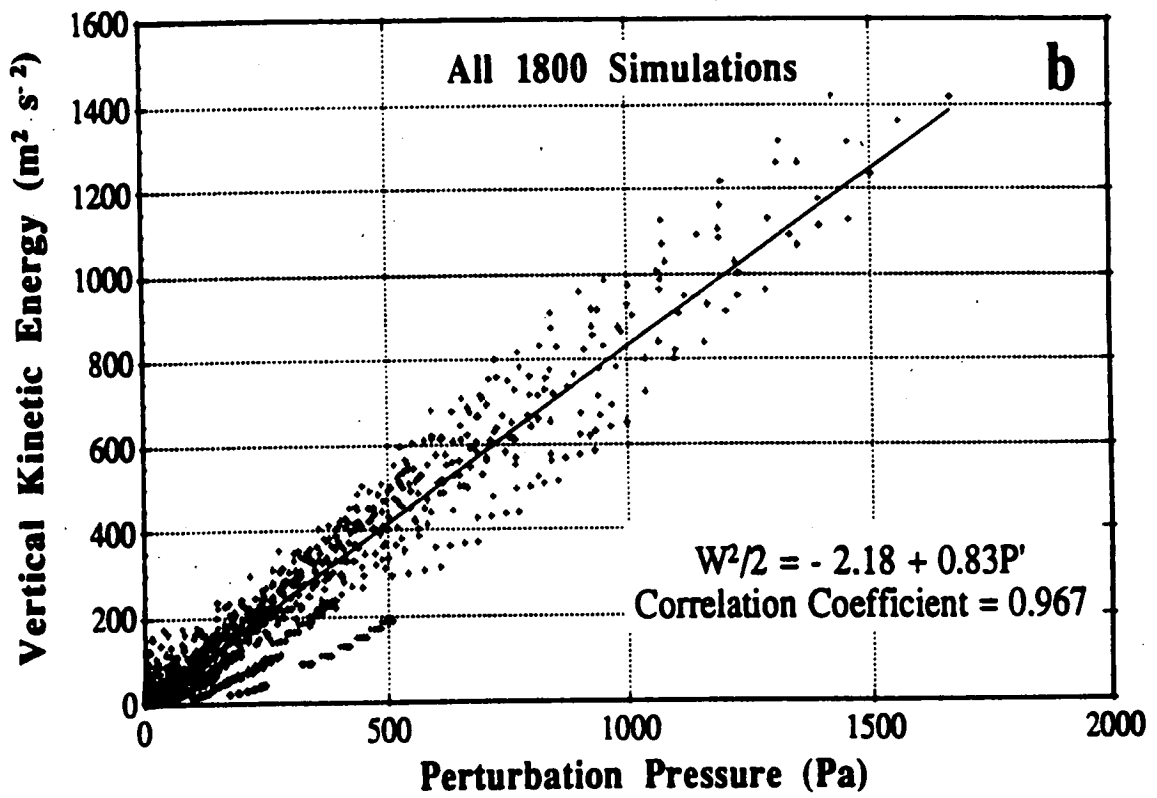
	Umax	Wmin
Droegemeier	46.7	-35.0
Krueger	45.1	-34.8
Droegemeier	52.5	-37.9
K & W 3-D	47.4	-37.9

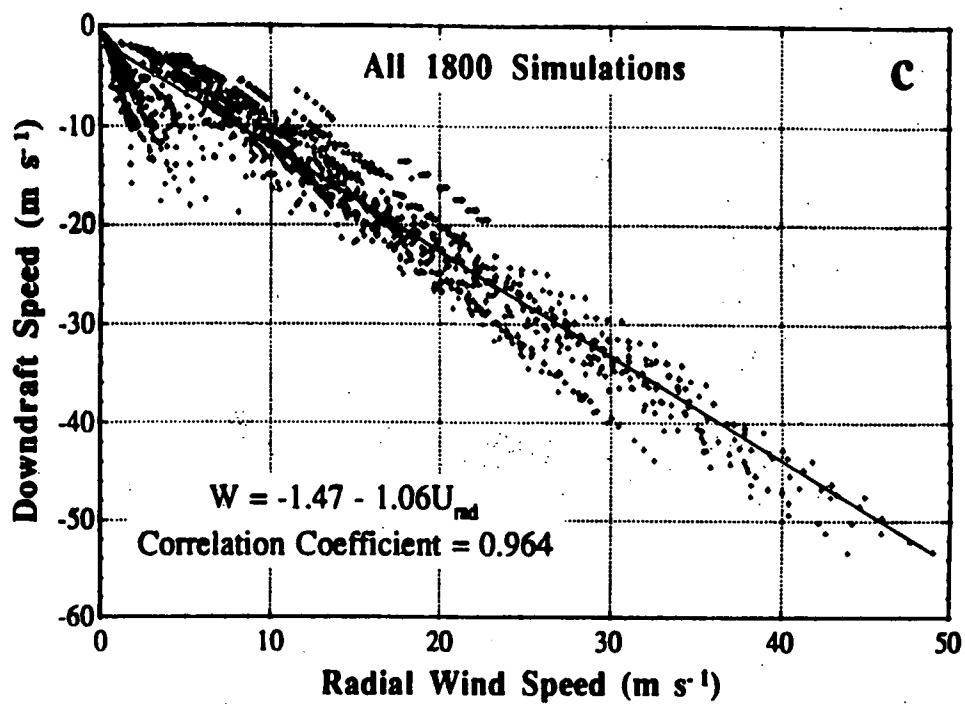


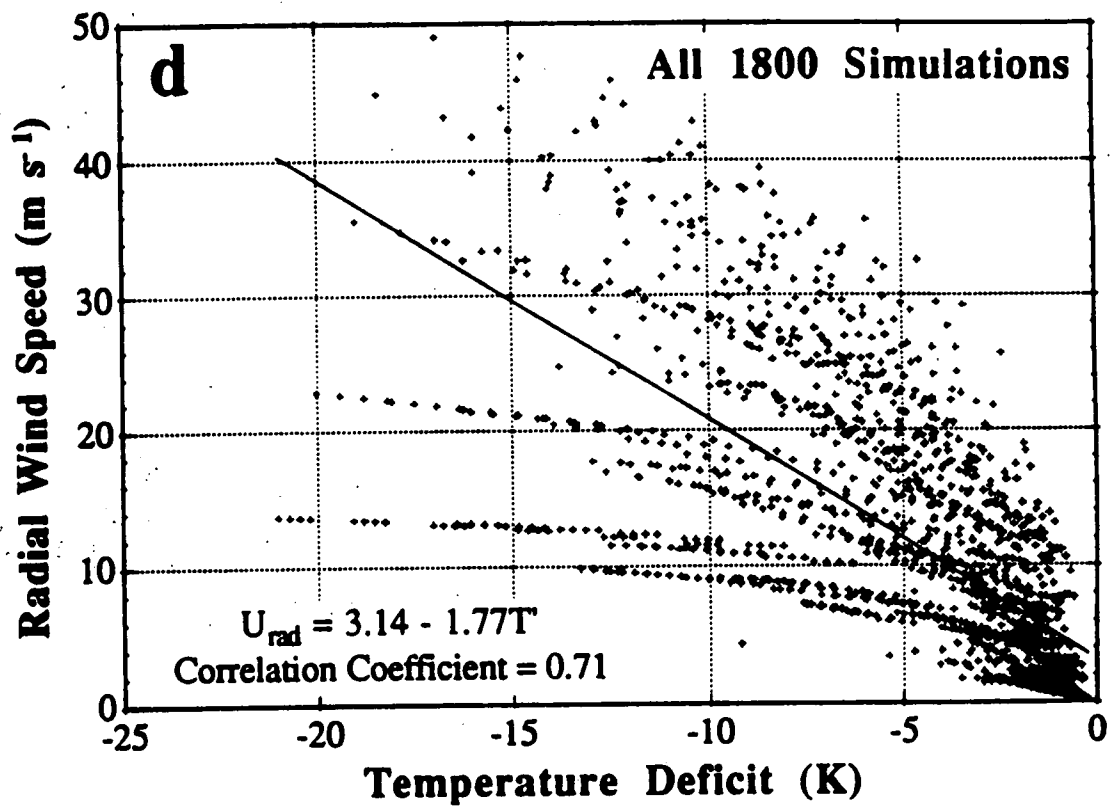


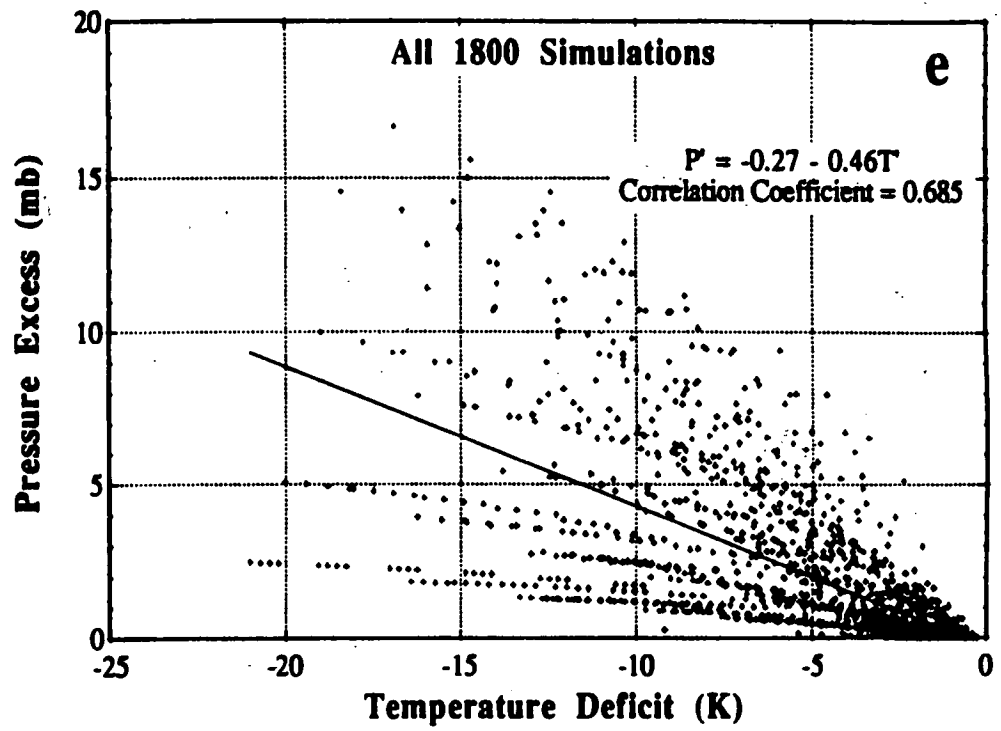


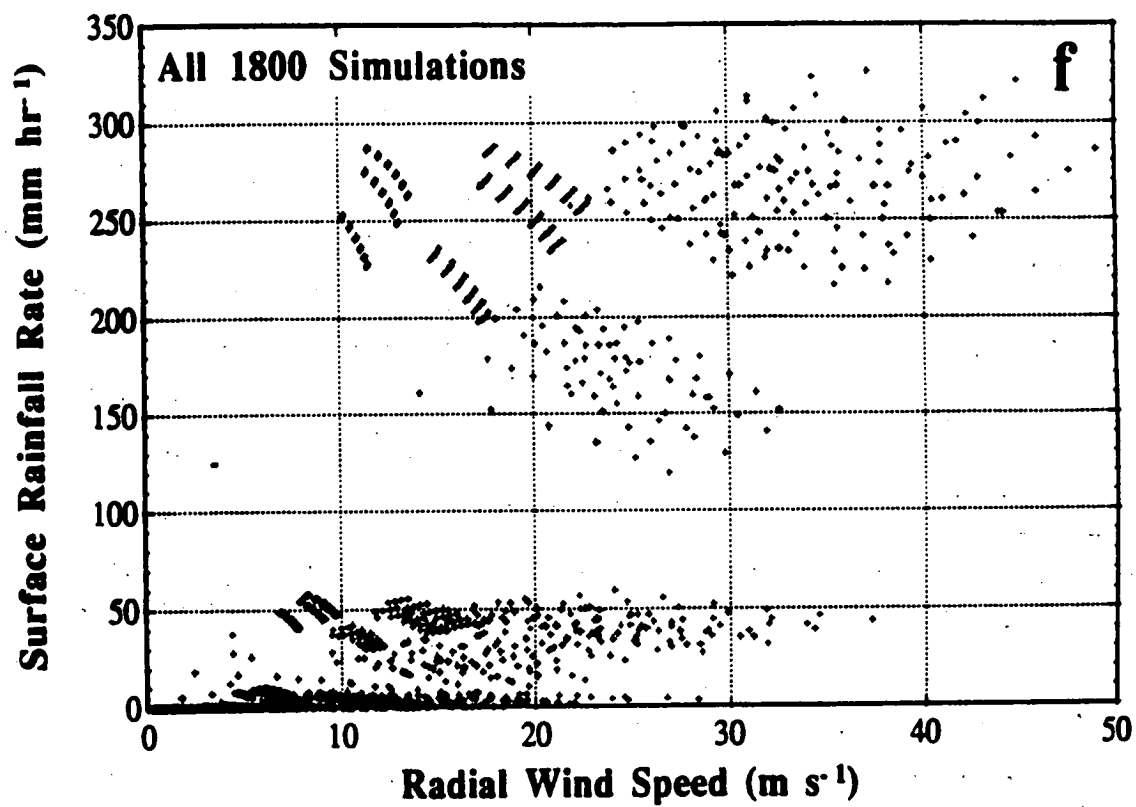


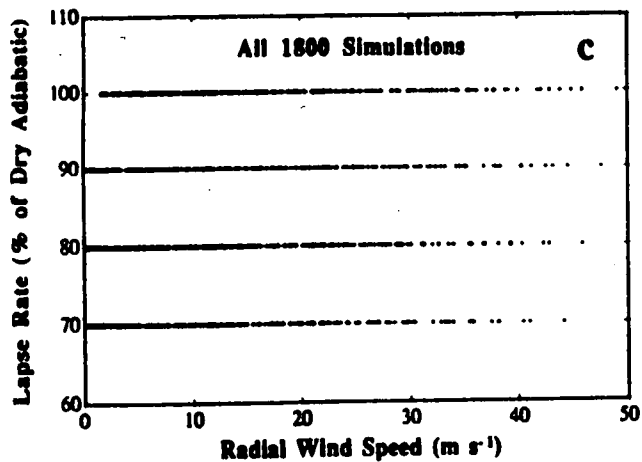
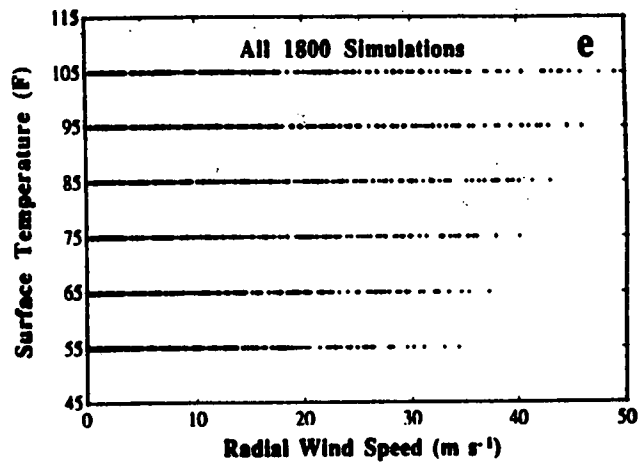
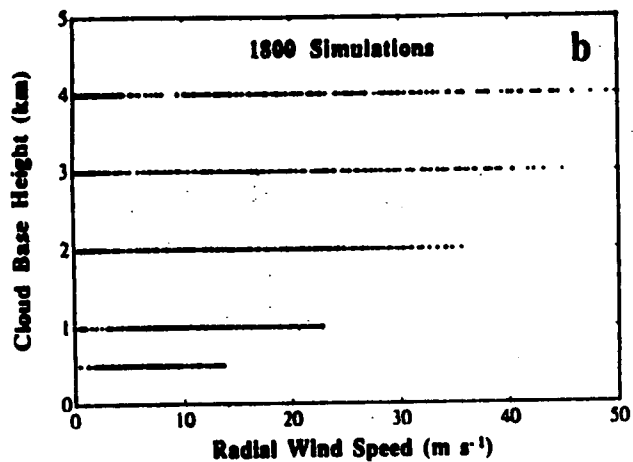
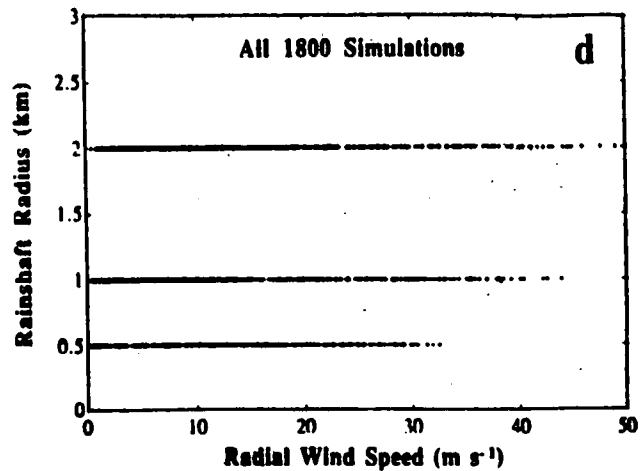
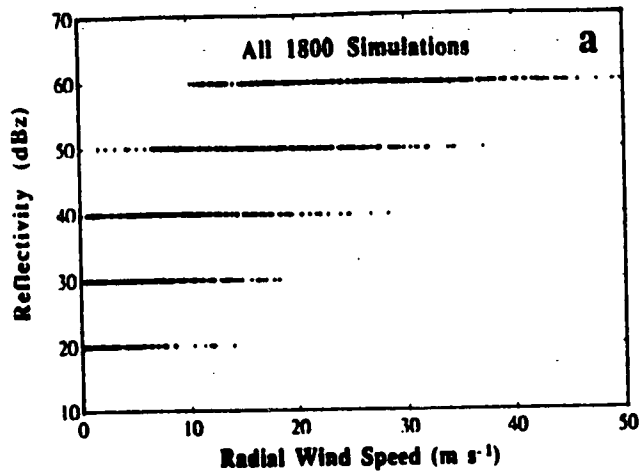












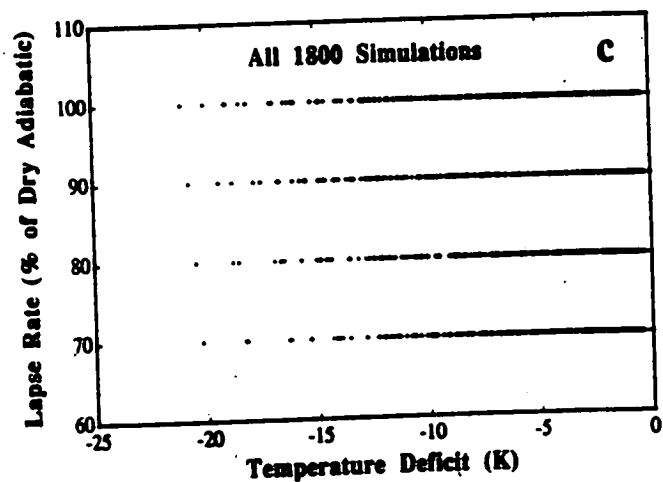
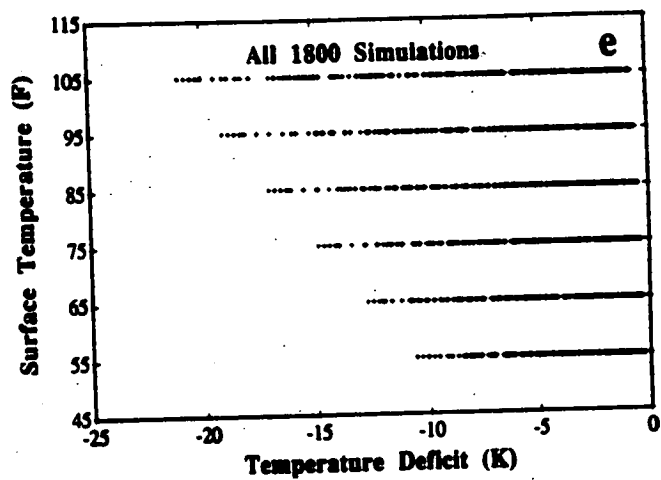
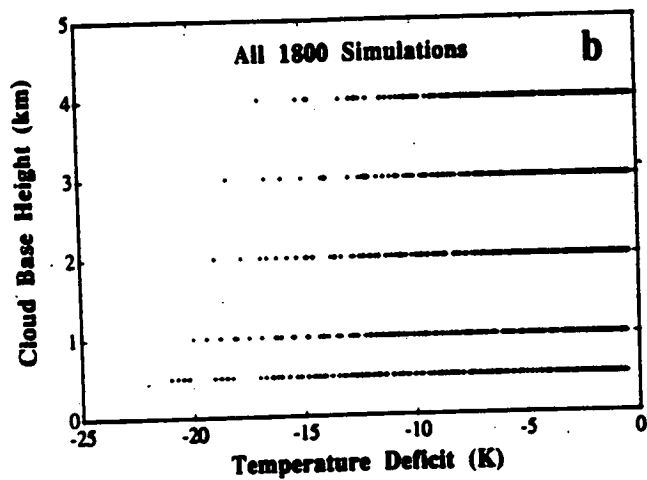
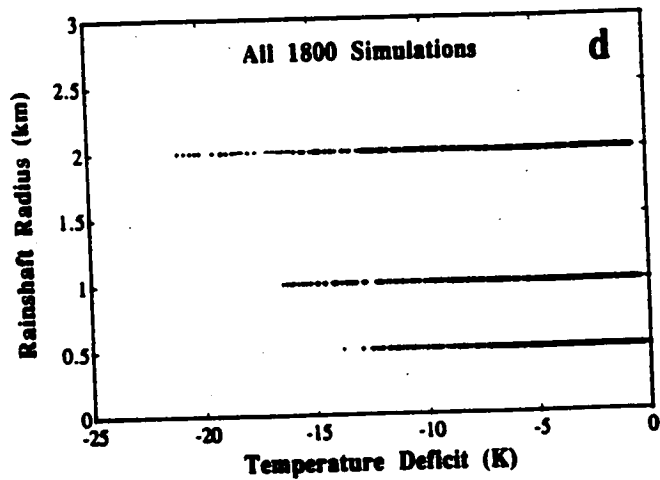
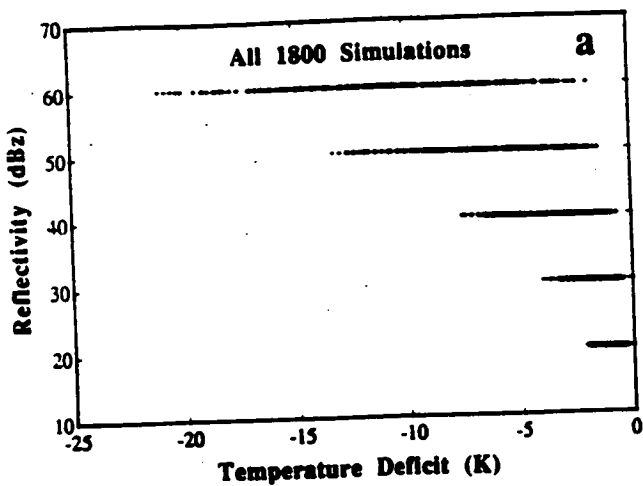


Table 5. Slope of linear fit between radial and downdraft wind speeds for all 1800 simulations as a function of rainshaft radius (R) and cloud base height (H), the ratio of which is defined as the aspect ratio (R/H).

Rainshaft Radius R (km)	Cloud Base H (km)	Aspect Ratio (R/H)	Slope
2.0	0.5	4.00	-0.60
1.0	0.5	2.00	-0.78
2.0	1.0	2.00	-0.75
2.0	2.0	1.00	-0.90
1.0	1.0	1.00	-0.93
0.5	0.5	1.00	-0.97
2.0	3.0	0.67	-0.95
2.0	4.0	0.50	-0.97
1.0	2.0	0.50	-1.03
0.5	1.0	0.50	-1.10
1.0	3.0	0.33	-1.04
1.0	4.0	0.25	-1.06
0.5	2.0	0.25	-1.16
0.5	3.0	0.17	-1.17
0.5	4.0	0.13	-1.17

Table 6. Probabilities (%) of radial wind speed classified according to model input parameters for the set of 1800 simulations.

ALL indicates that the associated parameter varies among all values used in the Subset.

Input Variable					Wind Speed			
LR	Tsfc	Refl	CB	Rad	$\geq 10.3 \text{ m s}^{-1}$ ($\geq 20 \text{ kts}$)	$\geq 12.9 \text{ m s}^{-1}$ ($\geq 25 \text{ kts}$)	$\geq 15.4 \text{ m s}^{-1}$ ($\geq 30 \text{ kts}$)	$\geq 18.0 \text{ m s}^{-1}$ ($\geq 35 \text{ kts}$)
ALL	ALL	ALL	ALL	ALL	44.50	35.17	28.22	22.61
100	ALL	ALL	ALL	ALL	59.11	45.56	36.89	29.11
90	ALL	ALL	ALL	ALL	45.33	37.11	29.78	24.00
80	ALL	ALL	ALL	ALL	39.56	31.11	24.44	19.78
70	ALL	ALL	ALL	ALL	34.00	26.89	21.78	17.56
ALL	105	ALL	ALL	ALL	48.67	40.67	33.33	26.33
ALL	95	ALL	ALL	ALL	48.00	39.33	31.33	26.00
ALL	85	ALL	ALL	ALL	46.33	37.00	29.67	25.33
ALL	75	ALL	ALL	ALL	45.33	34.33	28.00	23.00
ALL	65	ALL	ALL	ALL	42.33	31.67	25.33	20.00
ALL	55	ALL	ALL	ALL	36.33	28.00	21.67	15.00
ALL	ALL	60	ALL	ALL	98.89	85.28	78.61	70.56
ALL	ALL	50	ALL	ALL	74.17	62.50	46.94	35.00
ALL	ALL	40	ALL	ALL	36.39	22.50	13.61	7.22
ALL	ALL	30	ALL	ALL	11.11	5.28	1.94	0.28
ALL	ALL	20	ALL	ALL	1.94	0.28	0.00	0.00
ALL	ALL	ALL	4.0	ALL	49.44	45.56	39.72	34.44
ALL	ALL	ALL	3.0	ALL	53.06	46.39	41.11	35.56
ALL	ALL	ALL	2.0	ALL	56.11	46.94	38.33	31.67
ALL	ALL	ALL	1.0	ALL	45.00	31.67	21.94	11.39
ALL	ALL	ALL	0.5	ALL	18.89	5.28	0.00	0.00
ALL	ALL	ALL	ALL	2.0	52.00	43.33	35.50	29.00
ALL	ALL	ALL	ALL	1.0	45.17	37.33	29.33	25.17
ALL	ALL	ALL	ALL	0.5	36.33	24.83	19.83	13.67

LR = Lapse Rate (% of Dry Adiabatic)
Tsfc = Surface Temperature (F)
Refl = Reflectivity Factor (dBz)
CB = Cloud Base Height (km)
Rad = Rainshaft Radius (km)

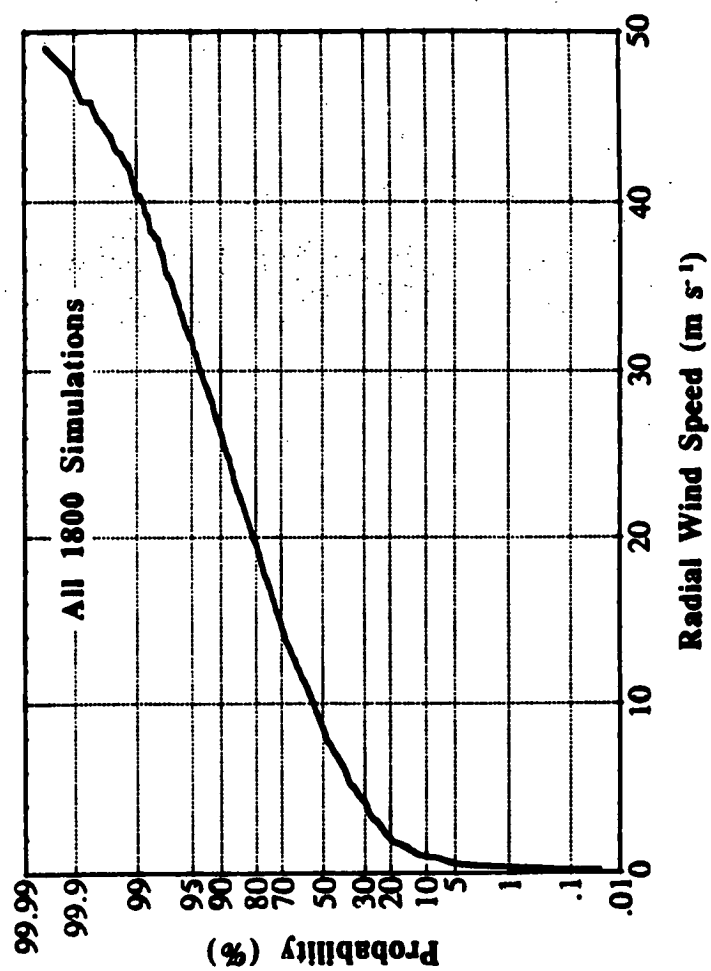


Table 7. Probabilities (%) of radial wind speed classified according to model input parameters for a subset of 114 simulations defined below.

ALL indicates that the associated parameter varies among all values used in the Subset.

Input Variable					Wind Speed			
LR	Tsfc	Refl	CB	Rad	$\geq 10.3 \text{ m s}^{-1}$ ($\geq 20 \text{ kts}$)	$\geq 12.9 \text{ m s}^{-1}$ ($\geq 25 \text{ kts}$)	$\geq 15.4 \text{ m s}^{-1}$ ($\geq 30 \text{ kts}$)	$\geq 18.0 \text{ m s}^{-1}$ ($\geq 35 \text{ kts}$)
ALL	ALL	ALL	ALL	ALL	60.53	41.23	32.46	21.05
100	ALL	ALL	ALL	ALL	60.53	41.23	32.46	21.05
ALL	105	ALL	ALL	ALL	60.53	42.11	34.21	21.05
ALL	95	ALL	ALL	ALL	60.53	42.11	31.58	21.05
ALL	85	ALL	ALL	ALL	60.53	39.47	31.58	21.05
ALL	ALL	60	ALL	ALL	100.00	85.19	66.67	55.56
ALL	ALL	50	ALL	ALL	66.67	55.56	48.15	22.22
ALL	ALL	40	ALL	ALL	55.56	22.22	22.22	11.11
ALL	ALL	30	ALL	ALL	28.57	14.29	0.00	0.00
ALL	ALL	20	ALL	ALL	25.00	0.00	0.00	0.00
ALL	ALL	ALL	2.0	ALL	85.71	64.29	57.14	42.86
ALL	ALL	ALL	1.0	ALL	61.54	38.46	33.33	15.38
ALL	ALL	ALL	0.5	ALL	27.27	15.15	0.00	0.00
ALL	ALL	ALL	ALL	2.0	60.00	46.67	33.33	26.67
ALL	ALL	ALL	ALL	1.0	66.67	47.22	36.11	25.00
ALL	ALL	ALL	ALL	0.5	54.55	27.27	27.27	9.09

Lapse Rate = 100% Dry Adiabatic
 $85 \text{ F} \leq \text{Surface Temperature} \leq 105 \text{ F}$
 $20 \text{ dBz} \leq \text{Reflectivity} \leq 60 \text{ dBz}$
 $0.5 \text{ km} \leq \text{Cloud Base Height} \leq 2.0 \text{ km}$
 $0.5 \text{ km} \leq \text{Rainshaft Radius} \leq 2.0 \text{ km}$
 $U_{\text{rad}} \geq 5 \text{ m s}^{-1}$

Table 8. Coefficients of multivariate linear regression equations for the radial wind speed (m s^{-1}) for all 1800 simulations (1799 degrees of freedom), using various combinations of predictors.

Shown are the predictors, the estimated standard deviation of model error (m s^{-1}), the leading constant, and the five regression coefficients. The units of the regressors are as shown in Table 3, except for the lapse rate, which is given by its decimal equivalent.

Predictor(s)	% Variance Explained	Est. Std. Dev. of Model Error	Regression Coefficients					
			Const	LR	Tsfc	dBz	CBHt	Rad
LR	3.7	9.8	-3.40	17.31	—	—	—	—
Tsfc	1.7	9.9	5.15	—	0.08	—	—	—
dBz	60.4	6.3	-10.69	—	—	0.55	—	—
CBHt	5.4	9.7	7.50	—	—	—	1.82	—
Rad	4.6	9.8	7.30	—	—	—	—	3.43
dBz, LR	64.1	6.0	-25.38	17.31	—	0.55	—	—
dBz, Tsfc	62.1	6.2	-16.83	—	0.08	0.55	—	—
dBz, CBHt	65.8	5.9	-14.51	—	—	0.55	1.82	—
dBz, Rad	65.0	5.9	-14.69	—	—	0.55	—	3.43
LR, Tsfc	5.5	9.7	-9.56	17.31	0.08	—	—	—
LR, CBHt	9.2	9.5	-7.22	17.31	—	—	1.82	—
LR, Rad	8.3	9.6	-7.41	17.31	—	—	—	3.43
CBHt, Tsfc	7.1	9.7	1.33	—	0.08	—	1.82	—
CBHt, Rad	10.0	9.5	3.48	—	—	—	1.82	3.43
Tsfc, Rad	6.3	9.7	1.14	—	0.08	—	—	3.43
LR, Tsfc, CBHt	10.9	9.5	-13.38	17.31	0.08	—	1.82	—
LR, Tsfc, dBz	65.9	5.9	-31.57	17.31	0.08	0.55	—	—
LR, Tsfc, Rad	10.1	9.5	-13.57	17.31	0.08	—	—	3.43
LR, CBHt, dBz	69.6	5.5	-29.22	17.31	—	0.55	1.82	—
LR, CBHt, Rad	13.7	9.3	-11.23	17.31	—	—	1.82	3.43
LR, dBz, Rad	68.7	5.6	-29.41	17.31	—	0.55	—	3.43
LR, Tsfc, CBHt, Rad	15.5	9.2	-17.39	17.31	0.08	—	1.82	3.43
LR, Tsfc, CBHt, dBz	71.3	5.4	-35.39	17.31	0.08	0.55	1.82	—
LR, Tsfc, Rad, dBz	70.5	5.5	-35.57	17.31	0.08	0.55	—	3.43
LR, CBHt, Rad, dBz	74.1	5.1	-33.23	17.31	—	0.55	1.82	3.43
LR, Tsfc, CBHt, dBz, Rad	75.9	4.9	-39.40	17.31	0.08	0.55	1.82	3.43

Table 9. As in Table 8, but assuming that the cloud base height is known (359 degrees of freedom) and takes the values shown in the left column.

Cloud Base Height	% Variance Explained	Est. Std. Dev. of Model Error	Regression Coefficients					
			Const	LR	Tsfc	dBz	CBHt	Rad
0.5 km	94.3	0.8	-6.61	1.56	0.02	0.23	—	1.27
	0.3	3.4	5.35	1.56	—	—	—	—
	0.9	3.4	5.17	—	0.02	—	—	—
	87.7	1.2	-2.30	—	—	0.23	—	—
	5.4	3.3	5.20	—	—	—	—	1.27
1.0 km	95.8	1.2	-17.31	6.46	0.04	0.40	—	2.48
	1.4	6.0	4.47	6.46	—	—	—	—
	1.2	6.0	6.89	—	0.04	—	—	—
	86.5	2.2	-5.85	—	—	0.40	—	—
	6.6	5.8	7.07	—	—	—	—	2.48
2.0 km	92.7	2.6	-37.66	17.90	0.07	0.61	—	4.11
	4.2	9.6	-2.38	17.90	—	—	—	—
	1.7	9.7	6.94	—	0.07	—	—	—
	79.9	4.4	-11.75	—	—	0.61	—	—
	6.9	9.4	8.04	—	—	—	—	4.11
3.0 km	89.3	4.0	-52.66	25.98	0.11	0.74	—	4.75
	5.8	11.7	-8.46	25.98	—	—	—	—
	2.6	11.9	4.46	—	0.11	—	—	—
	74.8	6.1	-15.86	—	—	0.74	—	—
	6.0	11.7	8.08	—	—	—	—	4.75
4.0 km	84.4	5.3	-63.63	34.6	0.14	0.78	—	4.57
	8.4	12.8	-15.99	34.6	—	—	—	—
	3.2	13.2	2.29	—	0.14	—	—	—
	68.2	7.6	-17.66	—	—	0.78	—	—
	4.6	13.1	8.14	—	—	—	—	4.57

Table 10. As in Table 8, but assuming that the reflectivity factor is known (359 degrees of freedom) and takes the values shown in the left column.

Radar Reflectivity	% Variance Explained	Est. Std. Dev. of Model Error	Regression Coefficients					
			Const	LR	Tsfc	dBz	CBHt	Rad
20 dBz	60.2	1.5	-9.08	10.34	0.02	—	-0.46	1.94
	24.8	2.0	-6.39	10.34	—	—	—	—
	1.7	2.3	0.98	—	0.02	—	—	—
	6.6	2.3	3.37	—	—	—	-0.46	—
	27.2	2.0	0.13	—	—	—	—	1.94
30 dBz	56.3	2.5	-18.04	20.73	0.03	—	-0.01	2.49
	37.6	3.0	-12.76	20.73	—	—	—	—
	1.8	3.8	2.30	—	0.03	—	—	—
	0.0	3.8	4.89	—	—	—	-0.01	—
	16.8	3.4	1.96	—	—	—	—	2.49
40 dBz	56.5	3.7	-25.22	26.84	0.07	—	0.67	3.85
	30.1	4.6	-13.77	26.84	—	—	—	—
	4.7	5.4	3.49	—	0.07	—	—	—
	2.5	5.4	7.62	—	—	—	0.67	—
	19.2	4.9	4.56	—	—	—	—	3.85
50 dBz	66.7	4.0	-21.52	19.01	0.12	—	3.04	4.36
	9.6	6.5	-0.27	19.01	—	—	—	—
	9.3	6.5	6.13	—	0.12	—	—	—
	32.2	5.6	9.51	—	—	—	3.04	—
	15.7	6.3	10.81	—	—	—	—	4.36
60 dBz	83.2	3.8	-13.11	9.65	0.14	—	5.85	4.55
	1.4	9.3	16.17	9.65	—	—	—	—
	7.2	9.0	12.69	—	0.14	—	—	—
	65.3	5.5	12.08	—	—	—	5.85	—
	9.3	8.9	19.07	—	—	—	—	4.55

Table 12. As in Table 8, but assuming that the rainshaft radius is known (599 degrees of freedom) and takes the values shown in the left column.

Rainshaft Radius	% Variance Explained	Est. Std. Dev. of Model Error	Regression Coefficients					
			Const	LR	Tsfc	dBz	CBHt	Rad
0.5 km	77.9	3.8	-29.05	15.27	0.05	0.47	1.02	—
	4.6	7.8	-4.60	15.27	—	—	—	—
	0.9	7.9	4.86	—	0.05	—	—	—
	69.7	4.4	-10.41	—	—	0.47	—	—
	2.7	7.9	6.25	—	—	—	1.02	—
1.0 km	77.1	4.9	-37.28	18.33	0.07	0.59	1.91	—
	4.0	10.0	-3.88	18.33	—	—	—	—
	1.5	10.2	5.81	—	0.07	—	—	—
	65.9	6.0	-11.80	—	—	0.59	—	—
	5.7	9.9	7.69	—	—	—	1.91	—
2.0 km	75.7	5.4	-39.82	18.35	0.11	0.59	2.53	—
	3.6	10.7	-1.73	18.35	—	—	—	—
	3.2	10.7	4.78	—	0.11	—	—	—
	59.9	6.8	-9.85	—	—	0.59	—	—
	8.9	10.3	8.55	—	—	—	2.53	—

Table 11. As in Table 8, but assuming that the surface temperature is known (299 degrees of freedom) and takes the values shown in the left column.

Surface Temperature	% Variance Explained	Est. Std. Dev. of Model Error	Regression Coefficients					
			Const	LR	Tsfc	dBz	CBHt	Rad
55° F	75.1	4.1	-28.95	18.10	—	0.46	0.90	2.24
	6.3	7.8	-6.21	18.10	—	—	—	—
	63.8	4.9	-9.07	—	—	0.46	—	—
	2.0	8.0	7.29	—	—	—	0.90	—
	3.0	8.0	6.56	—	—	—	—	2.24
65° F	76.2	4.3	-30.71	17.67	—	0.50	1.30	2.77
	5.0	8.6	-4.81	17.67	—	—	—	—
	63.8	5.4	-9.73	—	—	0.50	—	—
	3.5	8.7	7.48	—	—	—	1.30	—
	3.9	8.7	6.97	—	—	—	—	2.77
75° F	76.8	4.6	-32.42	17.30	—	0.54	1.68	3.24
	4.1	9.4	-3.61	17.30	—	—	—	—
	63.2	5.8	-10.41	—	—	0.54	—	—
	5.0	9.4	7.58	—	—	—	1.68	—
	4.5	9.4	7.32	—	—	—	—	3.24
85° F	77.4	4.9	-34.07	16.93	—	0.57	2.03	3.72
	3.4	10.1	-2.53	16.93	—	—	—	—
	62.5	6.3	-11.08	—	—	0.57	—	—
	6.4	10.0	7.60	—	—	—	2.03	—
	5.1	10.0	7.53	—	—	—	—	3.72
95° F	77.8	5.2	-35.81	16.89	—	0.60	2.37	4.14
	3.0	10.8	-1.85	16.89	—	—	—	—
	61.4	6.7	-11.64	—	—	0.60	—	—
	7.4	10.5	7.54	—	—	—	2.37	—
	5.6	10.6	7.68	—	—	—	—	4.14
105° F	77.7	5.5	-37.43	17.00	—	0.63	2.65	4.50
	2.7	11.4	-1.42	17.00	—	—	—	—
	60.3	7.3	-12.18	—	—	0.63	—	—
	8.7	11.0	7.47	—	—	—	2.65	—
	6.0	11.2	7.78	—	—	—	—	4.50

Table 13. As in Table 8, but assuming that the lapse rate is known (449 degrees of freedom) and takes the values shown in the left column.

Ambient Lapse Rate	% Variance Explained	Est. Std. Dev. of Model Error	Regression Coefficients					
			Const	LR	Tsfc	dBz	CBHt	Rad
70% of D.A.	71.9	5.0	-23.63	—	0.08	0.58	0.62	3.22
	2.0	9.3	2.73	—	0.08	—	—	—
	64.6	5.6	-12.29	—	—	0.58	—	—
	0.7	9.4	7.72	—	—	—	0.62	—
	4.6	9.2	5.26	—	—	—	—	3.22
80% of D.A.	74.7	5.0	-25.10	—	0.08	0.61	1.15	3.28
	1.9	9.8	3.81	—	0.08	—	—	—
	66.2	5.7	-12.44	—	—	0.61	—	—
	2.2	9.8	7.79	—	—	—	1.15	—
	4.3	9.6	6.38	—	—	—	—	3.28
90% of D.A.	78.8	4.7	-26.20	—	0.08	0.62	2.01	3.51
	1.7	10.1	5.49	—	0.08	—	—	—
	66.0	6.0	-11.62	—	—	0.62	—	—
	6.4	9.9	7.55	—	—	—	2.01	—
	4.6	9.9	7.66	—	—	—	—	3.51
100% of D.A.	82.8	4.1	-23.78	—	0.07	0.51	3.50	3.73
	1.5	9.8	8.57	—	0.07	—	—	—
	55.0	6.6	-6.38	—	—	0.51	—	—
	20.7	8.8	6.92	—	—	—	3.50	—
	5.6	9.6	9.92	—	—	—	—	3.73

Preliminary Comparison with JAWS Observations

- Model Data Subset Satisfying the Following:

$$U \geq 10 \text{ m s}^{-1}$$

$$2.0 \text{ km} \leq \text{Cloud Base} \leq 4.0 \text{ km}$$

$$75 \text{ F} \leq \text{Sfc Temp} \leq 95 \text{ F}$$

$$20 \text{ dBz} \leq \text{Reflectivity} \leq 40 \text{ dBz}$$

$$90\% \text{ D.A.} \leq \text{Lapse Rate} \leq 100\% \text{ D.A.}$$

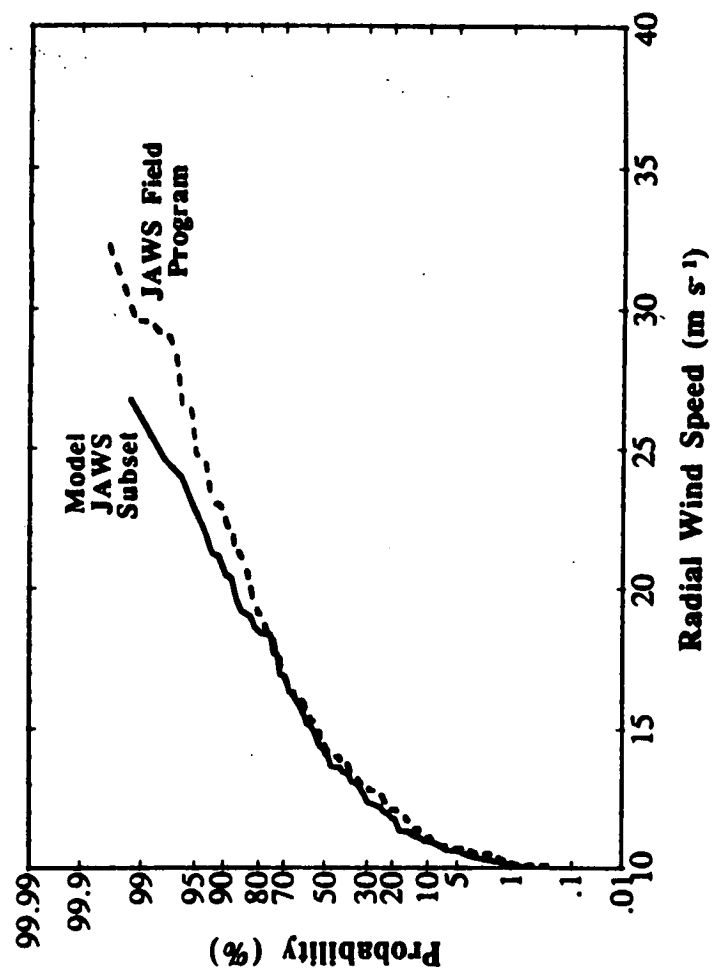
$$0.5 \text{ km} \leq \text{Rainshaft Radius} \leq 2.0 \text{ km}$$

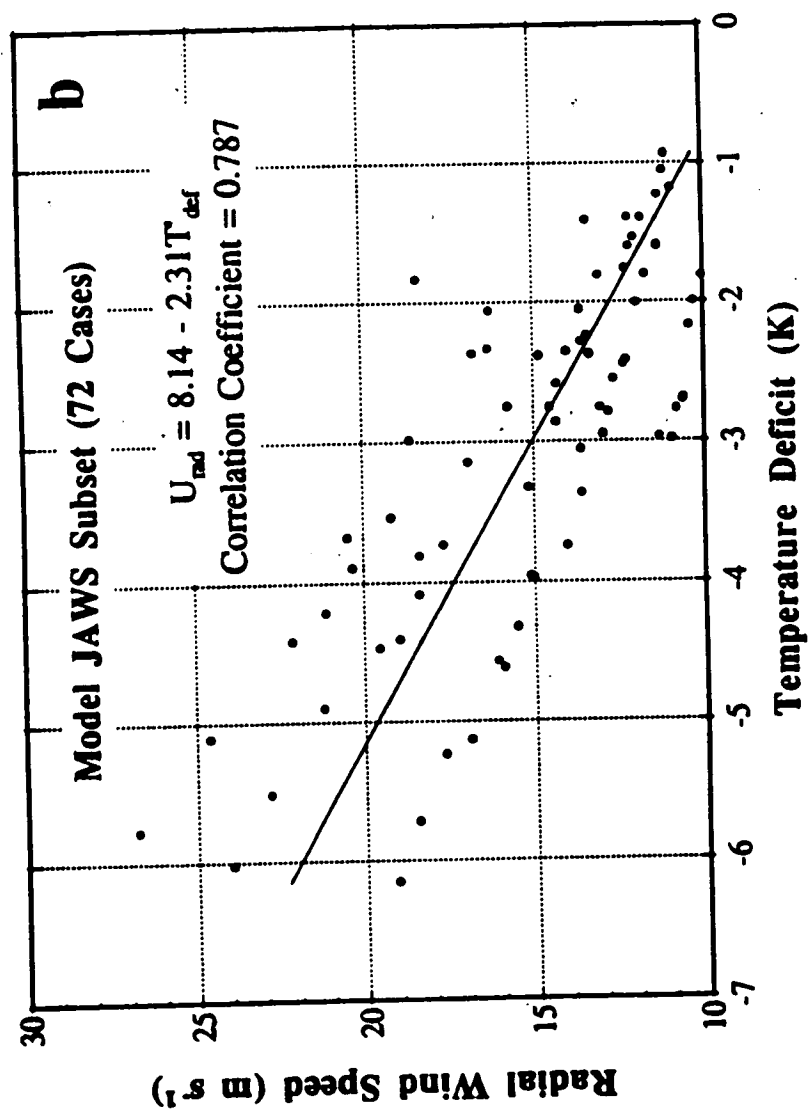
- 72 Simulations (vs 186 JAWS events)

Table 6. Probabilities of horizontal wind speed computed from the model data and JAWS observations.

Dataset	Wind Speed			
	≥ 20 kts	≥ 25 kts	≥ 30 kts	≥ 35 kts
JAWS Observations	98.39	76.88	42.47	23.12
All 1800 Simulations	44.50	35.17	28.22	22.61
†Model JAWS Subset	98.61	66.67	40.28	25.00

† Criteria: radial wind $\geq 10 \text{ m s}^{-1}$
 $2.0 \leq \text{cloud base height} \leq 4.0 \text{ km}$
 $75 \text{ F} \leq \text{surface temperature} \leq 95 \text{ F}$
 $20 \text{ dBz} \leq \text{cloud base reflectivity} \leq 40 \text{ dBz}$
 $90\% \text{ dry adiabatic} \leq \text{lapse rate} \leq 100\% \text{ dry adiabatic}$
 $0.5 \text{ km} \leq \text{rainshaft radius} \leq 2 \text{ km}$
(72 cases)





Preliminary Conclusions

- The Model Solution Space Contains Considerable Variability
- Solution Behavior is Physically Consistent
- Reflectivity is the Dominant Influence Most of the Time in Determining Radial Wind Speed
- Gross Statistical Comparisons with JAWS are Encouraging
- The "Numerical Field Experiment" Approach Appears Well-Suited to this Problem
- Several Avenues for Practical Application

Ongoing Work

- Inclusion of Ice Processes and Shallow Stable Layers
- "Pointwise" and Overall Statistical Comparisons with JAWS and Orlando TDWR OT&E Data
- Refinement of Parameter Space
- Evaluation of Probability Calculations for Operational Forecasting
- Further Development of Parametric Relationships Between Model Outputs and Inputs

**A "Numerical Filed Experiment" Approach for
Determining Probabilities of Microburst Intensity
Questions and Answers**

Q: Kim Elmore (NCAR) - I am fascinated by the work you did, and specifically how much of a predictor reflectivity was in general. For the equivalent JAWS simulations, how good of a predictor was reflectivity for intensity?. Do you remember?

A: Kelvin Droegemeier (University of Oklahoma) - We haven't actually done that break down for the JAWS data yet. Based on the other results, I would say it was probably a very strong influence.

Kim Elmore (NCAR) - Our experience in JAWS was that it wasn't a very good predictor of the outflow we would see. That was one of the major conclusions. Reflectivity, for the JAWS data, was not a good predictor.

Kelvin Droegemeier (University of Oklahoma) - I just had a student finish a Master's Thesis on a study of Orlando cases. What we have found and what tended to make that conclusion seem plausible in light of the fact that the reflectivity factor was the same and apparently similar environments, was the fact that low level effects like low level inversions in stable air change the outflow intensity. It does not take much stabilization in low levels to really change the outflow intensity. In fact you will see that if you stay around and look at the animation sequence. Now I know Fred and others of us who run models have actually dropped globs of rain into stable air for a long time. What this student did, for the first time, with a 3-D cloud simulation with ice, showed that the storms themselves forming beneath the low level stable air, were virtually unaffected by it. Once the rain came down and the outflow hit, that is when the radial winds were really diminished by virtue of the stable air.

Kim Elmore (NCAR) - We have seen, when gust fronts go by, that often once you stabilize a relatively deep part of the boundary layer that they do not make it through any more.

Kelvin Droegemeier (University of Oklahoma) - Yes; it doesn't have to be but maybe four or five hundred meters. It can be pretty shallow. One of the limitations of our study is that we did not put in the shallow stable layer. If you consider the parameters, you have to figure how thick is a layer and how cold is it. That is two more parameters and that would run it up to 20,000 simulations.

Kim Elmore (NCAR) - In JAWS, we also did not stratify the cases as to was there cold surface layer or not.

Kelvin Droegemeier (University of Oklahoma) - That is a tough thing to do. Usually they just skim the mesonet and you just never know.

Kim Elmore (NCAR) - Our gut feeling was; once we had a cold surface layer, if it had been around long enough to deepen, however much it had to deepen, and we did not even really know how much that was, that tended to shut it off.

Kelvin Droegemeier (University of Oklahoma) - I completely agree, I think that is the controlling influence for attenuating that stuff.

Q: Brac Bracalente (NASA Langley) - The reflectivity values you referred to are at the cloud level right at the high altitude where the rain first starts to fall. Did you do any correlating with the reflectivity levels at the outflow region? We have found that the peak shear did not necessarily occur where the heaviest rain was.

A: Kelvin Droegemeier (University of Oklahoma) - No, we have not done that but we could. In fact, if you stay around for the video tape you will see that the reflectivity near the ground or not too far above the ground is less than it is at cloud base height. I should have mentioned, in the absence of having ice in this case, we are assuming that once the precipitation falls below cloud base the only stuff that is important for the forcing that occurs that drives that microburst is the stuff that happens below cloud base. Obviously, that is not always the case, but that was the assumption in this case here. The reason we did that is so we do not have to consider all the possible soundings and wind profiles and everything that happens above cloud base where there is a lot of variability. So that was the other assumption.

Q: Fred Proctor (NASA Langley) - Define what you mean by your cloud base height in your model studies?

A: Kelvin Droegemeier (University of Oklahoma) - It is basically just the height at which the rain begins to fall, that is the simplest explanation.

Q: Fred Proctor (NASA Langley) - Is that the top of your model then?

A: Kelvin Droegemeier (University of Oklahoma) - Yes, and the vertical velocity is zero there.

Session III. Reactive System Technology

19930104 11

Session III. Reactive System Technology

N 93 - 19600
488723

30P

An Approach to Evaluating Reactive Airborne Wind Shear Systems

Joe Gibson, Martin Marietta

PRECEDING PAGE BLANK NOT FILMED

**AN APPROACH TO EVALUATING
REACTIVE AIRBORNE WINDSHEAR SYSTEMS
IN THE CONTEXT OF
GROUND-BASED SYSTEM DEPLOYMENT STUDY**

MARTIN MARIETTA

**JOE GIBSON
APRIL 14, 1992**

An Approach to Evaluating
Reactive Airborne Windshear Systems
in the Context of
Ground-based System Deployment Study

Joseph P. Gibson Jr
Martin Marietta
Air Traffic Systems
Washington, DC

ABSTRACT

An approach to evaluating reactive airborne windshear detection systems was developed to support a deployment study for future FAA ground-based windshear detection systems. The deployment study methodology assesses potential future safety enhancements beyond planned capabilities. The reactive airborne systems will be an integral part of planned windshear safety enhancements.

The approach to evaluating reactive airborne systems involves separate analyses for both landing and take-off scenario. The analysis estimates the probability of effective warning considering several factors including NASA energy height loss characteristics, reactive alert timing, and a probability distribution for microburst strength.

AGENDA

• **INTRODUCTION**

• **PURPOSE**

• **ANALYSIS**

• **SUMMARY**

PURPOSE

ANALYSIS TO SUPPORT DEPLOYMENT STUDY OF FUTURE GROUND-BASED SYSTEMS

- **TDWR OPTIONS**
- **ASR WINDSHEAR PROCESSOR**
- **LLWAS-3**

DEPLOYMENT STUDY METHODOLOGY ASSESSES POTENTIAL SAFETY ENHANCEMENTS BEYOND PLANNED SYSTEMS

- **PLANNED GROUND-BASED SYSTEMS**
- **PLANNED AIRBORNE SYSTEMS**

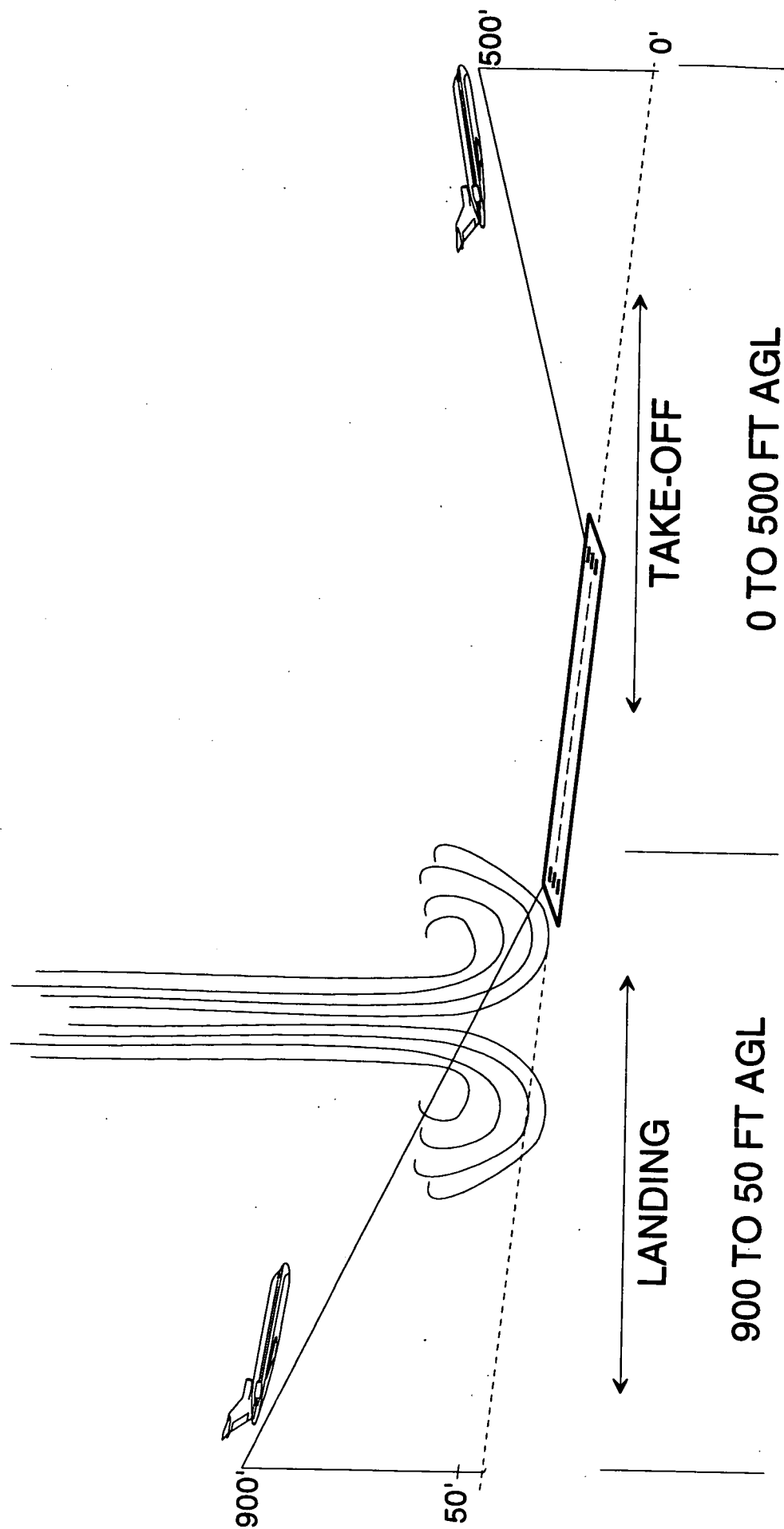
REACTIVE SYSTEMS ASSESSED

- **FORWARD-LOOKING ASPECTS UNCERTAIN**

Q-4

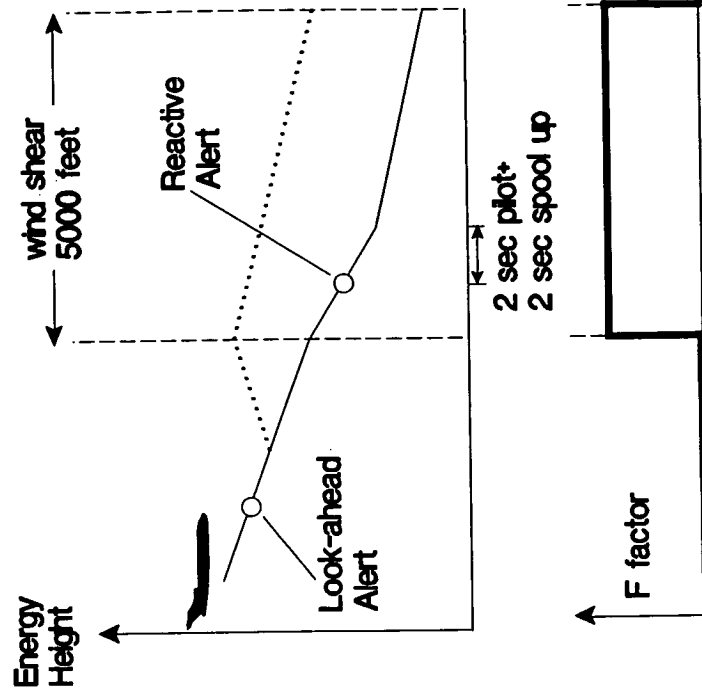
ANALYSIS OVERVIEW

- ANALYSIS PERFORMED FOR LANDING AND TAKE-OFF SCENARIOS



ENERGY HEIGHT ANALYSIS

- SCENARIO FOR NASA ENERGY HEIGHT ANALYSIS

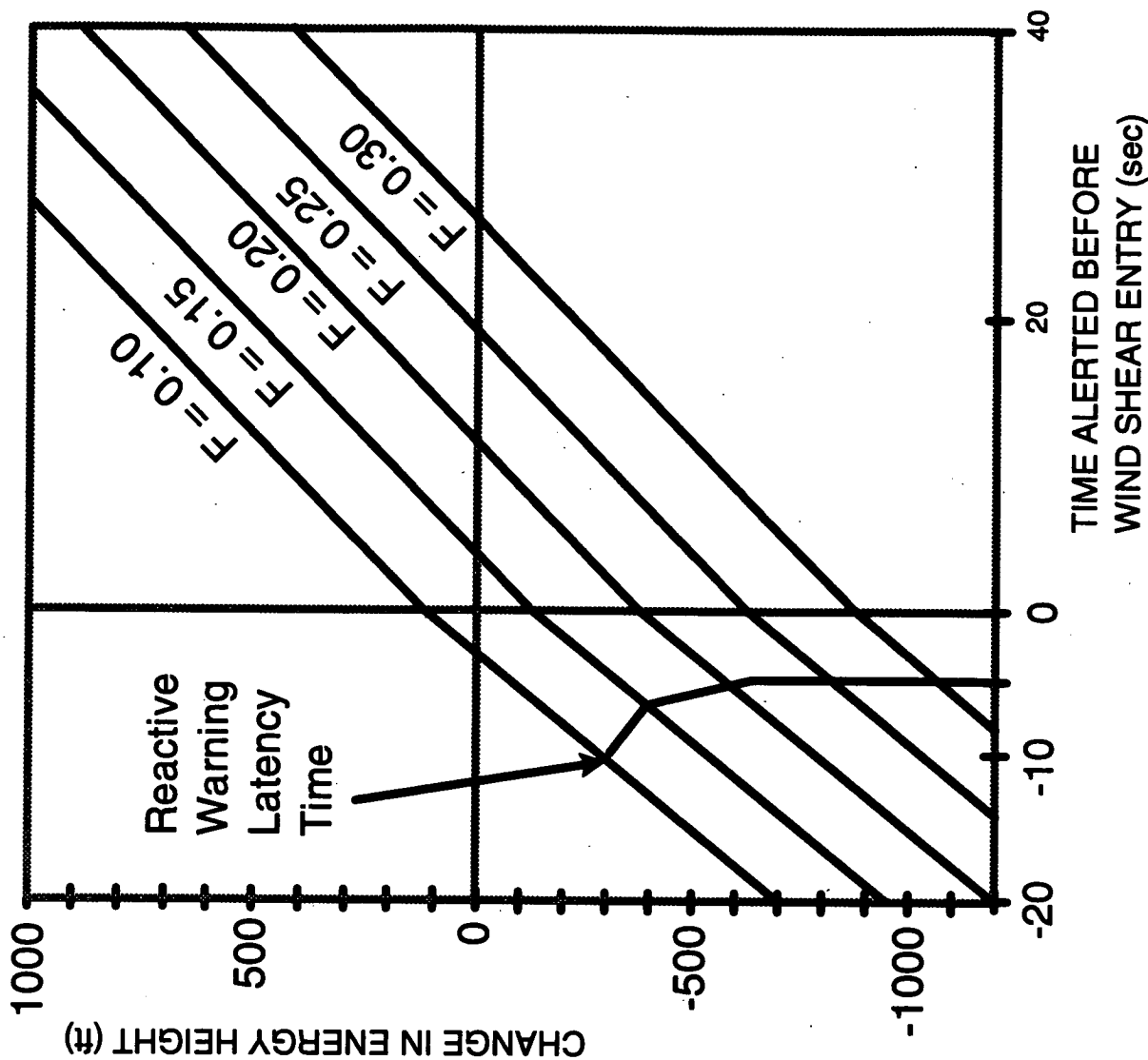
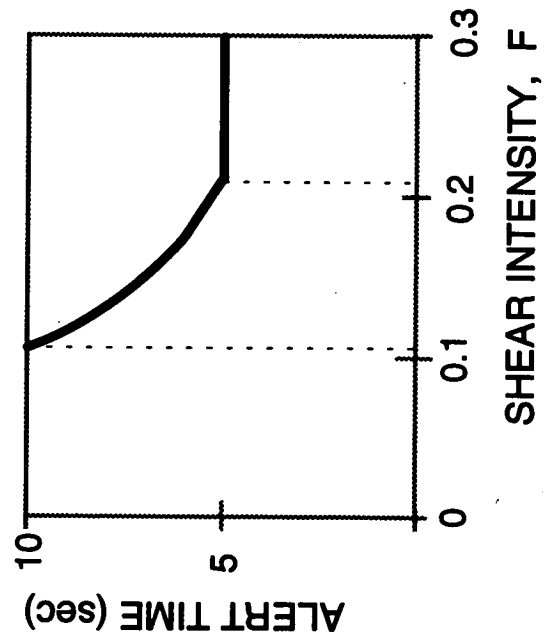


- AVERAGE AIRCRAFT PERFORMANCE AND MICROBURST HORIZONTAL SIZE
- CONSTANT F FACTOR ACROSS 5000 FOOT DISTANCE
- PILOT INCREASES POWER AND EXECUTES RECOVERY PITCH
- SIMULATED FULL RANGE OF ALERT TIMES AND WIND SHEAR STRENGTHS

ENERGY HEIGHT LOSS FOR REACTIVE SYSTEMS

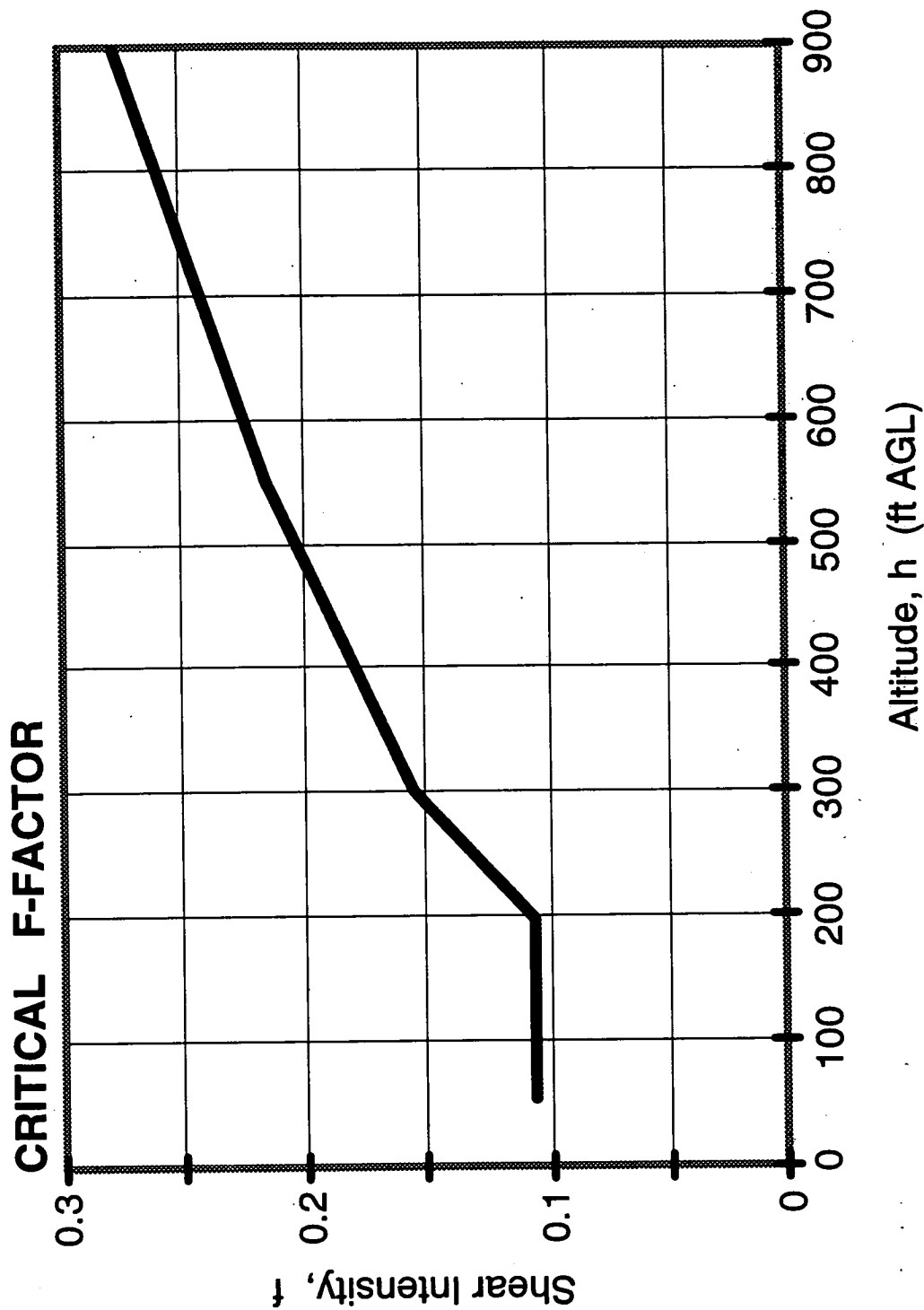
- ENERGY HEIGHT RESULTS
 - ALERT TIME
 - SHEAR INTENSITY, F
- DETERMINE ENERGY HEIGHT LOSS FOR REACTIVE SYSTEMS

REACTIVE ALERTING REQUIREMENTS (TSO-C117)



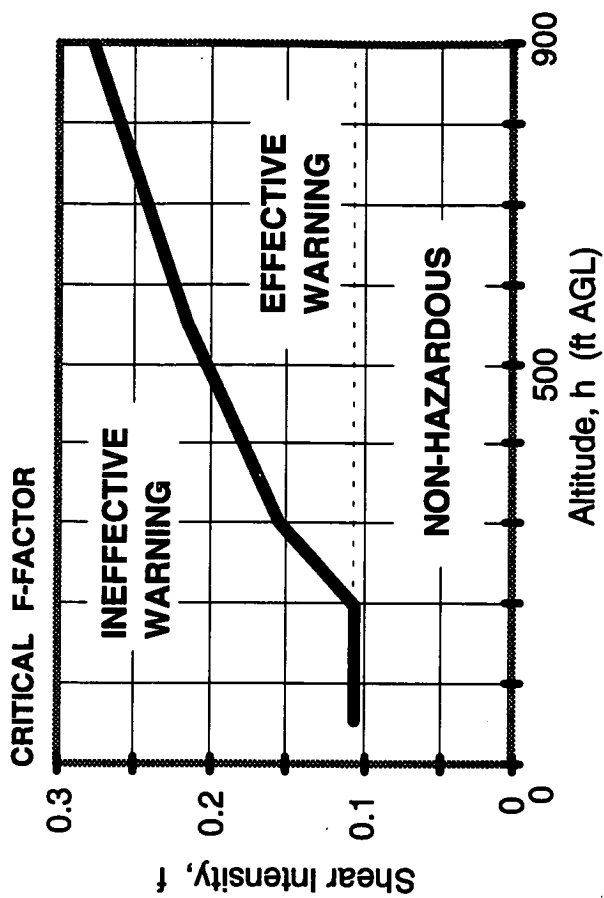
DETERMINATION OF CRITICAL F FACTOR

- FROM ENERGY HEIGHT LOSS, DETERMINE ALTITUDE LOSS.
- REACTIVE ALERT TIME
- ENERGY HEIGHT OFFSET

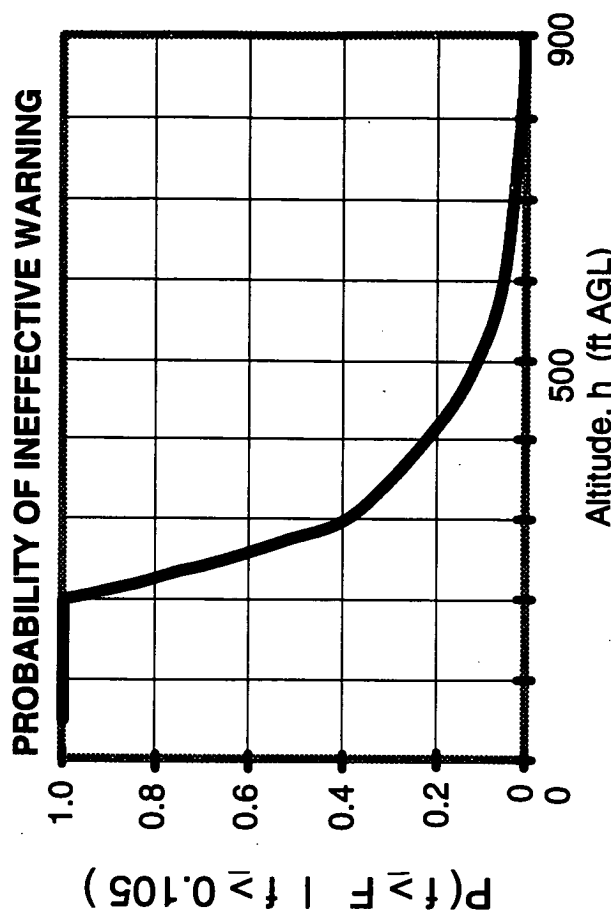
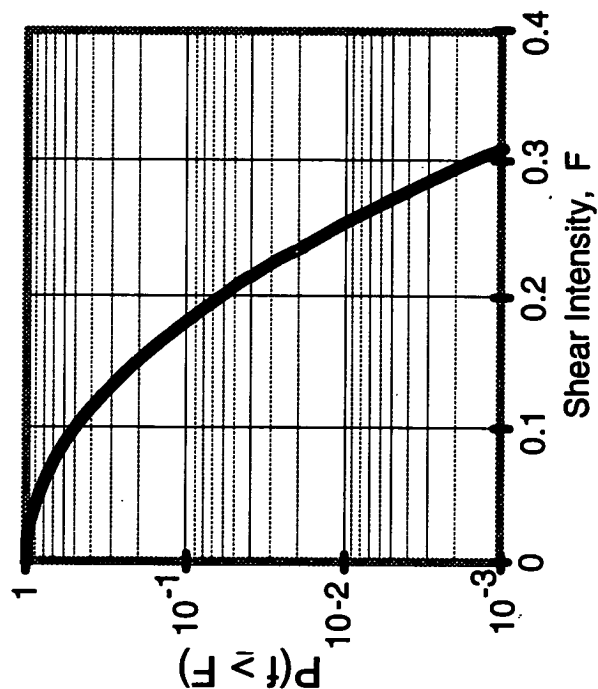


PROBABILITY OF INEFFECTIVE WARNING

- DETERMINE PROBABILITY OF EXCEEDING CRITICAL F-FACTOR GIVEN HAZARDOUS ENCOUNTER



- EXCEEDENCE PROBABILITY, $P(f \geq F)$ BASED ON OBSERVED MICROBURSTS



LANDING SUMMARY

- **PROBABILITY OF INEFFECTIVE WARNING AVERAGED OVER ALTITUDE RANGE**
 - **= .33**
- **PROBABILITY OF EFFECTIVE WARNING IS CONVERSELY**
 - **= .67**

TAKE-OFF

- **GROUND TO 50 FT AGL**
- **REACTIVE SYSTEMS NOT REQUIRED TO PROVIDED WARNING**
- **INEFFECTIVE FOR ROLLOUT**
- **50 TO 500 FT AGL**
- **CALCULATED SIMILARLY TO LANDING.**
- **HAZARDOUS THRESHOLD HIGHER, F_{HAZ}=.15**
- **OVERALL TAKE OFF PROBABILITY OF EFFECTIVE WARNING = 0.1**

OVERALL RESULTS

OVERALL PROBABILITY OF EFFECTIVE WARNING DETERMINED

- **LANDING WEIGHTED 67 % - TAKE-OFF WEIGHTED 33 %**

- **THREE POINT ESTIMATES DETERMINED**

- **OVERALL RESULTS**

- **HIGHEST 0.48**

- **MOST LIKELY 0.37**

- **LOWEST 0.24**

SUMMARY

- **REACTIVE EFFECTIVENESS DETERMINED CONSIDERING**
- **REACTIVE ALERT TIME REQUIREMENTS**
- **APPROACH/LANDING SCENARIOS**
- **AVERAGE AIR CARRIER AIRCRAFT MIX**
- **AVERAGE MICROBURST HORIZONTAL SIZE**
- **VARIED WIND SHEAR STRENGTHS**

An Approach to Evaluating Reactive Airborne Wind Shear Systems

Questions and Answers

Q: Dan Stack (ALPA) - I am curious whether or not you are including rejected landings or shall we say go-arounds in your landing criteria? Perhaps rejected landings and go-arounds should be a separate criteria.

A: Joe Gibson (Martin Marietta) - No I do not believe so.

Dan Stack (ALPA) - I can think of a couple of cases where a go-around was actually attempted. One was a US Air that ended up in the grass at Detroit, and about 15 years ago there was another one in Saudi Arabia where a go-around was attempted in a microburst and had gotten to 800 feet above the ground before they were blasted back onto the ground by a second microburst. So perhaps this rejected landing or a go-around concept should be included some place in your data.

A: Joe Gibson (Martin Marietta) - No we did not consider that, but it is a good point.

Q: Unknown - Could you expand on why you think the hazardous F-factor is higher in the takeoff configuration?

A: Joe Gibson (Martin Marietta) - Well, because the aircraft is up near full power, and therefore you can go through a higher strength microburst without it affecting your climb performance. When you are going in at approach airspeed you are going in slower and a microburst of comparable strength would effect you more on landing.

Mike Lewis (NASA Langley) - The curves that I showed in the last presentation would show just the opposite of that?

Joe Gibson (Martin Marietta) - Yes, I realize that. That was the assumption when I went in. I did this about six months ago.

Q: Bud Laynor (NTSB) - How did you consider the trade off of kinetic energy for potential energy when you were going through your studies? You talked in terms of energy height loss, but not in terms of airspeed, and yet you mentioned the pitching maneuver per the training aid?

A: Joe Gibson (Martin Marietta) - Yes, that energy height offset that I was talking about is basically to account for the slowing of airspeed and then losing kinetic energy to save you actual potential energy, which is the energy height, the height you are at. That was about a one hundred foot offset; considering that you could slow, you could lose some airspeed with out getting to stall.

Session III. Reactive System Technology

Panel Discussion

Kirk Baker, Federal Aviation Administration
Dr. Roland Bowles, NASA Langley Research Center
Joe Gibson, Martin Marietta
Howard Glover, Sundstrand
Doug Ormiston, Boeing
Rosa Oseguera, NASA Langley Research Center
Dr. Paul Robinson, Lockheed Engineering & Sciences
Terry Zweifel, Honeywell

PRECEDING PAGE BLANK NOT FILMED

Reactive System Technology - Panel Discussion

Panel Members:

Kirk Baker,	Los Angeles Certification Office, FAA
Roland Bowles,	NASA Wind Shear Program Office, NASA Langley
Joe Gibson,	Air Traffic Systems, Martin Marietta
Howard Glover,	Reactive Wind Shear Systems, Sundstrand
Doug Ormiston,	Reactive Wind Shear Systems, Boeing
Rosa Oseguera,	NASA Wind Shear Group, NASA Langley
Paul Robinson,	NASA Wind Shear Group, Lockheed Engineering
Terry Zweifel,	Reactive Wind Shear Systems, Honeywell

Roland Bowles (NASA Langley) - We composed some questions that we thought were pertinent and would fuel some discussion, and distributed them to the panel members. I will just review them briefly.

1) Current industry status of reactive technology.

- Percent equipage to date in the system for those who have opted to equip with reactive system technology.
- Operational successes that any of you may want to relate.
- Operational problems and solutions as you see them.

We have an expert here from the FAA on equipage; his name is Frank Rock. In fact he is an expert on all of this. Frank, what is the current fleet equipage percentage now?

Frank Rock (FAA) - I do not have the exact number, but it was quoted at the last meeting we had and if I remember correctly it was about 50%.

Roland Bowles (NASA Langley) - Operational successes? You fellows who design and build and implement them, is the technology out there working for you? Is it paying off? Have you saved lives as a result of this technology?

Howard Glover (Sundstrand) - I guess one way of looking at it is that I have not heard of a fatal Wind Shear accident in a while. I asked around our place for some statistics, and I was surprised at what I found. I won't go into the gory details, but Sundstrand manufactures a couple of different flavors of Wind Shear detection systems. One of them contains a Wind Shear algorithm which is designed by Boeing and delivered on all new Boeing aircraft. The other is one that we have designed ourselves and is essentially intended for older aircraft, the so-called analog aircraft. There are approximately 2,500 of our systems flying, and they have probably been flying in those numbers for about a year. That is an average I would say. That is several million flight hours I believe, unless my arithmetic is totally hosed up. That is for a typical airline operation. We have only heard of a single save in that whole time, and that is the Atlanta 767 that somebody

mentioned this morning. That is amazing. So either it is happening and we are not hearing about it, or the frequency of encountering the Wind Shear is considerably less, because of the avoid factor, which all the pilots are now being trained to do, is paying off. That is the only conclusion that I can come to. I suspect that it is the correct one. I guess the conclusion that operators are not reporting events is probably true also. But on reflection, the avoidance, both by use of information from the ground and also pilot reports, is paying off.

Unknown - What about invalid alerts?

Howard Glover (Sundstrand) - Nuisances. We won't get too deep into the distinction between system failure induced alerts and nuisance alerts. Originally, they were quite frequent the thing said wind shear and there wasn't one. Well, actually there was a wind shear, but it was not hazardous. Rosa Oseguera mentioned this morning several ways of compensating a reactive system to take care of operational factors. One of the worst operational factors that we had problems with was the down wind turn that she mentioned. When you turn from flying into the wind to down wind, the aircraft sees an effective wind shear. We had compensated for that but not enough. We found that at least one carrier during flight training operations was making forty five degree bank turns in surface wind conditions of sixty knots or more. That will do it everytime. So we had to tailor our system to that. Another factor was that pilots quite naturally tend to carry excess airspeed when they suspect wind shear might be present. To a reactive system that can look like an effective increase in the wind shear intensity. We also added compensation for that excess airspeed to reduce the unwanted warning. Since we did all of those things we have had relatively few nuisance alerts. In fact I could not find any reports, other than sensor failures, in the last six months. Sensor failures is a whole other story. Obviously, if you are depending on aircraft sensors and they fail then you can induce an apparent wind shear alert.

Roland Bowles (NASA Langley) - Terry, do you have any comments about your successes?

Terry Zweifel (Honeywell) - We have been out in the industry now since about 1985 or so and have had on the order of 10 valid alerts by pilots. In some cases they were apparently quite critical wind shears that the pilot was able to get out of and wrote us a nice report. I tend to agree with the idea that having these devices coupled with the training in avoidance has made a major impact on the number of alerts that has occurred, even possible accidents.

Paul Robinson (Lockheed) - Can I ask Howard Glover how you compensate for the wind shear alert going off in the down wind turn?

Howard Glover (Sundstrand) - In the down wind turn we have bank angle as an input. We assume that if a bank angle above a certain threshold is sustained for a while, the pilot or the flight control system is doing it and the aircraft is in an intentional turn. Now I have heard it argued that we know that the kind of turbulence you get in a wind shear encounter induces bank angles of that order, I say yes, but the wind shear warning has gone off before that, in our simulations anyway.

Paul Robinson (Lockheed) - So you are effectively reducing the gain on the system?

Howard Glover (Sundstrand) - Exactly, yes.

Roland Bowles (NASA Langley) - I think that introduces the next question. Is there design space remaining to improve reactive system technology? Is it possible to look at perhaps better performance at lower cost? Is the gust rejection or turbulence problem solved? Are the time to alert performance of these systems optimized? And the last one relates exactly to Paul's question; do you need three axis implementation? You can let the physics do the walking through the yellow pages for you there, rather than degaining the system as a function of bank angle. Would that be a worth while improvement or would it be considered excessive cost? Any comments along those lines?

Paul Robinson (Lockheed) - I would like to present something which backs up what Mike Lewis presented this morning. This deals with the gust rejection filters, the time to alert, and the parameter on which the system should alert. Mike mentioned that the hazard is defined as a one kilometer averaged F-factor. I would like to show you this chart here. The red line is the F-factor that was experienced by the In Situ system while penetrating Event 143. It is filtered using a second order filter. If we take the raw unfiltered data and calculate the backward one kilometer average of the F-factor we get the black line. As you can see it is a lot noisier than the In Situ F-factor we are using, but it illustrates two points. One is that if you are going to work on an average F-factor of 0.105 or more you require some filtering in order to get the alert at the correct time and of the correct volume. The other point is that the filter does a lot better job at noise suppression. So you are really gaining two things here, noise suppression, and you are actually calculating an averaged F-factor on which to alert. This might put up a new spin on the gust rejection filter problem.

Roland Bowles (NASA Langley) - We are asking this question from the perspective of the technologist. Let me ask this, is there any drivers on the airline side to improve performance, or are they perfectly happy with the product they have? Do they want improved performance, perhaps even at lower costs? Or is the customer clambering for something better? Any other comments about design space remaining for this technology to improve situations?

Howard Glover (Sundstrand) - I think I would get fired if I said there was no design space left. Yes, of course, there is. But you hit it right on the head a moment ago. Are the improvements necessary? No, the customers are not beating on us for that. They are beating on us for all the usual things that customers do. More reliability of the equipment, etc.

Terry Zweifel (Honeywell) - I would like to make a few comments relative to the turbulence rejection and time to alert. The real problem with reactive systems is that you have to have the heavy filtering. The filter that Paul just showed is not a light filter, it is a very heavy filter, and you have to have that for the turbulence suppression. Conversely, that filter is the very thing that keeps it from alerting faster. A lot of studies that we have done at Honeywell and I know that others have done throughout the industry show, that unfortunately, with the simple type filters that we are looking at this is apparently as good as we can do. There are other concepts that we have looked at, but have not really got to the point of production readiness. Smart filters for example, using some of the atmospheric parameters that Kelvin Droegemeier was talking about. Maybe you can make those filters a little less heavy in certain conditions. So I think there is some

room to grow in that area. But right now as I see it that is about the only area you are going to get a faster detection time out of.

Roland Bowles (NASA Langley) - You are really beating your head against a vicious trade off. The physics is compelling. You are either going to get a lot of false alerts and good response time, or a lot of delay?

Terry Zweifel (Honeywell) - The filter itself determines how many nuisance alerts you are going to have.

Roland Bowles (NASA Langley) - To what extent do you think the application of reactive system technology can be made aircraft independent or aircraft non specific. In other words, can one box work for all airplanes? Would that be useful? Are there manufacturers that are thinking along those lines?

Howard Glover (Sundstrand) - I think all of the reactive system manufacturers have essentially one system, for all transport category aircraft anyway. In fact, I think inherent in the reactive system is an independence from the aircraft performance; as far as wind shear detection is concerned anyway. As far as recovery guidance is concerned, obviously it has to be somewhat specific to the aircraft. Terry, do you disagree with that?

Terry Zweifel (Honeywell) - I agree one hundred percent. In fact, we have done studies on that and have actually submitted a report to the FAA comparing L-1011's, DC-9's, 727's, 737's, the whole gambit, and the detection times just do to the algorithms are virtually identical. There are of course differences in what sensors they have, how the boxes are mounted on the airplane, that sort of thing. The basic detection algorithms have not changed for any of the airplanes so naturally you would hope that it would detect the same. So yes, I would agree with that. There is physically no reason that they should be different, given roughly the same long period frequencies and that sort of thing. It is not necessarily true, as you mentioned, on the lighter airplanes, the Gulf Streams perhaps, and some of those.

Roland Bowles (NASA Langley) - I think for heavy airplanes, 100,000 pound category or heavier, you are in good shape. I think the light ones could pose a challenge. I guess that leads us into the one that I think a lot of people are about ready to engage in, and that is, the industry view of the FAA certification criteria as exemplified in the TSO C-117. Is the TSO a useful standard? Is the TSO content technically sound? What are the current problems in applying the TSO? And, are industry and government willing to modify the TSO where appropriate? If that is a reasonable thing to do, what kind of process would you have to go through to do that?

Kirk Baker (FAA) - Right now the requirement documents that we use to certify reactive systems are AC 25-12, AC 120-41, and TSO C-117. The minimum performance requirements for the system are referenced in TSO C-117. One of the problems that we have seen is a discontinuity between AC 25-12 and TSO C-117. AC 25-12 brings out the way you demonstrate the system, but it does not specifically have hard requirements like the TSO does. Today we've only had one application for TSO C-117 that we are considering in the Long Beach Office. What we have looked at so far has demonstrated to us that there is a definite lack of interpretation of

what the TSO really says, and how you interpret the performance requirements. This is our goal: that all applications for type certificate or type certificate and supplemental type certificate STC's will be required to meet the minimum performance standards of the TSO. No one has demonstrated that to us yet. I think this is because of the complexity of the TSO. I think the FAA has an obligation to make this happen; to clearly define the FAA policies for reactive systems and approval under TSO C-117. One of the ways that Roland had indicated, was possibly amending the TSO. If we can't use it and we can't seem to implement it then maybe we need to change it. Well, I am doing something right now, in the ACO, to try and better provide the FAA's interpretation of what the TSO requirements are. I have sent that document out and I believe some of you have received that document already. If you haven't I do have copies here and you are welcome to take some. This policy statement is in a draft form right now and we have coordinated it through all the ACO's. It specifically spells out our interpretation of the requirements, and how you should meet the requirements in performance and guidance. We are soliciting your comments right now on our interpretation. I think that is one way of determining whether we need to change the TSO. What I would propose is to come to an agreement on what those policies and interpretations should be. Then I would like to amend AC 25-12 to include a statements which references the TSO as the minimum performance standard. But, in order to do this we need your comments as soon as possible. That is basically, I think, the FAA's position right now on certifying and approving systems under the TSO. We will need those comments in by April 30, 1992.

Terry Zweifel (Honeywell) - One obvious comment there would be on your statement to amend AC 25-12 to include a statement which references the TSO. That kind of makes the TSO an advisory circular, doesn't it? What if I have this wonderful box and I want to go certify it are you going to certify it under AC 25-12? If so, do I have to go out and run the whole TSO? For those of you who may not be familiar with it, the TSO is not a small test. It takes approximately four weeks to run this set of tests. So if you are trying to build boxes for all kinds of airplanes you are getting into some very involved testing. Obviously we as manufacturers would just as soon not do that unless we had to. That is my concern. In essence the TSO is just becoming a part of an AC and there is no TSO.

Kirk Baker (FAA) - Well the AC is one way to certify a system. I don't think you are creating an AC out of the TSO. The TSO has minimum performance requirements listed in it, times to detect. That is something that the AC doesn't have. There shouldn't be a disconnection there. What I see happening in the industry, is everybody wants to continue to certify their systems under the AC 25-12 to establish practices with various ACO's. One thing that promotes is non standardization and ACO shopping. Because one ACO does not treat an applicant the same as another. That is one of the reasons that I think the TSO is a valuable document. It could create some standardization. It is a minimum performance standard. I think that goes right along with a generic type, airplane independent system. I know the industry feels that they are generic, but they have never demonstrated it. We have always gone and demonstrated on the type airplane that needed it.

Terry Zweifel (Honeywell) - My concern is that if you continue doing it that way, what you end up with is that we AC every possible type of airplane. There is no longer any need for the TSO. It doesn't accomplish anything. If you take that approach, you think why TSO to begin with.

Howard Glover (Sundstrand) - I would invert that. Our experience is that we had to do the same amount of testing to certify, in addition to TSO certification, whether or not meet we the TSO. In other words, when we go to the certification office, they still want to see it on the simulator specific to the type of aircraft were going on. We still have to ground and flight test on the aircraft that we are applying for the supplementary type certificate for. The biggest potential factor in variation of performance from installation to installation, is the sensors on the aircraft, and that is not addressed by the TSO at all.

Kirk Baker (FAA) - Those are installation specific requirements.

Terry Zweifel (Honeywell) - That is why you need the AC.

Kirk Baker (FAA) - Exactly, I was going to add that point. That is why I think, if we can somehow be convinced in the FAA that the systems are generic detection wise, than the TSO could become a useful document. Because once you demonstrated your performance and function of detection then again you would still have to go out and demonstrate installation specifics like sensor combinations and guidance requirements. But the detection portion would be taken care of under the TSO. That is one advantage I see of the TSO. I am not a real fan of the TSO myself, but it is with us and we have to try and use it. That is why I am trying to disseminate and get the FAA to make some interpretations of what the requirements are of the TSO and standardize those. Then disseminate them to industry for your review and comment. If we can live with our interpretation, then we will go ahead and publish that as a memorandum policy letter to all of the ACO's along with probably some guidance on the installation specifics. Again, just because you have the TSO doesn't mean you can just go stick it on an airplane.

Terry Zweifel (Honeywell) - No, admittedly. The problem from the manufacturers point of view is that building simulators to certify all these systems on is a very expensive proposition. Where do you find DC-8 simulators that you can try your reactive system on. They are very hard to come by and you end up struggling with that. The idea of the TSO, I thought, would be that you could take this box which was TSO'd and I wouldn't need to build that DC-8 simulator. I know the detection laws are OK. That to us was the big advantage. I was afraid you were trying to tell me, "that is nice but we won't do that, you are still going to have build the DC-8 simulator."

Kirk Baker (FAA) - No, I think we can tackle the detection issue. Guidance is another question altogether, obviously. The rule has been changed. Guidance is not a requirement on older airplanes. DC-8 being one of them.

Howard Glover (Sundstrand) - Kirk, if you are willing to revisit AC 25-12 are you willing to revisit TSO C-117, and reconvene the committee for one session?

Kirk Baker (FAA) - Certainly, if the comments from industry strongly oppose our interpretation and convey to us that there is a need to amend the TSO then that is what we will do. That is a lengthy process.

Terry Zweifel (Honeywell) - That is the concern I have. If it will take 50 years then it is going to be of no value to anyone.

Kirk Baker (FAA) - That is why I am trying to promote this other way. That is, by coming to an agreement on the interpretation of the requirements in the TSO. With that knowledge base, then amend the AC 25-12. We want to enforce the idea that any certification of a reactive system has to meet the minimum performance standards of the TSO. That is standard FAA policy. Right now that is not happening.

Terry Zweifel (Honeywell) - I am not sure what you are referring to. We, by the way, happen to be an applicant for the TSO, in case you haven't deduced that?

Kirk Baker (FAA) - We haven't seen that yet and you may convince us otherwise. From the data that I have looked at so far, I don't think you demonstrated the system the way we interpreted it. For instance, the wind axis separately as opposed to in combination.

Terry Zweifel (Honeywell) - I don't know if you want to get into the details of the TSO?

Kirk Baker (FAA) - I don't think we really do.

Roland Bowles (NASA Langley) - I don't think we have time today. The intent here is to expose a willingness on the FAA's part to sit back and garner comments from the industry, look at what your comments are, and if appropriate, put a process in place to alter or at least amend the TSO. In terms of you who have actually used it. What are the areas that are sensitive to you? What is most difficult? If it takes four weeks, what are the stumbling blocks in the TSO?

Terry Zweifel (Honeywell) - One thing is this running the turbulence test.

Roland Bowles (NASA Langley) - I totally disagree with the whole turbulence approach. That is one we are going to purpose.

Howard Glover (Sundstrand) - It isn't just the time taken for the turbulence test, Roland, which is excessive. I think it is 250 hours, something like that. It is the fact that each run of the turbulence test is, for example done at constant altitude. We have to have a system which takes into account aircraft performance instantaneously. If the aircraft is in takeoff configuration it should be climbing. If it is in an approach configuration it should be descending at 700 feet per minute, roughly. None of that is taken into account by the turbulence model. In fact it is totally artificial for our system to fly level at 500 feet above the ground. That does not make sense, and yet here you are doing it as a test.

Terry Zweifel (Honeywell) - I don't argue that. It does give you an indication of what your turbulence sensitivity is.

Paul Robinson (Lockheed) - But it doesn't have to be done like that. The turbulence testing process can be simplified based on the work that Roland has been doing at NASA. A follow on to that is the inputs for Wind Shear detection, using actual microburst F-factor inputs or windfields. There doesn't seem to be too much representative of what we saw in the field in 1991, that goes through the system in terms of predicting time to alert, and missed alerts in the TSO. That would be another problem, the weather inputs.

Terry Zweifel (Honeywell) - Are you saying that the wave forms are not realistic?

Kirk Baker (FAA) - They are not realistic.

Terry Zweifel (Honeywell) - The problem is you would have to come up with an infinite number to represent every conceivable microburst thing. How do you say this five is representative and this five isn't?

Roland Bowles (NASA Langley) - What we would like to contribute to your process is to suggest a significant revision, though not complicated or more complex, turbulence realization for consideration in the TSO. And then also, to consider the applicant complying with the nuisance criteria by a direct calculation of a performance number compared to a curve. Is he above it or below it? This ability to predict what the nuisance rate or level exceedance rate may be is based on well founded scientific and accepted aviation computational principles. Let me put it another way. I think it makes no sense to sit there and run at one constant altitude an airplane simulation for 2500 hours with a fixed RMS turbulence, and count an exceedance. What I think we want to do is ask the question, "how often will you get a nuisance due to operational turbulence based on well founded available data, per operation." Use three minute approaches and three minute departures, and Monte Carlo that. That is the operational number you want. Not whether or not one turbulence realization run for 2500 hours will give you an exceedance. Howard, do you see what I am suggesting?

Howard Glover (Sundstrand) - I agree with you entirely.

Roland Bowles (NASA Langley) - And, we can do that problem by calculation, rather than simulation. We would like to lay this out for you Kurt, and see how the industry responds to it. Here is some data that shows how well we predicted it as compared to measurements. The measurements are based on data that was provided courtesy of Boeing in their Southwest program. Our problem is getting this kind of operational data to compare the predictions to. This is what our system looked like, and notice in both cases, the measurements are falling under the tail of the calculation. Which says if we had a higher population or a higher statistical sample we are likely to pull this up and they would agree even more closely. We can't pursue it here because of the complexity of it. But this is the approach we will recommend to you. It could really cut down on the cost of complying with that nuisance demonstration that you have in the TSO.

Terry Zweifel (Honeywell) - Why do you need actual operational data? That is really just a mathematical exercise of running through the process?

Roland Bowles (NASA Langley) - Strictly to convince us that the prediction is true.

Terry Zweifel (Honeywell) - How do you get that? How do you gather all that data operationally, turbulence levels and all that?

Roland Bowles (NASA Langley) - That will be embodied in the turbulence model and we base that on literally 3000 hours of low altitude turbulence measurements by the whole B-52 fleet. About 7000 hours of data out of Canadian and US turbulence measurements in different terrain

and different atmospheric stability at low altitude. That statistical model has been put together.

Terry Zweifel (Honeywell) - Is that the one in the TSO?

Roland Bowles (NASA Langley) - No. It came out of Slick's deck.

Terry Zweifel (Honeywell) - I guess what I was trying to get at is that once you define what the turbulence is then all you have to do is sit down and run it through the filters.

Roland Bowles (NASA Langley) - Precisely, you define the turbulence realization, you define your gust rejection filter network and by calculation show that with that stochastic input across that ensemble of statistics you fall either above or below the exceedance line. I think it could cut the cost considerably, and it would be actually more valid than what we are doing now. This is the way we prove that the wings won't come off of airplanes due to extreme gust loads. The TSO may be useful but it could be more useful, and less costly to apply. I think there is some room for improvement, or maybe it's clarification, of the technical content in the TSO. So, we will respond as will the industry and we will see where we go.

Kirk Baker (FAA) - Yes, I think that is very important.

Roland Bowles (NASA Langley) - The final subject. How does industry view hybrid systems technology based on the integration of reactive and predictive technology? What are the expected problems, expected improvements in safety, and perhaps cost? I have heard people say that reactive system technology is non throw away. I have said it. I think that is where I heard it, actually. I do believe it is non throw away technology. So, is there some industry sense that hybrid devices may be useful if the cost can be controlled. Would that not get us out of some of the dilemmas on certifying predictive systems as a stand alone device. Any comments along that line?

Howard Glover (Sundstrand) - I think one of the keys to convincing airlines to put money into anything other than the reactive system is the benefit to cost ratio. If you can make the predictive system do something other than detect this Wind Shear event, which is going down in frequency as far as encounters are concerned, then that is the best way to do it. Things such as was mentioned today like clear air turbulence detection, wake vortex detection, perhaps even terrain detection. If you can do that and demonstrate it, then I think it is probably something that the industry would go for. If you can't do that then I don't believe that they will. Except in rare occasion.

Sam Shirck (Continental Airlines) - I think I would be remiss if I left anyone with the impression that our airline in particular, and I think American and Northwest also, are really enamored with the reactive systems. I think it was the best technology that we were able to produce at the time, but I don't think it is the answer at all. Joe Gibson presented some facts there that would indicate that on takeoff we have only got one chance out of ten of survival in the right type of shear. That is what I got out of what you said. As a pilot, I can tell you I am not wild about those odds. And I think I can speak for the airline, that I don't think we would stay in business with those type of odds. So we are hoping that we can get certification of a predictive

type system that is stand alone for at least the retrofit aircraft. The better of all worlds would be to back it up with a reactive system. In the future I don't think you will be able to buy an airplane without a reactive system that is embedded in the flight control laws of the aircraft. I don't think it is going to be possible to do it. But a predictive system is something that we are definitely striving for and I think we are very close. One of the things that kind of bothers me, I guess it is a comment more than a question, I heard just a few minutes ago that we were using a two second pilot response time and a two second engine spool time. I think accepted pilot response time in the past on RTOs which is a critical situation, has been 2 1/2 seconds. I would like to see at least some recognition that we stick with the same ground rules. And, for those that think that the engines on the ground loving 727 are going to spool in two seconds have got another thought coming. That won't happen.

Roland Bowles (NASA Langley) - Your point is well taken Sam. We have had some successes out there with this technology, but there is one around the corner where we may dig a whole and have to go back to the drawing board.

Russell Targ (Lockheed) - I was worried about the exact thing that Sam just spoke to and that is the data that Mr. Gibson just presented. In the pilot's wind shear handbook we learn that a average wind shear encountered in the JAWS study had an F-factor of about 0.2 and they warned that a heavy weight jet encountering such an average wind shear had about a 50% chance of experiencing undesirable contact with the ground. Now that is three year old analyses, and we have a whole panel of experienced reactive investigators here. I wondered, if you consider this F-factor of 0.2 to be an average wind shear that one might encounter, what is the likelihood of having an accident even after you have enunciated a wind shear occurrence that you are flying into.

Roland Bowles (NASA Langley) - Well, this is a rare opportunity for me, this is a time I get to challenge Russell. No statistic came out of the JAWS program with regard to an average F-factor of 0.2 at all. What we do have is a statement based on a 498 microburst sample with a lot of data provided by Lincoln and the NCAR guys, using the same algorithm that we were using to uplink the F this past summer, that suggest that this is the probability of equaling or exceeding a given level of F. So, about half of them are greater than 0.12. A 0.2 or bigger, based on this data, would occur at a frequency of one in one hundred, roughly. I don't know where you got that number but it was clearly not true.

Russell Targ (Lockheed) - Where I got the number was from the histogram that appears in the JAWS study where they say that an average Denver-Stapleton dry microburst would correspond to a 40 or 50 knot headwind change.

Roland Bowles (NASA Langley) - That is not an F-factor, that has nothing to do with airplane energy loss.

Russell Targ (Lockheed) - If you say that you lose that over a kilometer.

Roland Bowles (NASA Langley) - But that was not the case. Some of them were five kilometers wide.

Kim Elmore (NCAR) - I am trying to remember what the numbers were, but I think a typical size was a little over three kilometers and typical intensity was something on the order of 14 meters per second, or something like that. Of course, we did not know what F-factor was back then. 0.2 would be far bigger than what we saw on the average.

Russell Targ (Lockheed) - I have no desire to quarrel over what the average F-factor in the universe is. What I would like to know is if I encounter such an average F-factor as is indicated here, what is my likelihood of surviving?

Roland Bowles (NASA Langley) - I think Joe gave you the answer to that in terms of a system effectiveness number. Again effectiveness of a system is not the ability to detect it, it is the ability to prevent an accident. Let's face it, there are some events in this world that I don't care if you get the reactive system alert in two seconds or four seconds or a millisecond, if you are in it you may not survive. There are some out there that big. But these tend to be relatively rare.

Joe Gordan (Safe Flight) - I think everybody is missing something here and that is what the accident studies have shown. The fact is that given all the accident studies, any reactive system would have saved that accident. You can pick numbers out, Mother Nature does some funny things, but that is not what the evidence has shown.

Roland Bowles (NASA Langley) - You can make a compelling case that for the vigil pilot who is right on top of it, knowing what is coming, he can survive. The point is, nobody knows what the effectiveness of the system is. As we heard, we have only gotten a few alerts out there in the system and we sort of know what the false alert problems are.

Terry Zweifel (Honeywell) - I will just make a few more comments relating to that. When you say it is a 0.2 F-factor shear, the question is not is it in a 0.2 F-factor shear, the question is for how long? There is another assumption that is being made and that is, if you are in a shear and the shear is 50 knots that you will lose 50 knots of airspeed. That does not happen in reality. You do lose airspeed, but you will not lose the entire amount of the shear. So that means your kinetic energy relative to the air is not as bad as it appears in some of these studies.

Roland Bowles (NASA Langley) - That's right, and that is why we need to change that curve in the TSO from wind speed change to something more meaningful in terms of performance impact on airplanes.

Terry Zweifel (Honeywell) - One more comment on the accident models. What Joe said is exactly true. There is not an accident case that anyone's reactive system can't detect and fly out of. In fact, in many cases we ran them 2 and 2 1/2 times the actual value and you still could fly out. So if there was a conception somehow that the reactive systems are just totally ineffective, it clearly is not true. They are not the final answer, I don't think anyone is promoting that. But they also can do a lot more than seemed to be coming out in some of the papers here.

Session IV. Airborne Doppler Radar / Industry

19930104/2

Session IV. Airborne Doppler Radar / Industry

N 93 - 19601

488725

22

RDR-4B Doppler Weather Radar With Forward Looking Wind Shear Detection Capability
Steven Grasley, Allied-Signal Aerospace

PRECEDING PAGE BLANK NOT FILMED

RDR-4B Doppler Weather Radar With Forward Looking Windshear Detection Capability

**Bendix/King ATAD
Status Of Development Activity**

**Steven S. Grasley
Sr. Radar Product Manager**

Allied-Signal Aerospace Company
Bendix/King Air Transport Avionics Division



Bendix/King ATAD Position

**Committed to the development of airborne
weather radar with Forward-Looking Windshear
Detection/Avoidance capability**

**Logical Extension For Current Airborne
Weather Radar**

Allied-Signal Aerospace Company
Bendix/King Air Transport Avionics Division



RDR-4A Technical Baseline

- More Than 4,500 Currently Delivered
- Latest Generation
- Solid State Transmitter
- Fully Coherent
- Doppler Turbulence Detection Capability

Can Be Modified For Windshear Detection Capability

Allied-Signal Aerospace Company

Bendix/King Air Transport Avionics Division



RTA-4A Characteristics

Transmitter Peak Power	125 Watts (nominal)
Pulse Width	6 and 18 μ secs (alternating)
Pulse Repetition Rate	380 Hz Weather Mode 1600 Hz Doppler Mode
Maximum Range	320 nmiles
Operating Mode	Pulsed Coherent
Frequency	9.345 GHz
Noise Figure	5 dB Minimum
Dynamic Range	50 dB Minimum
Gain Control	60 dB Minimum
Weight	24.5 lbs

Allied-Signal Aerospace Company

Bendix/King Air Transport Avionics Division



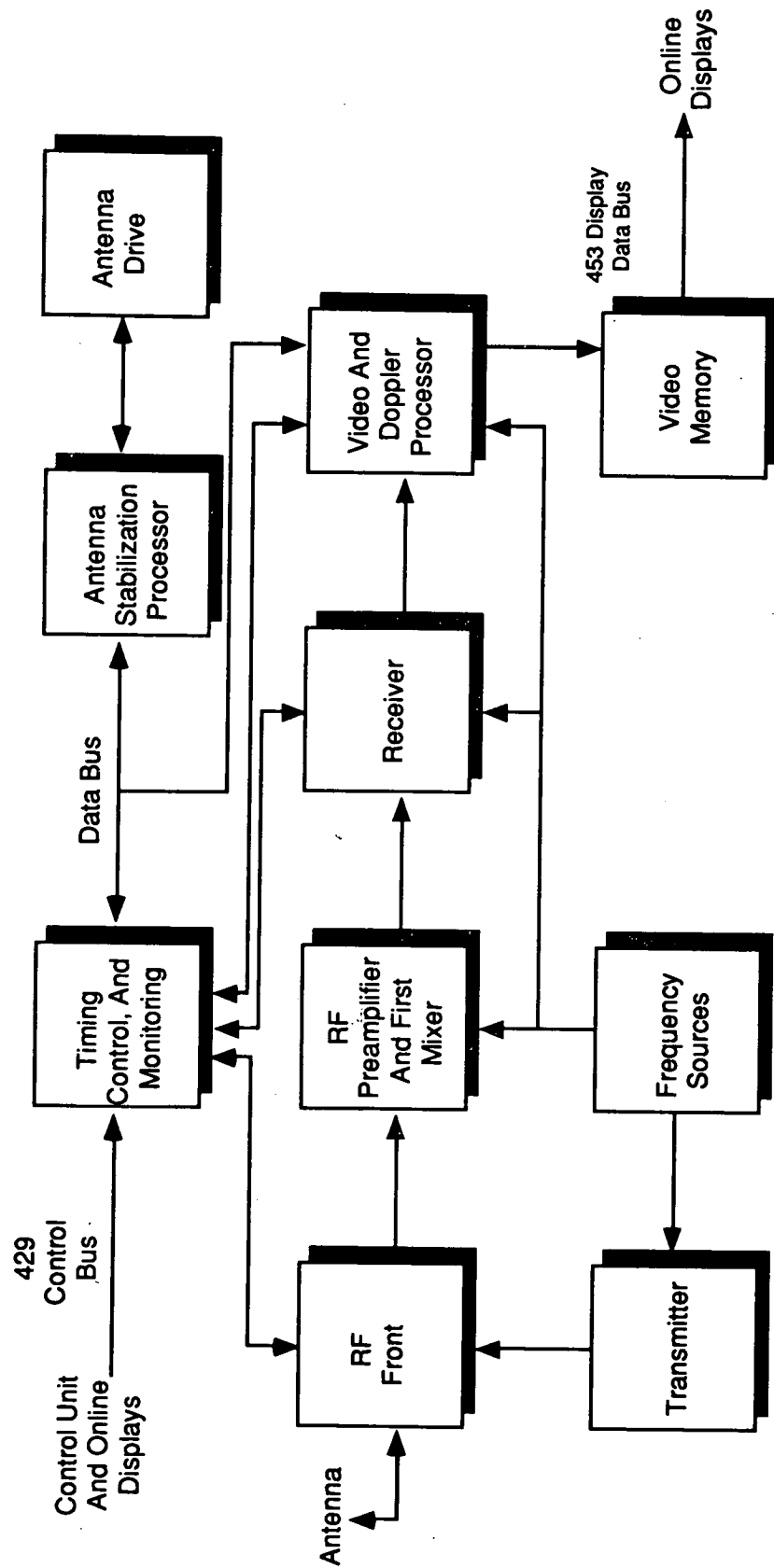
RDR-4 Antenna Characteristics

Radiator	30" Flat Plate (REA-4B) 24" Flat Plate (REA-4A)
Gain	35 dB with REA-4B 33 dB with REA-4A
Beam Width	3.3° REA-4B 3.8° REA-4A
Frequency	9.345 GHz \pm 30 MHz
Stabilization Type	Line-Of-Sight
Stabilization Limits	<u>DAA-4A</u> <u>DAA-4B</u>
Tilt	$\pm 15^\circ$ $\pm 15^\circ$
Pitch	$\pm 25^\circ$ $\pm 15^\circ$
Combined Tilt/Pitch/Roll	$\pm 45^\circ$ $\pm 35^\circ$
Azimuth Scan	180° 160°
Stabilization Accuracy	$\pm 0.25^\circ$ Static / $\pm 0.5^\circ$ Dynamic
Weight	DAA-4A/REA-4A: 28.5 lbs DAA-4A/REA-4B: 26.7 lbs DAA-4B/REA-4A: 12.7 lbs

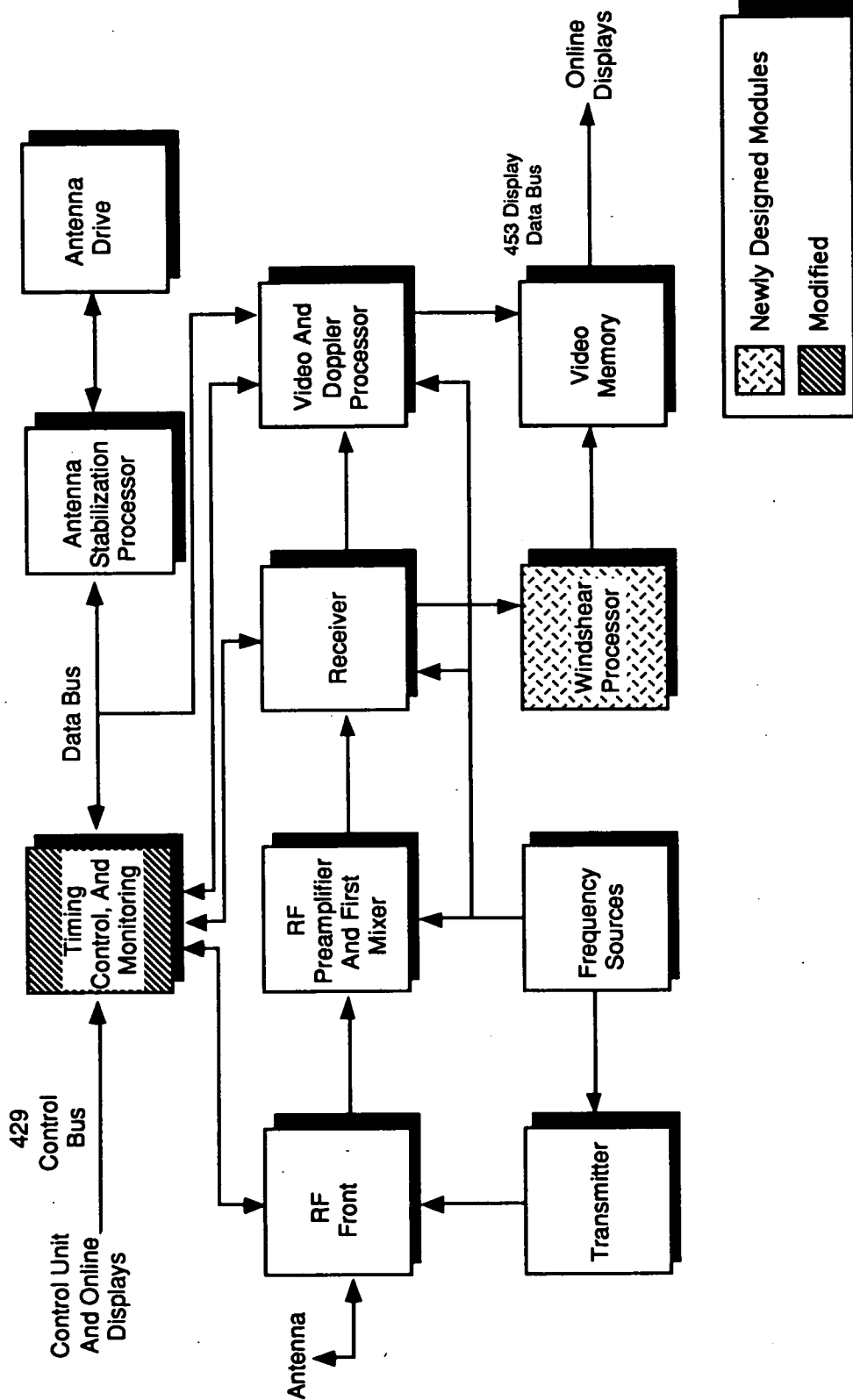
Modifications of RDR-4A to RDR-4B

- **Receiver/Transmitter**
 - Add Windshear Detection Hardware and Software
 - Add Windshear Mode Control Software
 - Add Windshear Data To The Output Buses
- **Indicator**
 - Add Windshear Data Display Capability
 - Add Windshear Mode Selection (May Also Apply To Control Panel)
- **Antenna**
 - No Modifications Required
- **Aircraft**
 - No Mechanical Modifications
 - Some Wiring Changes Might Be Required For Interfaces
 - No Radome Changes Required

RDR-4A Functional Block Diagram



RDR-4B Functional Block Diagram



Allied-Signal Aerospace Company

Bendix/King Air Transport Avionics Division



RDR-4B Characteristics

	WEATHER AND MAP MODE		TURBULENCE DETECTION	WINDSHEAR DETECTION
	125 Watts (Nominal)			
TRANSMITTER PEAK POWER				
PULSE WIDTH	6 and 18 μ sec Alternating	6 μ sec	2 μ sec	
PRF	380 Hz	1600 Hz	6000 Hz	
MAXIMUM RANGE	320 nmi	40 nmi	10 nmi	
OPERATING MODE	Pulsed Coherent			
FREQUENCY	9345 \pm 2 MHz			
SYSTEM NOISE FIGURE	5 dB			
ANTENNA SCAN	180°		\pm 40°	
ANTENNA GAIN	35 dB			
ANTENNA BEAMWIDTH	3.3° Elevation 3.4° Azimuth			
TILT CONTROL	\pm 15°	Manual	Automatic	

Allied-Signal Aerospace Company

Bendix/King Air Transport Avionics Division



Development/Test Plan

■ Prototype Completed	1991
■ Proof-of-Concept Flight Test	1992
■ Certification Testing	1992-1993
■ Production	1993

CV-580 Testing Capability

- RDR-4B Prototype Installed
- Real-time, Reconfigurable Computer Displays
- High Speed Data Recording
- TDWR Data Link To Correlate With TDWR and NASA Testing (Planned)

CV-580 Test Results

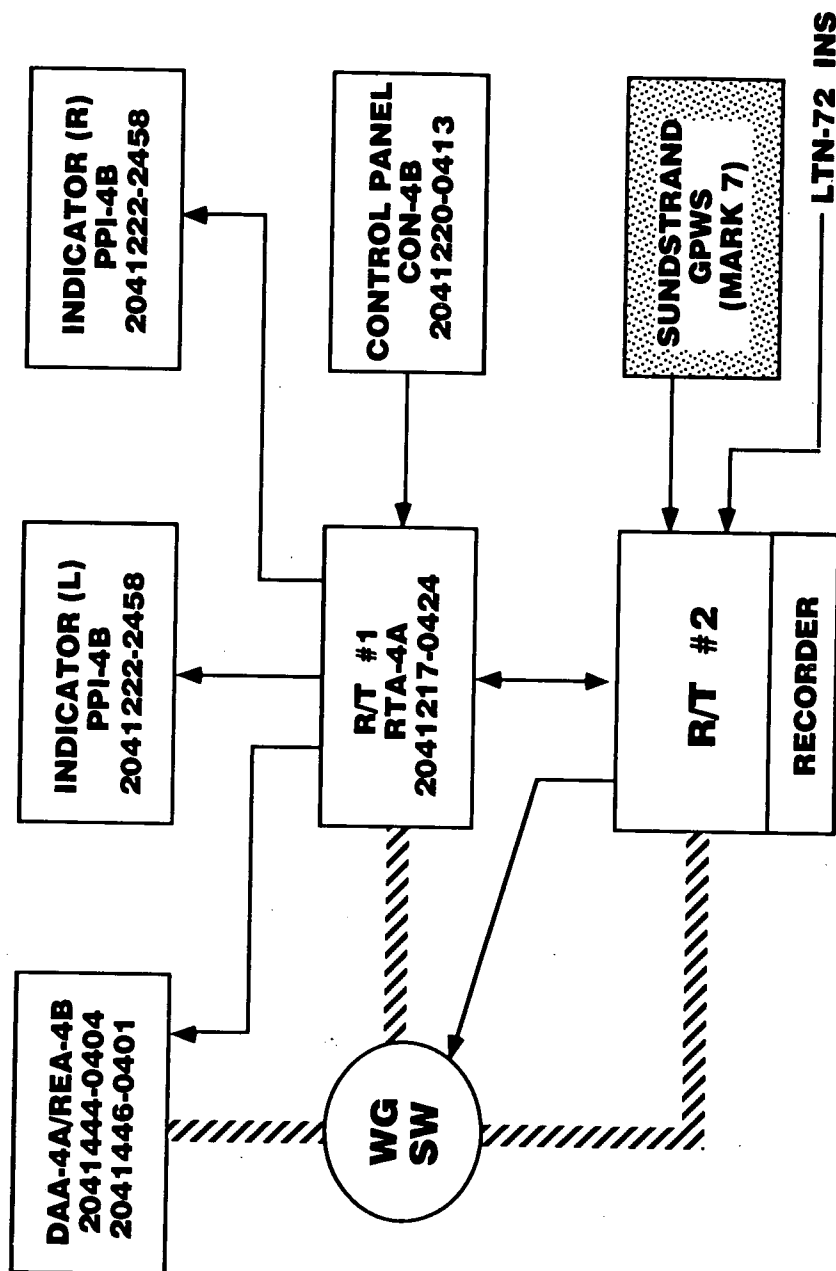
■ Flight Testing To Date

- Clutter Cancellation Techniques Verified
- Wind Velocity Calculation Techniques Verified
- Several Microbursts Recorded - Ft. Lauderdale Area

■ Continuing Testing 1992-93

- Further Refinement of Processing Techniques
- Verification of "Dry" Microburst Detection Capability
- Correlation of Data With Ground Based Radars At Denver & Orlando
- Correlation of Data With NASA B737 Activity
- Certification Proof-of-Concept Flight Tests
- Performance Verification of Production Configuration

Continental A300 Test Configuration



Allied-Signal Aerospace Company

Bendix/King Air Transport Avionics Division



Continental Data Recording Program Operational Considerations

- Recording Is Fully Automatic
- Windshear R/T Is Always Powered
- Almost Transparent To Flight Crews
 - Weather Updates On One Sweep Instead Of The Usual Two
 - No Crew Intervention Required
- Data Recorder Is Replaced Once A Week

Continental A300 Test Results

- Data Being Gathered On Take-Off/Landing During Revenue Operation
- Data Analysis On-Going
- No Windshear Events Yet Identified
- Data Gathering To Continue Through 1992

Allied-Signal Aerospace Company

Bendix/King Air Transport Avionics Division



Display Considerations

■ Bendix/King ATAD Proposal:

- Hazard Factors In Colors
- Aural Alert and Visual Alert With Flashing Symbol On PPI Or EFIS

■ FAA / SAE / Airlines Proposal:

- Symbolic Display Super Imposed On Weather
- Alert With Chime And Yellow Light
- Warning With Audio And Red Light

Key Goals: Simple, Useful, Minimum Mods/Cost

General Development Accomplishments

- System Design Complete
- Prototype Built & Flight Tested
- Production Design In Process
- Certification Concept Defined

Allied-Signal Aerospace Company

Bendix/King Air Transport Avionics Division



Remaining Issues

(From Items Identified At Third Conference)

■ Technical:

- Establishment Of Hazard Thresholds
- Definition Of Display Characteristics

■ Operational:

- Means Of Selecting Windshear Mode
- Displays
- Aural Alerts
- Interaction With Reactive Windshear System

RDR-4B Doppler Weather Radar
With Forward Looking Wind Shear Detection Capability
Questions and Answers

Q: Roland Bowles (NASA Langley) - Do you feel that you understand and have a clear path in mind for certification as per the industry government activities on the interim standards document and other certification related questions? Secondly, do you plan in the next six months to move forward with the certification program?

A: Steve Grasley (Allied-Signal) - I think we understand what has been done to date. It certainly is not absolutely clear how certification will ultimately be accomplished. There is still a number of issues that remain open. The MOPS is being firmed up and that is one of the critical things that we are going to need. It is going to take another meeting or two I believe. John Wright is kind of leading up that activity and he shaking his head in agreement. It is going to take a little bit longer before that is done. As far as moving forward within the next six months to do some certification, it is quite dependent on those issues. There is also some of the exempted airlines who are quite interested in moving forward. We'll support them if we are in a position to do that. If they want to move forward and get going with it then we will certainly support whatever they would like in that area.

Q: Kirk Baker (FAA) - You mentioned in your talk that you used some inputs for antenna tilt management, could you elaborate on what those are?

A: Steve Grasley (Allied-Signal) - The key issue is to steer the antenna beam in the outflow areas so we can get the measurements that we need and limit the amount of ground clutter that we get through the main beam. The inputs are defined by the new and evolving 708-A interface specification, radio altimeter is really the key one. We know how high we are above the ground and approximately where we want to be looking, in terms of tilt angle, so we can steer the beam into that region. As I mentioned, one scan did weather and one scan would do wind shear processing. You are looking at two different types of phenomenon in that case. You want to see the weather in front of you as well as the wind shears. The idea being that we could steer the beam during weather based upon what the pilot has selected and the weather of interest to the pilot, but then to get back down and do the scan in the wind shear mode right where we want it, through the region of interest in the microburst event. The radio altimeter data is primarily used to know our height above the ground, so we can steer the beam properly.

Q: Bruce Steakley (Lockheed) - What is the residual sensitivity of your system after your clutter cancellation techniques?

A: Steve Grasley (Allied-Signal) - I do not know the numbers right off the top of my head. We can certainly give you a little more background on that a little bit later. Certainly, we are not seeing things drastically different from what was seen in the NASA flight test in terms of sensitivity. It is very similar. It was encouraging.

Q: Ernie Baxa (Clemson University) - Can you say anything about the clutter rejection

algorithms for the wind shear detection mode?

A: Steve Grasley (Allied-Signal) - We have verified that the way that we are doing it is working. I am probably not at liberty in this particular forum to talk about specifics of that, we might be able to do that in another way. So far we are satisfied with the way our clutter rejection processing is working and we have good evidence to show that it does a good job. We can see the wind shears and get rid of the clutter data. I am sure that is not really the answer you were looking for, but it will have to do for today.

Q: Bob McMillan (GTRI) - You mentioned earlier in your talk that the Bendix radar can detect turbulence. Given the tenuous nature of back scatter from clear air atmospheric inhomogeneities, what is the reliability of detecting turbulence at useful ranges?

A: Steve Grasley (Allied-Signal) - We certainly make no claim to be able to detect clear air turbulence. You need something to see and something to bounce energy off of. Our objective in turbulence detection is to detect it in weather conditions. We are not attacking the clear air turbulence problem at this time, not from a radar perspective anyway.

Q: Pete Saraceni (FAA) - How well do you predict the 4B radar will see a dry microburst?

A: Steve Grasley (Allied-Signal) - I think we pretty much agree with what the NASA folks have said about the capability of detecting a dry microburst, as well as what the Collins and Westinghouse folks have said. You are basically into physics and the technology available today. Somewhere in the zero, down in the fairly low dBZ range we can get useful detection at reasonable detection ranges. What exactly can we see and how far away can we see it? That is to be determined this year. That is going to be a major objective of our activity and testing this summer, this storm season. We can see something that is currently classified as dry, but exactly how much? That is what we will find out.

Q: Dave Hinton (NASA Langley) - You suggested that pilots wanted to have the option of manually selecting the wind shear mode above 2500 feet. Do you believe that there is any operation requirement for wind shear avoidance above 2500 feet? Is there any safety hazard from wind shear at those altitudes?

A: Steve Grasley (Allied-Signal) - No, we don't think there is any issue of hazard at those kind of altitudes. When you start getting into shear type conditions above those things people tend to say that is turbulence of some sort more than wind shear. I did suggest that pilots wanted the option of manually selecting it. You get a wide range of inputs and desires on capabilities when you start talking to pilots. They want all kinds of neat stuff. Are we going to end up providing that option to be able to select wind shear above 2500 feet? No, that is not the intention at this point and time. We have just gotten inputs that said it would be kind of neat to look.

Q: Dave Hinton (NASA Langley) - Do you believe that Doppler technology can support wind shear detection at those altitudes given that downdraft estimation may be unreliable above 2500 feet and there may be little or no microburst outflow for the Doppler system to detect.

A: Steve Grasley (Allied-Signal) - That is true. We don't necessarily believe the radar Doppler technology can really provide you any benefit at that altitude. As I mentioned earlier, we do not believe there is really a wind shear hazard at those kind of altitudes.

1993010413

Session IV. Airborne Doppler Radar / Industry N93-19602

488727

34P

Airborne Doppler Radar Research at Rockwell International
Roy Robertson, Rockwell International

NASA / FAA

FOURTH COMBINED AIRBORNE WINDSHEAR

REVIEW MEETING

APRIL 14-16, 1992

ROCKWELL INTERNATIONAL
COLLINS AIR TRANSPORT DIVISION

ROY E. ROBERTSON



TOPICS

COLLINS 1991 WINDSHEAR FLIGHT PROGRAM

SYSTEM CONSIDERATIONS



FLIGHT PROGRAM OBJECTIVES

- **DETERMINE FEASIBILITY OF RADAR WINDSHEAR DETECTION**

- **PERFORMANCE ASSESSMENT**

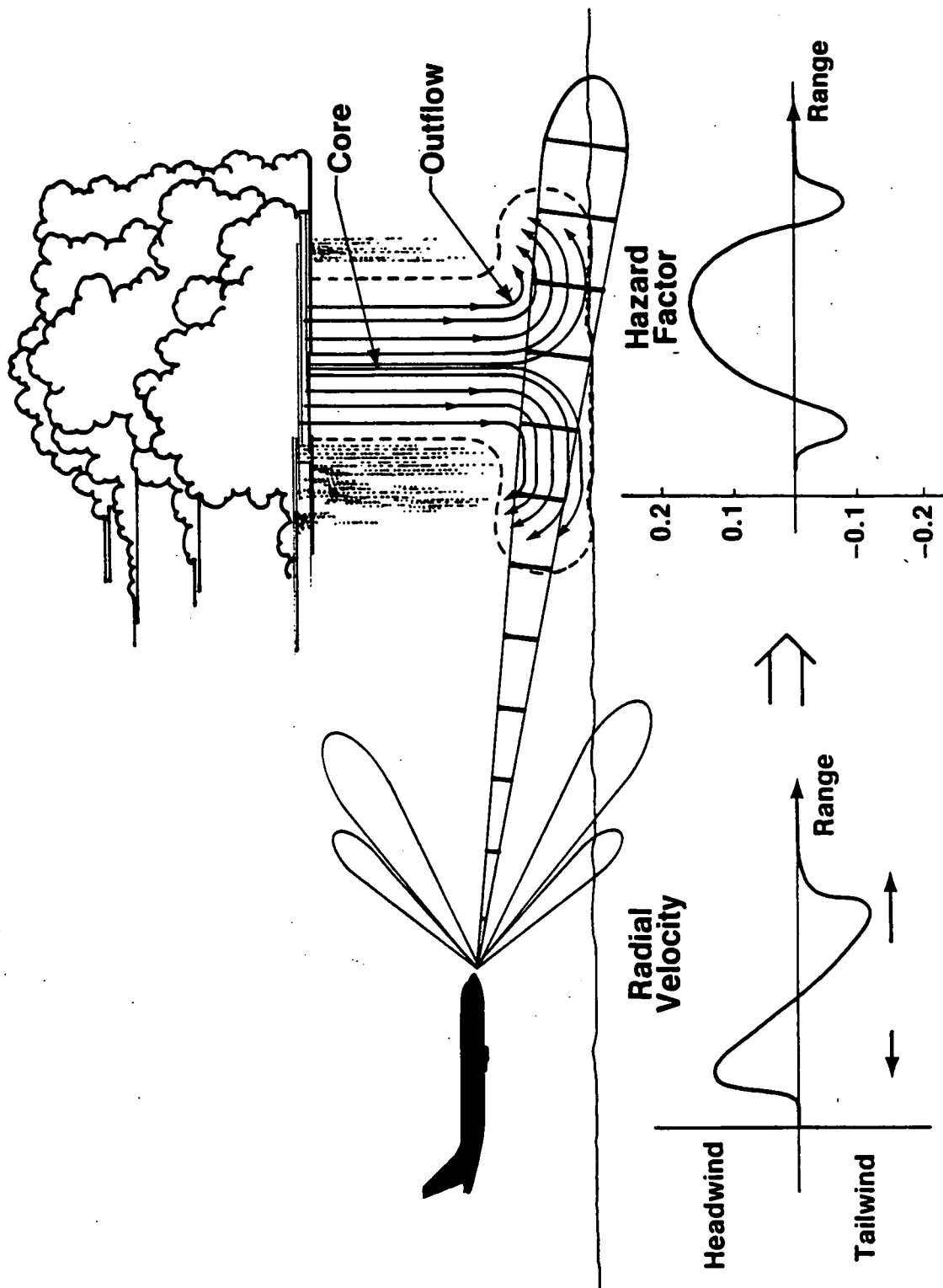
3-WAY DATA CORRELATION:

- AIRBORNE RADAR
- GROUND RADAR (TDWR)
- AIRCRAFT DATA

- **DETERMINE WINDSHEAR PRODUCT REQUIREMENTS**



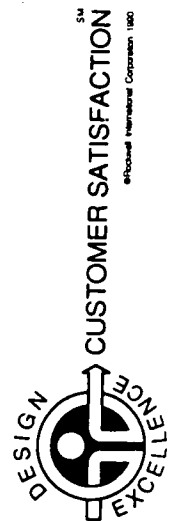
RADAR WINDSHEAR DETECTION



VC2045.1

FLIGHT PROGRAM PREPARATION

- **GROUND SUPPORT**
 - SITE SELECTION
 - GROUND RADAR
 - FLIGHT COORDINATION
- **AIRCRAFT**
 - EQUIPMENT
 - PERFORMANCE
- **OPERATION**
 - PROCEDURES
 - TRAINING
 - SAFETY CRITERIA
 - ATC

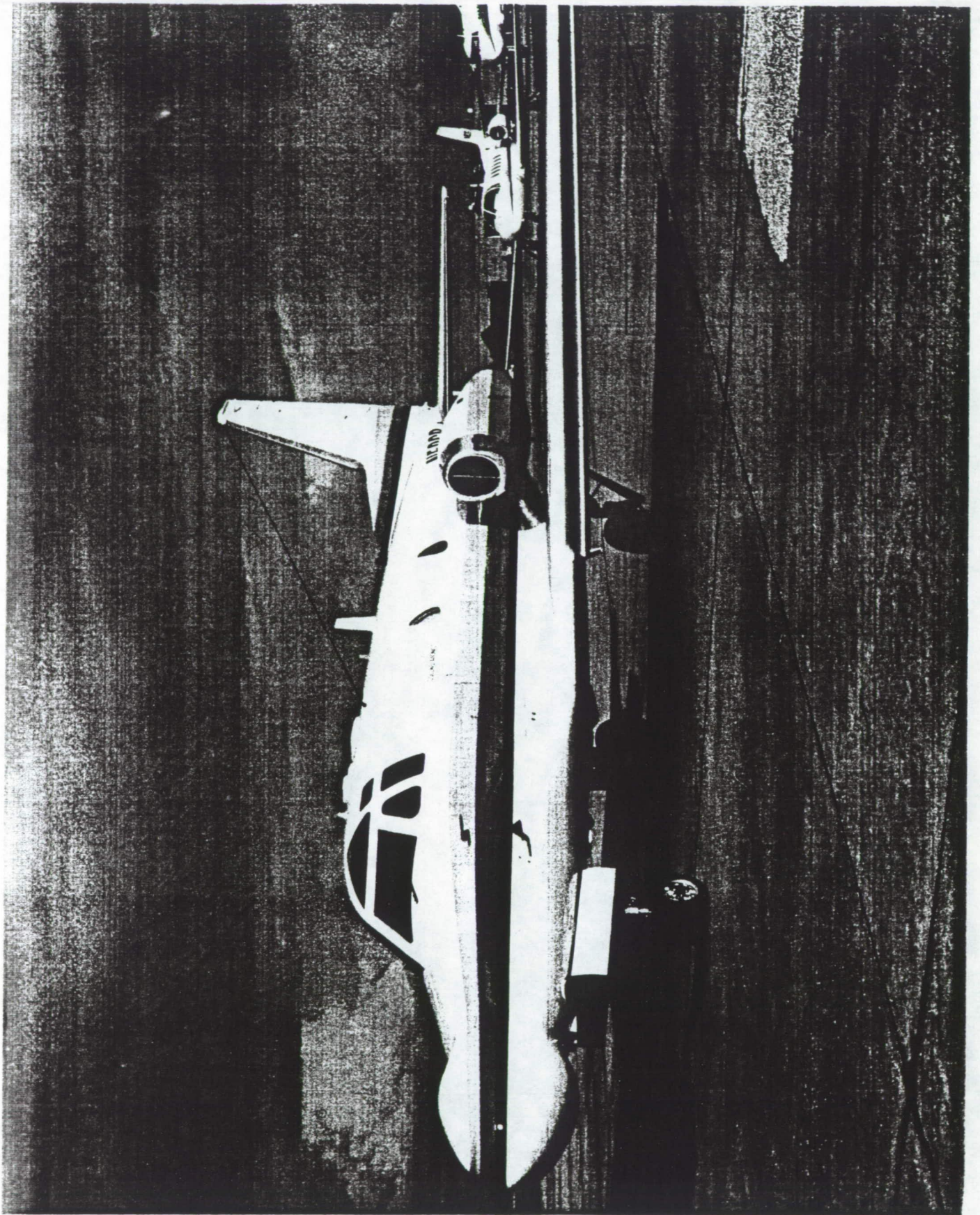


ORIGINAL PAGE IS
OF POOR QUALITY



ORIGINAL PAGE IS
OF POOR QUALITY





AIRCRAFT READINESS

- INSTRUMENTATION AND RECORDING

- WINDSHEAR RADAR
- POSITION (GPS)
- RADIO ALTITUDE
- ATTITUDE ACCELERATION
- AIR DATA
- NAVIGATION DATA
- TIME CODE
- COCKPIT VIDEO CAMERA

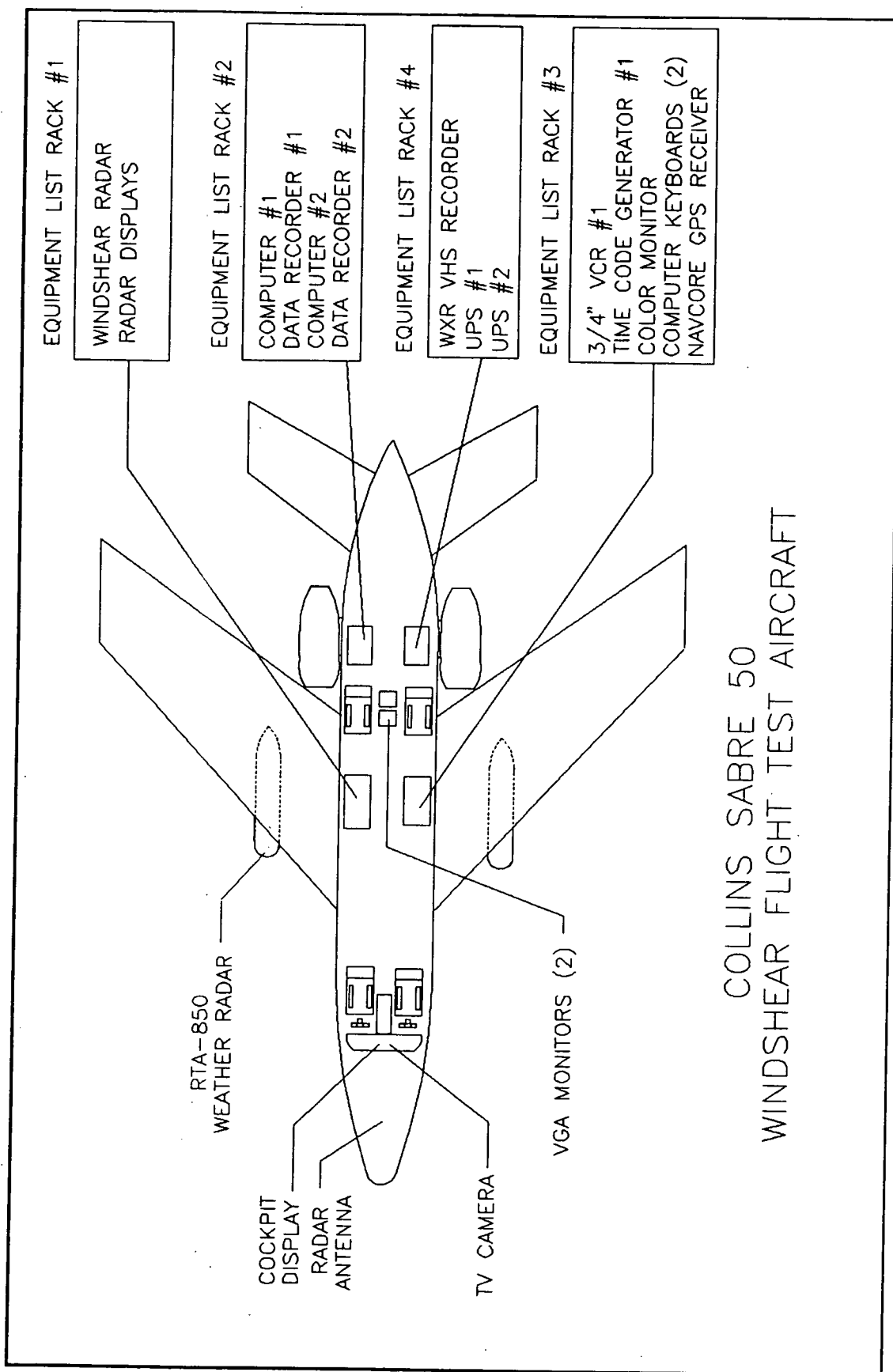
- AIRCRAFT MODIFICATIONS

- ANGLE OF ATTACK INDICATOR
- STALL WARNING SYSTEM, STICK SHAKER
- CONTINUOUS IGNITERS
- TCAS
- LARGER ENGINES

- PERFORMANCE TESTS

- CLIMB, ACCELERATION (F=APPROX 0.19)





COLLINS SABRE 50
WINDSHEAR FLIGHT TEST AIRCRAFT

FLIGHT OPERATIONS

- **GROUND SIDE**

- WEATHER MONITORING - AIRCRAFT LAUNCH DECISION
- LOCATE MICROBURST FORMATION
- HAZARD ASSESSMENT
- RADIO EVENT COORDINATES TO AIRCRAFT
- CONTINUOUS FLIGHT MONITORING
- DATA LOGGING/RECORDING

- **AIRCRAFT**

- GROUND WEATHER RADAR COMMUNICATIONS
- NAVIGATION SETUP
- ATC COORDINATION
- HAZARD ASSESSMENT
- OBSTACLE CLEARANCE
- DATA RECORDING
- RADAR OPERATION
- PENETRATION FLIGHTS

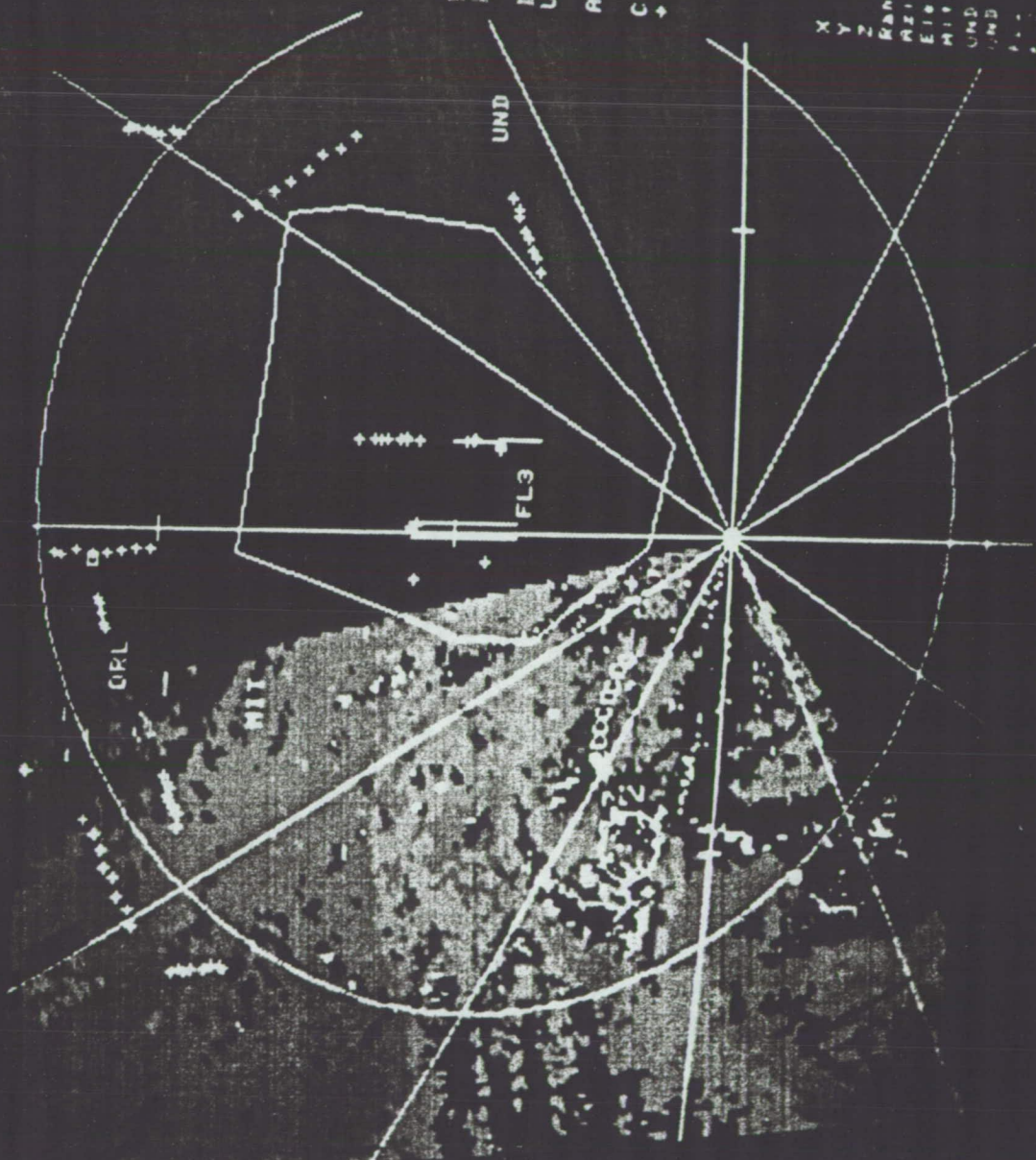


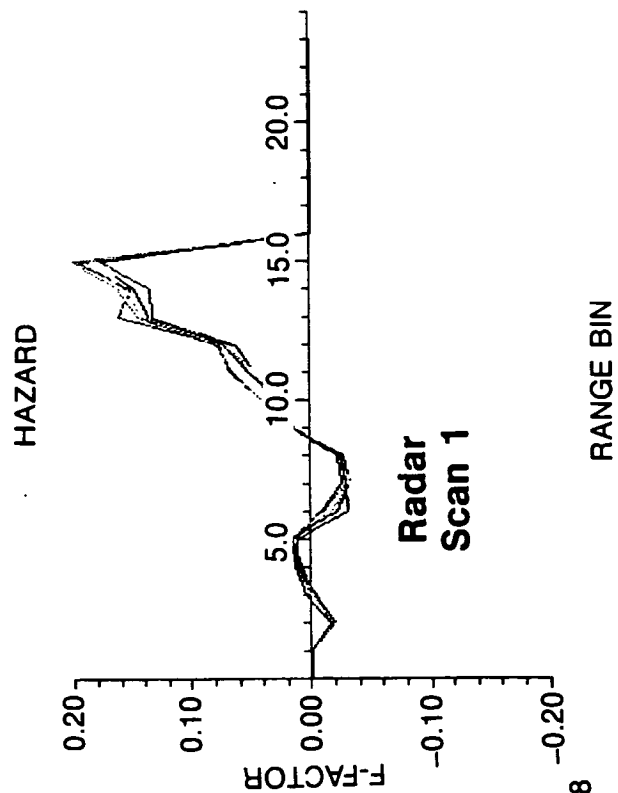
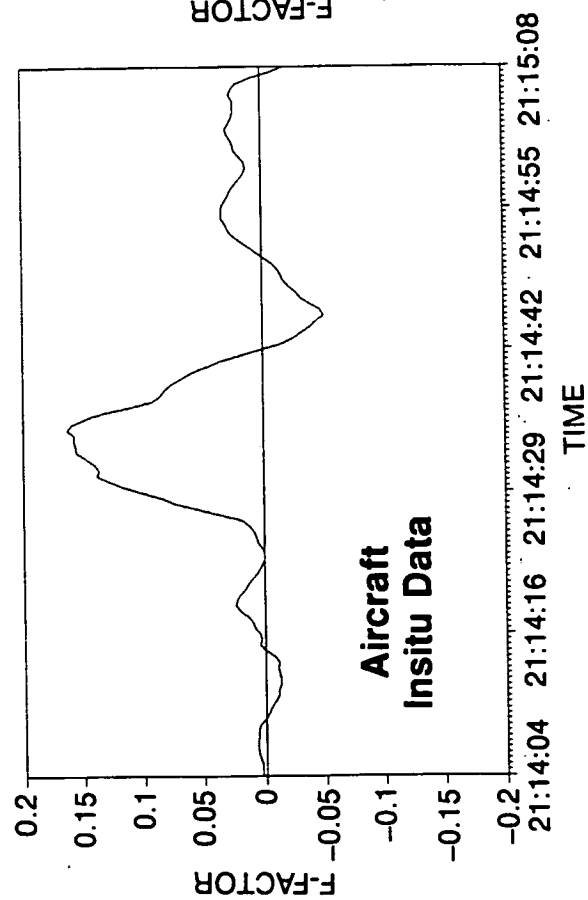
FLOWS (FL-2)
 Orlando
 21 14 07 on 09 20 11
 FPI Y1111 530 11
 Elevation 0 3 deg

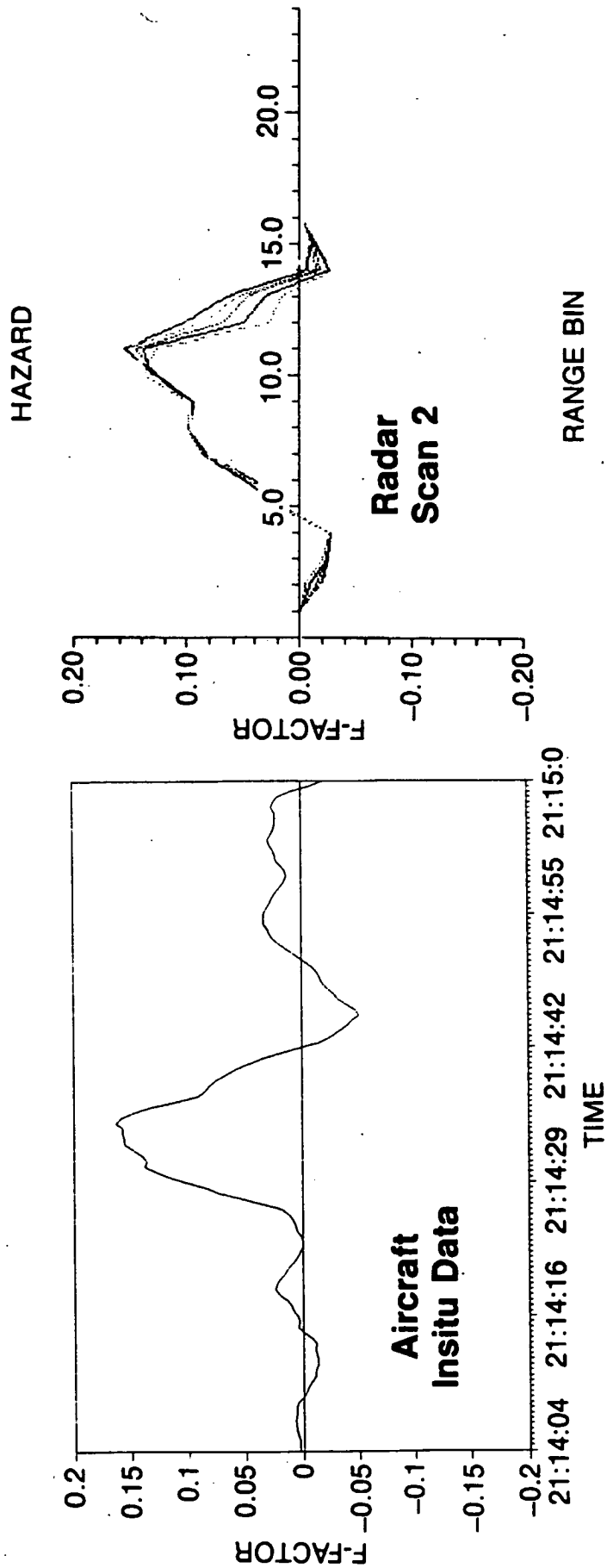
VELOCITY

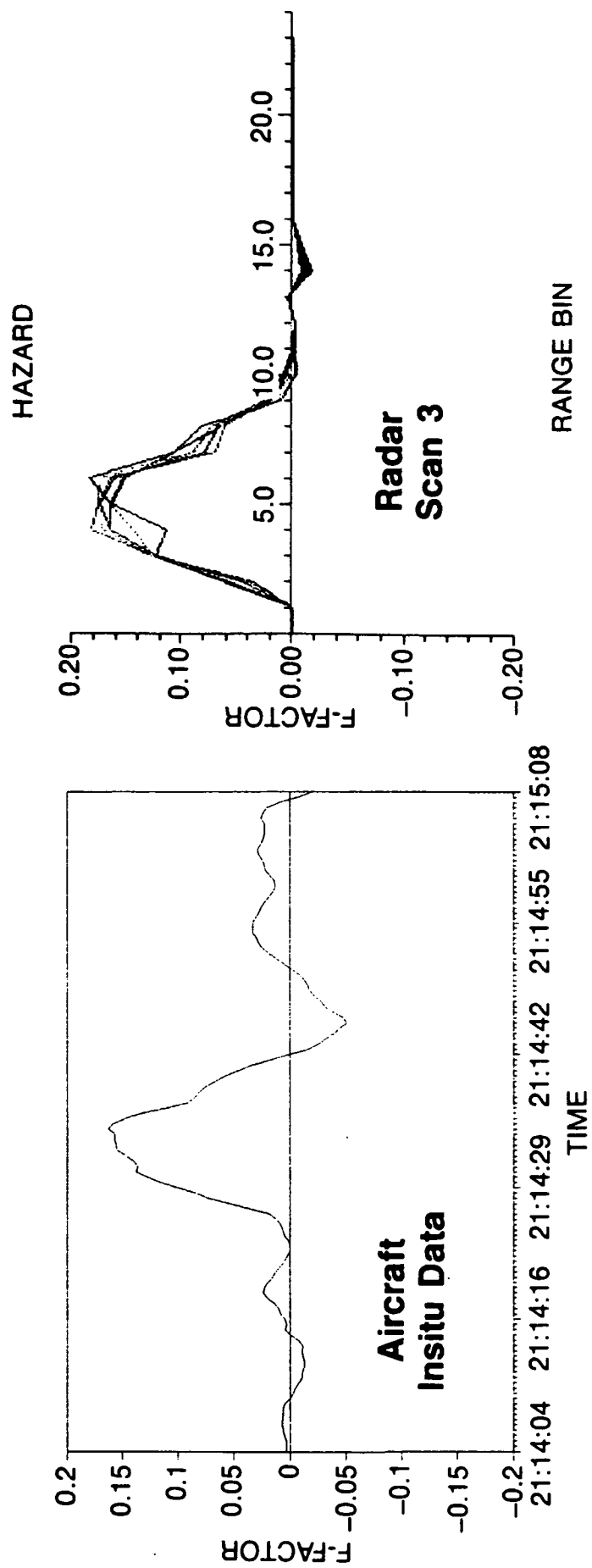


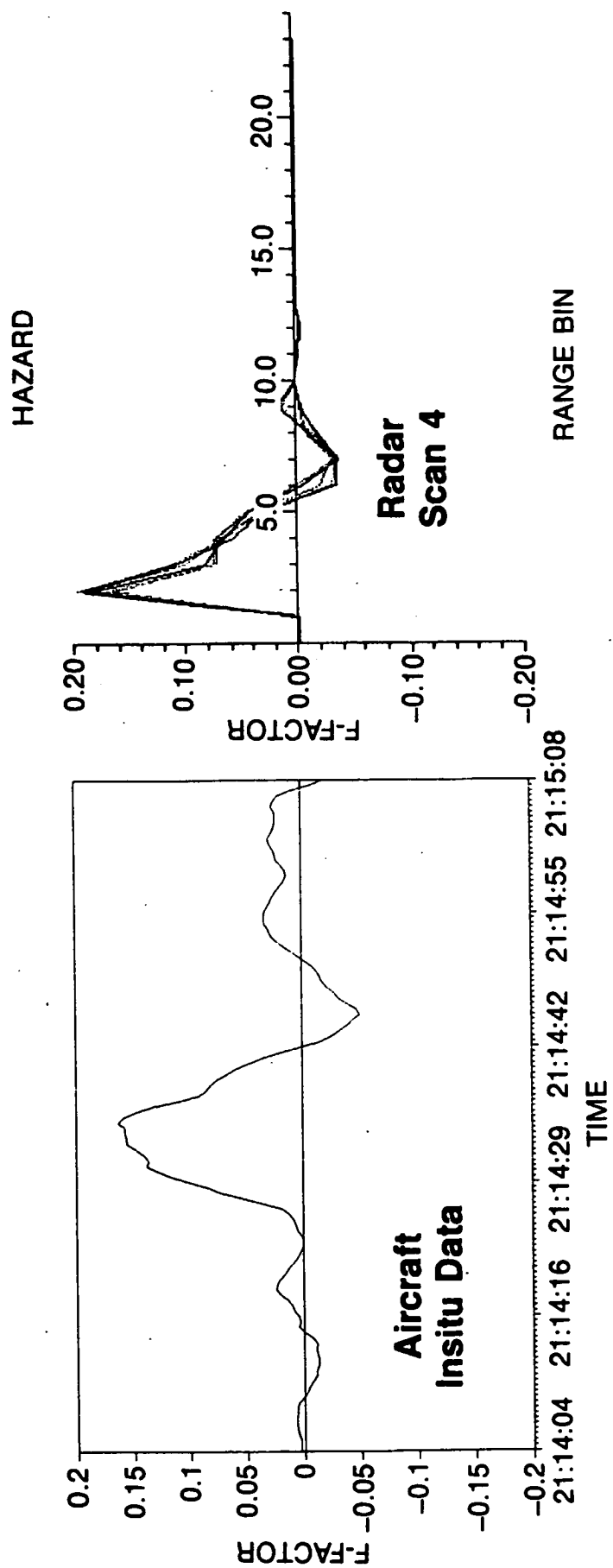
Aircraft Recon Data
code krtm elev mm 33
C 0355 09 15 14 05
+ AREA

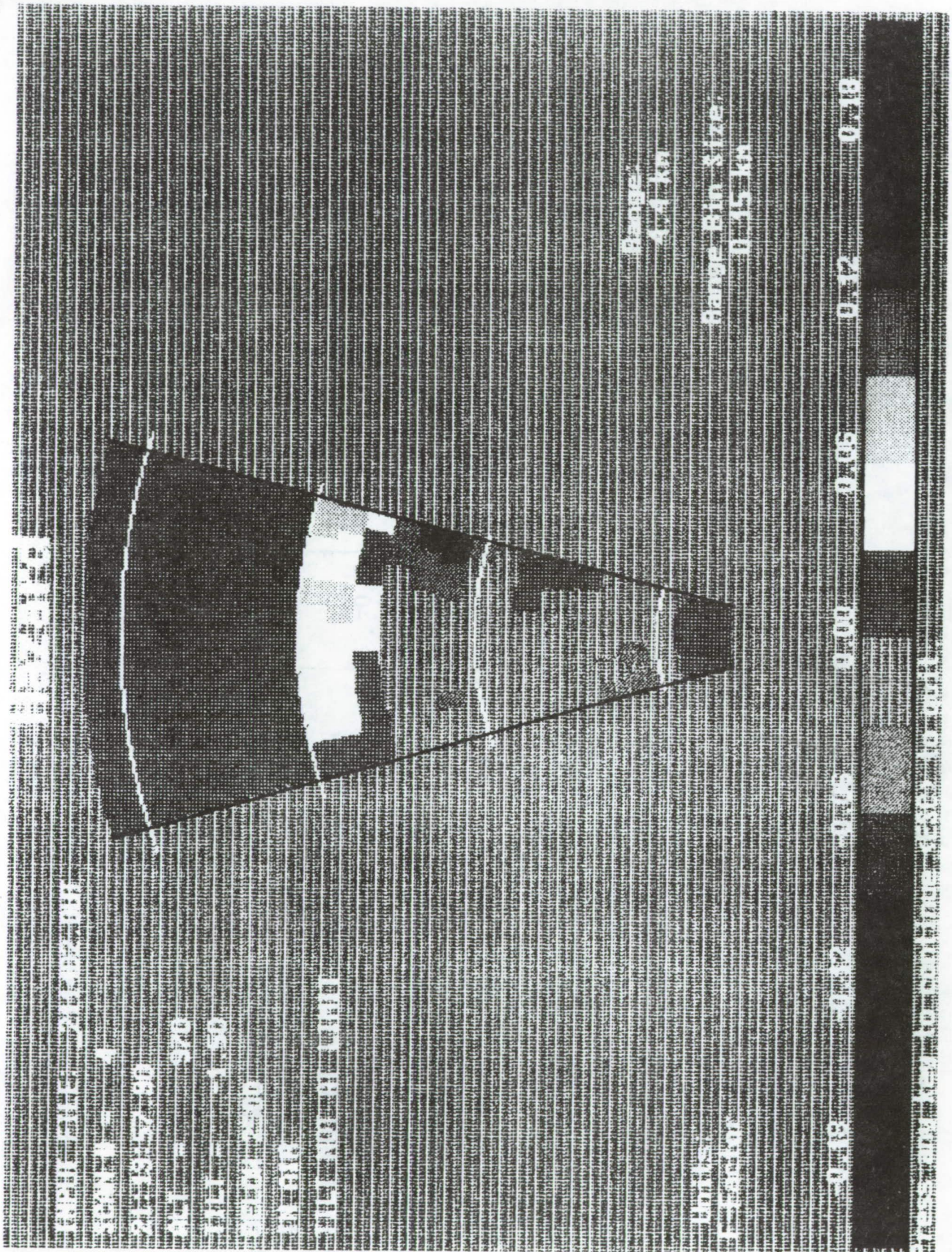


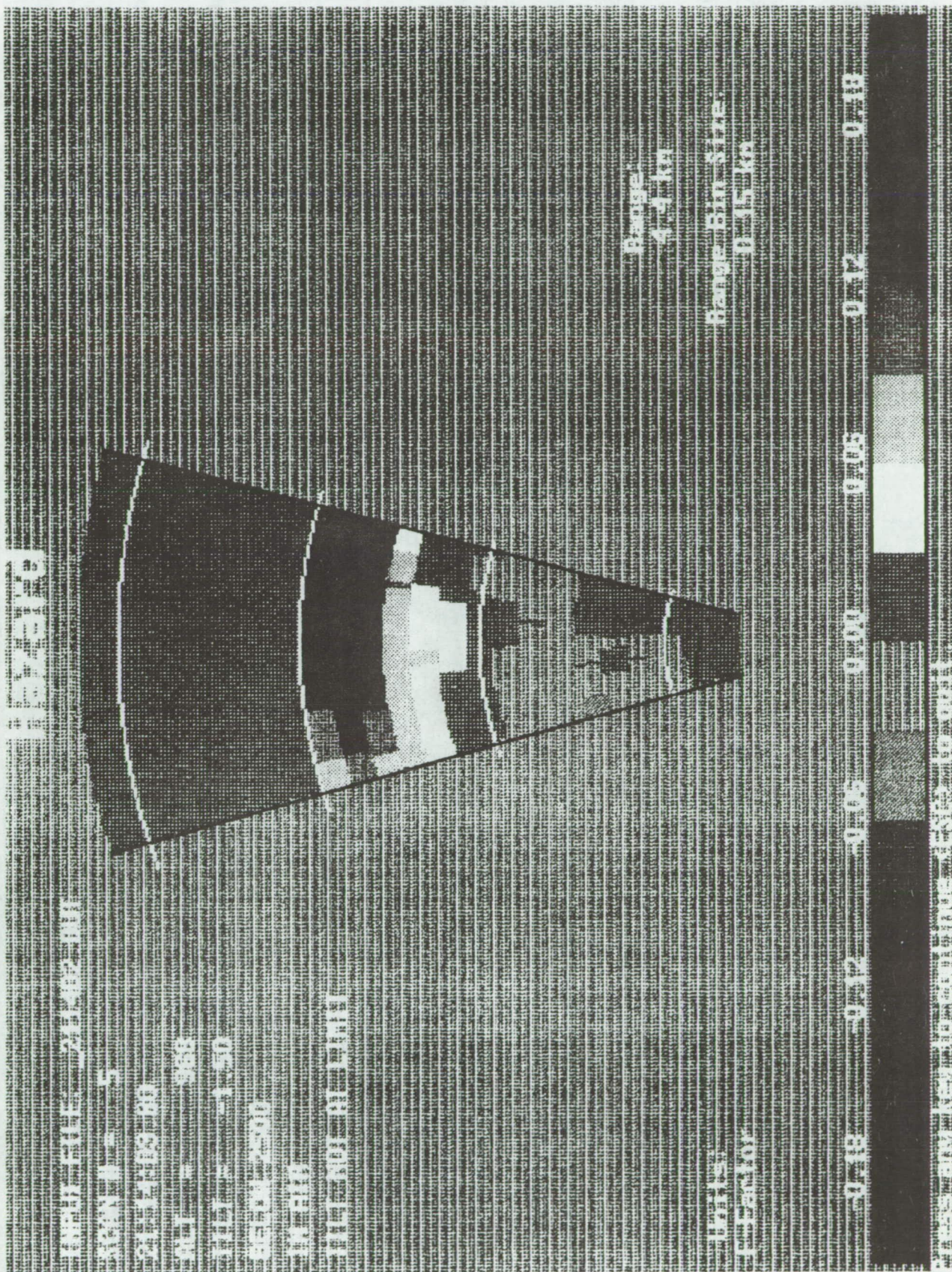




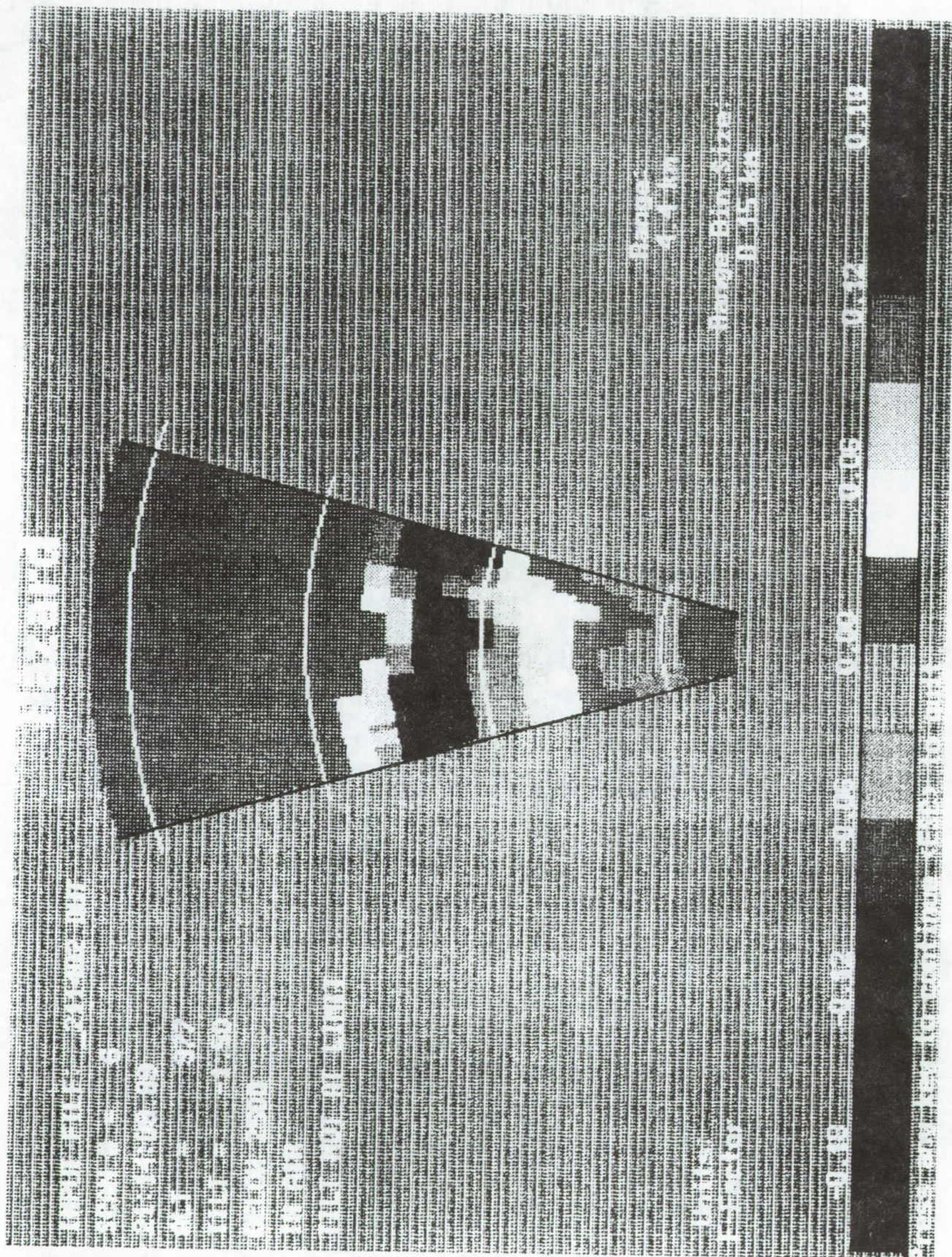


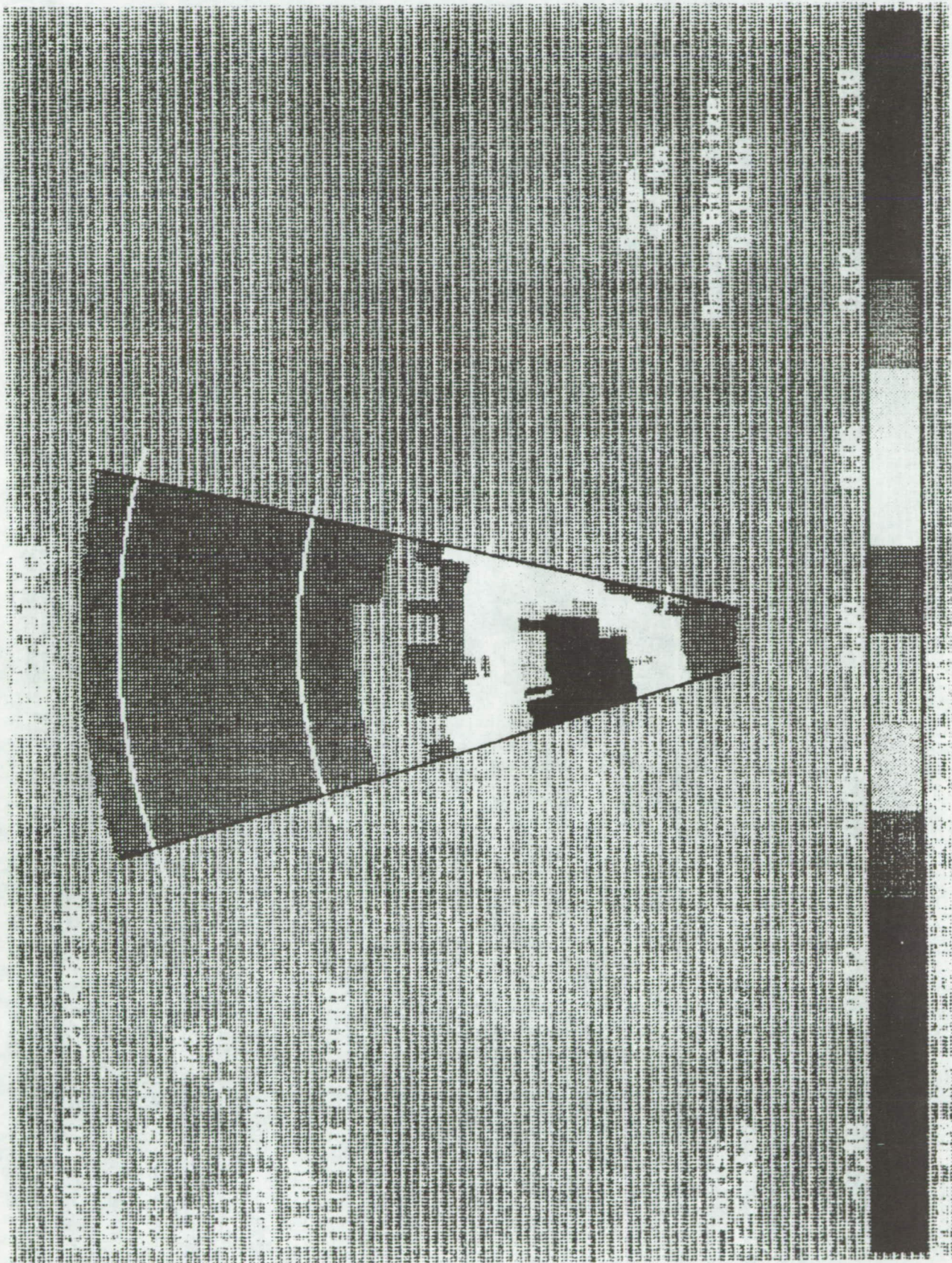




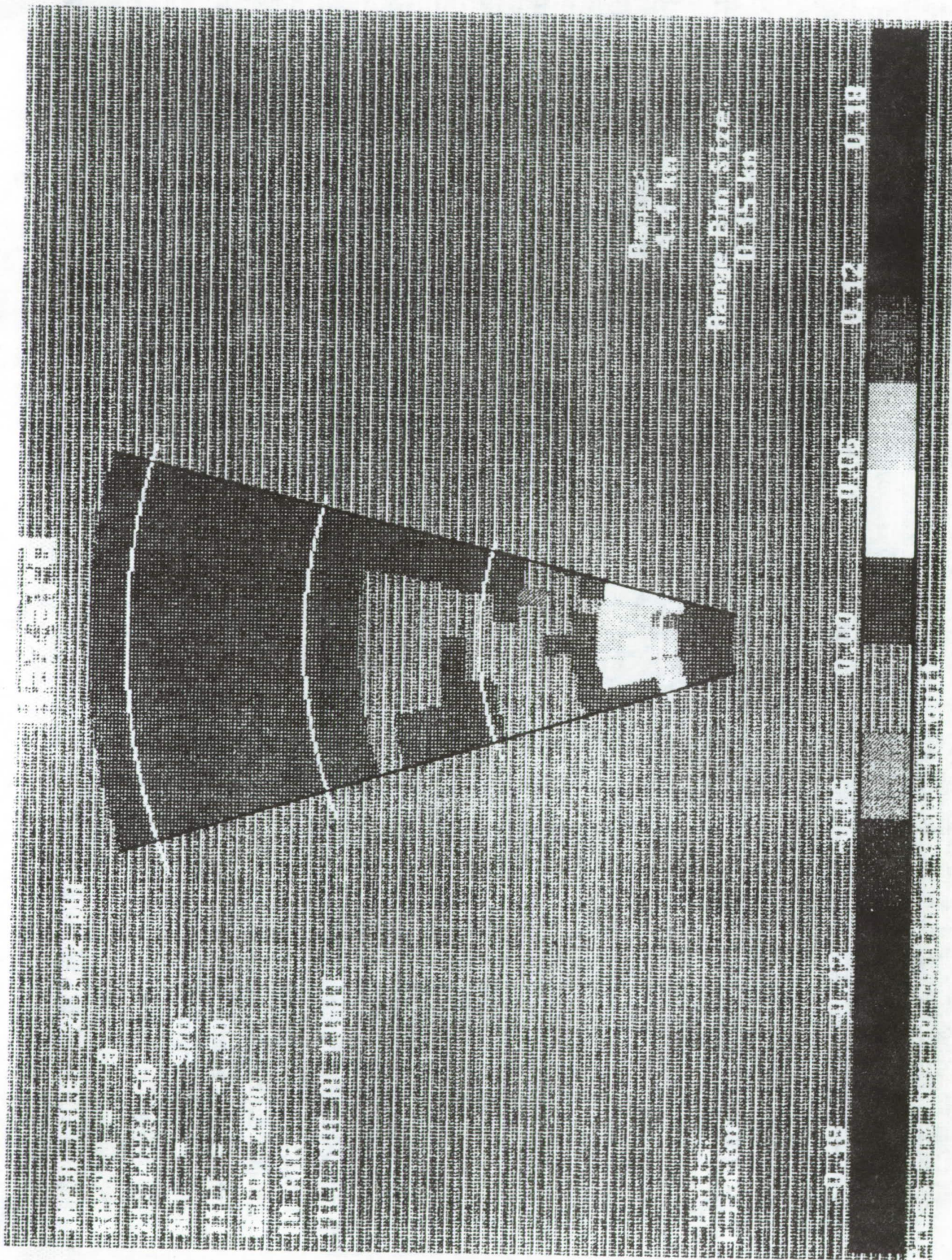


ORIGINAL PAGE IS
OF POOR QUALITY





ORIGINAL PAGE IS
OF POOR QUALITY



FLIGHT PROGRAM

CONCLUSIONS:

- EXCELLENT CORRELATION
 - AIRBORNE RADAR
 - AIRCRAFT INSITU
 - GROUND RADAR (TDWR)
- RADAR WINDSHEAR DETECTION IS FEASIBLE
- NEED FLIGHT DATA ON DRY EVENTS



SYSTEM CONSIDERATIONS

WARNING STRATEGY

- TWO LEVELS OF ALERTING
 - CAUTION <5 NAUTICAL MILES $\pm 25^\circ$ COVERAGE
 - WARNING <1.5 NAUTICAL MILES
- PRIMARY CREW ALERT
 - AURAL ALERT
 - "CAUTION" OR "WARNING" INDICATOR
- WINDSHEAR DISPLAY SECONDARY
 - HAZARD ASSESSMENT / ESCAPE MANEUVER
 - AUTOMATIC OR MANUAL
 - SYMBOLIC OVERLAY ON WEATHER

**CAUTION - TIME TO ASSESS HAZARD; AVOIDANCE
WARNING - GO AROUND**



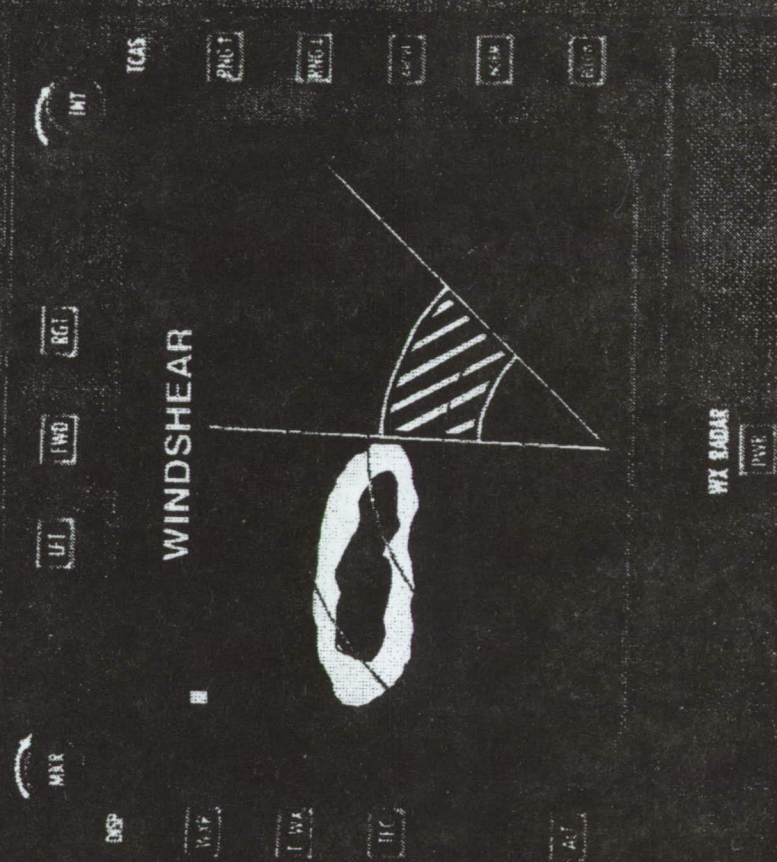
WINDSHEAR RADAR

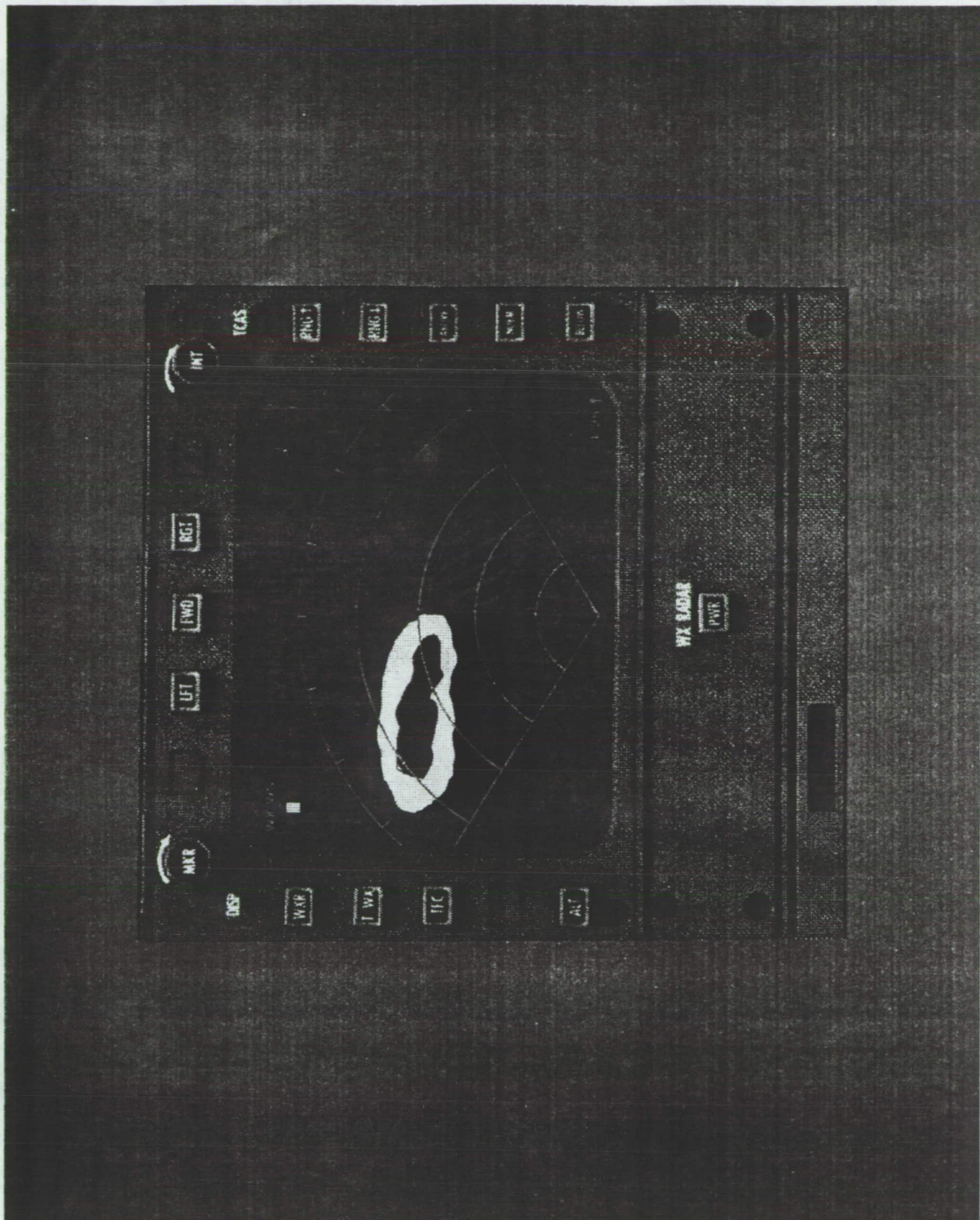
DISPLAY CONSIDERATIONS:

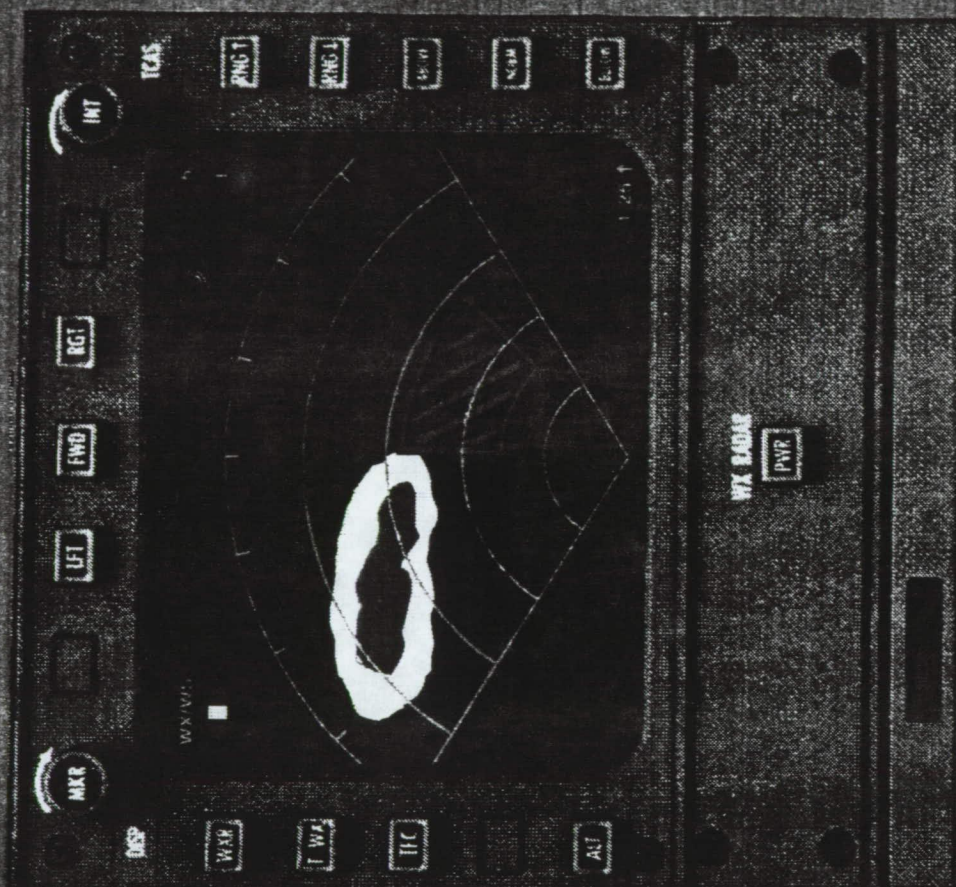
- HAZARD FACTOR DISPLAY
 - MAY OR MAY NOT BE ASSOCIATED WITH REFLECTIVITY CORE
 - DIFFICULT TO CORRELATE WITH VIEW AHEAD
- SYMBOLIC REPRESENTATION
 - OVERLAY ON WEATHER OR HAZARD DISPLAY

CONCLUSION: WINDSHEAR SYMBOLIC OVERLAY ON WEATHER DISPLAY GIVES MOST COMPLETE PICTURE OF WEATHER SITUATION

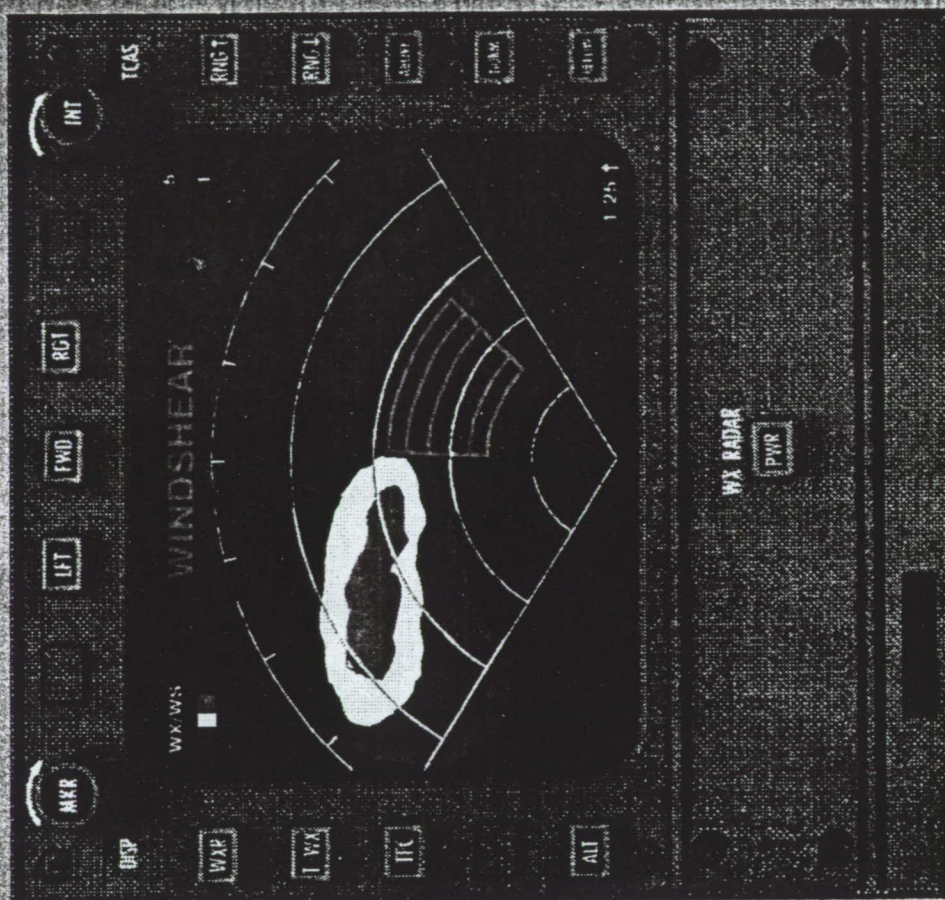












Airborne Doppler Radar Research at Rockwell International

Questions and Answers

Q: Roland Bowles (NASA Langley) - How did you estimate the downdraft, or did you estimate it in your total hazard calculation? Secondly: you post processed the airplane data through the In Situ algorithm; what did you think about the veracity of the algorithm?

Roy Robertson (Rockwell) - I will answer the second question first. Yes, we did post process the data. We collected the aircraft data from a different set of sources than what is on the B737. We had to piece together some of the In Situ inputs. The air data came from one source and the accelerometer data came from a different source, so we had to do a little work getting the filtering constant of the input data to agree. We also had some effort getting the angle of attack input calibrated. The algorithm seemed to have a fairly high sensitivity to angle of attack. Once we got those initial things worked out, we felt that the algorithm was doing very well. For downdraft estimation we used the first cut estimate that Dave Hinton had provided to the Lincoln Labs guys that had the altitude of the radar beam as a input parameter to the hazard factor calculation.

Q: Branimir Dulic (Transport Canada) - What is the price range and when will the system be in full operation, and the weight?

A: Roy Robertson (Rockwell International) - Price range? I am in engineering not marketing, so I would be stepping into some really deep problems if I said anything about that. Availability, we expect the system to be operational and finished with certification in 1993, and weight is roughly 30 pounds for the RT and something less than that for the antenna.

1993010414

488729
18p

Session IV. Airborne Doppler Radar / Industry

N 93 - 19603

Acquisition and Use of Orlando, Florida and Continental Airbus Radar Flight Test Data

Mike Eide, Westinghouse Electric

Bruce Mathews, Westinghouse Electric

PRECEDING PAGE BLANK NOT FILMED

Fourth Combined Manufacturers' and Technologists'
Airborne Wind Shear Review Meeting

April 14-16, 1992

Fort Magruder Inn, Williamsburg, Virginia

*Acquisition and Use
of
Orlando, Fla. and Continental Airbus
Radar Flight Test Data*

by

Mike Eide
Flight Test Pilot

Bruce Mathews
Radar Systems Engineering

Westinghouse Electric Corp.
Electronic Systems Group
Baltimore, Maryland

Abstract

Westinghouse is developing a lookdown pulse Doppler radar for production as the sensor and processor of a forward looking hazardous windshear detection and avoidance system. A data collection prototype of that product was ready for flight testing in Orlando to encounter low level windshear in corroboration with the FAA-Terminal Doppler Weather Radar (TDWR). Airborne real-time processing and display of the hazard factor were demonstrated with TDWR facilitated intercepts and penetrations of over 80 microbursts in a three day period, including microbursts with hazard factors in excess of .16 (with 500 ft. PIREP altitude loss) and the hazard factor display at 6 n.mi. of a visually transparent ("dry") microburst with TDWR corroborated outflow reflectivities of +5 dBz. Range gated Doppler spectrum (I,Q,FFT) data was recorded for subsequent development and refinement of hazard factor detection and urban clutter rejection algorithms.

Following Orlando, the data collection radar was supplemental type certified for in revenue service on a Continental Airlines Airbus in an automatic and non-interfering basis with its ARINC 708 radar to allow Westinghouse to confirm its understanding of commercial aircraft installation, interface realities, and urban airport clutter. A number of software upgrades, all of which were verified at the Receiver-Transmitter-Processor (RTP) hardware bench with Orlando microburst data to produce desired advanced warning hazard factor detection, included some preliminary loads with automatic (sliding window average hazard factor) detection and annunciation recording. The current (14-APR-92) configured software is free from false and/or nuisance alerts (CAUTIONS, WARNINGS, etc.) for all take-off and landing approaches, under 2500 ft. altitude to weight-on-wheels, into all encountered airports, including Newark (NJ), LAX, Denver, Houston, Cleveland, etc.

Using the Orlando data collected on hazardous microbursts, Westinghouse has developed a lookdown pulse Doppler radar product with signal and data processing algorithms which detect realistic microburst hazards and has demonstrated those algorithms produce no false alerts (or nuisance alerts) in urban airport ground moving vehicle (GMTI) and/or clutter environments.

Introduction

The Westinghouse Technical Direction is to provide a forward looking detection and avoidance system of low level windshear based upon a pulse-Doppler lookdown radar sensor to the commercial air transport market. The design of this system is for a "quiet, dark cockpit" with low false alert and nuisance alert rates. To be used, its warnings must be trusted and its hardware performance reliable.

Detection of microbursts employs an X-Band radar sensor designed to criteria which has made Westinghouse a leader in reliable lookdown airborne radar. Specific for this application are the demands of operating in an urban clutter environment and its attendant moving vehicle background. Our design approach is to temper initial, analytic designs based on experience with data from encounters with both microbursts and airport urban clutter.

However, it is difficult to obtain simultaneously interesting/stressing microbursts and appropriate clutter. These two series of flight tests have been respectively concerned to record radar data for microburst detection algorithm refinement and to observe and develop clutter rejection processing into a robust variety of urban airports with an in-revenue service aircraft reality. Signal and data processing algorithms subjected to input data collected in flight against actual microburst hazards verifies the detection capability of software upgrades to a radar in revenue service and demonstrate by superposition both hazard detection and low false alert criteria.

Overview

The Westinghouse involvement with airborne forward looking windshear detection radar (see figure 1) began in 1989. After talks with NASA LaRC, a flight test into nearby urban airports was conducted using a modified APG-68 (F-16) radar [1]. Data was collected along approach glideslopes using NASA "typical" waveforms. A number of antenna lookdown angles were examined to establish a baseline on antenna sidelobe rejection and appearance of ground moving discrete^s and traffic. Airport selection excluded stressing second time around urban clutter.

Westinghouse initiated a major development program. Receiver/transmitter/processor (RTP) units were designed, assembled, and software equipped to gather microburst data at the tailend of the microburst season. The design included pre-prototype component and design techniques. RTP configuration conformed to ARINC 708. The design included an FFT based signal processor and real time data processor.

The data collection radar was delivered to the Westinghouse owned and operated BAC-1-11 at the end of August with signal processing algorithms installed. Vectored by TDWR to areas of evolving or potential microburst activity, pilot decisions about fly-through utilized a realtime hazard factor display. Pre-processed radar data (FFT) was collected on over 100 microbursts over a 3 day period, including a run which produced 500 ft. loss in altitude.

The Orlando flights served as a checkout for installing the R/T into a Continental Airbus. Unlike Orlando, only VCR format data would be collected on the Airbus. The radar operated in an autonomous, non-interfering basis with the installed ARINC 708 type antenna system. VCR format data has been collected on 682 flight (1682 flight hours from 4-SEP-91 thru 8-APR-92) for take-off and approaches over altitudes from weight-on-wheels to 2500 ft. into a variety of urban airports including Cleveland, Denver, Newark, L.A., San Fransisco, Houston.

The initial software configuration on the Continental Airbus included only the signal processing algorithms as configured in the Orlando flights. These included neither complete clutter rejection nor total hazard factor algorithms. The software has been recently updated to include (1) refinement in the signal processing designed to reject GMTI-clutter while not impairing windshear detection, (2) computation of a total (vertical plus horizontal) hazard factor and (3) detection logic for total hazard factor. Effectively, the equipment is nominally configured for false alert scoring.

Radar and Instrumentation Design Considerations

Hazard factor accuracy may seem like an abstract and inaccessible quantity, but first order estimates of hazard factor accuracy can be controlled in sensor design by examining the sensitivity of the hazard factor to various measurement accuracies, particularly the accuracy of measuring outflow radial velocity and the distance over which the change in outflow velocities take place.

In fact, once these sensitivities are recognized, budgets for controlling the contribution from any single source can be allocated into the design. While the effects of sidelobe clutter, GMTI discretes, and other "clutter residue" contributions may be analytically elusive, accuracy limits of the hardware, the algorithmic processes, and/or waveform design may be established early in the design process.

In general, there may be several contributors to the Doppler velocity accuracy budget besides the signal-to-noise limitation, but the signal-to-noise limitation on Doppler velocity accuracy is most fundamental to when (at what range) the radar algorithmic processes can be expected to produce good velocity maps which produce good hazard factor maps. Minimal outflow reflectivities (and Doppler velocities) which produce marginally accurate hazard factors can be small if larger amplitude sidelobe/mainlobe ground moving vehicles or sidelobe discretes are inhibited from entering the velocity map.

range

Imperfect accuracy in the dimension over which the winds change will produce errors. Over-resolving sensors like radar will cut the microburst outflow into several pixels on a fine range grid, making the measurement of the outflow diameter relatively accurate in comparison to non-resolving sensors (e.g. infrared).

When the microburst is well resolved in range, a series of velocity measurements for the range pixels along an azimuth line may be used to construct an approximation to the horizontal windshear. Least mean square type approximations will be accurate over linear regions of shear (i.e. hazards) if the velocity measurements for each pixel are accurate.

Limits on velocity accuracy are usually set by the Doppler filter 3 dB. bandwidth. Non-resolving (i.e. pulse pair) Doppler sensors must resort to large signal-to-noise ratios to maintain accurate velocity measurements. Resolving (i.e. FFT spectrum analyzer) Doppler sensors can provide accurate Doppler velocity measurements at low signal-to-noise ratios.

The importance of low signal-to-noise ratio velocity accuracy is that the reflectivity of the outflow may be correspondingly less reflective, i.e. "dry".

According to NASA-LaRC, a minimally small, hazardous microburst will have the hazard area extend over about $D_\mu = 1000$ meters. Allowing some overlap by the approximating ensemble, the least mean square type slope estimator may begin to operate when diameter of the microburst hazard is subtended by the LMS window (population) of n_e points,

$$D_\mu \sim n_e \Delta R$$

$$\Delta R \sim D_\mu / n_e$$

Substituting for the range gate ΔR , with $(V/g) = (80/9.81) = 8.15$ sec, a 10% hazard factor accuracy on a nominal hazard factor of .105 yields [2],

$$\delta F/F = .10 \sim \{(8.15)/[2(1000)(.105)]\} [n_e \delta v / (n_e - 2)^{.5}]$$

Re-arranging, the velocity accuracy (δv) per point must be small,

$$\delta v \sim 2.58 (n_e - 2)^{.5} / n_e$$

For signal-to-noise limits, the velocity resolution Δv contributes to defining the velocity accuracy, $\delta v \sim \Delta v / (2 S/N)^{.5}$. Squaring both sides of the equation, the relationship between Doppler resolution and signal-to-noise becomes, approximately :

$$(\Delta v)^2 / (S/N) \sim 2(2.58)^2 (n_e - 2) / n_e^2$$

Consequently, range gated FFT spectrum analyzers can furnish fine Doppler resolution and, hence, accurate hazard factors at low S/N ratios due to minimal outflow reflectivities.

Accurate hazard factor processes at low S/N must avoid larger S/N returns, e.g. mainbeam clutter, sidelobe clutter, ground moving traffic, spurious, etc. The RTP assembly contains a stable oscillator (STALO), Receiver, Signal Processor, Solid State Transmitter, and Low Voltage Power Supplies. The STALO and receiver provide stability and spurious free operation in the presence of large mainbeam clutter. The receiver and STALO are departures for their attention to minimum detectable velocity and interference. The transmitter is solid state, based upon GaAs MMIC power amplifiers. A powerful signal processor is provided. This furnishes the numerical signal processing engine to accomplish an FFT spectrum analysis with proprietary algorithms to reject/sort clutter and GMTI with no consequence to windshear. Such algorithms are demanding because they must be executed at input data rates.

The signal processing effectively furnishes velocity (range x azimuth arrayed pixel) maps of the horizontal wind fields before and along the glideslope of the aircraft. Map data is available at a reduced rate. Data processing of these maps furnishes total hazard factor estimates along the aircraft approach or departure altitude profile. The final output stages of the warning system utilize a graphic processor to transform the radar coordinate maps into PPI formatted data as well as colour code the VCR displays. The processor design also supports high speed porting of the I&Q input data, the FFT data, etc. for instrumenting/data collection purposes.

"The Name of the Game" (see figure 2) for low level windshear warning is to sort windblown rain return ~~for~~^{from} other returns, including mainbeam urban (STAE) clutter, sidelobe distributed clutter, sidelobe and/or mainlobe GMTI. "Conditioning" preserves the signal integrity and minimizes spreading of mainbeam clutter through the downconversion process to analog-to-digital (ADC) conversion. "Signal Processing" includes those algorithms which are accomplished at the coherent processing interval (input data rate). With FFT spectrum analysis processing, there is a whole filterbank of Doppler candidates to describe the Doppler of the wind in a single range x azimuth beam (velocity map) pixel. The signal processor chore must smartly reduce the data entering the subsequent data processing stages by orders of magnitude. Pulse-pair and spectral averaging processes are simple and less demanding largely because they accept/include as eligible many Doppler returns which may not be windshear. "Data Processing" means the processing of the wind velocity maps to produce a total (i.e. both horizontal and vertical component) hazard factor map. It also may include the detection of average hazard factor areas. These different levels of radar data become the principal intermediate stages for observing radar performance and recording/instrumenting/displaying data.

Prior to the Orlando flights, Westinghouse assembled and delivered the data collection radar hardware to the software/systems integration bench. Real beam map and supporting modes were first developed and checked out at the bench and in local flight tests. Windshear mode development proceeded with several local flights through August. Initial development of the windshear signal processing utilized NASA-LaRC FORTRAN computer models of microbursts [3] and glideslope geometry, modified by Westinghouse to include its own models of multiple time around echo (MTAE, STAE) and distributed sidelobe clutter.

The objectives of the ORLANDO flights were to collect data on microbursts and to demonstrate airborne real-time processing and hazard factor display. The Orlando flights were conducted with signal and data processing operating (loading the timeline) but with ~~only~~ cursory signal processing enabled only. In general, the many thresholds and adjustable processing parameters in the signal processing algorithm were "de-sensitized" to insure that any and all Doppler reports would be passed to the VCR map displays. The objective was to unhinderedly collect any available data on microbursts. Real time processing of the wind blown rain return into velocity maps and hazard factor maps would allow the pilot and test crew to penetrate the microbursts, collect *in situ* (SUNDSTRAND) data, and otherwise corroborate the airborne displayed and recorded data with TDWR.

The installation on the BAC-1-11 (see figure 3) utilized a configuration in anticipation of the Continental Airbus installation to follow. A typical ARINC 708 (i.e. retrofittable) 30 inch flat plate phased array antenna was controlled through the sequencer. Data collection would include I&Q pulse and gated FFT radar data, INU, and air data input to the SUNDSTRAND reactive device in addition to the VCR formatted displays.

The BAC-1-11 operated in a fashion with the air traffic controllers and TDWR radar operators not unlike the preceeding NASA flights. Safety of flight considerations included minimum altitude limitations and air space restrictions. Using the voice and data link established by NASA earlier, the TDWR operators would vector the aircraft to the vicinity of the microburst. Based on pilot observations and TDWR radar reflectivity, Doppler, and/or hazard factor, the aircraft might penetrate the microbursts.

The Westinghouse flights were greatly aided by the fact of the real time airborne radar instrumentation display (see figure 4). The aircraft was directed to the vicinity of microburst activity by the TDWR, and the pilot used the radar display to locate a particular cell, assess the flight safety, and navigate through with little problem. As the data collection proceeded and the radar demonstrated its abilities to locate microbursts at long range, Westinghouse could approach general areas of activity and pick among evolving events. The VCR display format for both the Orlando and the Continental flight tests was constructed to the arguable convenience of engineers, and crowded a lot of instrumentation into a small space. Range (out to 8 n.mi. in range gates of 300 m.) x Azimuth ($\pm 23^\circ$) (B Scope) maps were provided for two bars of azimuth data, one bar at a lower elevation angle than the other. Each pixel on the screen represents a range gated angle cell of 16 colour shade coded data.

The maps at the top of the VCR format are unscaled amplitude (i.e. S/N). The "bland" colour palette employs red as a large amplitude signal and blue-green as minimal (near noise). The upper bar is on the right and the lower bar is on the left. Below these amplitude maps are the velocity maps for the respective bars. Green indicates zero velocity, yellow-red indicate tailwinds of increasing magnitude and blue indicates increasing headwinds (± 24 m/s or 3 m/s per colour shade). The odd rectangular window on the left is a B-scope lower bar horizontal hazard display. Most

people will find the PPI format of "total" hazard factor in the lower right corner most assessable. Hazard factor colour quantization spanned ± 2 (0.025 per shade). The space not used by the colour coded maps allows numerical discrete data. Activity of the signal processing numeric words provides engineers indications of proper activity of critical stages of the process. Along the bottom are indications of azimuth and elevation antenna position, aircraft location (lat.-long.), altitude, etc. Space was also allocated for SUNDSTRAND reactive hazard factor display and alphabetic annunciation.

The BAC-1-11 was vectored to some 80 different microburst events by the TDWR operators. Many of those events included multiple "isolated" cells and complex "line" events. In all, the radar collected data on over 100 microbursts in three afternoons of flight.

VCR tapes of the instrumented VCR format and views of the intercepts out the windshield will be shown.

The first video begins with a full screen display of the VCR instrumentation format. The amplitude, velocity, and hazard factor maps at the start of this run are full of activity in progress at near and very far (8 n.mi.) ranges. The cells of interest are being discussed by the pilot and TDWR. The airborne radar operator begins directing the pilot's attention to a beginning event. The audio contains conversation between the pilot and crew over the intercom and with the air traffic rf communication including the TDWR. The video transitions to a view out the pilot's windscreen with the instrumentation shrinking into the lower left corner of the screen. Subsequently, only the total hazard factor PPI map (true perspective) is shown. The visual shows little sign of outflow in the rain cell. As the penetration evolves, the microburst develops hazard factor displays portraying many shades of colours, including nearly .2 (top red). TDWR corroboration (post-flight de-briefing) placed the hazard factor along the flight path at .16, and the audio includes a pilot report of 500 ft. altitude loss for a penetration which began at an altitude under 2000 ft.

The second video segment begins as the plane (windscreen visual) emerges from a prior run on a rain core. The plane maneuvers slightly under TDWR direction, approaching a lake. Careful visual inspection of the lake surface will reveal an outflow. The air volume above the lake is clear. The radar display picks up indicated outflow activity in both the upper and lower bars of its scan patterns, and the hazard display shows a weak hazard factor at about 6 n.mi. as the aircraft turns and steadys under radar operator/radar display direction. Post flight de-briefing with TDWR corroborated a microburst forming with an outflow of +5 dBz. reflectivity. As the BAC-1-11 approaches, pilot comments indicate little or no visual ~~appearance~~ of a reflective rain core. The final audio remarks indicate the physical encounter with the windshear.

An outflow reflectivity of +5 dBz. at 6 n.mi. offers a rough calibration of the minimum detectable outflow reflectivity performance of the Westinghouse radar. As we introduced earlier, the RTP was installed aft of the pilot cockpit with additional waveguide run losses. We should expect to see lower reflectivities at shorter ranges, so, together with the range scaling and the ^{refuse} ~~additional~~ losses of a typical air transport installation, we may interpret an equivalent detectable reflectivity at 1.5 n.mi. (30 seconds of warning) of -5 dBz. *This particular microburst happens to be the least reflective outflow which we encountered, and the minimum detectable outflow reflectivity the Westinghouse radar system may expect is considerably) smaller (better) than -5 dBz.*

Continental Airlines Airbus Flight Testing

The Continental Airbus installation has given Westinghouse a opportunity to collect data and observe radar operation in the commercial airframe environment. The object of the Continental flight test was to place a radar of expected performance into a typical airline installation environment and observe its performance in the clutter and ground moving target/traffic environments as provided by the approaches and take-offs of its schedule. This objective was not in principle concerned with encountering microbursts and verifying/evaluating equipment detection performance. The salient design reasons for the flight test addressed the false alert and accuracy aspects of the radar design. Certainly, the interest was to perceive how and to what extent clutter, including mainbeam clutter, sidelobe clutter, ground moving ^{vehicle} ~~vehicle~~ traffic, etc. and any other phenomena encountered within the operational conditions of the aircraft approach and/or departure, including rf interference, will be evident to the radar. Such perceptions may allow some assessment of the false alert potential, but more likely, they furnish opportunities to Westinghouse to refine or add to its design.

Radar systems are dependent upon other systems on the aircraft for their satisfactory operation. Radomes and radome maintenance, mounting, vertical reference, altitude, etc. are furnished by the aircraft. Independent of any urban clutter - false alert concerns, there is much to be observed to insure a sensitive pulse-Doppler radar can properly operate, come what may with clutter.

Given that suitable hosting is provided, the regular flight patterns of an in-revenue service aircraft expose the radar to a variety of mainlobe, sidelobe, and second time around (STAE) urban and airport vicinity ground moving vehicular clutter.

The data collection radar system was supplied to Continental for installation. After supplemental type certification [4], the radar began supplying VCR display formatted video tapes at regular intervals. The installation of the Westinghouse equipment allowed non-interfering operation of the data collection radar with the on-board radar transparent to the pilot/crew. Whenever the radar was not being used, the Westinghouse radar would turn on automatically at altitude or takeoff using supplied aircraft discrettes and altitude data. The installation is largely an exploitation of the dual RTP operation expected for ARINC 708 equipment.

After returning to Baltimore, a different, more vivid colour palette was introduced to highlight activity. In general, the velocities of the outflows did not begin to approach 24 m/sec, so the velocity scale was reapportioned to ± 16 m/sec. The I and Q data recorded during the BAC-1-11 Orlando flights could be re-played through the RTP to produce new VCR displays and maps. The new palette uses a black background for zero activity. The amplitude scale indicates max (saturating) amplitudes by white decreasing to red, yellow, blue, green. The new velocity scale uses black for zero doppler with yellow, red as increasing magnitude tailwinds and green, blue, purple as increasing magnitude headwinds. The hazard factor uses black as zero, with yellow, red, magenta as increasing hazardous windshear and green to blue as increasing performance enhancing windshear.

The Orlando flights collected a mountain of radar data on microbursts. In general the clutter background was not worst case urban clutter, but some data was collected in/over the Orlando airport when it was closed to air traffic by the storms. This data allowed empirical studies of signal processing thresholds to reject non-windshear and ensure that windshear-like returns are retained without apparent loss. *In situ* data collection was limited. Air data collection was included at the last moment and its quality/collection is under examination and is questionable. TDWR radar data, available each day immediately after the respective flights, was used to "calibrate" the reflectivity/sensitivity of the radar, Doppler, and horizontal hazard processes of the data collection hardware and signal processing algorithms. Given their often differing perspectives on the events, the airborne and ground based radars produced excellent agreement in velocity and hazard factor and time and physical registration.

The Continental installation was initially equipped with unmodified Orlando signal processing algorithms. These algorithms were tailored to ensure that windshear would not be inadvertently edited/rejected, etc. Hence, the initial installed software configuration furnished only the simplest of mainbeam clutter processing as a means of rejection. Subsequent software updates included total hazard factor construction and a sliding window detection (400 m. range window with an window average $F=.105$ threshold) and optimized signal processing. All subsequent software loads were developed in the signal processing lab using the spare RTP unit as a test bed. The range gated in-phase and quadrature A/D data recorded during the flights for particular (i.e. hazardous) cases was played through the unit to check the performance of the PROMS (programmable read only memory chips) ~~which~~ destined for the Continental Airbus. Hence, the signal and data processing algorithms updating the Continental were verified to produce hazard factors, cautions, and warning alerts in correspondence to the corroborated Orlando microbursts. ***The software updates retain detection performance during periods of urban airport approach clutter false alert rejection algorithm observation, experimentation, and refinement.***

The latest software load included parameters and thresholds for the signal processing algorithms as determined empirically from reprocessing the Orlando flight test data.

The video segment shows ^asample in-revenue service landing approach for two different software loads in side-by-side comparison into the same (Newark) airport. Although the PPI total hazard factor display of the earlier (incomplete) software load shows some caution and hazard factor activity (from the spurious returns entering the velocity map from sidelobe leakage of discrete targets), it might well be considered remarkably "clean" were it not for the other PPI display being absolutely free of any such false cautions and/or alerts, even down to minimum altitude (weight on wheels). This video short indicates the power of the combined signal and data processing of the final configuration.

The map/instrumentation displays of these two runs were not, of course, collected simultaneously. However, the results portrayed are representative of the false alert performance to be viewed on all the landing approaches and takeoffs of the respective configurations.

The Continental flight tests have allowed Westinghouse to observe the commercial air transport operating and clutter environments. The equipment has performed largely as expected. Software loads have demonstrated by superposition the power of signal processing in rejecting sidelobe/vehicle traffic leakage while fully retaining microbursts, i.e. the signal processing algorithms and data processing algorithms operated satisfactory on the collected microburst data without any detection losses. The thresholds for sidelobe/GMTI rejection were empirically determined to retain microburst windshear by training with the Orlando microburst data. The Continental flight test data argues that a combination of modern signal and data processing algorithms can eliminate false alerts without compromising necessary detection performance..

Summary

1. Westinghouse has provided a new design pulse-Doppler lookdown radar for the air transport market.
2. With the help of the FAA and TDWR and the procedures established with them during the NASA LaRC flights, unprocessed quantitative (FFT) airborne data was collected in Orlando on over 100 separate microbursts, including real time hazard factor maps.
3. Westinghouse demonstrated the first airborne real-time detection of microburst windshear using airborne radar signal, data and hazard factor processing.
4. With the help of Continental Airlines, clutter data on many urban airports has been sampled within the context of the Westinghouse design.
5. Westinghouse has used the raw (I,Q,FFT) data collected in Orlando on hazardous microbursts to verify that its subsequent software loads have retained the necessary hazard detection performance. [False alert suppression has not been achieved at the expense of detection performance.]
6. Westinghouse has demonstrated airborne real time sidelobe/GMTI clutter rejection and a potential for satisfactory false alert operation. [Demonstration of 100,000 flight hour false alert times takes a long time.]

*Demonstrated
Detection and Avoidance Range Sensing of Hazardous Windshear
AND.
Low False Alert Techniques in Urban Airport Clutter*

References

1. B.Mathews, "Sabreliner Flight Test for Airborne Windshear Forward Looking Detection and Avoidance Radar Systems", Airborne Wind Shear Detection and Warning Systems, Third Combined Manufacturers' and Technologists' Conference, Oct. 16-18, 1990, NASA Conf. Pub. 10060, pt2, DOT/FAA/RD-91/2-II, p 715-754
2. I.Miller and J.Freund, Probability and Statistics for Engineers, Prentice Hall, 1965, p 233-235
3. C.L.Britt, User Guide for an Airborne Windshear Doppler Radar Simulation (AWDRS) Program, NASA Contractor Report 182025, DOT/FAA/DS-90/7, June 1990
4. G.Tsoucalas, "Continental Airlines Certification Plan", Westinghouse Predictive Windshear Radar Installation on Continental Airbus A300-B4 Aircraft", REF: FAA Project No. ANM1001-2145, (undated) 1991

Success by Empirical Refinement

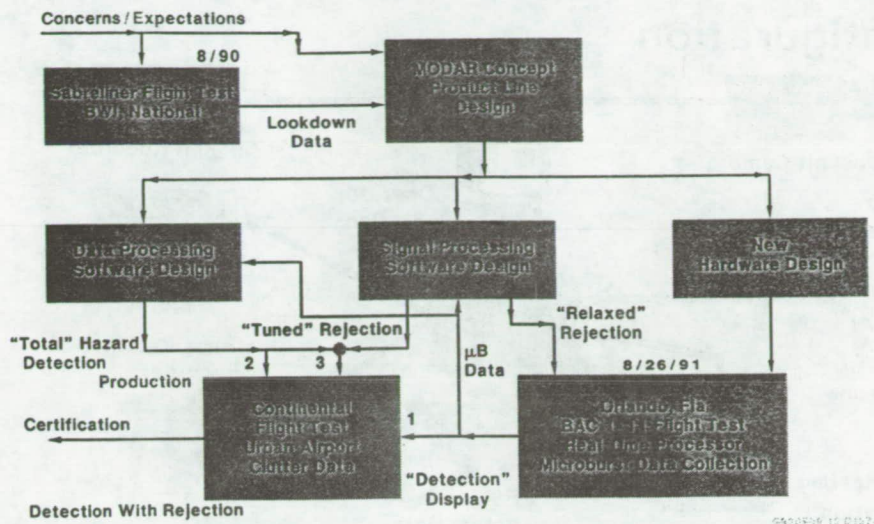


fig. 1 Overview of Approach

Low false alarm rate radar design must address mainbeam and sidelobe realities, particularly for sensitive detection near urban airports. Westinghouse has stressed the empirical detailed understanding of both microburst and urban airport clutter radar return in its design approach.

The Name of the Game ... Separate the Wind Return from Clutter

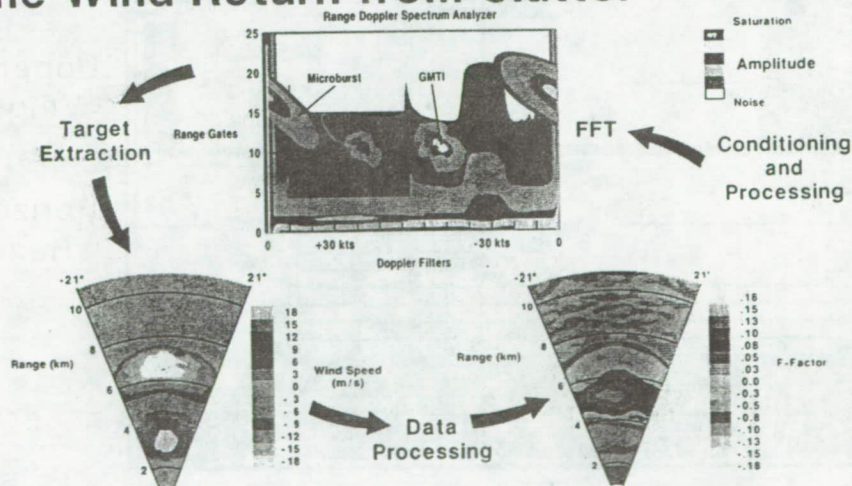


fig. 2 the Name of the Game... Separate the Wind Return from Clutter

Clutter and ground moving vehicular traffic returns must be separated from microburst outflow returns. This begins with a hardware design attendant of pulse Doppler realities and continues through digital algorithms to keep the wind blown rain and disregard non-windblown rain-like returns.

BAC1-11 Data Collection Configuration

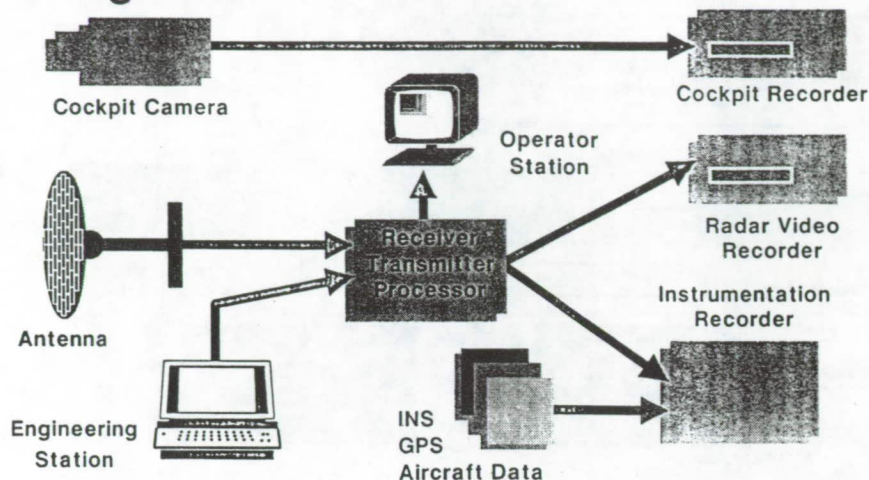
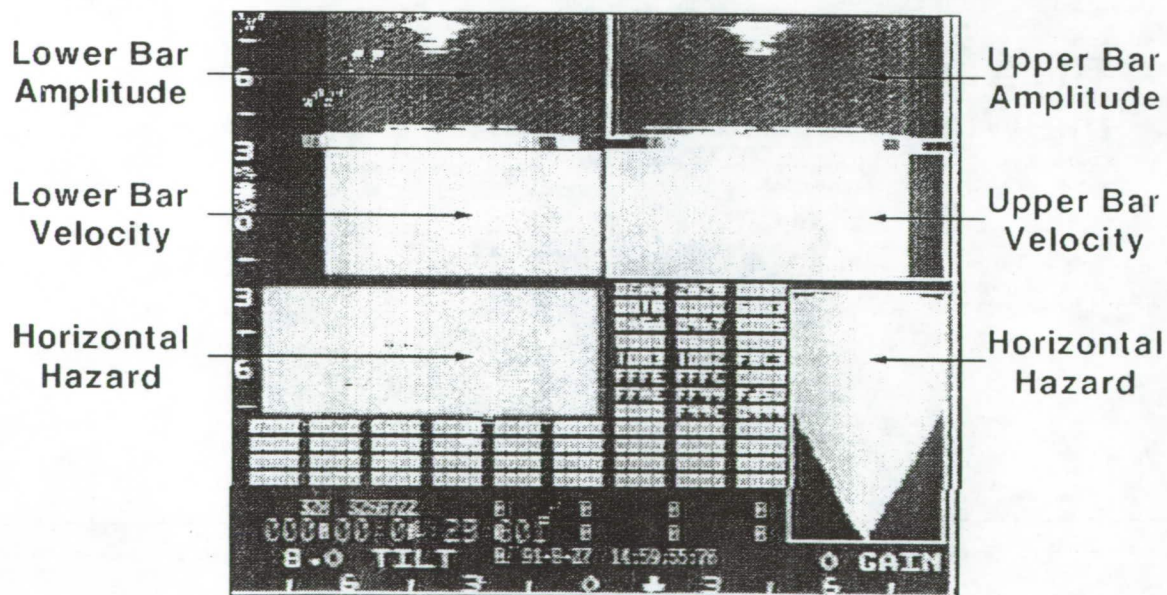


fig. 3 BAC-1-11 Installation

The BAC-1-11 installation includes ports for recording a variety of radar instrumentation and aircraft data.



G920909.02 BD351

fig. 4 VCR Instrumentation Format

The VCR format allowed collection of a great quantity of data of differing types. The discrete words included aircraft data and general processor health/activity parameters. The velocity display covered ± 24 m/s in Orlando with 16 colour shades (± 16 m/s on Continental Airbus). The hazard factor map covered $-0.2 \leq f \leq +0.2$

Acquisition and Use of Orlando, FL and Continental Airbus Radar Flight Test Data Questions and Answers

Q: Roland Bowles (NASA Langley) - Do you consider the ground clutter problem, both fixed and ground moving, solved?

A: Bruce Mathews (Westinghouse) - Yes, I do. The only thing I see remaining is a demonstration of the hazard factor accuracy in the presence of competing clutter.

Q: Roland Bowles (NASA Langley) - On a couple of the charts I saw the words "proven performance." On what kind of scientific basis do you claim proven performance, and would that be admissible in your certification initiative?

A: Bruce Mathews (Westinghouse) - I am not sure what is admissible to certification. We are engineers we are not scientist, we are not doing science. We have a great deal of faith and understanding in the principles of radar. We believe what we see, and it correlates very well with the TDWR. When they say they have an outflow reflectivity and velocity and we get the same thing, that is what we expect, and we are getting it. We do have a limited amount of In Situ data that we collected. We do not have a great deal of faith in it and there is not much we can do because it is limited.

Q: Roland Bowles (NASA Langley) - Do you plan to get it?

A: Bruce Mathews (Westinghouse) - We plan to get it this summer.

Q: Roland Bowles (NASA Langley) - Can you show us how your radar correlated, in your one hundred events, with the TDWR data?

A: Bruce Mathews (Westinghouse) - I think we can show that, yes. But, I don't have a viewgraph to show it right now.

Q: Roland Bowles (NASA Langley) - Dave Hinton talked about this yesterday, and I think Steve Campbell will further elaborate on it. Depending on how you flew and where you were relative to the divergent center, the TDWR could be viewed as significantly overestimating. We went through a very careful selection criteria to pull out the microburst encounters that really warranted detailed inspection. I would appreciate it if you could show us sometime what you have done, maybe later in the conference.

A: Bruce Mathews (Westinghouse) - Well, we are hoping to get that data. We do not have In Situ data, so we can't give you that kind of analysis. That is all there is to it. The data we have from our Sundstrand is very unsatisfactory.

Q: Jim Evans (MIT) - First, I would like to make a comment on the value of In Situ data. One of the key issues is the altitude dependence of the outflows, and where you are measuring versus where you should be measuring. We are flying our tests up at 1000 feet or above and we think the threat is a lot worse at lower altitudes. I think that is the first point we ought to recognize.

The value of In Situ is somewhat limited here because in fact you are not totally realistic as to where you should be flying. But that leads to another question. At what altitude where you attempting to measure in the measurements that we saw here? That is a very important issue in terms of your overall system performance and it has important implications. You did not really say at what altitude your antenna measures?

A: Bruce Mathews (Westinghouse) - We showed a two bar scan. We have one bar which we call an upper bar which points up and its principle purpose is to look at the reflective core and to make a higher altitude measurement of the outflow. As you can see in some of the displays, there was a stronger outflow in that upper bar than in that lower bar. The lower bar looks as near to the glide slope as a function of altitude as we dare. We tend to pick the beam up to keep the receiver from saturating, to stay in linear operation and to avoid unwanted clutter and saturation effects in the receiver. We picked the beam up as we come down in altitude. Now for these flight test in Orlando that beam was probably not doing a lot because we were flying fairly level at 1000 feet. When we land into Newark we are picking the beam up as a function of altitude controlling the beam with aircraft data. That is why the Continental Air Bus flight is important, to see how well that algorithm works. Some of the adjustments we wave made were to pick that up a little bit faster, because we saw a little bit more three sigma chatter in the elevation accuracy of the antenna than we had anticipated. Summarizing, we seek to make an estimate or a statement of the hazard factor along the glide slope that the pilot is flying. We look with two beams, one well above the glide slope and one very near to the glide slope to make that estimate.

Q: Pete Sinclair (Colorado State University) - How was the vertical motion determined?

A: Bruce Mathews (Westinghouse) - Westinghouse determines the vertical hazard factor using an algorithm which we would say is an extension of the NASA work that Dan Vicroy has reported. Because we have a two elevation bar scan, we measure the outflow velocities at two altitudes. Now, if you have two points you can draw a line between them. If you have a linear polynomial and you integrate it like you would for a conservation of mass principle, like Dan uses in his treatment of vertical estimation, you would get a quadratic polynomial, and that is what we do.

Q: Pete Sinclair (Colorado State University) - Was aircraft data or radar data used in this calculation?

A: Bruce Mathews (Westinghouse) - It is all radar data.

Q: Pete Sinclair (Colorado State University) - At what altitude is the calculation valid?

A: Bruce Mathews (Westinghouse) - The altitude is the altitude along the glide slope, that is what the calculation is made for. It is for every range gate along the glide slope. There is a separate vertical hazard factor calculated for each one of those range gates.

Session V. Doppler Related Research

1993010415 488731
30P

N93-19604

Session V. Doppler Related Research

Vertical Wind Estimation from Horizontal Wind Measurements
Dan Vicroy, NASA Langley Research Center

PRECEDING PAGE BLANK NOT FILMED

Vertical Wind Estimation From Horizontal Wind Measurements

Dan D. Vicroy

Flight Management Division
Vehicle Operations Research Branch
NASA/FAA Wind Shear Review Meeting

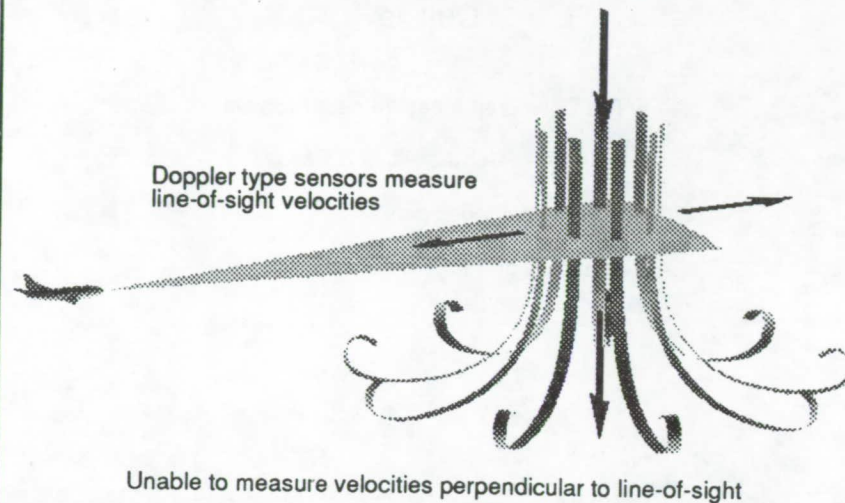
April 14-16, 1992

Outline

- The Downdraft Measurement Problem
- Initial Research Activities & Results
- Current Methodologies
- Summary and Future Activities

This presentation will begin with a brief description of the downdraft measurement problem for airborne Doppler based systems and the importance of the downdraft in assessing the hazard posed by a microburst wind shear. This will be followed by a review of research on the feasibility of using simple microburst models to compute the downdraft from horizontal wind measurements. The current methodologies for computing the vertical wind will then be discussed. A summary of the results and the plan for future research will conclude the presentation.

Downdraft Measurement Problem



Two of the airborne forward-look sensor technologies being tested to provide advanced warning of wind shear are Doppler RADAR and LIDAR. Both measure the Doppler shift of reflected light or radio waves from the aerosols, rain drops and other debris in the air, to determine the line-of-sight relative velocity of the air. An inherent limitation of this type of system is its inability to measure velocities perpendicular to the line-of-sight. The presence of a microburst can be detected by measuring the divergence of the horizontal velocity profile, yet, the inability to measure the downdraft can result in a significant underestimate of the magnitude and spatial extent of the hazard.

Wind Shear Hazard Index***The "F-factor"*****For straight and level flight**

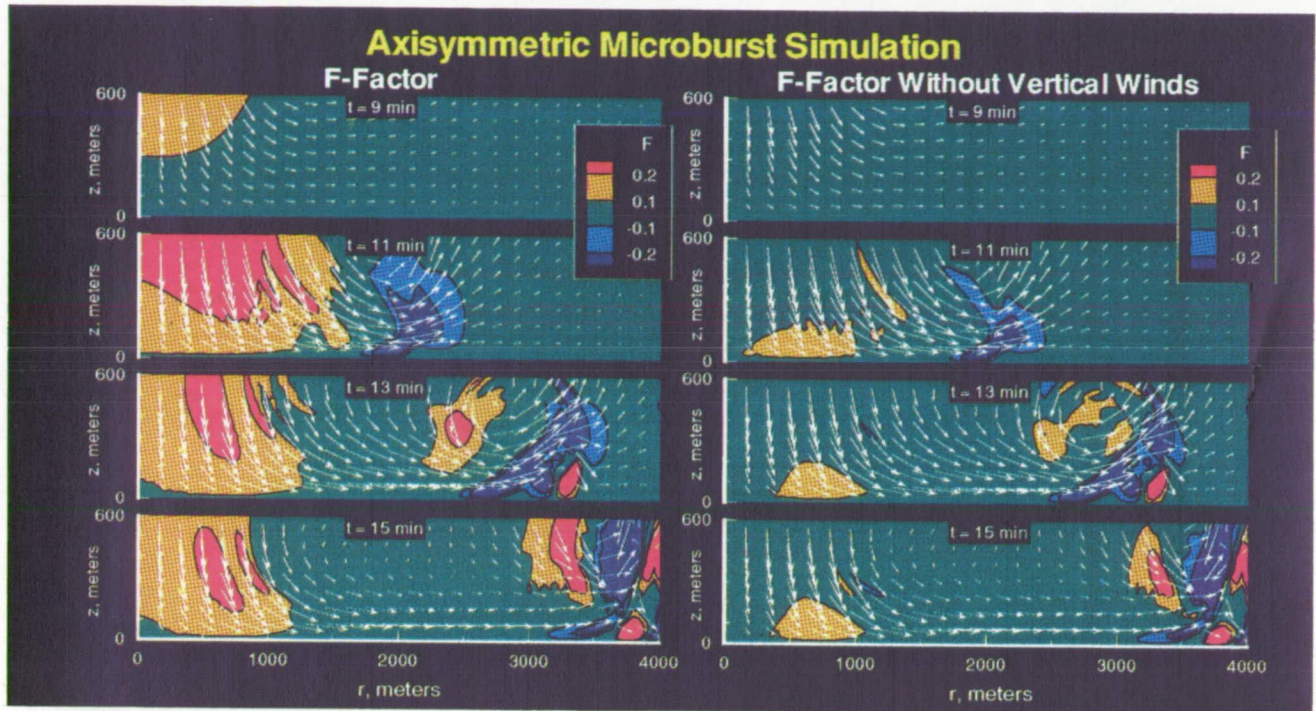
$$F = \frac{\dot{u}}{g} - \frac{w}{V}$$

Related to the potential rate of climb

$$\dot{h}_p = V \left(\frac{T - D}{W} - F \right)$$

The magnitude of the hazard posed by a microburst to an airplane can be expressed in terms of the "F-factor"[†]. The F-factor is a nondimensional hazard index that is directly related to the potential rate of climb capability of the airplane in wind shear. For straight and level flight the F-factor is a simple function of the rate of change of the horizontal wind (\dot{u}), the vertical wind (w), the acceleration due gravity (g), and the airplane's airspeed (V). Positive values of F indicate a performance-decreasing situation, and conversely, negative values indicate a performance-increasing condition.

† Bowles, Roland L.: *Reducing wind shear Risk Through Airborne Systems Technology*. 17th Congress of the International Congress of Aeronautical Sciences, Stockholm, Sweden, September 1990.



This chart shows F-factor contour plots and the wind velocity vectors for an axisymmetric microburst at four stages in its life cycle. This microburst was generated with the Terminal Area Simulation System (TASS) high-fidelity atmospheric model.[†] The F-factor contours were computed for an airplane flying level at 130 knots. The contours on the left include the vertical wind in the F-factor calculation while the contours on the right do not. The contours on the right represent the detectable hazard from solely horizontal wind measurements. The magnitude and spatial extent of the detectable hazard is clearly diminished. This chart illustrates the need for some means of estimating the magnitude of the vertical winds from the horizontal wind measurements.

[†] Proctor, F. H.: *The Terminal Area Simulation System. Volume I: Theoretical Formulation*. NASA CR-4046, April 1987.

Initial Research Activities

- Focused on downdrafts in microbursts
- Tried three microburst downdraft models of varying complexity
 - Linear model
 - Empirical model
 - Ring Vortex model

The initial research objective was to determine the feasibility of computing the downdraft of a microburst from horizontal wind measurements using simple microburst models. No attempt was made to compute updrafts or vertical winds from other weather phenomena, such as gust fronts, since these were considered performance increasing and thus were not hazardous. Three microburst downdraft models were tested. The three models represented varying degrees of complexity. The linear model was the simplest and the ring vortex model was the most complex.

Linear Downdraft Model

Based on:

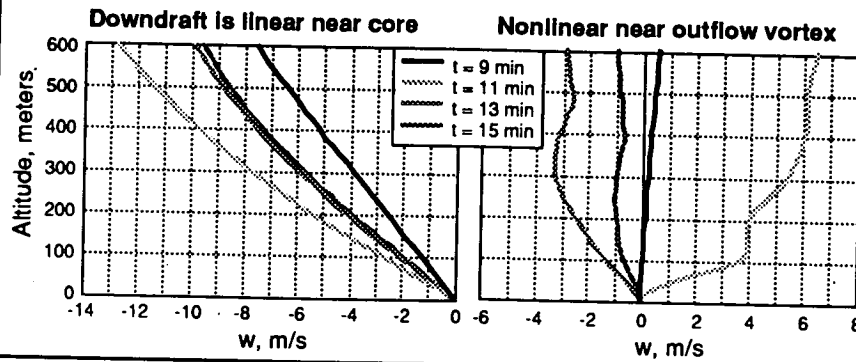
Conservation of mass

$$\frac{\partial u}{\partial r} + \frac{\partial w}{\partial z} + \frac{u}{r} = 0$$

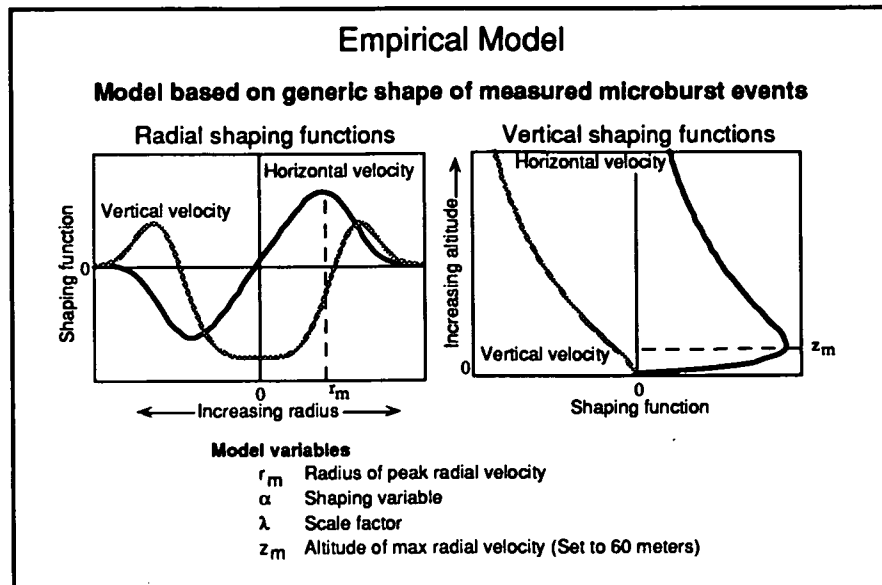
Linear variation with altitude

$$w = -z \left(\frac{\partial u}{\partial r} + \frac{u}{r} \right)$$

$$w = \frac{\partial w}{\partial z} z$$



The "linear model" is the simplest of the three models tested. It is based primarily on the principle of conservation of mass, which is expressed on this chart in cylindrical coordinates. If the vertical wind is assumed to be zero at the ground and vary linearly with altitude, then the vertical wind can be expressed as a simple function of the radial velocity profile. The linear assumption appears reasonable in or near the core of the microburst but poor near the outflow vortex.

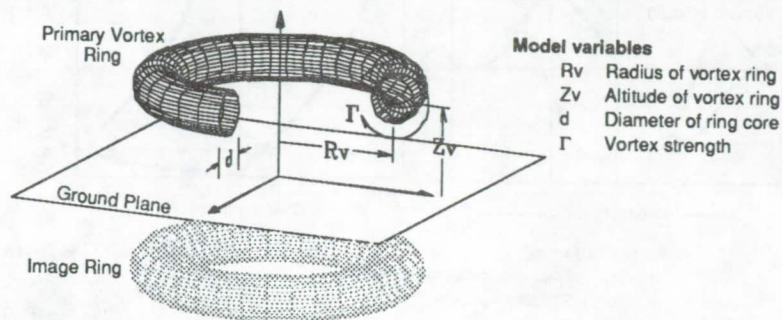


As the name implies, this model is based on measurements of several microburst events. The empirical model is an axisymmetric, steady-state model that uses shaping functions to satisfy the mass continuity equation and simulate boundary layer effects[†]. The shaping functions are used to approximate the characteristic profile of the microburst winds. The empirical model is fully defined through four model variables: the radius and altitude of the maximum horizontal wind, a shaping variable, and a scale factor.

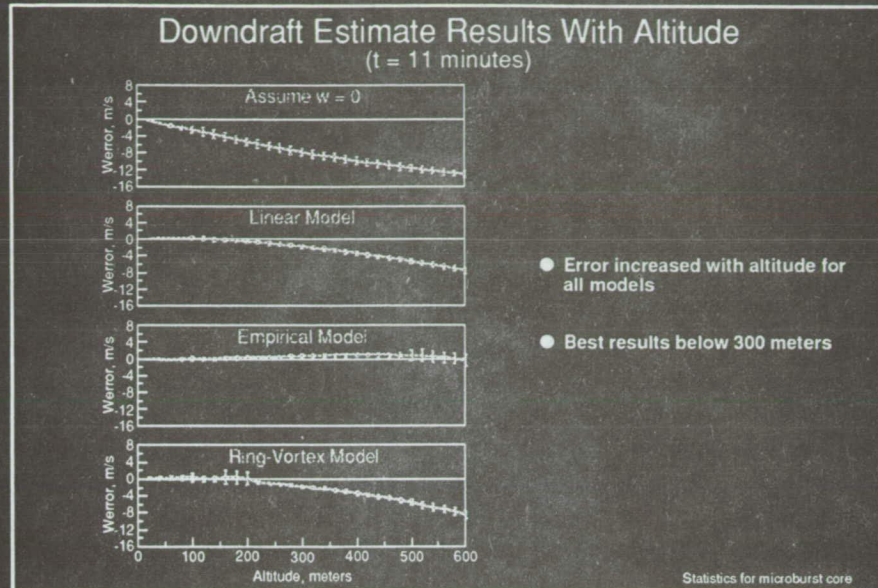
[†] Vicroy, Dan D.: *A Simple, Analytical, Axisymmetric Microburst Model for Downdraft Estimation*. NASA TM-104053, DOT/FAA/RD-91/10, February 1991.

Ring-Vortex Model

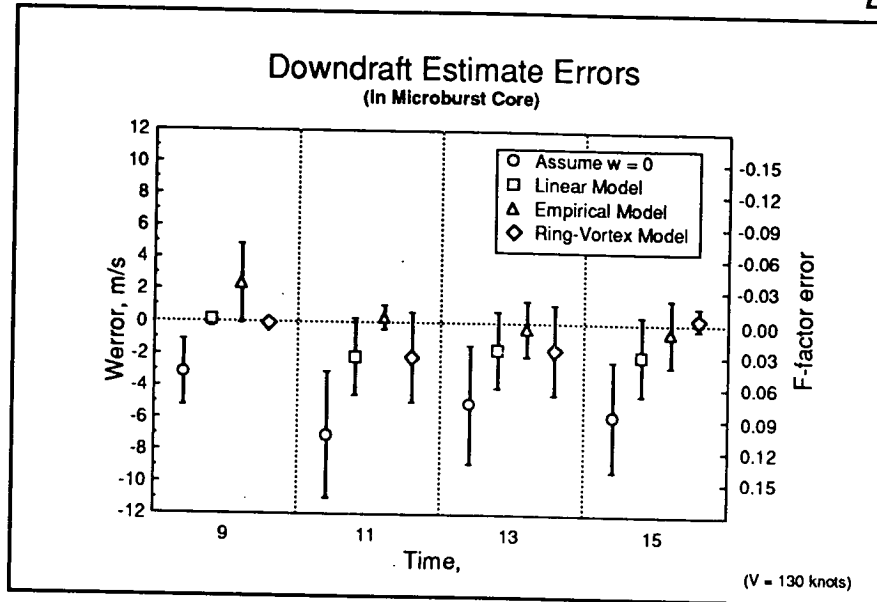
Model based on theoretical simulation
of microburst flow characteristics



The ring-vortex model is a theoretically derived model based on the assumption that the flow field generated by a vortex ring near a flat plate is similar to that of a microburst. This model has a primary vortex ring located above the ground and a mirror image ring located equidistant below the ground plane. The mirror image ring is used to satisfy the no-flow through the ground boundary condition. The vortex ring model is defined by four model variables: the radius and altitude of the primary vortex ring, the diameter of the viscous core, and the circulation strength.



An example of the mean and standard deviation of the downdraft estimate errors from the three models is shown here for the TASS axisymmetric microburst presented earlier. The errors are shown for each altitude at which a downdraft profile was estimated. Also shown is the error that results from assuming no downdraft ($w=0$). The errors were computed in the downdraft region of the microburst as the actual minus the estimated value. The errors increased with altitude for all of the models and all worked well below 300 meters. The empirical model worked particularly well in this example but had less favorable results in other test cases.



The total mean and standard deviation of the downdraft error over the full altitude range (0 to 600 meters), is shown here for each of the four stages of the microburst. Also shown in the figure is the corresponding F-factor error for an airspeed of 130 knots. None of the models had significantly better performance than the others. The linear model worked well for all the cases at altitudes below 200 meters. The empirical model produced the best results for the 11 and 13 minute cases. The 11 minute case is near the time of maximum shear and is perhaps the most critical from a hazard perspective.

NASALaRC

Initial Research Results

- Downdraft estimation errors increased with altitude
- No significant improvement with increased model complexity
- Model fitting technique requires knowledge and tracking of divergence center

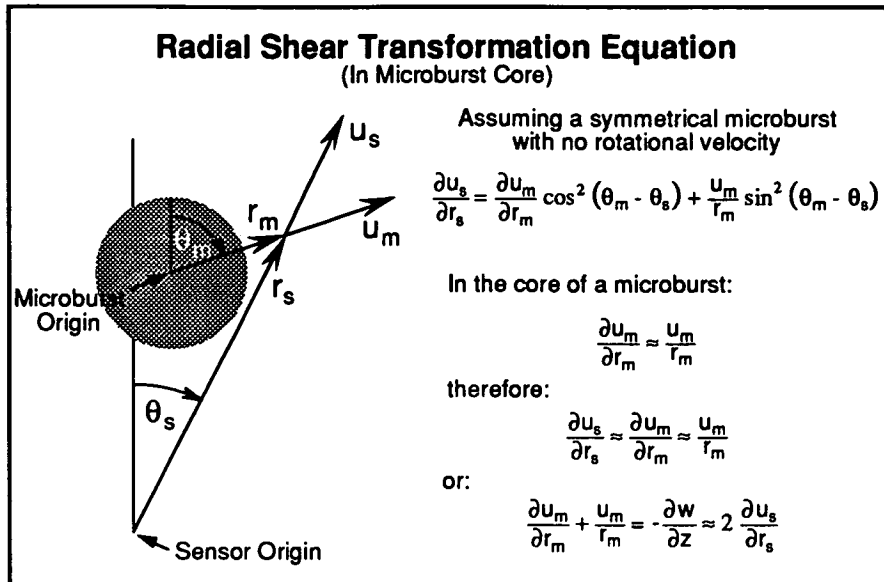
The primary result of this initial study was to establish that simple microburst models could be used to estimate the downdraft from horizontal wind measurements. For the three models tested the downdraft estimate errors increased with altitude and there was no significant improvement with model complexity. One difficulty of the model based downdraft estimation technique is the requirement that the model be referenced about the divergence center of the microburst. This requirement poses system implementation issues such as identification and tracking of the divergence center, which were not addressed in this study. Details of this initial study can be found in AIAA paper 91-2947 "Assessment of Microburst Models for Downdraft Estimation" by Dan D. Vicroy.

NASA **LaRC**

Current Research Efforts

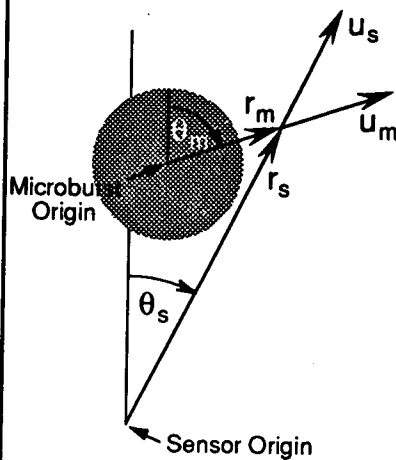
- Transformation of radial shear from microburst to sensor referenced coordinate system
- Development of new vertical wind estimation techniques
- Application of new techniques to '91 flight test data

The new wind shear hazard criterion, which was introduced by Mike Lewis (NASA LaRC) in an earlier presentation, defines the hazard as the F-factor averaged over one kilometer. Since the F-factor is now being averaged, the updrafts as well as the downdrafts must be computed. This required a restructuring of the techniques discussed earlier. This was accomplished by first translating the microburst-referenced wind field to a sensor referenced coordinate system. Simplifications were made to this transformation which manifested new vertical wind estimation techniques from Doppler sensor measured winds. These techniques were then tested using measured winds from the '91 flight tests to determine their viability.



This chart shows the radial shear transformation equation from a microburst-centered coordinate system to a sensor-referenced coordinate system under some simplifying assumptions. If the radial shear is assumed to be linear in the microburst core, then the transformation equation becomes a simple equality. If this equality is then applied to the mass conservation equation, a simple equation for the vertical velocity gradient as a function of the sensor measured radial shear is obtained.

Radial Shear Transformation Equation (Outside Microburst Core)



Assuming a symmetrical microburst
with no rotational velocity

$$\frac{\partial u_s}{\partial r_s} = \frac{\partial u_m}{\partial r_m} \cos^2 (\theta_m - \theta_s) + \frac{u_m}{r_m} \sin^2 (\theta_m - \theta_s)$$

Outside microburst core:

$$\frac{u_m}{r_m} \rightarrow 0 \text{ as } r_m \rightarrow \infty$$

therefore: $\frac{\partial u_s}{\partial r_s} \approx \frac{\partial u_m}{\partial r_m} \cos^2 (\theta_m - \theta_s)$

or: $\frac{\partial u_s}{\partial r_s} \geq \frac{\partial u_m}{\partial r_m}$

For large r_m

$$\frac{\partial u_m}{\partial r_m} + \frac{u_m}{r_m} = -\frac{\partial w}{\partial z} \approx \frac{\partial u_m}{\partial r_m} \leq \frac{\partial u_s}{\partial r_s}$$

This chart uses the same transformation equation as the previous chart but assumes that the measurements are made outside the microburst core. As the distance from the microburst core increases, simplifying assumptions can be made which result in an inequality relationship between the vertical wind gradient and the sensor measured radial wind.

Vertical Shear Approximation

$$\frac{\partial u_s}{\partial r_s} \geq 0$$

Assume inside microburst core:

$$\frac{\partial w}{\partial z} = -2 \frac{\partial u_s}{\partial r_s}$$

$$\frac{\partial u_s}{\partial r_s} < 0$$

Assume outside microburst core:

$$\frac{\partial w}{\partial z} = -\frac{\partial u_s}{\partial r_s}$$

or

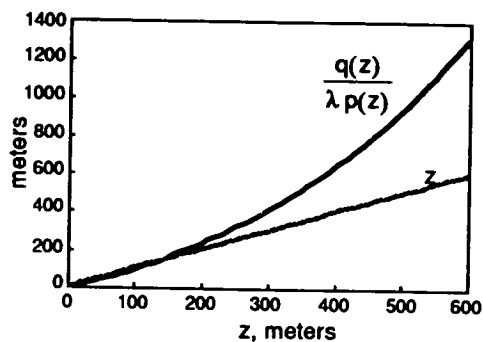
$$\frac{\partial w}{\partial z} = -\frac{1}{2} \left(3 \frac{\partial u_s}{\partial r_s} + \left| \frac{\partial u_s}{\partial r_s} \right| \right)$$

By combining the results of the previous two charts a simple approximation for the vertical wind gradient as a function of the sensor measured radial wind can be postulated.

Vertical Wind Estimation Methodology

Linear Method

$$w = z \frac{\partial w}{\partial z}$$

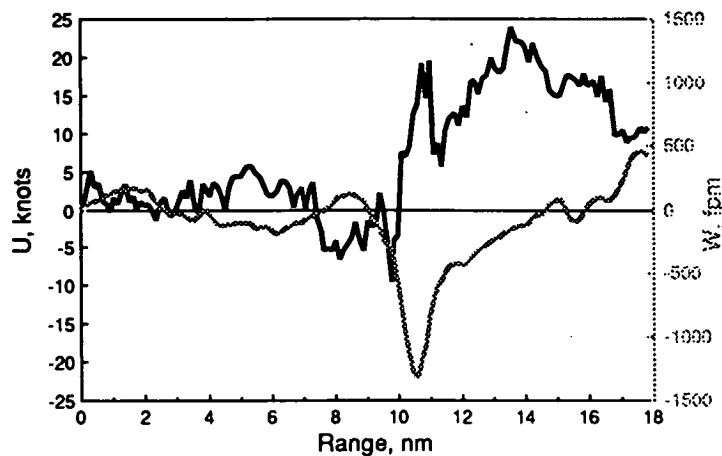


Empirical Method

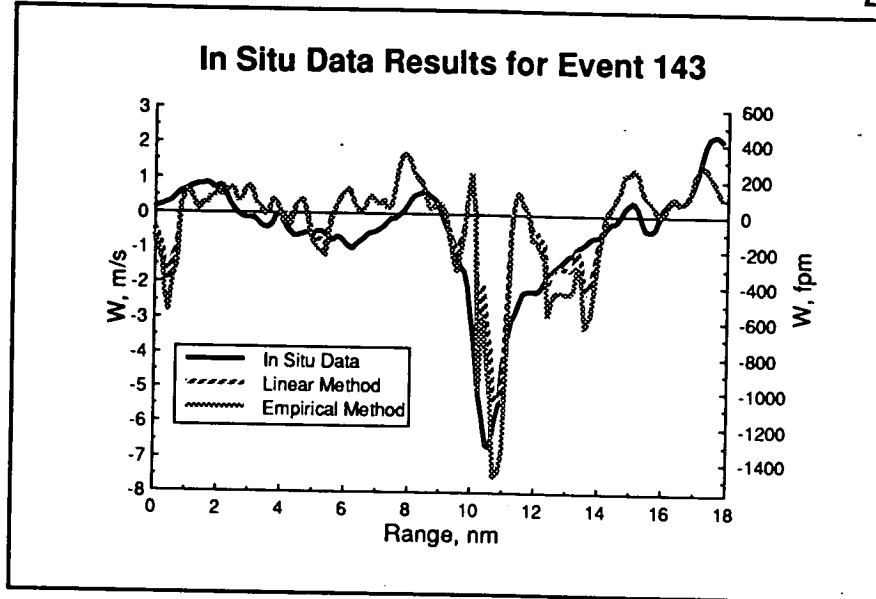
$$w = \eta(z) \frac{\partial w}{\partial z}$$

$$\eta(z) = \begin{cases} \frac{q(z)}{\lambda p(z)}, & \frac{\partial w}{\partial z} \leq 0 \\ z, & \frac{\partial w}{\partial z} > 0 \end{cases}$$

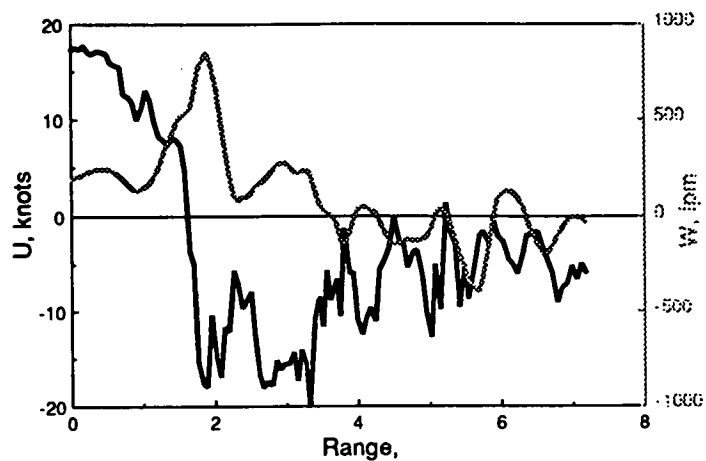
With an estimate of the vertical wind gradient in hand, the next step was to develop methodologies for computing the vertical wind from the vertical wind gradient. Two methodologies were developed. The simplest was the previously tested linear method. The other method was a derivation of the empirical model used in the initial study. The vertical shaping functions were used to define an altitude dependent function for computing the downdraft in the microburst core, and the linear method is used to compute the updrafts outside the microburst core.

Event 143 In Situ Data Winds

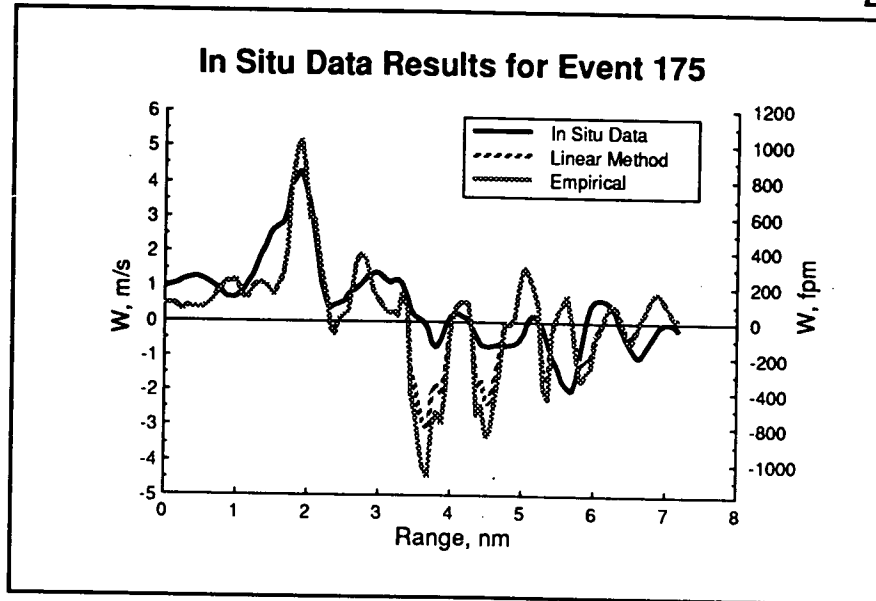
A quick test of the two new methodologies was conducted using the In Situ measured winds from microburst and gust front penetrations during the '91 flight tests. Presented on this chart are the horizontal (U) and vertical (W) wind measurements of microburst event 143. The horizontal wind was used as input into the vertical wind estimation methodologies. The measured vertical wind was used to compare with the estimated value.



The vertical wind estimation results are shown on this chart for the new linear and empirical methods. As can be seen there is very little difference between the two methods for this particular case. The difference between the two methods only manifests itself at altitudes above 400 meters. This data was obtained at an altitude of about 300 meters. In general the vertical wind estimate follows the measured vertical wind profile. However, localized fluctuations in the horizontal wind profile resulted in spikes in the vertical wind estimation. This would indicate that the horizontal wind profile may need to be filtered to provide a smooth input for vertical wind estimation.

Event 175 In Situ Data Winds

As mentioned earlier, the vertical estimation methods were also tested using gust front data. Presented on this chart are the horizontal and vertical wind measurements of gust front event 175.



Once again, the difference between the two methods is small at the altitude at which this data was collected. The methods estimated the updraft fairly well, but considerably over estimated two downdrafts. The current methodologies assume any divergence is a microburst and compute the downdraft accordingly. This can lead to the large downdraft estimates shown here. Some signal processing may be required to test the extent of the divergence and classify as a microburst or a local fluctuation accordingly.

Results Summary

- Simple analytical models are sufficient for computing vertical winds at altitudes below 600 meters (~2000 ft).
- May need to tailor the vertical shear approximation to signature of radial shear measurement (how linear is the shear measurement over a given range?)
- Estimate of vertical wind is sensitive to "noise" in radial shear value

The preliminary data obtained to date would indicate that the simple analytical methods discussed here should be sufficient for estimating the vertical winds from horizontal wind measurements. However, there is still some signal processing research required to improve the vertical wind estimates and reduce the sensitivity to local fluctuations in the horizontal wind profile.

Future Activities

Focus:

System implementation issues

- Clutter
- Resolution

Signal processing?

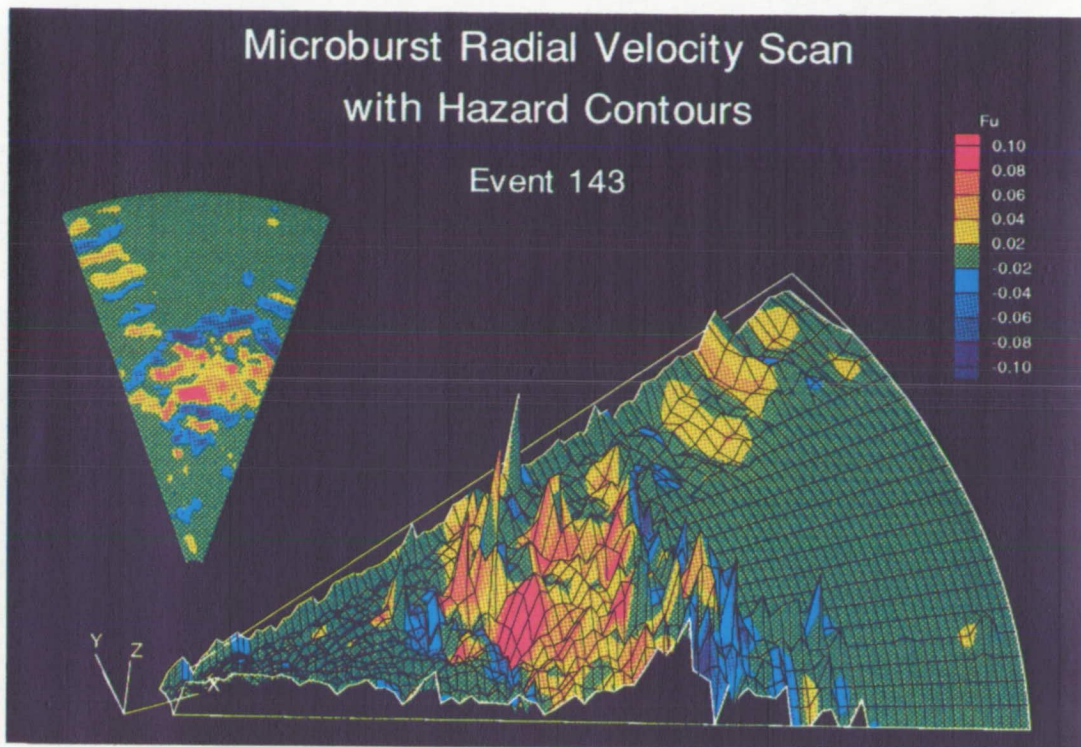
Approach:

Use sensor simulations with high fidelity asymmetric microburst models

Compare simulation results with flight test data

Future research efforts will focus on the system implementation issues for utilizing the two vertical wind estimation methodologies. The signal processing required to distinguish small scale vertical wind fluctuations from larger scale microbursts will be a large part of this research. The forward-look sensor characteristics, such as signal-to-noise ratio and range gate resolution, must be accounted for in the signal processing.

Sensor simulations with high fidelity asymmetric microburst models will be used to develop the signal processing. Once developed, the simulation results can be tested against flight test data to assess the "real world" performance.



This last chart is used to illustrate the signal processing problem. Shown here is a surface plot of the horizontal wind measurement from a range/azimuth scan of an airborne Doppler radar. Included on the surface plot are the F-factor contours. Clearly, the signal processing will play an important role in hazard identification.

Vertical Wind Estimation from Horizontal Wind Measurements

Questions and Answers

Q: Craig Wanke (MIT) - I have a question about determining whether you are inside the core or outside the core. Do you need somehow to estimate in real time where the core of the microburst is or to know your distance from it somehow, to apply this?

A: Dan Vicroy (NASA Langley) - I probably wasn't very clear on that. Part of the problem with the model base approaches that I showed early on was that they were all referenced to the center of the microburst. Consequently, you did have to track the microburst and determine where the center of divergence was. We decided that was definitely not a good approach. The second methodology that I showed, which is the current implementation, just looks at the sign of the divergence, and if it is a positive divergence then you assume that you are in a microburst core and if it is a negative divergence then you are outside of the microburst core. That is probably too simplistic. Perhaps what you need to do is tailor the vertical shear approximation by doing a linearity check. If it is a positive divergence and that divergence is fairly linear over a given range, then perhaps you can assume that you are in a microburst core and then estimate the vertical wind accordingly. If it is not very linear over the appropriate range, then you can say that is just turbulence or a small downdraft and you would not want to treat it as a microburst.

Q: Pat Adamson (Turbulence Prediction Systems) - From the dual Doppler analysis, particularly in the Denver area, it was not uncommon to have 2:1 asymmetric events, as well as dry events with a low signal to noise. Have you done any error calculations on the estimation of vertical winds under those conditions?

A: Dan Vicroy (NASA Langley) - I haven't yet. That is part of that future work that we hope to wrap up by the end of the summer. The microburst simulations that I will be using from Fred will all be asymmetric, they will not be axisymmetric.

Fred Proctor (NASA Langley) - I have looked at a couple of very asymmetric events using this technique and it does surprisingly well.

488753
40p

1993010416

N93-19605

^

Session V. Doppler Related Research

Microburst Characteristics Determined from 1988-91 TDWR Testbed Measurements

Paul Biron, MIT Lincoln Laboratory

Mark Isaminger, MIT Lincoln Laboratory

**MICROBURST CHARACTERISTICS
DETERMINED FROM 1988-91 TDWR TESTBED
MEASUREMENTS**

**PAUL J. BIRON
MARK A. ISAMINGER**

**M.I.T. LINCOLN LABORATORY
15 APRIL 1992**

(PRESENTED BY J. EVANS)

PRECEDING PAGE BLANK NOT FILMED

Vugraph Text - Biron/Isaminger Papers

Vugraph #1 "Outline"

Under FAA sponsorship, the MIT Lincoln Laboratory has conducted experimental windshear measurements at a number of locations since 1985:

1985:	Memphis, TN
1986:	Huntsville, AL
1987-88:	Denver, CO
1989:	Kansas City, MO
1990-91:	Orlando, FL

The principal sensor was the TDWR testbed radar (S-band with 1° beamwidth through 1990, C-band with 0.5° beamwidth since 1991). Supporting sensors have included the UND C-band Doppler radars (1986-91) the MIT C-band Doppler radar (1991) and a sizable surface mesonet (measuring average and peak temperatures, humidity and winds 1/minute).

This paper presents some recent results (extending those in the paper by Wolfson, et al. at the 19th Conference on Decision and Control) germane to airborne windshear system design and certification. We will first discuss the data analysis procedure and the associated caveats. The relative frequency, severity and duration of microburst hazards at the various locations is important for determining the tradeoffs between safety and operational impact of false alerts which are encompassed in detection system thresholds.

We next consider radar/lidar design issues such as reflective in microbursts and the vertical structure of outflows. A companion topic, gust front characteristics, is discussed in a paper by Klinge, et al. at the vugraphs end of this talk. Finally, we provide recent surface thermodynamic data associated with microbursts.

OUTLINE

- **ANALYSIS PROCEDURE/CAVEATS**
- **NUMBER OF EVENTS**
- **HAZARD LEVELS AND DURATIONS**
- **RADAR/LIDAR DESIGN FACTORS**

REFLECTIVITIES

SIZES

- **THERMODYNAMICS**
- **SUMMARY**

Vugraph #3 "Assessment Procedure"

The TDWR testbed radar meteorologists have compiled gross microburst structure information on a large number of the microbursts. The meteorologist inspects the TDWR surface scan radial velocity field with the TDWR microburst detection algorithm overlaid on the image. The meteorologist clicks the mouse on the radial velocity image pixels characterizing the maximum and minimum velocity associated with a microburst as well as the midpoint. The velocity values, locations and corresponding reflectivity values are stored in a computer data base. The shear is estimated by the equation $S = \Delta V / \Delta R$ where ΔV is the velocity difference and ΔR (i.e., the "width") the distance between maxima and minimum velocities.

Thus, localized high shear regions such as discussed by Campbell and Proctor in this conference are not captured by this approach, (i.e., the shears computed generally are a lower bound to shear averaged over typical distances such as 1-2 km).

Since only horizontal velocities are considered, and the degree asymmetry is not known, the vertical component is not directly considered. It should also be noted (see Campbell paper in this conference) that the altitude at which the surface tilt measured may have biased velocities downward. The data base considers microbursts at ranges out to at least 30 km and, one expects (from geometrical arguments) that the bulk of the data is a relatively long range where horizon effects tend to create a beam volume at higher altitude.

In some cases, we have high resolution vertical profiles from RHI scanning on microbursts at close range. The 1991 data is particularly useful in this respect due to the 0.5° beamwidth.

ASSESSMENT PROCEDURE

- EXPERIENCED RADAR METEOROLOGIST ASSESSMENT OF MICROBURST OUTFLOWS AND CORES AIDED BY TDWR MICROBURST ALGORITHM PRODUCT OUTPUT
- RESULTS STORED IN COMPUTER DATA BASE FOR SUBSEQUENT ANALYSES
- CAVEATS:
 - SHEAR ESTIMATES REPRESENT AVERAGE OVER OUTFLOW REGION- LOCALIZED "HOT SPOTS" NOT CONSIDERED
 - ASYMMETRY NOT CONSIDERED-WOULD AFFECT VERTICAL VELOCITY ESTIMATES FROM HORIZONTAL DIVERGENCE
 - OUTFLOW ALTITUDE ESTIMATES SIGNIFICANTLY EFFECTED BY 3 D SCAN PATTERN USED AND DISTANCE TO OUTFLOW- MOST ACCURATE RESULTS WITH RHI'S USED IN KC AND ORL

Vugraph #4 "Dist. of MB Strength"

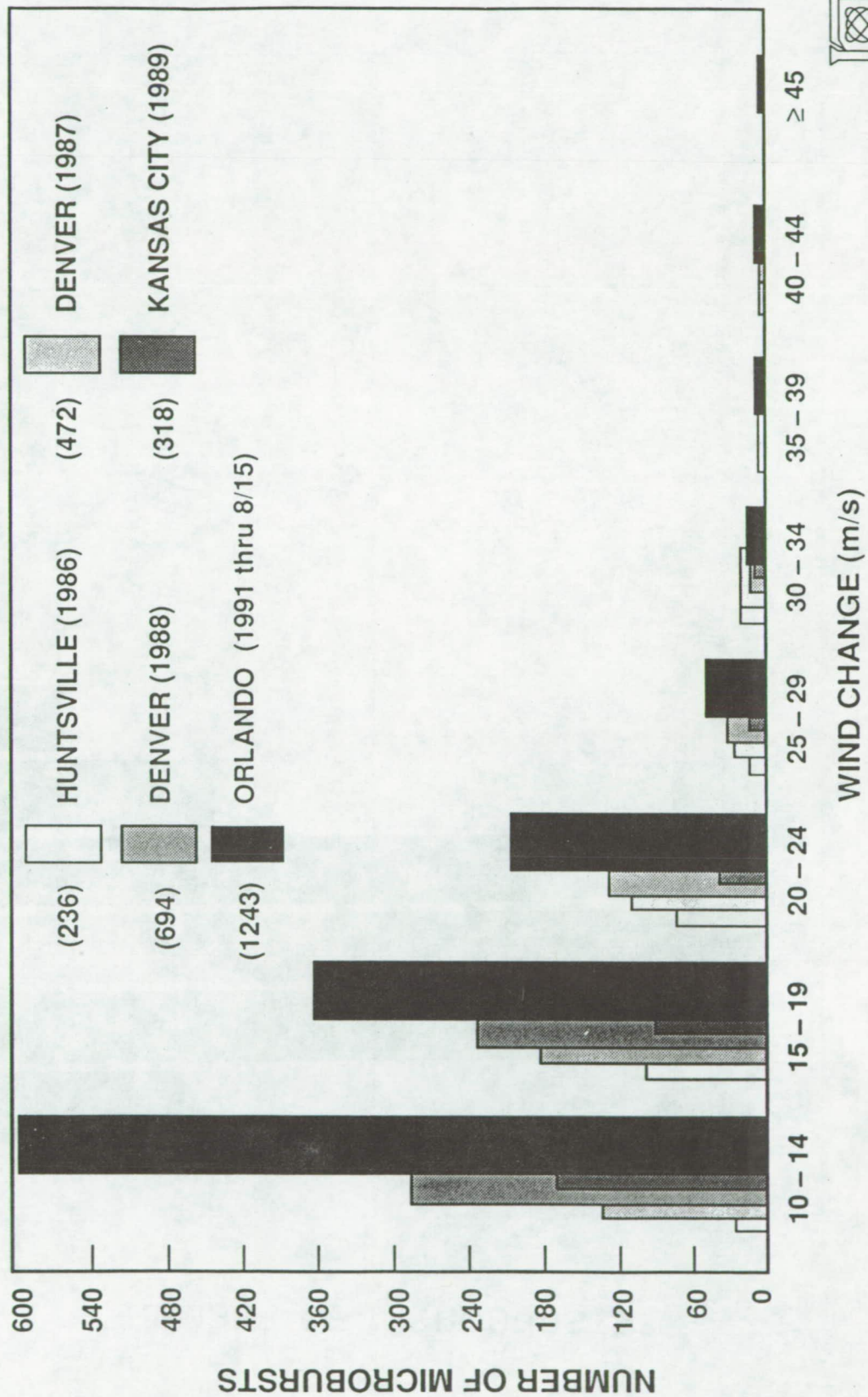
The number of microbursts detected in real time (shown in parentheses next to the bar code) varies considerably between the various locations. The Huntsville results were biased low (by a factor of approximately 2) by lack of real time automatic detection algorithm outputs. The Kansas City data reflects a year with far fewer thunderstorms than normal. Orlando was clearly the most active location with a total of over 1600 microbursts observed through October 1991.

The next three vugraphs show the observed ΔV ΔR converted the F factor estimates using the equation

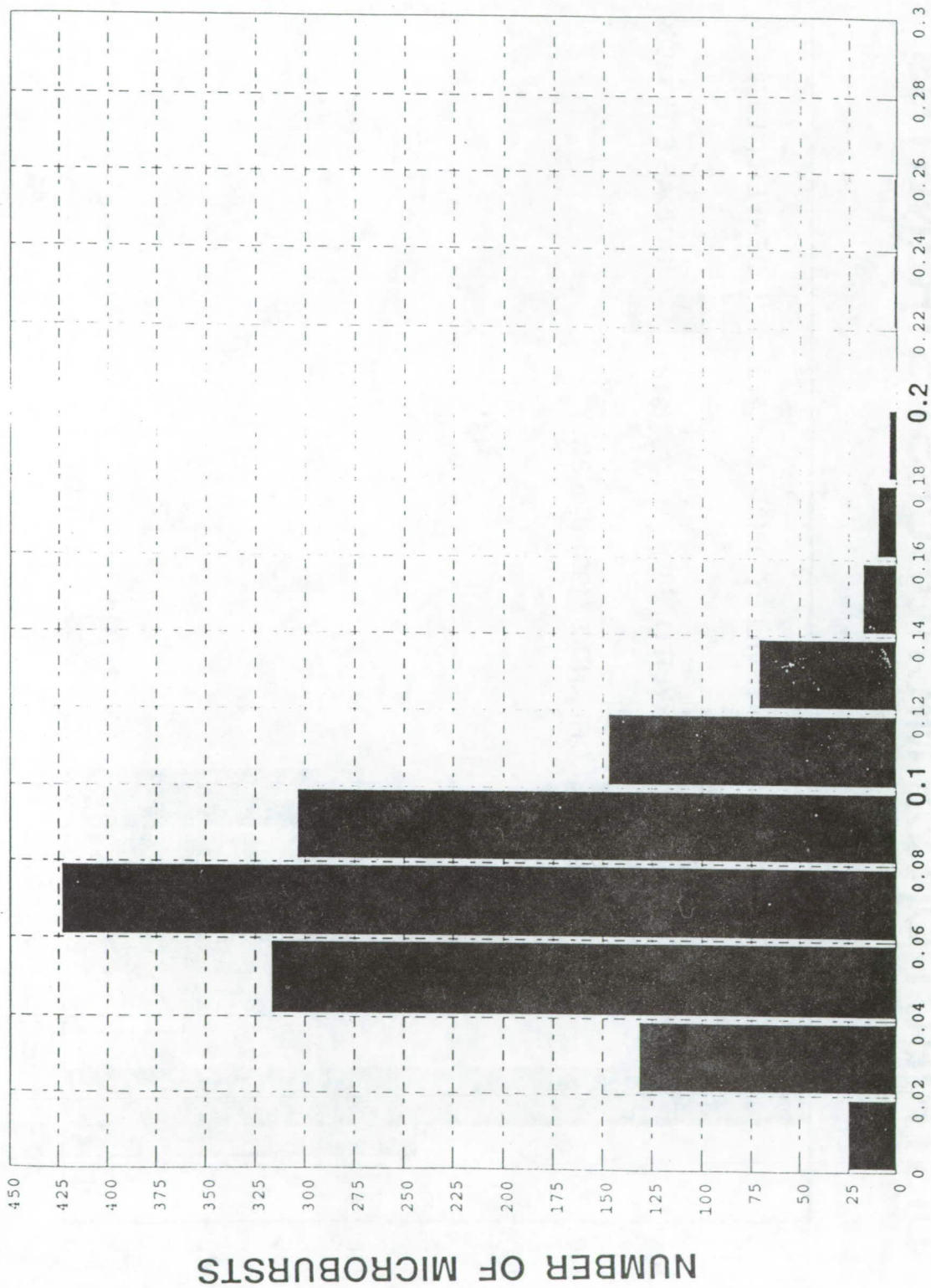
$$F = K \cdot \Delta V / \Delta R$$

corresponding to a flight at a ground speed of approximately 130 knots. We see that all locations have at least 100 such events with Orlando having over 300 such events in 1991.

DISTRIBUTION OF MICROBURST STRENGTHS

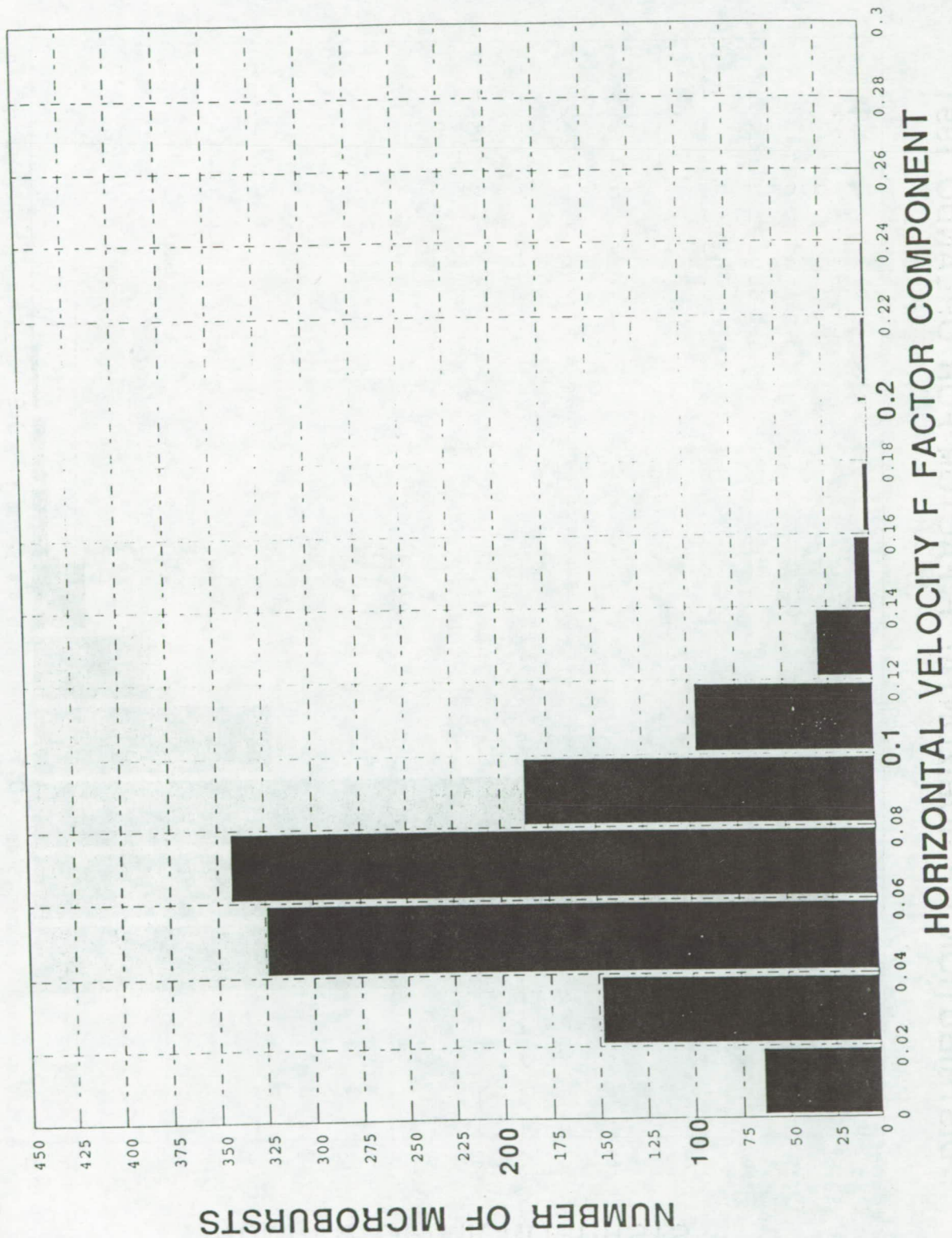


DISTRIBUTION OF HORIZONTAL F FACTOR FOR DENVER 1988
MICROBURSTS

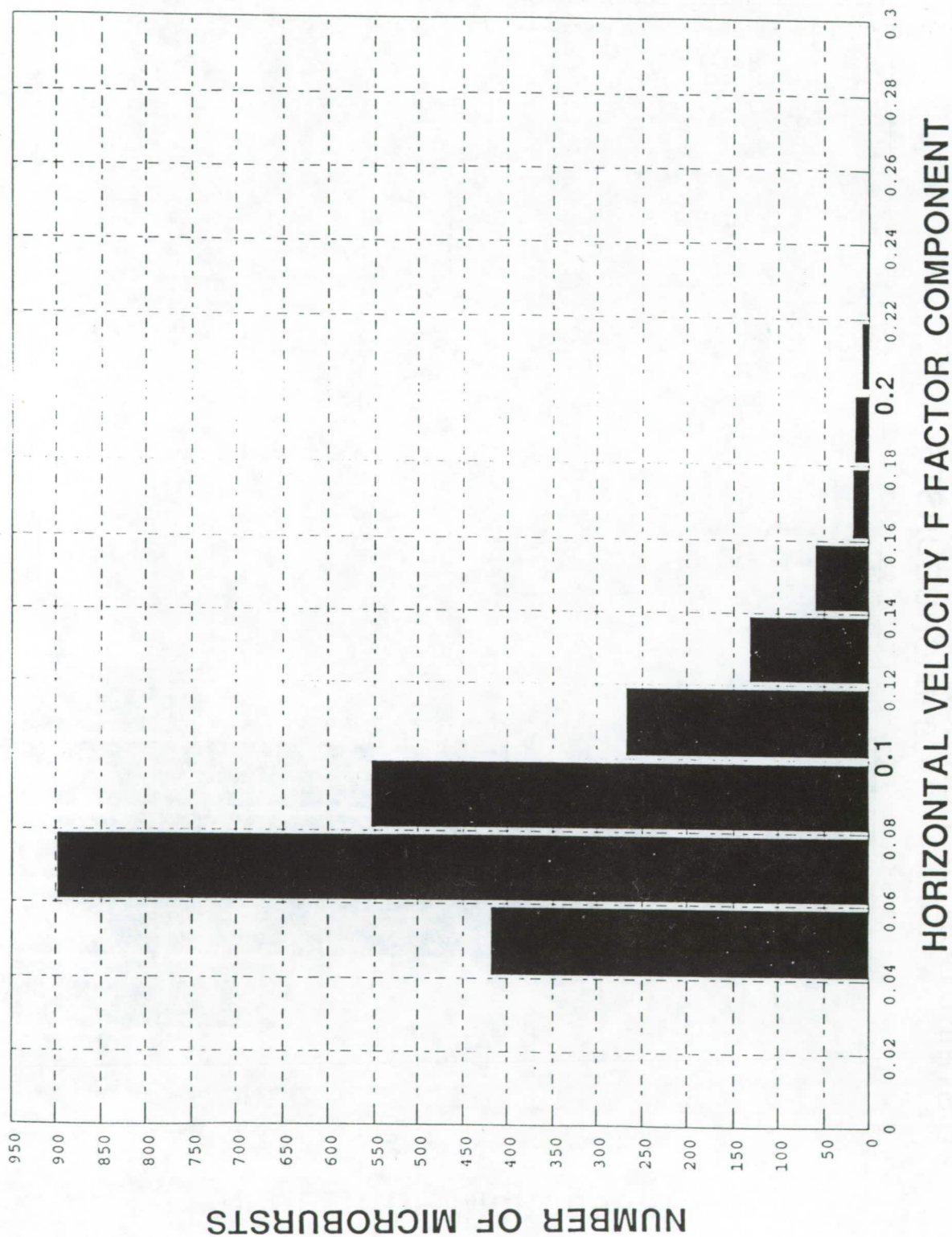


HORIZONTAL VELOCITY F FACTOR COMPONENT

DISTRIBUTION OF HORIZONTAL F FACTOR FOR KANSAS CITY 1989 MICROBURSTS



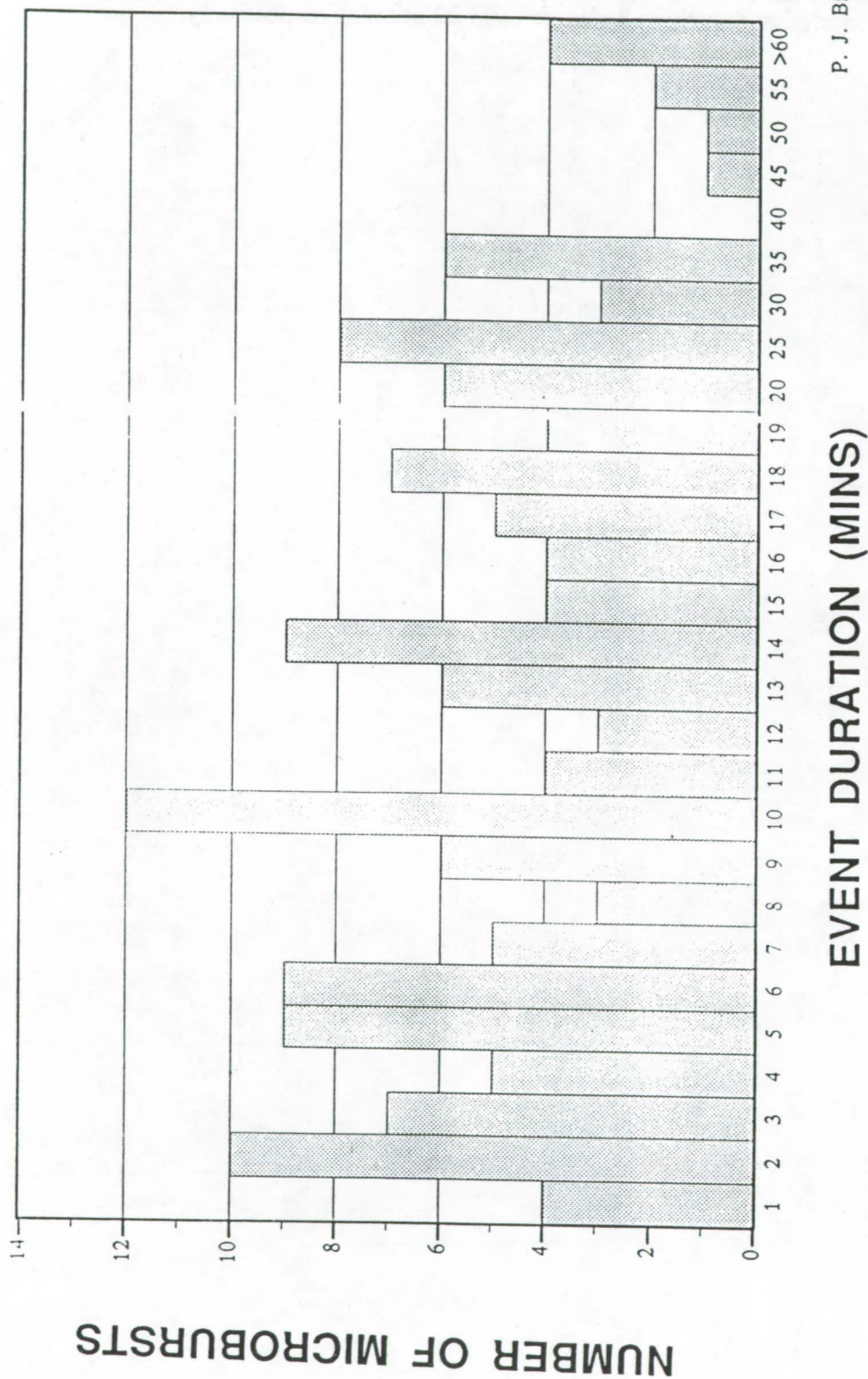
DISTRIBUTION OF HORIZONTAL F FACTOR FOR ORLANDO 1991



Vugraphs 7 - 8 "Duration of MB..."

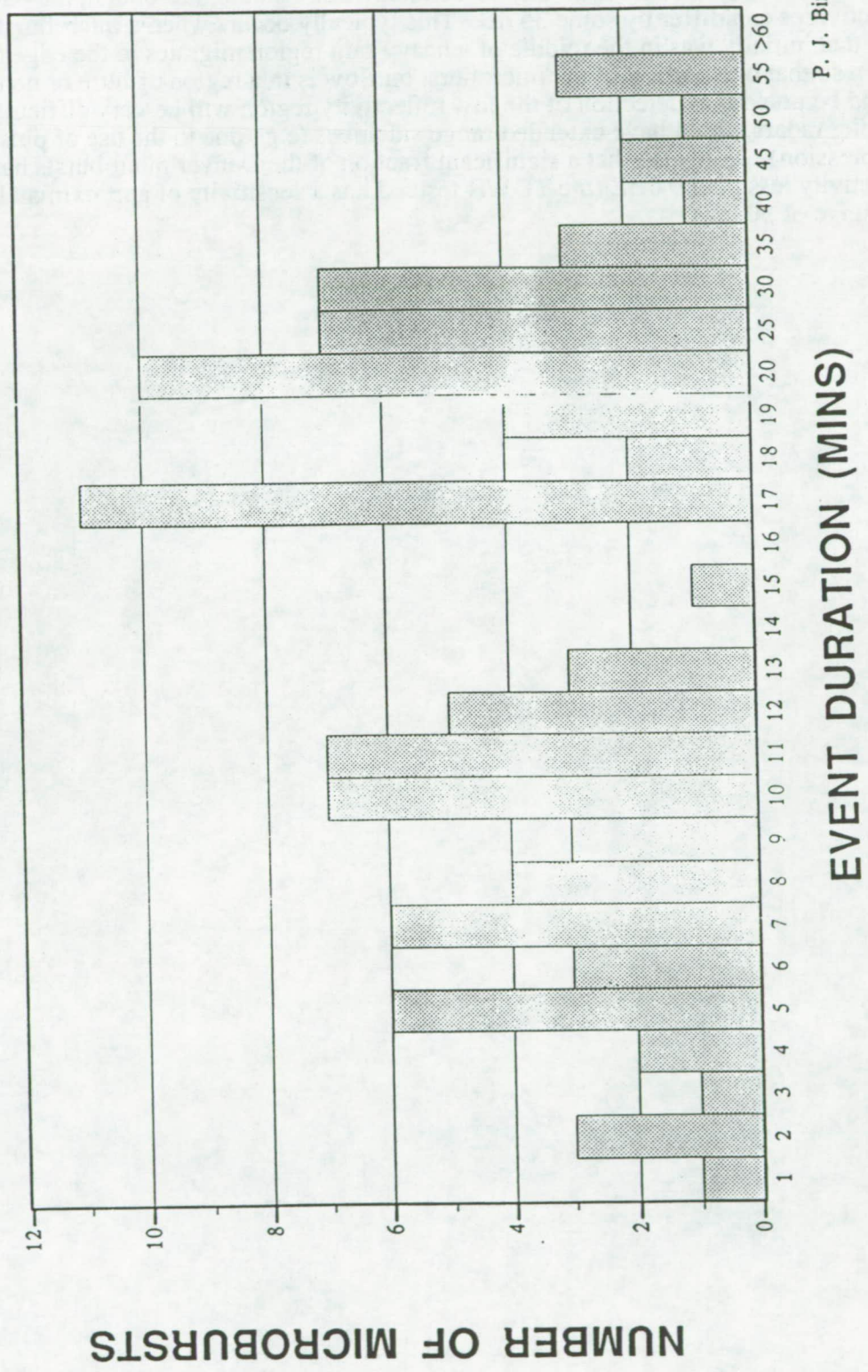
The Denver microbursts are seen to have almost an uniform distribution of duration out to 35 minutes duration. By contrast, Orlando appears to have a bimodal distribution with modes centered at durations 8 minutes and 20 minutes respectively.

DURATION OF DENVER MICROBURSTS WITH $\Delta V > 15$ M/S



P. J. Biron

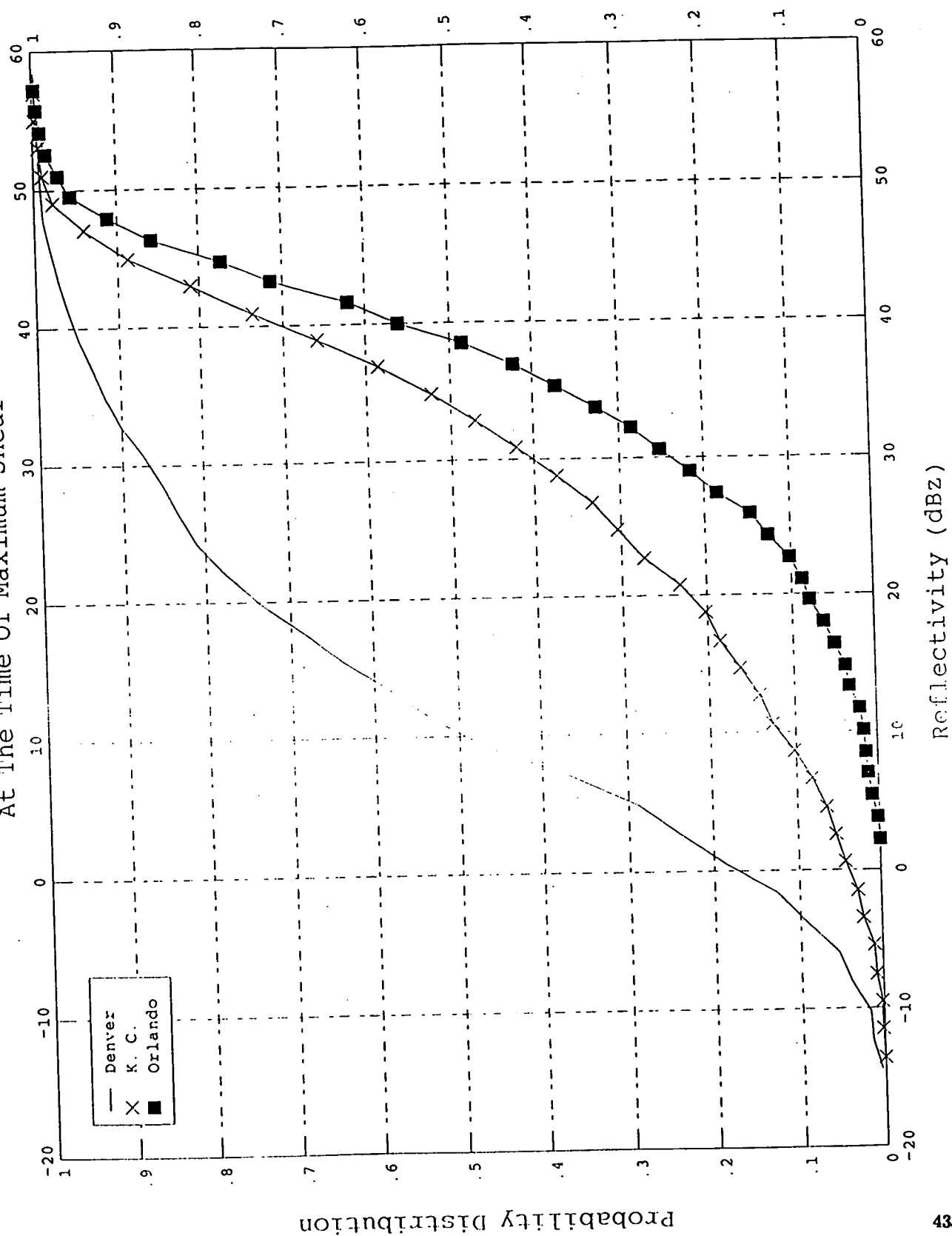
DURATION OF ORLANDO MICROBURSTS WITH $\Delta V > 15$ M/S



Vugraph #9

The range in outflow reflectivities at the velocity maxima and minima at individual locations vary 40-50 dB. Denver is seen to have a median reflectivity of 10 dBZ which is some 25 dB lower than Kansas City or Orlando. For a single microburst, the outflow reflectivities can differ by some 35 dB. This typically occurs when a microburst downdraft that initially was in the middle of a heavy rain region migrates to the edge of the rain region so that one portion of the microburst outflow is in a region of little or no rain. It should be noted that detection of the low reflectivity region will be very difficult for Doppler radars which have extended range sidelobes (e.g., due to the use of pulse compression). Note also that a significant fraction of the Denver microbursts have reflectivity less than 0 dBZ (the TDWR testbed has a sensitivity of approximately -5 dBZ at a range of 50 km).

Summer Microburst Outflow Reflectivity At The Time Of Maximum Shear



Vugraph #10 "Summer MB Maximum Reflectivity"

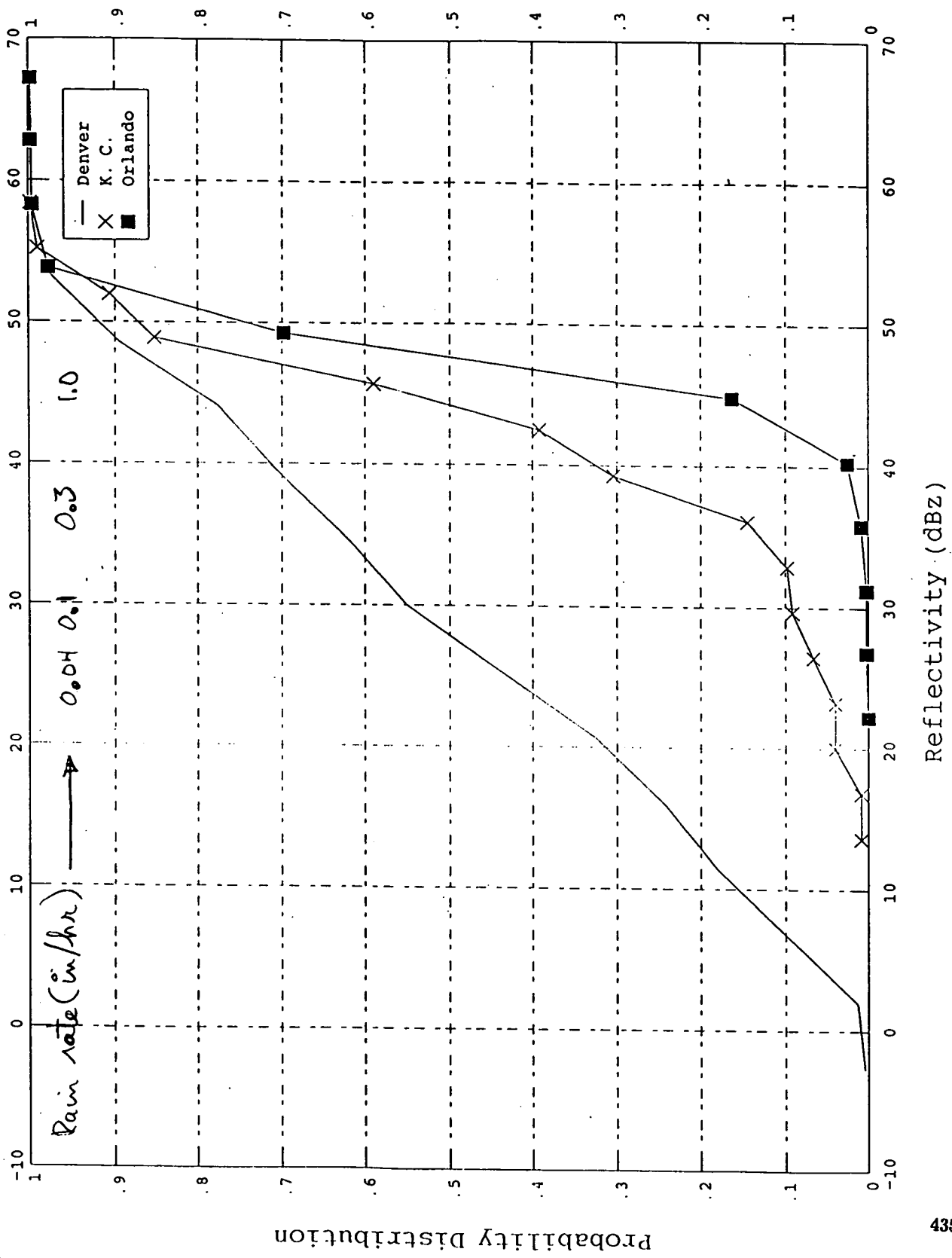
The core reflectivities are seen to be higher (e.g., by 10 - 15 dB for median levels) than the outflow reflectivities. Note also that the range of core reflectivities is much less than the outflow reflectivity. Most of the literature to date has focused on core reflectivities. Thus, although most microbursts in Orlando are very wet, (nearly all core reflectivities > 40 dBZ), over 10% of the outflows are fairly dry (< 20 dBZ).

The rain rates shown at the top of the figure were computed from the relationship

$$Z = 295 R^{1.43}$$

where R is the rainfall rate in mm/hr and Z is the reflectivity factor in mm⁶/m³. Note: the rain rates sketched in on the corresponding vugraphs during the verbal presentation were erroneously labeled as inches/hr, but were actually mm/hr. At the meeting, the threshold of rain that would raise concerns about attenuation for laser systems was stated to be about 1 inch/hour. We see that approximately half of the Orlando microbursts will have rain rates exceeding 1 inch/hour. Thus, Orlando testing will be useful in addressing the ability of laser systems to work in heavy precipitation.

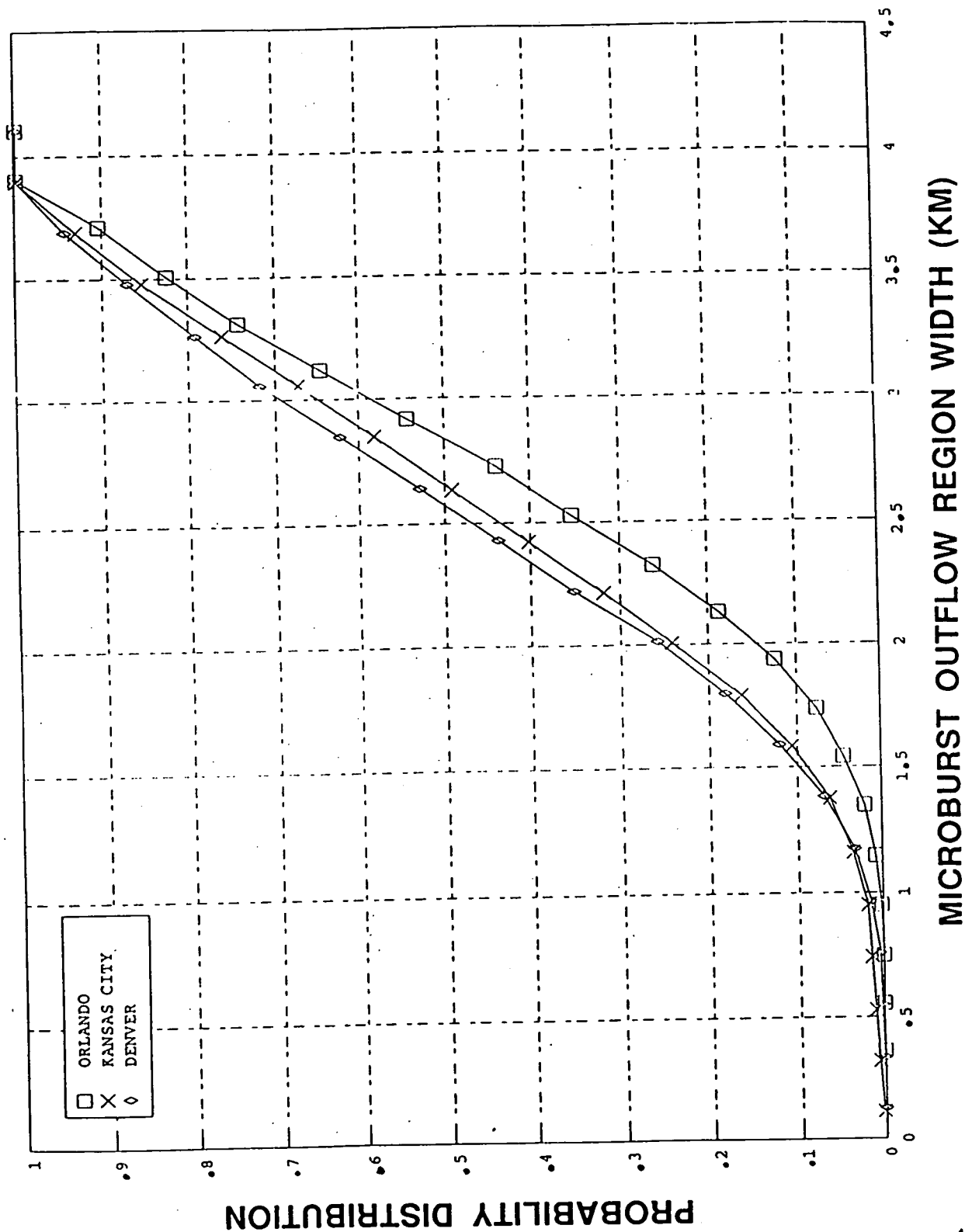
Summer Microburst Maximum Reflectivity



Vugraph #11 "MB Outflow Region Widths"

The spatial scale of microburst outflows is important for design of spatial filtering algorithms. The outflow size is seen to be quite similar with Orlando having slightly larger widths. A number of outflows are less than 1 nmi wide.

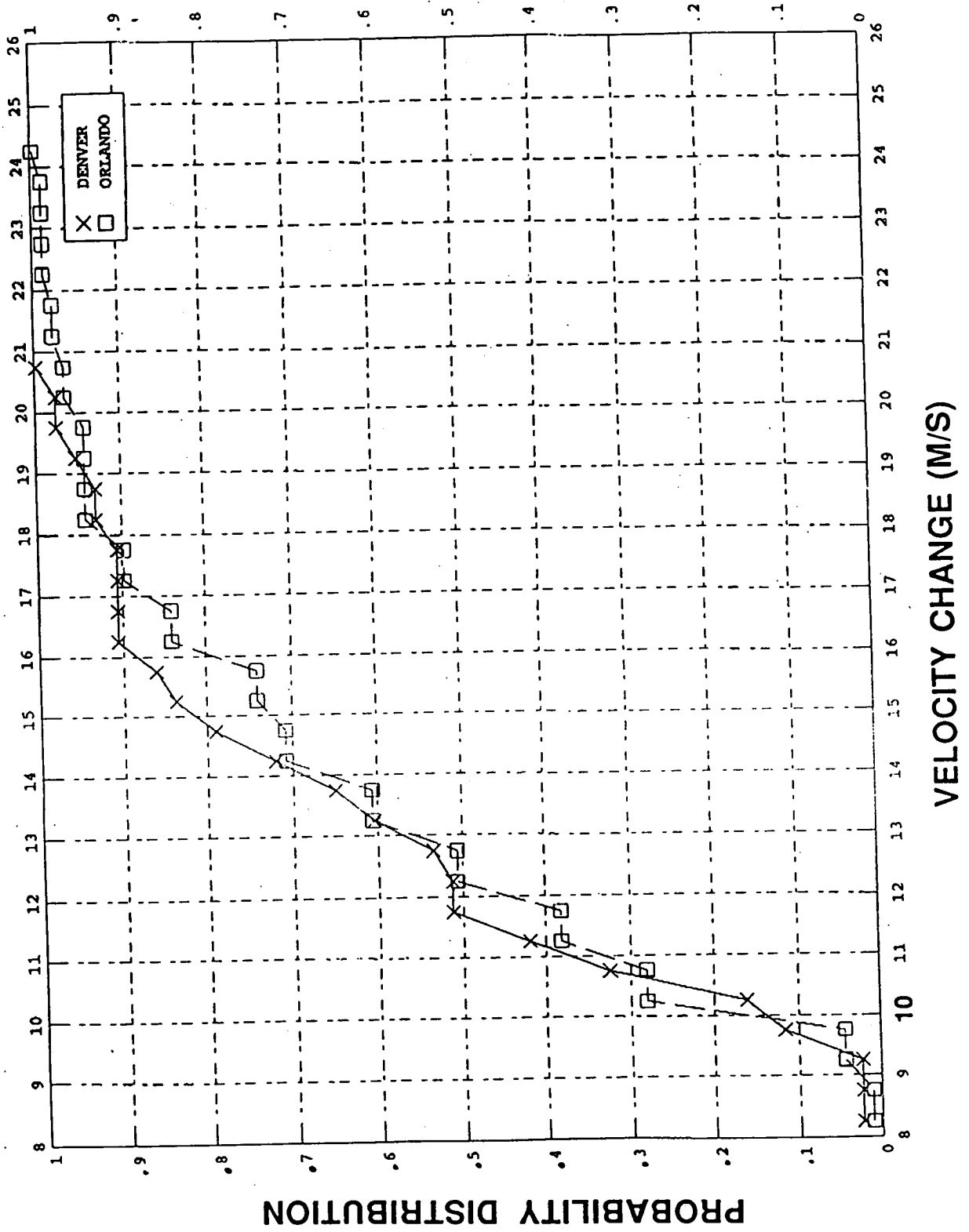
MICROBURST OUTFLOW REGION WIDTHS



Vugraph #12 "Strength Distribution...

Since small events pose a difficult detection challenge, the magnitude of the wind changes associated with these is of concern. We see that the bulk (i.e., 70%) of these correspond to a wind change of less than 30 knots. However, there are some strong (> 40 knot) small events.

STRENGTH DISTRIBUTION OF SMALL (WIDTH < 2 KM) DENVER AND ORLANDO MICROBURST EVENTS



Vugraph #13 - 15 "Vertical Structure of Orlando MB"

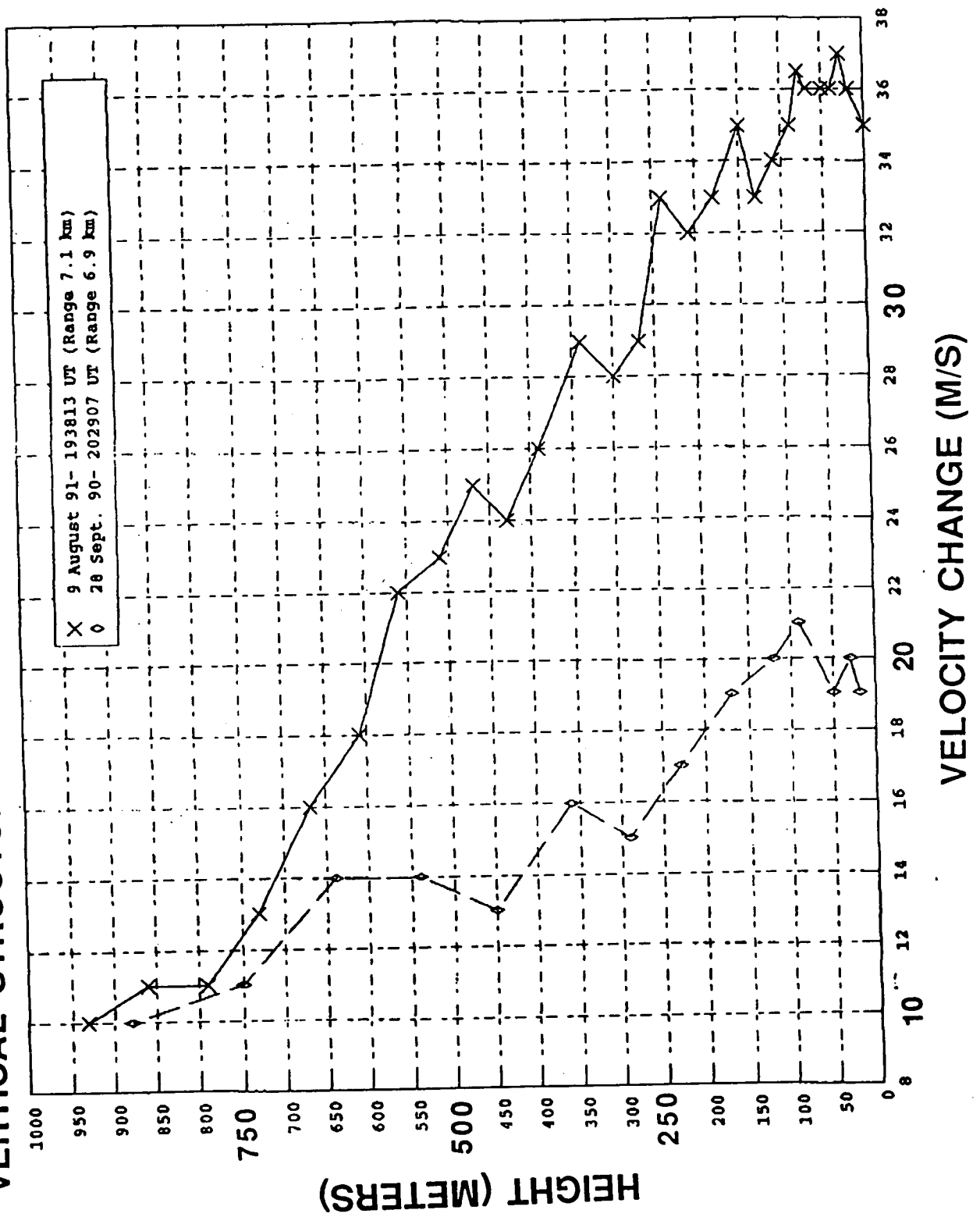
The vertical structure of microburst events is a key issue in forward looking sensor design. The bulk of the reported results on vertical profiles have been flawed by the prior vertical resolution associated with:

- 1) the use of PPI scans with relatively widely spaced elevation angles and/or
- 2) the inclusion of data from long ranges where the radar beam vertical extent is large relative to the microburst variation with height.

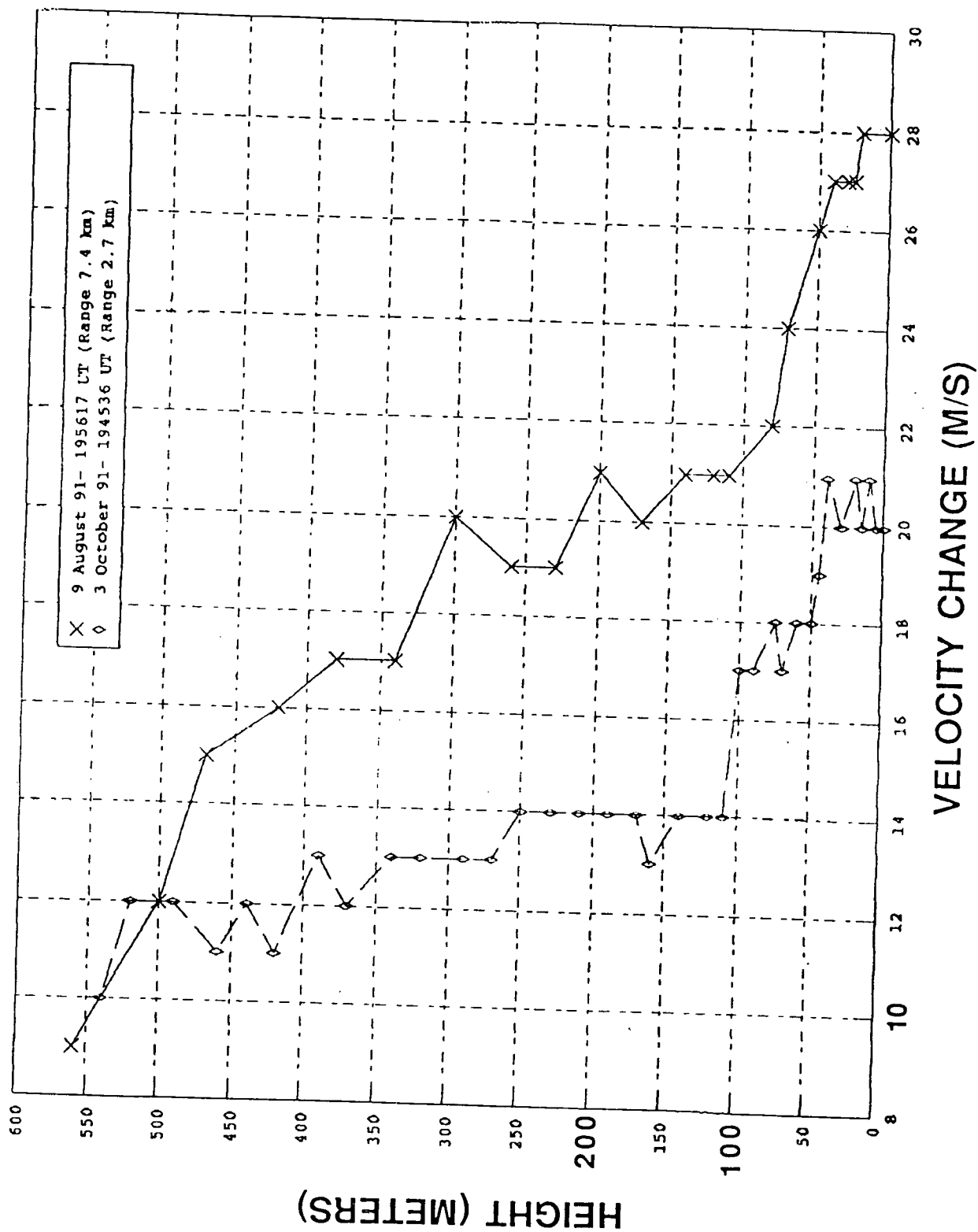
In Orlando, we are attempting to improve this situation by taking advantage of the narrow beamwidth (0.5°) of the TDWR testbed. Microbursts within 10 km (corresponding to a beamwidth vertical extent $< 80\text{m}$) are scanned using RHI scans to provide closely spaced vertical measurements.

We see a wide variation in vertical profile between events and during an individual event. The drop off in velocity from the surface to 300m AGL is about 6 knots (15-30%) for the 9 August event at 1938 GMT and for the 28 September event. By contrast, we see similar drop off between the surface and 100m AGL for the 3 October event and the 9 August event at 1956 GMT. The August 1991 events show a 33-50% drop off in velocity at 150m AGL.

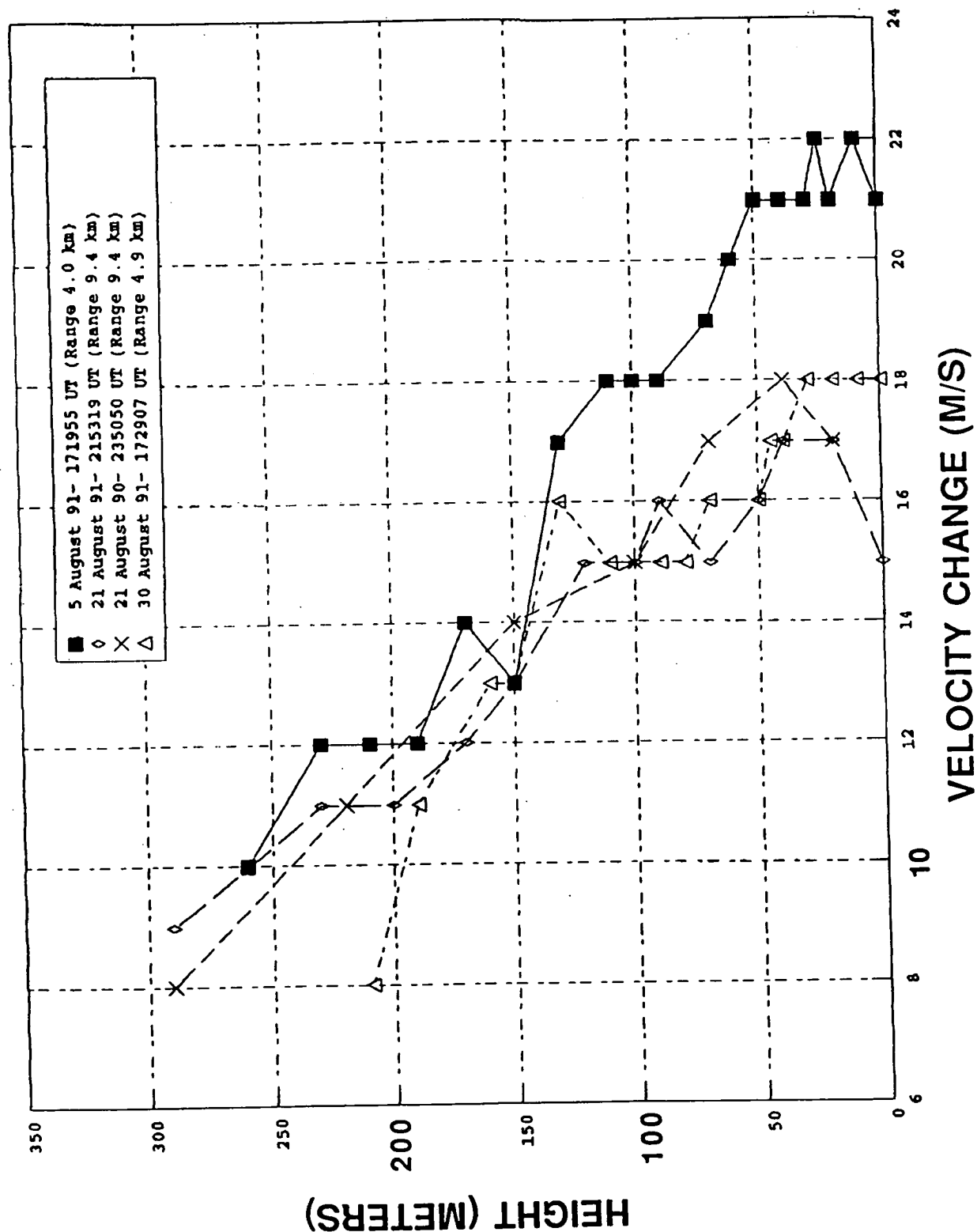
VERTICAL STRUCTURE OF ORLANDO MICROBURST OUTFLOWS



VERTICAL STRUCTURE OF ORLANDO MICROBURST OUTFLOWS



VERTICAL STRUCTURE OF ORLANDO MICROBURST OUTFLOWS

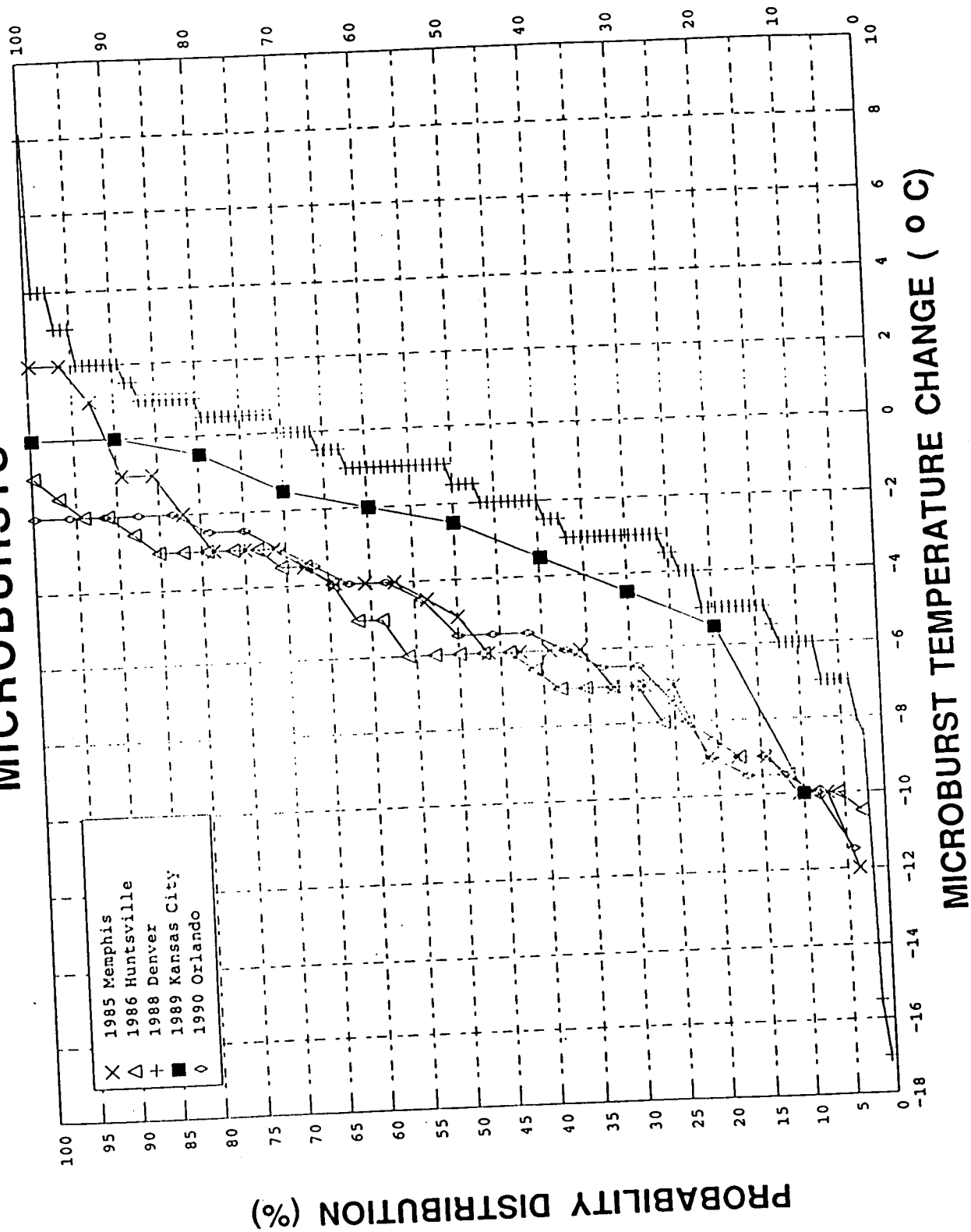


Vugraph #16 "Temperature Changes"

The surface mesonet system used with the TDWR testbed measures temperature every 7 seconds and records the 1 minute average and peak values. The figure shows the temperature changes associated with all microbursts ($\Delta V \geq 10$ m/s) which impacted the mesonet. We see that there is a wide variation in temperatures at the surface with a significant fraction of the events having temperature drops less than 2° C.

It should also be noted (see attached article by Klinge-Wilson, et al) that most gust fronts have temperature changes of -7°.

TEMPERATURE CHANGES ASSOCIATED WITH MICROBURSTS



SUMMARY

- MANY EVENTS HAVE HORIZONTAL DIVERGENCE CORRESPONDING TO $F > 0.1$ AT ALL LOCATIONS
- WIDE RANGE OF REFLECTIVITIES WITHIN INDIVIDUAL MICROBURSTS AND BETWEEN DIFFERENT MICROBURSTS
- EVENTS WITH RHI SCANNING SUGGEST MOST OUTFLOW DEPTHS ARE LESS THAN 300 M AGL AND THAT COVERAGE TO 50-100 M IS HIGHLY DESIRABLE
- SIGNIFICANT FRACTION OF STRONG MICROBURSTS HAVE SMALL SIZES (< 2 KM)
- HIGH RESOLUTION TRIPLE DOPPLER ANALYSES FROM ORLANDO WILL ASSIST IN DEFINING OUTFLOW VELOCITY STRUCTURES

CHARACTERISTICS OF GUST FRONTS *

Diana Klinge-Wilson and Michael F. Donovan
Lincoln Laboratory, Massachusetts Institute of Technology
P. O. Box 73; Lexington, MA 02173

1. INTRODUCTION

A gust front is the leading edge of a thunderstorm outflow. A gust frontal passage is typically characterized by a drop in temperature, a rise in relative humidity and pressure, and an increase in wind speed and gustiness.

Gust front detection is of concern for both Terminal Doppler Weather Radar (TDWR) and Next Generation Weather Radar (NEXRAD) systems. In addition, airborne systems using radar, lidar, and infrared sensors to detect hazardous wind shears are being developed (Bowles and Hinton, 1990). The automatic detection of gust fronts is desirable in the airport terminal environment so that warnings of potentially hazardous gust front-related wind shears can be delivered to arriving and departing pilots. Information about estimated time of arrival and accompanying wind shifts can be used by an Air Traffic Control (ATC) supervisor to plan runway changes. Information on expected wind shifts and runway changes is also important for terminal capacity programs such as Terminal Air Traffic Control Automation (TATCA; Spencer, *et al.*, 1989) and wake vortex advisory systems.

In addition, the convergence associated with gust fronts is often a factor in thunderstorm initiation and intensification. Knowledge of gust front locations, strengths, and movement can aid forecasters with thunderstorm predictions.

Current gust front detection systems generally are reliable in that the probability of false alarms is low. However the probability of detecting gust fronts with these systems is less than desired (Evans, 1990). Improved characterization of gust fronts is a key element in improving detection capability.

Typically, the basic products from the algorithms are the location of the gust front (for hazard assessment) and its propagation characteristics (for forecasting). This paper discusses the thermodynamic and radar characteristics of gust fronts from three climatic regimes, highlighting regional differences and similarities of gust fronts. It also compares propagation speeds, estimated by two techniques, to measured propagation speeds.

2. DATA AND METHODOLOGY

Measurements made as a part of the Federal Aviation Administration (FAA) TDWR operational demonstrations held in Denver, CO (1988); Kansas City, MO (1989); and Orlando, FL (1990) are used to characterize gust fronts. To support the operational demonstrations, a 30- to 40-station mesoscale network (mesonet) of automatic weather stations, with an average inter-station spacing of 1.4 - 2.1 km, was sited at each airport to measure surface winds, temperature, relative humidity, pressure, and rainfall amounts every minute (Wolfson, 1989). Only gust fronts that passed through the mesonet were considered in this study.

The requirement that a gust front pass over the mesonet limited the number of gust fronts available for analysis. Ten Denver, nine Kansas City and 13 Orlando gust fronts were chosen. Mesonet data were used to determine the surface thermodynamic and kinematic characteristics of gust fronts, while reflectivity thin line characteristics were derived from the TDWR testbed radar (FL-2). Wolfson, *et al.* (1990) present statistics on gust front strength, length, duration, propagation, depth, and temperature difference between the ambient and outflow air. This paper extends that analysis by characterizing the thermodynamic structure and radar reflectivity thin line signatures of gust fronts from the different climatic regimes.

Gust front temperature and relative humidity were taken from the mesonet data. Figure 1 shows a time series

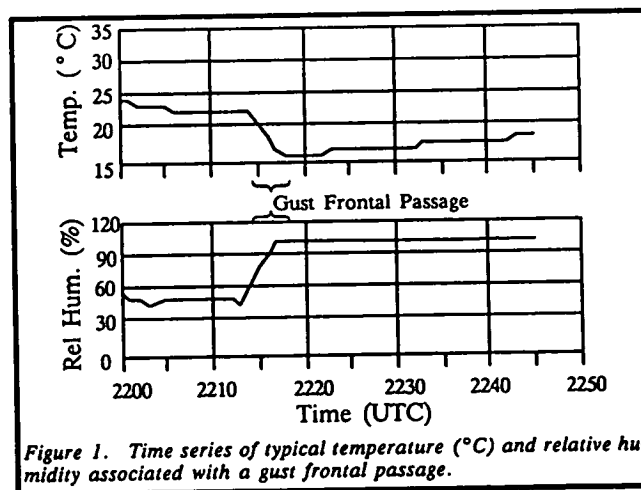


Figure 1. Time series of typical temperature (°C) and relative humidity associated with a gust frontal passage.

plot of the typical temperature and relative humidity associated with a gust frontal passage over a mesonet station. The sharp decrease in temperature and rise in relative humidity at 2215 UTC mark the passage of the gust front. For

*The work described here was sponsored by the Federal Aviation Administration. The United States Government assumes no liability for its content or use thereof.

this gust front, the ambient temperature was 23°C, the outflow temperature was 18°C, and the temperature difference was 5°C. The ambient relative humidity was 50%, the outflow relative humidity was 100%, and the relative humidity difference was 50%. These data were tabulated for each station that experienced the passage of a gust front. The data were then averaged to derive characteristic temperatures and humidities for each gust front.

Gust front propagation speeds and reflectivity thin line characteristics were derived from single-Doppler radar data. The average and peak reflectivities, as well as the average reflectivity ahead of and behind the thin line, were extracted from each gust front event that exhibited a thin line. An event is a single observation of a gust front on a radar volume scan as determined by subjective analysis. Thus, a single gust front scanned five times by the radar would result in five gust front events.

3. GUST FRONT CHARACTERISTICS

Figure 2 provides the distribution of some temperature and relative humidity characteristics of Denver, Kansas City, and Orlando gust fronts. Negative temperature differences indicate that the outflow air was cooler than the ambient air. Averages computed from these data are presented in Table 1. For one Kansas City gust front the outflow was slightly warmer and less moist than the ambient air.

Table 1. Averages of maximum outflow temperature ($\max \bar{T}_{gf}$), minimum outflow temperature ($\min \bar{T}_{gf}$), outflow temperature (\bar{T}_{gf}), ambient temperature (\bar{T}_{amb}), ambient-outflow temperature difference ($\Delta \bar{T}$), maximum outflow relative humidity ($\max \bar{RH}_{gf}$), minimum outflow relative humidity ($\min \bar{RH}_{gf}$), outflow relative humidity (\bar{RH}_{gf}), ambient relative humidity (\bar{RH}_{amb}), and outflow-ambient relative humidity difference ($\Delta \bar{RH}$). Temperatures are in °C and relative humidities are in percent.

	Denver	Kansas City	Orlando	All
$\max \bar{T}_{gf}$ (°C)	30	27	29	30
$\min \bar{T}_{gf}$ (°C)	18	14	20	14
\bar{T}_{gf} (°C)	24	21	25	23
\bar{T}_{amb} (°C)	29	25	32	29
$\Delta \bar{T}$ (°C)	-5	-4	-7	-6
$\max \bar{RH}_{gf}$ (%)	82	100	100	100
$\min \bar{RH}_{gf}$ (%)	23	53	65	23
\bar{RH}_{gf} (%)	50	86	84	74
\bar{RH}_{amb} (%)	30	74	58	54
$\Delta \bar{RH}$ (%)	20	12	26	20

Kansas City outflows exhibit the greatest range in outflow temperatures (13°C), followed by Denver and then Orlando. Kansas City average ambient and average outflow

temperatures are colder than Denver and Orlando temperatures, but the average temperature difference between the outflow and ambient air is smallest in Kansas City.

The relative humidity data show that outflows are driest in Denver. On average, the largest difference in ambient-outflow relative humidity is associated with Orlando, followed by Denver and Kansas City.

Outflows from thunderstorms have been shown to be dynamically similar to density currents (Charba, 1974). A density (gravity) current is generated whenever a fluid of greater density moves through a fluid of lesser density. The motive force of the gravity current is the hydrostatic pressure difference between the two fluids. Equation 1 expresses gust front propagation speed in terms of the depth of the outflow head and the difference in virtual temperature between the warm and cold air (Seitter, 1983). This equation

$$V = k' \left[gH \frac{\Delta T_v}{T_v} \right]^{1/2} \quad (\text{Eqn. 1})$$

where:

- V = gust front propagation speed
- k' = redefined Froude number ($'1$)
- g = acceleration of gravity
- H = depth of gust front head
- ΔT_v = difference in virtual temperature between warm and cold air
- T_v = virtual temperature of the warm air.

was used to estimate the propagation speed of the Denver, Kansas City, and Orlando gust fronts for comparison to measured propagation speeds, as deduced from radar data. Head depth was estimated from radar data and virtual temperature was estimated from temperature and relative humidity. The comparison of propagation speeds computed from Seitter's technique and measured propagation speeds is given in Figure 3. In two Denver and three Kansas City cases, the gust fronts did not propagate away from the leading edge of the parent storm and outflow depth could not be estimated. These gust fronts are not represented in Figure 3.

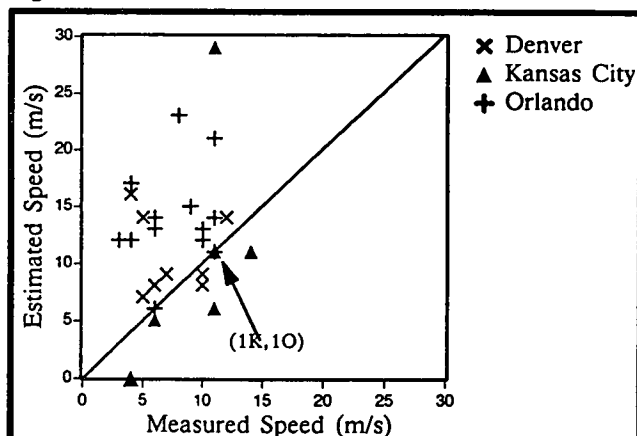


Figure 3. Estimated versus measured gust front propagation speed. Estimated values were computed from Seitter's technique. In cases where data points overlap, the numbers of points for each location (D: Denver, K: Kansas City, O: Orlando) are shown in parentheses.

GUST FRONT THERMODYNAMIC CHARACTERISTICS

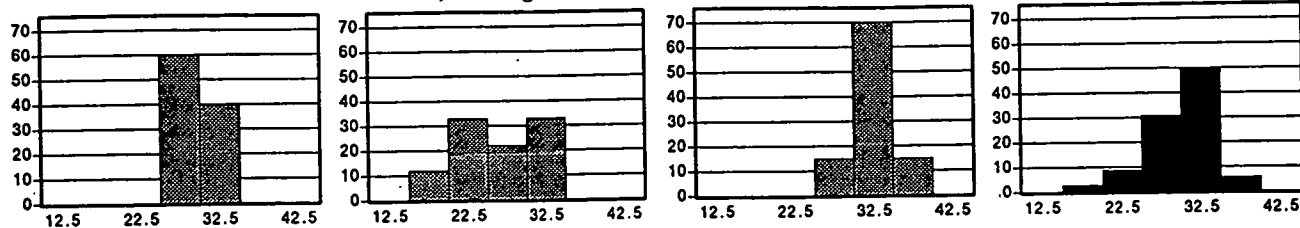
Denver 1988

Kansas City 1989

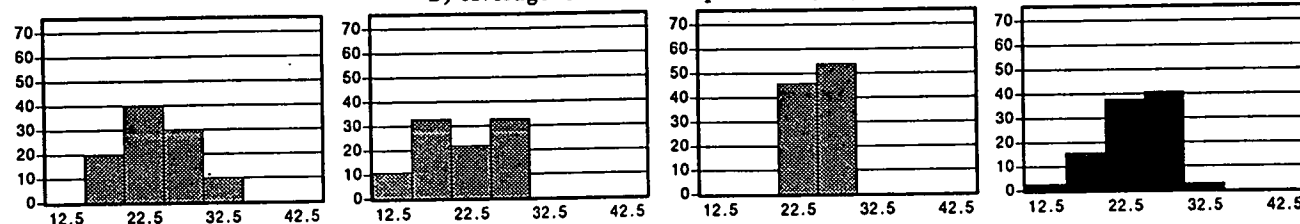
Orlando 1990

ALL

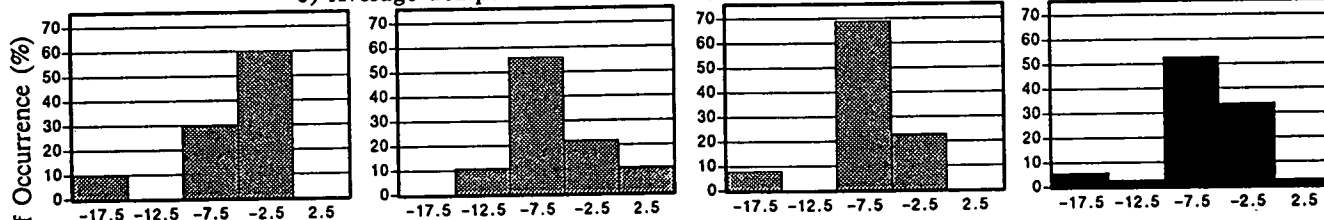
a) Average Ambient Temperature ($^{\circ}\text{C}$)



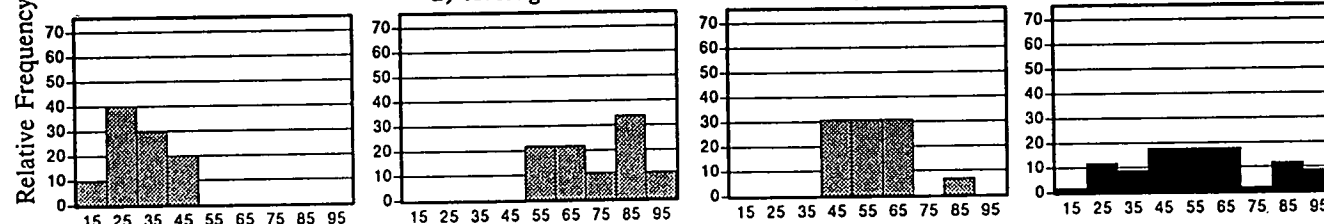
b) Average Outflow Temperature ($^{\circ}\text{C}$)



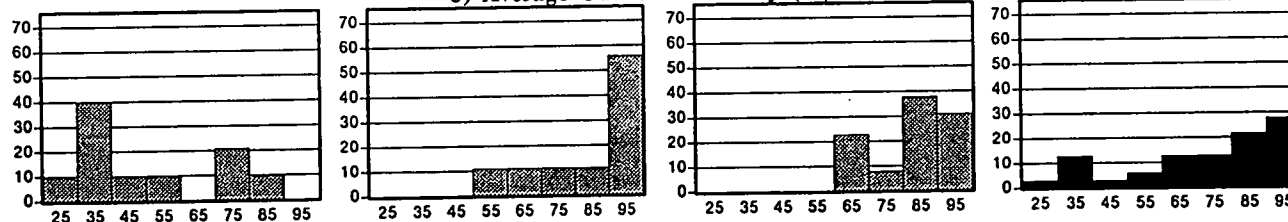
c) Average Temperature Difference ($^{\circ}\text{C}$) (outflow minus ambient)



d) Average Ambient Relative Humidity (%)



e) Average Outflow Humidity (%)



f) Average Relative Humidity Difference (%) (outflow minus ambient)

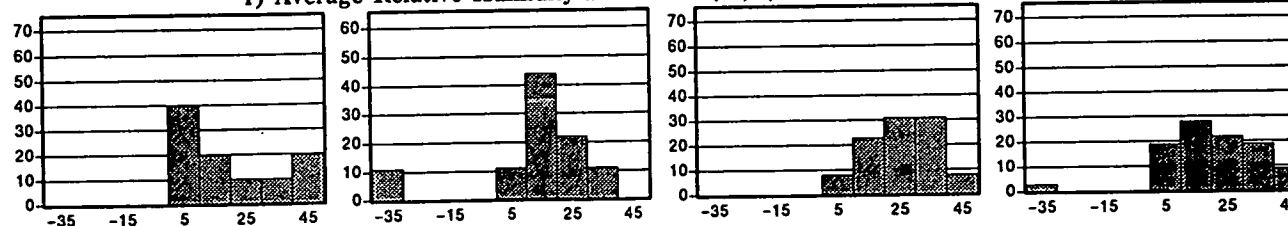
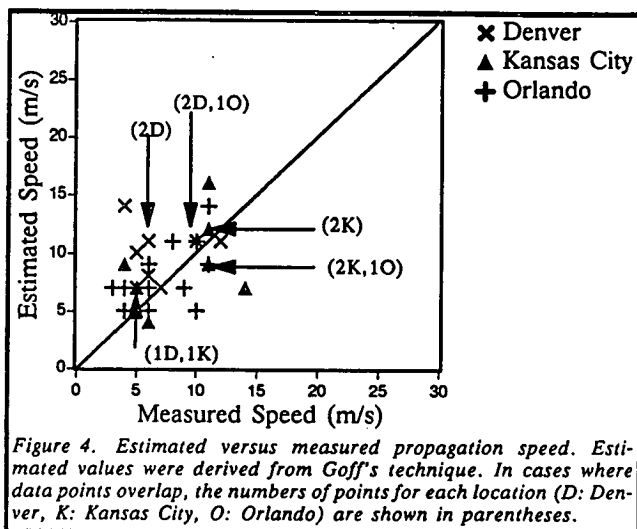


Figure 2. Relative frequency (%) of the average (a) ambient temperature ($^{\circ}\text{C}$); (b) outflow temperature ($^{\circ}\text{C}$); (c) temperature difference ($^{\circ}\text{C}$) between the outflow and ambient air; (d) ambient relative humidity (%); (e) outflow relative humidity (%); and (f) relative humidity difference (%) between the outflow and ambient air. The values on the abscissa are the midpoints of the interval.

Goff (1976) found that propagation speed was roughly 67% of the maximum wind speed in the outflow. This estimate of propagation speed is compared to the measured speeds in Figure 4.



Propagation speed is generally overestimated using Seitter's technique, although the estimated speeds for Kansas City gust fronts were less than the measured values. Goff's technique also tends to overestimate propagation speed, but to a lesser degree than Seitter's technique. The average differences and average absolute differences between the measured and estimated speeds are given in Table 2. The two techniques provide about the same performance for Denver gust fronts, but Goff's estimate is better for Kansas City, Orlando, and over all.

Table 2. Average and average absolute differences between estimated and measured propagation speed for Denver, Kansas City, Orlando, and All locations.

Location	Average Difference	Average Absolute Difference
Seitter's Technique		
Denver	3.3	4.0
Kansas City	0.8	5.2
Orlando	6.3	6.3
All	4.2	5.4
Goff's Technique		
Denver	3.0	3.2
Kansas City	0.1	3.0
Orlando	0.8	2.4
All	1.3	2.8

Figure 5 shows gust front duration, propagation speed and outflow depth as functions of the ambient-out-

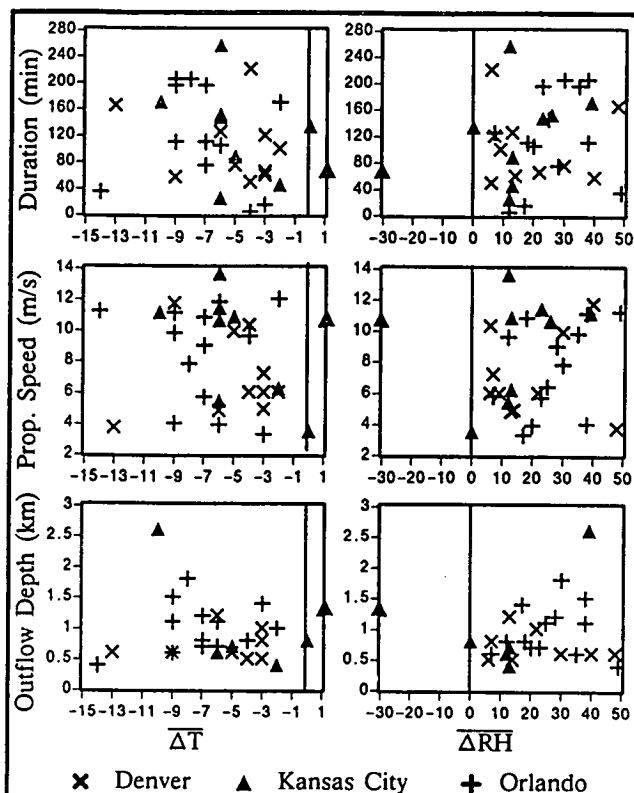


Figure 5. Gust front duration, propagation speed, and outflow depth as functions of the average ambient-outflow temperature difference (ΔT) and relative humidity difference (ΔRH).

flow temperature and relative humidity differences for gust fronts at the three sites. Since the gust front motive force is the hydrostatic pressure difference between the outflow and ambient air, one would expect those outflows exhibiting the largest temperature differences to move fastest and last longest. The data do not support this expectation, possibly because the velocity of the opposing ambient flow is not considered. In addition, gust front strength is determined from Doppler velocities. Since the radar senses only the along-the-beam component of the flow, strength estimates may be incorrect.

Reflectivity data from gust front events is provided in Figure 6. For detection algorithms, it is important to know not only the reflectivity characteristics of the thin line, but also the reflectivity characteristics of the air on either side of the thin line. For this reason, reflectivities ahead of and behind the gust front are given. Mean values for the measured variables are shown in the upper right corner of each plot. There appears to be no strong regional influence on the peak and average reflectivities in the thin line or in the average reflectivity behind the thin line (i.e., in the cold air). However, the reflectivities of the air ahead of the thin line (i.e., in the warm air) are lower in Denver (-7 dBZ) than in Kansas City (-4 dBZ) and Orlando (-3 dBZ), although these differences are small. If the thin line is visualized as a "wrinkle in a rug" then the wrinkle is higher, and therefore possibly easier to detect, in Denver.

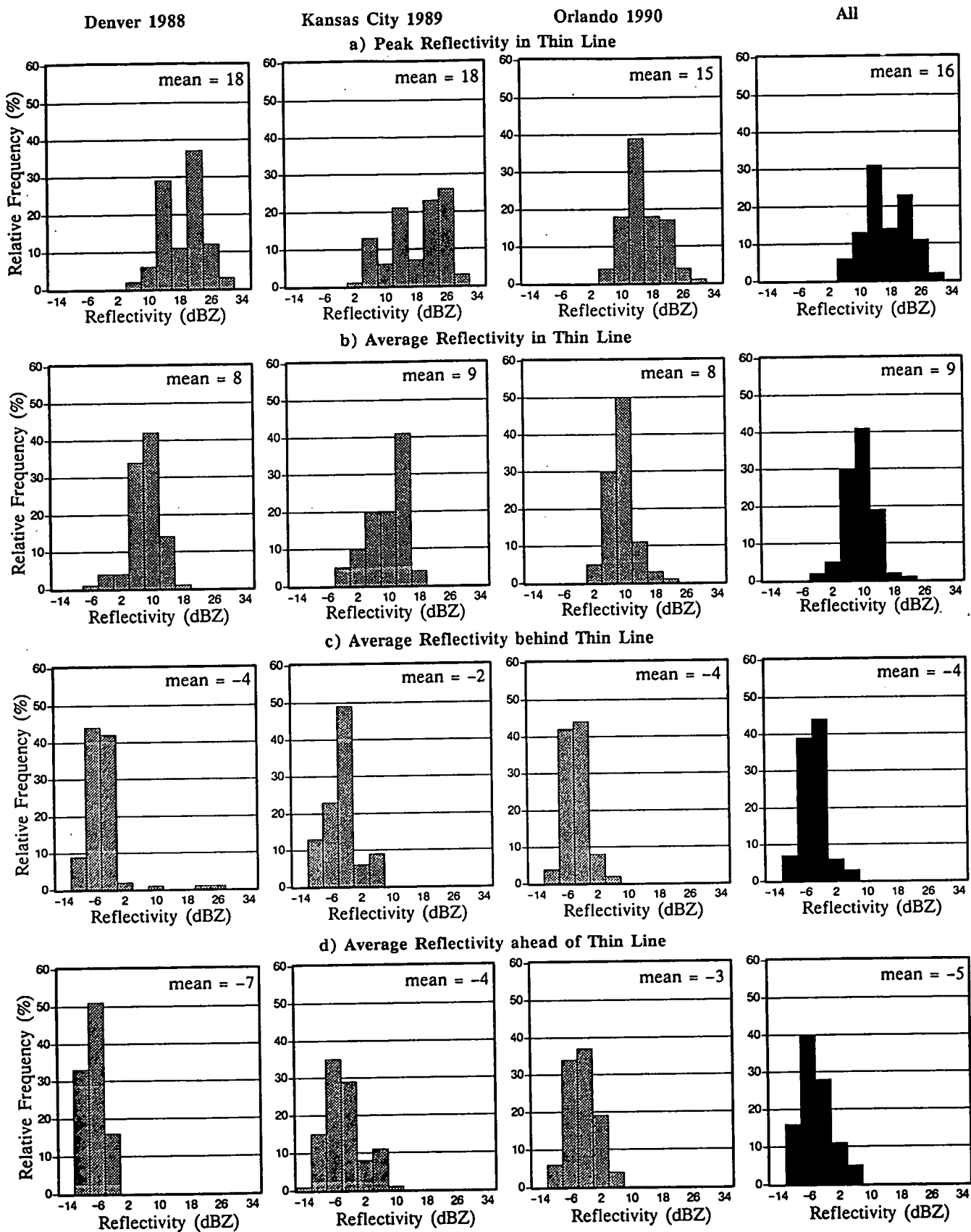


Figure 6. Reflectivity characteristics of gust fronts represented by relative frequency of events at three airports (Denver, Kansas City, and Orlando) for the measured variable. The rightmost graph in each row shows the relative frequency of the measured characteristic for all gust fronts (ALL).

4. SUMMARY

The key to detecting gust fronts is the accurate characterization of the phenomena. Some algorithms rely heavily on radar signatures of gust fronts, while others are based upon sensors that measure temperature changes across the gust front. Regardless of the sensor used to detect gust fronts, it is important to understand the differences and similarities in gust fronts over a variety of climatic regimes.

This paper has shown for the cases studied here that Kansas City outflows are colder than Denver and Orlando outflows; and that Denver outflows are driest. However, the ambient-outflow temperature and relative humidity differences are greatest in Orlando.

Two techniques were used to estimate gust front propagation speed. Seitter's method, which used virtual temperature and outflow head depth, overestimated propagation speed. Goff's method also overestimated propagation speed, but to a lesser degree.

Reflectivity thin lines were also analyzed. The values of reflectivity in the thin lines showed no regional bias. However, the reflectivity of the ambient air was lowest in Denver, which may make Denver thin lines easier to detect.

5. REFERENCES

- Bowles, R. L. and D. A. Hinton, 1990: Windshear detection: airborne system perspective, Windshear - One Day Conference, London, England, 1 November 1990.
- Biron, P.J., and M.A. Isaminger, 1989: An analysis of microburst characteristics related to automatic detection from Huntsville, AL and Denver, CO. Preprints, *24th Conference on Radar Meteorology*, Tallahassee, Amer. Meteor. Soc., 269-273.
- Charba, J., 1974: Application of g-current model applied to analysis of squall-line gust front, *Mon. Wea. Rev.*, **102**, pp. 140-156.
- Evans, J. and D. Turnbull, 1990: Development of an automated wind-shear detection system using Doppler weather radar. *IEEE Proceedings*, **77**, 1661-1673.
- Evans, J.(ed.), 1990: Results of the Kansas City 1989 Terminal Doppler Weather Radar (TDWR) Operational Evaluation Testing, DOT/FAA/NR-90/1 (ATC-171), 78 pp.
- Goff, R. C., 1974: Vertical Structure of Thunderstorm Outflows, *Mon. Wea. Rev.*, **104**, pp. 1429-1440.
- Merritt, M.W., D.L. Klinge-Wilson, and S.D. Campbell, 1989: Wind shear detection with pencil beam radars. *The Lincoln Laboratory Journal*, **2**, 483-510.
- Seitter, K. L., 1983: Numerical simulation of thunderstorm gust fronts, Air Force Geophysics Laboratory Rept. No. AFGL-TR-83-0329, Envir. Res. Paper No. 862, 34 pp.
- Spencer, D. A., J. W. Andrews and J. D. Welch, 1989: An Experimental Examination of the Benefits of Improved Terminal Air Traffic Control Planning and Scheduling, *The Lincoln Laboratory Journal*, **V. 2, No.3**, Fall 1989, pp. 527-536.
- Wolfson, M., D. Klinge-Wilson, M. Donovan, J. Cullen, D. Neilley, M. Liepins, R. Hallowell, J. DiStefano, D. Clark, M. Isaminger, P. Biron, B. Forman, 1990: Characteristics of thunderstorm-generated low altitude wind shear: A survey based on nationwide terminal doppler weather radar testbed measurements, *Proceedings of the 29th Conf. on Decision and Control*, Honolulu, HI, pp. 682-688.
- Wolfson, M.M., 1989: The FLOWS automatic weather station network. *J. Atmos. Oceanic Technol.*, **6**, 307-326.

Microburst Characteristics Determined from 1988-91 TDWR Testbed Measurements Questions and Answers

Q: Roland Bowles (NASA Langley) - In the discussion of your vertical structure charts, for those two events, where was the event relative to the radar?

A: Jim Evans (MIT) - The top event is at a range of seven kilometers. This is scanned vertically and you can see the little x's on all the data points that are actually measured as individual measurements. In the blue event the radar range is 2.7 kilometers, and this is a half degree beam. What we have told them to do is when they see a microburst within about 7 or 8 kilometers to go into an alternative scan pattern and mix in RHI with PPI so that we get very high resolution on the outflows. We have been concerned ourselves about what altitude should we be setting our beams for the TDWR. So we have been trying to understand this whole issue of what the structures are. You have to do it at close range and the fact that we have a half degree elevation beam helps a lot. When we do RHI scanning we measured a whole bunch of angles, so they are pretty closely spaced, particularly at the bottom.

Q: Roland Bowles (NASA Langley) - There is a least one publication that came out of Lincoln that was excellent, were you published a great deal of your findings on half velocity point distribution; the altitudes at which the velocity was half peak. Do you have plans to publish, for those data that you can resolve the peak outflow, those distributions?

A: Jim Evans (MIT) - I think we probably need to put out a yearly report that takes all the ones from the preceding year and just reports them so that people in the community can use it. There is a very thick report that has data all the way up through about 1989 and maybe a little bit of 1990, and contains everything we knew about outflow structure in the vertical domain. We will continue to put out that report and we will continue to try to scan these things as best we can.

Roland Bowles (NASA Langley) - That would be valuable for people working with airborne systems.

Jim Evans (MIT) - It is an absolutely key parameter both for ground based and airborne systems.

Q: Mike Lewis (NASA Langley) - It looks like you have a lot of good data there. When talking about the summary of F-factor values, over what distance are those values taken or are they in fact variable distances?

A: Jim Evans (MIT) - The radar range is keeping track of all the microburst at least all the way out to 30 kilometers. The point I made was that if you start saying that the probability of the microburst occurring is proportional to area you find out that you tend to be weighted to long distances as opposed to short distances.

Q: Mike Lewis (NASA Langley) - Not range from the radar, but over what length were those F-factors values calculated?

A: Jim Evans (MIT) - It is simply taking the difference of the maximum and minimum velocities over whatever distance that occurred. So it is variable. That is an average shear over the outflow region. You may have localized hot spots, which Steve Campbell will talk about. That is one of the caveats and I want to emphasize that this is really a lower bound on what the F's would be if you looked over say one kilometer.

Mike Lewis (NASA Langley) - Essentially, any time you talk about F you need talk about both magnitude and length.

Jim Evans (MIT) - Yes, I understand. The advantage of this particular data is that it is a very large data base. You could take some selective events and go back and reprocess and probably work out a correction.

Q: Mike Lewis (NASA Langley) - You made some points about the core reflectivity versus the outflow reflectivity. Perhaps the message is not quite so bad for radar manufacturers trying to measure that low reflectivity area, because, while the maximum velocities would perhaps be in that outflow area the maximum shears are still in the core. That is the kind of region that we are trying to measure and trying to protect from, and that perhaps is the region of somewhat higher reflectivity.

A: Jim Evans (MIT) - Well, I think Steve will be showing some examples of where the highest shears are in his paper, which I believe is tomorrow. You can decide for yourself whether or not they are in the core.

Steve Campbell (MIT Lincoln Laboratory) - In general, is not necessarily true that the strongest shear is where the strongest reflectivity is. When Jim said cores, he meant reflectivity cores and that is not necessarily where the highest shear is.

Mike Lewis (NASA Langley) - O.K. I thought you were talking about the downdraft core.

Jim Evans (MIT) - The other thing that you have to understand is that in an awful large fraction of the events, particularly in a place like Denver, have multiple outflows bumping into each other. That is why there is asymmetry. Nobody can make an asymmetrical microburst by itself, but they tend to occur in families and that is what is ugly about the whole process.

Mike Lewis (NASA Langley) - My last point is that you mentioned a couple of times about the differences of measuring at a flight test altitude of 1000 feet versus lower altitudes. It seems to me, for the research purpose of determining if your shear detection system is measuring real shear, it is perfectly O.K. to measure at 1000 feet and confirm or deny the measurement with either In Situ measurement, or an estimate from TDWR, at the same altitude. It is not necessarily a flawed flight test to measure at a 1000 feet even if the maximum shear is at 300 feet or so, as long as you confirm your data by other 1000 feet measurements. If the shear from that confirmation equals the shear that your detector is predicting then you are doing a good job.

Jim Evans (MIT) - I guess I disagree. I think we are going beyond that. It isn't the proof that you can measure velocity, I could do it at 3000 feet. The key issue that you the airline buyer and

the air passenger ought to ask is; do I have a system that can measure the hazard where the plane has got to fly or infer it properly. That is the key issue. My point is this, if you try to point your antenna down at minus three degrees the clutter challenge goes up dramatically. You may have a system that is viable at measuring shear and velocities at 1000 feet and it is not viable at measuring down at 50 feet. That is the question I think you have to ask the system designer.

Mike Lewis (NASA Langley) - If you are talking about the clutter differences, then I agree completely.

Jim Evans (MIT) - I am talking about the clutter. Low reflectivity microburst have cross sections that are typical of what the military talks about as low observable vehicles. It is not easy to build look down shoot down fighters.

I showed some probability distributions of microbursts as a function of outflow reflectivity and some people asked about the ones that are low reflectivity events with high F values, what would be their distribution? We will try to do that. I thought maybe we could do it for the conference, but I think that is a little too much to promise. We do have it stored in a database. In principle there ought to be no problem in just putting in some more side conditions. That is one of the nice things we have been able to do by having these in a computerized database. Anyone who is interested in finding out about low reflectivity events with high Delta V's or high F-factors and want the characteristics of those, give me your business card and as soon as we get the results run off we will get it to you. We will give it to Roland as well.

Q: Branimir Dulic (Transport Canada) - Why do we think the number of events in Huntsville was underestimated?

A: Jim Evans (MIT) - It was not due to post processing. The number we showed for Huntsville was from the real-time log of microbursts. Subsequently, there was a limited replay operation where we were trying to decide if the radar missed microbursts. We compared the radar to surface wind measurements. We would pick certain days that they had found microbursts by looking at the surface wind measurements and they go back and look at the radar data. What they discovered in doing that was that we did not miss very many events, but the real-time log was missing about half the events that had been picked up in the post processing. It had missed about half of those that had come down over our mesonet, our wind sensors. So on the basis of that, I would presume that we missed about half. What happened was the humans watching the displays in real-time you will see a really strong microburst over here and they might miss another one over some other place that wasn't so distinct. That is the kind of thing that a computer does very well and humans get distracted. Because it was a careful but limited after the fact analysis that show we missed about half, I think that is probably true in general.

1993010417

488736
208

N93-19606

Session V. Doppler Related Research

Algorithms for Airborne Doppler Radar Wind Shear Detection

Jeff Gillberg, Honeywell

Mitch Pockrandt, Honeywell

Peter Symosek, Honeywell

Earl Benser, Honeywell

PRECEDING PAGE BLANK NOT FILMED

ALGORITHMS FOR AIRBORNE DOPPLER RADAR WIND SHEAR DETECTION

**Jeff Gillberg
Mitch Pockrandt
Peter Symosek
Earl T. Benser**

**Honeywell Inc.
Systems and Research Center
3660 Technology Drive
Minneapolis, Minnesota 55418**

ABSTRACT

Honeywell has developed algorithms for the detection of wind shear/microburst using airborne Doppler radar. The Honeywell algorithms use three dimensional pattern recognition techniques and the selection of an associated scanning pattern forward of the aircraft. This "volumetric scan" approach acquires reflectivity, velocity and spectral width from a three dimensional volume as opposed to the conventional use of a two dimensional azimuthal slice of data at a fixed elevation. The algorithm approach is based on detection and classification of velocity patterns which are indicative of microburst phenomenon while minimizing the false alarms due to ground clutter return. Simulation studies of microburst phenomenon and X-band radar interaction with the microburst have been performed and results of that study are presented. Algorithm performance in detection of both "wet" and "dry" microbursts is presented.

SLIDE 1

Title Slide

SLIDE 2

The development of algorithms for detection of wind shear/microburst using airborne Doppler radar is a part of a larger Honeywell effort for the development of an Enhanced Situation Awareness System (ESAS). This multifunction system will increase pilot situation awareness through provision of landing guidance in adverse weather, detection of severe weather, detection of severe weather, detection of microburst/wind shear, detection of wake vortices and clear air turbulence. This integrated system seeks to provide the above functionality with minimal impact to the aircraft and minimal requirements for additional hardware.

SLIDE 3

The Honeywell remote windshear detection research has concentrated on development of algorithms which are not based on any particular sensor technology. The algorithms

require measurements of air mass velocities that could be provided by laser doppler velocimeters, other types of laser radar as well as Doppler weather radar. The algorithm approach is based on detection and classification of velocity patterns which are indicative of microburst phenomenon while minimizing the false alarms due to ground clutter return. These algorithms have been developed and tested using the NASA-Langley Airborne Windshear Doppler Radar Simulation (AWDRS) and modeling of X-band Doppler radar characteristics.

SLIDE 4

The core of the Honeywell approach is the use of three dimensional pattern recognition techniques and the selection of an associated scanning pattern forward of the aircraft. This "volumetric scan" approach acquires reflectivity, velocity and spectral width from a three dimensional volume as opposed to the conventional use of a two dimensional azimuthal slice of data at a fixed elevation. For each volume element (voxel) in azimuth-elevation-range space the radar provides measurements of reflected power, mean velocity and spectral width. Receiver noise characteristics are measured and used to enhance the quality of the received data. Four separate types of features are then identified including regions of positive and negative divergence, regions of high reflectivity, regions of rotation and regions with similar spectral width. These regions are then collectively assessed by a three dimensional association algorithm which identifies three dimensional features which are associated clusters of the four basic feature types listed above. These three dimensional features are then compared with known attributes of microburst phenomenon and temporally tracked to identify those three dimensional features which are indications of microbursts.

SLIDE 5

These algorithms have been developed and tested using the NASA-Langley Airborne Windshear Doppler Radar Simulation (AWDRS) and modeling of X-band Doppler radar characteristics. We have modified the software for operation on our Sun workstations. It has also been modified to provide data from a simulated volumetric scan pattern and provides simulated output characteristic of that expected from nominal X-band Doppler radar using a Honeywell 12-inch flat plate antenna which produces an 8° beamwidth. We have been using the axisymmetric models developed in the past and are now upgrading the software to include the newer three dimensional models recently released.

SLIDE 6

The Honeywell approach was developed to minimize probability of false alarms at an acceptable detection capability. This is accomplished by the use of full three dimensional correlation approaches which reject those features which are characteristic of ground clutter and are not supported by measurements throughout the three dimensional scanning volume. Temporal tracking is used to assure the rejection of transient phenomenon. Additional information is also used to reduce false alarm rate including thresholding using the F-Factor hazard level, assessment of spectral width characteristics and comparison of the physical size of the hazard with known phenomenological understanding and aircraft upset requirements.

SLIDE 7

The volumetric velocity and hazard region data for a "wet" microburst (core reflectivity of 60 dBz) event is shown for three elevation scans at 0°, 20° and 40° elevations. This

data is simulated for a 1kW radar utilizing a Honeywell 12-inch antenna with a pulse repetition frequency of 6kHz and a pulse width of 1μsec. As is shown there is a large region at near ground level where significant hazard is identified. Note the extension of velocity and hazard features above in the 20° and 40° slices.

SLIDE 8

The reflectivity, Doppler velocity, intermediate data and final identified hazard region data for a "wet" microburst (core reflectivity of 60 dBz) event is shown. This data is simulated for a 1kW radar utilizing a Honeywell 12-inch antenna with a pulse repetition frequency of 6kHz and a pulse width of 1μsec. As is shown there is a large region at near ground level where significant hazard is identified. Note the rejection of spurious hazard regions surrounding the actual hazard region.

SLIDE 9

The volumetric velocity and hazard region data for a "dry" microburst (core reflectivity of 25 dBz) event is shown for three elevation scans at 0°, 20° and 40° elevations. This data is simulated for a 1kW radar utilizing a Honeywell 12-inch antenna with a pulse repetition frequency of 6kHz and a pulse width of 1μsec. As is shown there is a large amounts of clutter at near ground level. Note the extension of hazard features above in the 20° and 40° slices which eliminates most of the ground clutter as potential microbursts.

SLIDE 10

The reflectivity, Doppler velocity, intermediate data and final identified hazard region data for a "dry" microburst (core reflectivity of 25 dBz) event is shown. This data is simulated for a 1kW radar utilizing a Honeywell 12-inch antenna with a pulse repetition frequency of 6kHz and a pulse width of 1μsec. As is shown there is a large amounts of clutter at near ground level. Note the rejection of the significant level spurious hazard regions surrounding the actual hazard region

SLIDE 11

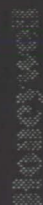
Honeywell is continuing the development of algorithms for detection of wind shear/microburst using airborne Doppler radar as well as developing data fusion approaches to utilize data provided from remote sensors as well as in-situ sensors for an overall integrated wind shear detection system. We anticipate testing of the algorithms using flight test data in 1992 and continued development of optimal guidance approaches exploiting data from remote sensors and in-situ sensors.

Algorithms for Airborne Doppler Radar Wind Shear Detection

Jeff Gillberg
Mitch Pockrandt
Peter Symosek
Earl T. Benser



Systems and Research Center
3660 Technology Drive
Minneapolis, Minnesota 55418



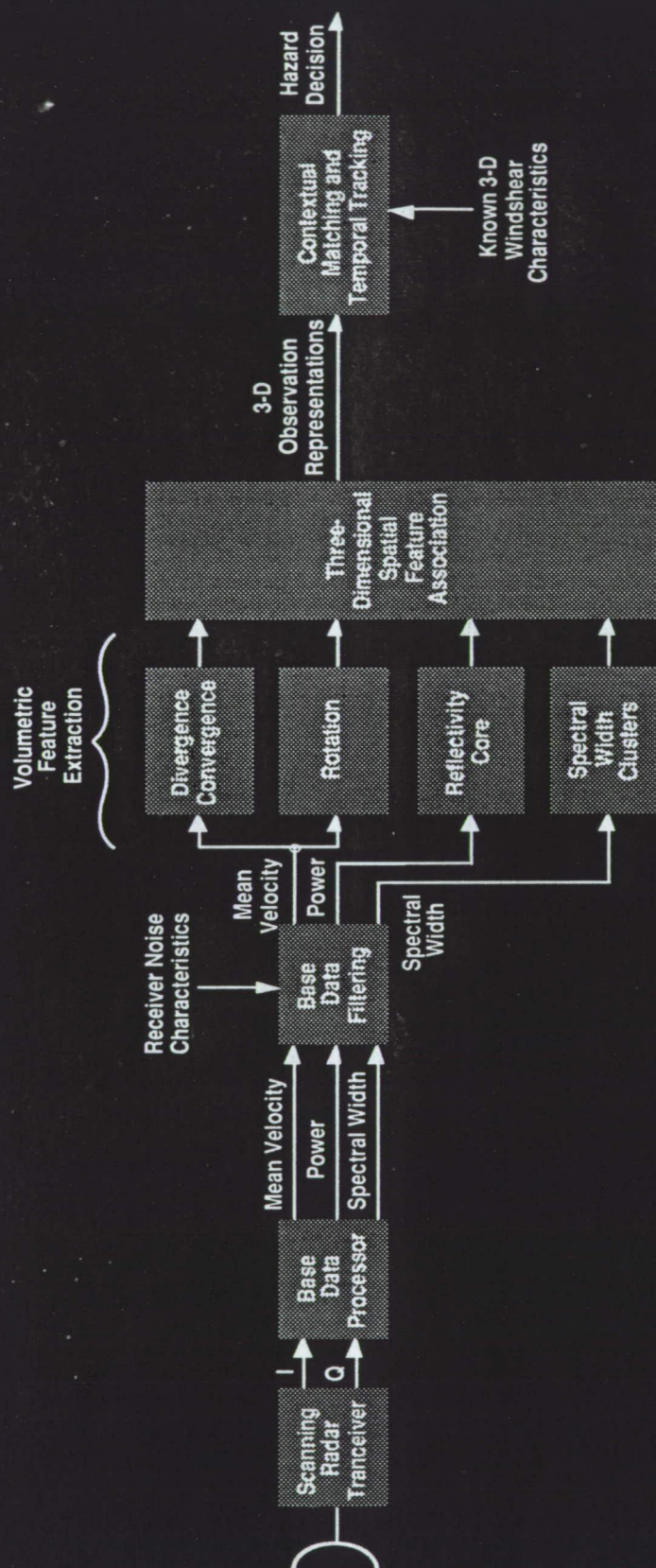
Enhanced Situation Awareness System (ESAS)

- Growing interest in ESASs for military and commercial aircraft
- ESAS required to provide situation awareness through
 - Adverse weather landing guidance
 - Detection of severe weather
 - Detection of microburst/wind shear
 - Detection of wake vortices
 - Detection of clear air turbulence

110107-4011

Honeywell Remote Wind Shear Detection Research

- Honeywell algorithm is not sensor-specific—velocity measurements required
 - LDV
 - Laser radar
 - Weather radar
- Based on locating velocity patterns indicative of hazardous wind shear while eliminating problems caused by ground clutter
- Microburst-specific algorithms developed and tested using NASA-Langley simulated data and X-band radar sensor model

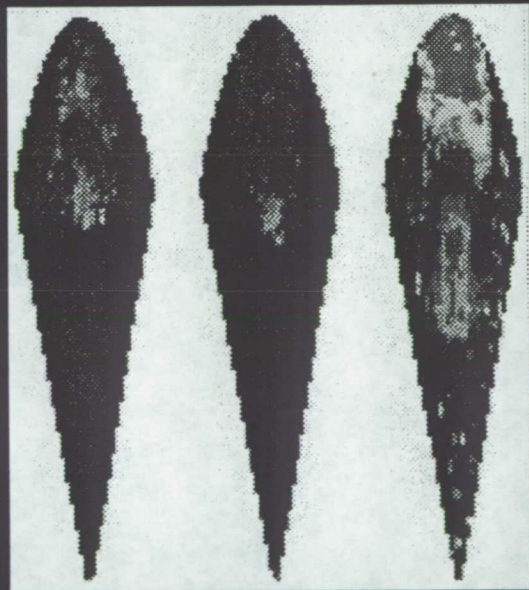


Honeywell

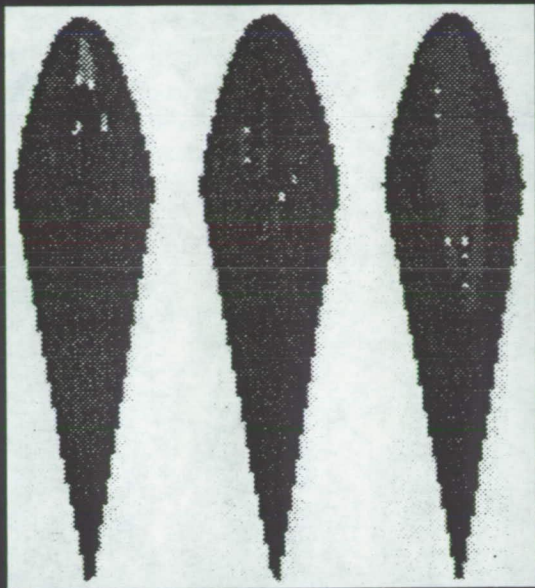
Radar/Microburst/ Clutter Modeling

- Utilized NASA-Langley airborne windshear doppler radar simulation (AWDRS)
- Modified software/parameters
 - Hosted on Sun workstation
 - Volumetric scan pattern
 - Generic X-band doppler radar parameters
 - Pattern for 12" Honeywell antenna (8° beamwidth)
- Currently upgrading to use the newer 3-D microburst models

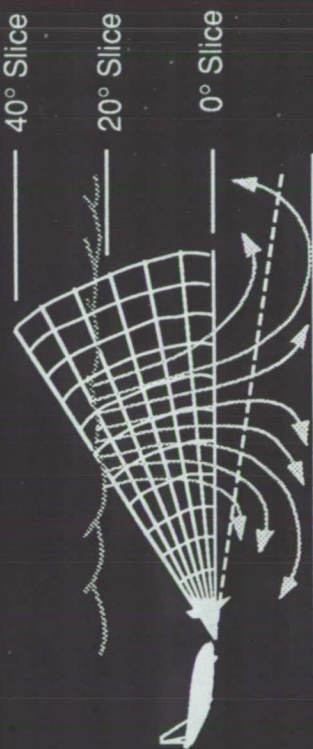
Volumetric Feature Grouping Identifies Microburst Windshear "Wet" Microburst



Doppler Velocity "Slices"

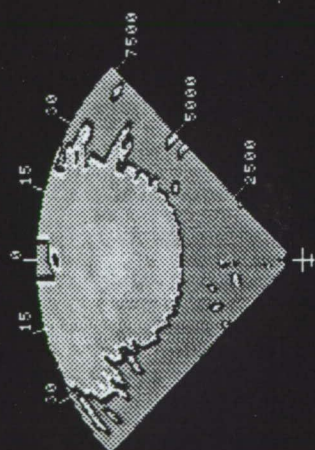


Identified Hazard Region "Slices"

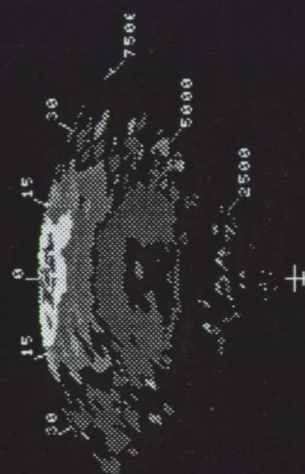


Algorithms for Airborne
Doppler Radar
Wind Shear Detection

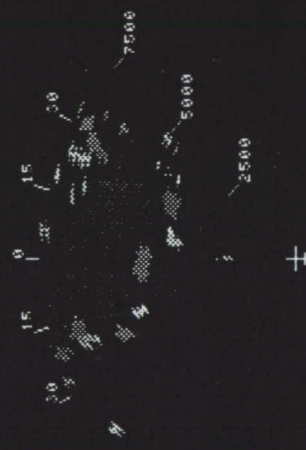
Honeywell's Wind Shear Detection Algorithm Removes Ground Clutter "Wet" Microburst



Reflectivity



Doppler
Velocity
Data



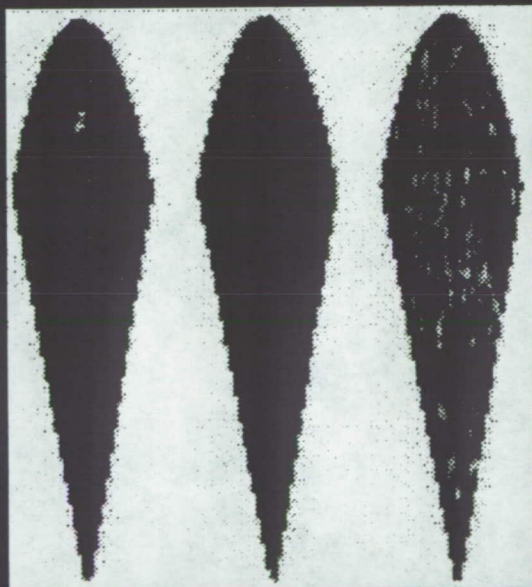
Intermediate
Result



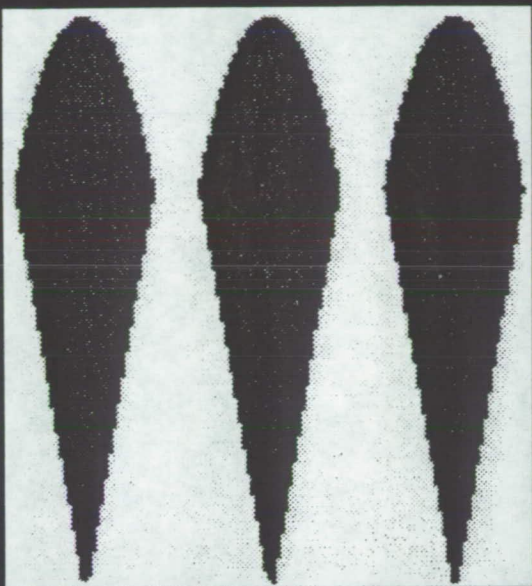
Hazard
Regions
Identified
by
Detection
Algorithm

Honeywell

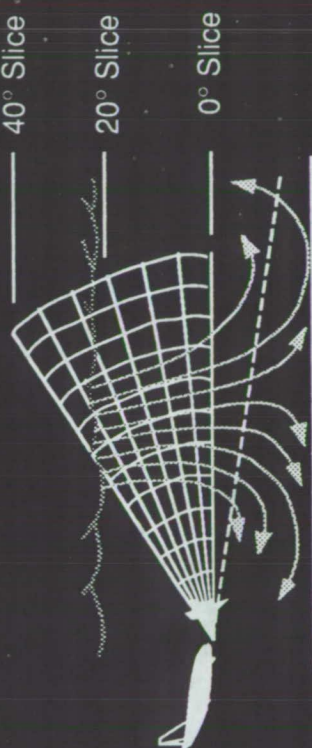
Volumetric Feature Grouping Identifies Microburst Windshear "Dry" Microburst



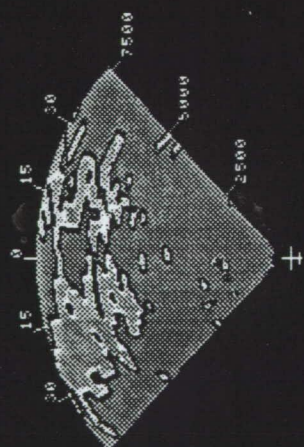
Doppler Velocity "Slices"



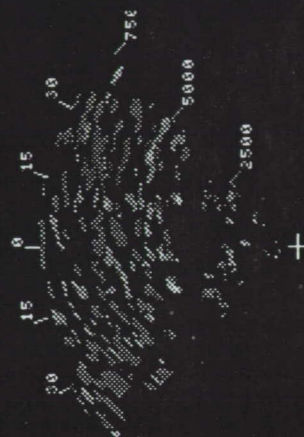
Identified Hazard Region "Slices"



Honeywell's Wind Shear Detection Algorithm Removes Ground Clutter "Dry" Microburst



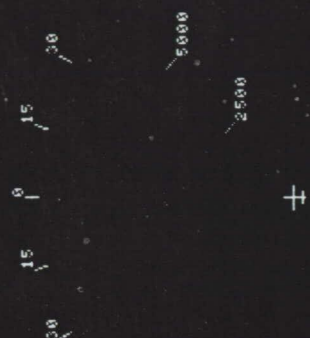
Reflectivity



Doppler
Velocity
Data



Intermediate
Result



Hazard
Regions
Identified
by
Detection
Algorithm

Honeywell

Future Plans

- Continued development and fusion with in situ/reactive sensors and algorithms
- Potential flight testing in 1992
- Development of optimal guidance algorithms using remote detection data

Algorithms for Airborne Doppler Radar Wind Shear Detection

Questions and Answers

Q: Kim Elmore (NCAR) - What did you use as a basis for using spectrum width estimates as an indicator of a hazard? Also, simply as a caveat, we found that in the Denver environment the use of rotation and convergence aloft does not seem to work very well as an estimation of whether the storm is actively producing a microburst or will produce one. It does work in the wet kind of environments in the South East, but it doesn't seem to work very well for us. Jim Wilson and Rita Roberts spent quite some time on that and finally threw up their hands in despair. How do you plan to address that, if this is going to be a primary constituent of the hazard determination. Secondly, what did you use as the basis to utilize spectrum width as a hazard estimation?

A: Earl Benser (Honeywell) - Right now there is a minimum and maximum spectral width threshold set that are used. We also look for areas that are of common spectral width for the volumetric feature recognition. So those are the two approaches that we have been using in terms of spectral width thresholding for detection. In terms of the correlation of all the volumetric features simultaneously, we do not necessarily demand that they are all simultaneously present, but we use the lack of all features as a part of the clutter rejection approach.

Q: Kim Elmore (NCAR) - I am curious as to where you got your information to form a hypothesis about spectral width associations.

A: Earl Benser (Honeywell) - I guess I am not necessarily familiar with those details of the activity.

Kim Elmore (NCAR) - Again, I wound up spending a lot of time chasing spectral width on Denver storms, and we found that it was next to useless. It was extremely viewing angle dependent. It may well be that you have done some sort of correlation with your beam width and what kind of spectral width you can expect from a meteorological aspect. That may have some utility. But, the work we did with our radars showed that it was not necessarily a good indicator.

Earl Benser (Honeywell) - As I understand it, and again I am not necessarily familiar with the details of that particular part of the algorithm, there are spectrum widths that are consistent with the type of phenomenon we are looking at. Things that have very little spectral width tend to be point targets as opposed to distributed targets that have relatively moderate spectral widths. The large spectral widths, as I understand it, are somewhat noisy. Anyway, the basic point is that there is activity going on in that area. I am not really familiar with the details.

Q: Paul Robinson (Lockheed) - From your slides it looks like you could estimate the hazard at zero degrees relative to the horizon, but you had the airplane flight path that looked like it was three degrees down. Does that not mean that you are looking at a hazard that the airplane may not encounter and perhaps underestimating that hazard?

A: Earl Benser (Honeywell) - The analysis that was presented today showed results where we looked at zero up to 40 degrees in 10 degree slices. Our activity right now is looking at specific scan pattern issues with respect to overall scan rate, scan range, and scan resolution.

Q: Paul Robinson (Lockheed) - Is there some reason why the program may not work looking three degrees down?

A: Earl Benser (Honeywell) - We do not have any reason to believe that it should not work. We have not completed the testing. Zero degrees was the initial completed activity.

Q: Dan Vicroy (NASA Langley) - Are you estimating a vertical winds? The fact that you are doing multiple vertical scans allows you to do some pretty interesting things in the vertical domain.

A: Earl Benser (Honeywell) - We have not gotten that far in our efforts. To date we have been looking at merely the in-plane velocity information, for detection of areas with consistent shear numbers for feature identification. We have not gotten to the point to either map out the vertical velocity structure within the events or to develop an F-factor estimate based on that initial data.

Session VI. Airborne Doppler Radar / NASA

PRECEDING PAGE BLANK NOT FILMED

1993010418

Session VI. Airborne Doppler Radar / NASA

N 93 - 19607

488738
228

NASA Experimental Airborne Doppler Radar and Real Time Processor for Wind Shear Detection

P. Schaffner, NASA Langley Research Center

Dr. M. Richards, Georgia Institute of Technology

W. Jones, NASA Langley Research Center

L. Crittenden, Research Triangle Institute

PRECEDING PAGE BLANK NOT FILMED



***NASA Experimental Airborne Doppler
Radar and Real-Time Processor
for Windshear Detection***

**P. Schaffner, NASA LaRC
Dr. M. Richards, GTRI
W. Jones, NASA LaRC
L. Crittenden, RTI**

Experimental Radar System Capabilities

- o Independent Data Frames 128 Pulse Repetition Periods per Frame
- o Selectable Transmitter Parameters
 - o PRF (9581, 4791, 3755, 2395, 1198 Hz)
 - o Pulse Width (1, 2, 4, or 8 μ s)
 - o Dual X-Band Transmit Frequencies
- o Selectable Antenna Parameters
 - o Scan Pattern (az, el, az/el)
 - o Scan Rate (3 Frames/1.5°)

Experimental Radar System

Capabilities

Continued

- o Independent AGC for each Range Bin (>60 dB)
- o Fast I.F. Gain Control (<0.5 μ s)
- o Selectable Range Bin Sampling of up to 124 bins to be recorded and processed out of 81 to 843 (depending on PRF & pulse width available from R/T unit)

Experimental Radar System

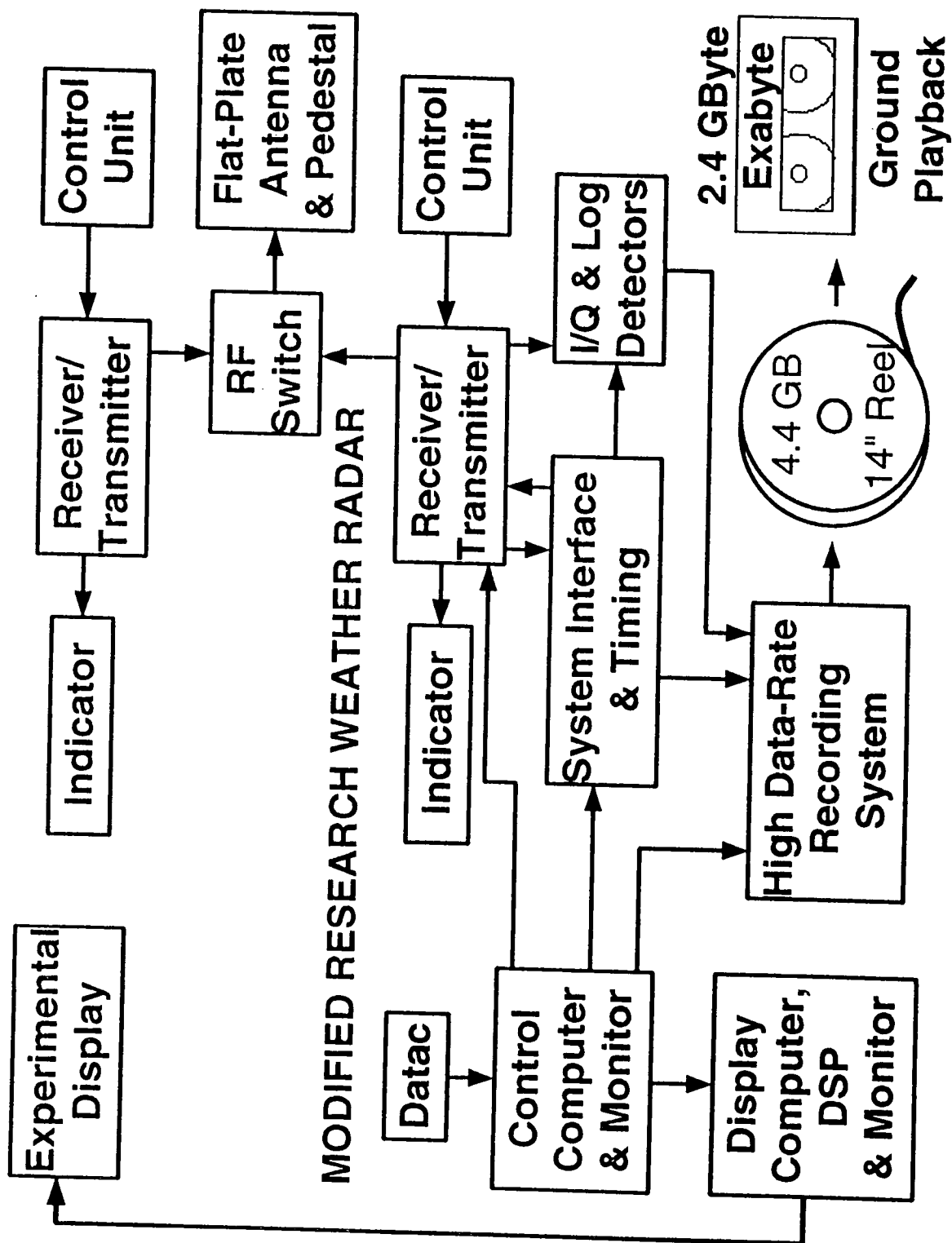
Capabilities

Continued

- o **Capability of skipping 0, 1, 2, or 3 Range Bins for each one selected**
- o **"Second Range Mode" in which every other transmit pulse is inhibited in order to study effects of range aliasing**

Experimental Radar System Block Diagram

PILOT'S STANDARD WEATHER RADAR



Wind shear Radar Signal and Data Processor (WRSDP)

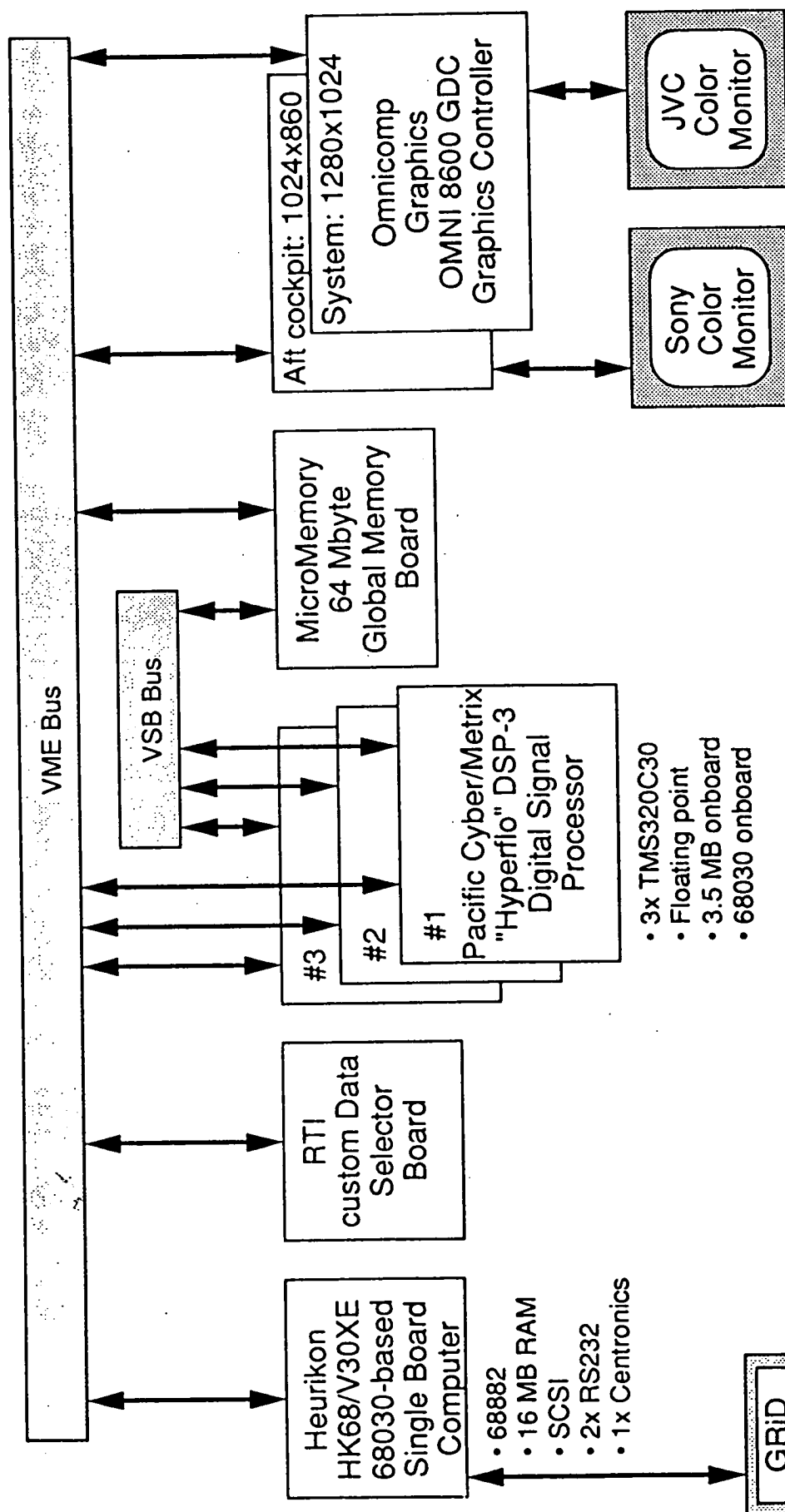
- o Developed under contract to NASA Langley Antenna and Microwave Research Branch (AMRB) by Research Triangle Institute (RTI) with subcontractor Georgia Tech Research Institute (GTRI)
- o VME-bus based computer, Motorola 68030 host running the OS-9 real time operating system
- o Three Pacific Cyber/Metrix DSP-3 boards each containing 3 TI TMS320C30 processors running at 33 MHz (Total mfg. rating 300 MFLOPS)

Wind shear Radar Signal and Data Processor (WRSDP)

continued

- o **Two high resolution graphics boards and monitors, hard and floppy disk drives, 64 MByte VME/VSBB bus memory board**
- o **Custom data selector board designed by RTI to allow use of data from radar, tape, or on-board simulation**
- o **GRiD 386 laptop computer, with separate keypad, for system console**

WRS DP HARDWARE ARCHITECTURE



Additional hardware features:

- 390 MB system hard disk
- 1.4 MB 3.5" floppy disk
- MuPAC VME enclosure
 - 12 slots
 - 500 W power supply

WRSDP System Design Goals

- o Flexible research tool for in-flight display and post-flight data analysis
- o Implement signal processing algorithms for real-time Doppler mean and variance estimation
- o Provide additional algorithms to calculate received power and signal spectra
- o Implement hazard detection, tracking, and alert algorithms
- o Support up to 6 simultaneous displays on 2 monitors

Q-6

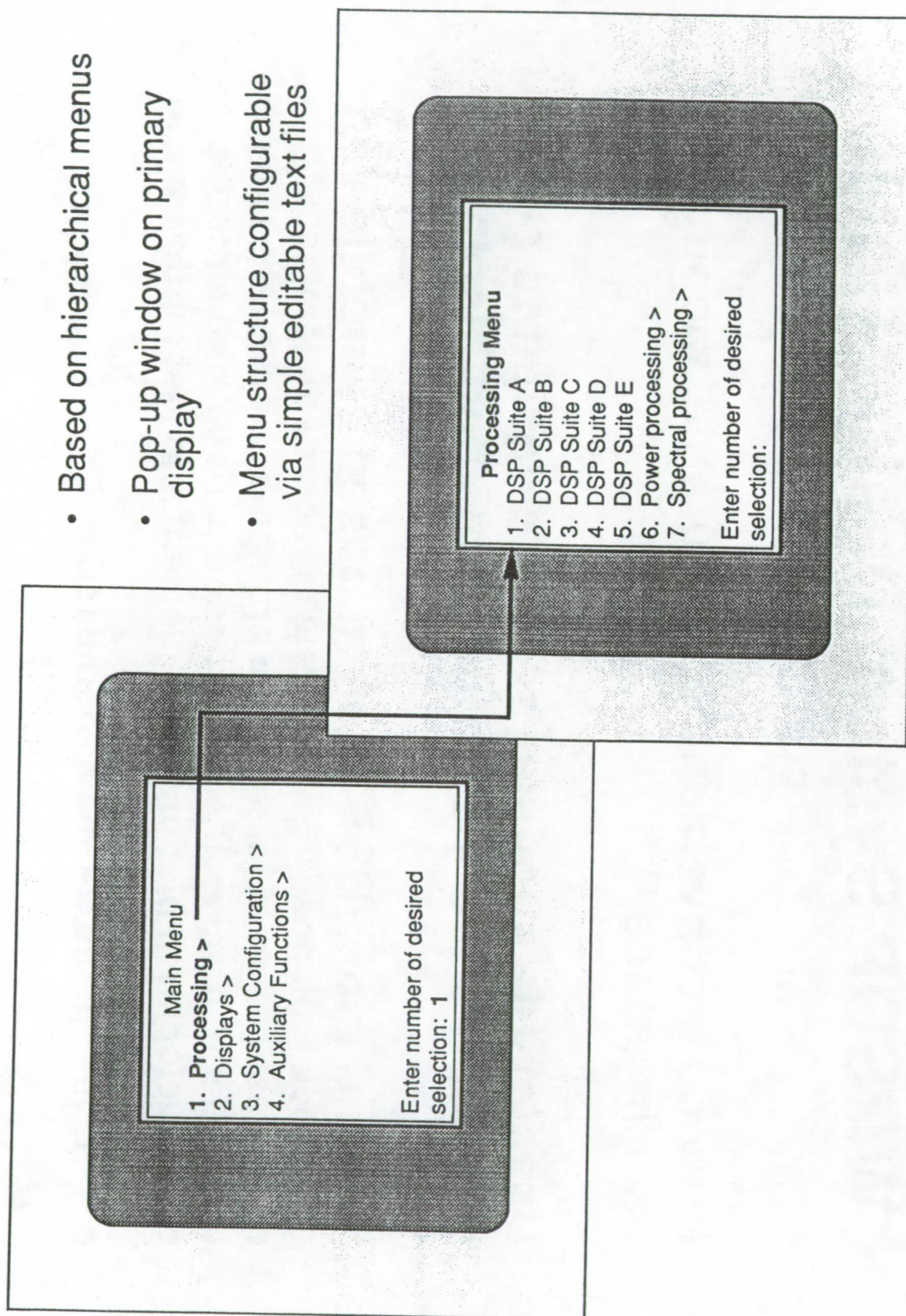
WRSDP System Design Goals

continued

- o **Provide a convenient, configurable, menu driven user interface**
- o **Use flexible, modular software design to support development of new algorithms and displays**
- o **Second radar/DSP system based in mobile van**
 - o Quick look post-flight analysis of recorded flight data
 - o Investigation of interference problems between the two radars
 - o Collection of weather data for comparison with aircraft data
 - o Development platform to implement and test hardware and software modifications
 - o "Live" spares for the airborne radar

USER INTERFACE

- Based on hierarchical menus
- Pop-up window on primary display
- Menu structure configurable via simple editable text files



DSP Software Development Tools

- o On Sun Workstation
 - o TMS320C30 C Compiler
 - o SPOX DSP Library
 - o TMS320C30 Simulator
 - o EMACS and vi editors
 - o Revision Control System (RCS)
 - o TCP/IP, NFS, Terminal Emulation, printing services
- o On Heurikon 68030 Host
 - o PC/M DSPdebug utility

OS-9 Software Development Tools

- o On Heurikon 68030 Host
 - o Microware OS-9 Operating System and Utilities
 - o uMACS editor
 - o C and gcc
 - o Make utility
 - o Source and system debuggers
 - o TCP/IP and NFS
 - o Absoft FORTRAN

WRSDP Digital Signal Processing

- o Basic purpose of DSP suites is the estimation of Doppler velocity mean and variance in each range-azimuth resolution cell
- o Choice of 4 different sets of DSP algorithms ("suites") currently provided for real-time use in performing these estimates
- o Other algorithms will be developed for post-flight analysis of data

WRSDP Digital Signal Processing

Continued

- o The DSP suites are formed from various combinations of:
 - o Clutter filters
 - Time Domain - FIR or IIR
 - Frequency Domain - Line Editing
 - o Spectrum Estimators
 - Fourier Transform, Autoregressive model, or none
 - o Frequency Estimators
 - Time-domain pulse pair, frequency domain pulse pair, first moment

DSP SUITES

SUITE	FILTER			SPECTRUM ESTIMATOR			FREQUENCY ESTIMATOR		
	FIR	IIR	LINE EDIT	NONE	FOURIER	AR	Time domain pulse pair	Freq. domain pulse pair	First moment
A		X		X			X		
B		X	X		X				X
C	X			X			X		
D		X	X		X			X	
E		X	X			X			X

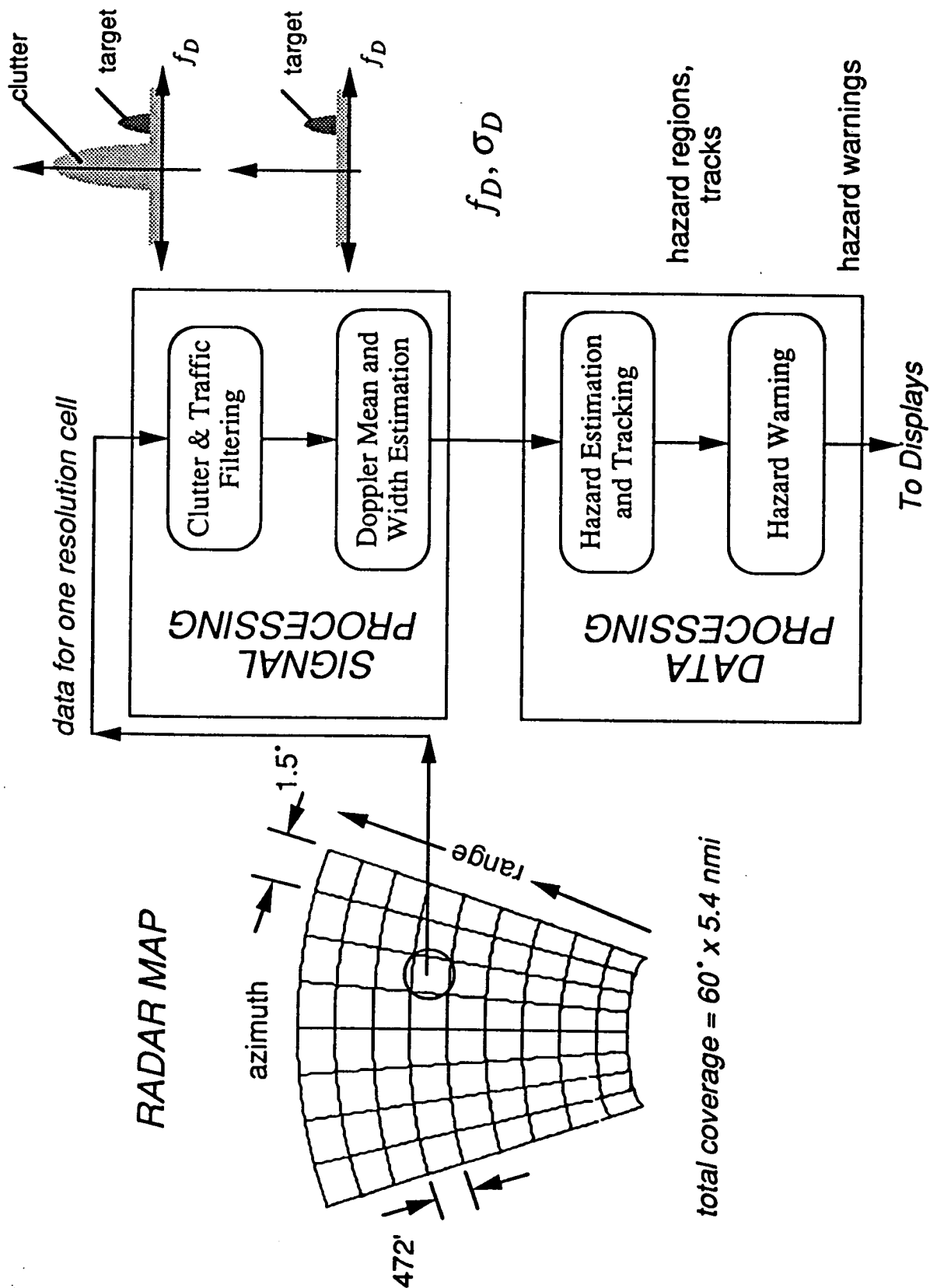
WRSDP Display Operational Modes

- o **Derived Velocity versus Range along range line**
- o **Received Power versus Range along range line, in dBm or dBz**
- o **FFT of selected Range Bins across 1 frame of 128 pulses**
- o **Color map of velocity/range over full azimuth scan**
- o **Color maps of power/range over full azimuth scan**
- o **Color map of hazard/range over full azimuth scan with wind shear tracking and alarm algorithms**

WRSDP Division of Functions

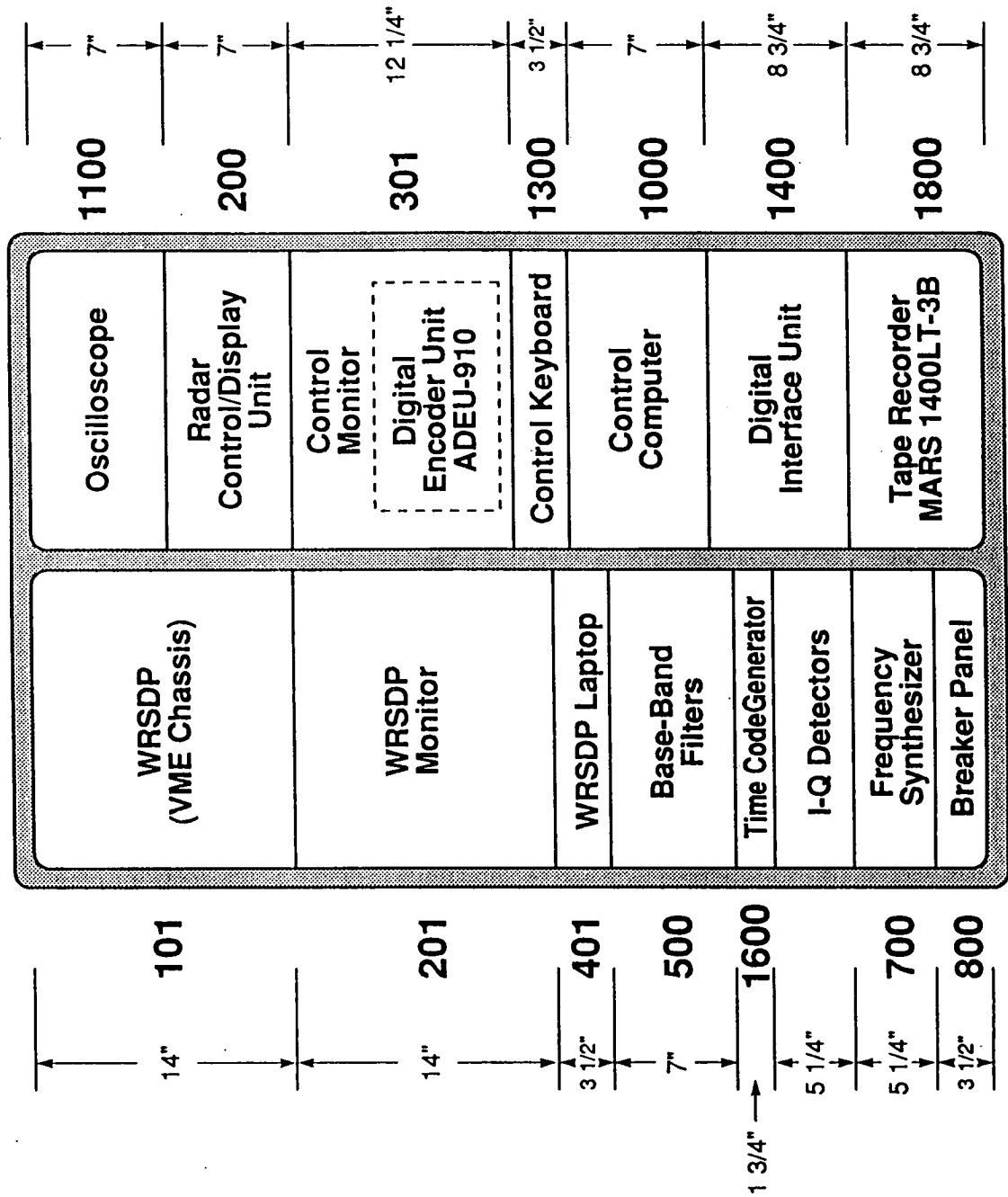
- o **Signal Processing - on DSP boards**
 - o Test signal injection
 - o Data flow and process control
 - o DSP algorithm suites
- o **Data Processing - 68030 host**
 - o User interface menu system
 - o Hazard detection and tracking
 - o Graphics calculations
 - o Diagnostics, start-up, load DSP images, tape control, etc.

STRUCTURE OF WRSDP SIGNAL & DATA PROCESSING ALGORITHMS



WINDSHEAR RADAR FLIGHT EXPERIMENT

Aircraft Console Equipment Arrangement



Summary

- o Airborne Wind Shear Radar System was flown in 1991 and successfully collected clutter, microburst and gust front data
- o WRSDP system has been tested and confirmed to be operational in laboratory with 4 algorithm suites implemented
- o Airborne Wind Shear Radar/WRSDP system currently being installed on NASA 737 for 1992 flight tests
- o Second system for Van/Playback/Quick-look being assembled and tested in laboratory

1993010419

Session VI. Airborne Doppler Radar / NASA

N93-19608

488740

18P

Ground Clutter Measurements Using the NASA Airborne Doppler Radar: Description of Clutter at the Denver and Philadelphia Airports

S. Harrah, NASA Langley Research Center

Dr. V. Delnore, Lockheed Lockheed Engineering & Sciences

M. Goodrich, Lockheed Lockheed Engineering & Sciences

C. Von Hagel, NASA Langley Research Center



***Ground Clutter Measurements Using the
NASA Airborne Doppler Radar:
A Description of Clutter at the
Denver and Philadelphia Airports***

S. Harrah, NASA LaRC
Dr. V. Delnore, Lockheed
M. Goodrich, Lockheed
C. Von Hagel, NASA LaRC

GROUND CLUTTER MEASUREMENTS USING THE NASA AIRBORNE DOPPLER RADAR: A DESCRIPTION OF CLUTTER AT DENVER AND PHILADELPHIA AIRPORTS

STEVEN D. HARRAH *
DR. VICTOR E. DELNORE **
MICHAEL S. GOODRICH **
CHRIS VON HAGEL *

Detection of hazardous wind shears from an airborne platform, using commercial sized radar hardware, has been debated and researched for several years. The primary concern has been the requirement for "look-down" capability in a Doppler radar during the approach & landing phases of flight. During "look-down" operation, the received signal (weather signature) will be corrupted by ground clutter returns. Ground clutter at and around urban airports can have large values of Normalized Radar Cross Section (NRCS) producing clutter returns which could saturate the radar's receiver, thus disabling the radar entirely, or at least from its intended function.

The purpose of this research was to investigate the NRCS levels in an airport environment (scene), and to characterize the NRCS distribution across a variety of radar parameters. These results are also compared to results of a similar study^{1,2} using Synthetic Aperture Radar (SAR) images of the same scenes. This was necessary in order to quantify and characterize the differences and similarities between results derived from the real-aperture system flown on the NASA 737 aircraft and parametric studies which have previously been performed using the NASA airborne radar simulation program.

This presentation describes the research and results obtained to date. These results were derived from data collected during the 1991 NASA Wind Shear Flight Experiment and include: the collection of data, analysis of incidence angle effects and polarization sensitivity, a comparison of NRCS statistics derived from the NASA radar and the ERIM SAR, an examination of intra-image features and inter-image repeatability, and an engineering summary of these results.

* NASA Langley Research Center, Hampton, VA 23665

** Lockheed Engineering and Sciences Company, Hampton, VA 23666

¹ D. Gineris, S. Harrah, and V. Delnore, "Analysis of Synthetic Aperture Radar (SAR) Data for Wind Shear Radar Clutter Modelling," *Proceedings of the Airborne Wind Shear Detection and Warning Systems: Second Combined Manufacturers' and Technologists' Conference*, Williamsburg, VA, October 18-20, 1988, pp. 225-244.

² S. Harrah, V. Delnore, and R. Onstott, "Clutter Modelling of the Denver Airport and Surrounding Areas," *Proceedings of the Airborne Wind Shear Detection and Warning Systems: Third Combined Manufacturers' and Technologists' Conference*, Hampton, VA, October 16-18, 1990, pp. 785-836.

GROUND CLUTTER MEASUREMENTS USING THE NASA AIRBORNE DOPPLER RADAR:

A DESCRIPTION OF CLUTTER AT DENVER AND PHILADELPHIA AIRPORTS

- **Summary of Ground Clutter Flights**
Locations & Measurements
Research Objectives
- **Landing Scene NRCS Statistics**
Measurement Repeatability
Incidence Angle Effects
Polarization Sensitivity
- **Specific Terrain NRCS Statistics**
Measurement Repeatability
Correlation to SAR Images
Incidence Angle Effects
- **Dynamic Range of Clutter Returns**
Antenna Pointing
Incidence Angle Effects
Polarization Sensitivity
- **Conclusions**
Application for Radar Design
FY' 92 Flight Plans

GROUND CLUTTER MEASUREMENTS USING THE NASA AIRBORNE DOPPLER RADAR: A DESCRIPTION OF CLUTTER AT DENVER AND PHILADELPHIA AIRPORTS

Summary of Ground Clutter Flights

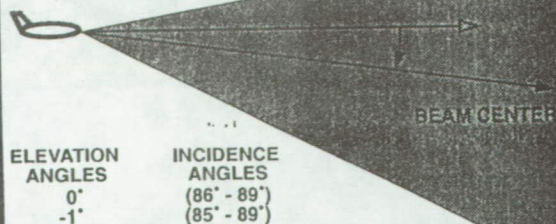
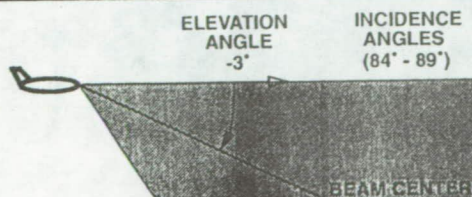
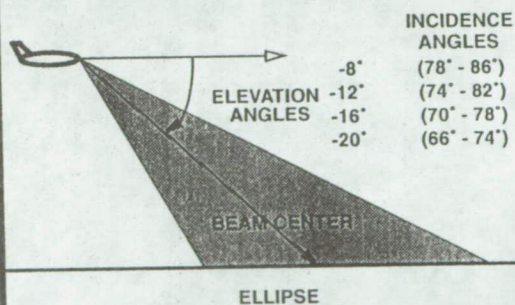
- Denver
 - 22 Approach/Landings (Runway 26 & 35)
 - Over 1 Hour of Recorded Final Approach Time
 - 22 Level Flights (~1000' AGL) (Runway 26 & 35)
 - Approx. 2,000,000,000 I&Q Samples
- Philadelphia
 - 31 Approach/Landings (Runway 27)
 - Over 1 Hour of Recorded Final Approach Time
 - Approx. 1,500,000,000 I&Q Samples
- Research Objectives
 - Evaluate Ground Clutter NRCS
 - Evaluate AGC Performance
 - Polarization & Antenna Tilt Management

GROUND CLUTTER MEASUREMENTS USING THE NASA AIRBORNE DOPPLER RADAR: A DESCRIPTION OF CLUTTER AT DENVER AND PHILADELPHIA AIRPORTS

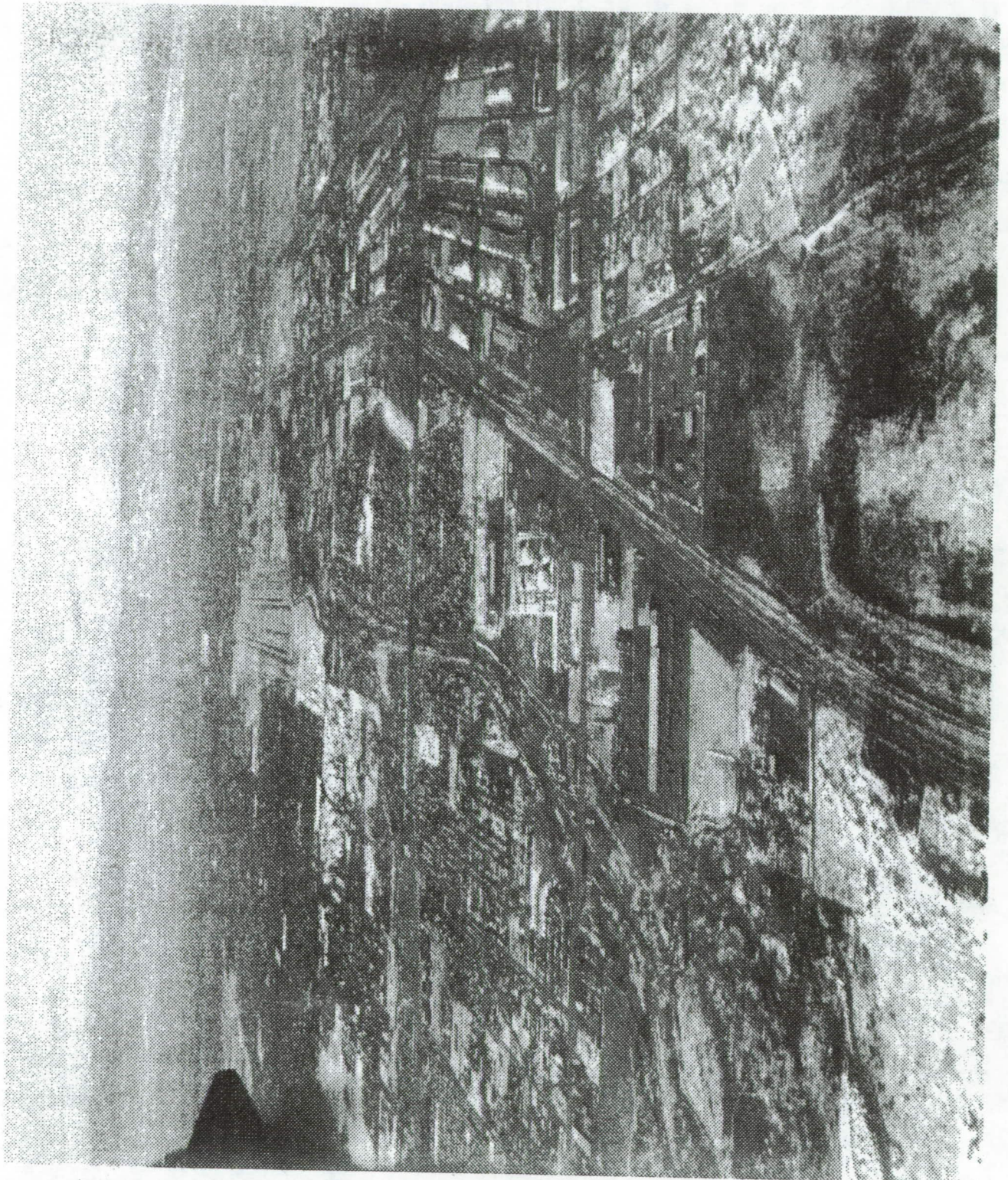
RADAR EQUATION GROUND CLUTTER CALCULATIONS

$$\bar{P}(R) = \frac{P_T G^2 \lambda^2}{(4\pi R)^3} \sigma^o \int_0^\infty \frac{|W(R-r)|^2 dr}{\sin \gamma} \int_0^\pi \int_0^{2\pi} A(\theta, \phi) d\phi d\theta$$

σ^o = Normalized Radar Cross Section



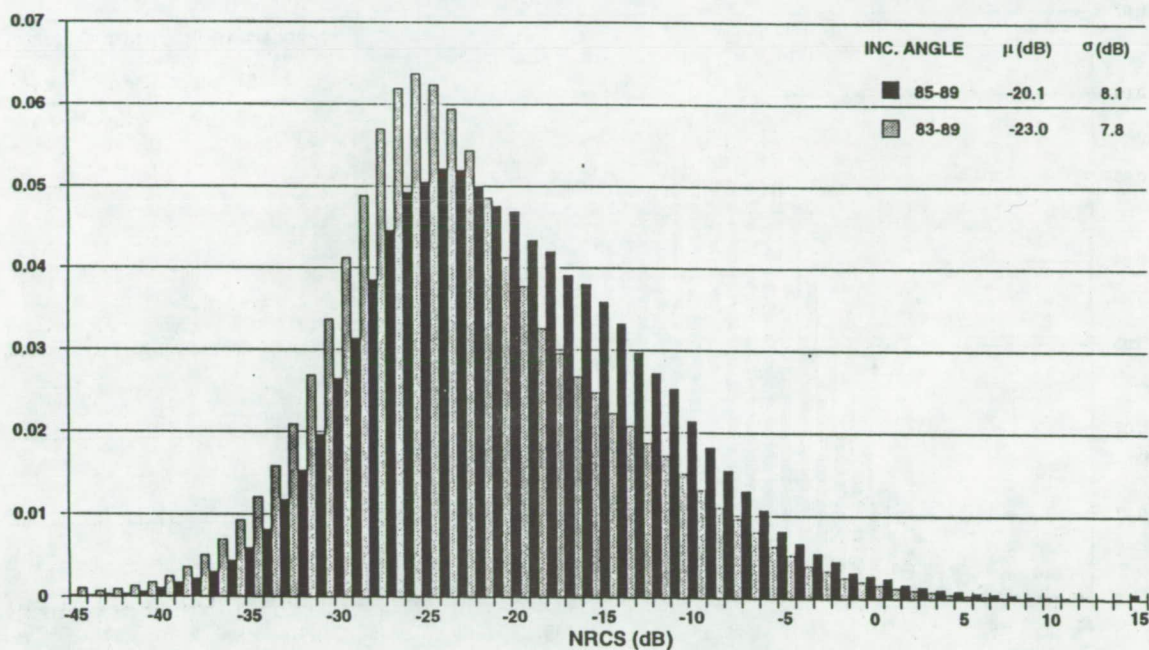
ORIGINAL PAGE
BLACK AND WHITE PHOTOGRAPH



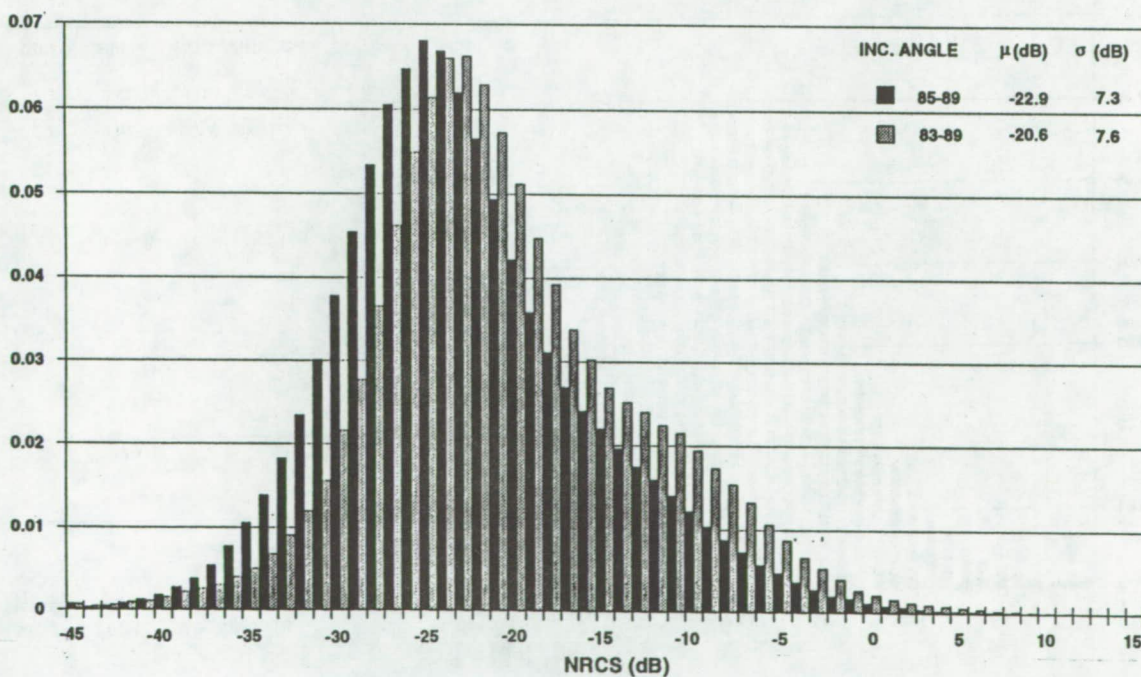
NASA WINDSHEAR RADAR 1991 FLIGHT EXPERIMENT



FINAL APPROACH GROUND CLUTTER NRCS (DENVER) INCIDENCE ANGLE EFFECTS : HH POLARIZATION



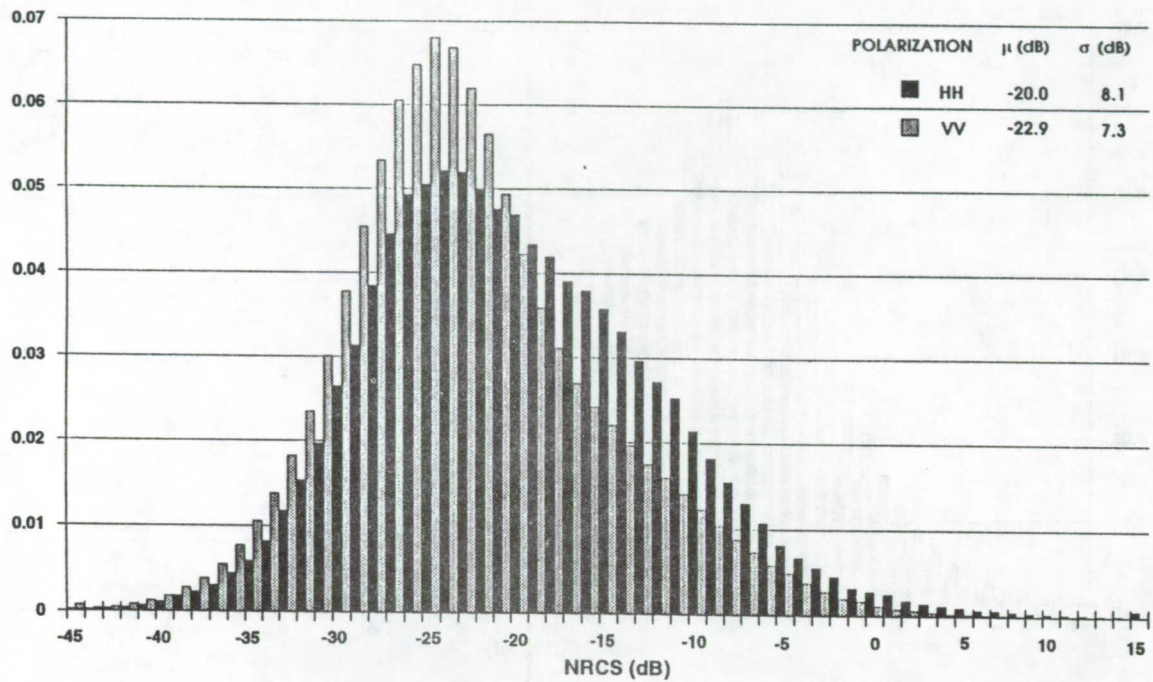
FINAL APPROACH GROUND CLUTTER NRCS (DENVER) INCIDENCE ANGLE EFFECTS : VV POLARIZATION



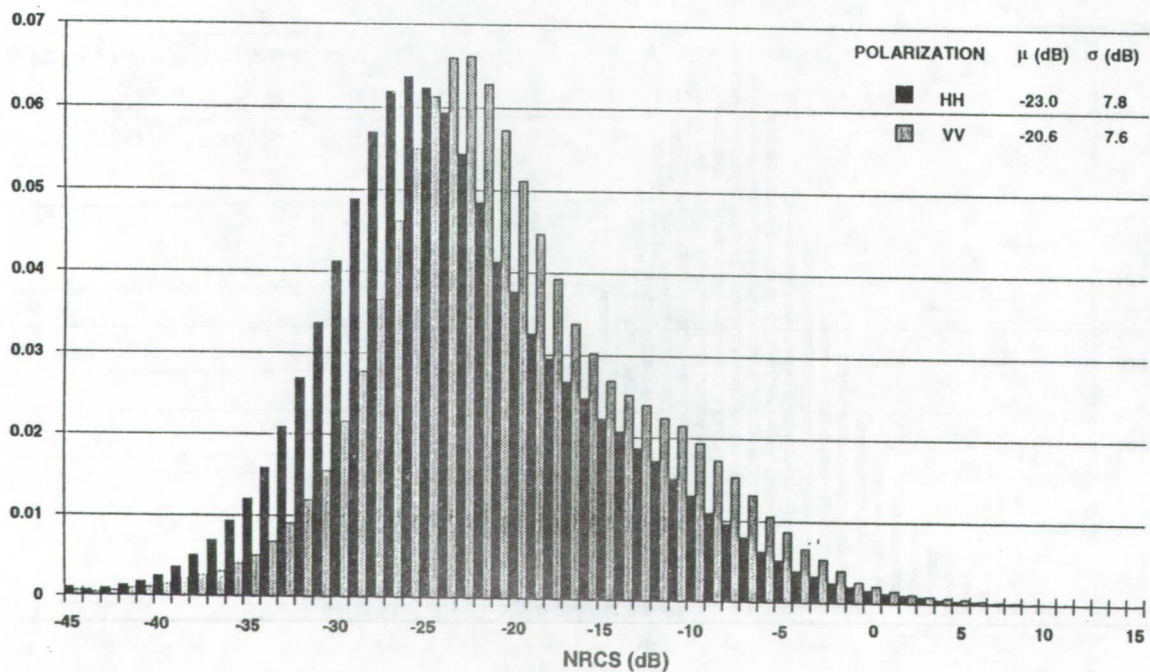
NASA WINDSHEAR RADAR 1991 FLIGHT EXPERIMENT



FINAL APPROACH GROUND CLUTTER NRCS (DENVER) POLARIZATION SENSITIVITY : -1 ELEVATION



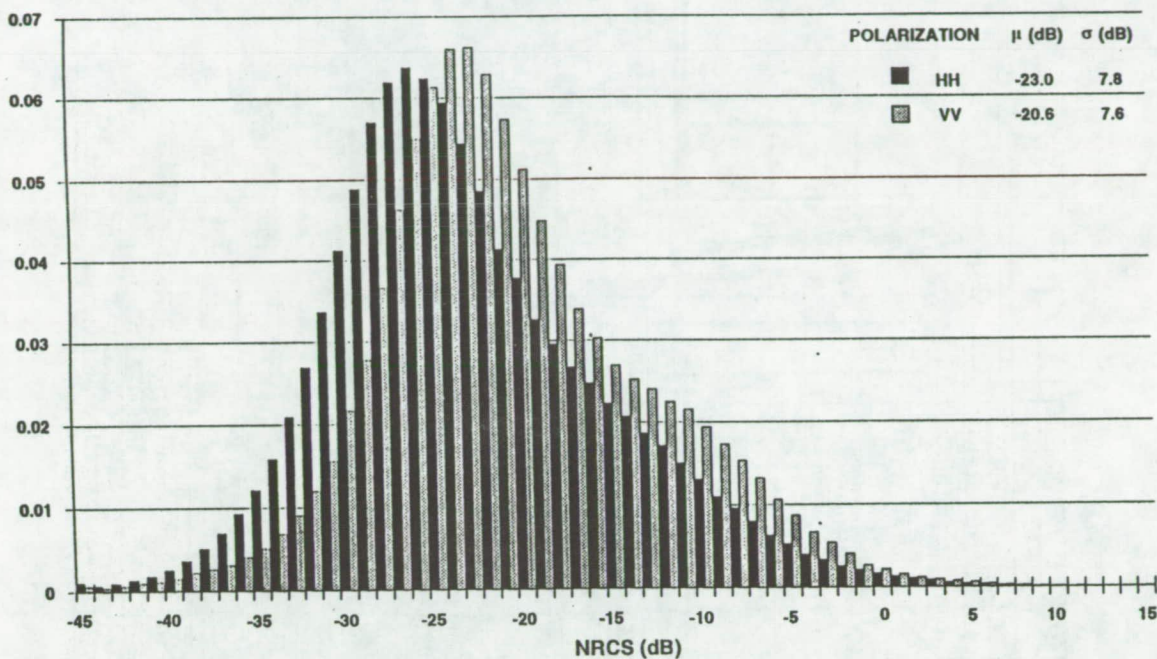
FINAL APPROACH GROUND CLUTTER NRCS (DENVER) POLARIZATION SENSITIVITY : -3 ELEVATION



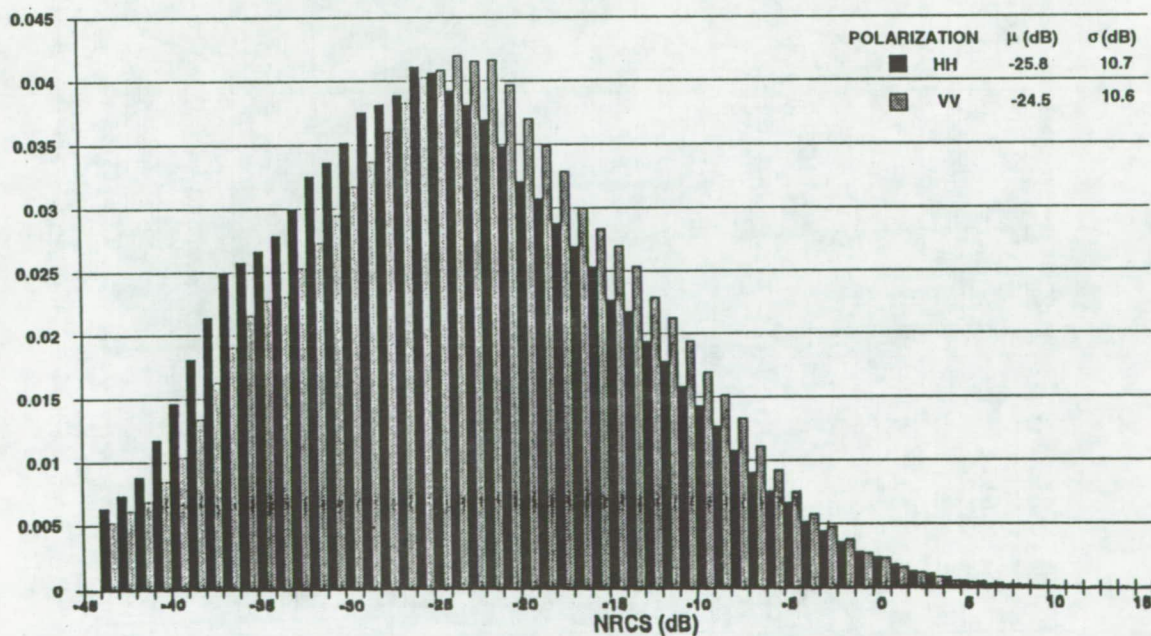
NASA WINDSHEAR RADAR 1991 FLIGHT EXPERIMENT



FINAL APPROACH GROUND CLUTTER NRCS (DENVER) POLARIZATION SENSITIVITY : -3 ELEVATION



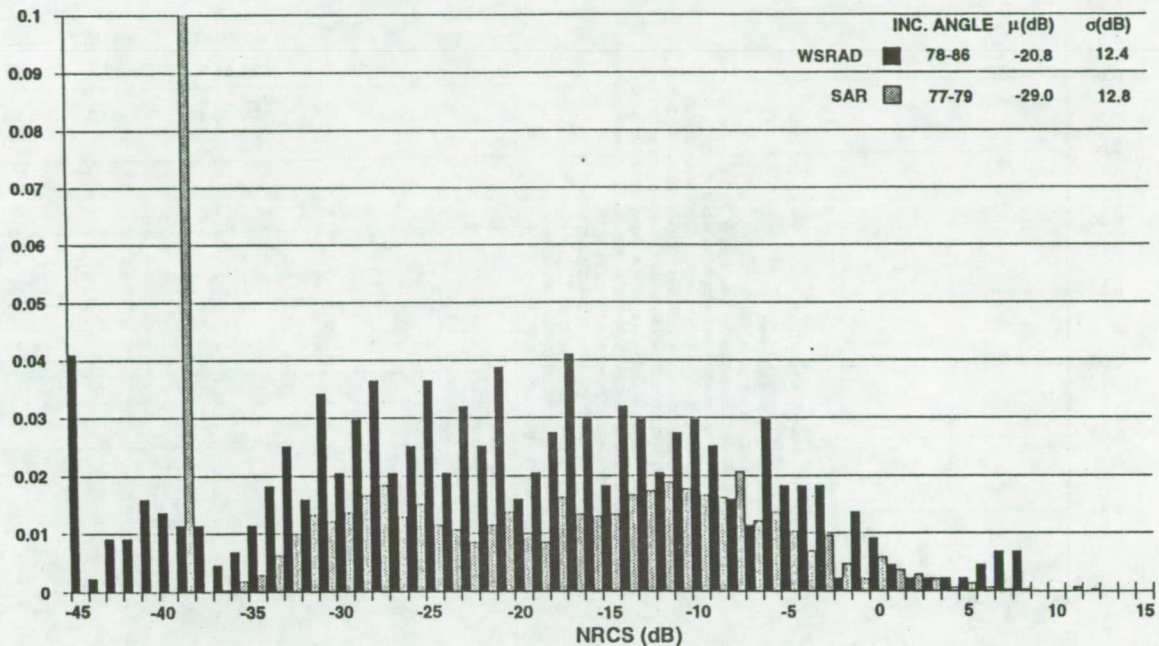
FINAL APPROACH GROUND CLUTTER NRCS (PHILADELPHIA) POLARIZATION SENSITIVITY : -3 ELEVATION



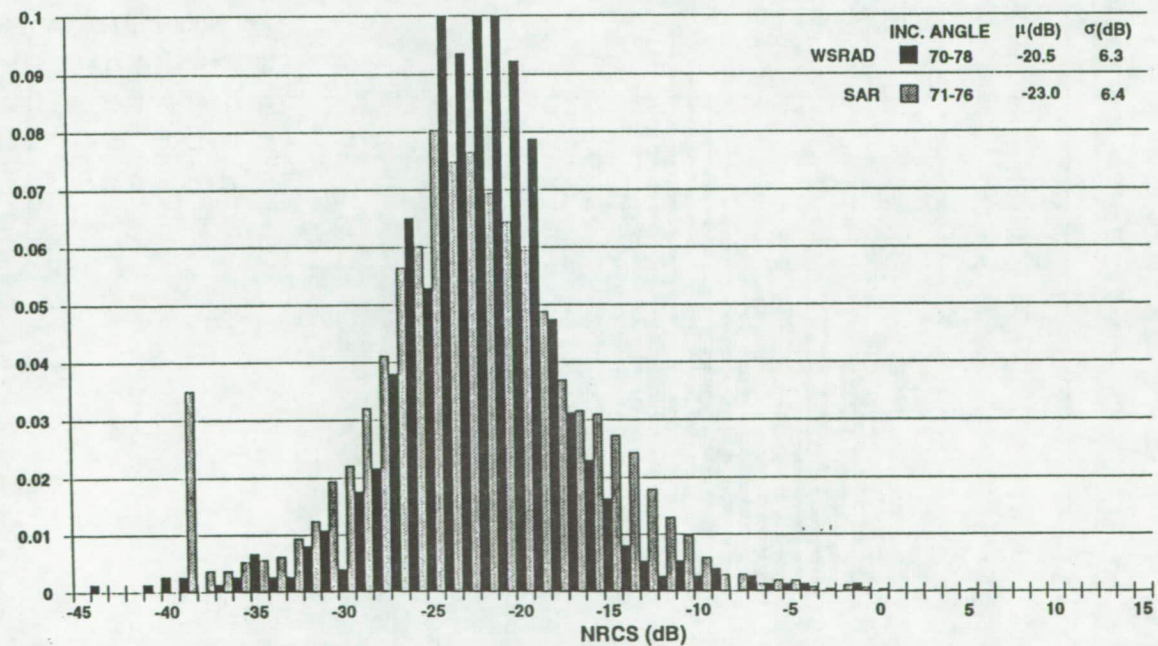
NASA WINDSHEAR RADAR 1991 FLIGHT EXPERIMENT



**NRCS HISTOGRAM (DENVER TERMINAL)
WSRAD & SAR COMPARISON**



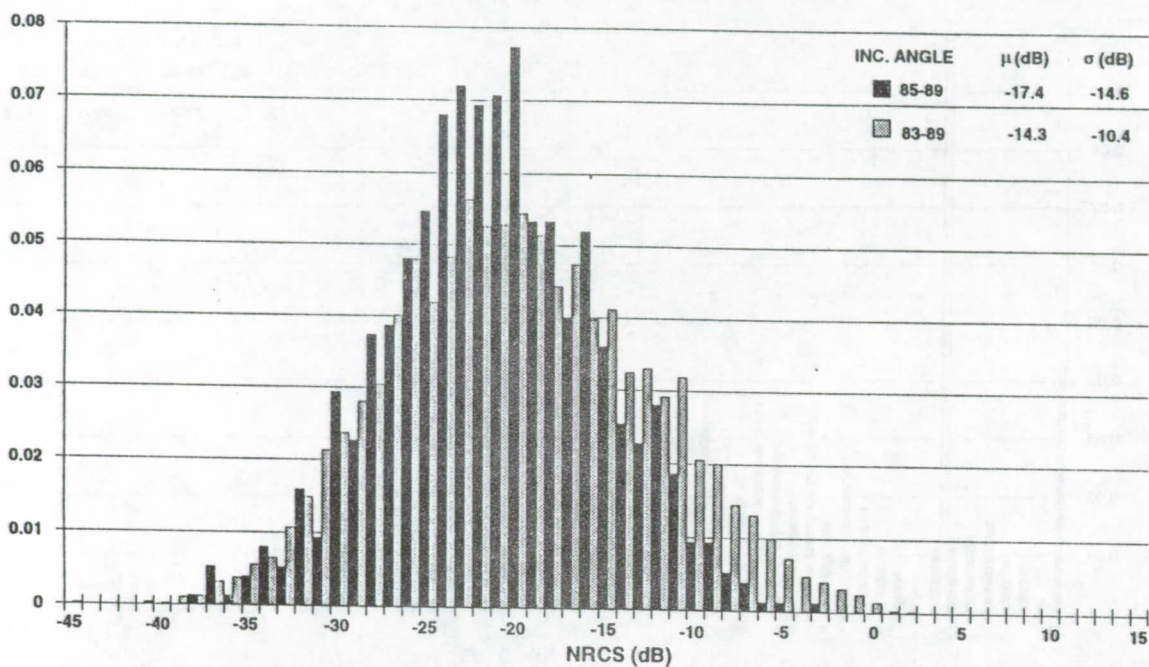
**NRCS HISTOGRAM (DENVER PARKS)
WSRAD & SAR COMPARISON**



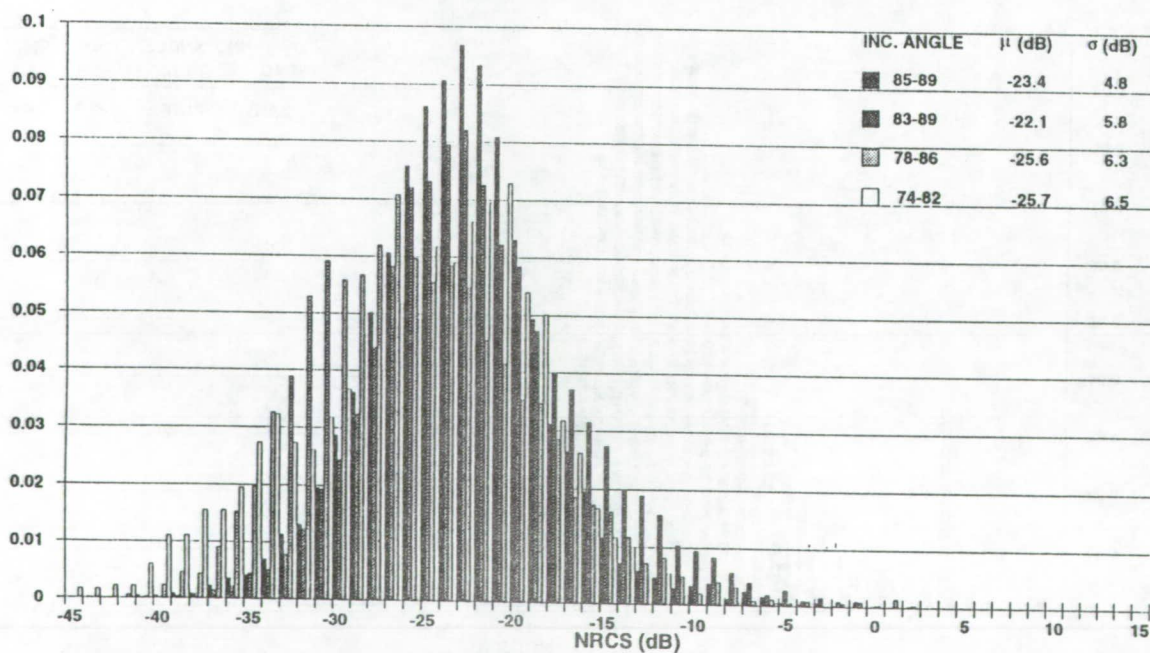
NASA WINDSHEAR RADAR 1991 FLIGHT EXPERIMENT



NRCS HISTOGRAM (DENVER URBAN)
MEASUREMENT REPEATABILITY

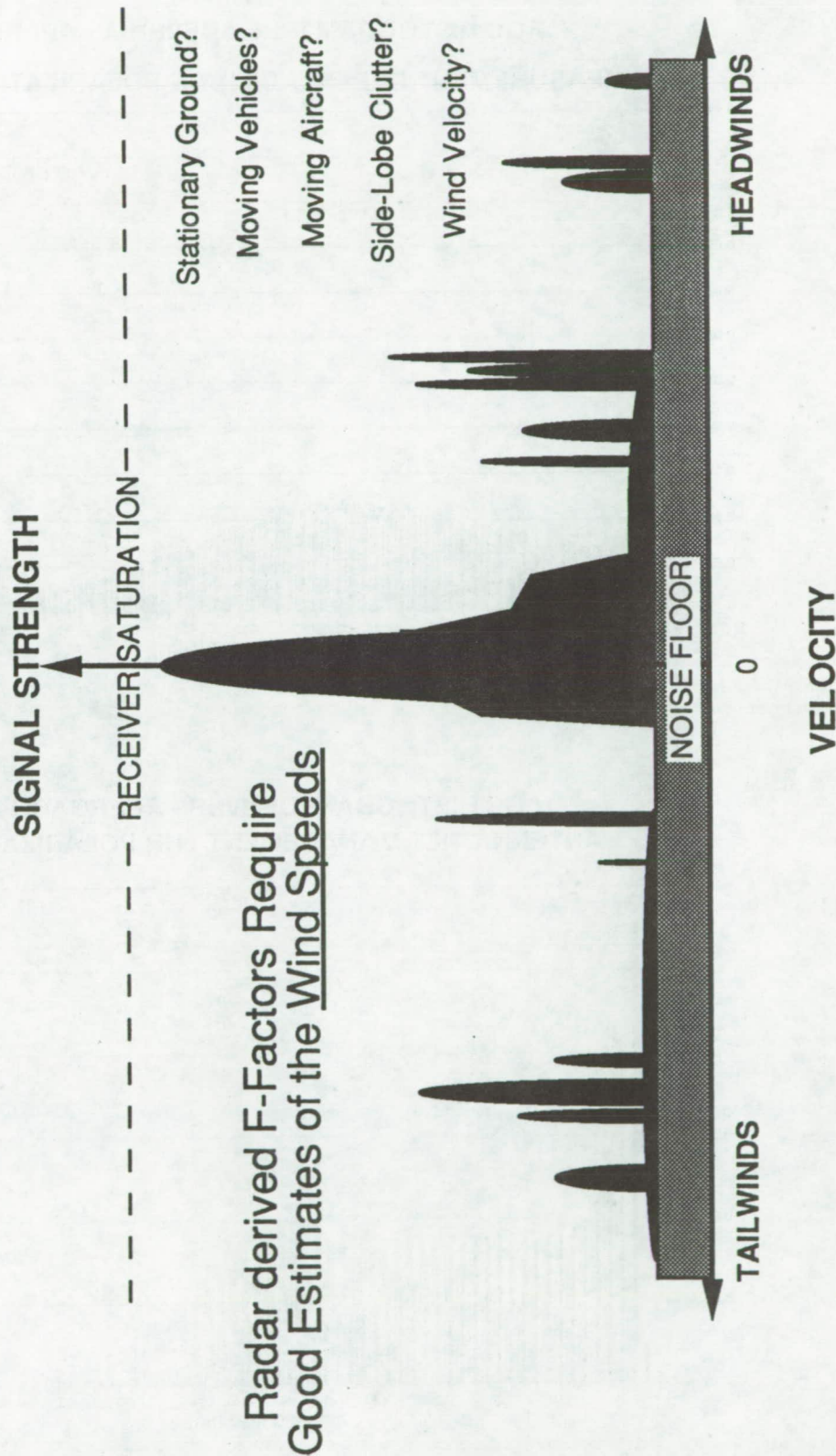


NRCS HISTOGRAM (DENVER RESIDENTIAL)
INCIDENCE ANGLE INSENSITIVITY



AIRBORNE WIND SHEAR DOPPLER RADAR SIGNAL

Proper Antenna Tilt Management
Allows The Radar Signal to be
Processed to give Velocity Information



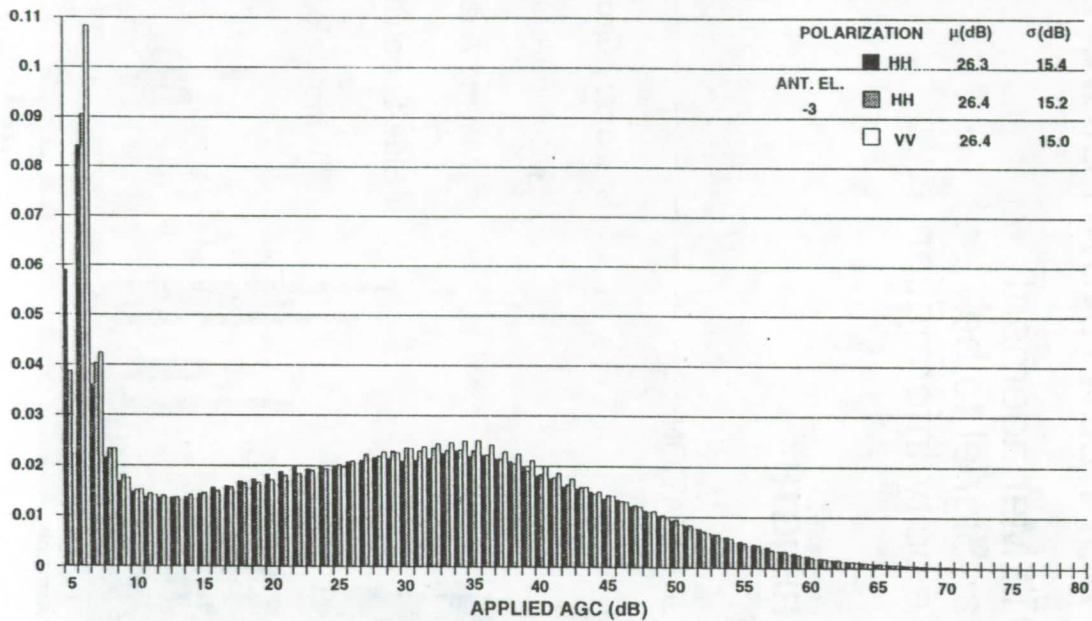
Radar derived F-Factors Require
Good Estimates of the Wind Speeds

NASA WINDSHEAR RADAR 1991 FLIGHT EXPERIMENT

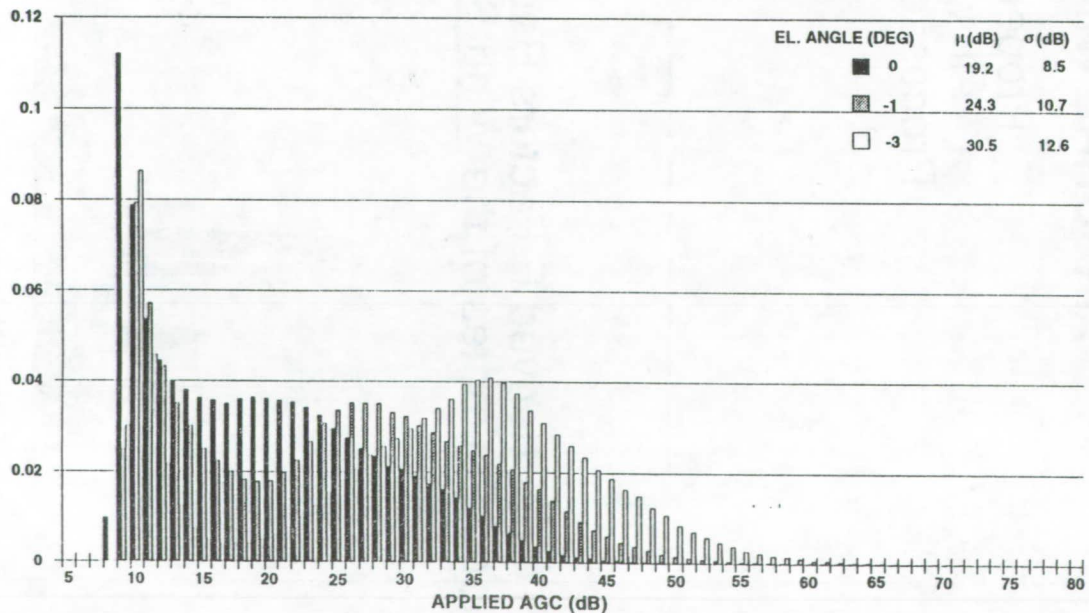


AGC HISTOGRAM (PHILADELPHIA - APPROACH 27)

MEASUREMENT REPEATABILITY & POLARIZATION SENSITIVITY



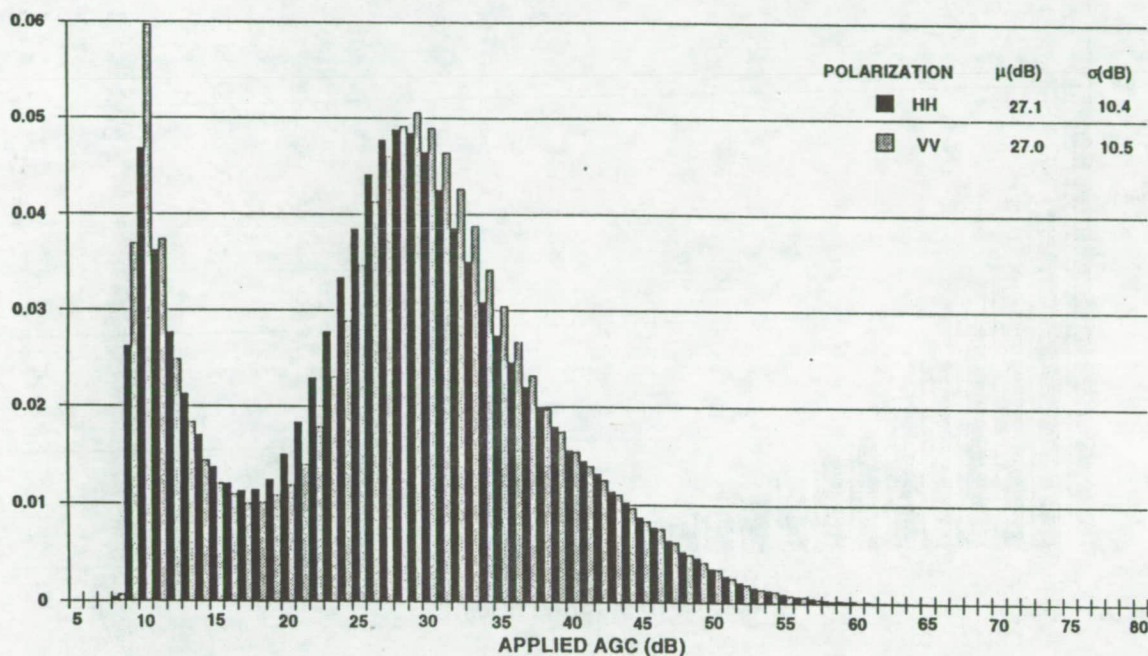
AGC HISTOGRAM (DENVER - APPROACH 26) ANTENNA TILT MANAGEMENT : HH POLARIZATION



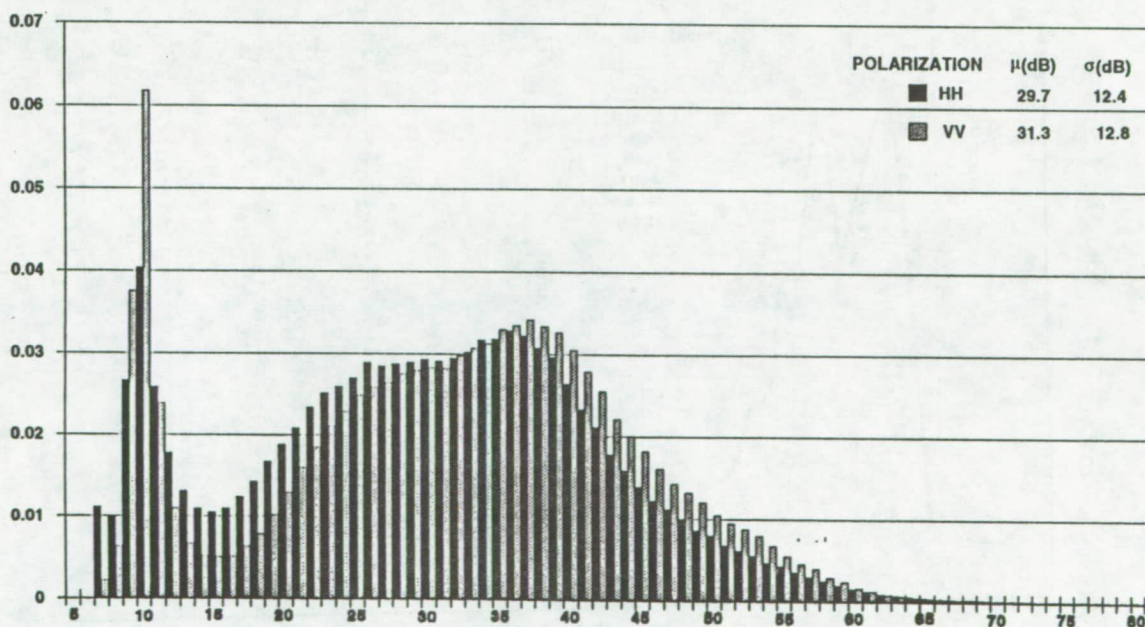
NASA WINDSHEAR RADAR 1991 FLIGHT EXPERIMENT



AGC HISTOGRAM (DENVER - APPROACH 35)
POLARIZATION SENSITIVITY : -1 ELEVATION



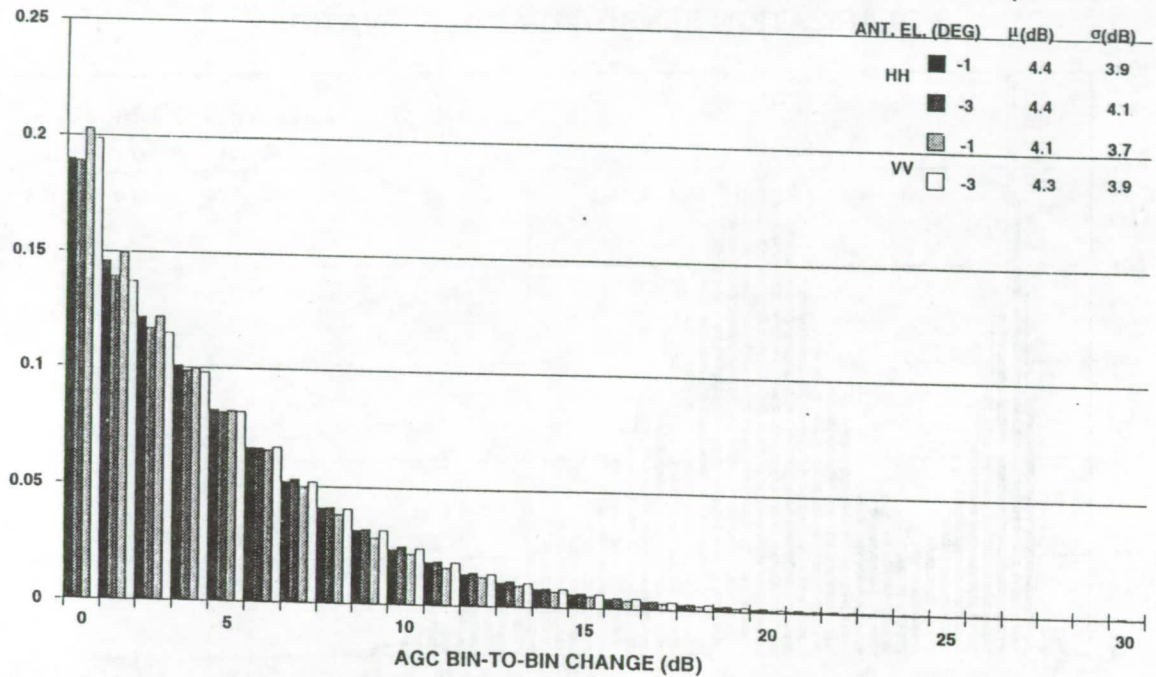
AGC HISTOGRAM (DENVER - APPROACH 35)
POLARIZATION SENSITIVITY : -3 ELEVATION



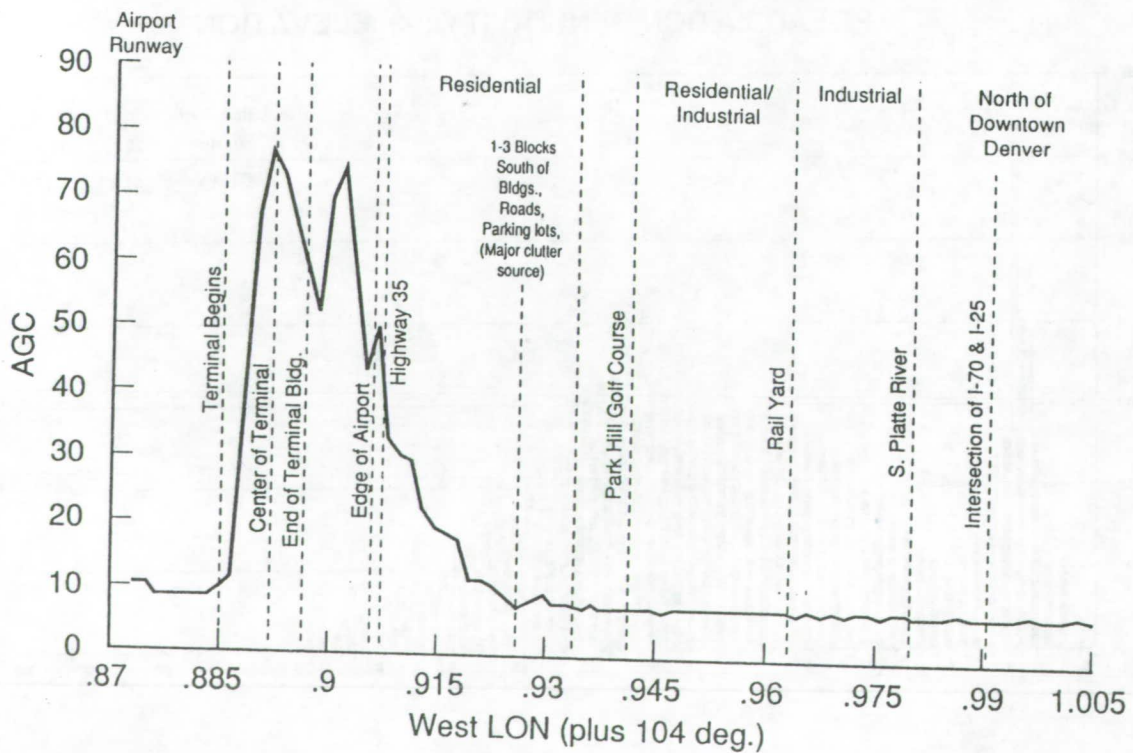
NASA WINDSHEAR RADAR 1991 FLIGHT EXPERIMENT



BIN-TO-BIN $d(\text{AGC})$ HISTOGRAM (DENVER - APPROACH 35)



STAPLETON TERMINAL



**GROUND CLUTTER MEASUREMENTS USING
THE NASA AIRBORNE DOPPLER RADAR:
A DESCRIPTION OF CLUTTER AT DENVER AND PHILADELPHIA AIRPORTS**

Conclusions 1991 Flight Experiment

- **NRCS Incidence Angle Effects**

Use Uncorrected NRCS from SAR Maps in Simulation
Man-Made Clutter Insensitive to Incidence Angle

- **NRCS Polarization Sensitivity**

Angular Dependency to Polarization Sensitivity
6 dB or Less of Separation HH - VV

- **Comparison with SAR Derived NRCS Statistics**

Natural Targets Show Good Agreement with SAR
SAR Maps Should Produce Realistic Clutter in Simulation
Reasonable Fidelity (Dynamic & Spatial Variations)

- **AGC Incidence Angle Dependency**

6 dB/1° Lower AGC Mean at Angles of Interest
2 dB/1° Lower AGC Std. Dev. at Angles of Interest

- **AGC Polarization Dependency**

1-3 dB Reduction Using VV (@ -1°)
1-3 dB Reduction Using HH (@ -3°)

- **Bin-To-Bin AGC Independent of Tilt & Polarization**

- **Implications for 1992 Flight Experiment**

Re-Investigate a Few Key Terrain Features
Increase Database for Polarization Study
Continue to Examine Moving Clutter

**Ground Clutter Measurements Using the NASA Airborne Doppler Radar:
Description of Clutter at the Denver and Philadelphia Airports
Questions and Answers**

Q: Jim Evans (MIT) - What is the instability residue of the radar transmitter? What is the signal wave form which has been used to obtain data? What are the antenna side lobes, in elevation, with the radome on? How is the data below the receiver sensitivity represented in the clutter histograms?

A: Steve Harrah (NASA Langley) - After talking to Collins, we would prefer not to openly disclose the instability residue values. If you would like to talk to Collins they are more than willing to share that information with you. The wave form is basically a simple rectangular pulse. The antenna side lobes are basically a half of a dB below what they are with the radome off. Those levels are typically 30-35 dB down for the first side lobe. In my clutter analysis I made sure, through the equations that were implemented, that we only looked at ground clutter targets which fell within four degrees of the center of the beam. In that respect, I don't believe we saw anything that did not have a significant amount of AGC applied to them. By that, it tells me that they weren't down in the noise.

Q: Jim Evans (MIT) - Will clutter measurements be conducted with realistic profiles at ugly clutter locations?

A: Steve Harrah (NASA Langley) - We are planning on making some additional measurements this year as I stated in my conclusions and future work statement. We are going to try and look at the urban clutter in Denver. As you suggest further on down in your comments to use runway 8. We will try and work that into the schedule and as long as we can get ATC to agree with it. In addition to that, we are going to make a trip to Washington this year we think, and maybe some other uglier clutter sites.

1993010420

Session VI. Airborne Doppler Radar / NASA

N 93 - 19609

488742

24p

Spectrum Characteristics of Denver and Philadelphia Ground Clutter and the Problem of Distinguishing Wind Shear Targets from Moving Clutter

A. Mackenzie, NASA Langley Research Center



***Spectrum Characteristics of
Denver and Philadelphia Ground Clutter
and the Problem of Distinguishing
Windshear Targets from Moving Clutter***

A. Mackenzie, NASA LaRC

Abstract

Spectral analysis of 1991 wind shear flight data has provided information about the power spectral density, spectral width, and velocity of ground clutter detected by the wind shear radar at several major airports. Ground clutter must be recognized and separated from weather targets before wind shear can be computed. Information will be presented characterizing and comparing ground clutter and weather target spectra. The information includes: (1)spectral widths of stationary ground clutter seen at various scan and tilt angles, (2)power spectral density and velocity of moving ground clutter relative to the stationary ground clutter, and (3)spectral widths and velocities of weather targets. The presentation will also include summary numerical results in the form of histograms and example numerical results in the form of spectral plots.

OUTLINE

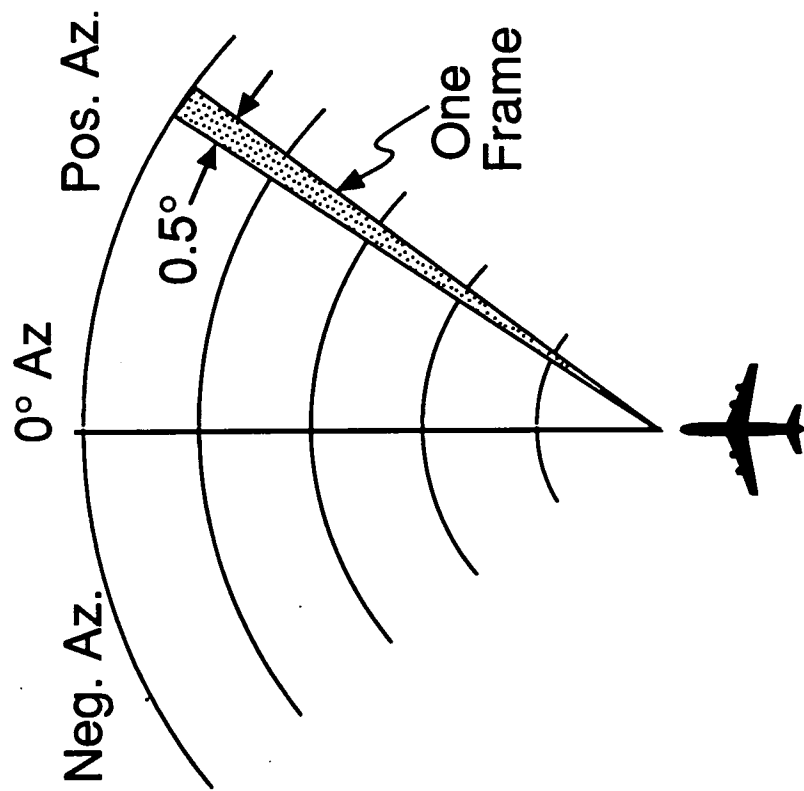
- DATA FRAME AND RANGE BIN GEOMETRY
- STATIONARY GROUND CLUTTER SPECTRA
 - Velocity Compensation
 - Spectral Width
- WEATHER SPECTRA: WIND SHEAR EXAMPLE
- MOVING GROUND CLUTTER SPECTRA
 - Histogram of Velocities
 - Histogram of Power Spectral Densities
Relative to Stationary Ground Clutter
 - View Across the Scan

Data Frame and Range Bin Geometry

In the usual mode of operation, the radar antenna scans in azimuth while keeping a fixed tilt. During the transmission of 128 pulses, the antenna moves through 0.5 degrees of its scan. Data collected from these transmitted pulses are called one data frame. Range bins are spherical shells concentric about the radar. Each bin is 144 meters thick. During one data frame, 128 samples are collected from each range bin.

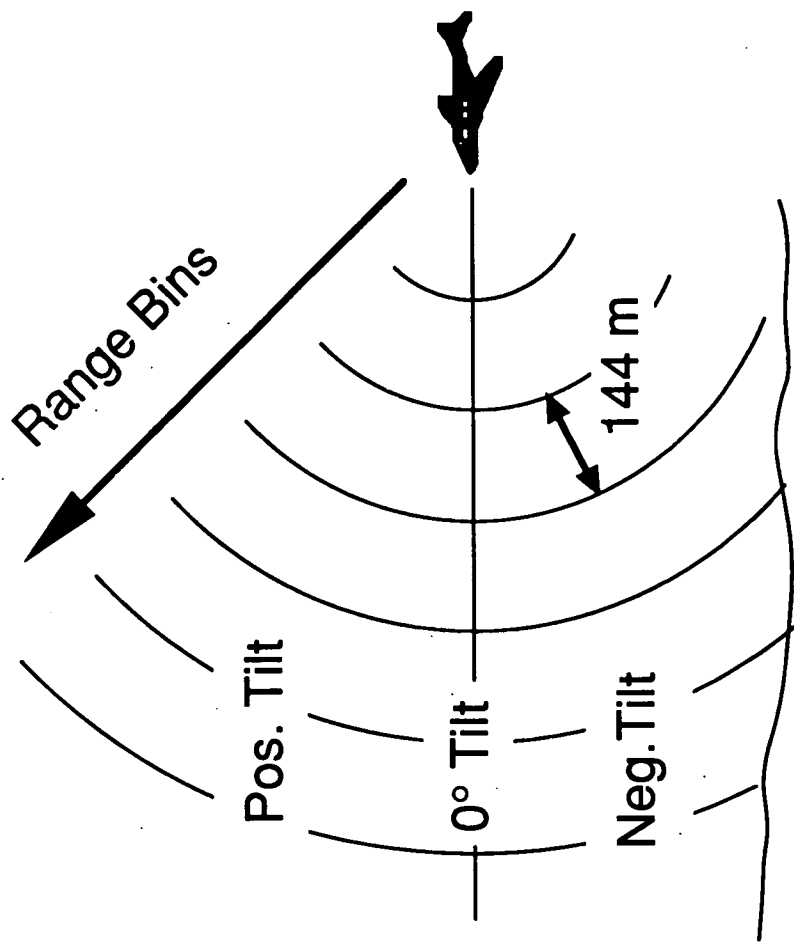
DATA FRAME AND RANGE BIN GEOMETRY

TOP VIEW



128 pulses transmitted during one frame

SIDE VIEW

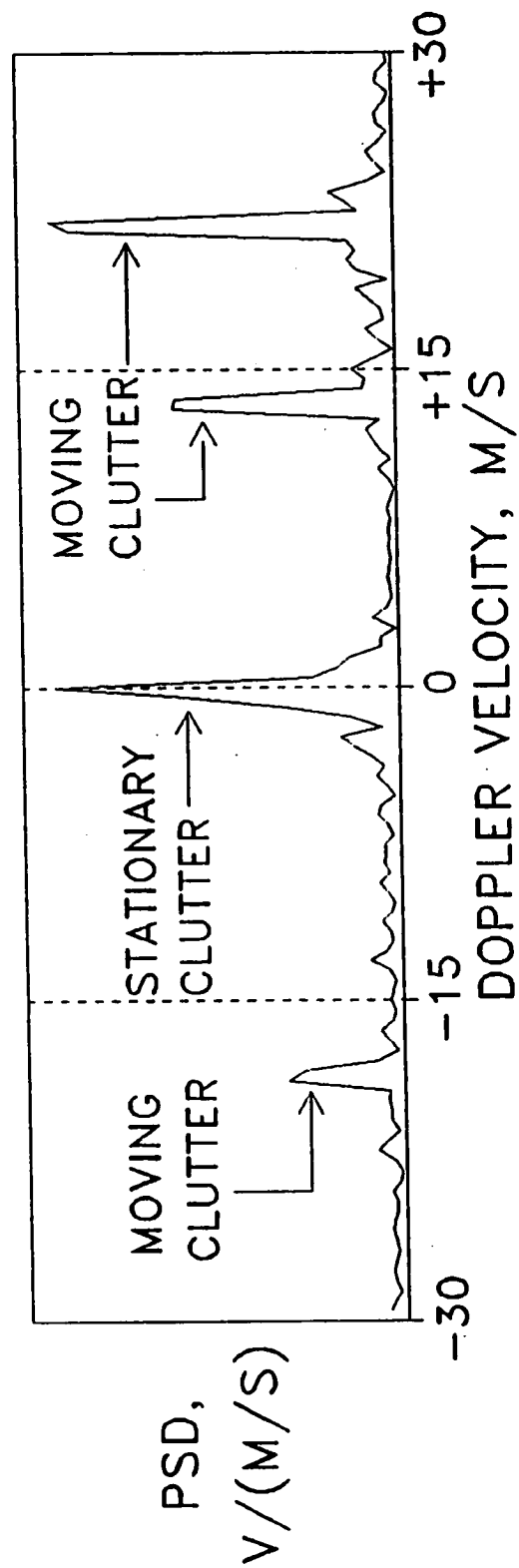
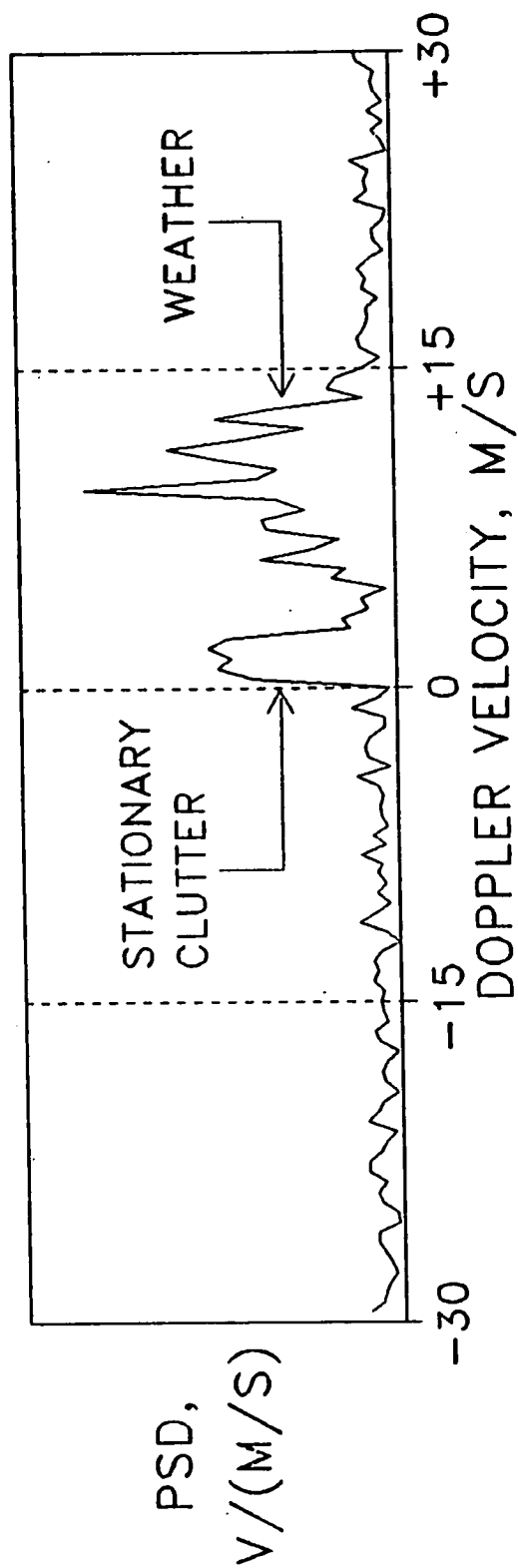


128 samples received from each range bin

Comparison of Weather and Clutter Doppler Spectral Shapes

After an FFT has been performed on a 128-point I,Q voltage time series, a 128-point Doppler velocity spectrum may be drawn from the magnitudes of the results. The spectrum represents power spectral density versus the detected radial velocities of targets in one range bin. A pulse repetition frequency of 3755 Hertz yields a velocity Nyquist interval of -30 to +30 meters per second. The lower plot shows a typical stationary ground clutter spike, which appears as a tall, pointed peak. The upper plot shows a typical weather spectrum, which looks like a collection of adjoining peaks in one area of the total spectrum. Moving clutter may appear as one or more distinct velocity peaks. Clutter may have higher or lower power spectral density than the weather target.

COMPARISON OF WEATHER AND CLUTTER DOPPLER SPECTRAL SHAPES

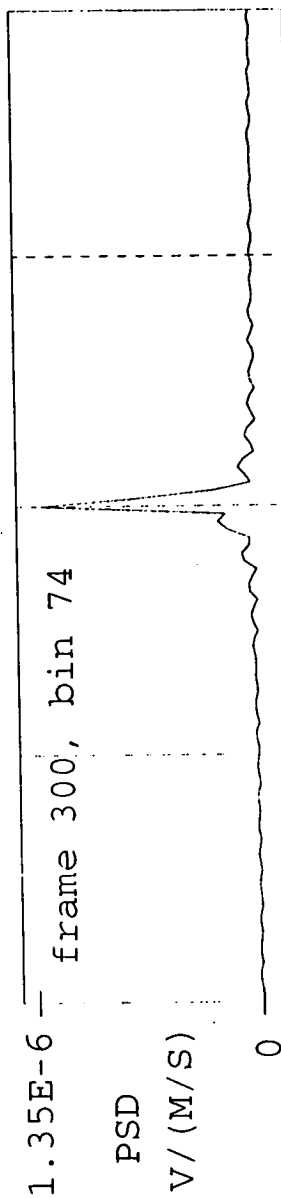


The Effect of Velocity Compensation on Stationary Ground Clutter

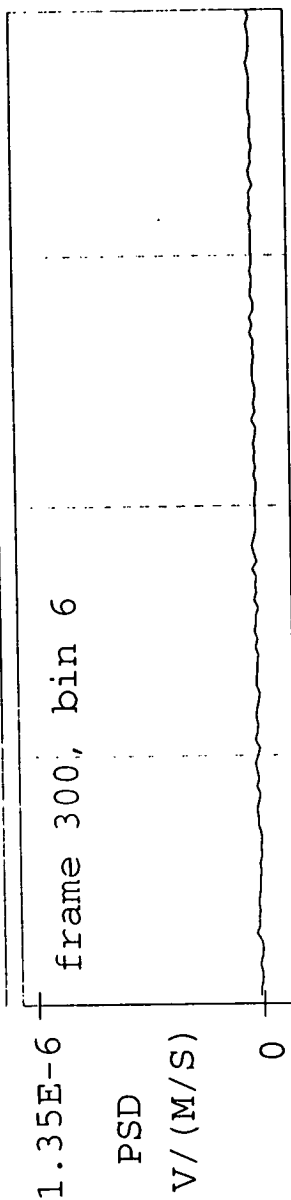
The radar receiver compensates in hardware for the apparent motion of the ground toward the airplane at the center of the antenna beam. For most range bins, this compensation puts the stationary ground clutter at the center of the velocity spectrum, which is zero meters per second. The velocities of stationary ground clutter not near the beam center will appear with an offset from zero, given by the equation at the bottom of the opposing page. The spectra shown are from a landing approach to the Philadelphia Airport. In most cases, stationary ground clutter from the near range bins, such as bin 6, is too far down on the antenna beam power pattern to be seen above the noise. However, an occasional very highly reflective object may appear in the spectrum with a velocity offset. Case 3 shows one of these occurrences.

THE EFFECT OF VELOCITY COMPENSATION ON STATIONARY GROUND CLUTTER

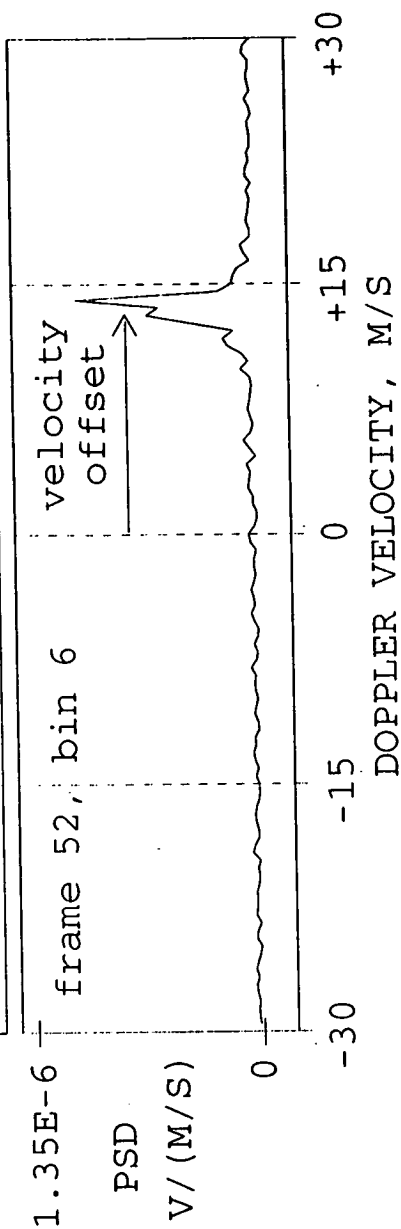
CASE 1:
MID OR FAR
RANGE BINS



CASE 2:
"USUAL"
CLUTTER IN
NEAR RANGE
BINS



CASE 3:
"UNUSUALLY
REFLECTIVE"
CLUTTER IN
NEAR RANGE
BINS



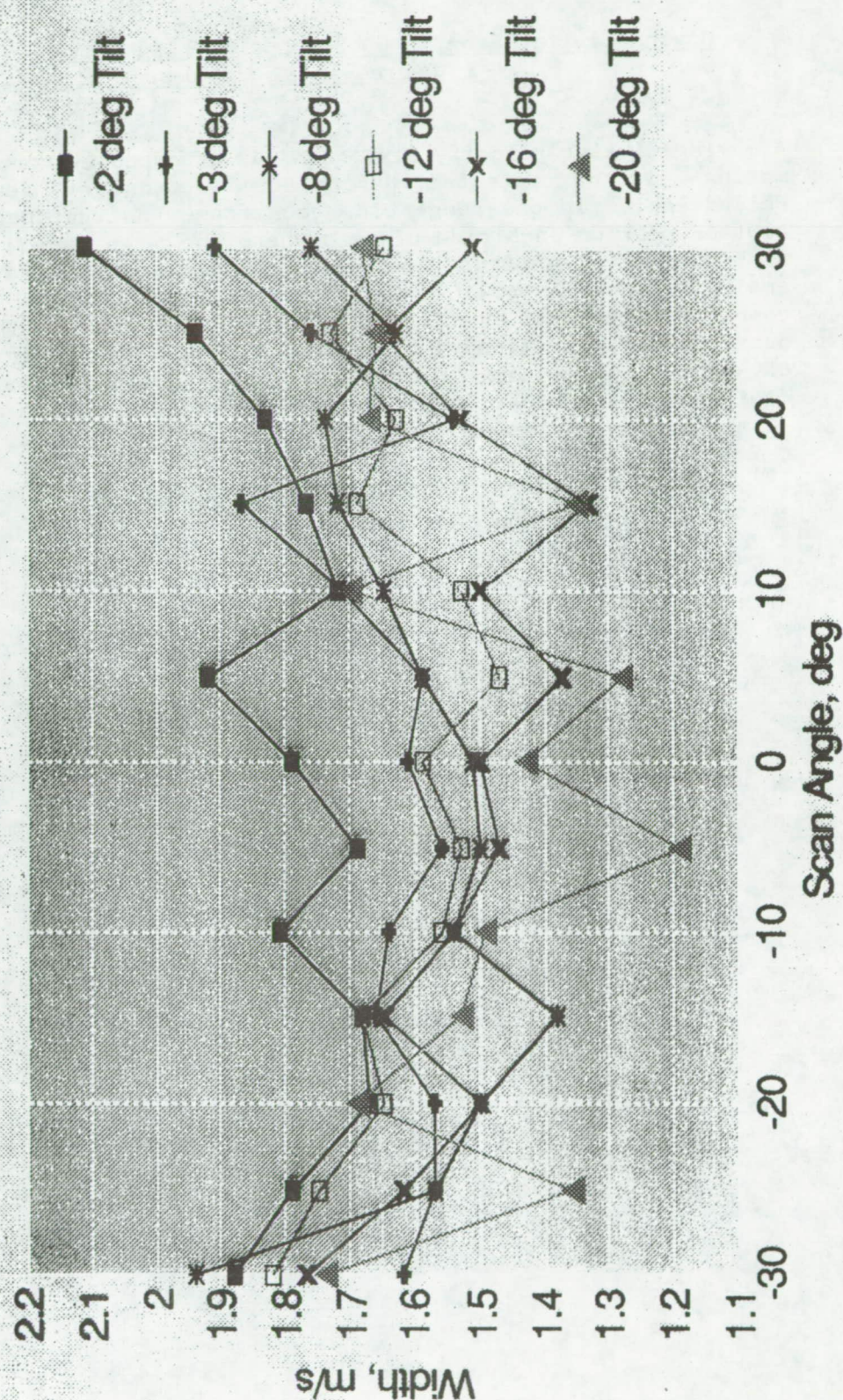
VELOCITY OFFSET = GOUNDSPEED * [COS(BORESIGHT DEPRESSION ANGLE)
- COS(CLUTTER DEPRESSION ANGLE)]

Spectral Width Versus Scan Angle

An initial look at Denver stationary ground clutter has yielded these spectral widths estimated by pulse pair processing. The data were taken from six level flights in clear weather over the Stapleton Airport, each flight with the antenna set at a different tilt angle. Average spectral widths were calculated versus scan and tilt angle, using those range bins where the antenna boresight intersected the ground. Data frames were excluded if their spectral width was more than 3.5 meters per second, since higher widths indicated the presence of moving clutter. The plot shows the width increasing toward the edges of the scan and decreasing as the antenna is tilted further downward.

SPECTRAL WIDTH VS SCAN ANGLE

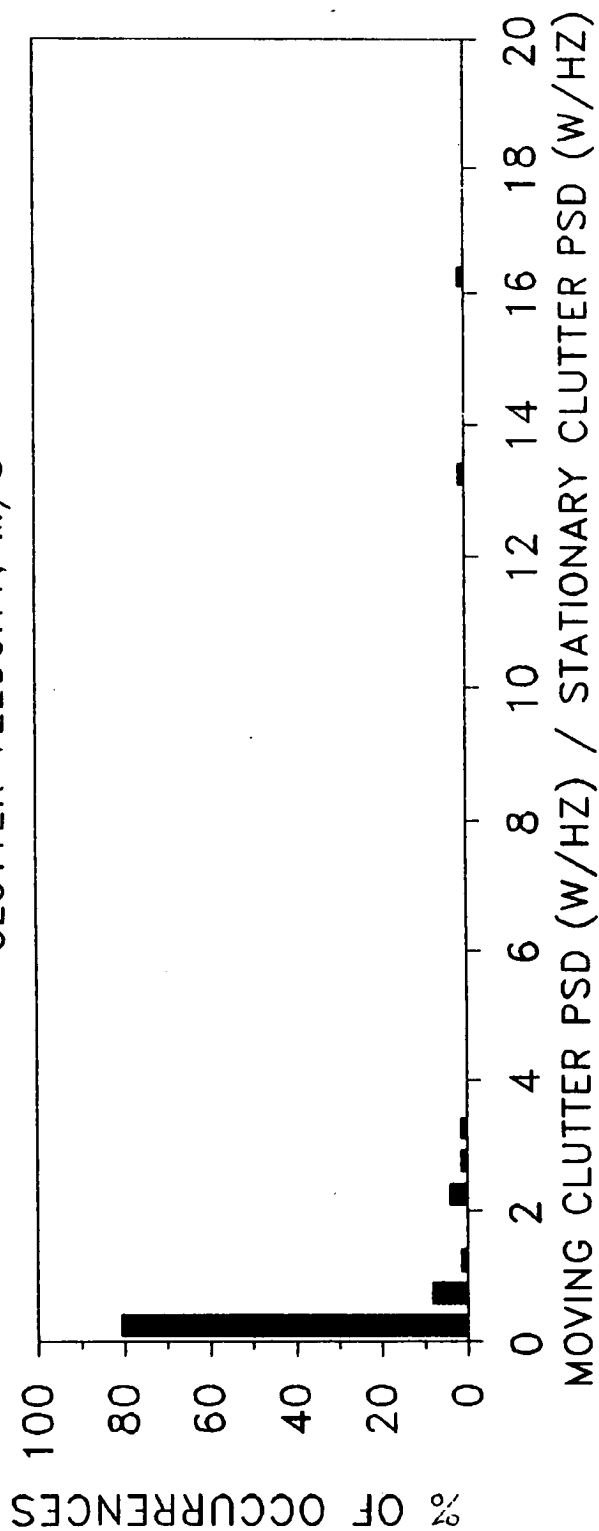
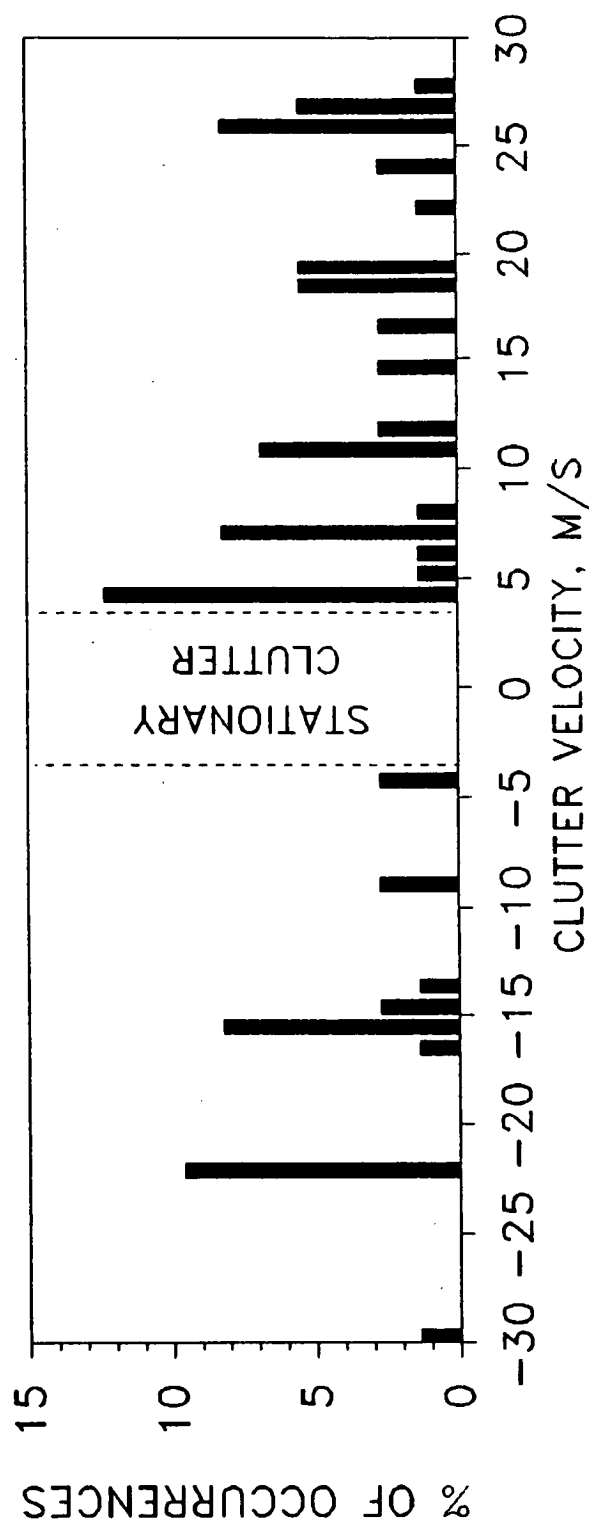
Stationary Clutter at Denver



Moving Clutter Seen in 30 Seconds of Flight Over Philadelphia:
-3 Degree Tilt, ±30 Degree Scan

A moving clutter velocity histogram was produced by counting instances of moving clutter detected during 30 seconds of level flight over Philadelphia. In one range bin, each frame was searched for the largest clutter peak on each side of zero where the power spectral density of the peak was more than four times the average power spectral density for the entire frame. A power spectral density histogram was produced by comparing the power spectral density of each peak to the power spectral density of the stationary clutter in the same frame. In over 90 per cent of cases, the moving clutter was less reflective than the stationary clutter. In the other 10 per cent of cases, the moving clutter was up to 16 times more reflective than the stationary clutter.

MOVING CLUTTER SEEN IN 30 SECONDS OF FLIGHT OVER PHILADELPHIA : -3 DEG. TILT, + 30 DEG. SCAN

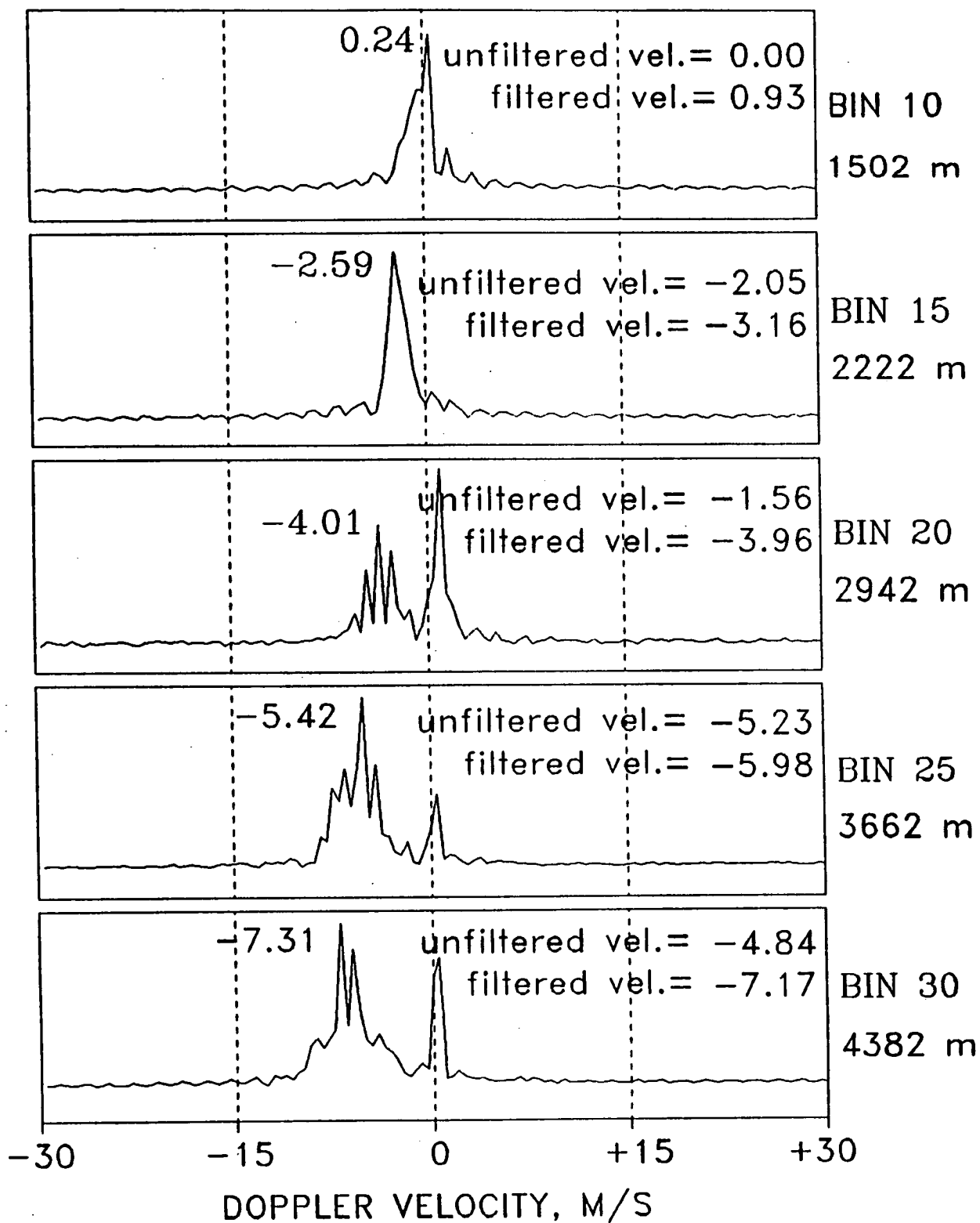


Wind Shear Viewed Along the 0.25-Degree Azimuth Line

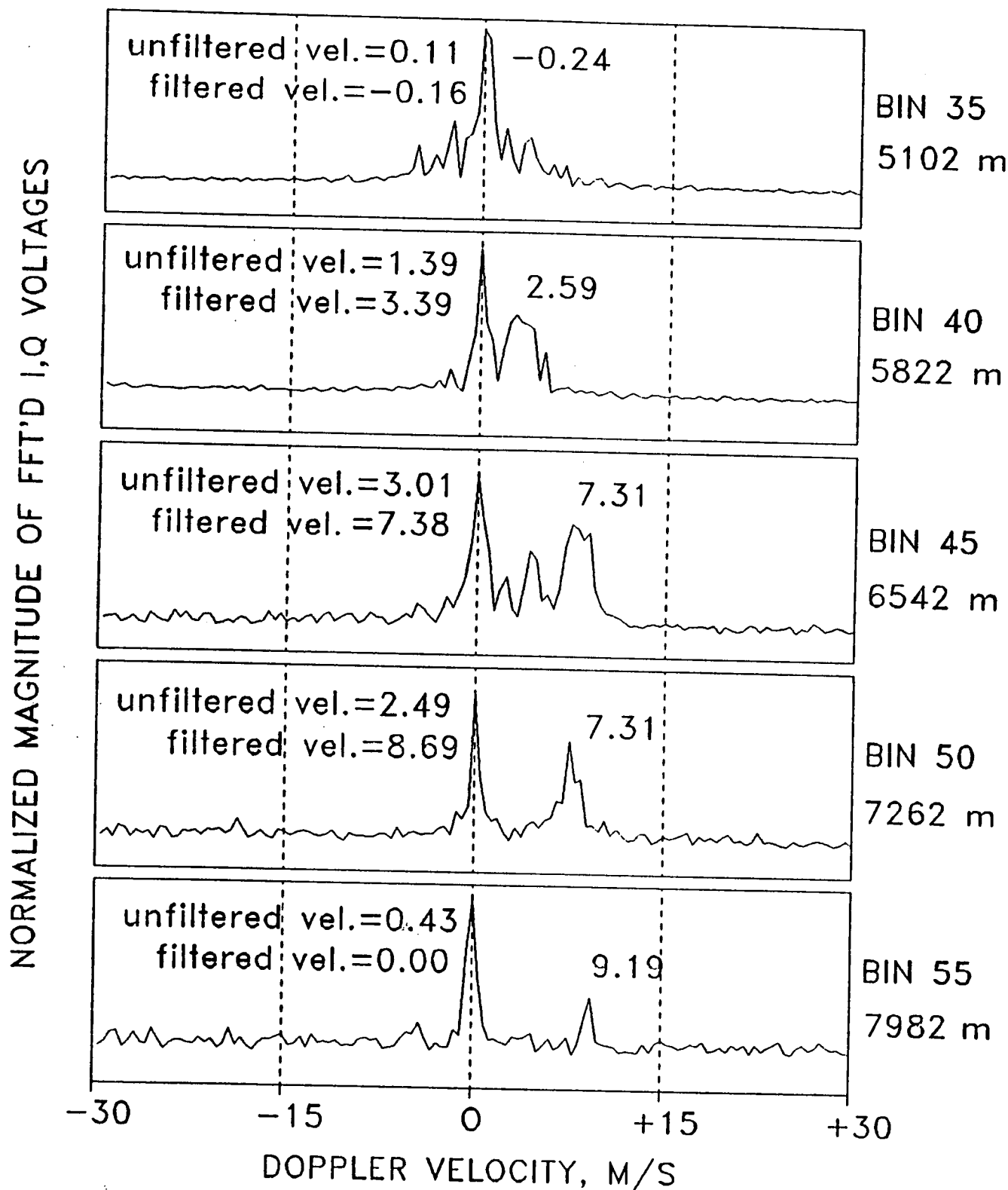
Looking along the 0.25-degree azimuth frame from range bins 10 to 55, we see weather velocities changing from near zero meters per second to -7 meters per second to +9 meters per second. Stationary ground clutter is also present in each bin. Pulse pair processing estimates of mean wind velocity are biased by stationary clutter velocity if no filtering is done. Improved wind velocity estimates are obtained by filtering out the stationary clutter prior to pulse pair processing. The filtered velocity map labeled "frm 1054" in the upper right corner shows weather velocities calculated for the above mentioned range bins in the center of the scan.

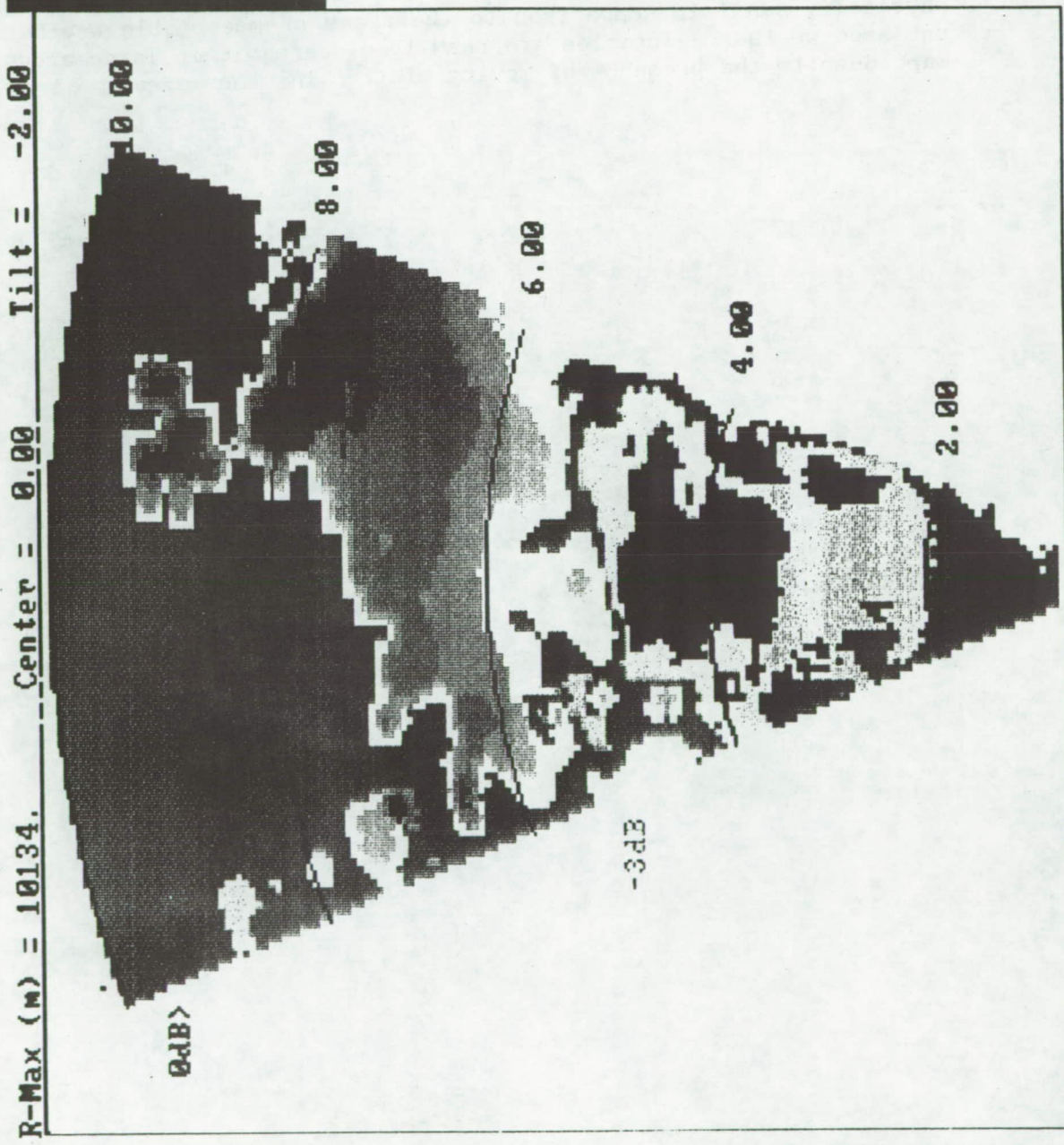
WIND SHEAR VIEWED ALONG THE 0.25° AZIMUTH LINE

NORMALIZED MAGNITUDE OF FFT'D I,Q VOLTAGES



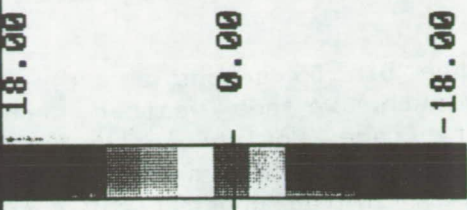
WIND SHEAR VIEWED ALONG THE 0.25° AZIMUTH LINE (CONTINUED)





CURSOR

LAI	28.5
LON	-81.2338
RG	5458.
AZ	0.
TILT	-3.49
FRM	1054
BIN	4
VAL	



DATE 6:20:91

TIME 20:45:21

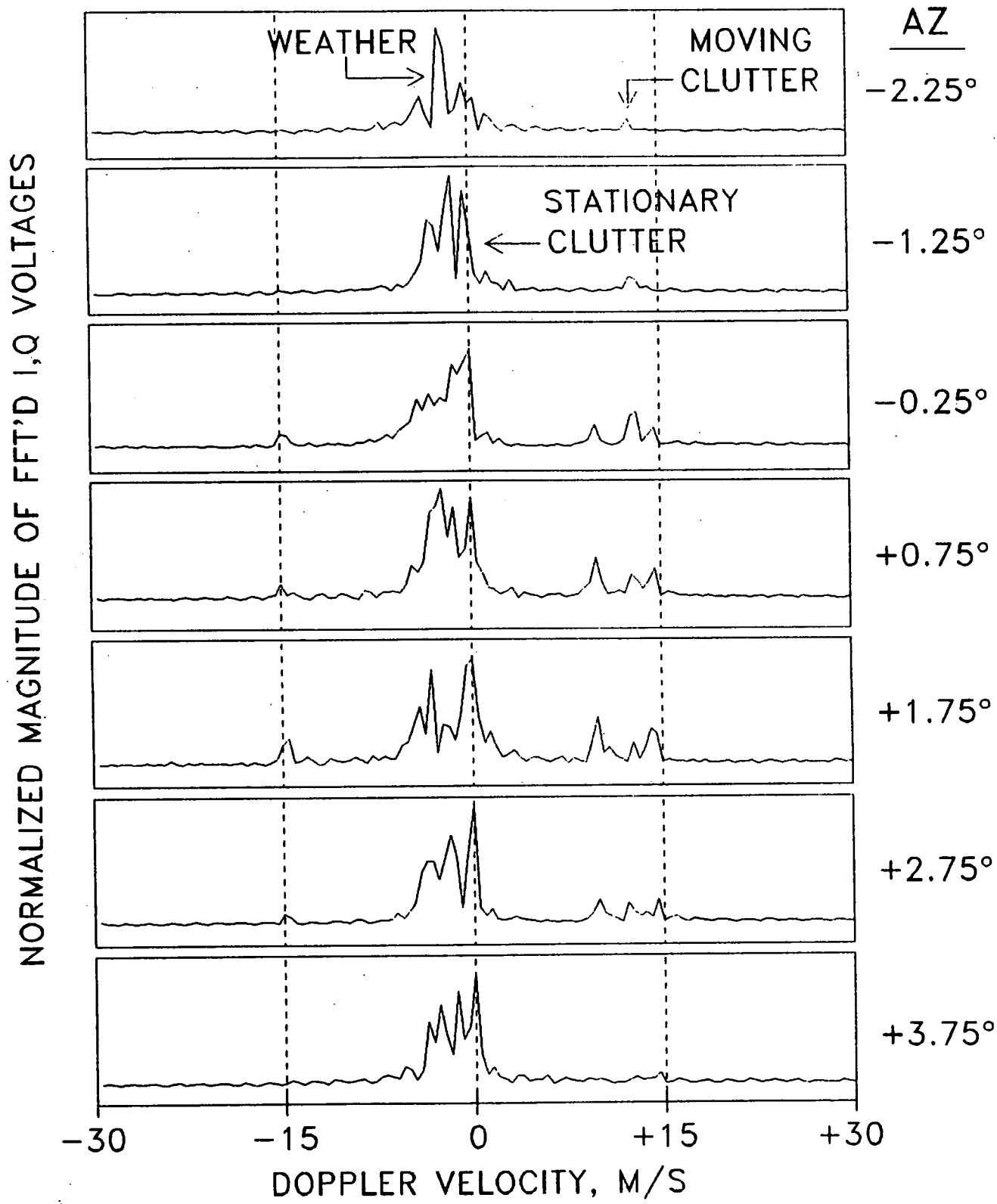
FRAME # 1096

R-Min (m) = 781. Alt (ft) = 1090. FILTERED WIND VELOCITY

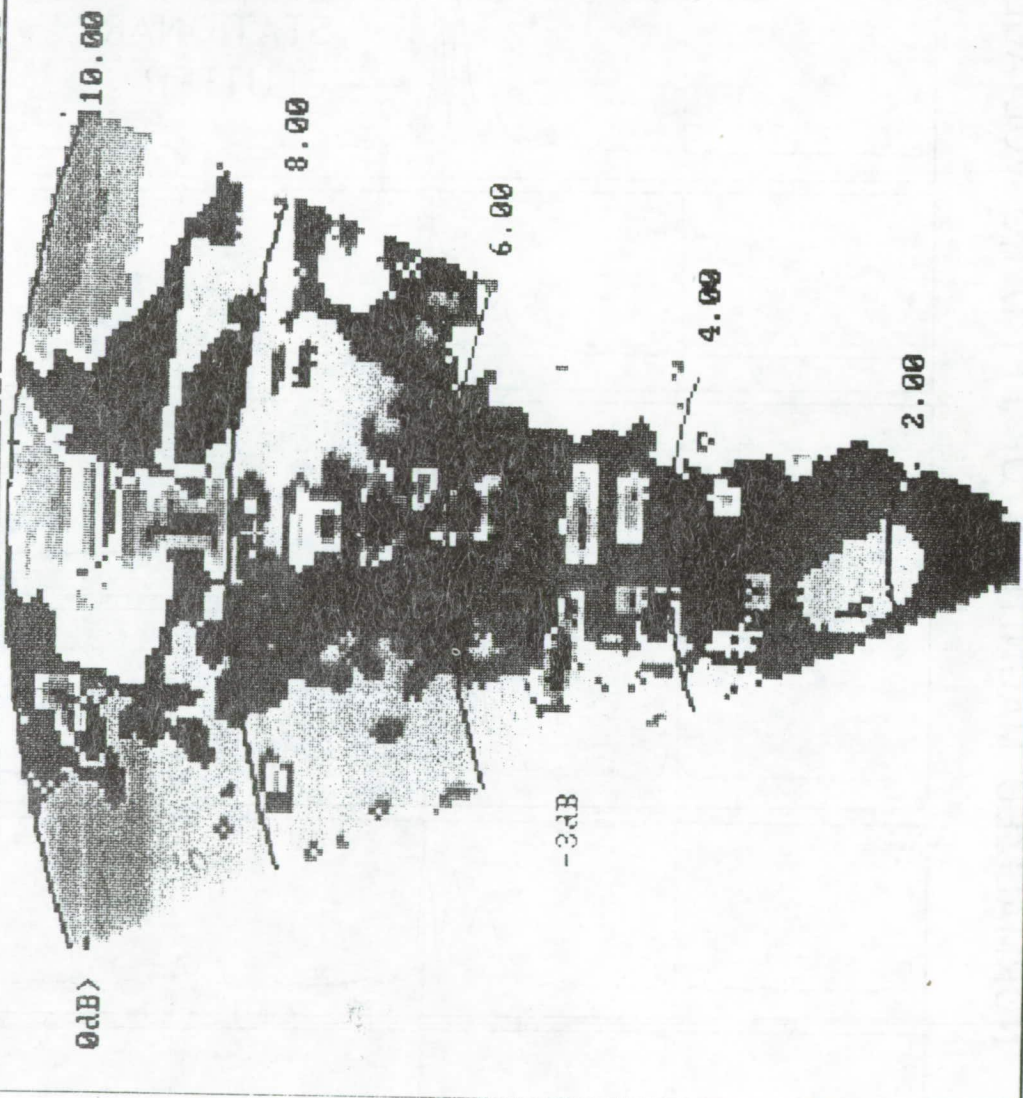
Comparison of Doppler Spectra from Range Bin 55
at Various Azimuth Angles

Looking at range bin 55 across a series of frames at -2.25 to +3.75 degrees in azimuth, we see weather accompanied by stationary ground clutter in every frame. Moving clutter appears, grows stronger, and fades as the antenna scans across a highway. In the filtered velocity map labeled "frm 142" in the upper right corner, the highway appears as a series of contrasting rectangular areas in a line down the center of the scan. Since only stationary clutter was filtered out before calculating the map velocities, some of the velocity estimates on the map are biased by the moving clutter. However, the areas of moving clutter are physically small in comparison to the areas of measurable weather. Thus, unbiased weather velocities are readily discernable in large areas of the map, despite the presence of moving clutter in other areas.

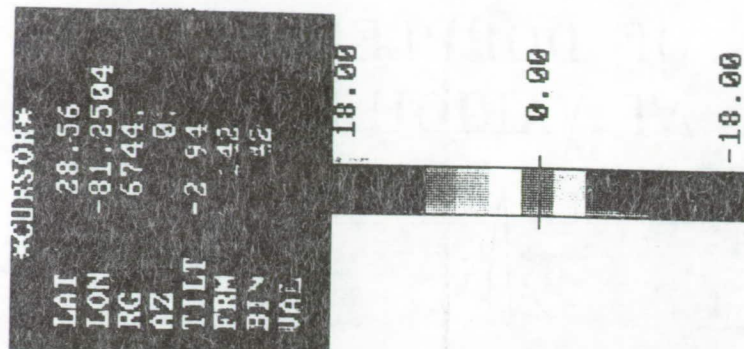
COMPARISON OF DOPPLER SPECTRA FROM RANGE BIN 55 AT VARIOUS AZIMUTH ANGLES



R-Max (m) = 10134. Center = 0.00 Tilt = -2.00



R-Min (m) = 781. FILTERED WIND VELOCITY Alt (ft) = 1134.



DATE 6:20:91

TIME 20:44:50

FRAME # 184

CONCLUSIONS

- Spectral width of stationary ground clutter is about 2 m/s at the edges of a ± 30 -degree scan.
- In all range bins, stationary ground clutter can be eliminated by velocity filtering.
- Weather spectra usually have greater spectral width than ground clutter spectra.
- Weather spectra may have higher or lower power spectral densities than clutter spectra.
- Although weather and clutter may be indistinguishable in single data frames, they may be distinguished in a map of the entire scan, due to the wider physical extent of the weather phenomenon.

Spectrum Characteristics of Denver and Philadelphia Ground Clutter and the Problem of Distinguishing Wind Shear Targets from Moving Clutter
Questions and Answers

Q: Jim Evans (MIT) - One of the important questions in reviewing the ability to reject ground clutter by filtering is what the base noise of your system is. What is the base noise of the system you are using in terms of instability residues?

A: Ann Mackenzie (NASA Langley) - You mean the noise of the receiver system?

Q: Jim Evans (MIT) - Well, it has to do with your transmitter system and the amplitude in phase variations it may apply as it puts out pulses, plus and noise in your local oscillator. What you will see when you analyze the spectrum, if you just sat on the ground and bounced the signals off of a nice target, is a big spike at zero velocity and then you will see a noised floor from anywhere from twenty to fifty or sixty dB down, that is almost flat. It turns out that is one of the expensive items in trying to build a pulse coherent radar, and it is an important element in terms of trying to understand the significance of your results. That is why I asked the question; what is the instability residue of your system? You can not build a system that puts out exactly to a thousandth of a dB the same pulse amplitude every time it transmits.

A: Brac Bracalente (NASA Langley) - I would like to address that. This is a design that was provided to us by Collins. All I can tell you is that it has a very stable low noise level. Our noise sensitivity is down around minus 110 dBZ and we see signals down that low. I can't tell you what the exact number is, that is something you will have to talk to Collins about. All I know is that it is a low number.

Q: Jim Evans (MIT) - That is not the right number. The number I am asking about is signal dependent noise?

A: Brac Bracalente (NASA Langley) - Are you talking about the clutter noise generated by jitter phase instability.

Q: Jim Evans (MIT) - Phase and amplitude instabilities either at the transmitter or the receiver.

A: Brac Bracalente (NASA Langley) - I can not give you the exact number on that. All I know is that it is pretty low. I think it is at a low enough level to not be a problem in the operation of the system.

1993010421

Session VI. Airborne Doppler Radar / NASA

N 93 - 19610

488744
24P

Comparison of Simulated and Actual Wind Shear Radar Data Products

Dr. C. Britt, Research Triangle Institute

L. Crittenden, Research Triangle Institute



Comparison of Simulated and Actual Windshear Radar Data Products

**Dr. C. Britt, RTI
L. Crittenden, RTI**

Comparison of Simulated and Actual Windshear Radar Data Products

**Charles L. Britt and Lucille H. Crittenden
Research Triangle Institute
Research Triangle Park, NC 27709**

**Abstract for Proposed Technical Talk for the
Fourth Combined Manufacturers' and Technologists'
Airborne Wind Shear Review Meeting
Williamsburg, Virginia
April 14-16, 1992**

Abstract

Prior to the development of the NASA experimental wind shear radar system, extensive computer simulations were conducted to determine the performance of the radar in combined weather and ground clutter environments. The simulation of the radar used analytical microburst models to determine weather returns and synthetic aperture radar (SAR) maps to determine ground clutter returns. These simulations were used to guide the development of hazard detection algorithms and to predict their performance.

The structure of the radar simulation will be reviewed. Actual flight data results from the Orlando and Denver tests are compared with simulated results. Areas of agreement and disagreement of actual and simulated results are pointed out.

COMPARISON OF SIMULATED AND ACTUAL WINDSHEAR RADAR DATA PRODUCTS

Charles L. Britt, Ph.D
Lucille H. Crittenden

VIEWGRAPH TITLES

Slide 1 -

Introduction - Comparison of Simulated and Actual Windshear Radar Data Products by Charles L. Britt and Lucille H. Crittenden.

Slide 2-

This is an overall flow chart of the Radar Simulation program developed for NASA by RTI personnel. The simulation inputs include: 1) a NASA-developed microburst data base for simulation of microburst radar returns; 2) synthetic aperture radar (SAR) maps from the Environmental Research Institute of Michigan (ERIM) for calculation of stationary ground clutter; and 3) a discrete target data base for simulation of moving ground clutter. A Monte Carlo technique is used to calculate the in-phase (I) and quadrature (Q) signals for each range cell of the radar. These signals are processed to power, velocity and hazard index using various signal and data processing algorithms.

Slide 3-

An example of a synthetic aperture radar (SAR) map of the Denver area. This map is used to determine the ground clutter level in the simulation.

Slide 4 -

This chart shows how the NASA flight test data is used to drive the simulation to permit direct comparison of simulated and actual radar data products.

Slide 5-

An example of a Denver ground scattering coefficient (σ_0) map obtained from NASA flight test data in July 1991. The location of runway 26R at Denver Stapleton airport is shown on the map. It should be noted that although the radar map is in σ_0 units, the actual values of σ_0 are valid only in the region where the antenna beam center intercepts the ground. Slides 10 and 11 show true σ_0 levels corrected for antenna pattern effects.

Slide 6-

An example of a simulated Denver ground scattering coefficient (sigma-zero) map using the NASA flight test data to provide aircraft position data for the simulation. This map is plotted for the same instant of time slide 5.

Slide 7-

This is a plot comparing simulated ground clutter levels with ground clutter levels obtained from flight tests. An ERIM supplied algorithm was used in the simulation to correct for the difference in incidence angles between the angles used in obtaining the SAR data and the angles required by the simulation.

Slide 8-

Plot similar to slide 7 except the ERIM incidence angle correction is not used for the simulation. Better correlations between flight and simulated data are obtained in this case. In both cases, an antenna tilt of -3 degrees is used.

Slide 9-

Plot of the frequency of occurrences of various clutter levels for flight and simulated data. The simulation used the SAR maps with no correction for incidence angle differences.

Slide 10-

Values of ground scattering coefficient (sigma-zero) obtained from a sample of flight data on a Denver approach to runway 26R. The aircraft altitude was 620 feet when the data were taken.

Slide 11-

Data taken under conditions similar to slide 10 except obtained from the simulation. The SAR clutter maps used in the simulation were uncorrected for incidence angle differences. Note that the mean value of sigma-zero is somewhat larger in this simulated case.

Slide 12-

Correlation calculations to determine if the simulation and flight data are properly registered spatially. The highest correlation is obtained with a lag of 2 range bins (288m) in the simulation using the SAR clutter maps. This indicates a difference of this magnitude in the coordinate systems used. For future comparisons of flight and simulated data, this registration error will be corrected.

Slide 13-

Conclusions from the results to date in the comparison of simulated and flight test data products. The comparison of simulated and flight data will continue.

COMPARISON OF SIMULATED AND ACTUAL WINDSHEAR RADAR DATA PRODUCTS

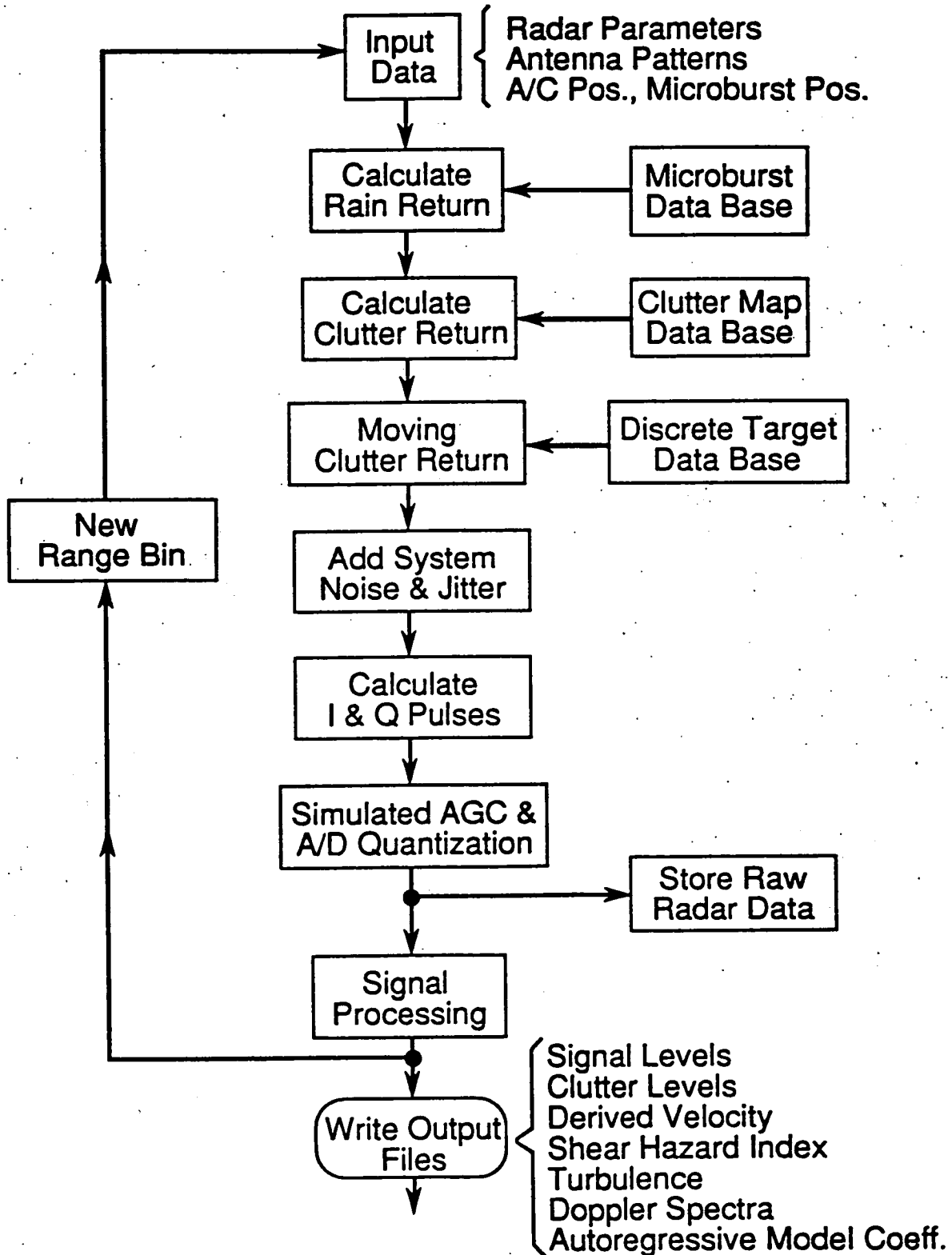
Charles L. Britt, Ph.D

Lucille H. Crittenden

**Research Triangle Institute
525 Butler Farm Rd. Suite 108
Hampton, VA 23666**



RADAR SIMULATION

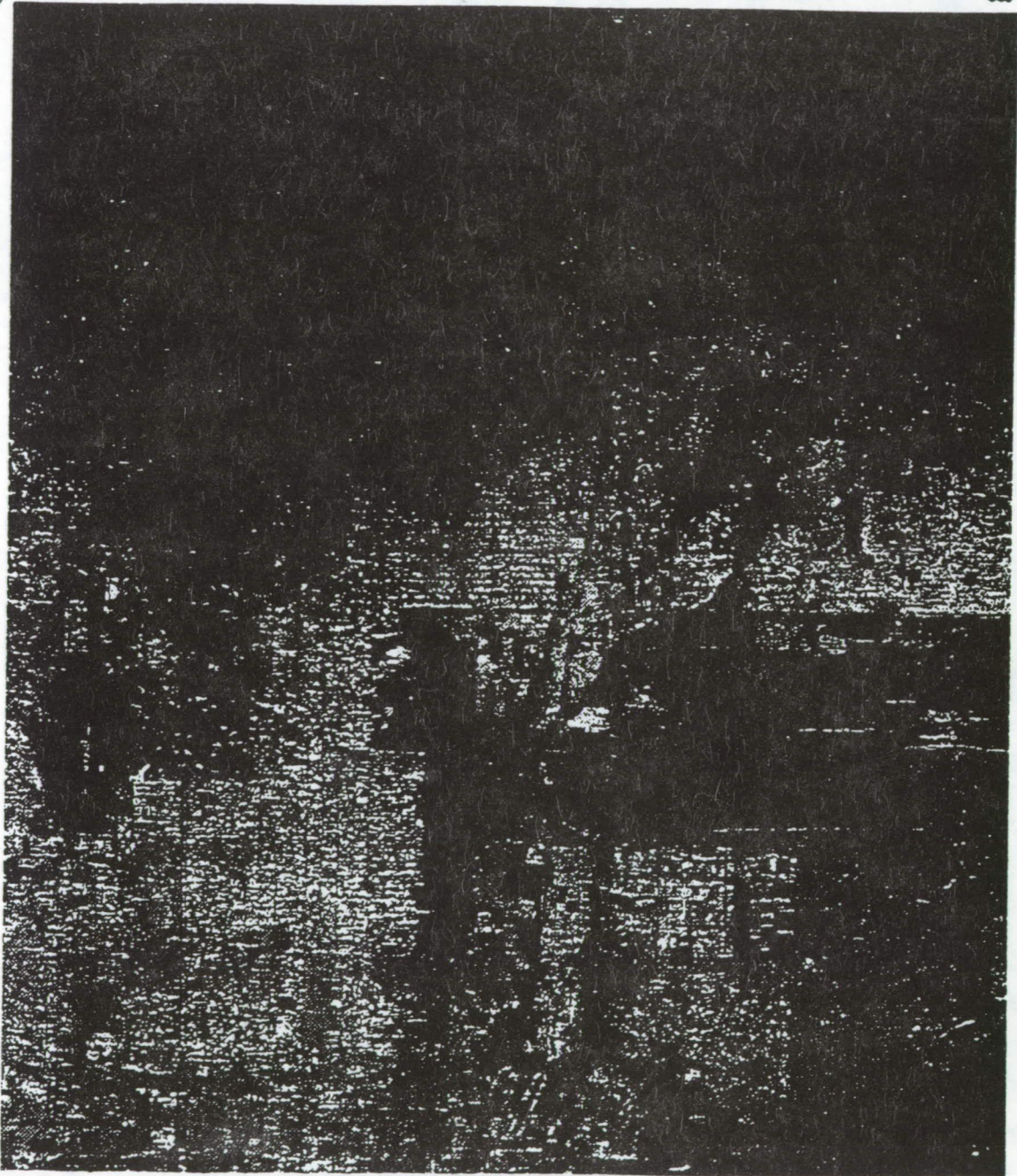


DENVER STAPLETON INTERNATIONAL
Image 1, 2nd Strip West
915 records, 683 elements/rec.

90¹

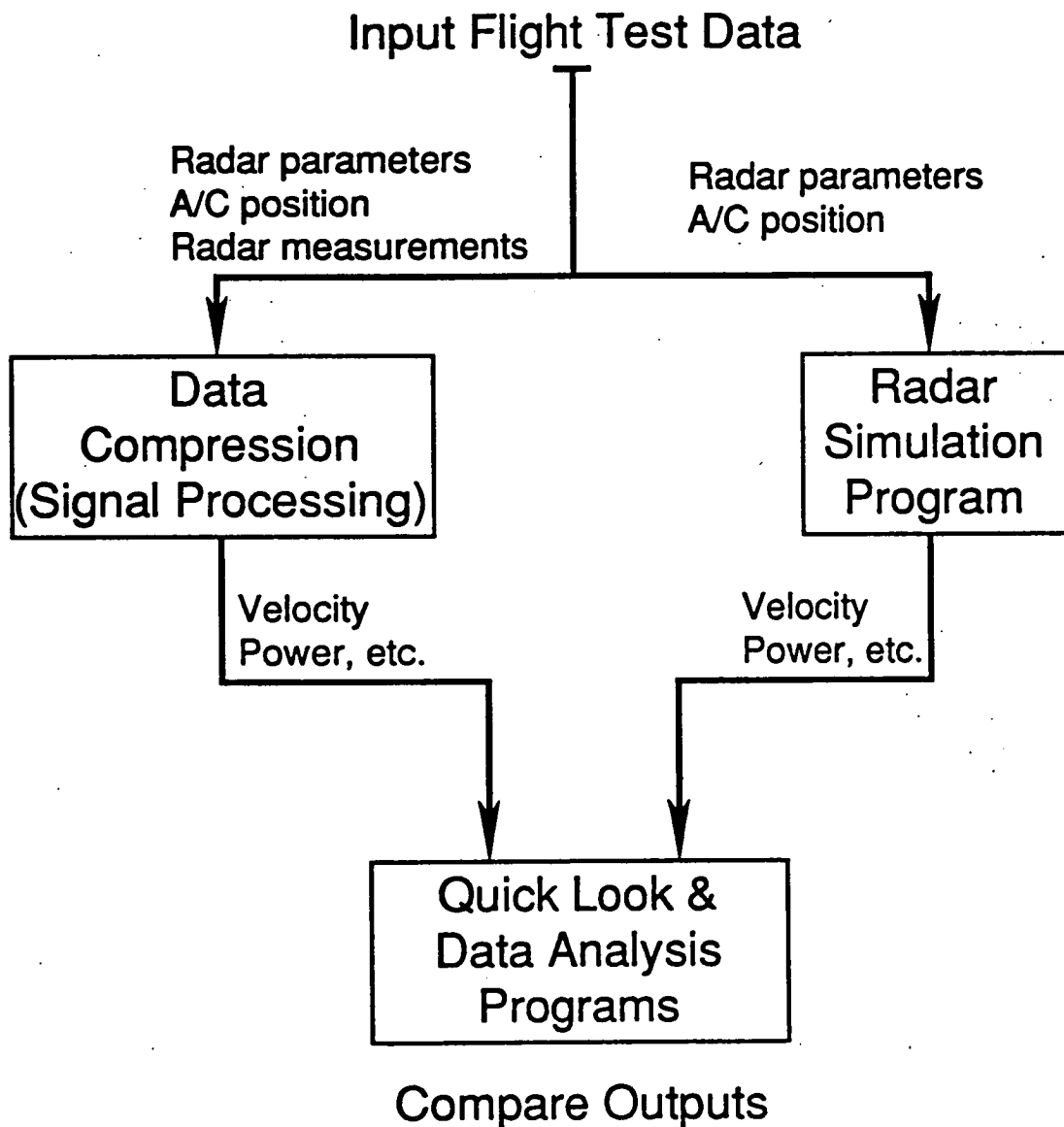
683

80
-16.5
-20.0
SCALE
40 db units



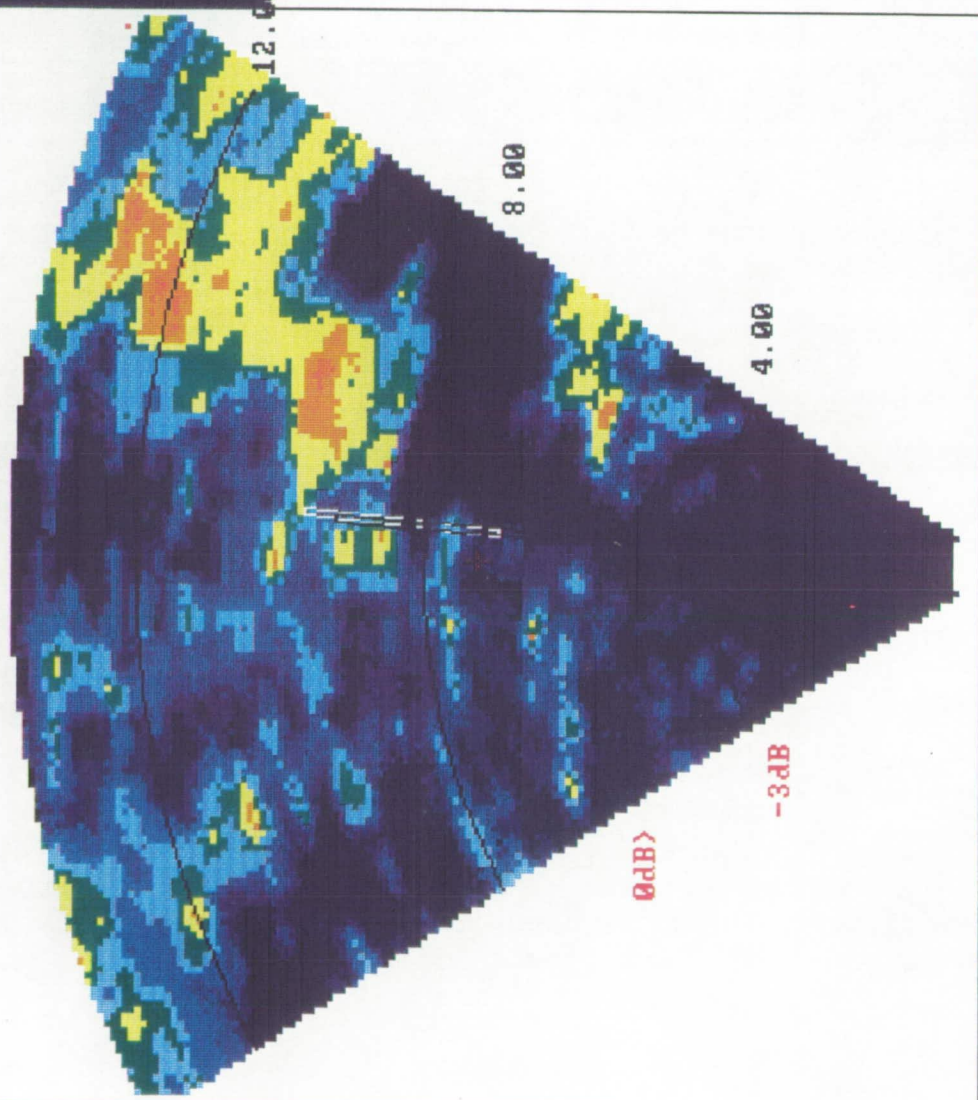
ORIGINAL PAGE IS
OF POOR QUALITY

COMPARISON OF SIMULATED AND ACTUAL RADAR DATA PRODUCTS



R-Max (m) = 13876. Center = 0.00 Tilt = -3.00

CURSOR
LAT 39.7503
LON -104.8723
RG 7328.
AZ 0
TILT -2.38
FRM 1117.
BIN 46.
VAL -37.34



R-Min (m) = 781. SIGMA ZERO - DB Alt (ft) = 998.

DATE 7: 7:91

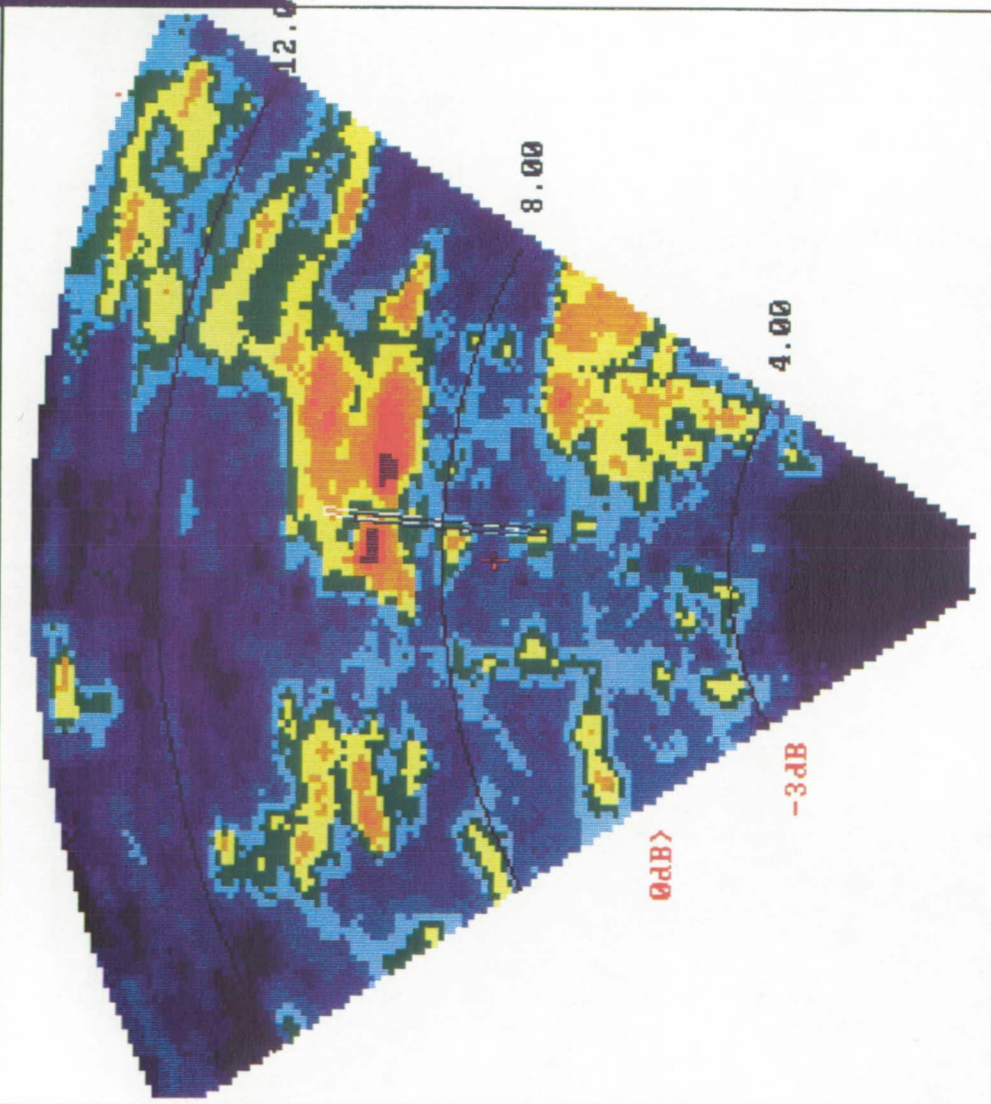
TIME 22:23: 1

FRAME # 1185

ORIGINAL PAGE
COLOR PHOTOGRAPH

P.550

R-Max (m) = 13876. Center = 0.00 Tilt = -3.00



CURSOR

LAT 39.7503
LON -104.8723
RG 7328.
AZ 0.
TILT -2.38
FRM 1117.
BIN 46.
VAL -34



DATE 7: 7:91

TIME 22:23: 1

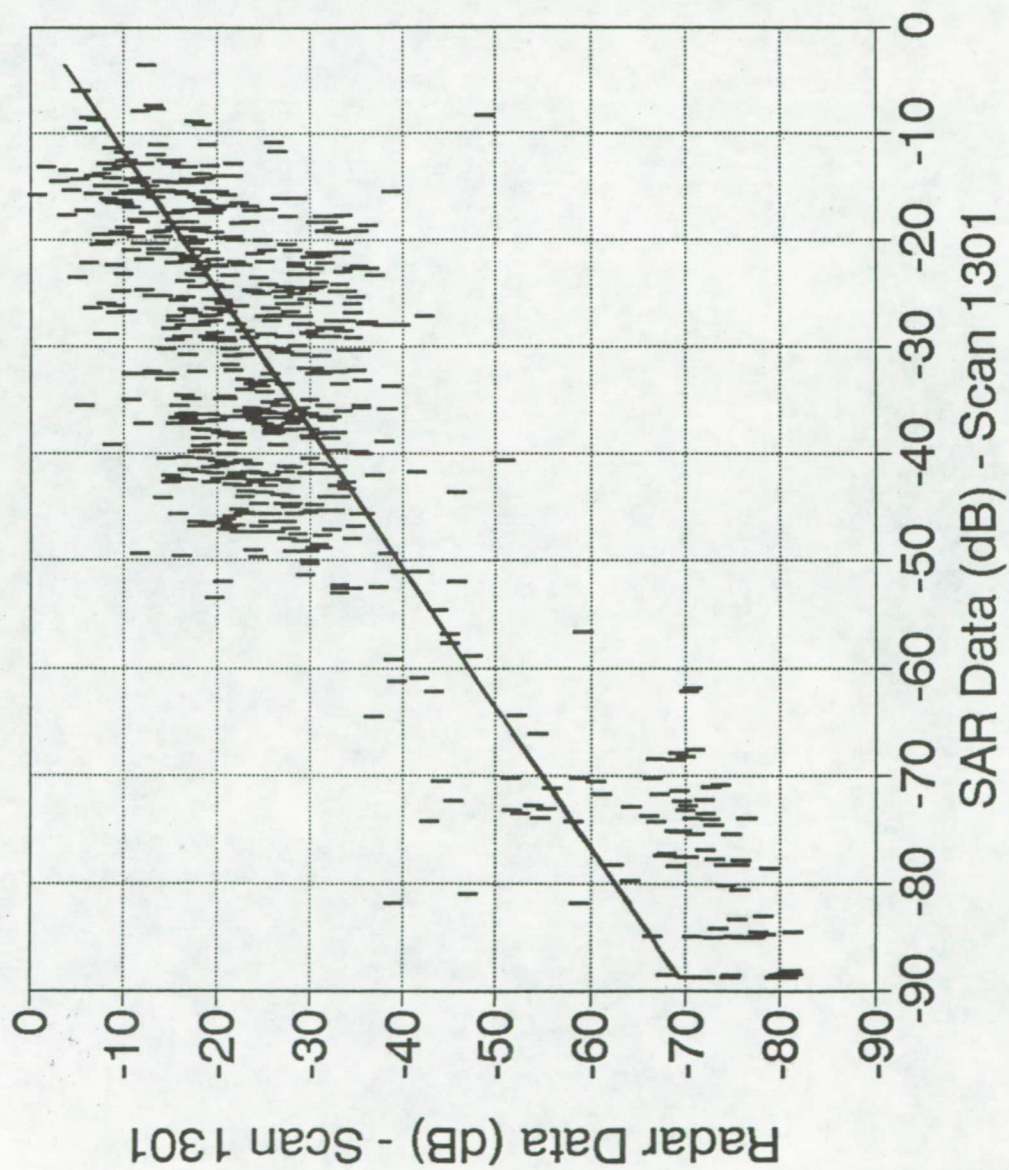
FRAME # 1193

R-Min (m) = 781. SIGMA ZERO - DB Alt (ft) = 998.

ORIGINAL PAGE
COLOR PHOTOGRAPH

Clutter Level Comparison-Denver

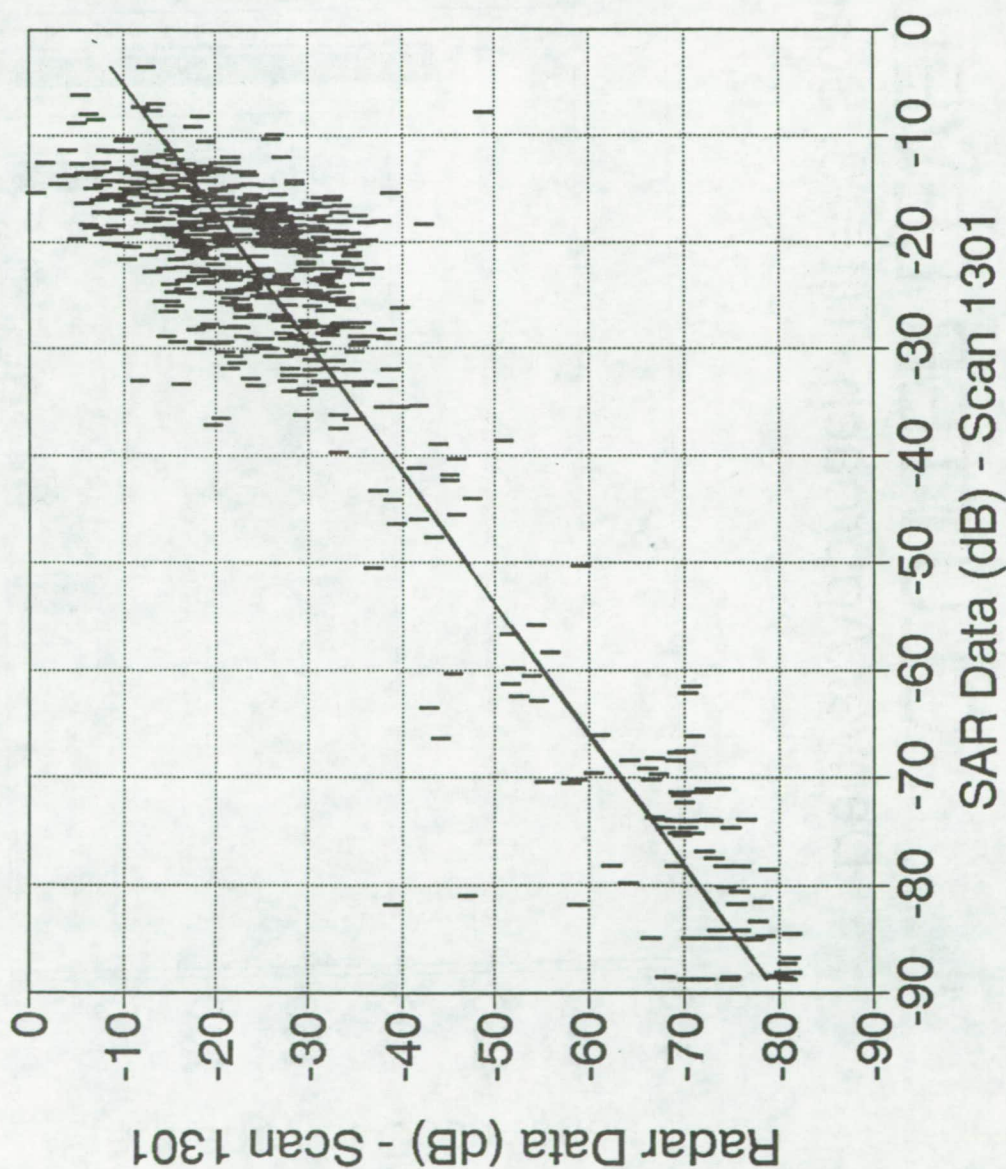
Incidence Angle Differences Corrected



RTI

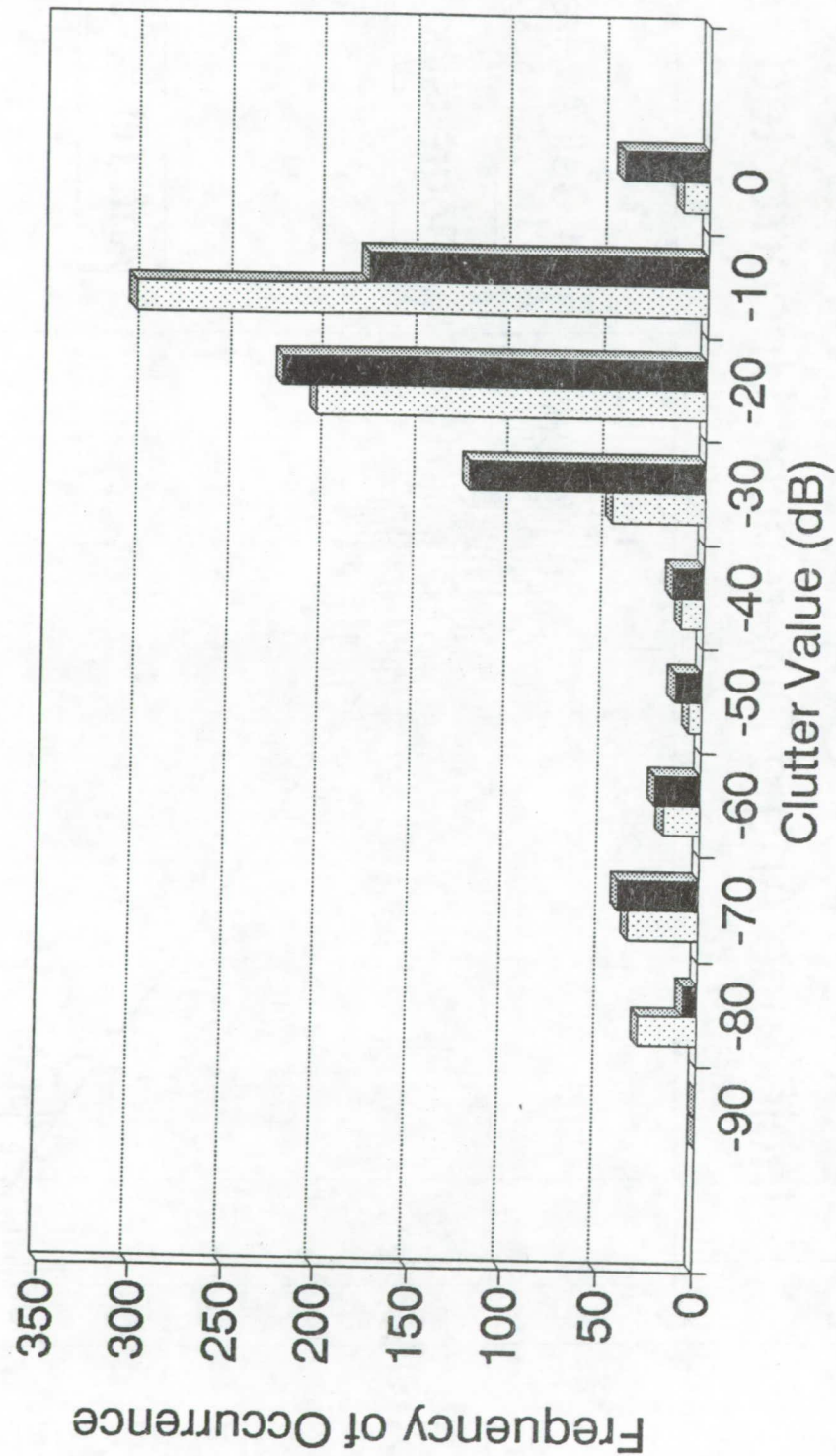
Clutter Level Comparison-Denver

Incidence Angle Differences Uncorrected



CLUTTER LEVELS

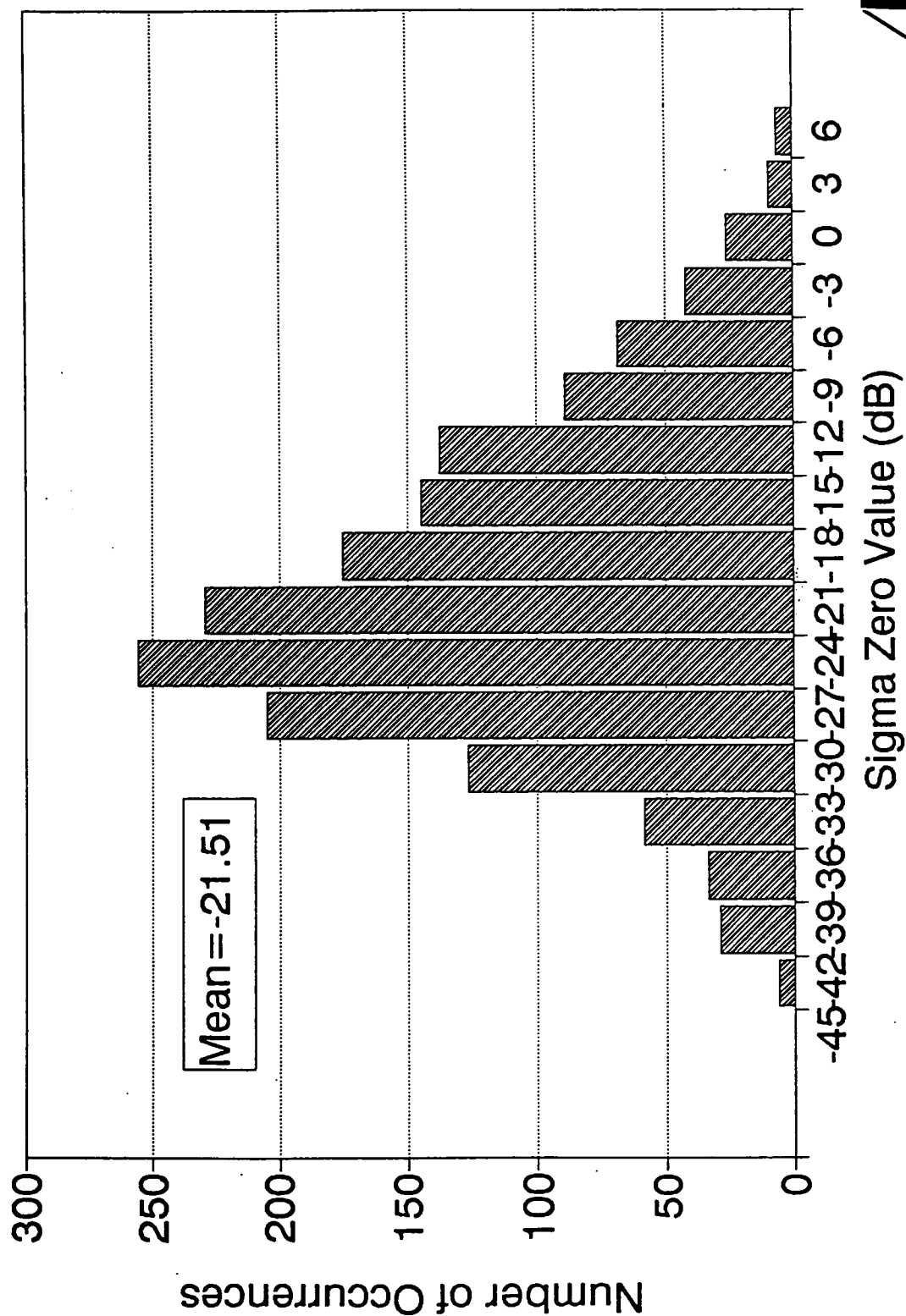
Denver Approach, Tilt=-3, Scan 1301



SAR Data (No Adj.) Radar Data

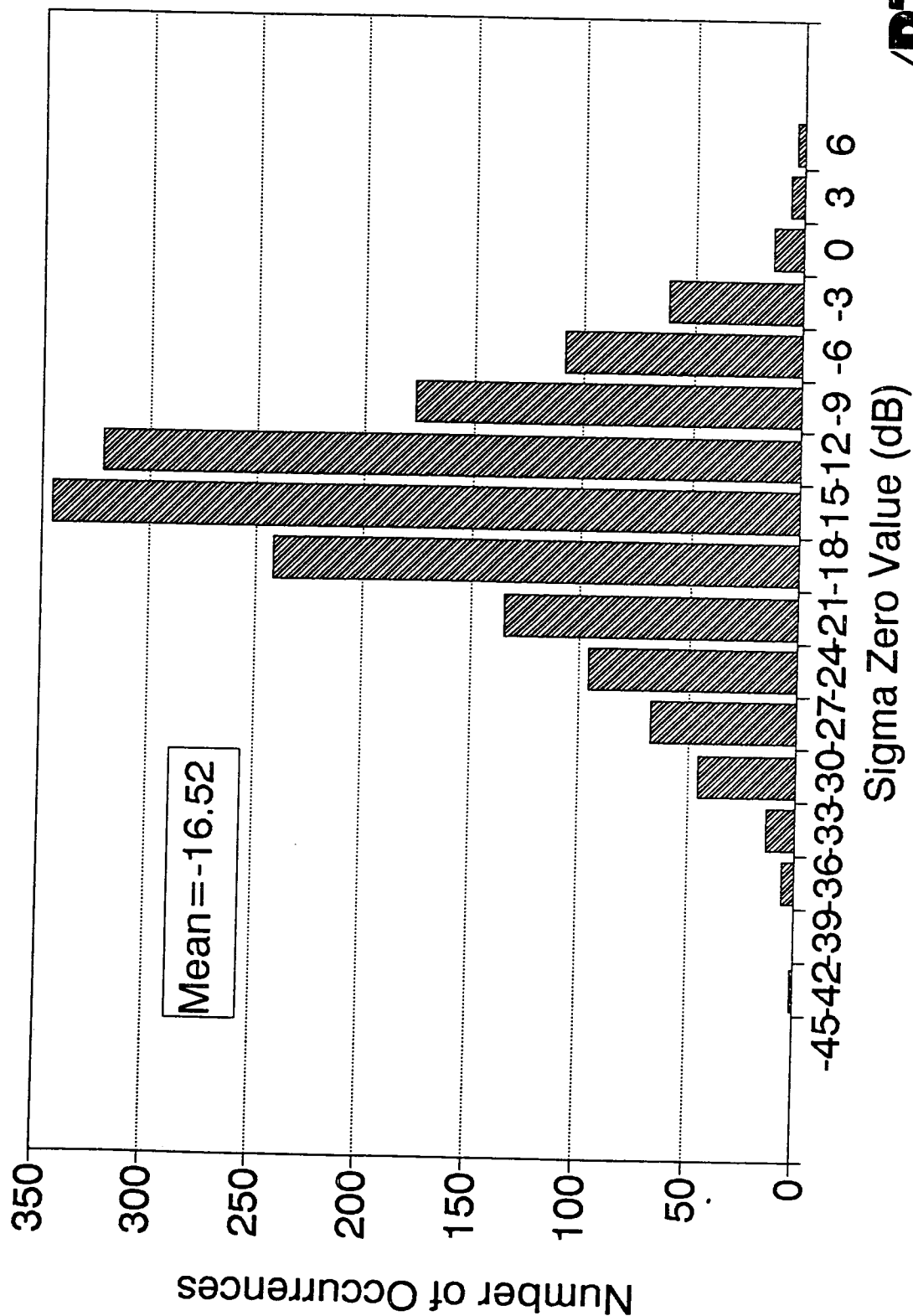
SCATTERING COEFFICIENT

Flight, DN1C2S1.M6, Frms 1791-1915



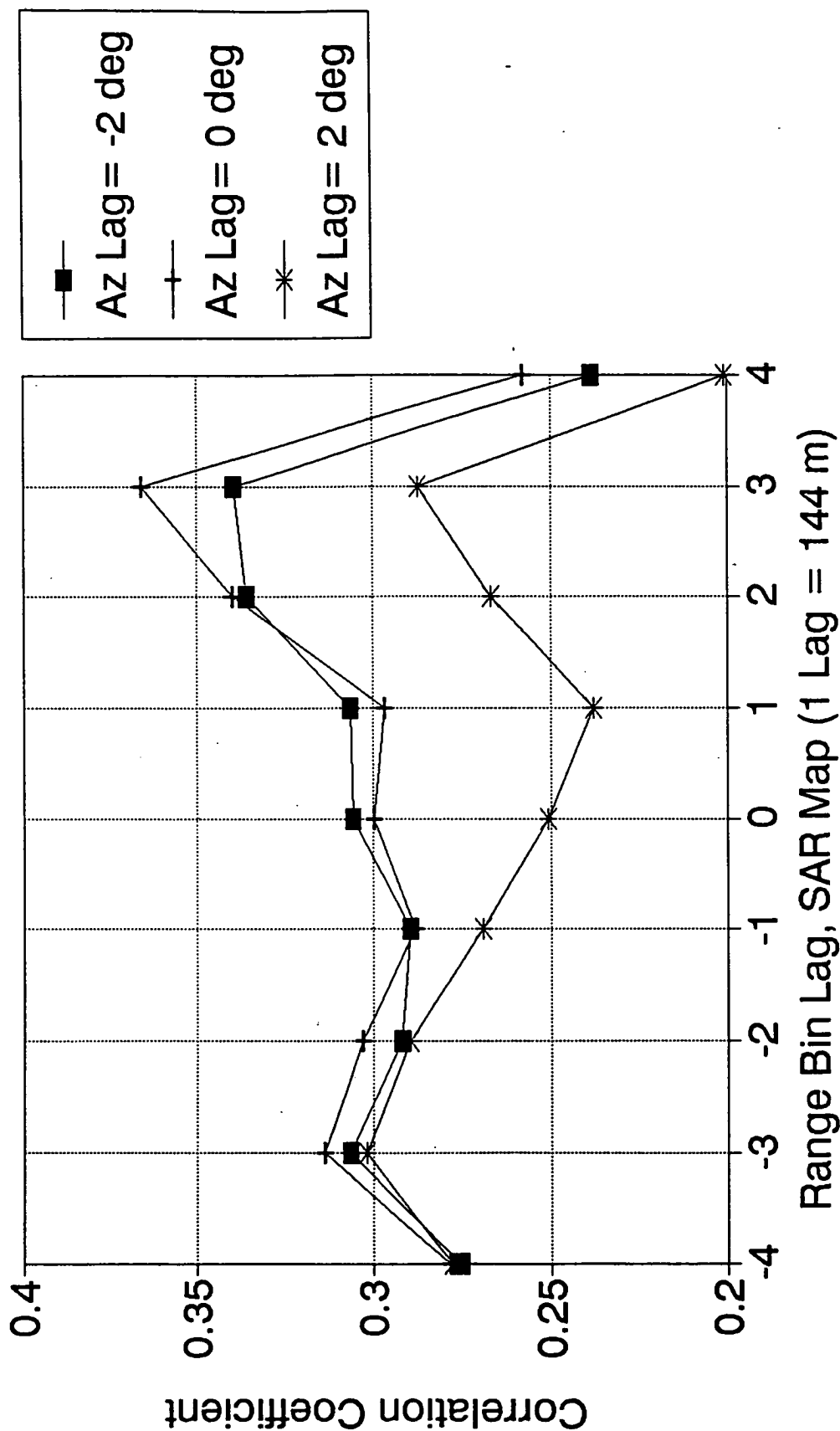
SCATTERING COEFFICIENT

Sim, DN1C2S1.M6, Frms 1791-1915



SAR MAP & DATA CORRELATION

Sigma Zero, Denver Approach, Tilt = -3



CONCLUSIONS

- **SIMULATION IS EXCELLENT TOOL FOR PREDICTION OF RADAR PERFORMANCE**
- **FOR ACCURATE CLUTTER FROM SAR MAPS IMPROVED INCIDENCE ANGLE CORRECTION ALGORITHMS MUST BE DEVELOPED**
- **USE OF NASA COLLECTED CLUTTER DATA WITH SIMULATED MICROBURSTS MAY PROVE TO BE THE BEST SIMULATION MODE**

/RTI

Comparison of Simulated and Actual Wind Shear Radar Data Products Questions and Answers

Q: Bruce Matthews (Westinghouse) - I think you have made a case that you have a good simulation of clutter, but how would you include that simulation of clutter into a radar? When would that be adequate?

A: Les Britt (RTI) - You mean to check the radar to certify it or something like that?

Q: Bruce Matthews (Westinghouse) - In your summary you state: "Simulation is an excellent tool for prediction of radar performance." You have just talked about a clutter model. How does that clutter model reflect what the radar equipment is? Do you have models for that also?

A: Les Britt (RTI) - We have in our simulation a baseline radar system which is basically our experimental system. That is what we use. We tried to simulate the flight system as well as we could, and that is our radar model that is in the simulation. The same number of A to D bits and that sort of thing.

Q: Brac Bracalente (NASA Langley) - So I guess you could add somebody else's design in there by proper modifications for their particular radar?

A: Les Britt (RTI) - Yes, if we knew all the parameters we could put someone else's radar model in there.

Q: Bruce Mathews (Westinghouse) - Does NASA recommend the use of the ADWRS clutter simulation with manufacturer furnished parameters as an adequate or reasonable alternative to other means of simulation, such as an RF injection driven by the SAR clutter maps?

A: Les Britt (RTI) - I think this has to do with the certification or system evaluation. I can't speak for NASA, but I doubt if they recommend either one. I don't think anybody knows. I think it is up to the manufacturer or perhaps the RTCA to determine how to evaluate the system.

Q: Jim Evans (MIT) - The clutter power not at the aircraft velocity is a key element of radar simulation performance. How are you modeling transmitter receiver instability residues, and the antenna side lobes with radome on, especially those at negative elevation angles? What experimental measurements have been or will be done to validate the assumptions?

A: Les Britt (RTI) - I will take the second part first. The antenna model used in the simulation is actually a table of measured data taken with the antenna and radome, over plus or minus 90 degrees, in the NASA anechoic chamber. So it includes all the side lobes. The data was taken in two principle planes but it was searched in three dimensions for any spurs or little peaks, and we did find one small peak which is in the data. We modeled a full 3-D pattern using the two principle planes with an interpolation scheme to go between the two principle planes. The first part of the question was the transmitter receiver instability. I brought some slides to show how we do that in the simulation. For each range bin we generate a series of I&Q depending on how many pulses we simulate. Currently it is running around 128. We model the clutter in the return

with a Monte Carlo technique which uses a set of random phased scatterers. Each range bin is divided up into five or six thousand incremental areas, each one assigned a random phase which is held fixed over the 128 pulse variation. The transmitter error is modeled with a random phase error which is currently a white noise model. In other words, it is changed from pulse to pulse in accordance with a normal distribution, which is an input parameter. You input the variance and it pulls out a transmitter phase error which is modeled as a linear function. You can also put a frequency drip in there, if you want to. It is modeled from pulse to pulse. You can get more elaborate with the phase model but that is the one we are currently using. We use an RMS phase error now of 5 degrees. We have run it up to 10 or 20 to see what effect it has, but that is currently what we are using. How is it validated? Basically by estimates from Collins and what have you. We talked to some tube manufacturers when we went through this two or three years ago, to get some number to put in there. It does not represent every transmitter, but we feel like it represents ours fairly well.

19930104 22

N93-19611

Session VI. Airborne Doppler Radar / NASA

488746
260

NASA Airborne Radar Wind Shear Detection Algorithm and the Detection of Wet Microbursts in the Vicinity of Orlando, Florida

**Dr. C. Britt, Research Triangle Institute
E. Bracalente, NASA Langley Research Center**



***NASA Airborne Radar
Windshear Detection Algorithm and
the Detection of Wet Microbursts
in the Vicinity of Orlando, Florida***

**Dr. C. Britt, RTI
E. Bracalente, NASA LaRC**

**NASA Airborne Radar Windshear Detection Hazard Algorithm and the
Detection of Wet Microbursts in the Vicinity of Orlando Florida**

**Charles L. Britt
Research Triangle Institute
Research Triangle Park, NC 27709**

and

**Emedio Bracalente
NASA Langley Research Center
Hampton, VA 23665**

**Abstract for Proposed Technical Talk for the
Fourth Combined Manufacturers' and Technologists'
Airborne Wind Shear Review Meeting
Williamsburg, Virginia
April 14-16, 1992**

Abstract

The algorithms used in the NASA experimental wind shear radar system for detection, characterization and determination of windshear hazard are discussed. The performance of the algorithms in the detection of wet microbursts near Orlando is presented. The talk will also review various suggested algorithms that are currently being evaluated using the flight test results from Denver and Orlando.

**NASA AIRBORNE RADAR WINDSHEAR DETECTION HAZARD ALGORITHM
AND THE DETECTION OF WET MICROBURSTS IN THE VICINITY
OF ORLANDO FLORIDA**

Charles L. Britt, Ph.D
Research Triangle Institute

Emedio Bracalente
NASA Langley Research Center

VIEWGRAPH TITLES

Slide 1 -

Introduction - NASA Airborne Radar Windshear Detection Hazard Algorithms and the Detection of Wet Microbursts in the Vicinity of Orlando Florida

Slide 2-

Example of a hazard index display from the NASA experimental windshear radar system. The algorithms to be discussed are designed to provide for timely windshear hazard alerts in the presence of ground clutter with no false alarms triggered by the ground clutter.

This hazard map is from flight data taken at Orlando, Florida on 6/20/91 and represents a wet microburst (Event #143) with a peak hazard factor of approximately .15. The subsequent flight of the aircraft through the microburst confirmed the hazard index through in-situ measurements. Agreement between the radar predictions and in-situ measurements was excellent.

Slide 3-

Techniques used in the NASA experimental radar to enhance the detection of a windshear hazard.

Slide 4-

Example of a plot of received power level vs. radar range showing the operation of the fast-acting radar AGC and the wide dynamic range seen along a range bin of the radar. Data from Orlando flight through microburst event #143.

Slide 5-

Chart showing various signal processing techniques that are being evaluated to separate the ground clutter and weather signals. The flight data is processed using various combinations of these processing techniques.

Slide 6-

Example of the Doppler spectrum obtained in range bin #47, frame 366 of Orlando event #143 (a wet microburst penetration). The mean wind velocity is approximated 6 m/s.

In processing the radar data, a 2-pole time-domain IIR filter was used with no data weights. The ground clutter is located at frequency line #65.

Slide 7-

Doppler spectrum taken under the same conditions as slide 6, except that Hann data weighting is used.

Slide 8-

Doppler spectrum taken under the same conditions as slide 6, except that FFT processing, Hann data weighting and spectral line editing is used.

Slide 9-

Doppler spectrum taken under the same conditions as slide 6, except that autoregressive (AR) processing, Hann Data weighting, and spectral line editing is used.

Slide 10-

Radar velocity map of microburst event #143 using a 2-pole IIR filter with Hann data weights and time-domain pulse-pair velocity estimation.

Slide 11-

Radar velocity map similar to slide 10 except using a spectral domain (FFT) filter (line editing) with spectral domain pulse-pair velocity estimation.

Slide 12-

Criteria for determining a valid velocity measurement in each range bin.

Slide 13 -

Algorithms used for calculation of the hazard factor.

Slide 14-

Plot illustrating the technique of least-squares hazard estimation. Five wind velocity measurements along a range line are used to estimate the slope of the velocity/range line which is proportional to the radial hazard index. In some cases, a weighted least squares technique is used whereby the velocity measurements are weighted by the value of spectral width. Measurements with smaller values of spectral width are given more weight in the slope calculation. This calculation is made for each range bin along a range line to provide an estimate of hazard for each range bin.

Slide 15-

Algorithms used to determine the extent of the hazard.

Slide 16-

Technique for determining the area and centroid of a hazard region as it appears on the radar map. The hazard region is a region of the radar map where the total hazard index is above a threshold value ($\sim .105$)

Slide 17-

Criteria used to display windshear alert on the radar display.

Slide 18-

Summary of the various thresholds used in processing flight data. The set of baseline thresholds given in the chart provide good results in the detection of windshear hazards and the elimination of false alerts. These thresholds are still under evaluation.

Slide 19-

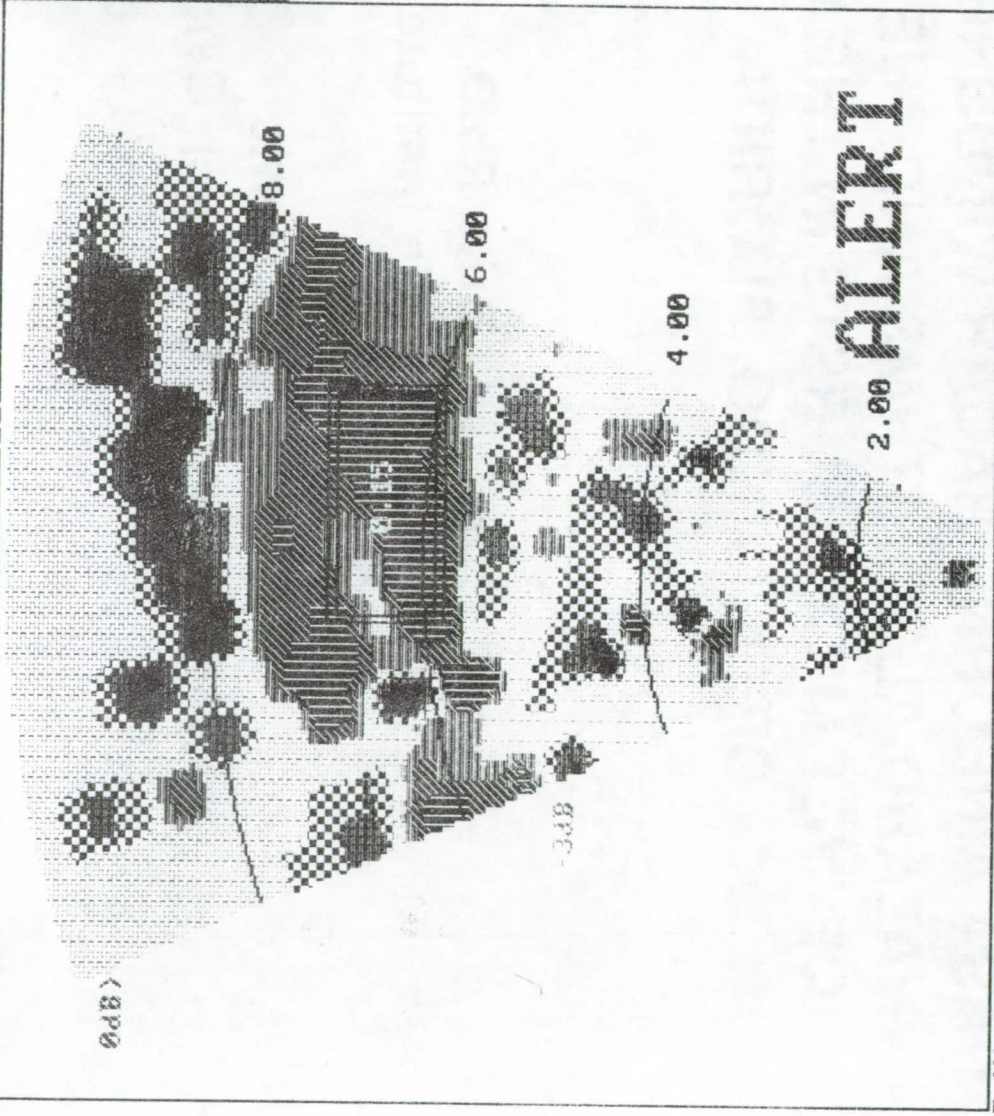
Conclusions from evaluation of signal and data processing algorithms to data.

**NASA AIRBORNE RADAR WINDSHEAR DETECTION
HAZARD ALGORITHMS AND THE DETECTION
OF WET MICROBURSTS IN THE VICINITY
OF ORLANDO, FLORIDA**

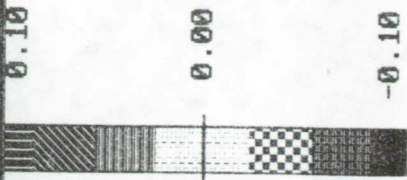
**Charles L. Britt, Ph.D
Research Triangle Institute**

**Emedio Bracalente
NASA Langley Research Center**

R-Max (m) = 9991. Center = 0.00 Tilt = -2.00



CURSOR
LAT 28.5751
LON 11.2365
RG 5386
AZ 0
TILT -3.53
FRM 884
BIN 33
VAL



DATE 6:20:91

TIME 20:45:12

FRAME # 886

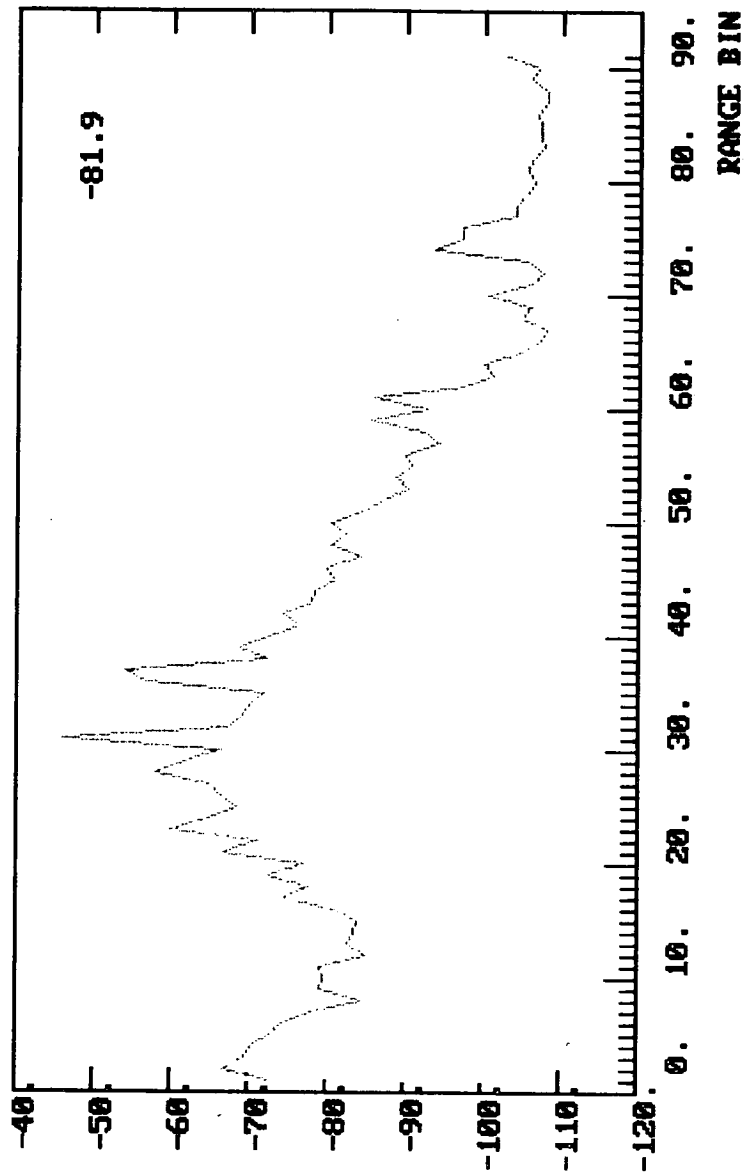
R-Min (m) = 781. TOTAL HAZARD FACTOR Alt (ft) = 1089.

DETECTION OF HAZARD

- Independent AGC for each range cell with large dynamic range.
- Range limiting.
- Antenna tilt control.
- Stationary ground clutter filter.
- Weighted least squares hazard estimation.

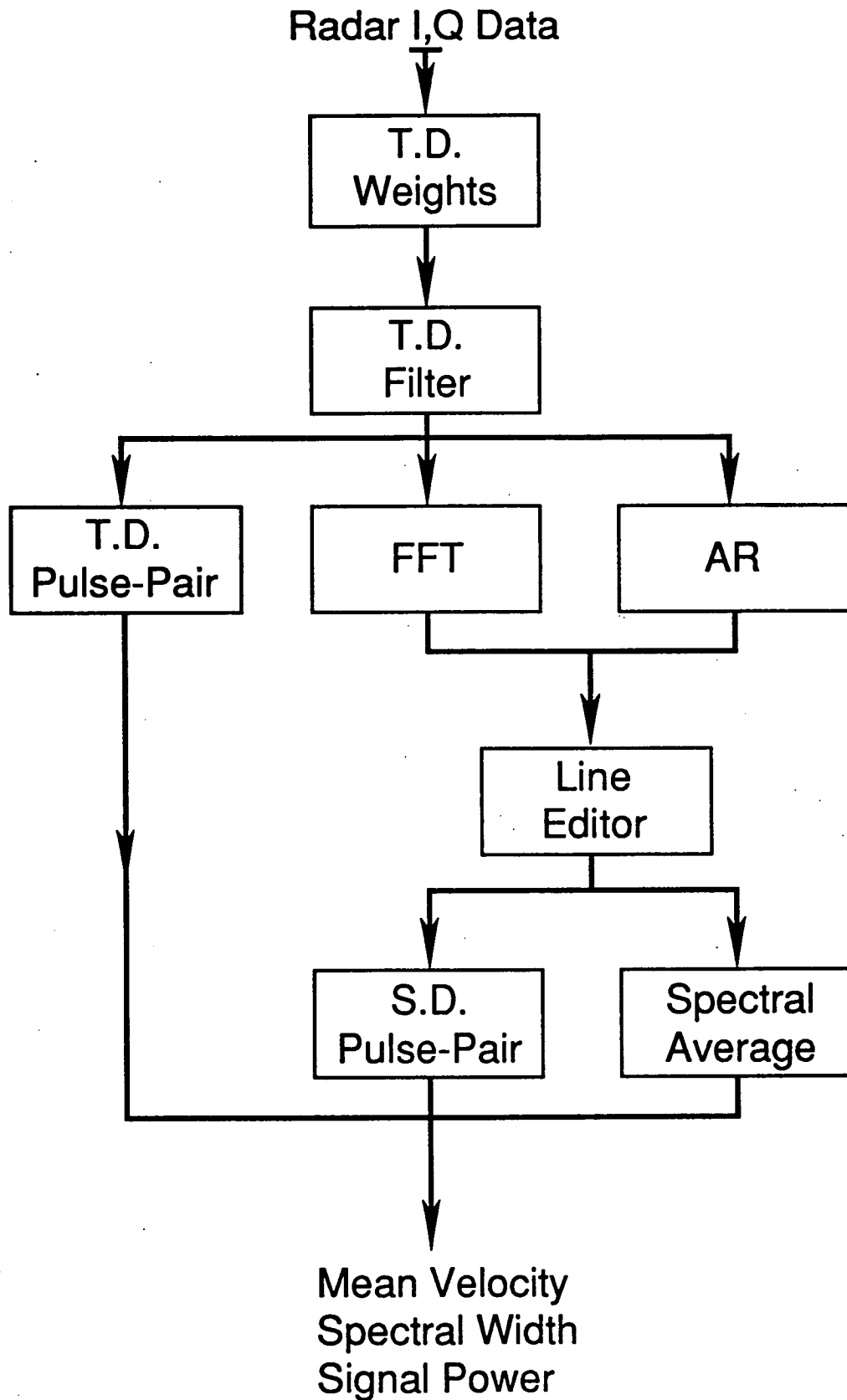
FRAME # 464
TILT = -2.0
ANT AZ = -4.8

POWER LEVEL (dBm) RG-MIN (m) = 781. RG-MAX (m) = 13876.



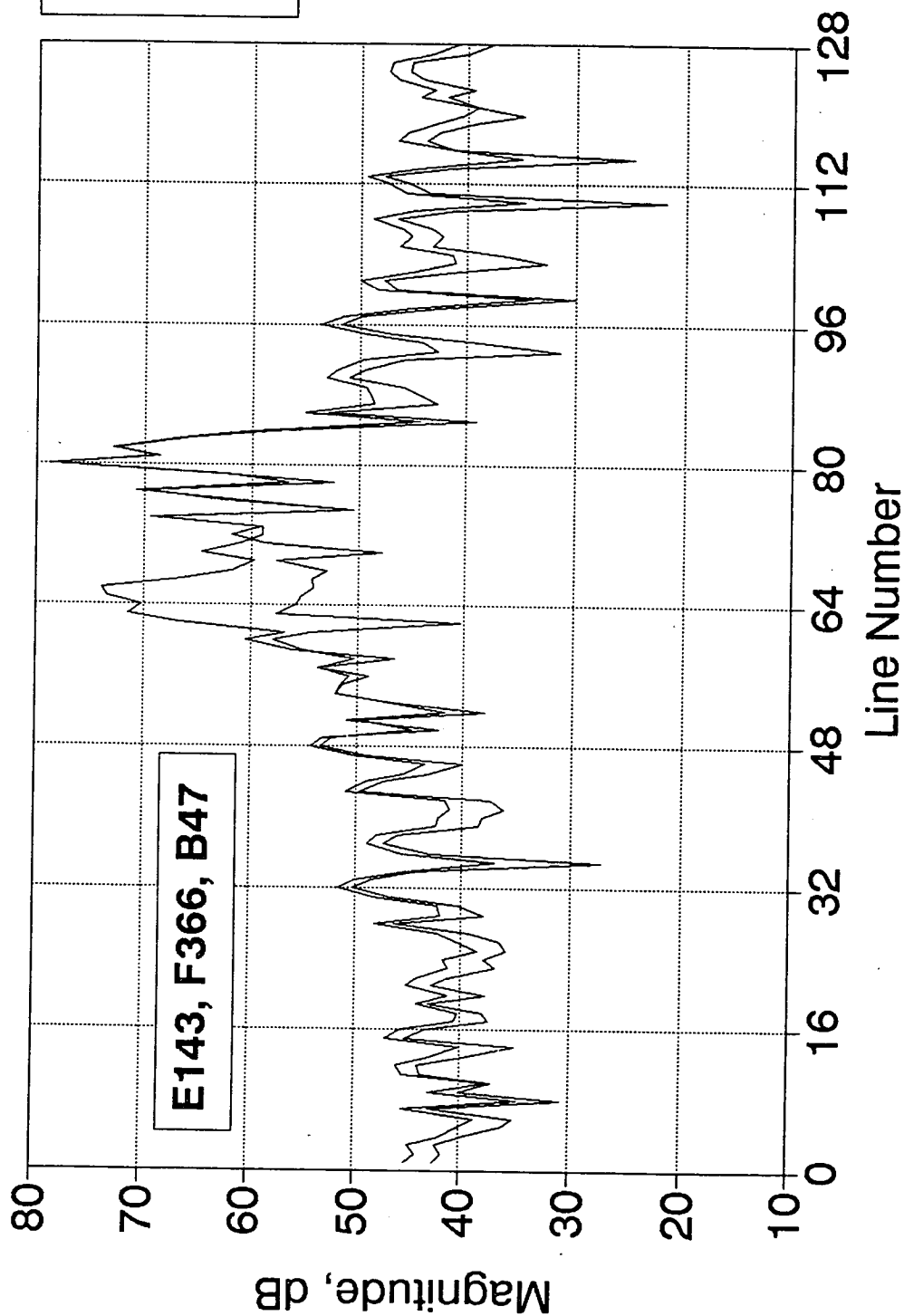
RECEIVED POWER VS. RANGE

SIGNAL PROCESSING ALGORITHMS



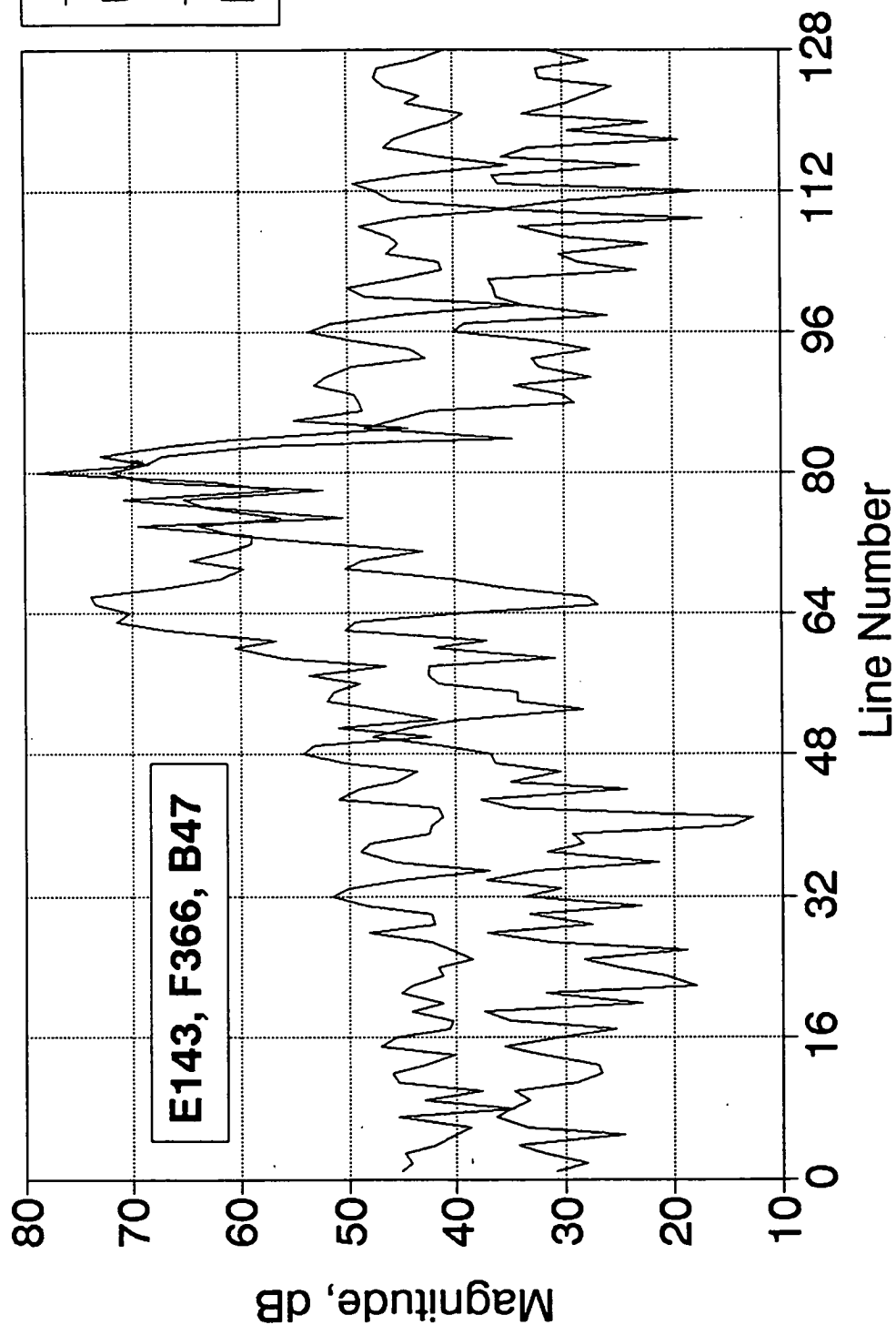
DOPPLER SPECTRUM

TD, No Wts., IIR-2 Filter



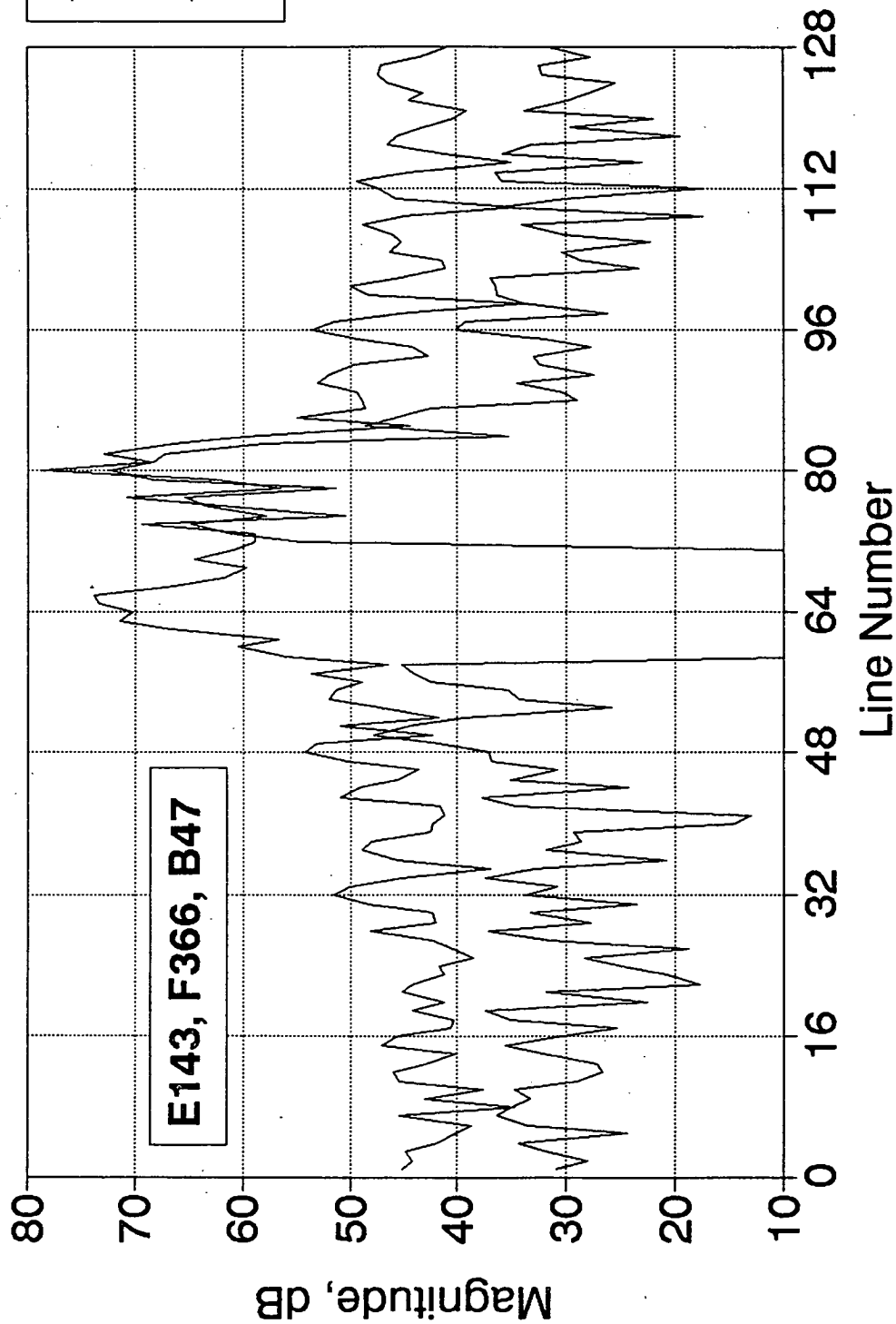
DOPPLER SPECTRUM

TD, Hann Wts., IIR-2 Filter



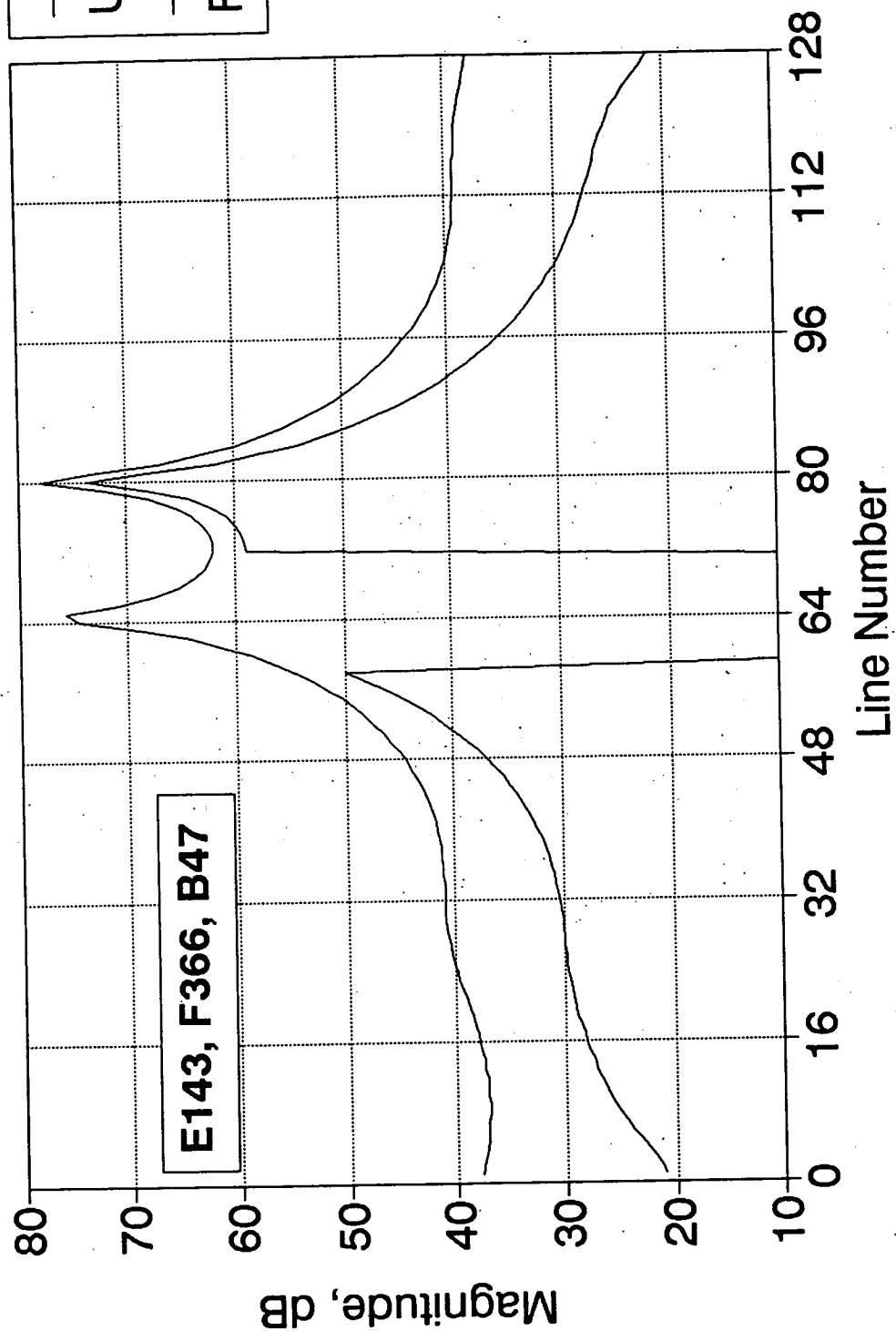
DOPPLER SPECTRUM

No TD Fil., FFT, Hann Wts., Line Edit



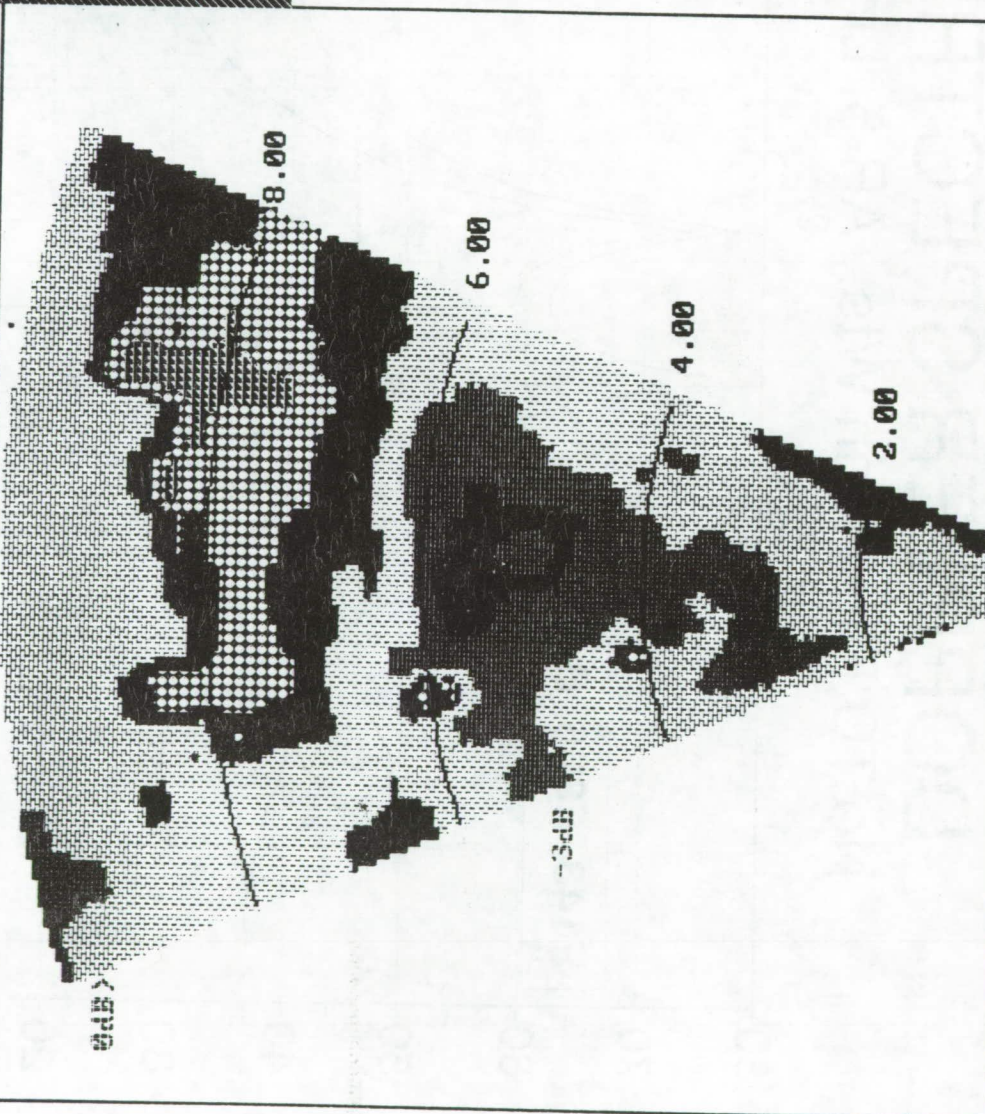
DOPPLER SPECTRUM

No TD Fil., Hann Wts., AR-5, Line Edit

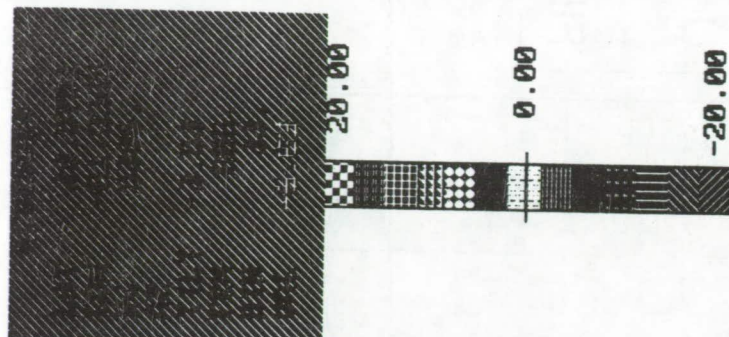


TIME-DOMAIN FILTER - IIR 2, HANN, PP

R-Max (m) = 9991. Center = 0.00 Tilt = -2.00



R-Min (m) = 781. FILTERED WIND VELOCITY Alt (ft) = 1089.



DATE 6:20:91

TIME 20:45:12

FRAME # 868

SPECTRAL DOMAIN FILTER - LINE EDIT



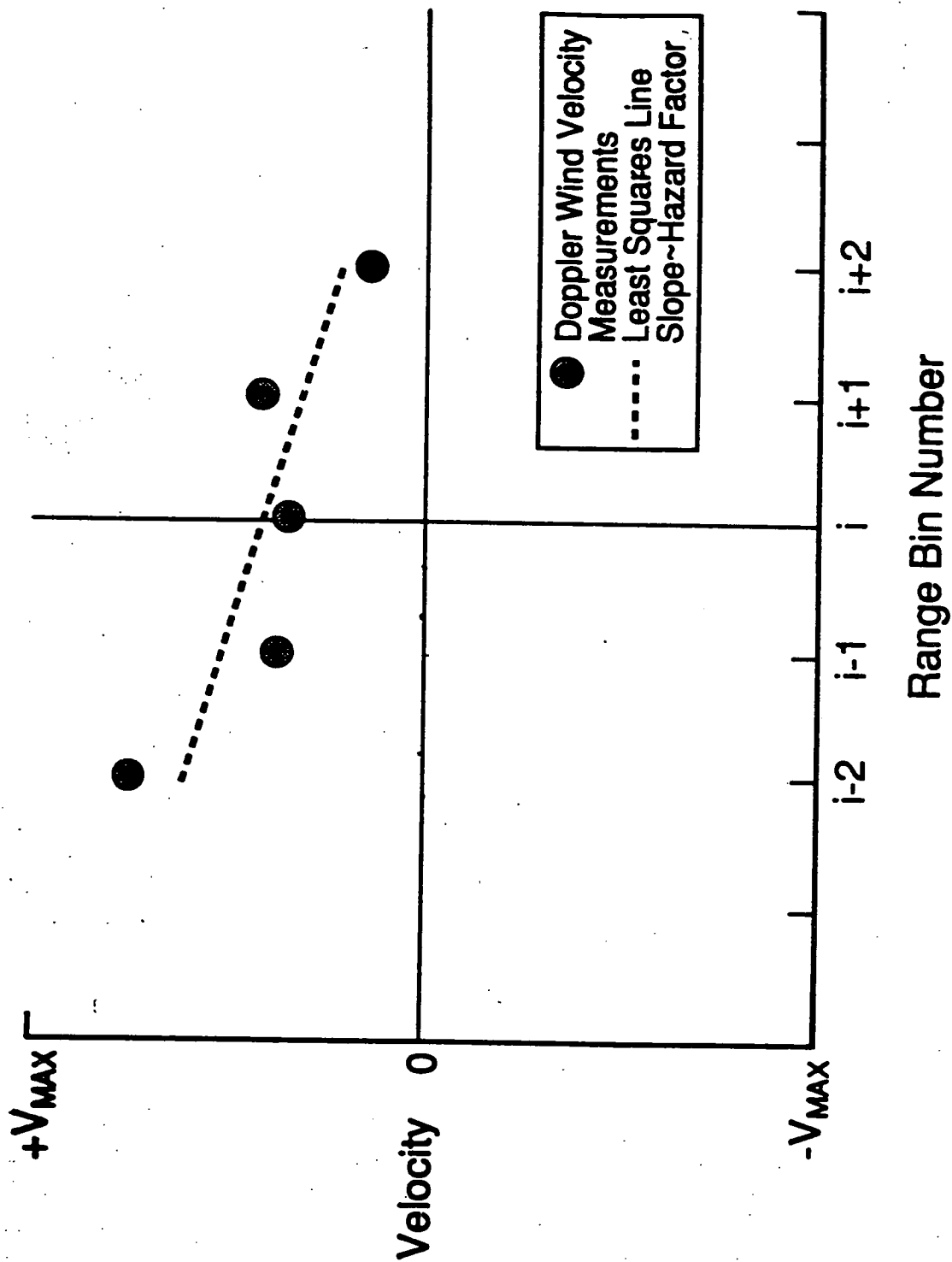
VALID VELOCITY MEASUREMENT

- 1. SIGNAL LEVEL ABOVE LEVEL THRESHOLD**
- 2. SPECTRAL WIDTH BELOW WIDTH THRESHOLD**
- 3. PROVISION FOR LOW-PASS FILTERING OF VELOCITY DATA**

CALCULATION OF HAZARD FACTOR

- 1. LEAST-SQUARES FIT TO VELOCITY OVER 5 RANGE BINS TO ESTIMATE VELOCITY SLOPE.**
- 2. VALID F-FACTOR CALCULATION IF LEAST-SQUARES RESIDUAL IS LESS THAN A RESIDUAL THRESHOLD.**
- 2a . ALTERNATIVELY, A WEIGHTED LEAST-SQUARES ALGORITHM IS USED; WEIGHTS ARE SPECTRAL WIDTHS.**
- 3. FROM THE RADIAL F-FACTOR AND THE ALTITUDE OF THE RANGE CELL, THE VERTICAL F-FACTOR IS ESTIMATED AND ADDED TO THE RADIAL TO FIND THE TOTAL F-FACTOR.**

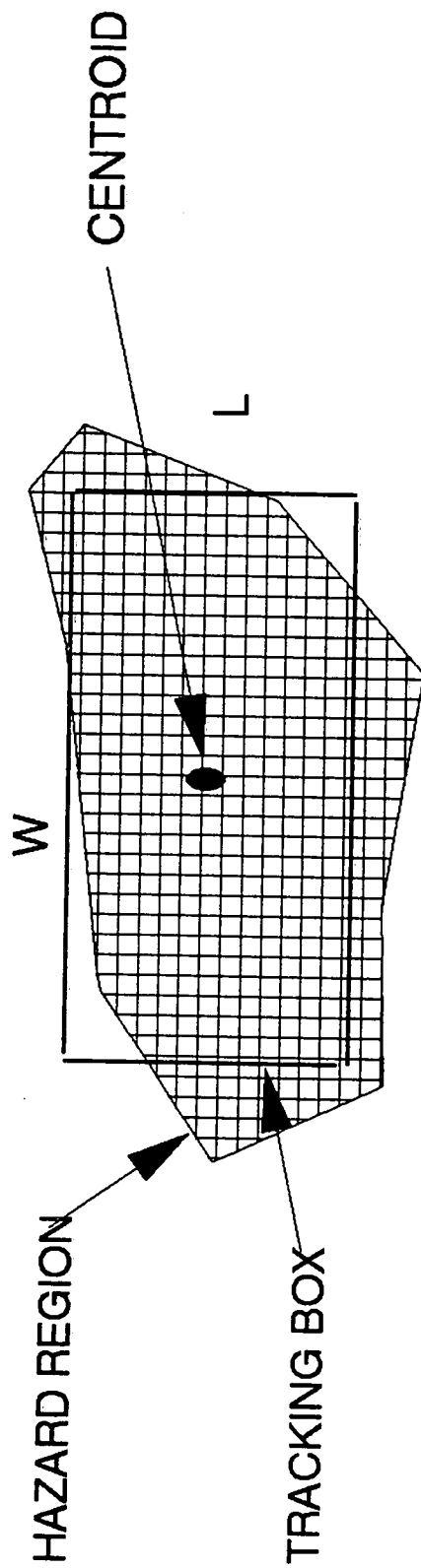
WEIGHTED LEAST SQUARES HAZARD ESTIMATOR



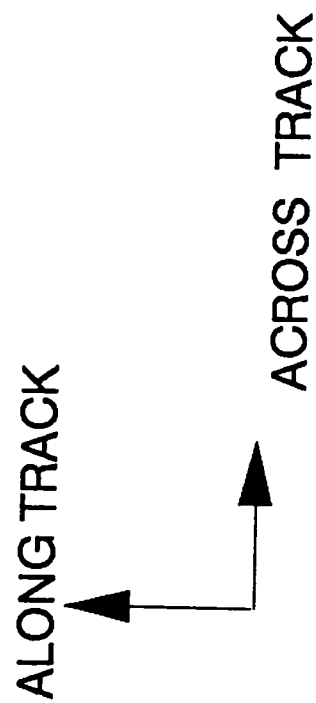
C-7

DETERMINATION OF HAZARD

- 1. AVERAGE THE BIN HAZARD FACTORS OVER A LENGTH OF APPROX. 1000 METERS.**
- 2. CALCULATE AREAS OF RADAR SCAN WITH HAZARD FACTOR ABOVE THE HAZARD FACTOR THRESHOLD.**
- 3. CALCULATE THE AREA OF THE HAZARD REGION.**
- 4. IF HAZARD REGION IS GREATER THAN AN AREA THRESHOLD, A HAZARD EXISTS IN THE SCAN.**



$L \times W = \text{AREA OF HAZARD REGION}$



WARNING CRITERIA

- 1. CENTROID OF HAZARD AREA IS TRACKED FROM
SCAN-TO-SCAN USING TRACK-WHILE-SCAN ALGORITHMS.**
- 2. IF THE HAZARD REGION PERSISTS OVER THE
SCAN COUNT THRESHOLD, AND IF THE TIME-TO-CLOSEST-
APPROACH IS LESS THAN THE TIME THRESHOLD, AN
ALERT IS DISPLAYED.**

SUMMARY OF BASELINE THRESHOLDS

SIGNAL LEVEL	>	-107 dBm
SPECTRAL WIDTH	<	8 m/s
TOTAL HAZARD INDEX	>	.105
LEAST-SQUARES RESIDUAL	<	3 m/s
AREA OF HAZARD	>	.2 sq km
SCAN COUNT	>	2
TIME-TO-CLOSEST APPROACH		10-40 secs

CONCLUSIONS

- USING BASELINE ALGORITHMS & THRESHOLDS ON FLIGHT AND SIMULATED DATA GIVES:

NO FALSE ALARMS ON CLUTTER
TIMELY ALERTS ON ORLANDO WET MICROBURSTS
AND SIMULATED DENVER DRY MICROBURSTS

- ADDITIONAL DATA RUNS REQUIRED TO SELECT BEST SIGNAL PROCESSING ALGORITHMS

- DIFFERENCES IN PROCESSING ALGORITHMS ARE SUBTLE - A FIGURE OF MERIT IS NEEDED FOR PROPER EVALUATION

**NASA Airborne Radar Wind Shear Detection Algorithm and the Detection of Wet
Microbursts in the Vicinity of Orlando, Florida
Questions and Answers**

Unknown - When you weight the least squares fit for shear on spectral width, isn't that going to make you unduly sensitive to any clutter that does get through your other filtering? I assume a false return would have very low spectral width wouldn't it?

A: Les Britt (RTI) - Yes, you are right. There have been suggestions to threshold on both ends of the spectral width, on very narrow spectral widths which may be a moving target and on the high end too, which is noise.

1993010423

488747

300

N93-19612

Session VI. Airborne Doppler Radar / NASA

**Signal Processing for Airborne Doppler Radar Detection of Hazardous Wind Shear as Applied to
NASA 1991 Radar Flight Experiment Data**

Dr. E. Baxa, Clemson University



***Signal Processing for
Airborne Doppler Radar Detection of
Hazardous Windshear as Applied to
NASA 1991 Radar Flight Experiment Data***

Dr. E. Baxa, Clemson University

Outline

- Platform Stability Analysis - aircraft attitude variations
- Microburst Detection Without Conventional Ground Clutter Rejection
 - autoregressive modelling
 - microburst tracking
- Adaptive Filtering for Ground Clutter Rejection With Low SCR
 - adaptive noise cancelling
 - simulated microburst in real clutter data
- Analysis of Out-of-Range Returns
- Groundspeed Corrections From Radar Returns
 - identification of error
 - asimuthal bias
- Additional On-going Research Work

4th CMTAW meeting

Radar Systems Laboratory
Electrical and Computer Engineering
Clemson University

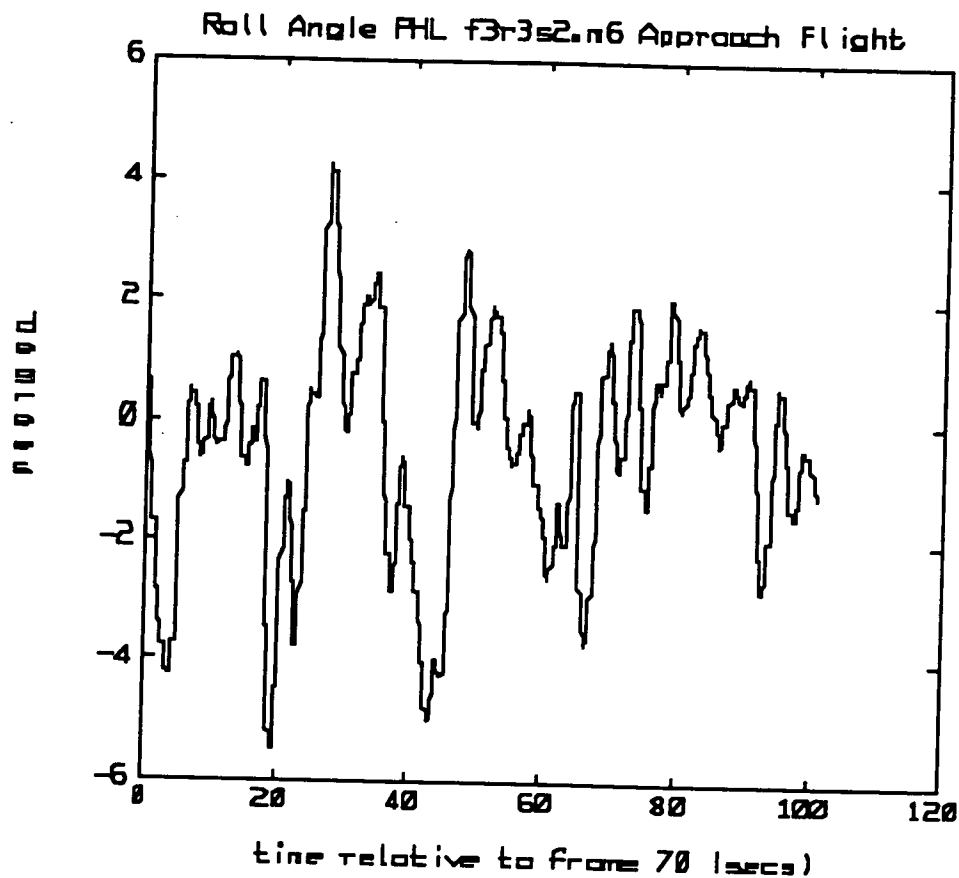
Apr. 15, 1992



Abstract

Radar data collected during the 1991 NASA flight tests have been selectively analyzed to support research directed at developing both improved as well as new algorithms for detecting hazardous low-altitude windshear. Analysis of aircraft attitude data from several flights indicated that platform stability bandwidths were small compared to the data rate bandwidths which should support an assumption that radar returns can be treated as short time stationary. Various approaches at detection of weather returns in the presence of ground clutter are being investigated. Non-conventional clutter rejection through spectrum mode tracking and classification algorithms is a subject of continuing research. Based upon autoregressive modelling of the radar return time sequence this approach may offer an alternative to overcome errors in conventional pulse-pair estimates. Adaptive filtering is being evaluated as a means of rejecting clutter with emphasis on low signal-to-clutter ratio situations, particularly in the presence of discrete clutter interference. An analysis of out-of-range clutter returns is included to illustrate effects of ground clutter interference due to range aliasing for aircraft on final approach. Data are presented to indicate how aircraft groundspeed might be corrected from the radar data as well as point to an observed problem of groundspeed estimate bias variation with radar antenna scan angle. A description of how recorded clutter return data are mixed with simulated weather returns is included. This enables the researcher to run controlled experiments to test signal processing algorithms. In the summary research efforts involving improved modelling of radar ground clutter returns and a bayesian approach at hazard factor estimation are mentioned.

Roll Angle vs. Time PHL f3r3s2.m6



4th CMTAW meeting

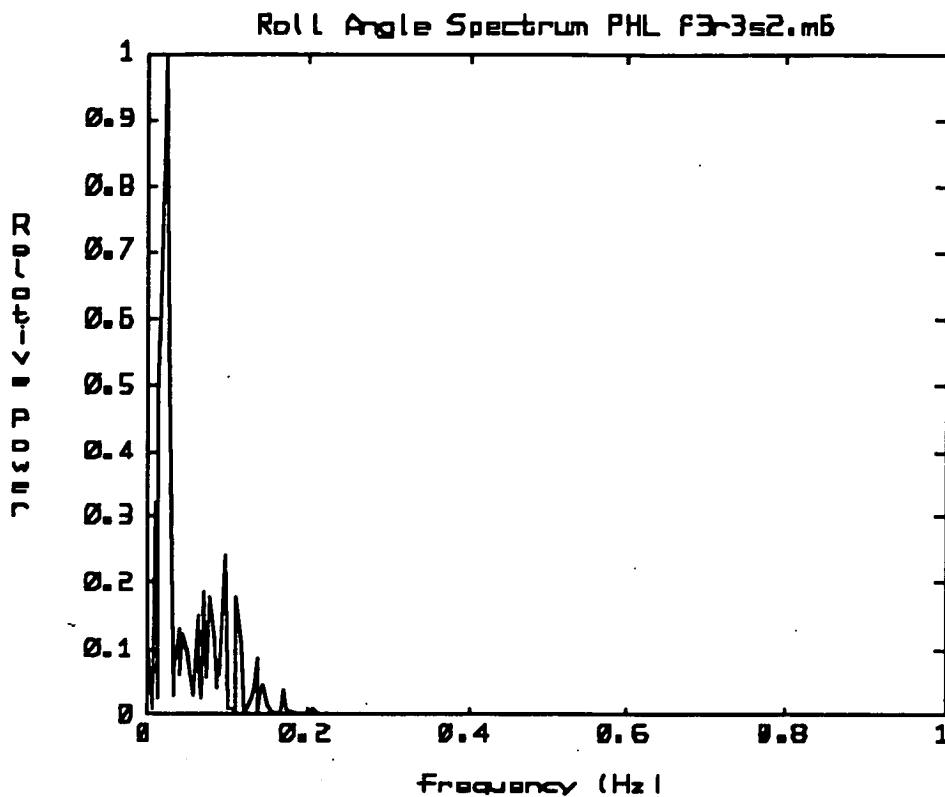
Radar Systems Laboratory
Electrical and Computer Engineering
Clemson University


Apr. 15, 1992

NOTES

Roll angle variation with time during approach to runway 27 at PHL. Data were recorded from DATAC with each frame of radar data at a frame rate of 29.25 frames per second.

Roll Angle Spectrum PHL f3r3s2.m6



4th CMTAW meeting

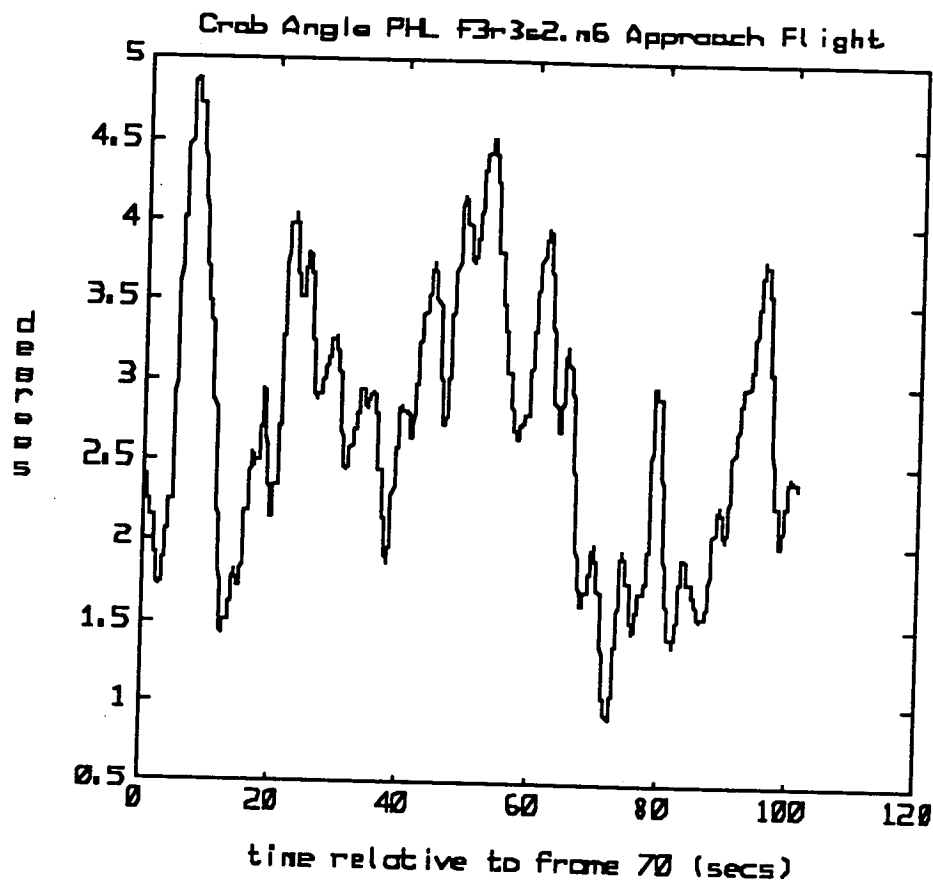
Radar Systems Laboratory
Electrical and Computer Engineering
Clemson University


Apr. 15, 1992

NOTES

Frequency spectrum of roll angle time variation during approach to runway 27 at PHL. Data were recorded from DATAC with each frame of radar data at a frame rate of 29.25 frames per second.

Crab Angle vs. Time PHL f3r3s2.m6



4th CMTAW meeting

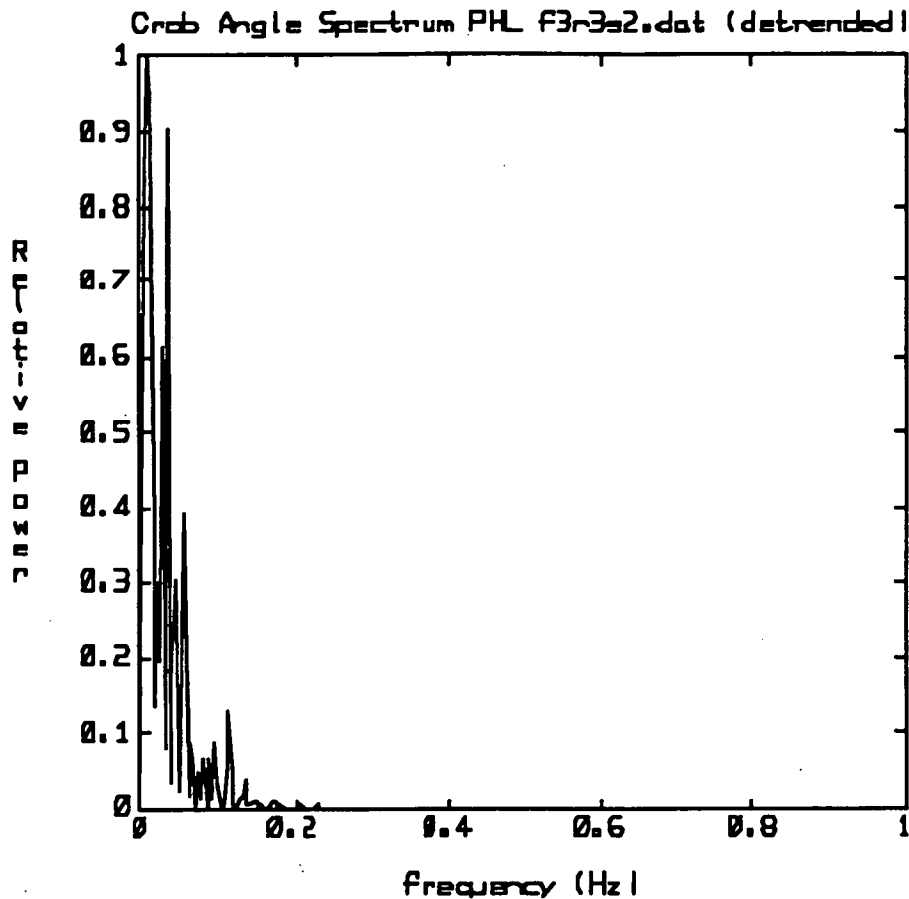
Radar Systems Laboratory
Electrical and Computer Engineering
Clemson University


Apr. 15, 1992

NOTES

Crab angle variation with time during approach to runway 27 at PHL. Data were recorded from DATAC with each frame of radar data at a frame rate of 29.25 frames per second.

Crab Angle Spectrum PHL f3r3s2.m6



4th CMTAW meeting

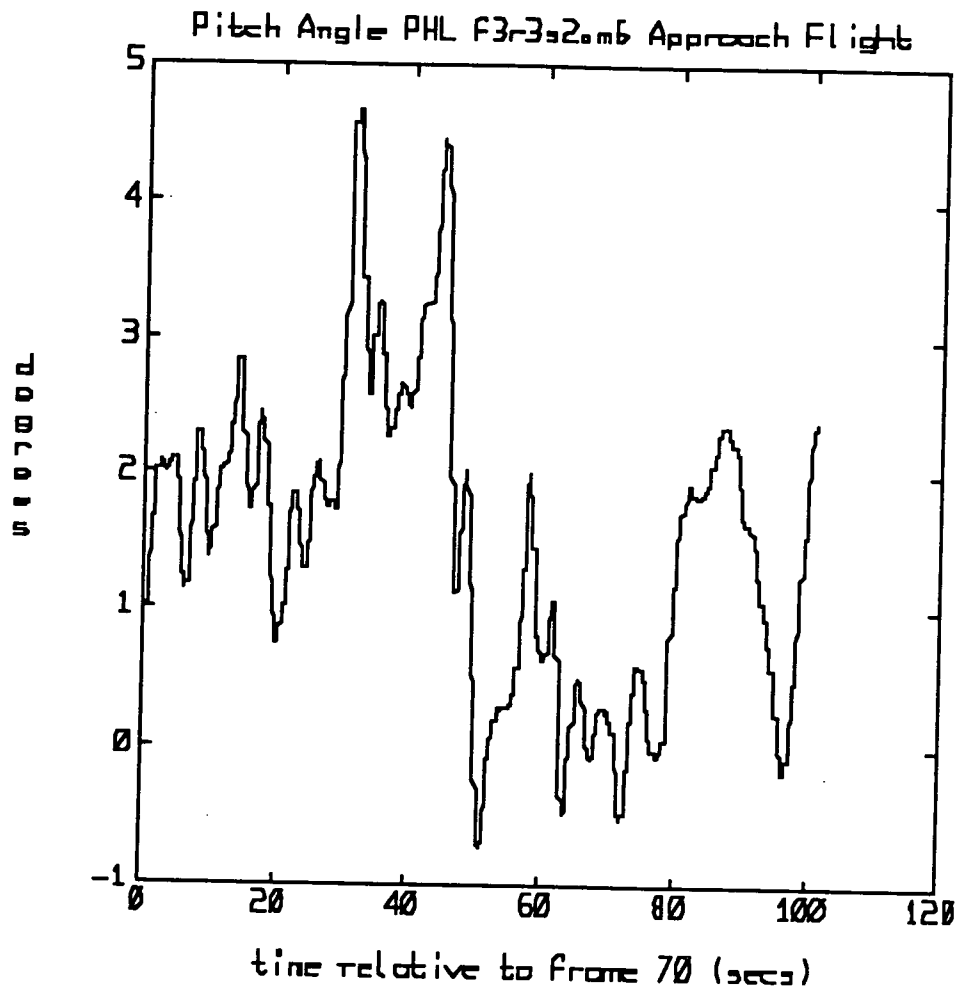
Radar Systems Laboratory
Electrical and Computer Engineering
Clemson University


Apr. 15, 1992

NOTES

Frequency spectrum of crab angle time variation during approach to runway 27 at PHL. Data were recorded from DATAC with each frame of radar data at a frame rate of 29.25 frames per second. Crab angle mean was removed prior to spectral analysis.

Pitch Angle vs. Time PHL f3r3s2.m6



4th CMTAW meeting

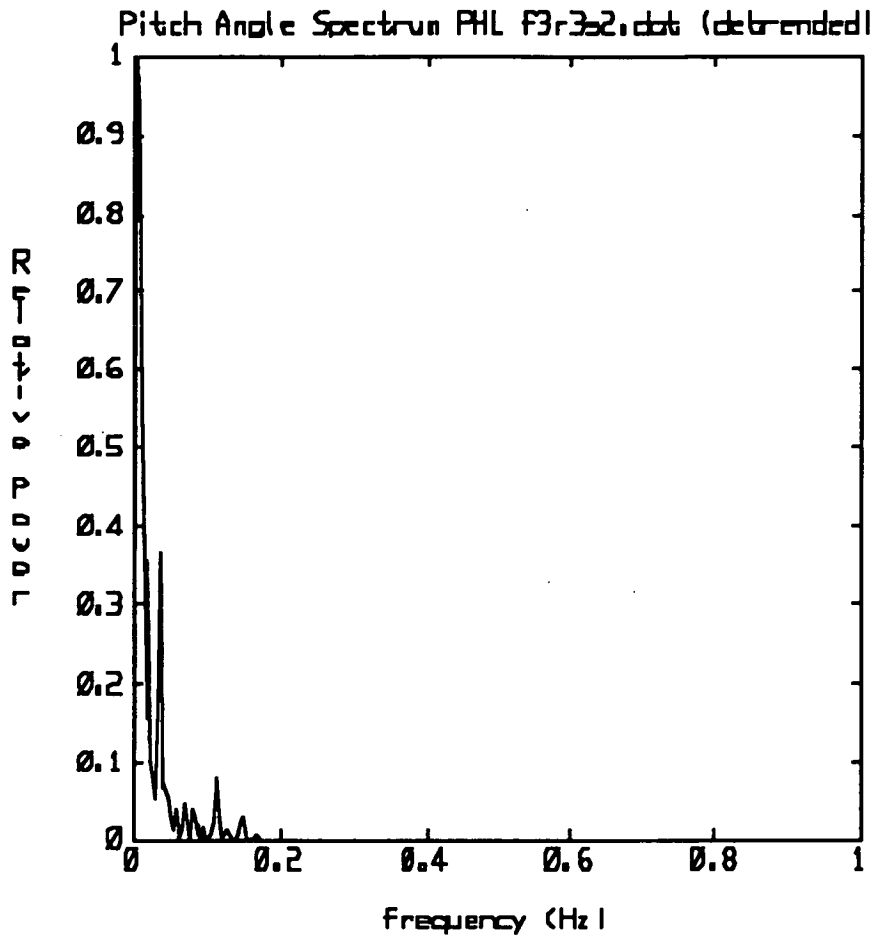
Radar Systems Laboratory
Electrical and Computer Engineering
Clemson University


Apr. 15, 1992

NOTES

Pitch angle variation with time during approach to runway 27 at PHL. Data were recorded from DATAC with each frame of radar data at a frame rate of 29.25 frames per second.

Pitch Angle Spectrum PHL f3r3s2.m6



4th CMTAW meeting

Radar Systems Laboratory
Electrical and Computer Engineering
Clemson University

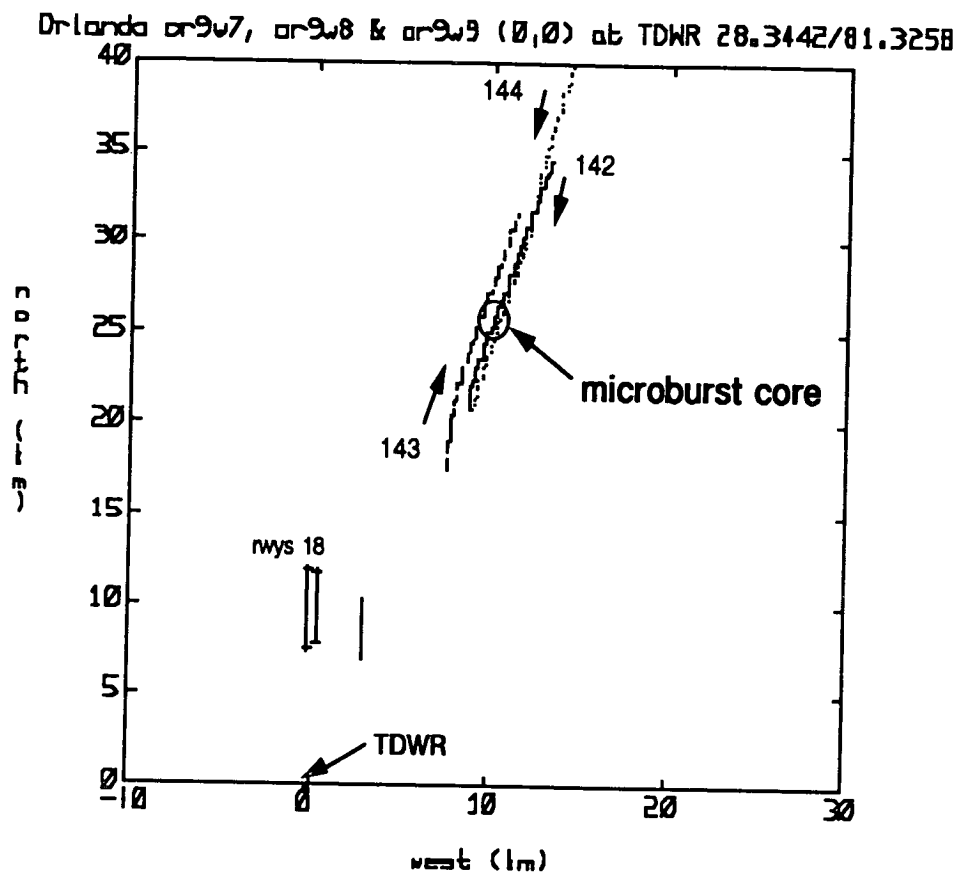
Apr. 15, 1992



NOTES

Frequency spectrum of pitch angle time variation during approach to runway 27 at PHL. Data were recorded from DATAC with each frame of radar data at a frame rate of 29.25 frames per second. The mean value of pitch angle was removed before spectral analysis.

Orlando Flights Though Events 142,143,144



4th CMTAW meeting

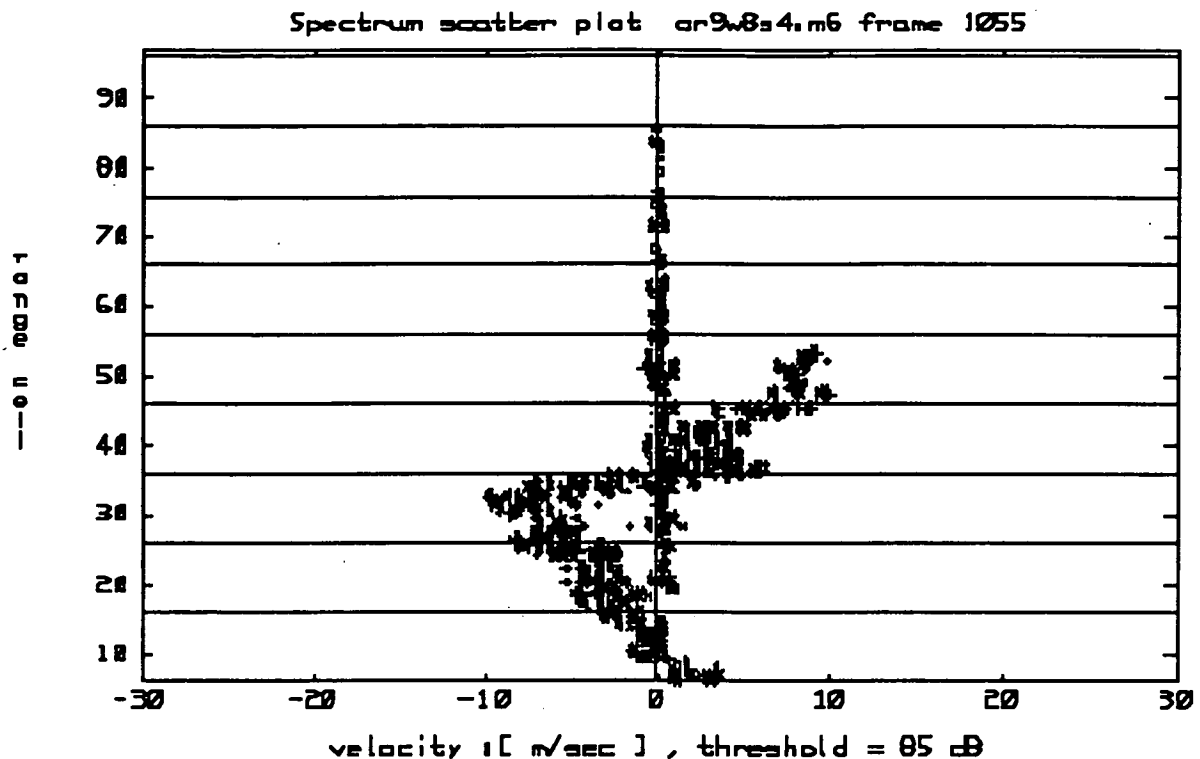
Radar Systems Laboratory
Electrical and Computer Engineering
Clemson University

Apr. 15, 1992

NOTES

Ground tracks of three legs of the NASA flight through the microburst in Orlando on day 171. This event was numbered 142 on the first pass, 143 on the second, and 144 on the third. The aircraft was at about 1100 feet traveling in excess of 200 knots. The indicated position of the microburst is an estimate of the core position based upon radar data. The TDWR is at 0,0 on this plot.

Event 143 Orlando 1991



4th CMTAW meeting

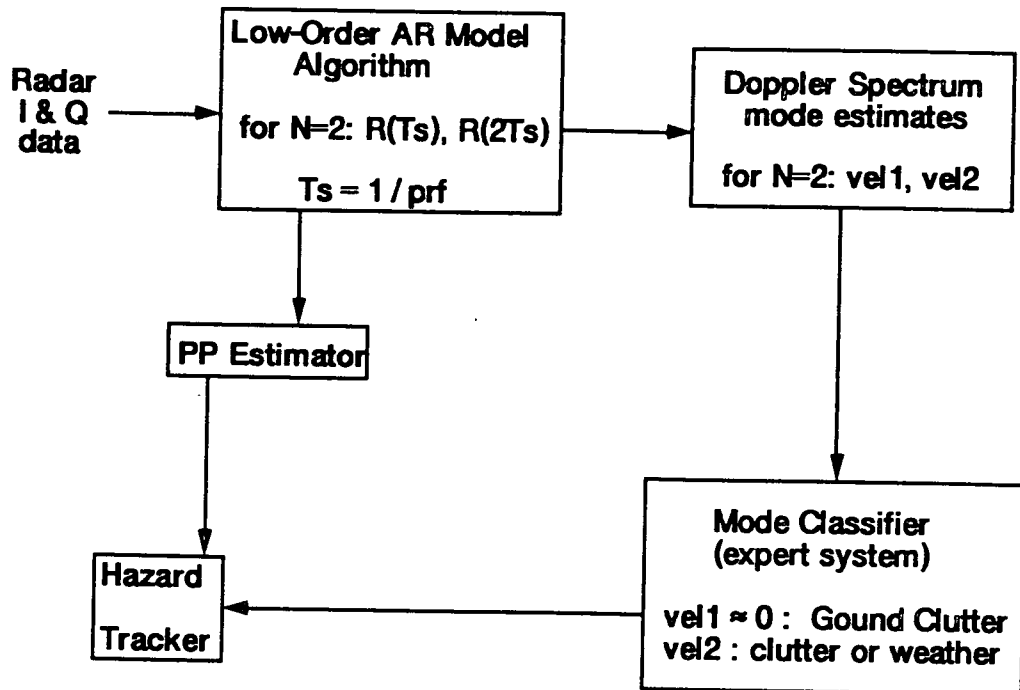
Radar Systems Laboratory
Electrical and Computer Engineering
Clemson University


Apr. 15, 1992

NOTES

During the flight through event 143 at Orlando a snapshot of the radar return looking into the microburst is analyzed using a Fourier transform of the I & Q sequence (96 samples) taken at an antenna azimuth of -0.25 degrees. The aircraft was on the track labeled 143 on the previous slide and located at about 8 km west and 22 km north of the TDWR. The range cell at the zero crossing of the "s-curve" characteristic is about range cell 35 which is approximately 5 km ahead of the aircraft. In the presentation the Doppler power spectrum has been thresholded and then a point density plot is used to indicate spectrum intensity. Doppler windspeed is on the abscissa. Range cells from 6 to 96 are indicated on the ordinate. No clutter rejection filtering has been used.

Autoregressive (AR) Modelling of Radar Return



4th CMTAW meeting

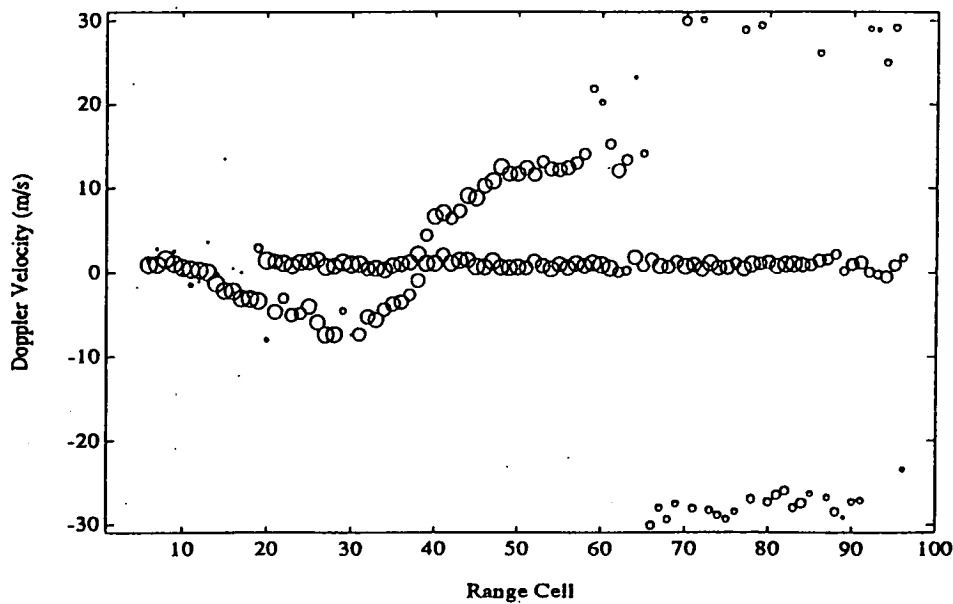
Radar Systems Laboratory
Electrical and Computer Engineering
Clemson University

Apr. 15, 1992

NOTES

Linear modelling of the I & Q sequences as if they were the output of a linear all-pole model driven by white noise is being used to investigate the feasibility of detecting modes in the return Doppler spectrum without the use of clutter rejection filtering. In situations where the clutter is particularly strong or may tend to bias spectrum mean estimates even when attempts at clutter rejection are made, this method is viewed as a possible alternative. It also provides a method for estimating a spectrum as an alternative to the FFT. A second order AR model is comparable to the pulse pair algorithm in terms of processing load and can give a useful spectrum estimate for further processing.

AR Based Velocity Estimates for Event 143



4th CMTAW meeting

Radar Systems Laboratory
Electrical and Computer Engineering
Clemson University

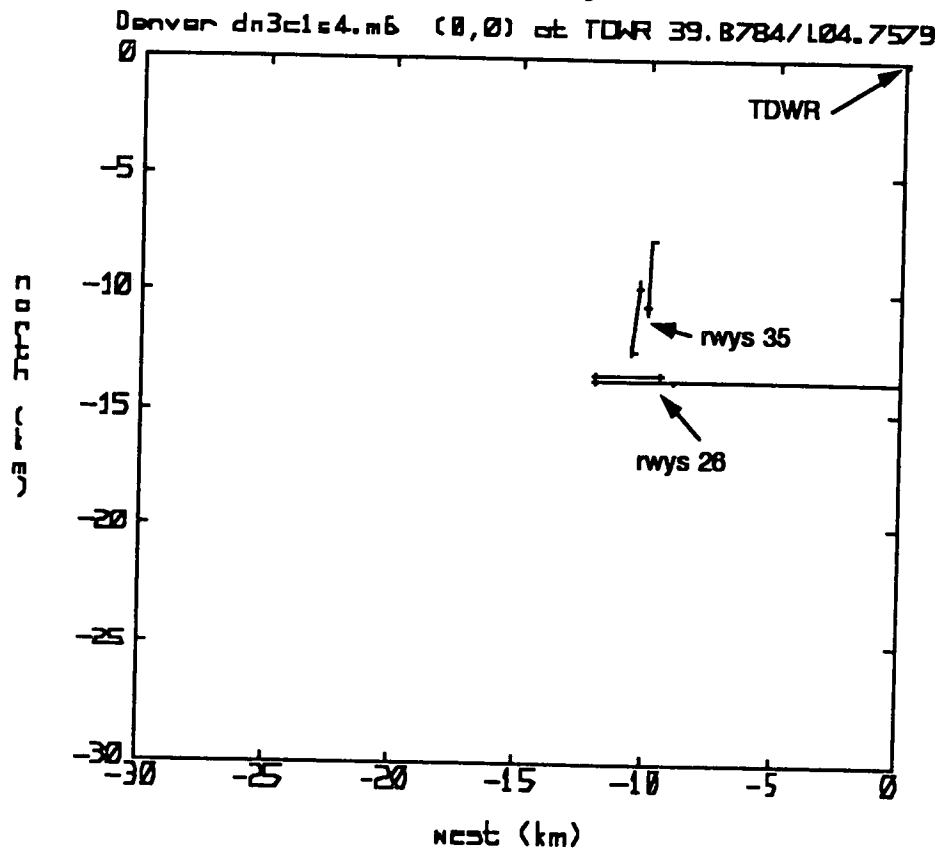
Apr. 15, 1992

NOTES

The snapshot of event 143 in Orlando at a time very near to that shown in the earlier scatter point plot is shown here after autoregressive modelling. Again no clutter rejection filtering has been used. The bubble center locations indicate the spectrum mode Doppler velocity estimates for each range cell. The size of the bubbles indicate relative mode strengths. The small bubbles near + 30 m/s and - 30 m/s in range cells 65 and above are indicative of returns at ranges where the return is weak with very little specular structure. Investigation is continuing to use these methods coupled with an expert mode classification algorithm to detect hazardous windshear.

Ref: M.W. Kunkel, "Spectrum Modal Analysis for the Detection of Low-Altitude Windshear with Airborne Doppler Radar," Radar Systems Lab TR-15, ECE Dept., Clemson University, Feb. 1992.

DEN rwy 26 Flyover



4th CMTAW meeting

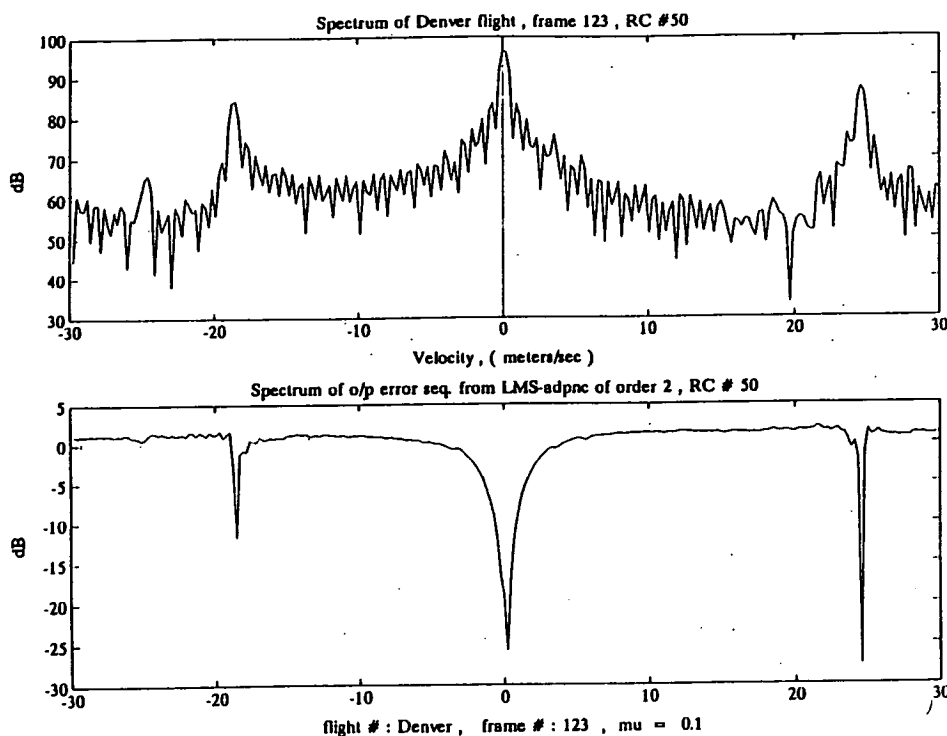
Radar Systems Laboratory
Electrical and Computer Engineering
Clemson University

Apr. 15, 1992

NOTES

This is a ground track plot of one of several clutter flights over runway 26L at Denver Stapleton. Generally these flights were at altitudes of 1400 to 1500 feet at groundspeeds near 200 knots. Various antenna elevations were used. Results here include data from horizontal elevation (0 degrees) and -1 and -3 degrees (below horizontal). The position plot is relative to the location of the TDWR (0,0).

Ground Clutter Doppler Spectrum (DEN rwy 26 Flyover) 1440 ft alt., AZ=0, EL=-1



4th CMTAW meeting

Radar Systems Laboratory
 Electrical and Computer Engineering
 Clemson University


Apr. 15, 1992

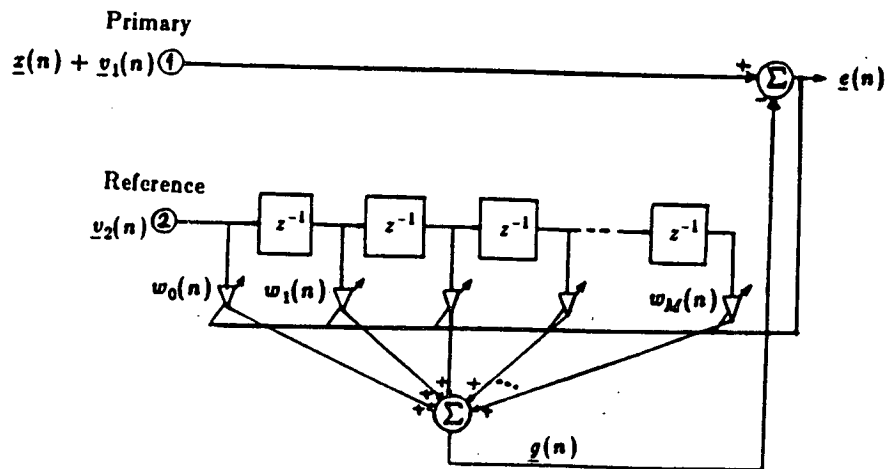
NOTES

A typical clutter FFT spectrum is shown which includes "discrete clutter" modes at about -18 m/s and +25 m/s in addition to the main lobe clutter near zero Doppler. These modes away from zero are due to returns from interstate highway I-70 which passes under runway 35. Also shown is the impulse response of a second order adaptive clutter rejection filter with the I & Q sequence used for the illustrated spectrum also used as a training sequence for the adaptive filter. Notice that the adaptive filter places notches at each of the strong clutter modes even with only a second order filter. The filter is an adaptive noise canceller using the LMS algorithm and is shown in block diagram form in the next figure.

Adaptive Noise Canceling with LMS Filter

LMS Algorithm: $\underline{w}_i(n+1) = \underline{w}_i(n) + \mu \underline{e}(n) \underline{v}_2(n-i), 0 \leq i \leq M$

where $\underline{e}(n) = \underline{x}(n) + \underline{v}_1(n) - \underline{g}(n) = \underline{x}(n) + \underline{v}_1(n) - \underline{w}_n^T \underline{y}_{2,n}$.



Tapped-delay-line model

Adaptive noise-canceller configuration summary.

4th CMTAW meeting

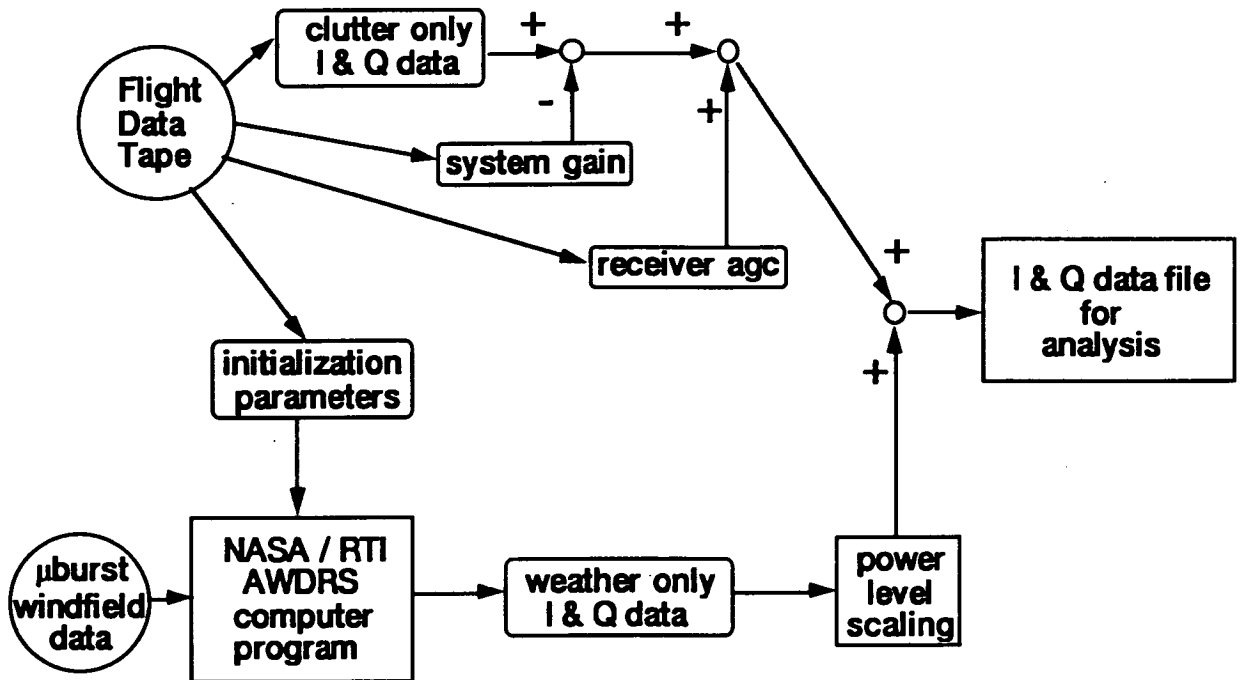
Radar Systems Laboratory
Electrical and Computer Engineering
Clemson University

Apr. 15, 1992

NOTES

An adaptive noise canceller can be used to optimally reject clutter from a radar return if a reference clutter sequence is available and that sequence is highly correlated with the ground clutter portion of the primary return and uncorrelated with the weather portion of the primary return. As shown earlier a low order tapped delay type adaptive filter may be very effective and is being investigated as an alternative for very low signal to clutter ratio situations.

Analysis of Modelled Microbursts in Real Clutter



4th CMTAW meeting

Radar Systems Laboratory
Electrical and Computer Engineering
Clemson University

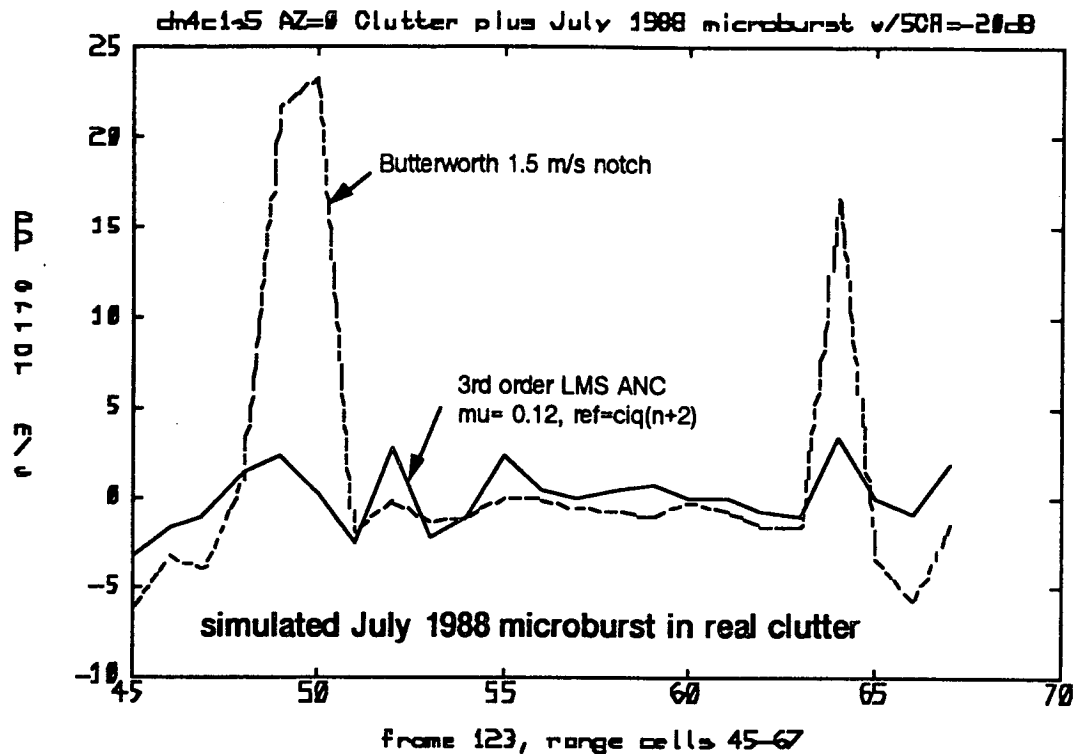

Apr. 15, 1992

NOTES

To investigate very low signal to clutter ratio situations the NASA simulation model is being used in conjunction with actual recorded ground clutter returns. The simulation model is set up with a microburst windfield from a previously observed microburst. It can be placed at any location for which clutter data have been recorded. Simulated I & Q data are then simply added to the archived clutter I & Q data after proper scaling and used for analysis of signal processing algorithms. The weather signal to clutter ratio can be controlled as desired by the user.

Adaptive Noise Canceling Clutter Rejection Results

post clutter rejection filter pulse-pair mean estimate error



4th CMTAW meeting

Radar Systems Laboratory
Electrical and Computer Engineering
Clemson University

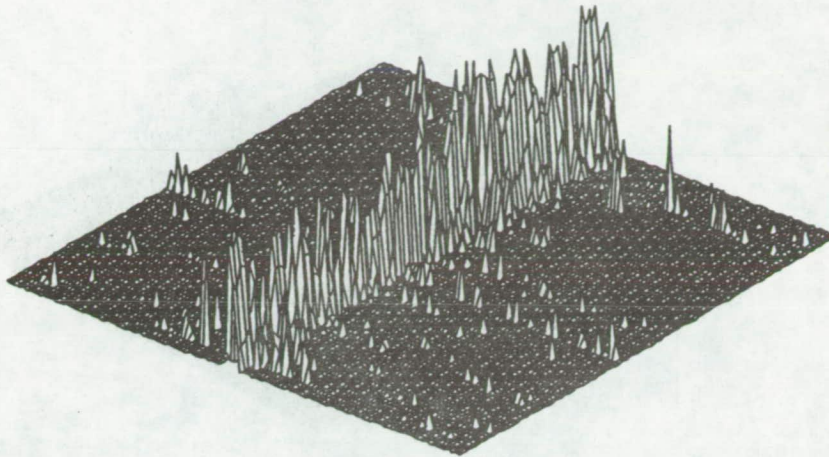
Apr. 15, 1992

NOTES

The LMS based adaptive noise canceller described earlier was used to investigate detection of the July 11 1988 Denver microburst in the presence of actual radar ground clutter data recorded in 1991. The weather return levels were scaled to maintain a constant average signal to clutter ratio of -20 dB in each range cell. The pulse pair estimate of Doppler spectrum mean was then computed after filtering with an adaptive noise canceller using the recorded and time delayed clutter data as a reference input. Results were compared to similar processing after filtering with a fixed 1.5 m/s notch Butterworth filter. The adaptive filter is much better where discrete clutter interference is present (near range cells 50 and 64). This should improve hazard factor estimates.

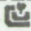
DEN rwy 26 Flyover, EL=0, 3755 prf, 1-14km

dn2clas1 Frame 153 rc 6-96 96 samples at PRF



norm 80-100dB -30,+30m/s Doppler velocity spectra

4th CMTAW meeting

Radar Systems Laboratory
Electrical and Computer Engineering
Clemson University


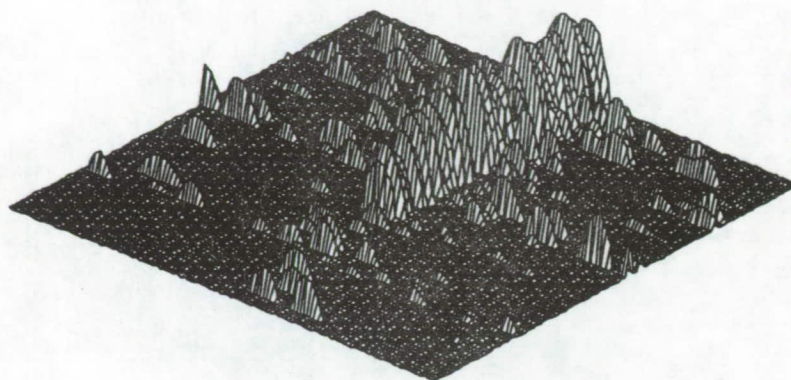
Apr. 15, 1992

NOTES

This and the next 8 slides analyze the effect of out-of-range returns in the Denver data when the aircraft was flying over runway 26 headed west with the radar antenna oriented toward the mountains. Three views show the radar Doppler spectra for range cells 6-96 at the 3755 prf. Data at 1877.5 prf were also recorded and analyzed to show what is in range cells 6-96 without second time around returns and what is in the extended range cells that aliases into the closer range cells when operating at the higher prf. Three different antenna elevation angles are shown. Out-of-range interference is significant at the horizontal elevation (EL=0) and is reduced to a negligible level at EL=-3 degrees. Some spectrum aliasing is also noted in the reduced prf plots since the Doppler range is halved to -15,+15 m/s.

DEN rwy 26 Flyover, EL=0, 1877.5 prf, 1-14km

dn2clas1 Frame 153 rc 6-96 16 samples at PRF/2



norm 70-100dB -15,+15m/s Doppler velocity spectra

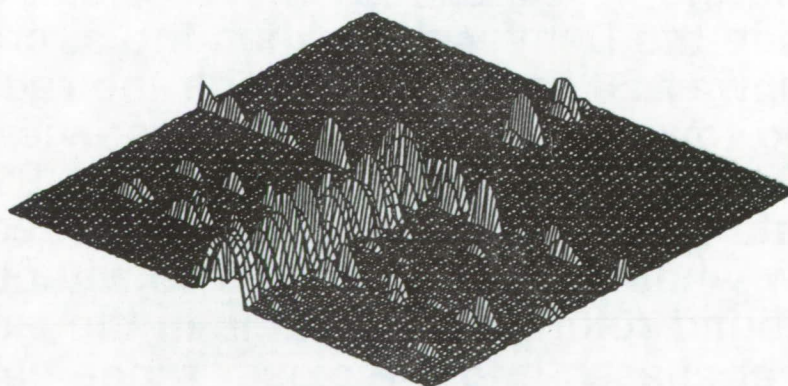
4th CMTAW meeting

Radar Systems Laboratory
Electrical and Computer Engineering
Clemson University

Apr. 15, 1992

DEN rwy 26 Flyover, EL=0, 1877.5 prf, 42-56km

dn2clas1 Frame 153 rc 284-374 15 samples at PRF/2



norm 70-100dB -15,+15m/s Doppler velocity spectra

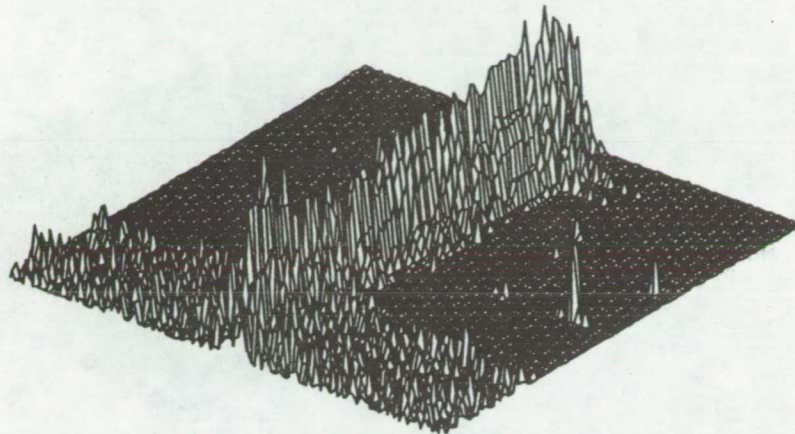
4th CMTAW meeting

Radar Systems Laboratory
Electrical and Computer Engineering
Clemson University

Apr. 15, 1992

DEN rwy 26 Flyover, EL=-1, 3755 prf, 1-14km

dn4cls5 Frame 123 rc 6-96 96 samples at PRF



70-100dB -30,+30m/s Doppler velocity spectra

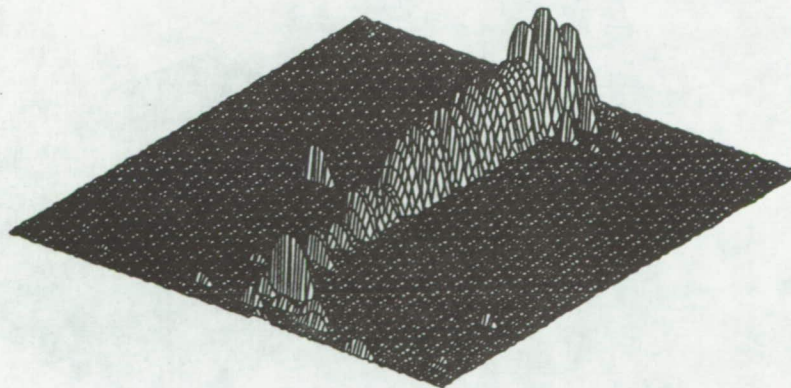
4th CMTAW meeting

Radar Systems Laboratory
Electrical and Computer Engineering
Clemson University

Apr. 15, 1992

DEN rwy 26 Flyover, EL=-1, 1877.5 prf, 1-14km

dn4cls5 Frame 123 rc 6-96 16 samples at PRF/2



70-100dB -15,+15m/s Doppler velocity spectra

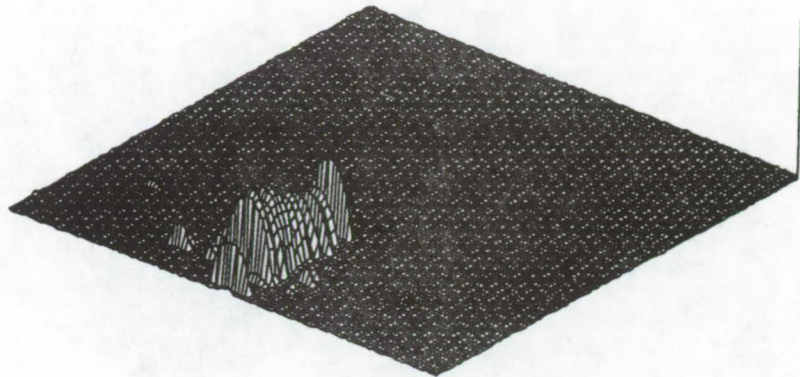
4th CMTAW meeting

Radar Systems Laboratory
Electrical and Computer Engineering
Clemson University

Apr. 15, 1992

DEN rwy 26 Flyover, EL=-1, 1877.5 prf, 42-56km

dn4cls5 Frame 123 rc 284-374 15 samples at PRF/2



70-100dB -15,+15m/s Doppler velocity spectra

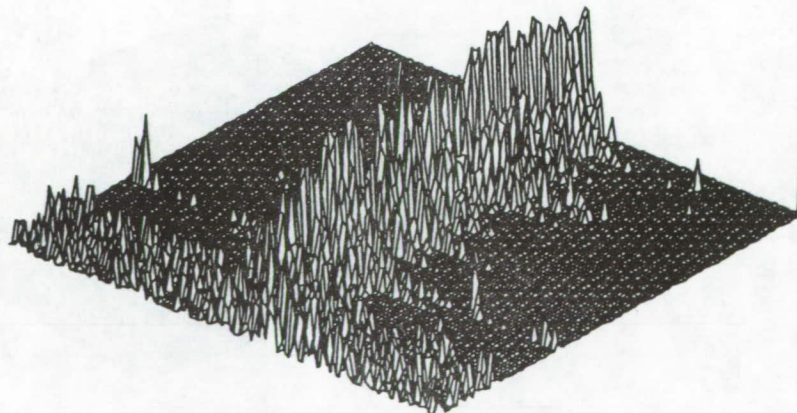
4th CMTAW meeting

Radar Systems Laboratory
Electrical and Computer Engineering
Clemson University

Apr. 15, 1992

DEN rwy 26 Flyover, EL=-3, 3755 prf, 1-14km

dn3cls3 Frame 210 rc 6-96 96 samples at PRF



70-100dB -30,+30m/s Doppler velocity spectra

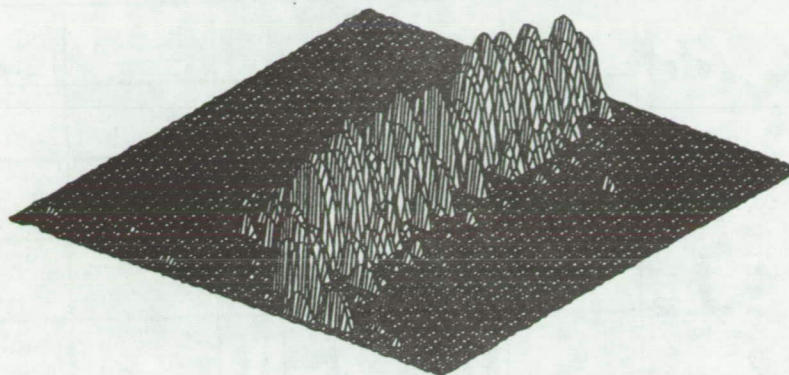
4th CMTAW meeting

Radar Systems Laboratory
Electrical and Computer Engineering
Clemson University

Apr. 15, 1992

DEN rwy 26 Flyover, EL=-3, 1877.5 prf, 1-14km

dn3cls3 Frame 210 rc 6-96 16 samples at PRF/2



70-100dB -15,+15m/s Doppler velocity spectra

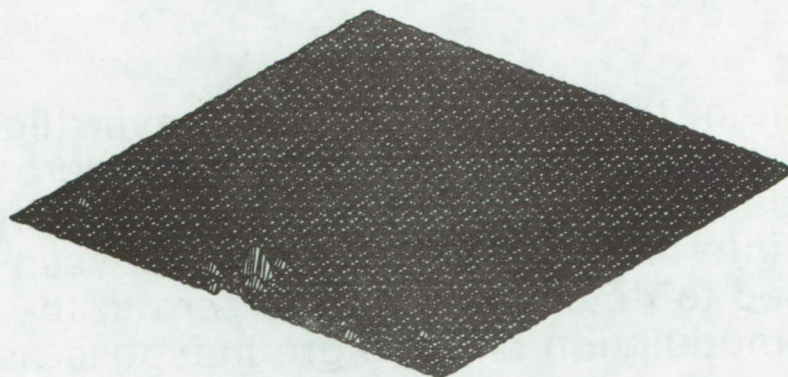
4th CMTAW meeting

Radar Systems Laboratory
Electrical and Computer Engineering
Clemson University

Apr. 15, 1992

DEN rwy 26 Flyover, EL=-3, 1877.5 prf, 42-56km

dn3cls3 Frame 210 rc 284-374 15 samples at PRF/2



70-100dB -15,+15m/s Doppler velocity spectra

4th CMTAW meeting

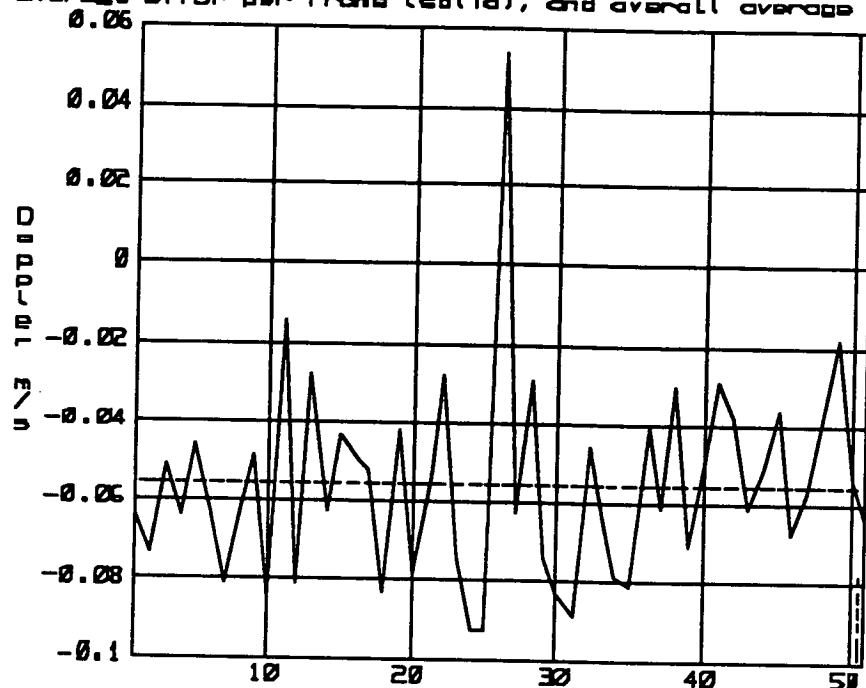
Radar Systems Laboratory
Electrical and Computer Engineering
Clemson University

Apr. 15, 1992

Mean Groundspeed Error from Radar Return - DEN

dn2c6as1.m6, EL=0, all times with corrected AZ \approx 0, rc 6-96

average error per frame (solid), and overall average (dashed)



Frame of look-ahead azimuths (91 range cells corrected)

4th CMTAW meeting

Radar Systems Laboratory
Electrical and Computer Engineering
Clemson University

Apr. 15, 1992

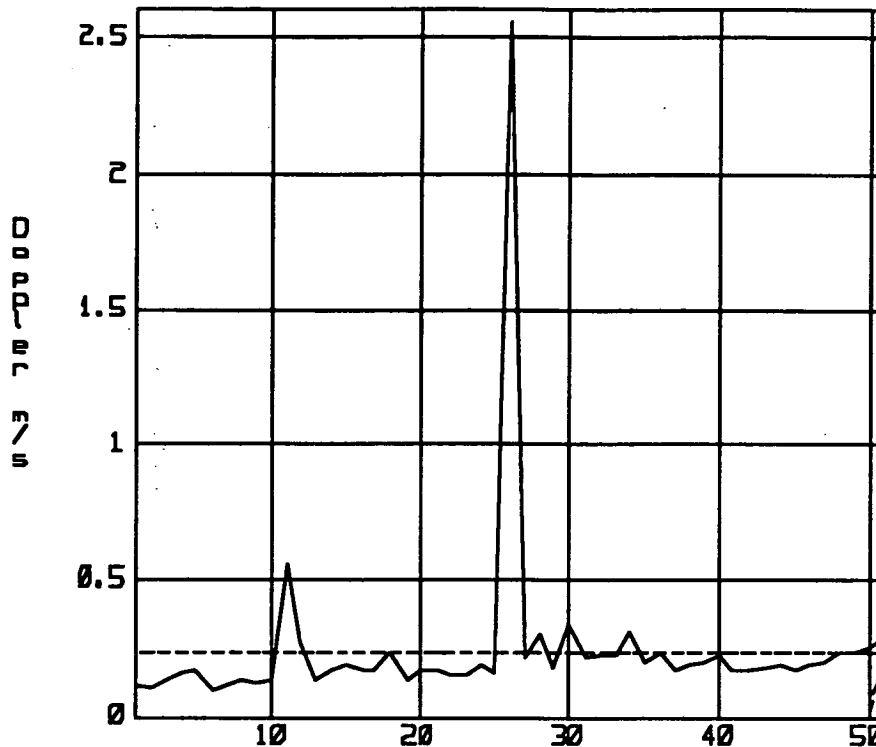
NOTES

One of the Denver runway 26 overflights is analyzed to determine any difference from zero of the Doppler location of the ground clutter mainlobe. This difference is interpreted as a difference between the groundspeed used to determine Doppler zero in the radar demodulation and the groundspeed as measured by the radar. In each frame of 128 radar pulses the spectrum peaks in all range cells have been averaged to get a "frame" mean. These are then plotted for each frame when the corrected antenna azimuth was 0 degrees. A slight bias of approximately 0.055 m/s is noted.

St. Dev. Goundspeed Error from Radar Return - DEN

dn2c6as1.m6, EL=0, all times with corrected AZ ≈ 0 , rc 6-96

Standard deviation per Frame (solid), and overall st. dev. (dashed)



Frame of look-ahead azimuths (91 range cells corrected)

4th CMTAW meeting

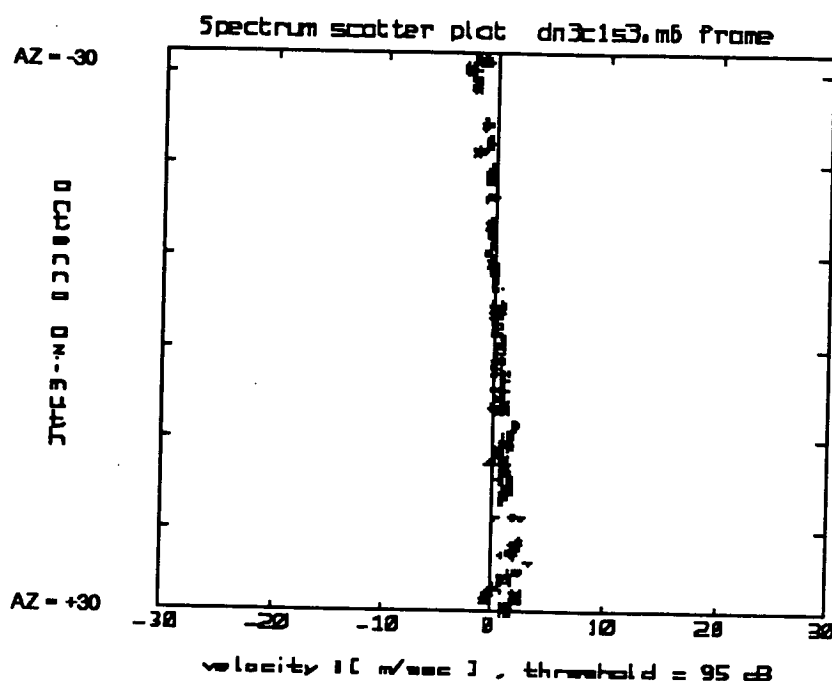
Radar Systems Laboratory
Electrical and Computer Engineering
Clemson University


Apr. 15, 1992

NOTES

The situation described in the previous slide has been analyzed to estimate the standard deviation in the "groundspeed error" as determined from the radar measurement.

Groundspeed Correction Bias vs. Antenna Azimuth



4th CMTAW meeting

Radar Systems Laboratory
Electrical and Computer Engineering
Clemson University

Apr. 15, 1992

NOTES

During each flight experiment the airborne radar antenna was in a scanning mode, typically covering -30, +30 degrees azimuth relative to the A/C longitudinal axis. A small bias error in the ground speed that varied linearly as a function of azimuth angle was noted in virtually all data sets. This error remained after routine correction for the geometric variation of zero Doppler as a function of azimuth angle. In addition, the slope of this bias varied depending on the antenna scan direction. This figure illustrates a counterclockwise scan from a DEN rwy 26 flyover. FFT spectra of data records from 61 frames at 1 degree increments across the scan were thresholded so that the central ground clutter peak is represented as a cluster of points showing how the Doppler spectrum peak varies with azimuth angle. All data are from the range cell where the antenna boresight intersects the ground.

Additional On-going Research Work

- 1. Real time algorithm development**
- 2. Adaptive clutter rejection filtering**
- 3. Modelling of weather radar returns**
 - autoregressive modelling
 - linear models based on fractals
 - non-linear models based on chaotic systems theory
- 4. Optimal Bayesian methods for Hazard Factor estimation**
 - use Doppler spectra as windspeed probability density
 - transform to F-factor probability density
 - estimate "most probable" F-factor map in protection volume

4th CMTAW meeting

Radar Systems Laboratory
Electrical and Computer Engineering
Clemson University


Apr. 15, 1992

References

- Baxa, E.G., Jr., " Airborne Pulsed Doppler Radar Detection of Low-Altitude Windshear - A Signal Processing Problem," Digital Signal Processing 1, pp. 186-197, Academic Press, October 1991.
- Kunkel, M.W., "Spectrum Analysis for the Detection of Low-Altitude Windshear with Airborne Doppler Radar," Radar Sys. Labs. TR-15, ECE Dept., Clemson Univ., Clemson, SC 29634-0915, February 1992.
- Baxa, E.G., Jr. and Lee, J., "The Pulse Pair Algorithm as a Robust Estimator of Turbulent Weather Spectral Parameters Using Airborne Pulse Doppler Radar," NASA CR4382, DOT/FAA/RD-91/17, 1991.
- Keel, B.M. and Baxa, E.G., Jr., "Adaptive Least Square Complex Lattice Clutter Rejection Filters Applied to the Radar Detection of Low Altitude Windshear," Proc. Int. Conf. Acoust., Speech, Sig. Proc., ICASSP-90, Albuquerque, pp. 1469-1472, Apr. 1990.

REPORT DOCUMENTATION PAGE			Form Approved OMB No. 0704-0188	
Public reporting burden for this collection of information is estimated to average 1 hour per response, including the time for reviewing instructions, searching existing data sources, gathering and maintaining the data needed, and completing and reviewing the collection of information. Send comments regarding this burden estimate or any other aspect of this collection of information, including suggestions for reducing this burden, to Washington Headquarters Services, Directorate for Information Operations and Reports, 1215 Jefferson Davis Highway, Suite 1204, Arlington, VA 22202-4302, and to the Office of Management and Budget, Paperwork Reduction Project (0704-0188), Washington, DC 20503.				
1. AGENCY USE ONLY (Leave blank)		2. REPORT DATE September 1992		3. REPORT TYPE AND DATES COVERED Conference Publication
4. TITLE AND SUBTITLE Airborne Wind Shear Detection and Warning Systems - Fourth Combined Manufacturers' and Technologists' Conference			5. FUNDING NUMBERS WU 505-64-12-01	
6. AUTHOR(S) Dan D. Vicroy, Roland L. Bowles, and Robert H. Passman, compilers				
7. PERFORMING ORGANIZATION NAME(S) AND ADDRESS(ES) NASA Langley Research Center Hampton, VA 23665-5225			8. PERFORMING ORGANIZATION REPORT NUMBER	
9. SPONSORING / MONITORING AGENCY NAME(S) AND ADDRESS(ES) National Aeronautics and Space Administration Washington, DC 20546-0001			10. SPONSORING / MONITORING AGENCY REPORT NUMBER NASA CP-10105, Part 1 DOT/FAA/RD-92/19-I	
11. SUPPLEMENTARY NOTES Dan D. Vicroy and Roland L. Bowles: NASA Langley Research Center, Hampton, Virginia Robert H. Passman: Federal Aviation Administration, Washington, DC				
12a. DISTRIBUTION / AVAILABILITY STATEMENT Unclassified—Unlimited Subject Category 03			12b. DISTRIBUTION CODE	
13. ABSTRACT (Maximum 200 words) The Fourth Combined Manufacturers' and Technologists' Conference was hosted jointly by NASA Langley Research Center (LaRC) and the Federal Aviation Administration (FAA) in Williamsburg, Virginia, on April 14-16, 1992. The meeting was co-chaired by Dr. Roland Bowles of LaRC and Bob Passman of the FAA. The purpose of the meeting was to transfer significant ongoing results of the NASA/FAA joint Airborne Wind Shear Program to the technical industry and to pose problems of current concern to the combined group. It also provided a forum for manufacturers to review forward-look technology concepts and for technologists to gain an understanding of the problems encountered by the manufacturers during the development of airborne equipment and the FAA certification requirements. The present document has been compiled to record the essence of the technology updates and discussions which follow each.				
14. SUBJECT TERMS Microbursts; Wind Shear; Aircraft Hazards; Doppler Radar; Infrared; LIDAR			15. NUMBER OF PAGES 621	
			16. PRICE CODE A99	
17. SECURITY CLASSIFICATION OF REPORT Unclassified	18. SECURITY CLASSIFICATION OF THIS PAGE Unclassified	19. SECURITY CLASSIFICATION OF ABSTRACT	20. LIMITATION OF ABSTRACT	

NSN 7540-01-280-5500

Standard Form 298 (Rev. 2-89)
Prescribed by ANSI Std. Z39-18
298-102

PRECEDING PAGE BLANK NOT FILMED